FUEL FOR THE FUTURE

Processed High Quality Coals for Low- and Zero-emissions Power

George Domazetis

Fuel for the Future

Fuel for the Future:

Processed High Quality Coals for Low-and Zero-emissions Power

By

George Domazetis

Cambridge
Scholars
Publishing

Fuel for the Future:
Processed High Quality Coals for Low- and Zero-emissions Power

By George Domazetis

This book first published 2019

Cambridge Scholars Publishing

Lady Stephenson Library, Newcastle upon Tyne, NE6 2PA, UK

British Library Cataloguing in Publication Data
A catalogue record for this book is available from the British Library

ISBN (10): 1-5275-3683-1
ISBN (13): 978-1-5275-3683-8

Dedicated to Thalia

TABLE OF CONTENTS

PREFACE

The greatest global challenge today is perhaps the impact of increasing levels of Greenhouse gases (GHGs) in the atmosphere and the consequences that flow from this, viz. increasing temperatures, melting ice and glaciers, higher sea levels, and climate change. The primary contributor to the GHG levels is the widespread use of fossil fuels for power generation, transport, agriculture, industry, and domestic sectors. The problems are exacerbated by various factors, such as large scale deforesting, low efficiency in fossil fuel usage, the increasing demand for transport and power generation.

It is important to foster a balanced debate on this important problem. The drive to reduce poverty and improve living conditions worldwide also calls for urgent action. An important factor in improving living conditions for developing countries is secure and affordable power. Low cost and abundant fuels have been crucial to the growth of developed economies, and it is reasonable to offer the same advantages to the economies of developing nations. It also needs to be stated that a secure and affordable power supply is necessary for all economies. The drive to lower the cost of renewable sources of power is also an important contributor to lower emissions.

The world is faced with a dilemma. If fossil fuels are used at an increasing rate the problems from higher levels of GHG will become greater, and both developed and developing nations will suffer, with the poorer countries experiencing the greatest difficulties. It is highly unlikely, however, that the world would shut down all coal-fuelled power generation, or cease using fossil fuels, as the consequences of this would be traumatic.

It is obvious that many initiatives and innovations are required to address these difficulties, including political, economic and technological ideas. Some of these include reducing the carbon footprint in our daily lives, utilising renewable power generation where it is economically competitive, increasing the efficiency of fossil fuels electricity generation with the goal of zero-emissions plants, enlarging carbon sinks such as forests, and developing power distribution systems that better enable communities to meet the variable demand for power. The nature of the problem requires a worldwide effort that ultimately is about the human spirit and the belief that we can share the challenges together, and together achieve our collective goal. Such a collective effort would ensure energy security, provide access

for all nations to reliable and affordable energy, and enable economic growth, while protecting the planet for future generations.

The ultimate goal is to take advantage of plentiful and relatively cheap fossil fuel to generate electricity with zero emissions, without an unacceptable increase in the price paid for power. This goal is technically feasible – however, even if coal-fuelled power generation with zero-emissions is developed and implemented, this in itself will only slow down the increasing levels of GHGs. Other sectors need to reduce emissions significantly to avoid the consequences of increasing global temperatures. For example, transportation may undergo a transition to electricity-driven vehicles, and this would be boosted by the availability of a low emission and affordable electricity supply.

This volume discusses the research and development of low rank coals, carried out within the context of addressing the environmental impact of these coals when used to generate electricity. Low rank coals make up about half of the world's coal deposits and are widely used due to their low cost. Currently these operate with the highest carbon emission intensity. Research that can take advantage of the low cost of low rank coal, and achieve low or zero emissions, has the potential to provide affordable electricity, thereby achieving the twin goal of secure, affordable power with a reduction in emissions. The concept is to chemically process these coals into high quality fuel, with high efficiencies in processing and power generation. The research discussed in this volume deals predominately with low rank coals, and how high quality fuel may be produced with the properties required for maximum performance of new power generating plants, and coal gasification. The process does not discharge any pollutants to the environment, and new coal power plants would be designed for low emissions, with the ultimate goal of converting these into zero-emissions plants. This concept would include the capture and utilisation of carbon dioxide as a feedstock to manufacture valuable materials.

It is hoped that ultimately this coal treatment process will be developed commercially and thus make a significant contribution to the overall effort at combating the problem(s) arising from the increasing concentration of GHGs in the atmosphere.

The research discussed in this volume is the result of fruitful collaboration between Clean Coal Technology Pty Ltd and La Trobe University in Australia. It is with considerable pleasure that I highlight the contributions made by staff and post-graduate students at the University, particularly Professors B. D. James (deceased) and J. Liesegang, whose support and input proved invaluable to the success of the project. Contributions by staff in the Departments of Chemistry, Physics, and Earth

Sciences, particularly Mr J. G. H. Metz, Dr R. Glaisher (deceased), Dr P. J. Pigram, and Dr I. Potter, are gratefully acknowledged. I am grateful to Professor J. Hill for his interest and involvement. The work by M. Raoarum and P. Barrila provided an especially useful contribution to the project. Facilities and welcome support were provided by the Victorian Partnership for Advanced Computing Facility, Melbourne, and the Australian Partnership for Advanced Computing National Facility (currently the National Computational Infrastructure), Australian National University, Canberra.

ABBREVIATIONS

Acid washed
aw
As received
ar
Atomic absorption spectroscopy
AAS
Binding energy
BE
Carbon capture and storage
CCS
Carbon-13 nuclear magnetic resonance cross-polarisation with magic angle spinning ^{13}C NMR CP/MAS
Chemical oxygen demand
COD
Circulating fluidised bed combustion
CFBC
Clean Coal Technology Pty Ltd/La Trobe University
CCT/LTU
Combined heat and power
CHP
Commonwealth Scientific and Research Organisation
CSIRO
Computational fluid dynamics
CFD
Computer-controlled scanning electron microscopy
CCSEM
Cost of electricity
COE
Density functional theory
DFT
Di-methyl ether
DME
Direct coal-fuelled turbine combined cycles
DCFTCC

Direct coal-fuelled turbine
DCFT
Distributed activation energy model
DAEM
Dry ash free basis
daf
Dry basis
db
Electron paramagnetic resonance
EPR
Externally-fired combined cycles
EFCC
Fischer-Tropsch
F/T
Force field
FF
Fourier-transform infra-red spectroscopy
FTIR
Gas chromatography/Mass spectrometry
GC/MS
Global Warming Potential index
GWP
Greenhouse gases
GHGS
Heat of formation
ΔH_f
Higher heating value
HHV
Inductively coupled plasma atomic emission spectroscopy
ICP-AES
Integrated gasification combined cycles
IGCC
Internal rate of return
IRR
International Energy Agency
IEA
Kelvin (degrees)
K
Laser-induced breakdown spectroscopy
LIBS

Life cycle assessment
LCA
Lower heating value
LHV
Megajoules per kilogram
MJ/kg
Megawatt hour
MWh
Megawatts
MW
Milligrams per litre
mg/L
Milligrams
mg
Million metric tons
MMT
Molecular dynamics
MD
Molecular mechanics
MM
Multiple high-resolution transmission electron microscope
HRTEM
Net present value
NPV
Nitrogen oxides
NOx
Normal temperature and pressure
NTP
Operating and maintenance cost
O&M
Parts per million
ppm
Pressurised fluidised bed combustion
PFBC
Proton exchange membrane electrolysers
PEM
Pulverised coal
PC
Reverse osmosis
RO

Scanning electron microscopy and energy dispersive x-ray analysis
SEM-EDX
Semi-empirical quantum mechanics
SE-QM
Single point self-consistent field
1scf
Solid oxide electrolysis cell
SOE
Substitute natural gas
SNG
Sulphur oxides
SOx
Supercritical
SC
Thermal gravimetric and differential thermal analysis
TG/DTA
Time of flight – secondary ion mass spectrometry
TOF-SIMS
Total dissolved solids
TDS
Total organic carbon
TOC
Turn over frequency
TOF
Ultra-supercritical
USC
United States Environment Protection Agency
US EPA
Water gas shift
WGS
X-ray absorption near edge structure
XANES
X-ray diffraction
XRD
X-ray fluorescence
XRF
X-ray photoelectron spectroscopy
XPS

CHAPTER ONE

COAL-FUELLED POWER GENERATION AND THE NEED FOR CLEAN TECHNOLOGIES

It is understood that the unrestricted use of fossil fuels may lead to levels of greenhouse gases (GHGs) that would result in the "overheating" of the globe and cataclysmic climate change. The general perception is that the increase in GHGs emissions, especially from fossil-fuelled plants, must be reduced to low or zero-levels. Some insist that coal-fuelled power generation and coal mining operations should cease.

There is also the view that emphasises the benefits and security derived from cheap and secure energy to expand and modernise economies. Developing countries, in particular, observe that developed nations have obtained the benefits of a secure and plentiful supply of energy, and demand they also derive such benefits for their economies.

Fossil fuels, and particularly coal, have become a source of controversy and political agitation.

Developed and developing economies are all dependant on an affordable and secure source of power. Electricity generation is a basic requirement for daily activities, clean water, and the disposal of sewage, which are critical in improving health and maintaining good living standards; it also contributes to lessening poverty and improving the well-being of countless human beings. This, however, may clash with the environmental hazards associated with fossil fuels' pollution, which may result in poor health as well as long term climate change. The climate change due to the rising concentrations of GHGs in the atmosphere poses long term hazards to all nations.

In view of these problems, we may ask, "What is the future of coal-fuelled power generation?"

Historically, electricity has been generated using coal, gas, diesel, nuclear, hydro and, recently solar, wind, and to a lesser extent bio-fuels. Fossil fuels are burnt and the heat is used to create steam that drives turbines connected to generators. Gas-fuelled turbine power plants burn gas, and the hot gases are expanded through turbines which are connected to power

generators. Coal-fuelled power generation has undergone significant improvements in efficiency, and with the additional advances in the management of power transmission and distribution, as well as economies of scale, coal became the dominant fuel for power generation worldwide.

Coal power generation is projected to remain the major source of electricity for the foreseeable future. The International Energy Agency (IEA) reports that coal fuels about 40% of the world's power generation, but there is a greater proportion of coal-fuelled power in many countries. The IEA also shows that improvements in power generation efficiency would be a significant step towards a reduction in CO_2 emissions from coal (Burnard and Bhattacharya, 2011). Projections of energy production in the USA show coal consumption decreased from 2017 onward, mostly replaced by gas, while data for China and India show these countries rely heavily on coal-fuelled power generation. The proportion of electricity generation using coal is large for many nations, even though effort is being expended in lowering emissions; e.g. the proportions of power generation using coal reported for the period from 2007 to 2011 are 79% for China, 49% for the USA, and 92% for Poland. Coal power generation in India accounts for 73% of electricity production, and although this proportion may decrease, reports indicate overall coal-fired capacity may increase substantially by 2040, despite considerable increases in wind and solar power. China is expected to produce 50% of its total power with coal, which is still projected to be the major fuel for power generation in 2050. The IEA Coal Information Overview provides details of coal use in regions around the world.*

Coal varies in rank (heating content), in composition, and in the amounts of pollutants such as sulphur and ash. Consequently, a variety of electricity generation technologies have been developed (and continue to be developed) in response to the particular coal properties. Historically, the majority of pulverised coal power plants are subcritical, and operate at lower efficiency levels (30% for low rank coal, 38% for black coal). New plants are being developed in an effort to reduce and eliminate CO_2 emissions. For example, oxy-combustion has been developed as an advanced technology to include capturing CO_2. Coals with high sulphur content can be used in fluid-bed combustion plants that retain sulphur with the ash, and sulphur oxides from pulverised coal power plants may be removed by cleaning flue gases. Pulverised coal combustion is the major technology for power generation; as the term implies, coal is crushed into a powder and fed to a coal burner with air. Coal gasification is a technology used to produce synthesis gas (mainly CO and H_2), and this can be used as fuel for power generation with gas turbines, or to provide synthetic household gas, or to

* For more information, see http://www.iea.org/topics/coal/.

produce liquid hydrocarbons, such as sulphur-free diesel. An overview of developments for clean energy is provided by Johnsson (2007), and a discussion of advances in modelling of coal combustion and gasification at the Sandia Laboratories is given by Hecht and Shaddix (2015).

Historically, progress in power generation has occurred through improvements in efficiency and economies of scale, which have ensured a secure and affordable power supply to underpin economic activity and improve living standards. The prolonged period of burning fossil fuels, however, has resulted in degradation of the environment, and air pollution, which can lead to poor health to populations, and now poses global changes to the climate, leading to more severe weather events and rising sea levels.

Coal's molecular matrix is composed mostly of carbon and hydrogen, with variable amounts of oxygen, nitrogen, and sulphur, with water- and ash-forming components; when pulverised coal is mixed with air in a coal flame, the combustion with oxygen produces carbon dioxide, water, pollutants such as sulphur and nitrogen oxides, and ash particulates. The environmental and health problems posed by the fossil-fuelled power generation sector (and also from the transport sector) have been discussed for decades and various programs have been implemented to reduce pollutants (such as removing sulphur and nitrogen oxide emissions) and to find measures that may ultimately remove the emission of all pollutants to the atmosphere. Because the problem is global, and because power generation is essential to nations and their economies, a large number of measures have been examined and continue to be discussed for changes to future power generation; these measures include new ways to use fossil fuels, increased use of solar and wind power, developing electric cars, increases in the efficiencies by the user of electricity (thereby lowering the demand), and advances in the management of electricity transmission grids to use a mix of power sources that would ensure lower emission intensities are maintained. The ultimate goal of these programs is the transition towards low- to zero-emissions power, by using a judicious combination of power generation from fossil, nuclear, bio-fuel, solar, wind and hydro sources. Of particular interest is the concept of zero-emissions fossil fuel power generation that includes the capture of CO_2 for use as a feedstock for the synthesis of valuable products, thereby offsetting the costs for the capture of CO_2. This strategy requires long term planning, and a radical change in the management of electricity transmission grids, but offers the promise of secure and affordable power for the foreseeable future, with a mitigation of CO_2 emissions. This is an exciting concept that, if successfully implemented on a commercial sale, would be a major factor to solving the problems of climate change attributed to using coal as a fuel. A secure and affordable

supply of electricity, with low emissions, would enhance economic activity and prosperity in regions with significant coal resources.

The economic and policy dimensions of global climate change have been discussed in the Stern Review (2006), which concluded, "The benefits of strong, early action considerably outweigh the costs" and estimated the annual worldwide costs of stabilising CO_2 to 500-550ppm at about 1% of the global GDP by 2050. The review identified four ways to achieve the desired reduction in emissions:

1. Reducing demand for emissions-intensive goods and services.
2. Increased efficiency, which can save money and reduce emissions.
3. Action on non-energy emissions, such as avoiding deforestation.
4. Switching to lower-carbon technologies for power, heat, and transport.

These general recommendations have been accepted by most governments and industries. There is universal agreement on the need to increase the efficiency of coal-fuelled power generation. The efficiency of fossil-fuelled plants is that proportion of the heat content of the fuel that produces electricity; power plants produce steam in boilers, and the steam drives turbine generators. Increasing the temperature of the steam increases the efficiency of power generation. Subcritical power plants operate at temperatures up to 374°C and pressures of 3,208 pounds per square inch (psi). Supercritical power plants (SC) operate at up to 566°C, and ultra-supercritical power plants (USC) may operate at up to 760°C and pressure levels of 5,000 psi. The environmental impact of fossil-fuelled plants is assessed by the emissions' intensity, reported as the kilograms of CO_2 per megawatts of electricity sent to the grid; higher efficiencies result in lower emission intensities.

The combination of higher efficiency in power generation and the relatively lower costs of coal provides a secure power supply, and can lead to lower emissions while slowing the increase in the cost of electricity to the end-user. The Stern Review highlights measures that may be taken nationally and internationally to limit the amount of CO_2 emitted to the atmosphere – these include placing a price on CO_2, the development of low-carbon and high efficiency technologies, and dealing with barriers to changing behaviour.

Due to the looming problems resulting from inefficient plants and the overuse of fossil fuels, major Clean Coal Technology Research, Development and Demonstration Programs (CCT RD&D) have been undertaken to examine a number of initiatives to minimise, and ultimately

negate, the environmental problems posed by the increasing use of fossil fuel, while maintaining the security and affordability of low cost coal-fuelled power generation. These programs have provided incremental improvements in efficiencies, but have not instigated the global radical changes that would result in the required reduction in emissions from fossil-fuelled power generation. While progress has occurred in the development of the implementation of higher efficiencies from SC and USC pulverised coal-fired technologies, lower efficiency sub-critical plants continue to be used for power generation. Generally, an SC plant operates at about 45% efficiency, and a USC plant may operate at ≥45% based on the lower heating value (LHV) of bituminous coals. Future developments in alloys may lead to a USC efficiency of 50% (LHV). Progress in circulating fluidised bed combustion (CFBC) plants utilising low-rank fuels would also result in lower emissions of SO_X and particulates.

While modern electricity production and distribution systems are increasingly reliant on a mix of power generation from coal, nuclear, hydro, and gas, the largest relative increase in power generation has been from solar and wind. The cost of renewables has continued to decrease and, as a result, these increasingly supply a higher proportion of power to communities. Grids are managed to cope with the intermittent nature of renewables. The IEA reports that renewable sources made up almost two-thirds of new net electricity capacity, amounting to about 165 gigawatts (GW), with 74 GW in China. Indeed, for the first time, additions of solar PV power outpaced the growth of other sources, including that of coal-fuelled power generation. Conventional low efficiency coal-fuelled plants are an undesirable option for future power generation (Katzer, 2017).

There is a diverse range of coal types, with variable properties, and thus coals of differing quality are available for power generation. Low quality coals would not be desirable as fuel for future cleaner power generation technologies. Low rank coals are problematic as fuels for subcritical plants, and these problems would increase if these coals are used to fuel future high efficiency plants. Technologies have been sought to improve the quality of coals; the motivation to process low rank coals into high quality fuel is their low cost per unit heat of the mined coal. This relatively low cost must be maintained with any high efficiency plant, and this may be realised by developing a concept that integrates the coal treatment process with the power generating plant, to achieve high thermal and power efficiencies. This concept is similar to operational combined heat and power plants. The coal treatment process is integrated with a power station to refine raw coal into high quality fuel designed for maximum performance of the high efficiency power plant. The major features of the high quality processed

coal are low to virtually zero ash, low sulphur and chloride content, high heating value, and the ability to use catalysts to enhance reactions between coal and steam for gasification.

The ultimate clean future for the coal project is zero-carbon emissions, by collecting CO_2 for use as a raw material for the production of valuable materials, such as methanol, or di-methyl ether (DME). The overall trajectory towards a zero-emissions commercially viable coal-fuelled power generation is common to all major CCT Programs.

The specific purpose of this volume is to discuss the research that is central to understanding the properties of low rank coals that render them as poor quality fuels, and from this outline the methodology required to process these for future use as high quality fuels in low- to zero-emissions concept(s). This research deals with low rank coals and the efforts undertaken to process these into high quality fuels; this is a portion of the much wider worldwide programs towards the development of low carbon emissions fossil-fuelled power generation systems. This volume discusses coal-fuelled power generation using high quality fuels obtained by processing low cost, low rank coals, and a strategy towards zero-emissions power. The discussion also draws on innovation achieved in the larger worldwide CCT Programs, such as low-NOx burners, higher efficiency plants, oxy-combustion, and the production of hydrogen.

A detailed treatment of all coal types and their use is beyond the scope of this volume; research on coal utilisation has been carried out over many decades, and a great amount of literature has been published on coal properties, coal combustion slagging and ash fouling, with additional literature dealing with clean coal programs. As a result, it is impractical to include all of the scientific literature dealing with all coals, and instead the information that has been selected mostly deals with low rank coals. As the treatment methodologies to produce low ash coal are primarily chemical, the major focus has been on understanding the chemistry required to render low rank coals into high quality fuels for future coal combustion and gasification.

Clean Coal Programs

Major programs have been undertaken worldwide to develop lower emission coal-fuelled power generation, with the twin goals to reduce, and eventually eliminate, environmental problems derived from using coal, and to provide secure and affordable power generation in the foreseeable future. Examples of these programs include the US Department of Energy Clean Coal Technology Program (DOE CCT), the Japanese Clean Coal Project

(JCOAL) and the European Commission Research & Innovation on Energy (EU). The DOE, JCOAL and EU programs are discussed briefly here to illustrate the nature of the worldwide effort. China has also made significant progress in implementing high efficiency power plants and renewable power.

The comprehensive DOE CCT Program seeks to improve current power generation plants, and to develop new technologies that would meet energy requirements economically while addressing environmental impacts. A general review of the USA's activities and the funding of technologies by Longwell et al. (1995) gives an assessment of the future goals of the DOE's coal research, development, demonstration and commercialisation programs extending to 2040. During this period, coal is projected to continue to fuel electric power generation, along with a growing use of gas. The DOE coal program addresses mainly power generation technologies, with an emphasis on environmental concerns and clean fuels; the review also addresses the barriers to higher efficiency in both power generation and fuel production, ways to reduce CO_2 emissions, control of air pollutants, and the discharge of solid wastes. This assessment also noted increases in efficiency would require extensive R&D to overcome a number of barriers. The highest efficiencies are obtained with gas turbine combined-cycle systems, and for these the production of a hot gas stream of sufficient purity is required, which is the major challenge to developing commercial plants. Critical components required for these advanced power generation plants include the continuous removal of slag from combustion chambers, high temperature filters for Pressure Fluidised-bed Combustion (PFBC) systems, a high temperature air/furnace heat exchanger for indirect fixed systems, a hot gas clean-up system for PFBC and for Integrated Gasification Combined-Cycle (IGCC) systems, and turbine blades that would operate at high temperatures and can cope with trace impurities that may escape the high temperature gas clean-up system. Fuel cells are also capable of clean operation and high efficiency, but their high cost is a major problem. Solutions to these challenging problems require a continued program of advanced research and component development. The large array of technologies considered will also require detailed systems studies and the development of realistic commercialisation strategies.

The DOE "Program Update of 2000" report discusses 38 projects, which included ways to control and lower emissions of sulphur dioxide (SO_2), nitrogen oxides (NOx), mercury and particulate matter for existing plants. The program includes developments in Fluidised-bed Combustion (FBC), IGCC, and Advanced Combustion/Heat Engines. Innovations are created to improve efficiencies and environmental performance for electricity

generation and the production of synthesis gas. A significant component of the DOE Program includes coal upgrading projects, such as the ENCOAL® Mild Gasification Project, the Advanced Coal Conversion Process, and methanol production at a commercial-scale demonstration plant with the Liquid Phase Methanol (LPMEOH™) Process (this produced 80,000 gallons/day of methanol for Eastman Chemical Company). Considerable reductions have been achieved in SOx and NOx emissions from US coal-fuelled power plants to meet regulations imposed by the Clean Air Act (DOE, 2001). The DOE CCT trajectory includes the development of new higher efficiency power plants, thereby decreasing the emission intensity ($kgCO_2/MWh$), and would meet the increasing demand for electricity. The Program culminates in the Vision 21 Plan; a wide range of power generation options are considered, including fuel cells and turbines fuelled with natural gas and coal – this anticipates a range of facilities that will be able to convert fossil fuels in a cost effective manner into electricity, process heat, fuels, and/or chemicals, with low CO_2 emissions (National Research Council, 2003).

Carbon dioxide capture for use in enhanced oil recovery has been pursued through joint industry- and DOE- funded arrangements. Currently, the expanded Petra Nova operational plant captures emissions from a 240 MWe generation facility situated at Houston, with a demonstrated ≥90% carbon capture rate. This facility is reported to capture ≥5,000 tons of CO_2 per day, used for enhanced oil recovery, which is expected to boost the production of oil by an additional 14,500 barrels per day. This offsets the costs of CO_2 capture, and for this particular example, predictions of enhanced oil recovery for the site are 60 million barrels of oil (at the price of oil, this represents a total revenue of $2-$3 billion). This is an example of a commercial CO_2 capture program. Currently, however, simple carbon capture and storage encounters energy penalties and costs; ultimately cost effective technologies with zero-emissions may be achieved by capturing CO_2 for use as a feedstock to produce valuable products such as liquids and plastics. The costs of CO_2 capture would be offset by returns from valuable products. The long term goal for zero-emissions has been accepted by major organisations; the central feature for this is the cost effective production of hydrogen, to be used in reactions with CO_2 to provide high value products.

The DOE has sought ways to improve the performance, and reduce the capital costs, of coal gasification. This includes work on advanced gasifiers configured with supporting systems that incorporate innovative technologies. The intent is to utilise highly efficient new reactors for smaller scale applications and superior products, with the use of low cost, low rank coals, and thereby expand opportunities for gasification systems with lower

feedstock costs. A significant development is that of gasifiers for higher hydrogen content in synthesis gas (syngas) production. Research has been conducted on advanced water-gas shift processes and catalysts to reduce the cost of high-hydrogen syngas production. The production of hydrogen, and higher quality syngas, are important ingredients in developing technologies with lower CO_2 emissions. Chemical looping is also being researched, in which oxygen is used through an oxidation-reduction cycling of an oxygen carrier, which is a single metal oxide, such as copper, nickel, or iron, or a metal oxide supported on a high-surface-area substrate, such as alumina or silica (Aston et al., 2013). The DOE funded a pilot scale operation and testing of syngas chemical looping for H_2, and Alstom carried out research on chemical looping for high-hydrogen syngas for power generation and/or liquid fuel production.* The production of syngas with a higher H_2 content may also be achieved by developing catalysts for the gasification of coal with steam, and the relevant chemistry is discussed in Chapter Seven of this volume.

The DOE reports the following activities during 2018:

> R&D is focused on developing and demonstrating advanced power generation and carbon capture, utilization and storage technologies for existing facilities and new fossil-fuelled power plants by increasing overall system efficiencies and reducing capital costs. In the near-term, advanced technologies that increase the power generation efficiency for new plants, and technologies to capture carbon dioxide (CO_2) from new and existing industrial and power-producing plants are being developed. In the longer term, the goal is to increase energy plant efficiencies and reduce both the energy and capital costs of CO_2 capture and storage from new, advanced coal plants and existing plants. These activities will help allow coal to remain a strategic fuel for the nation while enhancing environmental protection.†

The DOE also seeks to facilitate partnerships with industry, and academic researchers, in the areas of solid oxide fuel cells, stress and geomechanical impacts in the subsurface related to CO_2 storage, pre-combustion carbon capture, and advances in fossil power system operation and economic performance.‡

---

* For more information, see https://www.netl.doe.gov/research/coal/energy-systems.

† For more information, see https://im-mining.com/2018/11/13/advancing-coal-power-plants-future.

‡ For more information, see https://www.energy.gov/fe/science-innovation/office-clean-coal-and-carbon-management.

Japan imports its energy, and the goal of the Japanese effort is to ensure a secure and sustainable supply of coal; to this end, Japan relies on access to reserves of coal such as are found in the USA, Europe, China, Indonesia, India and Australia. The JCOAL Program undertakes activities to identify and characterise overseas coal resources, and provide assessments of the technological capabilities required by Japanese coal importers and users. Japan has a greater focus on developing plants of increasing efficiency (and a resulting lower coal use), such as SC and USC plants, as part of their power generation mix (JCOAL, 2007). The overall strategy of the Japanese CCT Program has been technical innovation in the use of coal to fuel their power generating industry. This extensive and wide ranging program places considerable emphasis on the future use of various forms of coal gasification technologies, such as IGCC and integrated coal gasification with fuel cell combined cycles. Additional effort has gone into coal-derived synthesis gas conversion into liquid fuel or chemical raw materials, such as methanol and DME, as an alternative to diesel, and gas to liquid hydrocarbons for diesel production. The ultimate goal of the JCOAL is also zero CO_2 emissions coal-fuelled plants.

The European Commission has allocated the largest portion of its funding to collaborative research and innovation, which includes renewable sources and improving the efficiency of electricity use in homes and offices in cities. The EU effort on CCT has been mainly on carbon capture and storage from high efficiency coal-fuelled plants. The EU Commission added the "Energy Technologies and Innovation" in 2013 to respond to new challenges and to consolidate research and innovation across Europe. The activities included the "Horizon 2020 Energy Challenge" which focuses on "Energy Efficiency", "Competitive Low-Carbon Energy" and "Smart Cities and Communities", and covers the full innovation cycle – from proof-of-concept to applied research, pre-commercial demonstration and market uptake. * The International Energy Agency (IEA) reported on EU achievements in the development of clean coal power generation technologies by improving the performance of pulverised coal-fired power plants, including reducing slagging and fouling of boilers, and improved environmental outcomes. The effort also included co-combustion and fluidised bed applications, the development and introduction of advanced power generation systems, and methods for CO_2 control (Minchener and McMullan, 2007). The IEA assessed the ongoing progress in coal-fuelled power generation and made a number of recommendations, including introducing policies that would reduce constructions of new subcritical

* For more information, see https://ec.europa.eu/info/publications/interim-evaluation-horizon-2020_en.

coal-fuelled plants, and instead encourage utilising commercially available, cost effective supercritical pulverised coal plants. The energy penalty associated with carbon capture and sequestration was also noted.

The DOE and JCOAL CCT programs have examined a wide range of coals to fuel various power generating plants, brought improvements in the environmental impact of current coal-fuelled subcritical plants, and contributed to the development and commercialisation of higher efficiency future plants. The DOE and JCOAL strategies are ultimately for future zero-emissions coal-fuelled systems that will include hydrogen in hybrid technologies based on enhanced coal gasification.

The US and China have undertaken a collaborative approach within the Clean Energy Research Centre, a program that encourages top researchers from both countries to develop technologies for clean energy. The program seeks technologies needed for an efficient and low-carbon economic future. This is wide ranging and includes advanced coal-fuelled technologies, and energy efficiency for buildings.

The uptake of higher efficiency SC and USC coal-fuelled plants has increased in China and Japan. Germany initially constructed SC and USC plants with steam temperatures of ≥550°C. Japan started constructing SC plants due to the 1970 oil crisis, and these power plants accounted for a significant proportion of generation plants in 1996, with an average annual growth of 27.3%. USC plants were introduced by 1993 and Japan was the driver of USC technologies during this period. China is reported to have built ten SC units during ~1990s, growing to 27 by 2010. From 2010 to 2020, larger power plants in China will be required to be SC, and about half of the new power plants will be USC (Horach et al., 2014). China has progressed the clean coal project, which includes USC coal-fired plants exceeding 100 GW, and the operation of a 250 MW integrated gasification combined-cycle demonstration power plant; the program includes water slurry gasification, dry feed pressurised gasification technology with a >2000 ton/day capacity, and the demonstration of CO_2 capture and storage, including enhanced oil recovery. Research on high temperature heat resistant alloy material has led to the demonstration of a 600 MW USC unit, which exceeds 700°C, to enable a system efficiency of 50-52%. A considerable proportion of China's coal reserves are low-rank coal and research is also ongoing to improve the quality of this coal.

Advanced higher efficiency coal-fuelled plants are developed by major suppliers of power generation plants. General Electric is part of a consortium undertaking a US DOE-led project to develop materials for USC plants that would operate with high pressure steam at 760°C. Siemens is developing new materials and turbines to operate at 600-700°C. Alstom

reports a design-ready 500 MW turbine to operate at 700°C, but are concerned with the costly alloys required for such a plant (We, 2011). SC and USC plants operate with high generating efficiencies, and where applicable, combined heat and power may provide up to 90% total thermal efficiency (Mohn, 2008; Santoianni, 2015).

The IEA has undertaken a study of how high efficiency, low emission coal-fired power plants may contribute to the reduction of carbon dioxide emissions in the major coal user countries: Australia, China, Germany, India, Japan, Poland, Russia, South Africa, South Korea and the USA. These countries have differing coal-plant fleet ages and efficiencies, and different local conditions and policies which impact on the capacity to implement advanced technologies. The study provides an overview of the differing trends for these countries, showing their dependence on an aging coal-fuelled fleet, and the prospects for growth, or decline, in coal-sourced electricity (Barnes, 2015).

The advanced power generation plant uses expensive alloys operating at high temperatures and pressures, and it is imperative that the coal used to fuel such plants does not cause the corrosion or fouling of heat transfer surfaces. Most coals, and especially low rank coals, contain aggressive ash-forming constituents that may cause corrosion, erosion and fouling of boilers. High moisture in low rank coals is also unwanted. Effort is required to produce high quality, non-fouling and low-cost fuel for new power generation plants. A plethora of physical and chemical approaches to upgrading all coals have been performed by various organisations, and the major ideas are discussed in this volume. Various organisations have examined novel ways to utilise low rank coal, particularly by upgrading high-moisture low rank coal by drying, but few (if any) of these are commercialised. Modern drying technologies have been developed in Germany and the US. RWE's WTA dryer and GRE's DryFining™ system have been demonstrated successfully at a commercial scale, while Vattenfall's PFD dryer has reached pilot scale. Dry lignite has been used to fuel a new power station in Grevenroich-Neurath near Cologne; this operates at 43% efficiency with a flexible response to demand. These are major advances in developing high efficiency lignite-fuelled power stations (World Coal, 2014).

While a large number of low rank coal drying processes have been examined, few chemical methods have undergone extensive research to produce high quality coal. A process developed by Clean Coal Technology Pty Ltd, and an R&D program in collaboration with La Trobe University (CCT/LTU R&D), is discussed in this volume; this process chemically removes ash constituents at elevated temperatures and then uses the same

heat to lower the moisture in coal. This process may also be used to add catalysts to low rank coals. The CCT/LTU R&D Program, which deals solely with the treatment of low rank coals, has defined process conditions to produce three high quality products with high heater content: (1) non-fouling coal, suited for high efficiency coal-fuelled plants such as SC and USC, (2) zero-ash coal suitable for direct coal-fuelled turbines, and (3) a catalytically loaded coal suited for the steam gasification of coal. The process is designed to be integrated with high efficiency coal-fuelled power generation plants, and is also integrated with gasification plants to produce high quality syngas.

Classifications of Coal and its Properties

Coal upgrading and beneficiation processing conditions are primarily based on the properties of the various coals, which are ranked as fuels based on their heat content. The low rank coals are peat, brown coal, lignite, and sub-bituminous, and the high rank coals are bituminous and anthracite. Table 1-1 shows the classification adopted by Coal Marketing International. Table 1-2 provides a range of properties for the majority of low rank coals. The US Geological Survey produced a detailed classification system for coals that includes elemental analysis, heating content, and accessibility for mining (Wood et al., 1983).

The heterogeneity of the coals poses considerable difficulties in developing chemical processes to improve their quality. Coal beneficiation has been practiced for a considerable period, with the majority of processes used to lower the ash content of high rank coals; some of these techniques may be applicable to sub-bituminous coals and lignites. The techniques for coal beneficiation are broadly physical, although recently chemical methodologies have been examined and discussed in the literature. The techniques discussed here are mostly for low rank coals, but occasionally high rank coal processes are also mentioned for illustration purposes.

An inexact, but useful, classification for coal processing is a division into two broad categories, namely hydrophilic (attracts and retains water) and hydrophobic (repels water). Low rank coals are hydrophilic due mainly to a greater proportion of oxygen functional groups within the organic coal matrix; these coals can be treated using aqueous acid-based chemistry. Hydrophobic coals can be washed with water to remove unwanted constituents, and as water is not absorbed by the coal, the treated coal can be separated from water without reducing the heating content. Hydrophilic coals will retain water and this must be removed after treatment to ensure a high quality product is obtained.

Table 1-1. Coal Properties and Rank*

	Moisture (ar)[a]	Volatile Matter (daf)[b]	Carbon (daf)	Calorific Value (ar)[c]	Oxygen (daf)
Peat	~75%	69 – 63%	<60%	3,500 kcal/kg	>23%
Lignite	35 – 55%	63 – 53%	65 – 70%	4,000 – 4,200 kcal/kg	23%
Sub-bituminous C	30 – 38%	53 – 50%	70 – 72%	4,200 – 4,600 kcal/kg	20%
Sub-bituminous B	25 – 30%	50 – 46%	72 – 74%	4,600 – 5,000 kcal/kg	18%
Sub-bituminous A	18 – 25%	46 – 42%	74 – 76%	5,000 – 5,500 kcal/kg	16%
High volatile bituminous C	12 – 18%	46 – 42%	76 – 78%	5,500 – 5,900 kcal/kg	12%
High volatile bituminous B	10 – 12%	42 – 38%	78 – 80%	5,900 – 6,300 kcal/kg	10%
High volatile bituminous A	8 – 10%	38 – 31%	80 – 82%	6,300 – 7,000 kcal/kg	8%
Medium volatile bituminous	8 – 10%	31 – 22%	82 – 86%	7,000 – 8,000 kcal/kg	4%
Semi-Anthracite	8 – 10%	14 – 8%	90%	7,800 – 8,000 kcal/kg	3.5%
Anthracite	7 – 9%	8 – 3%	92%	7,600 – 7,800 kcal/kg	4.5%
Meta-Anthracite	7 – 9%	8 – 3%	>92%	7,600 kcal/kg	5%

a – as received, often as-mined; b – dry ash free; c – kcal/kg= 0.0041868 MJ/kg.

As indicated by Tables 1-1 and 1-2, coal composition varies greatly, and coals can be found with properties outside those depicted in these Tables. Good quality high rank coals are exported, and their quality (and price) is

* For additional information see: http://www.coalmarketinginfo.com/advanced-coal-science/.

assessed by their heat, sulphur, and ash contents. Low rank coals are rarely exported, and most are used domestically for power generation. The cost of the coals roughly follows the classification in Table 1-1, with low rank coals having the lowest cost and high rank the most expensive. The heat content of low rank coals is generally low, as ash and moisture may account for between 50% and 70% of the weight of the mined coals.

Table 1-2. Range of properties of as-mined low rank coals.

Coal	H_2O wt%	Ash wt%	Volatile Matter wt%	Fixed Carbon wt%	Sulphur wt%	Chloride wt%	LHV⁺ MJ/kg
Brown Coal*	55 - 63	1 - 15	17 - 20	16 - 20	0.3 - 2	0.1 - 2	6 - 11
Lignite**	30 - 60	5 - 25	15 - 20	10 - 25	0.5 - 4	0.6	7 - 15
Sub-bituminous#	15 - 35	4 - 20	20 - 42	30 - 49	0.3 - 3	-	11- 23

* oxygen content at 24 - 28wt%; ** oxygen content 15 - 25wt%; # oxygen content 10 - 23wt%; ⁺low heating value

A useful comparison of the costs of various coals is based on the $/unit heat/unit weight (based on the average values of cost and the heating content). The cost per unit heat (AU$/GJ) is estimated at: brown coal 0.5-0.8; lignite 0.8-1.0; and thermal coal 4.7 (these values may differ as coal prices fluctuate due to changes in demand and supply, but the trend remains unchanged – a recent discussion on coal costs can be found in the IEA Report 'Production and Supply Chain Costs of Coal'; cf. Baruya, 2018).

Generally, the lowest cost per unit heat is that of low rank coals; a commercially viable treatment process for these coals would be possible if this cost comparison is sustained after treatment into high quality products.

Low rank coals exhibit a very wide range of ash and moisture, and treatment of high ash coals into high quality fuel would require significant effort, which may increase the costs of producing higher quality products. Consequently, a commercially viable process must consider the specific properties of a coal seam that need to be changed, and adopt a methodology that would ensure the advantage of the low cost of the mined coal is maintained. The properties of interest are the nature of the ash and moisture. Generally, the ash-forming constituents in low rank coals are sodium, magnesium, calcium, iron and aluminium species chemically associated with functional groups in the coal matrix, with alumina-silicate minerals and pyrites present as discrete extraneous particles, physically mixed with coal during mining; some of these extraneous mineral particles may also contain sodium (Na), magnesium (Mg), iron (Fe) and calcium (Ca). The ash-

forming constituents undergo chemical reactions in a coal flame; sodium forms vapour NaCl, NaOH, and Na_2SO_4 in combustion systems and Na_2CO_3, NaOH, NaCl (and perhaps sulphides) in gasification systems, and these react with silicates to form molten phases which deposit on heat transfer surfaces causing corrosion and fouling.

A feature of hydrophilic coals is the ability to dissolve the ash constituents with acid, and a variety of acid treatments may be developed to remove various proportions of ash. The costs of these treatment methods would be related to the type of acid and the amount consumed to remove the required amount of ash constituents. The efficiency of acid treatment is also an important aspect of ash reduction, as some ash-forming species may be removed at low acidity while others may require strong acids; elevated temperatures increase the ability to dissolve ash, but this requires acid resistant vessels for coal treatment. Acid treatment is attractive as it could also remove some sulphur pollutants along with ash-fouling constituents from the coal. The hydrophilic nature of low rank coals enables the penetration of acid through reasonably sized coal particles. Hydrophobic high rank coals are more difficult to process using acid due to the chemical nature of the ash constituents, and these coals need to be crushed into relatively small particles to expose encapsulated ash-forming particles to attack by acids. The behaviour of the various coals at elevated temperatures is also important to developing a viable process, and for this an understanding of the coals at a molecular level is required.

Coals are formed from mixtures of vegetation that have undergone very complex transformations over prolonged periods. Studies have been motivated by the utilisation of coals. High rank coals are used for heat and for the production of coke used in iron production. Low rank coals have received less attention because they are difficult to burn and cannot be turned into coke for iron production. With the advent of modern instrumental techniques, analytical chemists have been able to obtain a great deal of data on the composition of coals which have enabled insights on the way they have formed and on their behaviour as fuels. Advances in computer molecular modelling have also provided a powerful tool for chemists to understand the behaviour of coals. Computer simulations have also been employed to examine the intricacies of coal combustion and the formation of pollutants.

Coal-fuelled boilers are subjected to slagging and fouling by liquid silicates and corrosive ash deposits, which cover heat transfer surfaces and reduce heat transfer for generating steam. Ash deposit build-up can cause the shutdown of a power station in order for the boiler surfaces to be cleaned, thereby reducing the power output and adding costs for the

cleaning and maintenance of corroded surfaces. The large proportions of moisture and ash in low rank coals are significant "dead" mass flows, and require larger sized plants for given power outputs, resulting in higher capital costs. In spite of their low cost, the problems posed by low rank coals diminish their cost-competitive advantage. When emissions are included in these evaluations, low rank coals are often assessed as the least competitive fuels. The low cost of these coals has, however, motivated efforts to improve their quality.

Processing Low Rank Coals into High Quality Fuel

Coal beneficiation is any process performed on as-mined coal to obtain an improved product. Coal beneficiation processes include physical operations, chemical treatments, and microbial processes, and are usually designed to produce a fuel for advanced power generation technologies. Physical beneficiation processes involve gravity separation, centrifugal action, and magnetic techniques, to separate coal matter from its impurities. Generally, coal treatments are classified as wet (Kumar Sharma et al., 2015) and dry techniques (Zhao et al., 2014). The costs of coal processing would be offset by the following advantages:

- The composition, calorific value, and moisture content of the processed coal are improved, yielding a superior fuel that eliminates slagging and fouling, and the result is an increase in boiler availability and lower overall operating costs.
- A reduction in the sulphur content of coals will reduce sulphur oxide emissions after combustion, which in turn decreases flue gas desulphurisation requirements to meet environmental regulations.

Historically, low rank coal upgrading has been carried out to lower the moisture content, but the product was often of poor quality as it retained an ash fouling propensity.

An economical process would produce high quality non-fouling fuels from low rank coals by removing ash and moisture, and this has the potential to fuel power plants at lower costs with improved environmental performance.

Currently, with the emphasis on higher efficiency and lower emissions, it is unlikely that as-mined low rank coals will be used to fuel new power stations. Indeed, the future is bleak for as-mined low quality coals. The general outlook may be summarised as follows: Low quality coal often results in inefficiencies and costs to power plants. Yet more than 45% of the

world's coal is high-moisture and high ash. It has been recognised over a lengthy period the need to develop less energy intensive coal-drying technologies and higher quality coals. Efforts in coal drying are progressing in Australia, Germany and the United States, but efforts to develop large-scale integrated demonstration is required with the development of less energy- and water intensive technologies for coal beneficiation to reduce its ash and sulphur content. Success in developing more efficient coal-drying and beneficiation technologies will promote the wider use of low rank coals in new plants such as ultra-supercritical pulverised coal and IGCC applications.

The production of low-cost high quality coal from low rank coals would have a global impact. Large brown coal deposits are located in Germany and in Victoria (Australia). Large deposits of lignite and sub-bituminous coals are located in the USA, Europe, China, India, Indonesia and Russia. Germany mines more than 100 million tons of brown coal per year for power generation. Poland has large reserves of lignite, and mines about 57 million tons per year, which fuels 32% of its total power generation. Czech Republic mines about 50 million tons of lignite per year for power generation. Low quality lignite is also mined for power generation in Greece, Serbia, and Bulgaria.*

US coal production in 2016 was 743 million short tons, 17% lower than in 2015 due to low natural gas prices and warmer-than-normal temperatures during the 2015-16 winter that had reduced electricity demand. The retirements of some old coal-fired power generators, and lower international coal demand, have also contributed to declining US coal production.† The USA mines large quantities of lignite annually in North Dakota and Texas. Large quantities of sub-bituminous coal are also mined annually in the USA, particularly in Wyoming.

China has a large amount of coal resources, with recoverable reserves estimated at 115 billion tons; of these, 55% are bituminous and anthracite, 29% sub-bituminous and 16% lignite (of these, lignite deposits in Inner Mongolia account for ~72% and those in Yunnan for ~14%). Deposits of high sodium low rank coal are found in the Zhundong coalfields in Xinjiang autonomous region. China's coal production was estimated at 3.47 billion tons in 2011.‡

* These figures are indicative only, as coal usage has varied from year to year during the past decade.

† On coal production in the USA in 2016, see https://www.eia.gov/coal/.

‡ For more details, see http://www.sourcewatch.org/index.php/China_and_coal/.

Indonesia is one of the largest exporters of coal. Its reserves are 36 billion tons of coal, and over 21 billion tons of these are low rank. India has large deposits of mostly low rank coal.

R&D effort is required to find ways to efficiently process low rank coals into high quality fuels for high efficiency power generation plants. The goal of higher efficiency and lower emissions can only be achieved when the coal process is integrated with high efficient power plants, to use waste heat in the coal treatment.

Efforts to upgrade low quality coals by various organisations have been undertaken for many years (Meshram et al., 2015). Most approaches to upgrading these coals are stand-alone; such plants require burning coal to provide heat and power for the process, adding to CO_2 emissions, which would generally negate reductions in CO_2 emissions derived from using such upgraded coal to fuel higher efficiency power plants. Numerous upgrading methodologies produce coal dust and are plagued by problems from spontaneous combustion when the upgraded coal is stored for transport. Moisture reduction alone provides a product that burnt hotter and this exacerbates ash fouling, and this fuel would cause greater ash-related problems. Consequently, no low rank coal processing technology has progressed to large scale commercial production; the exception is fluid-bed drying of low-ash brown coal that has been developed into a commercial plant. The USA clean coal technology program also included a number of technologies that attempted to change the properties of low rank coals, but for the majority of cases, the properties of these processed coals were unsuitable for new high efficiency power generation plants.

It is noteworthy that a considerable portion of funding provided for major CCT programs (e.g. DOE, JCOAL, and EU) has been expended on improving current subcritical coal-fuelled plants. Yet the technologies that offer a reduction of emissions, such as supercritical, combined cycles, and combined heat and power generation, have been known for decades. The allocation of funding for work on well understood technologies has been due to the environmental difficulties posed by emissions of sulphur, nitrogen, mercury, and particulates. Emphasis has been placed on removing acid rain constituents (SOx and NOx) emitted by coal-fuelled subcritical power stations. These problems were addressed by adding flue-gas cleaning plants to remove sulphur and nitrogen oxides, which increased capital costs for coal-fuelled power generation. Considerable effort has also been expended on coal fluid-bed technologies, which may use sorbents in the fluid-bed to take up sulphur pollutants. Low NOx burners have also been commercialised; these innovations were added mostly to low efficiency, subcritical plants to enable compliance with clean air regulations. Some of

these innovations, however, may be used to enhance the performance of new coal-fuelled plants, such as the use of low NOx coal burners in SC and USC plants.

Various coal treatment methodologies have been tried, and the following examples illustrate the diverse range of methods reported in the scientific literature:

- The hydrothermal treatment heats brown coal/water slurries at elevated temperatures, and was developed to pilot scale by various organisations. The coal/water mixture is heated at temperatures of 300-400°C, and under these conditions, toxic and carcinogenic organic compounds are formed and these enter the aqueous phase (Li et al., 2002; Wiater et al., 2000; Nakajima et al., 2013). This process may decrease the water in brown coal from 60% to ~50% and would remove a proportion of water soluble ash material.
- Technologies for treating high rank coals have been developed to reduce sulphur (Couch, 1991), and to reduce ash, using either caustic (Meyers et al., 1992; Nowak, 1994) or hydrofluoric acid (Kindig and Reynolds, 1987; Lloyd and Turner, 1988); these methodologies have been applied particularly to produce ultra-low ash coal as fuel for direct fired turbine plants (Brooks et al., 2000).
- Hyper Coal has been obtained by extracting the organic matrix from the coal and separating this from the ash. Solvent extraction is usually carried out at 200-380°C under nitrogen, using organic solvents such as tetralin, 1methylnaphtalene, dimethylnaphthalene, and light cycle oil. After extraction, separation of the dissolved matter from solid matter is performed at room temperature (Okuyama et al., 2004).
- Coal moisture reduction methods include a back-pressure steam drying process using low grade heat from a power plant, and also a high pressure steam process to heat lignite to 230-280°C, and these remove moisture as liquid water containing dissolved inorganics. The energy requirements are 0.6 to 1.7 MJ/kg to remove liquid water, as compared to 3.0 to 4.5 MJ/kg to remove it as evaporated steam; these approaches can suffer from losses of coal fines and the production of polluting wastewater. Computer simulation studies have been reported on drying methods for integration into a Greek lignite-fired power plant (Kakaras et al., 2002).

Treatment methods are initially developed at a laboratory scale, as this enables a considerable number of analytical and characterisation techniques

to be employed, and for details on the impact of the treatment methods on coal quality to be obtained. Numerous laboratory experiments need to be carried out to establish conditions that would produce the required quality of a treated coal, and to examine the behaviour of such samples when heated at temperatures obtained in coal flames. These experiments provide a great deal of data while avoiding the expenses incurred in the construction and operation of a pilot plant. The analytical data of laboratory-treated coals can also be used in simulating the performance of these fuels in power plants, and also to examine the schematics for the integration of the coal processing and drying units with the power station, using software packages such as GateCycle™; this software may also be used to simulate the performance of ultra-clean (or virtually zero-ash) coal by adding a coal combustor to a combined-cycle plant. These simulations have indicated that it is possible to achieve overall thermal efficiencies greater than 80%, with a corresponding reduction in emissions (total thermal efficiency is the proportion of the heat from the fuel used to perform useful work in coal treatment and power generation); the efficiencies of power generation for these simulations are upward from 43% for SC plants to 50% for combined-cycle plants (Domazetis et al., 2008). Such an array of techniques also enables initial assessments of the likely economic and environmental outcomes for the various coal treatment methodologies.

As mentioned previously, upgrading processes must take into account the physical and chemical properties of the particular coal. For example, brown coal is a compressible substance, and it can undergo chemical decomposition when heated as a coal/water mixture. This makes it difficult to develop a chemical treatment process operating at elevated temperatures and pressures, as decomposition at elevated temperatures produces toxic waste, and attempts at separating the coal from water at high pressures by filtration compresses the coal into a dense solid, making processing extremely difficult, or even impossible. A viable process must also avoid producing polluting and toxic by-products, otherwise environmental regulations would prohibit such a commercial venture.

The ideal coal process would produce high quality coals (high heating content, low amounts of non-fouling ash, and low sulphur) at reasonable costs and without adding to emissions of CO_2, and the resulting fuel should be designed for non-problematic performance in high efficiency plants. Three categories of processed coal that meet these requirements can be envisaged:

- Non-fouling dry coal, for SC and USC power stations, and gasification plants.

- Ultra-clean coal (or virtually zero-ash) for direct-fuelled turbine combined-cycle power stations.
- Catalytic coals for enhanced steam gasification to provide greater amounts of hydrogen in synthesis gas.

Devising a process that would produce these three types of coals has required a comprehensive R&D program to provide a detailed understanding of the molecular features of low rank coals, the chemistry related to the ash-forming species, and the chemistry relevant to process conditions that would remove the constituents that are the cause for the poor performance of these fuels. Ash-forming species that are responsible for fouling of boilers from these fuels may be removed using acids. Effective acid treatment requires the penetration of the solid coal by the acid, and this is possible in hydrophilic low rank coals. Acid treatment at elevated temperatures without toxic by-products, followed by moisture reduction of the hot coal, is an attractive concept; however, considerable additional research and development is required to render such a concept as a practical proposition. Detailed R&D on catalytically active species added to low rank coals enables advanced catalytic steam coal gasification.

Acid treatment of low rank coals under conditions that avoid the formation of toxic organic pollutants has been developed by the CCT/LTU Program, which has undertaken work on a suite of low rank coals that are typical of deposits found worldwide. The Program has also shown how high thermal efficiencies can be achieved by using low-grade heat for the coal process, and thereby avoiding CO_2 emissions that would be incurred from a stand-alone coal processing plant (Domazetis et al., 2008; 2010). The CCT/LTU concept requires further development for the commercialisation of these new technologies, to produce low-cost, high quality fuel for high efficiency power plants, with a trajectory towards zero-emissions.

Coal-Fuelled Power Generation in a Carbon Constrained Future

Concerns about climate change resulting from the increased concentrations of GHGs in the atmosphere are the major drivers towards a low- or zero-CO_2 emissions future. There are numerous GHGs emitted into the atmosphere. The relative impact of these may be assessed by normalising them all to carbon dioxide (CO_2), using the Global Warming Potential index (GWP). The GWP provides a comparison of greenhouse warming for each gas against CO_2 set at 1, per unit mass, and per the length of time it remains in the atmosphere. CO_2 is chemically stable and stays in the

climate system for thousands of years (however, it can be fixed through the global carbon cycle). A number of studies by international groups and institutions have assessed the proportions of various gases that provide the GHGs total; for example, in 2014, estimates of the total were $6{,}870 \times 10^6$ metric tons of CO_2 equivalent, and the distribution to this total was CO_2 81%, methane 11%, nitrous oxide 6%, and fluorinated gases at 3% (US EPA Inventory, 2014).* The methane GWP is 28-36 over 100 years and also includes indirect effects, as CH_4 is a precursor to ozone, which is also a GHG. The nitrous oxide GWP is 265-298 for a 100-year timescale. The GWPs for chloro-fluorocarbons, hydro-fluorocarbons, hydrochloro-fluorocarbons, perfluorocarbons, and sulphur-hexafluoride can be in the thousands or tens of thousands; for example, the GWP values for CF_4, C_2F_6, SF_6 and NF_3 are 7,390, 12,200, 22,800 and 17,200, respectively. Some gases which are relevant to the manufacturing of the crystalline silicon photovoltaic solar cell and the film silicon module, can have a very high GWP (de Wild-Scholten et al., 2007).

The world's largest GHGs emitters on an absolute basis are China, the United States, and the European Union; on a per capita basis, GHGs emissions are highest in the United States and Russia. The major sectors in the global distribution of GHGs data for 2017, reported by the Centre for Climate and Energy Solutions, are electricity and heat, agriculture, transportation, and manufacturing. Generally, power generation accounts for a considerable proportion of CO_2 emissions, with cement, iron and steel, refineries, and petrochemical industries providing significant emissions. The quantitative data may vary from year to year, but qualitatively the major sources of increasing concentrations of GHGs to the planet's atmosphere are derived from the power, transport and agriculture sectors.† Energy consumption by sector and proportions by fuel for the USA are shown in Figure 1-1, which illustrates the dominant role of fossil fuels (oil, gas and coal). In regions such as China, India, Indonesia, and Poland, the proportion of coal-fuelled power generation is much higher than in the USA.

The political divides related to climate change make it difficult to obtain a consensus on measures required to reduce GHGs concentrations in the atmosphere (even if climate change sceptics are excluded from this discussion). A majority view exists for the necessity for secure power generation, with the realisation that a practical approach towards coal-fuelled power with lower carbon intensity should include systematically

* On the EPA's Overview of Greenhouse Gases, see https://www.epa.gov/ghgemissions/overview-greenhouse-gases.

† For more details, see the Intergovernmental Panel on Climate Change website at http://www.ipcc.ch/.

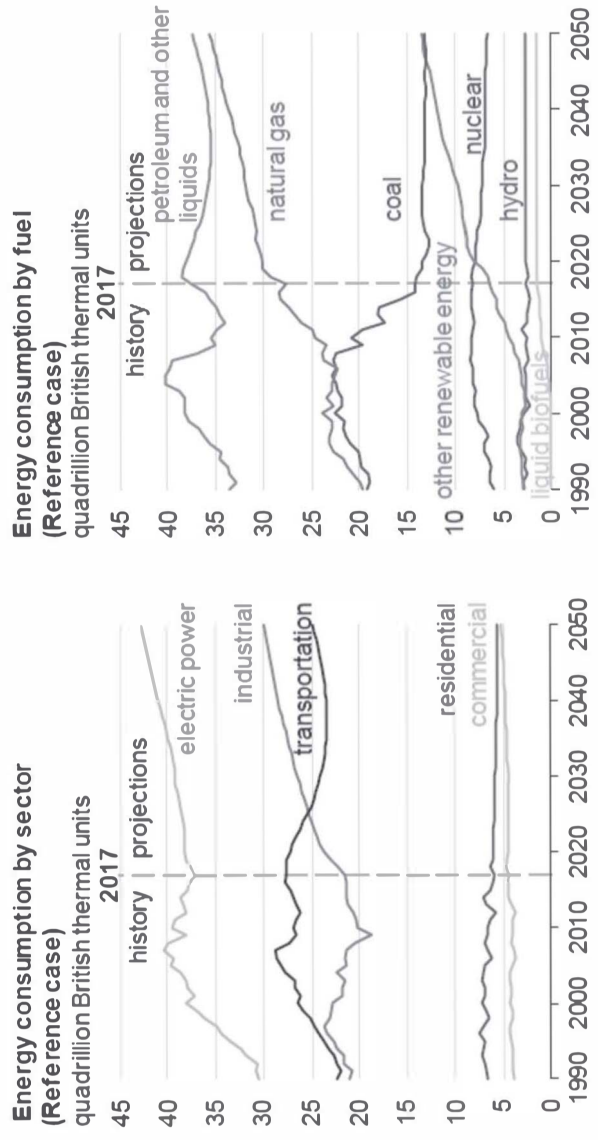

Figure 1-1. Energy consumption by sector and fuel. (U.S. Energy Information Administration, Annual Energy Outlook 2018, with Projections to 2050. https://www.eia.gov/outlooks/aeo/pdf/AEO2018.pdf)

closing old "dirty" coal-fuelled plants, plans to replace these with new fossil-fuelled plants of increasingly high efficiencies, and to design these new plants with the capability for commercially viable carbon capture and mitigation. Generally, it is uneconomical to modify old, low-efficiency plants with additional technology for the separation of CO_2 from flue gas with capture and sequestration – this is particularly so for old plants fuelled with low rank coal. It needs to be understood that simply adding renewables to meet the increasing demand for electricity does not reduce the total tonnage of GHGs being emitted to the atmosphere. The remedy would be to close all old high emissions coal plants, and to reduce emissions from other sectors, with the ultimate goal of operating low- to zero-emissions coal-fuelled plants. Higher efficiency on the demand side of power use would also contribute to lower overall emissions.

Public commentary on the need to reduce emissions is often crafted to criticise coal, although the emphasis should be on the inefficient use of all fossil fuels by the various sectors. Informed discussion on coal-fuelled power stations should emphasise the role regulations may play in bringing certainty to investors, but the politics are complicated and divisive, and public discussions present a wide range of views. On one side of the political divide, environmentalists regard coal as dirty, and promote renewable power as a commercially sound solution to the problems stemming from increasing levels of CO_2 in the atmosphere. On the other side of politics, the importance of coal to major economies is emphasised, exemplified by the following statement that recognises the importance of coal-fuelled power within the context of clean coal activities in China and USA:

> **Dirty Coal, Clean Future**: To environmentalists, "clean coal" is an insulting oxymoron. But for now, the only way to meet the world's energy needs, and to arrest climate change before it produces irreversible cataclysm, is to use coal-dirty, sooty, toxic coal in more sustainable ways. The good news is that new technologies are making this possible. China is now the leader in this area, the Google and Intel of the energy world. If we are serious about global warming, America needs to work with China to build a greener future on a foundation of coal. Otherwise, the clean-energy revolution will leave us behind, with grave costs for the world's climate and our economy. (Fallows, 2010)

Public announcements have also been made by organisations that are withdrawing funding from dirty coal projects, for example:

> The DBS bank will stop financing 'dirty-coal' or low-grade coal projects by the end of this year, but continue to support ventures in emerging markets that uses higher-quality coal, a top bank official has said. The Singapore-

> headquartered bank, which is rated among the largest in Asia, will also focus on funding renewable energy projects.... (Economic Times, 2018)

While some communities protest against coal:

> Community members in Newcastle, New South Wales, Australia, hang out coal-covered clothes and display signs reading 'No new mines' and 'No New Coal' to highlight the serious health and climate impacts of the Commonwealth Bank's lending policies. At the same time in Newcastle port Greenpeace activists occupy the world's largest coal port with the message, "CommBank's Coal Kills". (Greenpeace, 2017)

And environmentalists insist:

> Coal can never be clean. Here's why:
> - The burning of fossil fuels releases greenhouse gases into the atmosphere, increasing levels of CO_2 and other gases, trapping heat, and contributing to global climate change.
> - Coal combustion releases the greenhouse gases carbon dioxide (CO_2) and nitrous oxide (N_2O) during combustion. Coal-fired power plants release more greenhouse gases per unit of energy produced than any other electricity source.
> - Coal supplies around 33% of the energy used for electricity in the United States, which makes coal-fired power plants a prime target for reducing greenhouse gas emissions.
> - Luckily, coal-fired plants are closing down throughout the U.S. as the fuel becomes less profitable due to state and federal regulations, an aging fleet, and competition from other sectors such as natural gas, wind, and solar.
> - The coal mining process releases methane, which is 28-36 times more potent as a greenhouse gas than CO_2....
> - Carbon capture and storage (CCS) technologies have been marketed as a way to address climate emissions from burning coal, by pumping CO_2 produced through burning coal underground instead of into the air. However, the technology is extremely expensive, and even if the carbon can be sequestered, the coal-fired plant will still result in destructive coal mining as well as toxic coal ash as a by-product. (Green America)

These examples illustrate the widely divergent public perceptions, and the resulting complex political situations. Informed discussions can be found in numerous scholarly reports, reviews and books; the brief discussion here is to indicate factors that are relevant to the question, "What is the future of coal-fuelled power generation?" Public opinion, and the

various interest groups that have taken an active position on climate change, have created a perplexing political mix. 'Giddens's paradox' is an apt summary:

> Since no previous generation has ever had to confront the problem of human-induced climate change before, it is hard for the public to accept it as a reality, let alone an urgent problem, when stacked up against the diversity of other problems the world has. For reasons already given, we do not know the true level of risk in advance. (Giddens, 2015)

The major factors in this complicated situation were identified in the Stern Report as economics and politics arising from concerns on climate change. Governments need to agree on the particular actions necessary to deal with climate change-related global impacts, and to adopt policies that identify specific regional activities that may be undertaken to reduce emissions.

Nonetheless, specific areas and difficulties that must be overcome for adaptation to the many possible outcomes from climate change have hardly been defined, nor a systematic assessment of the required remedies. The possible barriers appear endless, and are mostly related to the institutional and social dimensions of adaptation; studies on barriers to mitigation are mainly carried out in developed countries. The impact of climate change on the poor countries, particularly that of extreme weather conditions, is troubling. It is widely recognised that climate change may undermine economic development, and this would adversely impact the poor and vulnerable groups through a decrease in food production, with mass migration from adversely affected regions, and consequential health problems and conflicts. The poor are especially vulnerable to shocks from climate variability because of their reliance on agriculture. The undesirable outcomes are expected to actualise in regions with a larger proportion of poor people, which would exacerbate their current economic inequalities. Since climate change is global, these cataclysmic outcomes may occur on a global scale. The poor are disproportionately exposed to flood risk in urban areas, such as are found in regions of Africa, India, Asia and the Pacific Islands. People in rich countries are not as dependent on production activities that are linked to weather contingencies, and have resources to protect themselves against the direct effects of adverse weather conditions.

It is clear that government policies are required that are based on comprehending the global impact of climate change, and that would initiate activities to manage the challenges of adaptation thereto; the focus needs to be on the economic development required to facilitate transformational adaptation, especially for poverty reduction in vulnerable regions. Such

initiatives require financial resources and investment in infrastructure carried out with the uncertainty imposed by the prospects of future changes to the climate (Castells-Quintana et al., 2018).

The Paris Accord (2015) recognises the impact on developing countries, summarised in the following section:

- ...also recognizing the specific needs and special circumstances of developing country Parties, especially those that are particularly vulnerable to the adverse effects of climate change, as provided for in the Convention,
- Taking full account of the specific needs and special situations of the least developed countries with regard to funding and transfer of technology,
- Recognizing that Parties may be affected not only by climate change, but also by the impacts of the measures taken in response to it,
- Emphasizing the intrinsic relationship that climate change actions, responses and impacts have with equitable access to sustainable development and eradication of poverty,
- Recognizing the fundamental priority of safeguarding food security and ending hunger, and the particular vulnerabilities of food production systems to the adverse impacts of climate change,
- Taking into account the imperatives of a just transition of the workforce and the creation of decent work and quality jobs in accordance with nationally defined development priorities,
- Acknowledging that climate change is a common concern of humankind, Parties should, when taking action to address climate change...

A general approach to reducing emissions requires global effort, with greater clarity in determining the most effective course of action. The role of higher quality coal for greater efficiency and lower emission intensity would contribute to lower emissions, but this is one of a number of measures needed to deal with the overall problem. When we factor in the constant high intensity emissions from old coal-fuelled plants, however, the situation becomes unpalatable. An important act towards a lower GHGs future would be for developed countries to replace old high emitting plants with economically viable new low emitting plants, to operate in concert with renewable sources of power.

An additional barrier towards clean coal utilisation in various developed countries, and to closing dirty plants, has been policies implemented for the deregulation and privatisation of power generation. The privatisation and deregulation of the power industry has resulted in ownership by the private

sector of old plants without CO_2 remediation features, and investors in such plants have expectations of long term returns, thus resisting closing any old plant and replacing it with a new high efficiency plant designed for CO_2 remediation. Governments have come to realise that regions are dependent of a secure supply of power, and simply closing old power stations would cause unacceptable disruptions, with dire consequences for communities and local economies. The result is uncertainties regarding future coal-based power generation, and this has been exacerbated by political pressures related to climate change. The principal areas of concern relate to the expense of replacing old plants, and a reluctance by the power generation industry to adopt promising new coal-based technology, because such new plants lack a record of prolonged commercial viability within a carbon constrained future.

The economics and politics of climate change have caused governments to encourage the expansion of renewable power generation, especially solar and wind, to meet increasing demand for power, which has resulted in an overall increase in costs to the consumer of electricity. Baseload generating capacity has been met in many cases by a refurbishment and life-extension of old plants, and because of this, the high CO_2 emissions from these old inefficient coal-fuelled power plants continue. Reductions in emissions intensity can generally be met by closing down the aging plants, and replacing these with new lower carbon intensity baseload plants without disruption in supply. It needs to be emphasised that any government policy that encouraged constructing new high efficiency coal-fuelled plants with lower carbon intensity must be accompanied with closing a large number of inefficient coal plants to significantly reduce emissions. The current situation in various regions is a lack of incentives to build new high efficiency power plants and a reliance on old plants for secure baseload power. When this situation occurs within a context of fear of an insecure power supply to a community, the result is continuing high carbon emissions. Simply adding renewables to meet increasing demand does not reduce total emissions from such regions. While recent trends are showing an increase in construction of higher efficiency plants, this needs to be accompanied with the closure of old plants.

It is estimated that about 20% of all power generation plants are approaching their end-of-life, and the power industry is facing challenges in replacing these old plants, while achieving the expected returns from these assets. Nonetheless, the power generating industry has undergone changes in the mix of power generating plants, in the management of the grid, and in adopting innovations such as digitising asset performance management to improve returns (Wan, 2017). Improvements in the efficiency of power

usage have also had an impact by lowering the demand for electricity. Grid systems manage baseload, peakload, and intermittent power supply, and smart grids are used in the distribution network, particularly with renewable power. Peakload is the maximum load during a specified period of time. Usually, peakload supply is obtained from all sources, including plants that can be brought online relatively quickly. Intermittent supply is from renewable, solar and wind, with the availability of these renewable energy resources dependent on uncontrollable environmental conditions, such as the weather and season. Such uncertainty makes it challenging to utilise renewable energy resources. These challenges have motivated innovations such as the development of technologies for smart grids, and new coal plants may be designed to vary output to compensate for the intermittent supply from renewables. A smart grid is an electricity network that can intelligently integrate the actions of generators and consumers to deliver sustainable electricity. The smart grid is developed with the capability of collecting information, and distributing energy demand, supply and price between consumers and utility companies in real time. The development of smart grids and localised renewable power generation is ongoing, and various scenarios have been discussed by Liu and Hsu (2018); battery storage is also touted as a way to overcome the variability of renewable power generation, but it is difficult to rationally justify the resulting high costs to consumers.

The embracing of innovation by the power sector would include developing a process for high quality low cost coal, designed for high efficiency power generation with the capture of CO_2 for use as a feedstock for valuable products. This trajectory may ultimately use SC- and USC-power stations with oxy-combustion, hybrid catalytic coal-steam gasification plants that produce liquids, and power using a combined-cycle plant fuelled by the tail gases from the liquids plant. Such future plants may include water electrolysis to produce oxygen and hydrogen, and the hydrogen would be used with CO_2 feedstock to produce a high value product such as methanol. The oxygen would be used for oxy-combustion power generation, which would emit a stream of CO_2 and water for capture. The result would be zero-emissions plants with revenue streams from power, hydrocarbons, and chemicals. This is a futuristic concept that may be developed by governments and industry; the various uses of CO_2 with the potential for mitigation measures have been widely discussed, such as by the DOE.*

Increasing the efficiency of coal power generation plants would result in lower CO_2 emissions intensity. For example, the efficiency of old brown

* See, for instance, https://www.netl.doe.gov/research/coal/carbon-capture/co2-use-and-reuse.

coal-fuelled plants in Australia is ≤30%, with emissions reported at 1200-1400 kg CO_2/MWh (see Chapter Nine), compared with emissions of about 670 CO_2 kg/MWh for advanced USC plants. The IEA reports global average efficiency of coal-fired plants is at 33%, with three-quarters of such plants operating at lower efficiency, and more than half of these are over 25 years old (IEA, 2012). The impact of increasing efficiency on lower CO_2 emissions from plants fuelled with low rank coal has been assessed by comparing the carbon intensities of old brown coal-fuelled subcritical plants with those for models of SC and combined-cycle plants fuelled with non-fouling processed coal. These give a general comparison of the reduction in carbon intensity with increasing power generation efficiency, as shown in Figure 1-2. The results in Figure 1-2 of CO_2 emissions intensities for SC plants, combined-cycle plants, and advanced gasification technology are obtained from models of fully integrated coal treatment plants with the three power generation options, while the data for subcritical power plants are obtained from current brown coal-fuelled power generation. Direct coal-fuelled combined-cycle plants can operate at 50% power generating efficiency, and in a CHP configuration, the overall thermal efficiency (total heat used for power and the coal treatment plant) is estimated at 80% (Domazetis, 2001; on CHP, see IEA, 2008 and DOE, 2013).

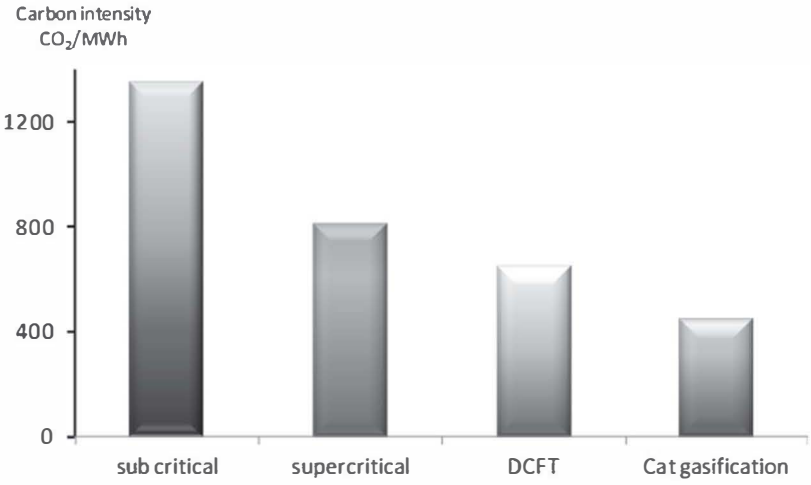

Figure 1-2. Reduction in carbon intensity of plants with increasing efficiency, fuelled with low rank coals.

The futuristic concept of the hybrid catalytic coal steam gasification power and liquids plant, discussed in Chapter Nine, is potentially a cost-effective approach to a zero-emissions plant that would provide power and valuable products for the foreseeable future – synthesis gas and CO_2/H_2 may be used to produce a number of valuable products (He et al., 2009; Behr and Heite, 2000; James et al., 2010; Isahak, 2015). The reaction between coal and steam would produce the syngas with higher hydrogen content from treated low rank coal-containing catalysts. Catalytic steam gasification of low rank coal is discussed further in this volume – the endothermic chemistry may be actualised, for example, by using plasma torch technology, thereby ensuring the maximum reaction between steam and coal. Currently, plasma gasification is used to gasify waste and work has been reported for coal-steam gasification (Galvita, 2007).

Oxygen-coal combustion would produce a stream of CO_2 and H_2O which can be captured on site, and this would avoid CO_2 separation from the flue gas of a power station. The uses of CO_2 include synthesis and enhanced oil recovery with CO_2 underground storage (Toftegaard et al., 2010).

The costs for water electrolysis to produce oxygen and hydrogen are mainly power-related; these are discussed in this volume, and it may be stated at this point that low cost power may be obtained during off-peak periods of demand, which may render this concept commercially attractive. In this way, the costs of CO_2 reduction would be offset by revenue streams from valuable products, such as methanol (Sakamoto, 2001). The future of coal is as a high quality fuel for high efficiency power generation with CO_2 remediation. This requires low cost, high quality coal, and processing low rank coals into lower-cost high quality fuels is a viable option.

References

Barnes, I. 2015. 'Upgrading the efficiency of the world's coal fleet to reduce CO_2 emissions', *Cornerstone*, 3 (1), 4-9. Available at: https://www.worldcoal.org/file_validate.php?file=Cornerstone_Volume3_Issue1.pdf.

Baruya, P. 2018. 'Production and supply chain costs of coal', IEA CCC Report Number CCC/289.

Behr, A. and Heite, M. 2000. 'Telomerization of Carbon Dioxide and 1,3-Butadiene: Process Development in a Miniplan', *Chem. Eng. Technol.*, 23, 952-955.

Brooks, K., Clark, B., Waugh, J., Langely, G. and Lothringer, B. 2000. 'Ultra-Clean Coal as a Gas Turbine Fuel', 10th Japan/Australia Joint

Technical Meeting on Coal, *Australian Coal Review*. Available at: http://www.australiancoal.csiro.au/

Burnard, K. and Bhattacharya, S. K. 2011. *Power Generation from Coal: Ongoing Developments and Outlook*, Paris: International Energy Agency.

Castells-Quintana, D., del Pilar Lopez-Uribe, M. and McDermott, T. K. J. 2018, 'Adaptation to climate change: A review through a development economics lens', *World Development*, 104, 183-196.

Centre for Climate and Energy Solutions, 'Global Emissions', *Centre for Climate and Energy Solutions*. Available at https://www.c2es.org/content/international-emissions.

Couch, G. R. 1991. *Advanced coal cleaning technology* (IEACR/44), London: IEA Coal Research.

De Wild-Scholten, M. J., Alsema, E. A., Fthenakis, V. M., Agostinelli, G., Dekkers, H., Roth, K. and Kinzig, V. 2007. 'Fluorinated Greenhouse Gases in Photovoltaic Module Manufacturing: Potential Emissions and Abatement Strategies', *22nd European Photovoltaic Solar Energy Conference*, Fiera Milano, Italy.

DOE, 2001. *Clean Coal Technology Demonstration Program: Program Update 2000*, National Technical Information Service, U.S. Department of Commerce.

DOE, 2013. *Combined Heat and Power*, Washington, DC: U.S. Department of Energy. Available at: https://energy.gov/sites/prod/files/2013/11/f4/chp_accomplishments_booklet.pdf.

Domazetis, G. 2001. 'Clean Coal as Fuel for Turbines', *Australian Coal Review*. Available at: www.australiancoal.csiro.au.

Domazetis, G., Barilla, P., James, B. D. and Glaisher, R. 2008. 'Treatments of low rank coals for improved power generation and reduction in Greenhouse gas emissions', *Fuel Processing Technology*, 89, 68-76.

Economic Times. 2018. 'DBS to stop funding 'dirty-coal' projects by year end', *Economic Times*. Available at: https://economictimes.indiatimes.com/industry/indl-goods/svs/metals-mining/dbs-to-stop-funding-dirty-coal-projects-by-year-end/articleshow/62850096.cms.

Fallows, J. 2010. 'Dirty Coal, Clean Future', *The Atlantic*. Available at: https://www.theatlantic.com/magazine/archive/2010/12/dirty-coal-clean-future/308307/.

Galvita, V., Messerle, V. E. and Ustimenko, A. B. 2007. 'Hydrogen production by coal plasma gasification for fuel cell technology', *Int. J. Hydrogen Energy*, 32, 3899-3906.

GateCycle™, 1998. Analysis Program, Version 5.20.0, Enter Software Inc. 1490 Drew Ave., Suite 180, Davis, CA 95616.

Giddens, A. 2015. 'The politics of climate change', *Policy Politics*, 43, 155-162.

Green America, 'Coal: Why Is It Dirty?', *Green America*. Available at: https://www.greenamerica.org/fight-dirty-energy/amazon-build-cleaner-cloud/coal-why-it-dirty.

Greenpeace. 2017. 'Dirty coal to dirty politics', *Greenpeace*. Available at: https://www.greenpeace.org.au/blog/dirty-coal-to-dirty-politics/

He, L-N., Wang, J-Q. and Wang, J-L. 2009. 'Carbon dioxide chemistry: Examples and challenges in chemical utilization of carbon dioxide', *Pure Appl. Chem.*, 81, 2069-2080.

Hecht, E. and Shaddix, C. 2015. 'Coal Combustion and Gasification Science', NETL Crosscutting Research Review Meeting, Pittsburgh, PA, USA, April 27, 2015. Available at: https://www.netl.doe.gov/.

Horach J., Chen Q., Rennings K. and Vögele S. 2014. 'Do lead markets for clean coal technology follow market demand? A case study for China, Germany, Japan and the US'. *Environmental Innovation and Societal Transitions*, 10, 42-58.

IEA. 2008. *Combined Heat and Power: Evaluating the Benefits of Greater Global Investment*, Paris: International Energy Agency. Available at: https://www.iea.org/publications/freepublications/publication/chp_report.pdf.

IEA. 2012. *Technology Roadmap - High-Efficiency, Low-Emissions Coal-Fired Power Generation*. Available at: https://webstore.iea.org/technology-roadmap-high-efficiency-low-emissions-coal-fired-power-generation.

Isahak, W. N. R. W., Ramli, Z. A. C., Hisham, M. W. M. and Yarmo, M. A. 2015. 'The formation of a series of carbonates from carbon dioxide: Capturing and utilisation', *Renewable and Sustainable Energy Reviews*, 47, 93-106.

James, O. O., Mesubi, A. M., Ako, T. C. and Maity, S. 2010. 'Increasing carbon utilization in Fischer-Tropsch synthesis using H_2-deficient or CO_2-rich syngas feeds', *Fuel Processing Technology*, 91, 136-144.

JCOAL. 2007. 'Future Outlook for CCT', in JCOAL, *Clean Coal Technologies in Japan: Technology Innovation in the Coal Industry* (Tokyo: JCOAL), 111-113. Available at: http://www.jcoal.or.jp/eng/cctinjapan/3otc.pdf.

Johnsson, F. 2007. 'Fluidized Bed Combustion for Clean Energy', *The 12th International Conference on Fluidization – New Horizons in Fluidization Engineering*, 47-62.

Kakaras, E., Ahladas, P. and Syrmopoulos, S. 2002. 'Computer simulation studies for the integration of an external dryer into a Greek lignite-fired power plant', *Fuel*, 81, 583-593.

Katzer, J. 2007. *The Future of Coal, Options for a Carbon Constrained Future. An Interdisciplinary MIT Study*. Available at: http://web.mit.edu/coal/.

Kindig, J. K. and Reynolds, J. E. 1987. US Patent 4695290.

Kumar Sharma, M., Priyank, G. and Sharma, N. 2015. 'Coal Beneficiation Technology for Coking & Non-Coking Coal Meant for Steel and Thermal Power Plants', *Am. J. Engineering Research,* 4, 55-63.

Li, C., Takanohashi, T., Saito, I., Iino, M., Moriyama, R., Kumagai, H. and Chiba T. 2002. 'The Behaviour of Free Radicals in Coal at Temperatures up to 300 °C in Various Organic Solvents, Using in Situ EPR Spectroscopy', *Energy Fuels*. 16, 1116-1120.

Liu, R-S., Hsu, Y-F. 2018. 'A scalable and robust approach to demand side management for smart grids with uncertain renewable power generation and bi-directional energy trading', *Int. J. Electrical Power Energy Systems,* 97, 396-407.

Lloyd, R. and Turner, M. J. 1988. US Patent 4780112.

Longwell, J. P., Rubint, E. S. J. and Wilson, J. 1995. 'Coal Energy for the Future', *Prog. Energy Combust. Sci*., 21, 269-360.

Meshram, P., Purohit, B. K., Sinha, M. K., Sahu, S. K. and Pandey B. D. 2015. 'Demineralization of low-grade coal – A review', *Renewable and Sustainable Energy Reviews*, 41, 745-761.

Meyers, R. A., Hart, W. D. and McClanathan, L. C. 1992. US Patent 5085764.

Minchener, A. J. and McMullan, J. T. 2007. *IEA Coal Research, Clean Coal RD&D*. Available at: www.iea.org.

Mohn, W. 2008. 'An Overview of the Ultrasupercritical boiler Materials Development Program'. Available at: https://www.netl.doe.gov/File%20Library/Research/Coal/Advanced%20Research/11-40Mohn.pdf.

Nakajima, T., Hasegawa, H., Takanashi, H. and Ohki, A. 2013. 'Ecotoxicity of effluents from hydrothermal treatment process for low rank coal', *Fuel,* 104, 36-40.

National Research Council. 2003. *Review of DOE's Vision 21 Research and Development Program*, Washington, DC: National Academies Press.

Okuyama, N., Komatsu, N., Shigehisa, T., Kaneko, T. and Tsuruya, S. 2004. 'Hyper-coal process to produce the ash-free coal'. *Fuel Process. Technol.,* 85, 947–967.

Paris Accord, 2015. *21st Conference of the Parties of the UNFCCC in Paris.* Available at: https://unfccc.int/process/the-paris-agreement/what-is-the-paris-agreement.

Sakamoto, Y., Zhou W. and Kawabe, T. 2001. 'Performance analysis of a CO_2 recycling system which utilizes solar energy', *Int. J. Energy Res.*, 25, 275-280.

Santoianni, D. 2015. 'Setting the Benchmark: The World's Most Efficient Coal-Fired Power Plants', *Cornerstone*, 3 (1), 39-42. Available at: https://www.worldcoal.org/file_validate.php?file=Cornerstone_Volume3_Issue1.pdf.

Stern Review. 2006. *The Economics of Climate Change*. Available at: http://www.sternreview.org.uk/.

Toftegaard, M., Brix, J., Jensen, P. A., Glarborg, P. and Jensen, A. D. 2010. 'Oxy-fuel combustion of solid fuels', *Prog. Energy Combustion Sci.*, 36, 581-625.

US Clean Coal Compendium, *Coal Processing of Clean Fuels.* Available at: http://www.netl.doe.gov/cctc/programs/program.html.

US EPA Inventory, 2014. *Overview of Greenhouse Gases.* Available at: https://www.epa.gov/ghgemissions/overview-greenhouse-gases.

Wan, S. 2017. 'Asset Performance Management for Power Grids', *Energy Procedia,* 143, 611–616.

We, C. 2011. Developing USC: A Leap of Faith? *Power Engineering International*, 19, 24-28.

Wiater, I., Born, J. G. P. and Louw, R. 2000. 'Products, Rates, and Mechanism of the Gas-Phase Condensation of Phenoxy Radicals between 500-840 K', *Eur. J. Org. Chem.*, 921-928.

Wood, Jr. B. G. H., Kehn T. M., Carter, M. D. and Culertson W. C. 1983. *Coal Resource Classification System of the U.S. Geological Survey (Geological Survey Circular 891)*, Denver, CO: U.S. Department of the Interior.

World Coal. 2014. 'Drying lignite – how and why?', *World Coal*. Available at: https://www.worldcoal.com/power/01102014/iea-ccc-report-on-drying-lignite-1381/.

Zhao, Y., Yang, X., Luo, Z., Duan, C. and Song, S. 2014. 'Progress in developments of dry coal beneficiation', *Int. J. Coal Sci. Technol.,* 1, 103-112.

CHAPTER TWO

COMPOSITION AND PROPERTIES OF LOW RANK COALS

Coal has been used as a fuel for centuries, and fossil fuels are the dominant source for energy worldwide. Currently there is a continued interest in the efficient use of coal and the development of clean coal technologies. Coal is a very complex material, consisting of heterogeneous organic matter with inorganics and minerals present in various forms, and such effort requires a detailed understanding of the fundamental properties of coal, using advanced techniques of coal characterisation. Consequently, a multidisciplinary approach is required to characterise the various coals. The extent of such characterisation also depends on the type of application and behaviour of coal in different energy systems.

Coal is formed by the transformation of organic matter by bio- and physico-chemical mechanisms that are generally termed as the coalification process; microorganisms cause the chemical decomposition of vegetal matter while temperature and pressure impact over geological times to render the substance into the various coal deposits. The main factors that determine the quality of a coal deposit are its heating content per unit weight, the behaviour of ash at combustion temperatures, and the amounts of pollutants formed on combustion from sulphur, nitrogen, chloride, and particulates which may contain various toxic substances.

The overall goal of a coal treatment process is to produce high quality coal at the lowest cost, and to achieve a significant improvement in the environmental impact from that fuel. It is essential that any coal treatment process does not create toxic substances due to breakdown of the organic molecular matrix of the coal, and to this end, it is necessary to obtain an understanding of the relevant properties of coal and its applications as fuel, using appropriate analytical and characterisation techniques. The challenges posed by the heterogeneous nature of coal make it necessary to use many techniques in studies of coal composition, the behaviour of coal as it is heated, and the causes for ash fouling and pollution. These techniques would also provide data that would ensure a coal treatment process is non-

polluting, by identifying conditions that produce toxic substances and ways to avoid these.

We may infer that any coal treatment process operating at elevated temperatures and pressures has the potential to release organic compounds into the wastewater, and these include toxic substances as by-products. The formation of toxic substances under extreme temperature and pressure has been confirmed in practice. An appropriate R&D program for a coal treatment process must obtain an in-depth understanding of:

- The composition and molecular characteristics of the coal, and especially any changes that may occur to the organic macromolecular matrix due to the process conditions.
- The chemistry of coal combustion and the gasification of the processed coal to ensure it is of the required quality.
- Particularly, the chemistry of ash formation, of sulphur, nitrogen, and chloride species, any correlation between treatment methods, and the reduction of ash fouling and polluting aspects of the resulting product.

A number of standard and specialist analytical and molecular modelling techniques are required for such an R&D effort, and the major ones are discussed in this chapter. These techniques have been used to obtain data relevant to the conditions for coal processes that impact on the quality and properties of the product, and to determine if any by-products had formed.

The characterisation of coals is carried out by determining its composition, assessing the coal macerals, and by establishing its physical properties (Speight, 2005; Doughten and Gillison, 1990; Choi et al., 1989). Conventional analysis data are used to assess standard aspects of coal samples, such as their heating values and degrees of pollution as a fuel. For example, measurements of volatile matter and char are related to the coal flame, which in turn is related to the design and operation of the coal burner. Analysis of ash-forming constituents in the coal suggests these are indicative of the ash fouling propensity, and physical properties are indicative of handling, dust formation and crushing behaviour. Porosity and moisture retention are related to a range of behaviours, and the hydrophobic/hydrophilic nature of the coals is important for the penetration of acids during acid extraction of ash constituents. Understanding the type of ash-forming inorganics and minerals in coal samples is of central importance in devising conditions for acid extraction of moieties that cause fouling.

The standardisation of tests and analysis techniques is important for a quantitative comparison of data on coal samples within a laboratory, between various laboratories, and between research groups. Standard procedures deal with sampling methods, accuracy and precision of analysis, and are necessary for the reproducibility and repeatability of data. The heterogeneity of low rank coal, however, precludes a selection of samples for universal standardisation – the composition of a coal sample may vary greatly within a seam, as will variations in different seams and from various locations worldwide. Consequently, the sampling and preparation of low rank coals are particularly important for any R&D effort on coal processing, because such a program must encompass all aspects of the coal type. It is necessary to prepare thoroughly mixed samples of a coal that would be used for a given suite of experiments. It is imperative that a thoroughly mixed sample is used to conduct such experimental investigations on coal upgrading, and each thoroughly mixed batch of a particular coal should always be used to represent a particular portion of a seam. This will ensure that data from a variety of techniques can be used to characterise that particular batch of coal, and the data obtained for each batch enable an assessment of the efficacy of the various treatment methodologies that are examined. Producing various batches of well-mixed samples for a variety of coals will also provide results that would be considered as representative of a range of low rank coals and in this way enable a general conclusion to be reached for a particular seam, and also be applicable to a range of other coal deposits. Additionally, a suite of chosen samples of different batches of low rank coals, crushed and mixed into individual batches that are representative of the properties of a range of the various low rank coals, is required to enable an assessment of the general conditions for treating these various coals.

Analytical techniques are also required to deal with any waste and wastewater produced by the various treatment methods to determine the changes to ash-forming species, to measure the extent of the removal of sulphur and chloride, and ultimately to determine the properties of the upgraded product as they relate to the fundamental aspects of coal utilisation, such as pyrolysis, combustion, and gasification.

The development of a practical coal treatment process requires a comprehensive research effort that includes the process conditions, the design of a coal treatment plant, and its implementation *via* integration with supercritical and ultra-supercritical power stations, to ensure power generation at high efficiency. Coal treated into a fuel for advanced catalytic gasification must produce synthesis gas with a higher hydrogen to carbon monoxide ratio than that obtained from conventional gasification of low

rank coal. Practical implementation of the coal treatment process must also take advantage of the low-costs of as-mined low rank coals.

Formation of Coal, Functional Groups, and Ash-Forming Components

The geochemical formation of coals is termed coalification, which denotes complex changes to buried vegetation; Figure 2-1 is a simplified illustration of this complicated process. A detailed discussion of the geology of coal formation is outside the scope of this book; the present discussion serves as background for an understanding of the complex compositional nature of coals. Insights into the nature of coals, especially at a molecular level, assist in devising suitable conditions of a coal treatment methodology, particularly as it is related to the chemistry of functional groups in low rank coals.

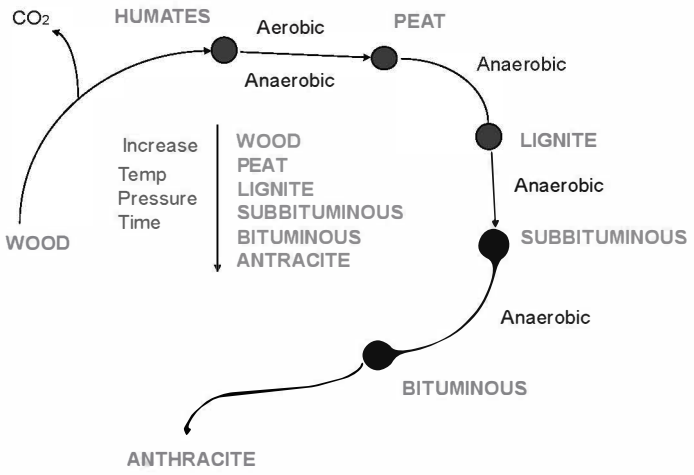

Figure 2-1. Simplified representation of the formation of coal and increasing rank.

Coals are ranked to reflect the geological age of coal deposits, and this ranking is routinely assessed by measuring the content of the moisture, volatile matter, ash, fixed-carbon, and calorific value of each particular rank. The low rank coals are termed peat, brown coal, lignite and sub-bituminous, and the high rank coals are termed bituminous and anthracite.

Coal deposits were formed over lengthy periods, under conditions where the rate of accumulation of vegetation was greater than losses through biodegradation of the organic matter; the earlier and initial deposits formed through these processes would have been of peat, which occurs when vegetation accumulates in swamps, river systems, flood plains, deltas and lake fringes. When water recedes from these accumulations, and further vegetation is deposited, it may be followed by the additions of varying amounts of soil that cover the accumulated vegetation. While the vegetation may initially have been converted into peat, if the conditions were right, and with additional time, these deposits would eventually have formed brown coal or lignite. In cases in which these deposits of vegetation were covered with greater amounts of soil, the resulting higher pressures and temperature are thought to continue the coalification process, ultimately forming high rank coal. Additional components are expected to form during the coalification of these deposits, such as gases and hydrocarbons, because the geochemical changes during coalification include the loss (or accumulation) of methane and carbon dioxide, with the progressive enrichment of organic carbon in the solid coal deposit. Additional mechanisms may include tectonic movements that covered large regions of vegetation, causing the accumulated vegetation to form deposits that would undergo coalification. Salt water is often invoked in the formation process, explaining the presence of sodium chloride. It is likely that a variety of conditions may have caused the burial of large forests, with additional accumulations of vegetation, and these may have ultimately become coal deposits.*

The deposits of buried vegetation would consist of a mixture of wood, bark, sap, leaves, and pollen, subjected to bacterial/fungal attacks and to the effects of pressure and temperature over geological periods. Soil and sand are also mixed with the vegetation, so the coalification process involves a complex mixture of organic compounds, dissolved inorganic salts that became chemically associated with organic functional groups, clay, sand, and other minerals present as extraneous particles. These particles may be embedded into the matrix of high rank coals as a result of greater pressures and lengthy periods of coalification. The resulting mixture (coal) would also contain organically bound sulphur and nitrogen which would be within the coal matrix, and in some cases small amounts of organically bound chloride. Consequently, coals may contain varying amounts of most of the elements in the Periodic Table.

The major components of the buried coal forming organic matter are lignin, cellulose, carbohydrates, proteins, resins, oils, fats and waxes. The ash-forming substances of low rank coals consist of water-soluble inorganic

* On coal formation, see https://www.worldcoal.org/coal/.

salts, inorganic compounds chemically associated with the organic matrix, and extraneous mineral and clay particles. Inorganics bound to the coal matrix are usually Na, Mg, Ca, Fe, Al and a variety of trace amounts of other inorganics such as P, Ti, Hg, K, Mn, Se, As (Wang et al., 2003; Lachas et al., 1999). Mineral particles present in the coal layer may be crystalline and amorphous; it is likely that over lengthy periods, chemically associated inorganics in the coal matrix may have originated from mineral particles mixed with the coal/water deposits that underwent coalification. For example, iron exists as complex iron-oxy/hydroxyl compounds and these may have been 'added' to the coal matrix over many centuries by the action of pressure, heat, and the hydrophilic environment on iron containing mineral particles found in the mixture. Minerals consist of sand, quartz, clays, pyrites, and other matter that form inter-seam layers and overburden, and similar material may have been mixed with the vegetation during coal formation. Some additional mineral matter may also be obtained from interseam deposits that are mixed with coal during mining. Ash, sulphur, and moisture can vary considerably for different deposits. Ash-forming constituents may comprise anywhere between 2wt% and 40wt% of the coal on a dry basis; for example, Bulgarian lignite contains 25-38wt% ash and up to 7wt% sulphur (air dry basis) (Vassileva and Vassilev, 2005), whereas German brown coals may contain 2-4wt% ash and 0.2-0.4wt% sulphur.

Coals are also classified based on macerals, considered the smallest components or subdivisions of coal, and reflect the materials from which the coal components originated; maceral analysis provides the microscopic constituents of coal based on its morphology and reflectance. There are three general maceral groups: *vitrinite*, *inertinite* (both various forms of wood/bark) and *liptinite/exinite* (plant resins, leaf, spores, and algae). These are subdivided into maceral subgroups, and finally into particular macerals. Several systems of nomenclature exist worldwide, and the Australian Standard (AS3856-1986), which has a modified system based on that used by the International Committee for Coal and Organic Petrology, gives a maceral classification that includes brown coal, described as (ASTM, Gammidge):

- **Maceral group** – *Vitrinite*
  Maceral subgroup – Telovitrinite
    Macerals: Textinite, Texto-ulminite, E-ulminite, Telocollinite
  Maceral subgroup – Detrovitrinite
    Macerals: Attrinite, Densinite
  Maceral subgroup – Gelovitrinite
    Maceral: Porigelinite

During peat formation (or the early stages of coalification), a gradual biotransformation of the lignin macromolecule is thought to occur by depolymerisation, demethylation, and demethoxylation. A decrease of cellulose materials is also observed. Lignin is the principal precursor to humunitic coal material, altered during coalification so that more condensed aromatic groups are present. Oxygen functional groups present in lignitic materials and an oxidative splitting of aliphatic chains in lignin provide a considerable amount of carboxyl functional groups in low rank coals.

Vitrinite is considered to result from fungal attacks on lignin, and involves the loss of methane from methoxy groups, followed by a series of re-arrangements and condensation reactions leading to furans, phenols and some cross linking. Internal redox processes involving the conversion of some enzylic alcohols to carboxylic acids may increase the proportion of carboxylate functional groups. The transformation of lignin, which contains many oxygen functional groups, into lignite is also thought to include dehydroxylation, β-O-4- ether cleavage and demethylation; this is one of a number of large complex macromolecules that constitute the organic matrix of low rank coals. Other molecules include humic acids, fatty acids and waxes, all containing varying amounts of oxygen functional groups. Monofatty acids in the range (C_{14}-C_{32}) are believed to be present at 3-7wt% of some coal seams (on a dry basis).

Humic acids may account for anywhere up to 30% of the brown coal organic mass, and these contain phenol and carboxyl groups, and thus may constitute a significant portion of the total oxygen functional groups in brown coals. Waxes and other more aliphatic materials are physically mixed with the coal matrix. The complexity of coals increases when the great varieties of plant (and mineral) material, with differing 'burial' conditions, are considered *in toto* as the coalification process (Hatcher, 1988; Stout et al., 1988). Other functional groups found in coal include: nitrogen-containing molecules derived from natural substances such as proteins and hetero-N-molecules, sulphur found as aliphatic and aromatic thiols, and small amounts of organo-chlorides. Sulphur and chlorine are also present as inorganics/minerals (e.g. pyrites and sodium chloride).

Attempts have been made to follow organic matter transformations during coalification at a molecular level, and to relate these to the rank and composition of coals, but these have met with limited success due to the complexity of coal formation (Carlson and Granoff, 1991; Jurkiewicz, 1987). Generally, the transformations of woody lignin have been extensively studied, but considerable uncertainty exists regarding the humin and biomass material comprising brown coal deposits. Elucidating the structure of humic substances is an on-going process and a number of

hypothetical structures have been formulated. A lignin-inherited block from humic substances has been proposed (Shevhenko and Bailey, 1996).

A useful, broad classification of coals may also be based on its hydrophilic or hydrophobic properties, because hydrophilic substances can be treated using aqueous-based methods. Low rank coals are hydrophilic and contain hydrogen-bonded water within the macromolecular matrix, and large amounts of water within its pores. The hydrophilic properties of low rank coals are due to the abundance of hydroxyl, carboxyl and other oxygen functional groups within the coal.

In the following sections, the major techniques used to characterise low rank coals are discussed, and this is followed by a discussion of how these techniques are used to assess the quality of processed high quality low rank coals.

Characterising Coal

Characterising coal is challenging because the substance is a complicated mixture of a variety of organic moieties and inorganic/mineral species; considerable effort has been expended to develop standardising methods that provide reproducible data for such a complicated substance. It is impossible for chemists to propose a single, unambiguous molecular structure for all coals because the substance is made up of many different molecules that are the result of an extremely complicated natural process (or numerous processes), which have undergone many transformations in a variety of geological environments. The major interest in coals, however, has been in their use as fuels, and consequently the primary purpose of coal characterisation and analyses is to determine its quality as a fuel for power generation and for gasification. Currently an additional interest has been on determining the process conditions that would yield high quality fuels at relatively low costs, and with benign environmental outcomes. It is understood that characterising coals requires measuring a wide range of chemical, physical, and mechanical properties; details of the numerous techniques used in such measurements are found in the references for this chapter; the current discussion deals with techniques relevant to low rank coal processing.

An analysis of coal is generally performed on the coal samples taken from the bulk material obtained at specified areas of a coal seam, and sampling protocols are adopted that provide samples representative of the bulk of the coal. Detailed discussions on sampling and analysis are provided by Speight (2005), and by the IEA Clean Coal Centre (Zhu, 2014). The coal mining industry uses a number of sample mixing methods, including

mechanical mixing devices, such as the riffle sample divider; these would be relevant for large scale operations – for small scale laboratory research, mixing can be done using established laboratory procedures.

The variety of analytical methods used for coal characterisation are for convenience regarded here as conventional and specialist techniques. The conventional methods are: ultimate and proximate analysis, calorific value, ash composition, and ash fusion temperature.

- *Ultimate analysis* provides the percentage elemental composition of carbon, hydrogen, sulphur, chloride and oxygen on a dry ash free basis (daf). The methods adopted are discussed in the literature and in standards publications. Oxygen is determined by difference, but in cases where a direct determination of major elements is required, other techniques are adopted – this is discussed below.
- *Proximate analysis* determines the coal components as solid and gaseous, expressed as the percentages of fixed carbon, volatile matter, moisture, and ash.
- *Ash analysis* is the elemental composition of the ash obtained from a coal sample, using standard methods.
- *Moisture* is determined by heating a sample of as-mined coal (often crushed to 200-micron size) in a crucible at 108±2°C to a constant weight. Once the sample has cooled to room temperature, it is weighed again and the loss in weight represents moisture. Loss of moisture must be prevented during sample preparation.
- *Volatile matter* is measured by heating a known weight of a sample of as-mined crushed coal in a covered crucible at 900±15°C in an inert atmosphere to a constant weight. The sample is cooled and weighed, and the loss of weight represents moisture and volatile matter. The remainder is fixed carbon and ash.
- *Carbon and ash* are determined by heating the crucible containing char and ash (after determining volatiles) in an oxidising atmosphere until all the carbon is burned. After cooling to room temperate, the weight of the residue is the ash, and the difference in weight from the previous weighing is the fixed carbon.
- *Calorific value* is determined using a bomb calorimeter that measures the heat released by burning the known weight of a coal sample in oxygen under pressure.

The physical and mechanical properties of coal include porosity, compressibility, dust formation, hardness and grindability. If a coal

processing method changes the composition of the organic matrix, the product from such a process would be characterised anew using all available techniques. If, however, the coal processing method is designed not to change the organic matrix (for example, physically removing some ash-forming particles by sieving at conditions that leave the organic matrix unaffected), the organic matrix of the resulting product would be similar, and characterisation techniques would focus on the behaviour of the product as a fuel (such as any change in fouling propensity as a result of the lower ash content).

R&D programs on treating low rank coals, utilise the standard techniques in assessing coal, and additional techniques are often required to obtain data that may provide a link between the conditions employed in the various treatment methodologies, and the quality and behaviour of the products. A number of advanced analytical techniques are required to provide information on the organic structure, and also data on the inorganic ash-forming matter that may remain in the treated coal. Advanced characterisation techniques have emerged which enable the examination of individual coal particles in greater detail, and also techniques that may identify various functional groups in coal; a number of these have been discussed by Vassilev and Tascón (2003).

The techniques discussed here have been used in studies of a number of coal samples that cover a range of properties typical for low rank coals. These are followed by a discussion of the data obtained with these techniques, particularly as they relate to the treatment processes and the end products. The data have been used to assess the properties and characteristics that cause the poor performance of low rank coals as fuel for power generation, and to devise conditions for the production of high quality treated coals that would lead to good performance in advanced power generation and gasification plants.

Studies of ash chemistry are particularly relevant as these provide general insights on the behaviour of inorganics and minerals during coal combustion and gasification. The remedy for the ash-related problems is to create processes that treat these coals to reduce many of the ashes forming inorganics to relatively low levels. Sulphur and chloride also need to be reduced or removed, while nitrogen pollution may be reduced by using low NOx burners.

A commercially viable coal treatment method needs to reduce moisture, and sulphur, chloride, and ash-forming constituents, from low rank coals, while catalytic coal steam gasification requires an understanding of the chemistry of catalysts added to the coal. Generally, viable treatment methods for low rank coals should encompass the following:

- Reducing moisture using low-grade (or waste) heat.
- Acid washing at elevated temperatures to reduce or eliminate ash constituents.
- Demineralisation to produce ultra-clean (or virtually zero-ash coal).
- Adding appropriate inorganic complexes to act as catalysts for steam gasification.
- Leaving the organic matrix unaffected, and avoid forming toxic organic waste during processing.

Not all coal treatment processes meet the above requirements, and various types are discussed in Chapter Six to illustrate the variety of major coal treatment methods examined to date. Ideally, the treated product would contain low levels of ash which can be experimentally demonstrated to be non-fouling, with a reduction or removal of inorganic forms of sulphur and chloride (to avoid corrosion and acidic emissions), and a higher heat content resulting from reduction in moisture. Analytical techniques would obtain details on the ash-forming species in the raw coal, and how the various treatment conditions, such as acidities and temperatures, result in the removal of the ash-forming species. Specialised techniques are also required to detect various forms of sulphur in coal, and also to detect and identify if any traces of toxic materials had formed during the coal treatment.

Chemical treatment methods for hydrophilic (low rank) coals use aqueous chemistry and this produces wastewater that must be analysed to identify the inorganic and organic constituents, and to establish if any toxic substances are present. The wastewater is cleaned and recycled in the coal treatment plant, and analytical techniques would also be used to assess the quality of the recycled clean water. The impact of the temperature of the coal/water mixture on the wastewater composition must also be systematically examined. Elevated temperatures in the treatment process enhance the action of acids to remove ash constituents, and this would increase production rates. At significantly high temperatures, however, a breakdown of the coal matrix occurs, producing toxins. The correct temperature for any coal treatment must be established experimentally.

The heat added to enhance the action of acid on ash reduction in coal may be low-grade heat obtained by integrating the coal process with the power plant, and this heat could also be used to reduce moisture, and in this manner, a non-fouling coal with higher heating content would be produced economically. Consequently, it is important to identify the appropriate temperature for coal treatment, as it must be below a level that would lead to a breakdown of organic matter in coal, and yet sufficient to enable rapid ash removal and moisture reduction.

The properties of low rank coals are diverse, and as mentioned previously, a comprehensive study of treatment methodologies for these should use a suite of well-mixed coal batches of specific samples of brown coal, lignite and sub-bituminous, representative of all low rank coals in their amounts of ash, pollutants, and moisture. This will enable the identification of the conditions for coal treatment of most of the low rank coals found worldwide.

Commercial considerations often require an assessment of a new (Greenfield) mine. Although details of such activities are outside the scope of this volume, generally, the same analytical techniques are used to assess numerous samples that provide a general composition of a coal deposit. This involves setting up a grid to map out the depth and breadth of the deposit. Samples of coal and inter-seam deposits are obtained by drilling at the identified points in the grid. The samples obtained by drilling are divided into uniform lengths for proximate, ultimate, and ash analysis, and to measure heat content. This approach maps out the overburden depth, the coal quality and seam depth, and inter-seam layers of clay and sand. The data from these samples may also be used to assess the types of conditions required to process the seam of coal into the required quality fuel.

Coal samples from operational mines can also be obtained from a conveyor feeding fuel into a boiler. The heterogeneity of brown coal, for example, is illustrated by Figure 2-2, which shows the variation in ash content of brown coal conveyed over a period of one month, and fed into a boiler at La Trobe Valley, Australia; variations in the ash content of brown coal greater than these are often observed.

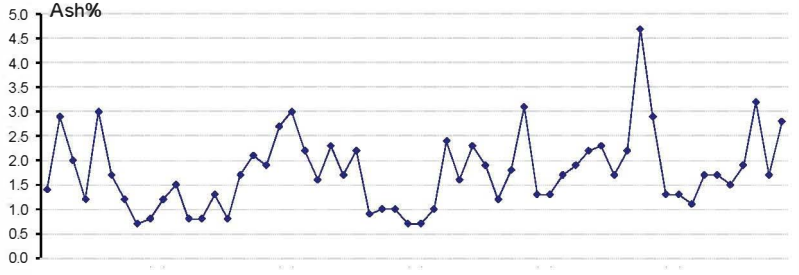

Figure 2-2. Example of the periodic variation of ash in coal fed to a power station boiler (for one month).

Real time monitoring of lignite quality variations would facilitate quality control of coal fed to a boiler, but conventional methods for the determination of coal ash are time consuming, and thus data of coal quality control can be

difficult to obtain in real time. Online analysis methods that provide similar accuracy to conventional methods, integrated with computerised systems, with the capability of providing the required quality control are needed (Galetakis and Pavloudakis, 2009). A number of online coal analyses techniques have been discussed (Zhu, 2014) but many have been shown to be expensive and some may use radioactive sources, requiring extensive health and safety measures.

An effective online analysis system of coal will be useful in any future coal treatment plants, as this may provide real time data of the raw coal prior to treatment, which can be used to vary the conditions of the treatment to the coal as it enters the treatment plant, and also enable real time coal quality control of the product. Laser-induced breakdown spectroscopy (LIBS) is an example of an instrumental technique with the potential to meet the required analytical and technical characteristics for an online coal analysis of mined coal fed to a processing plant, and an analysis of the product exiting such a plant. It is a rapid non-destructive method that provides elemental composition data of minor or major components. The instrumentation is robust, and available in a compact format. LIBS has been used to measure the elemental composition of coal samples with a range of slagging characteristics, and with ash fusion temperatures ranging from 955°C to 1480°C. The coals were analysed for Al, Ca, K, Mg, Na, Fe, Si, and Ti, and these values were correlated to the coal ash's initial deformation fusion temperature under reducing conditions; the accuracy obtained with LIBS was 15% of the values obtained by a conventional measurement of the elemental composition of these samples. The LIBS system was also tested offline at a power plant on three different coals; the field results were comparable to the average relative fusion temperature prediction according to the American Society for Testing and Materials' standardised measurements (Romero et al., 2010).

The high moisture in low rank coals presents a challenge to the accuracy of real time online analysis; the sample most often used in LIBS laboratory investigations is air-dried coal, which is assumed to have a relatively stable moisture content, and thus variations in moisture content are ignored. The online real time analysis of low rank coals, however, would be impacted by high moisture, and this has been demonstrated for high moisture coals, in that part of the moisture is evaporated under laser radiation. This means that part of the energy from the laser is used to dissociate and ionise the water vapour, and perhaps is reflected by the fast expanding moisture, thereby changing the absorption of laser energy by the solid coal. The result is a lower coal mass ablated by the plasma due to increasing moisture content, thereby emitting smaller line intensities (Chen et al., 2015).

Preliminary results from laboratory tests carried out on moving samples of coal (to mimic raw coal transported by a conveyor belt), using a LIBS system, indicate that the elements Al, Ca, Fe, Si, may be determined with reasonable accuracy. The study tested seven coals, but no information is provided on the impact of moisture in coal (Redoglio et al., 2016).

LIBS systems have also been used to analyse ash derived from coal-fuelled boilers. Sample preparation by pelletising ash is normally employed, although "on tape" sample preparation is suggested. In this study, a double-pulse approach in orthogonal reheating configuration was applied to enhance the repeatability and precision of the LIBS results. LIBS results are reported to be comparable with results from normalised analytical methods (Ctvrtnickova et al., 2010).

Microwave moisture meters have been discussed for rapid online moisture measurements, but these are limited to relatively low moisture, high rank coals. Recent work appears to extend the amount of moisture that may be determined with a novel microwave resonance sensor system operating at four resonance frequencies, which was optimised for moisture measurement within fluidised bed granulations (Peters et al., 2017).

It is noteworthy that the quality of the brown coal shown in Figure 2-2 varies from non-fouling coal (with less than 1wt% ash) to fouling coal (≥5wt% ash and relatively high levels of sodium). Selective mining, which mixes low ash coal with the correct proportions of high ash coal, providing a coal feed with a uniform ash of <2wt%, is an approach that may be used to reduce the fouling problems posed by the variable quality of this coal seam. The heat content, however, cannot be improved by this approach, and a successful outcome is predicated on having a sufficient quantity of low-ash coal to mix with high-ash coal. The variability and fouling propensity observed in such coal seams can be negated by using the appropriate coal treatment process.

While there are many techniques used to characterise coals (Gupta, 2007), the present discussion is confined to techniques required for studies on developing an effective low rank coal treatment methodology and to obtain information on the processed coals. The methodology for these studies commences with sample preparation, using a relatively large batch of coal delivered in airtight packaging to avoid loss of moisture. Each coal batch is identified by the location of the mine and the sampling position in the seam. It is then crushed and thoroughly mixed in the laboratory, and all work examining different treatment conditions for that coal would be carried out using this well-mixed sample. This procedure is necessary because the treatment conditions are varied systematically, and in this manner, the impact of each specific treatment can be assessed based on the

analysis of each treated product, obtained from the same batch of well-mixed coal.

Total moisture of the as-received coal should be measured with precautions taken to avoid losing moisture during coal crushing and mixing. The procedure requires that when the coal sample is obtained from the mine, it is immediately placed in an air tight container, and the initial moisture is determined by rapidly transferring a known weight of this coal to a crucible and placing this in an oven at 108°C, as required by the method. After the initial moisture has been measured, a well-mixed batch of coal is prepared from the raw coal. For example, the brown coal can be crushed using an IKA-Werke MF10 impact analytical mill, then passing it through a selected Mesh sieve. This batch of coal is then thoroughly mixed, and stored in an air tight polyethylene container. Some moisture would be lost during the crushing and mixing, and the amount lost can be determined by comparing the moisture of the crushed and sieved coal with the amount of moisture determined for the as-received mined sample (Domazetis et al., 2006).

The relative homogeneity of a well-mixed batch of coal is assessed by measuring the wt% ash for three portions obtained from the batch randomly – a variation of ≤0.3wt% (db) between the three portions' total ash is indicative of a well-mixed coal batch.

The various characterising methods are briefly discussed in this section to illustrate the insights and data obtained from these techniques. The samples used for the studies of treatment conditions are each analysed for moisture, ash, volatile matter, fixed carbon (proximate analysis), and elemental composition (ultimate analysis). After each treatment method, the treated coal is analysed. The changes to the ash chemistry resulting from the particular treatment method provide an assessment of the non-fouling nature of the products. The analysis of wastewater provides data required for water clarification. Treatments are carried out at elevated temperatures and an assessment of the loss of moisture for each temperature is made for each hot treated coal by placing it in a stream of nitrogen until it has reached room temperature. The moisture in each treated coal is then determined and the loss relative to the initial value is recorded against the treatment temperature.

Total moisture in coal samples can be determined by heating a weighed coal sample at 105-108°C to a constant weight, but all coal samples with >5wt% ash need to be heated in an inert atmosphere (nitrogen or helium), particularly if they contain significant amounts of Fe, or if they have been treated with catalytic complexes, due to the slow reaction of this coal with oxygen. Coal samples containing relatively large amounts of iron should be prepared for particular characterisation and analysis, such as SEM and XPS (see below) by grinding the coal under hexane (to avoid contact with air) to

decrease the particle size, and if necessary, followed by pressing into a pellet.

Proximate and ultimate analyses' methods are standardised and are carried out by commercial laboratories equipped (and certified) for this task; these methods generally report oxygen in coal by difference. Studies that involve catalysis require a direct measurement of oxygen in coal, and also additional analysis that can differentiate inorganic oxygen (due to minerals, and from metal complexes added to coal) from organic oxygen in the coal molecular matrix. It is also necessary to directly determine the total oxygen in the raw coal sample, and to compare this with the total oxygen in the same sample that has undergone treatment. Total oxygen can be measured using analytical methods, and differentiation between organic and inorganic oxygen is obtained using XPS. Direct determination of total oxygen may be done by using micro-analytical techniques (discussed below) – these provide a direct measurement of the total oxygen, but suffer from using a small sample weight; thus, it is necessary to thoroughly mix the coal sample, and obtain at least three measurements using the micro-analysis, to assess any variations due to the heterogeneous nature of the sample. Total oxygen measurements have also been undertaken by combusting coal followed by FTIR analysis of the combustion products, and by a chemical analysis of oxygen functional groups in brown coals (Solomon et al., 1990; Murata et al., 2000).

Total ash is determined by heating a known weight of dried crushed coal in air to burn off all organic matter, leaving a residue consisting of the inorganic and mineral substances. The ash is cooled to room temperature in a desiccator and weighed. Usually the coal sample is heated to 1100°C in a muffle furnace, but samples with relatively high amounts of volatile sodium and potassium should be heated to 900-950°C, to avoid loss of these substances as vapours. In exceptional cases, such as high sodium and potassium coals, samples may be heated at lower temperatures for a prolonged period, and the resulting weight measured until all char has been consumed, leaving the total ash.

Elemental Analysis

Standard ultimate and proximate analyses are performed on all coal samples. A direct determination of carbon (C), hydrogen (H), oxygen (O), nitrogen (N), chloride (Cl), and sulphur (S) can also be made for selected samples using micro-analytical techniques.* Microanalysis is based on the

* Ultimate analyses for the CCT/LTU research were carried out by the Australian Coal Industry Research Laboratory Ltd., and microanalyses for the CCT/LTU

complete and instantaneous oxidation of the coal sample into organic and inorganic combustion products. The sample is placed in a tin capsule with tungsten oxide and a copper catalyst, and dropped into a vertical quartz tube maintained at a temperature of 1020°C with helium carrier gas. Pure oxygen is mixed with the carrier gas as the sample is dropped into the tube. The mixture of gases is passed over a catalyst layer to achieve complete combustion, then through copper to remove excess oxygen and reduce nitrogen oxides to nitrogen. The resulting mixture is separated into carbon dioxide, water, sulphur dioxide and nitrogen, with a chromatographic column, and these are quantified using a thermal conductivity detector. Oxygen is determined using the same methodology, but without added oxygen in a helium carrier gas, and is reported as the total oxygen for the sample. Duplicate results are obtained for each element in the coal sample, and the error for all analyses is ±0.3wt%; variations in a batch of well-mixed coal are reported at between 0.3-0.5wt%.

X-Ray Fluorescence Analysis (XRF)

XRF is widely used to determine the elemental composition of solids, and in coal research, the analysis of inorganics that form ashes from coal. The principle of XRF is based on the excitation of individual atoms by an external energy source, resulting in X-ray photons emitted with a characteristic energy or wavelength. The elements in the sample may be identified and quantified by detecting and counting the number of photons of a particular energy emitted from a sample. The technique may be used to analyse elements from sodium to uranium, in concentrations ranging from a low of parts per million to a high percent. Quantification is done by calibration using standards in the appropriate concentration range*. XRF results of the elemental composition of the ash samples obtained from a number of coals are discussed below; each of these samples was prepared for analysis by pulverizing it to <65μm particle size using an automated mortar and pestle, and an accurate weight of 0.750g of the ash is thoroughly mixed with 4.000gm of fusion flux (Norrish 12:22 lithium tetraborate: lithium metaborate) and melted to form a pellet. The results for low rank coals discussed for the CCT P/L research were obtained with the Siemens

---

research were performed by the Campbell Microanalytical Laboratory, University of Otago, New Zealand.

* NMI, *Elemental Analysis using X-ray Fluorescence*. Available at: https://www.measurement.gov.au/Services/EnvironmentalTesting/Pages/Elemental%20Analysis-using-Xray-Fluorescence.aspx.

SRS303as XRF spectrometer with Rh end window, X-ray tube operating at 40mA/75kV.

X-Ray Powder Diffraction (XRD)

XRD identifies crystalline compounds from their diffraction patterns, and details of the technique are found in the literature. This technique can be used to detect changes in the minerals present in low rank coals that may occur from the treatment method, and this is discussed below. Finely ground samples of the coals, chars, and ashes are analysed, for example, by using an instrument such as the Siemens Kristalloflex D5000 Diffractometer and graphite monochromator over the 2θ analysis range from 4-70° using CuKα radiation. XRD peaks are analysed using Macdiff 4.2.5 software. The ashes from the various coals contain multiple phases, some of which are present as amorphous substances, and some as microcrystalline mixtures. The recognition of amorphous materials in partially crystalline mixtures can be performed using SIROQUANT, developed in Australia by the CSIRO.

Atomic Absorption (AAS), and Inductively Coupled Plasma Atomic Emission Spectroscopies (ICP-AES)

AAS and ICP-AES are used to measure concentrations of dissolved inorganics extracted from coal samples, in ash, and in wastewater samples from the various coal treatments. Standard procedures are used with commercially available instruments, such as the GC 933 plus Atomic Absorption Spectrometer (these techniques give comparable results to the elemental analysis of inorganics from XRF; Pyle et al., 1995). An example of the procedure is as follows: a sample of ash is accurately weighed and thoroughly mixed with a lithium borate fusion mixture (0.0500 gm ash and 0.2000 gm of fusion mixture) into a Pt/Au crucible and fused at 1050°C for 10 mins. 2 ml of concentrated HNO_3 and 1 ml of water are then added, and the mixture is swirled until it dissolves. The solution is cooled and transferred to a 50 ml volumetric sodium-free flask and diluted to 50 ml using ultra-pure water. The solution is kept in a sodium-free plastic container for ICP analysis, using, for example, the GC Integra XM-sequential ICP-AES spectrometer (Metz and Domazetis, 1999). Similar procedures have been reported for the analysis of ash samples from sub-bituminous coal (Hurley and Schobert, 1992).

AAS has been used to obtain additional insights into the behaviour of inorganics in coal particles heated to elevated temperatures, and particularly for detailed studies of sodium released from heated low rank coal particles,

because sodium is a major contributor to ash fouling from these coals. A modified AAS system has been employed by Domazetis and co-workers to measure the rates of volatilisation of inorganics from coal particles placed in a graphite tube furnace capable of low heating rates, and also at high heating rates similar to those found in coal flames. Coal particles of differing sizes were placed in the tube furnace, and on heating, the sample decomposes, atomisation occurs, and time-resolved atomic absorption profiles are obtained. The peak shape of the profile for the inorganic for each coal sample is determined by the particle heating rate, and the rate of atom formation and removal. Atom formation is described generally as a first-order rate process.

The apparatus used in the studies of vapour phase species from burning coal particles was a GBC Scientific Instruments Model 903 single beam absorption spectrometer equipped with a methane burner. The GBC instrument was also employed to measure the atomising profiles of inorganics obtained by heating coal particles placed in with the GBC System 2000 electrothermal atomiser, which consists of a pyrolytically-coated graphite tube furnace, capable of heating rates of up to 2000°C/sec. Inert gas is added to the graphite furnace to prevent oxidation.

A methane flat-flame burner equipped to admit coal particles in the centre of the flame was used to measure concentrations of atomic species in the flame; the methane flat-flame burner enabled a given rate of sized coal particles to be fed in the centre and readings of atomic species were measured at given positions. The burner was mounted on a computer controlled platform to enable accurate positioning for each measurement.

Temperatures for the tube furnace and flat-flame burner were measured using a thermocouple, two-colour optical pyrometry, and by operating the spectrometer in emission mode. These techniques gave similar results for heating rates from 120°C s^{-1} to 1000°C s^{-1}.

The AA data provided the concentrations of gaseous inorganic atomic species released from heated coal particles (these are discussed further below). The experimentally measured concentrations of gaseous inorganics, such as sodium species, were compared with the values for these species obtained from computer modelling of the chemical kinetics and thermodynamics of the combustion of these coals. The comparisons between measured and calculated values were used to ascertain the reliability of kinetics and thermodynamics computations. The work formed a portion of an assessment on the impact of volatile inorganics on boiler fouling fuelled by these low rank coals (Campisi and Domazetis, 1990).

Scanning Electron Microscopy with Energy Dispersive X-ray Analysis (SEM-EDX) and Computer Controlled Scanning Electron Microscopy (CCSEM)

SEM-EDX provides images of particles, and identifies the inorganics Na, Ca, Mg, Fe, Cl and S in the coal matrix, as well as the elemental composition of discrete mineral particles mixed with the coal. It has been used to examine samples after the coal had undergone any particular treatment; examination with SEM-EDX would give a good indication if the coal treatment had removed any or all inorganics, sulphur, and chloride. It would also show if the extraneous clay and sand particles consisted only of aluminium and silicon oxides, and if crystalline quartz particles were present in the sample. The technique can be used to detect all elements with atomic weight ≥ 6. This is done, for example, by using a JEOL 840A instrument with a Link Analytical Pentafet X-ray energy dispersive detector, using a thin window, which also permits the detection of carbon and oxygen. This is operated at 20kV with the detector resolution being 144eV. Samples are covered with either 20nm of carbon (for ash), or approximately the same thickness of platinum (for coal). Samples are dried in a desiccator prior to examination. A variety of sample preparation procedures can be employed, including pressed pellets and epoxy mounted samples, which are either polished or microtomed to reveal the particle interior. Pellets can be prepared by grinding the sample and pelletizing using a Perkin-Elmer hydraulic press at a pressure of six tons/m^2 for 2 min.

CCSEM is a technique used to determine the size, composition, abundance, and association of inorganics and mineral grains in coal samples. This is an efficient technique to assess coal samples from a commercial coal treatment plant. CCSEM utilises backscattered electron imaging combined with automated particle recognition, and can scan preselected areas to provide chemical analysis, providing the composition and size of coal particles, and identification of any mineral particles with the coal. The CCSEM system is automated to provide compositional data and classify any mineral particle types; mineral particle typing is based on data from standard minerals (Gupta et al., 1998; Microbeam Technologies).

X-ray Photoelectron Spectroscopy (XPS)

XPS is used to analyse the surface chemistry of a material for its elemental composition, and the chemical and electronic states of the elements. This technique has been extensively employed in studies of coal, ash, and samples from catalytic coal gasification.

XPS spectra are obtained by irradiating a solid surface with a beam of X-rays and measuring the kinetic energy of electrons that are emitted from the material. Peaks appear in the spectrum from atoms emitting electrons of a particular characteristic energy. The energies and intensities of the photoelectron peaks enable the identification and quantification of all surface elements (except hydrogen) in the surface region (0-20 nm depth) of samples from their binding energies (BE) of the core electron orbital. The BE shifts identify the types of bonding between atoms, differentiating between oxidation states. The BE peaks move to higher energy as the oxidation number of an element increases. The relative amounts of the identified species are obtained as at% of each element. The heterogeneous nature of the coal, and of the coal ash, requires samples to be well-mixed and ground into a fine powder under an inert atmosphere prior to analysis.

The XPS data discussed in this chapter were obtained using a Kratos Axis Ultra XPS spectrometer with monochromatised Al Kα radiation ($h\nu$ = 1486.6eV) operating at 150W. The spectrometer energy scale was calibrated using the Au $4f_{7/2}$ photoelectron peak at the BE of 83.98eV. Spectra were charge corrected with reference to [C-C] species at BE = 285.0eV. Survey and region spectra were collected at 100 eV and 40 eV pass energies, respectively. The analysis area was 700 μm x 300 μm. Spectra were quantified using the Kratos XPS elementary sensitivity factor data after background subtraction and the fitting of Gaussian (70%)/Lorentzian (30%) component peaks. The full width at half-maximum of the peaks was maintained as constant or within a chosen range for all components in a particular spectrum. Uncertainties for all fitted spectra were estimated to be 10% of the measured atomic concentrations. The practical detection limit for elements is ≤0.5 at%. Additional experimental and methodology details, particularly for the analysis of transition metals, are found in Aronniemi et al., (2005).

XPS is useful for obtaining data that would identify changes to the coal samples brought about by acid washing, by demineralisation, and from the transformations of coal samples used for catalytic gasification. The technique can distinguish between carbon functional groups, organic and inorganic functional groups of oxygen and sulphur, and inorganic species, and inorganic and organic forms of oxygen in coal and in char; this technique has been particularly useful in studies of the transformations of metallic species such as iron, derived from reactions between steam and treated coal, relevant to catalytic steam gasification (Kelemen et al., 2002; Grzyek and Kreiner, 1997).

Time of Flight – Secondary Ion Mass Spectrometry (TOF-SIMS)

TOF-SIMS is a surface analysis technique that sputters molecular fragments from the surface of the sample. The average depth of analysis for a TOF-SIMS measurement is approximately 1 nm. A pulsed ion beam is used to remove molecules from the very outermost surface of the sample; these are fragments removed from atomic monolayers on the surface that are then accelerated into a 'flight tube' and their mass is determined by measuring the exact time at which they reach the detector. Particles produced closer to the site of impact tend to be dissociated ions (positive or negative). Secondary particles generated farther from the impact site tend to be molecular compounds that are fragments of much larger organic macromolecules. By measuring the 'time-of-flight' of the particles from the time of impact to the detector on a scale of nano-seconds, a mass resolution is obtained at one part in a thousand of the mass of a proton, as well as a mass spectrum that surveys all molecular masses over a range of 1-10,000 atomic mass unit.

TOF-SIMS detects a wide range of inorganic and organic species in coal. The quantification of spectra is by reference to appropriate standards; reference standards are necessary due to the complexity of the ionisation process, the impact of the matrix, the primary ion properties, and the post-ionisation behaviour on the fragments and their yields. The detected fragments provide qualitative data on the functional groups on the surface of a coal sample. The high mass resolution of the technique enables different species to be distinguished, allows good peak assignments to be made, and thus identifies the various fragments; these are related directly to the constituents of the surface of the coal sample. The identification of such fragments is particularly valuable for the detection of any toxic and carcinogenic substances that may form from decomposition chemistry during treatment of the coal, particularly when these were subjected to high temperatures. This technique has, for example, identified organic chloro-moieties, which could form toxic substances if coal undergoes decomposition reactions when it is heated to elevated temperatures, and these would enter the wastewater.

The TOF-SIMS data discussed here were obtained from coal powders and pellets, using a TOF-SIMS IV (Ion-Tof GmH, Germany) instrument with a reflectron analyser, a Ga^+ ion source (25keV) and a pulsed electron flood source for charge neutralisation. The identification of the relevant peaks in the spectra was performed following appropriate calibration of the

mass scale, using an ion fragment library incorporated in the Ion-Tof spectral analysis package.

Fourier-Transform Infra-Red Spectroscopy (FTIR)

FTIR has been used in a wide range of studies, including coalification, coal pyrolysis, and the formation of ash (Ibarra et al., 1996; Song et al., 2017; Baxter et al., 1993). FTIR has been used in experiments that compare products from treated coals with untreated coals, during pyrolysis and gasification. This application of FTIR can be carried out, for example, by recording spectra with a Perkin Elmer 1720X FTIR Spectrometer equipped with a gas cell. CO_2, CO (and CH_4 when required) spectra are recorded in the region 4000-800 cm^{-1}; the concentration for CO_2 is obtained from calibration graphs based on the area of the peaks from 2394.96 cm^{-1} to 2283.3 cm^{-1}, the concentration for CO from the area of the peaks from 2226.09 cm^{-1} to 2047.06 cm^{-1}, and for CH_4 the area from 3300 cm^{-1} to 2800cm^{-1}. Calibration of the FTIR cell is performed by measuring these areas for a certified standard mixture of CO and CO_2. A calibration graph can be provided for concentrations of 0.048vol% to 5.270vol% for CO_2, and 0.024vol% to 2.650vol% for CO. The calibration graph for CO is linear over the concentration range 0 to 1.3vol% in nitrogen ($R^2 = 0.99$), and the CO_2 graph is over the concentration range 0 to 2.6% ($R^2 = 0.97$). For the CO_2 concentration range of 0-5vol%, however, some deviation from linearity can occur (R^2=0.93).

Coal Pyrolysis

Pyrolysis is performed by heating coal samples to increasingly higher temperatures in an inert atmosphere, and measuring the amounts of evolved gases and tars, and the weight of the resulting char. It has been observed that when coal samples are heated in an inert atmosphere, the result is the loss of oxygen functional groups to yield CO_2, CO, and H_2O, and bond breaking that forms tar and hydrocarbon molecular fragments. It has also been observed that low rank coals containing inorganic species may yield different proportions of products on heating; the impact of added inorganic species in low rank coals is of particular interest, and metal-mediated pyrolysis of low rank coals has been reviewed by Domazetis et al., (2009).

Studies of the thermal transformations of coal samples containing added inorganics are relevant to the formation of catalytically active species for steam gasification. Studies of such thermal transformations commence with studies of acid washed coal to establish a base line, and then samples of the

same coal with known amounts of added inorganic are subjected to the same temperature-time profile. Work by Domazetis and co-workers on pyrolysis and gasification has been carried out using a quartz tube reactor placed inside a Lindberg furnace. A constant flow (10.0ml/min) of nitrogen is maintained with a calibrated flow-meter, and temperatures are measured using a type J thermocouple with a digital thermometer, accurate to ±4 °C. Two sets of experiments are performed for these studies:

1. To determine the total weight loss of the coal sample at specific temperatures, and to measure the evolved CO_2 and CO concentrations at these same temperatures, and
2. To measure the evolved CO_2 and CO concentrations for a specific time-temperature ramp.

The first set of experiments commence with the coal sample being placed in a crucible and dried by heating it in an atmosphere of nitrogen, and after cooling it to room temperature, measuring the weight of the dry coal. The crucible with the dry coal is then placed in a tube furnace that has been heated to the selected temperature while maintaining the flow of N_2 (e.g. 150°C, 200°C, and so on), and the concentration of evolving gases is monitored periodically every 10-20 min for a period of 300-400 min, using a gas cell and the Perkin Elmer 1720-X FTIR instrument. The char remaining in the crucible sample is again cooled under nitrogen and weighed; the temperature of the furnace is increased (usually by 50 or 100°C) and the procedure is repeated. In this way, the total weight losses, and the total concentrations of evolved CO_2 and CO, are measured at points in a temperature profile. At high temperatures, any evolved CH_4 is also detected and quantified.

The second set of experiments is performed using a known weight of a coal sample heated at a set temperature-time profile, and the evolved CO_2 and CO concentrations are measured. In these, the coal sample remains in the tube furnace as evolving gases are determined at each temperature. Once steady state conditions are achieved, the furnace setting is changed to the next temperature and gas concentrations are measured. This is repeated with temperature increases usually of 50°C, to a final temperature of 500°C. These experiments provided weight loss vs temperature, ratios of CO_2:CO at given temperatures, and also changes in evolving CO_2 and CO with changing temperature-time profiles (Domazetis et al., 2006).

Similar experiments are conducted to study catalytic steam gasification. In these, the gas stream is an inert gas (N_2 or He) saturated with steam. FTIR, and gas-chromatography are used to measure the amounts of

evolving H_2, CO, CO_2 and CH_4 at given temperatures, for coal samples without the inorganic, and from the same coal samples treated to contain particular amounts of the inorganic of interest. All of these experiments used samples of the aw coal as the base data, and the same coal containing a known amount of added inorganic. Coal samples need to be dried thoroughly to ensure a reaction occurs only with steam added in the gas stream (drying may be carried out by heating the sample for 5-6 hours under nitrogen or helium at 110°C, and then storing in a desiccator to cool to room temperature).

A brief description of experimental details of laboratory steam gasification is as follows: a porcelain boat holding the coal sample is placed into the quartz reactor at a set temperature of between 200°C and 900°C, with helium gas passed at an accurate rate through a round bottom flask containing gently boiling water, to carry water vapour through the quartz reactor. The product gases exiting the quartz reactor are passed through a water trap cooled in an ice bath to remove excess water vapour, and a sample is obtained in an IR gas cell for FTIR analyses. Gas samples are also obtained for online gas-chromatography (GC) analysis with a sampling loop. GC analysis can be performed using a double column Shimadzu GC-4B PTF, with a silica gel 60/80 packed column, specific for H_2, CO, CO_2, and CH_4, and a thermal conductivity detector. The temperature of the column is kept constant at 65°C, the detector at 50°C, and the injection loop at 120°C; the GC flow rate of gases is 80 ml/min. Data are recorded with an eDAQ Powerchrom 280. The GC is calibrated using standard gas mixtures of H_2, CO, CO_2, and CH_4 in helium. Any impact of gas flow rate on the results can be tested by varying the He flow-rates from 20-50 ml per min for one set of experiments (high flow), and 2-10 ml per min for another set (low flow).

Thermal Gravimetric Analysis (TG) and Differential Thermal Analysis (DTA)

Thermogravimetry monitors the mass losses in a sample subjected to programmed heating; this is an instrumental analytical method that can be used to determine the losses of moisture and volatiles from coal samples over a given temperature profile. TG/DTA can also provide information on the ash chemistry occurring in the sample as it is heated. TG/DTA analytical pyrolysis has been used to characterise coals, and thermoanalytical curves for a number of low rank coals have been presented in a compilation (Liptay, 1971) that can be used in studies on the thermal behaviour of inorganics in brown coal (Domazetis et al., 1987; Domazetis and Buckman,

1987). Experiments can be carried out by using heating rates that may be varied from a few degrees per minute to 200 degrees per minute; usually an inert atmosphere is used for pyrolysis, although experiments may also be carried out in a reactive atmosphere. The technique has been developed to yield proximate analyses on small coal samples (ca. 20 mg) that are comparable to analyses obtained using standard methods (Beamish, 1994; Mayoral et al., 2001; Ma et al., 1991). Thermal analytical methods can also be used for the simultaneous comparison of the temperature loss/gain in the sample with that of an inert standard, to indicate whether the various reactions occurring in the sample are exothermic or endothermic.

A TG/DTA study has been reported for thirty coals and six density separated fractions with <15wt% ash. The technique has also been utilised in developing reaction kinetic models based on non-isothermal weight loss data. Furthermore, TG/DTA has been applied to the study of metal-mediated pyrolysis of cation-loaded brown coals (Cu, Zn and P acetates, and Fe, Ni, Co, Mn and Ca chloride) (Kok, 2003; Alonso et al., 2001).

Wastewater

Wastewater from coal/water mixtures is obtained by heating a known weight of crushed coal thoroughly mixed with a given volume of water, in a stainless steel pressure vessel equipped with a heating mantle and stirrer. The samples are heated to given temperatures, and the coal is filtered from the water. The coal/water ratio is varied, and the temperatures are increased by 20 degree increments over the range 100-230°C. The water is analysed for chemical oxygen demand (COD), total dissolved solids (TDS) and inorganics using AAS.

Chemical oxygen demand (COD) measures the dissolved organic mass in wastewater samples using the dichromate method.

Total dissolved solids (TDS) are determined by evaporating a 50ml sample of filtered wastewater sample to a constant weight using a steam bath. The dissolved inorganics in the sample are then determined by burning off the organics from a weighed portion of TDS in a muffle furnace at 600°C, and the loss in the TDS sample is recorded as total dissolved organics (TDO) (McKenry, 2001).

Other Techniques

The heterogeneous nature of coal continues to pose challenges for its characterisation, and these challenges motivate the continued utilisation of advanced methods and techniques, such as:

- X-ray computed tomography, which creates 3D images; this non-destructive technique is used in studies on coal cleaning, swelling and shrinking during coal drying, on changes during devolatilisation, and to understand breakage during handling (Mathews et al., 2017).
- ^{13}C NMR and ^{1}H NMR, which have been widely used for diverse studies on coals, including coalification, structural aspects such as the mobile-phase in coal and liquefaction, functional groups analysis and work on computer generated coal molecular structures (Schulze et al., 1990; Xiong et al., 2002; Erdenetsogt et al., 2010).
- Flash pyrolysis, which has been developed to study the release of tars, gases, and the formation of char from the different ranks of coal, and has provided insights in developing a number of kinetic models of coal devolatilisation chemistry.
- Computer coal molecular structures have been developed over many years for the various ranks of coal, and with advances in characterisation techniques, these have increased in utility, and with the availability of supercomputers, some structures have been studied using *ab initio* computations (Mathews et al., 2011).

Assessing the Quality of Processed Coals

The goal of research into coal treatment is to economically produce high quality fuel, and to ensure the treatment method does not produce pollutants. This goal is achieved when the organic matrix of the coal is relatively unchanged, the ash constituents that are the cause of fouling are eliminated, moisture is reduced, and the wastewater does not contain toxic substances. A thorough assessment of the final products is also required on their behaviour as a fuel for combustion and gasification. The chemistry of the combustion of the processed coal would differ on the absence of ash fouling. The chemistry of catalytic steam gasification of the processed catalytic coal, however, differs considerably from that of the gasification of untreated coal, and this area requires a thorough understanding of the phenomena. Consequently, techniques are required for assessing the treated coals as fuels for coal combustion, as are techniques to provide insights on the mechanisms of catalytic coal gasification.

The data obtained with these techniques are mainly for low rank coals that have undergone chemical processes to yield non-fouling coal and ultra-clean coal (very low amounts of ash). Additional data on environmental improvements are also considered. The data are used to compare each coal sample before and after it has been subjected to a variety of treatment methods, to assess the changes attributed to each of the conditions that may

be varied in these methods of treating the coal (e.g. temperature, pH, coal particle size). Additionally, understanding the chemistry of metal-mediated pyrolysis and catalytic steam gasification requires an examination of reaction pathways using molecular models of coal with semi-empirical and *ab initio* quantum mechanics molecular computations, and comparing the outcomes from these with experimental results.

The scientific literature contains accounts of high rank coals treated into low-ash coals, but such data are sparse for low rank coals; consequently, most of the following discussion deals with general details from the CCT P/L – LTU R&D Program, as this has provided comprehensive data on the treatment of low rank coals into the desired products with an environmentally benign impact. The data on the product coal consist of elemental and proximate analyses, the chemical composition of ash, and analysis using XRF, XPS, XRD, AA, SEM, and TOF-SIMS. Additionally, wastewater analysis shows the amount of organic substances released from the coal, and TOF-SIMS data of solids obtained from wastewater would identify any toxic organics, if they were present in the wastewater. Measurements of total ash before and after treatment show the reduction in ash, while XRD and elemental ash analysis show the ash components remaining in the treated coal. The fate of sulphur and chloride entities during coal treatment is of interest, as they are responsible for acidic condensates in flue gas and corrosion in boilers, and atmospheric pollution. Elemental analyses in combination with XPS analyses identify the inorganic forms of sulphur and chloride and may show if any of these are removed by the treatment methods. Data that show reductions in both iron and sulphur are consistent with reductions in pyrites and other forms of inorganic sulphur. Minor amounts of organic chlorides would be detected with TOF-SIMS.

Analysis of wastewater from the coal treatment is followed by treatment to provide distilled grade water for re-use in coal cleaning; the concentrated waste from this is analysed to ensure pollutants have not formed, and thus are not released into the environment. For example, Nakajima et al. (2013) have demonstrated that when coal mixed with water mixtures is subjected to low temperatures, it did not produce toxic substances in wastewater, but toxicity is pronounced when the coal water mixture is heated to high temperatures.

Data discussed here are for:

- CCT P/L acid treatment of low rank coals
- CCT P/L catalytic low rank coal
- Acid treatment of black coal
- Caustic treatment of black coal
- Solvent extraction of black coal

The elemental composition of coal consists of carbon, hydrogen, oxygen, sulphur, chloride and nitrogen, calculated on an ash- and moisture-free basis. Ash is also analysed for composition and this is reported as either oxides, or as elemental components, in the dry coal. A direct measure of wt%C, wt%H, wt%O, wt%N, wt%S and wt%Cl can be obtained by, for example, using microanalysis; this method uses a small sample amount, and a very thorough mixed bulk sample is required to ensure the data are representative of the batch of coal. The errors of the micro-analytical method are normally ±0.3wt%; an examination of the analyses for a number of brown coal samples display differences of ±0.5wt% for carbon, ±0.2wt% for hydrogen, and ±0.3wt% for oxygen. The detection limits of microanalysis for nitrogen and sulphur are ±0.2wt%, but the results indicate a greater variety for these samples, with error at ±0.4wt%. The direct determination of total oxygen in well-mixed coal samples is used in conjunction with XPS data to quantify the types of carbon groups, and the organic and inorganic forms of oxygen, chloride, and sulphur in coal. The heterogeneous nature of brown coal inevitably leads to variations in analytical results, and although these variations may be minimised by thoroughly mixing the samples, they cannot be completely eliminated.

Table 2-1 lists the elemental composition, and the wt% ash, of dry samples of untreated and treated brown coal from Germany and Australia; the latter are Victorian brown coal from the Loy Yang mine and South Australian lignite samples (labelled SAlignite). Table 2-2 compares the data of the organic matrix of these low rank coals (available data for hyper-coal are included) on a dry ash-free basis. Table 2-3 lists the analyses of the ash in these coal samples.

Table 2-1. Analysis of coal samples (wt% on db, variation ±0.3wt%).

Sample	%C	%H	%N	%O	%S	%Cl	%Ash
German	59.5	4.4	0.6	30.4	<0.3	<0.3	4.5
German*	63.8	4.3	0.9	30.8	0.3	0.2	0.4
SAlignite1	53.4	4.3	0.2	25.2	3.1	0.9	12.9
SAlignite1*	56.6	4.6	0.6	30.5	3.0	0.3	4.5
SAlignite2	48.6	3.8	0.4	28.2	4.9	1.0	13.2
SAlignite2*	59.7	4.8	0.7	28.8	4.3	0.3	1.4
Loy Yang#-A	63.3	5.2	0.6	28.2	0.4	ND	2.1
Loy Yang-B	62.6	4.9	0.3	26.9	0.9	0.3	4.1
Loy Yang*	65.2	5.0	0.5	28.6	0.4	0.1	0.1
Loy Yang**	65.4	5.0	0.5	28.8	0.4	<0.1	0.04

O determined by difference, Cl undetermined; * aw coal; ** de-mineralised coal.

Table 2-2. Elemental analysis of coal samples as wt% of dry ash free (daf).

Sample	%C	%H	%N	%O	%S	%Cl
German	62.3	4.6	0.6	31.8	<0.3	<0.3
German*	63.8	4.3	0.9	30.8	0.3	<0.3
SALignite1	61.4	4.9	0.2	28.9	3.6	1.0
SALignite1*	65.4	4.0	0.7	26.1	3.5	0.3
SALignite2	56.0	4.2	0.5	32.5	5.6	1.2
SALignite2*	63.6	4.3	0.7	26.4	4.5	0.3
Loy Yang#-A	64.7	5.3	0.7	28.8	0.4	0.1
Loy Yang-B	65.3	5.1	0.3	28.1	0.9	0.3
Loy Yang *	65.3	5.0	0.5	28.7	0.4	0.1
Loy Yang**	65.4	5.0	0.5	28.8	0.4	<0.1
Raw (for hyper-coal)†	84.7	5.4	2.3	7.1	0.6	nd
Treated (hyper-coal)†	85.3	5.3	2.4	4.0	0.4	nd

O determined by difference, Cl undetermined; * aw; ** de-mineralised; † black coal ash 6%; hyper-coal ash 0.1%; from Wang et al. (2005).

The samples of lignite in this batch are high ash and sulphur; the data show acid treatment of the coals removes inorganic sulphur and chloride, and significantly reduces the amount of ash.

Demineralisation reduces the ash of the German and Loy Yang samples to very low levels, without a detectable change to the organic matrix.

The data in Tables 2-1 and 2-3 show that between 98% and 67% of the ash can be removed by treatment with acid, and efficient demineralisation can reduce ash by >99.9%; chloride is virtually eliminated, but organic sulphur in the coal samples is not changed significantly – the types of sulphur identified with XPS are discussed below. The composition of the ash remaining in the acid-treated coals consists of aluminosilicate substances (clays) which are non-fouling.

Two Loy Yang coal samples were acid washed (aw) to remove inorganics from the coal, and also de-mineralised, to remove both inorganics and minerals, in order to produce coal with virtually zero-ash.

Table 2-3. Ash components in treated coals as a percentage of the dry weight of coal.

Sample	%SiO_2	%Al_2O_3	%Fe	%Mg	%Ca	%Na	%K	%Cl	%S
German*	0.01	0.01	1.3	0.2	0.7	+	+	+	+
German#	0.01	0.01	~0.01	+	+	+	+	+	+
SALignite1	8.0	2.2	0.2	0.8	0.7	1.2	0.1	0.2	0.9
SALignite1*	4.7	1.0	0.4	0.8	1.4	0.4	0.1	0.2	0.4
SALignite2	4.7	0.6	0.5	1.3	2.4	1.1	0.1	0.6	1.3
SALignite2*	2.2	0.1	0.3	0.1	+	+	0.0	+	0.1
Loy Yang*	0.1	0.1	0.3	0.1	+	+	+	+	+
Loy Yang*	3.8	1.5	0.2	+	+	0.1	+	+	+
Loy Yang#	0.1	0.0	+	+	+	+	+	+	+

* aw coal; # demineralised coal; + at or below analytical detection limits.

Table 2-4 Ash composition and total ash for ultra-clean low rank coals and black coals (ppm).

Sample	V	Na	Mg	Al	Si	K	Ca	Fe	Ti	Total (ppm) and (wt%)	
German	-	5-7	7-41	19-37	46-94	<5	23-97	42-149	8-27	230-460	0.02-0.05
Loy Yang	<3	10-20	< 2	20	20-233	<5	7-9	8-22	8-20	<99-322	0.01-0.03
CSIRO	7-12	58-540	5-12	0-8	35-78	9-29	22-36	43-215	470	649-1400	0.06-0.14
Hyper-coal	n/a (not available)			n/a	n/a	n/a	n/a	n/a	n/a	200-1000	0.02-0.1
Black coal HF/HNO_3		%Na_2O	%MgO	%Al_2O_3	%SiO_2	K_2O	CaO	Fe_2O_3	SO_3	(ppm)	wt% ash
		0.077	0.077	0.037	0.051	0.052	0.023	0.26	3.63	6300	0.63

The oxygen measured directly for samples with high ash content includes significant amounts of inorganic oxygen in minerals (e.g. Al_2SiO_5). The organic oxygen in the coal matrix may be estimated by correcting the value for total oxygen for inorganic oxygen. This approach may be illustrated for SAlignite, which is estimated to contain ~5% clay; the total oxygen value for the untreated coal is due to organic oxygen groups, oxygen from any $CaSO_4$ and Na_2SO_4, and from oxygen in silica and clay. The correction for inorganic oxygen yields organic oxygen of the aw coal sample at 25.7wt%.

The composition of the ashes of ultra-clean coals reported in the literature are shown in Table 2-4, with ash components reported as parts per million, and the total ash also as the wt% in the dry coal; elemental analysis of the ash from hyper-coal is not available in the literature, and only the total ash is shown. Data for black coal treated with HF/HNO_3 have been reported for various conditions, and the lowest reported ash level is shown. The CSIRO treatment of high rank coal using caustic, followed by neutralising the liquor with acid and separating the coal, produces coal with low amounts of ash, but relatively high levels of sodium. The importance of sodium levels in ultra-clean coals is discussed in this volume. High rank coal treated with HF/HNO_3 contains relatively large amounts of ash. The CCT/LTU Program demonstrated that low rank coals can be treated to reduce the ash content to 'background levels', with sodium at the detection limits of the available techniques.

The acid treatment of lignite removes sodium and potassium, with sulphur reductions of >90% for SAlignite1 and ~50% for SAlignite2. The high sulphur reduction is often accompanied with a reduction in iron, consistent with the removal of inorganic sulphur.

The acid washing of low rank coals at elevated temperatures (<200°C) has not changed the organic matrix of these samples, while the amount of ash was reduced, and this reduction was dramatic for demineralised coals. The organic matrix of hyper-coal appears to have undergone changes that resulted in a reduction of organic oxygen, and the coal treated with HF/HNO_3 is reported to undergo oxidation by HNO_3.

XPS and TOF-SIMS detect any changes to the functional groups that may occur during treatments (data are not available for hyper-coal and HF/HNO_3 treated coal). XPS identifies elements and their chemical environment and their proportion is obtained as a percentage of the detected atoms (at% values). The following information is obtained with XPS for low rank coals:

Table 2-5. C 1s BE and at% from XPS region scans of coals*

Sample	H-C-C (eV)	at%	C-O (eV)	at%	C=O (eV)	at%	O-C=O (eV)	at%	shake up (eV)	at%
As received coal										
German	285.0	52.6	286.4	16.7	287.5	4.7	289.0	4.0		
SAlignite1	285.0	51.0	286.3	18.5	287.6	3.8	289.1	5.8		
SAlignite2	285.0	43.8	286.5	17.6	287.9	5.8	289.1	5.2		
Loy Yang	285.0	55.8	286.5	16.2	287.6	4.6	289.1	4.2		
Acid washed coal										
German	285.0	50.4	286.6	19.5	288.2	4.3	289.5	4.4	291.5	1.2
SAlignite1	285.0	47.1	286.4	19.2	287.8	3.9	289.3	4.7	291.2	1.3
SAlignite2	285.0	52.2	286.5	15.6	287.6	4.6	289.3	4.7	-	-
Loy Yang	285.0	53.3	286.6	16.5	288.1	3.3	289.3	5.0	291.0	1.9

* Adapted with permission from Domazetis et al., Energy Fuel, 20, 1556, 2006. Copyright (2006). American Chemical Society.

Carbon in coal: The groups identified by XPS are carbon bound to carbon and hydrogen (C-C-H; BE 285.0 eV), carbon bound to oxygen (C-O; BE 286.4eV), carbon double bonded to oxygen (C=O; BE 287.5 eV), and carboxyl carbon (O-C=O; BE 289.1eV). The C 1s BE energies and at% values from the region scans for a number of as received (ar) and aw coals are listed in Table 2-5. The amounts of carbon from average at% values for aw brown coals (standard deviation in parenthesis) are: [C-C-H], 52.2 (2.4); [C-O], 17.2 (1.6); [C=O], 4.3 (0.8); [O-C=O], 5.3 (1.6). The total carbon in these samples may be estimated by adding the at% values for the particular carbons observed with XPS. Hydrogen is not detected with XPS and consequently the at% values are somewhat greater than those obtained from the ultimate analysis data – if these are corrected by assuming 5wt% hydrogen in the samples, XPS provides the average total at% C for the ar samples at ~72%±3%, and for the treated samples at ~73%±3%. These values are somewhat greater than those obtained from ultimate analysis, and XPS is thus considered a secondary analytical technique for these studies. The XPS data show about 27at% of the carbon in these coals is bound to oxygen.

Oxygen in coal: Table 2-6 contains the XPS assignment of oxygen functional groups bound to carbon for brown coal and lignite samples. The BE 1s values for oxygen bound to carbon are ~533eV (C-O) and ~532eV (C=O). Verification of the types and amounts of organic oxygen determined by XPS is done by comparing the values obtained for coal with those obtained from pure samples of organic substances, such as polyacrylic acid (BE O 1s (C=O) 531.7 eV; 1s (C-O) 533.3 eV), and for a mixture of polyacrylic acid and tartaric acid (BE O 1s (C=O) 532.2 eV and 1s (C-O) 533.4 eV). A mixture of polyacrylic acid and tartaric acid with added SiO_2 provides similar O 1s values, but with an increase in the relative intensity at 532.2 eV, due to oxygen from SiO_2. The average at% values for the respective oxygen groups in these coals are lower by about the same amount that the average at% for carbon is higher, when these values are compared to those obtained from ultimate analysis, and may be due to small differences in the composition of the surface of the coal samples.

The data in Table 2-7 include a comparison of the [C:O] ratios from the XPS data with the ratios obtained from the elemental analysis for the respective coals. The XPS [C:O] ratios observed for German and Loy Yang brown coals are higher, whereas those for the two lignites are lower. These different results are likely to be due to the heterogeneous compositions and differences in the surface of the coal samples. XPS obtains chemical information on the outermost atomic layers of a material, the analysis depth usually being within the range 0.5-5 nm. Data of [C:O] ratios for

homogeneous materials such as polyacrylic acid, tartaric acid, and poly(ethylene terephthalate) provide the expected values based on the molecular formula of these compounds. Thus the variation observed for these coals is due mainly to their heterogeneous nature as it is observed on the surface of the coal particles.

Table 2-6. BE and at% assignments for oxygen groups in aw coal samples*

Sample	BE C-O (eV)	at%	BE C=O (eV)	at%
German	533.5	12.3	532.1	6.1
SAlignite1	533.6	10.1	532.4	11.3
SAlignite2	533.5	11.4	532.2	8.9
Loy Yang	533.6	12.3	532.2	7.1

Table 2-7. Carbon and oxygen from elemental analysis and XPS, aw coals (wt%)*

Samples	analysis		XPS		[C:O] ratio	
	C	O	C	O	analysis	XPS
German	65.2	28.8	70.0	24.7	2.26	2.83
Loy Yang	65.3	27.7	69.2	24.2	2.28	2.86
SAlignite1	65.4	26.1	64.0	26.3	2.51	2.43
SAlignite2	63.6	26.4	65.3	25.8	2.41	2.53

The number of oxygen atoms per 100 carbon atoms obtained from the elemental analysis for aw coal samples ranged from 30 to 33, while that from XPS data for these samples is from 24 to 31. Comparable values of oxygen atoms per 100 carbons are 20.3 for North Dakota lignite, 18 for Montana lignite, 18.8 for Beulah Zap lignite, 23.3 for Texas lignite, and 23.5 for Alaska lignite. Various oxygen functional groups have also been measured with ^{13}C NMR for brown coals and lignites. Although the concentration of [COOH] and [C-O] groups could be evaluated by ^{13}C NMR measurements, the values obtained using this technique were not quantitative due to the low signal-to-noise ratio of the spectra. The value of [COOH] may be determined by chemical analysis and a calculated value obtained for [C-O] groups, and these results are of carbonyl oxygen groups at 14-18wt% of the sample, and ether oxygen groups at 17-28wt% of oxygen in coal, while the values of [OH] and [COOH] groups varied from coal to coal.

The XPS data provided the following at% distribution of carbon bonded to oxygen (average values, with deviation in parenthesis):

[C-O] = 17.2% (1.6); [C=O] = 4.3% (0.8); [OC=O] = 5.3% (1.6).

The at% distribution of oxygen groups is:

[C-O] = 11.1% (0.7); [C=O] = 7.7% (1.4) (this compares favourably with total carbonyl oxygen at 14-18% from ^{13}C NMR).

About 41% of the oxygen is identified by XPS as carboxyl and carbonyl, and 59% as hydroxyl, phenol and ether. From the distribution of C 1s as [C=O] and [O-C=O], the organic oxygen in brown coals can be distributed as 23% carboxyl, 18% carbonyl, and the remaining 59% distributed amongst phenol, hydroxyl, ether and methoxyl groups.

Inorganics in low rank coal: The identification and differentiation of inorganic oxygen groups by XPS is particularly useful in studies of brown coal samples containing transition metal complexes that underwent catalytic steam gasification. The region XPS scans of brown coal samples containing iron and nickel complexes display a peak at BE at 530 eV assigned to inorganic oxygen groups. XPS studies identify inorganic oxygen groups after coal samples containing iron species are heated in an inert atmosphere (N_2 or He), and from the identical coal samples heated in an atmosphere containing steam. The oxygen groups chemically bound to inorganics are observed at BE 1s values at 530-532 eV. The following BE values are observed for various inorganic oxygen groups: BE (O_2^-) at 530.0-529.9 eV, (OH^-) at 531.1 eV; BE O 1s values for iron oxides are at 531.3 eV and 530.1 eV, assigned to [Fe-OH] and [Fe-O] respectively, while values for CaO, TiO_2 and ZrO_2 are at 531-532 eV. The data have been used in molecular modelling and experimental studies of coal and char containing metal complexes.

The XPS spectra of iron compounds also display multiple Fe $2p_{3/2}$ envelopes for Fe^{3+} and Fe^{2+}, with satellite peak structures often ascribed to shake-up or charge transfer processes. $Fe2p_{3/2}$ BE values for Fe_2O_3 are at 710.8-711.0 eV and for FeOOH at 711.4 eV. Complicated Fe(III) 2p features are observed for coal samples containing significant amounts of monomeric and polymeric iron hydroxyl species.

The XPS region scans for German aw brown coal, the same coal with 12.4wt% of added iron, and char prepared from this coal under nitrogen at 500°C, identify the changes that occur to organic and inorganic functional groups in low rank coal samples containing an iron oxy hydroxyl complex.

The XPS features for these samples are similar for the aw coal sample and the same sample containing iron complexes, with additional peaks due to the iron hydroxyl complexes in the coal sample. The relevant data are: BE O 1s 530.7 eV, 532.0eV and 534.0eV; BE Fe(III)$2p_{3/2}$ 710.5eV. When this coal sample is heated under N_2 at 500°C, the XPS features of the resulting char are consistent with the presence of the iron oxide/hydroxyl complex: BE O 1s, 530.7 532.0 and 534.0 eV; BE Fe(III)$2p_{3/2}$, 710.5eV.

The XPS spectra for the char from aw coal, when compared to that of the char from the same aw coal plus the iron complex, identifies the chemical changes that occurred to the coal matrix; the C 1s at% ratios of C-CH, C-OH, and O-C=O at% for aw char (285 eV C-CH to 286 eV C-OH) were 2.7 to 3.4, but for the char containing iron, this ratio increased to 3.8-4.0. The bulk of the carboxyl groups disappeared, consistent with the loss of these groups during pyrolysis to form CO_2; the relative amount of inorganic oxygen (as iron oxides) increases as the coal mass decreases. The significance of these data is discussed in detail in subsequent chapters.

Sulphur in coal: Organic and inorganic forms of sulphur are detected with XPS, at detection limits of ~0.4wt%. The acid treatment of low rank coals removes inorganic forms of sulphur, while organic sulphur remains unaffected. Organic sulphur is present in coal as alkyl and aryl thiols, thiophen, and oxidised sulphur, such as sulfones (TOF-SIMS data, discussed below, shows organic S-N groups are also present). Inorganic sulphur is present as sulphate and sulphide (pyrites). Sulphur is detected at BE S $2p_{3/2}$ 160-170 eV. The XPS region scans of brown coal (ar and aw) generally provide two doublets for S $2p_{3/2}$ at 164 and 169.0 eV, which are attributed to thiol sulphur and oxidised sulphur, respectively. The relevant BE values are: thiols S $2p_{3/2}$ 162.0-163.3 eV, thiophen S $2p_{3/2}$ 164.1 eV, sulfoxides S $2p_{3/2}$ 167.9 eV, sulfones S $2p_{3/2}$ 168.1-168.4 eV, and sulfonic S $2p_{3/2}$ 169.5-170.4 eV. BE S $2p_{3/2}$ at 163.3eV is assigned as sulfidic and the S $2p_{3/2}$ at 164.1eV as thiophenic. The BE S $2p_{3/2}$ peak for inorganic sulphate salts is at 169-170 eV and inorganic sulphides at 160.0-161.2 eV.

Changes in the relative intensities of the sulphur peaks for aw coals are consistent with the removal of inorganic sulphur by acid treatment. The region scan for sulphur in SAlignite1 coal (ar and aw), for example, shows a significant reduction in the inorganic sulphide (S $2p_{3/2}$ at 164.1 eV). The XPS region scans for aw SAlignite1 provides peaks due to reduced and oxidised sulphur; the S $2p_{3/2}$ peak at 164 eV is due to thiol sulphur, and the S $2p_{3/2}$ peak at 169 eV is due to oxidised sulphur. The relative at% concentrations of un-oxidised to oxidised sulphur was 1.4:1 in the treated coal, compared to the ratio of 3.5:1 for the untreated coal, consistent with the removal of inorganic sulphur by the acid treatment of the coal sample.

The region scan for the untreated SAlignite2 sample also contains the features of un-oxidised and oxidised sulphur, with a relative at% ratio of 0.7:1. The region scan for the aw SAlignite2 sample indicates smaller amounts of oxidised sulphur, consistent with the removal of inorganic sulphur; while it is unclear from this if pyrites were removed by the acid, this may be inferred from the data which show a reduction in the iron content and a reduction in inorganic sulphur.

The region scans for ar, aw, and demineralised Loy Yang and German brown coals occasionally provided peaks above the noise that can be assigned to organic sulphide and/or thiophen sulphur, at S $2p_{3/2}$ 164.1eV. The amount of sulphur in these coals (0.2-0.4wt%) was at or below the detection limits of XPS.

Chloride in coal: The BE Cl 2p values for organic chloride are at 199-201 eV; e.g. for C_6H_5Cl, the Cl $2p_{3/2}$ is at 200-201 eV, and for CH_2=CHCl the Cl $2p_{3/2}$ is at 199.6-200.3 eV, while inorganic chloride is detected at BE Cl $2p_{3/2}$ at 198 eV and Cl $2p_{1/2}$ at 200 eV. The region scans for the coal samples provide BE values of Cl $2p_{3/2}$ 197.6 to 198.6 eV, and Cl $2p_{1/2}$ 199.3 to 200.2 eV; inorganic chloride is detected in SAlignite1 and SAlignite2 at BE Cl $2p_{3/2}$ at 198.5 eV and BE Cl $2p_{1/2}$ at 200.5 eV. The XPS data are consistent with mainly inorganic chloride in coal (as NaCl), but the organic Cl 2p peaks are hidden by the peaks from inorganic chloride when the amount of organic chloride is low. The detection of small amounts of organic chloride is carried out using TOF-SIMS, and this is discussed below.

Wastewater: Samples of wastewater obtained from coal/water mixtures heated to between 100-200°C were examined with XPS as solids obtained after evaporating the water. A mixture of inorganic and organic components was identified with XPS. The region scan for C 1s consisted of features due to [C/CH] and [C-O] groups, and a smaller amount from the [O-C=O] group, indicating that mainly organic hydroxyl and a small amount of carboxylic acids are present in the sample. The region scan for oxygen consisted of a broad peak at BE 532-533 eV that could not be resolved. Considerable amounts of chloride (Cl $2p_{3/2}$ 197.6 eV), some oxidised sulphur (S $2p_{3/2}$ 169.4 eV), and some Na, Fe, Ca, Mg, Si, Al species were observed. The data are consistent with dissolved inorganic chlorides and sulphates/sulphides, and some organic moieties, solubilised in the water.

TOF-SIMS is a sensitive technique that can be used to detect a wide range of inorganic and organic species in coal.* Positive and negative mass spectra are obtained for untreated and treated coal samples. The observed

* This discussion has been modified with permission from Domazetis et al., Energy Fuels, 20, 1556-1564, 2006, Copyright (2006). American Chemical Society.

hydrocarbon fragments are consistent with a macromolecular matrix consisting predominantly of single phenyl groups connected by aliphatic units, with an abundance of oxygen functionalities, and smaller amounts of organic sulphur, nitrogen and chloride groups.

Negative fragments TOF-SIMS spectra. The major negative mass fragments obtained with TOF-SIMS for coal samples (relative intensities shown in brackets, normalised to O^- = 100) are typically: O^- (100), OH^- (59), CH^- (47), C^- (20), and C_2H^- (19). Fragments of lower intensity are: S^- (6), CN^- (3), and Cl^- (2). All of the brown coals provide similar major negative fragments, but their relative intensities differ; for example, the intensities of the major fragments for German brown coal were $O^- > CH^- > OH^-$ and $> C_2H^-$, but for SAlignite1, they were $O^- > OH^- > CH^- > C^-$ and $> C_2H^-$.

The negative sulphur fragments for aw coals were S^-, HS^-, SOH^-, SO_3H^-, SO_4^- and SO_4H^- (S^- the most intense). The organic fragment was $C_2H_4S^-$. Each of the brown coals provides differing intensities of these fragments. Generally, coal samples with larger amounts of sulphur provided peaks of greater intensity.

The negative chloride fragments observed for the aw brown coals are shown in Table 2-8, with intensities listed relative to Cl^- = 100 (Cl^- is the highest intensity fragment, HCl^- is not detected). The data compare to that for chlorinated bituminous coals which contain organic fragments such as C_6H_5Cl, $CHCl_2$, CCl_3, and $C_7H_5Cl_3$. The positive fragments are also consistent with organic chloride in brown coal. The detection of organo-chloride is significant because water soluble organo-chloride compounds (and organo-sulphur compounds) may form toxic pollutants if they enter the wastewater.

Table 2-8. Negative chloride fragments from aw brown coals.

Fragment	m/z	Rel Int
Cl^-	34.970	100
CCl^-	46.972	0.2
ClO^-	50.966	0.4
$C_2H_3Cl^-$	61.992	0.7
$COCl^-$	62.968	1.1
$C_3H_7Cl^-$	78.021	0.4

Positive fragments TOF-SIMS spectra. The positive fragments from the brown coals compare with TOF-SIMS data from high rank coals (Buckley and Lam, 1996; Sun, 2001). Fragments such as $C_nH_{(n+1)}^+$, $C_nH_{(2n-1)}^+$, and

$C_nH_{(2n+1)}^+$ predominate, with the most intense being $C_2H_3^+$, followed by (in decreasing intensities) $C_3H_5^+$, $C_2H_5^+$, $C_3H_7^+$, $C_4H_7^+$, CH_3^+, $C_4H_9^+$, $C_2H_2^+$, $C_4H_5^+$, CH_2^+. The hydrogen depleted fragments $C_nH_{(n-1)}^+$ are not abundant. Fragments indicative of aromatic groups, with their relative intensities, are: $[C_2H_3]^+$(100), $[C_5H_5]^+$ (7.8), $[C_6H_5\text{-}C_2H_5]^+$ (3.9), and $[C_6H_5\text{-}CH_2]^+$ (1.8).

Oxygen containing fragments are observed from hydrocarbons, such as $C_4H_7^+/C_3H_3O^+$ (m/z 55), $C_2H_3O_2^+/C_3H_7O^+$ (m/z 59) and C_4H_5O/C_5H_9 (m/z 69). The intensity ratios of these fragments are 11:1, 9.6:1 and 8.2:1. The values are comparable to those observed from the polymer poly(methylmethacrylate) (Briggs et al., 2000). Oxygen fragments obtained from phenol containing polymers, such as poly(4-vinyl phenol), and from oxidised polyethylene are also similar to the fragments obtained from brown coal (e.g. CHO^+, $C_2H_2O^+$, $C_2H_3O^+$, $C_2H_5O^+$, C_3HO^+, $C_3H_3O^+$, C_2HO^+, $C_7H_5O^+$, $C_7H_7O^+$ CHO_2^+, $C_2H_3O_2^+$, and $C_4H_7O^+$) (Liu et al., 2001).

Thermogravimetric-photoionisation mass spectrometry of coals has provided $C_nH_{2n}O$ fragments indicative of the fragmentation of alkenols and aldehydes (Zoller and Johnston, 1999). These series have been observed only for n=1 to 4 in the brown coal studies, i.e. up to $C_4H_8O^+$. The TOF-SIMS data are thus indicative of a polymeric substance containing phenolic and carboxyl groups linked by hydrocarbons. Fragments indicative of significant amounts of condensed phenyl groups are not observed.

Relatively low intensity sulphur-containing positive fragments are obtained for brown coal samples. The sulphur fragments originate from thiol and sulfone groups in the coal. A number of sulphur and nitrogen fragments are observed, with the C:H ratios for the fragments $C_4H_9SN^+$, $C_5H_{11}SN^+$ and $C_6H_{12}SN^+$ indicating aliphatic moieties (e.g. $[H_2NCH_2\text{-}CH_2\text{-}CH{=}CH\text{-}SH]^+$). The fragments S^+, HS^+, H_3S^+, S_2^+ are low intensity, and $C_2H_3S^+$, $C_2H_5S^+$ were observed for the SAlignite1 sample. The Loy Yang and German coals provide the fragments CH_2S^+, CH_3S^+, $C_4H_{12}O_4S^+$ and $C_4H_7S^+$ and are indicative of organic sulphate and thiol groups. The SAlignite1sample contains oxidised sulphur fragments ($C_7H_6SO_3^+$, $C_6H_{16}O_4S^+$, $C_7H_{13}O_4S^+$, $C_8H_{14}O_4S^+$, and $C_9H_{13}O_2S^+$), which may originate from aromatics and substituted phenols, e.g. $C_6H_7S^+$, $C_7H_6SO_3^+$, $CH_3\text{-}(O)C_6H_3\text{-}SO_2^+$, $CH_2(C_6H_4)SO_3^+$, $C_6H_5CHSO_3^+$. The sulphur groups, oxidised sulphur groups, and S-N containing fragments indicate polluting organo-sulphur species that may be released into the wastewater from coal treatment processes.

The positive chloride-containing fragments listed in Table 2-9 originate from organic chloride in brown coals and lignite. The major fragment for SAlignite1 and Loy Yang brown coal is $C_{11}H_{18}Cl^+$, and for the German brown coal is $C_{15}H_{12}Cl^+$. The fragment $C_{11}H_{18}Cl^+$ may be part of either an

aliphatic or aromatic functional group in the coal organic matrix. The fragments $C_{11}H_{18}Cl^+$ and $C_{15}H_{12}Cl^+$ (German brown coal) may be derived from phenyl-alkyl and aliphatic moieties in the coal sample. Fragments from these coals are similar to those from chloride-containing polymers such as polyvinyl chloride (e.g. CH_2Cl^+, $C_3H_5Cl_2^+$) (Briggs et al., 2000; Auriet et al., 2001).

Table 2-9. Positive chloride fragments from brown coals

Fragment	m/z	Fragment	m/z
CCl^+	46.970	$C_{11}H_{18}Cl^+$	185.104
CH_2Cl^+	48.988	$C_{12}H_8Cl^+$	187.035
$C_3H_5Cl_2^+$	110.977	$C_{14}H_{17}Cl^+$	220.098
CCl_3^+	116.904	$C_{15}H_{11}Cl^+$	226.060
$C_5H_7O_2Cl^+$	134.013	$C_{15}H_{12}Cl^+$	227.066
$C_{10}H_9Cl^+$	164.043	$C_{15}H_{14}Cl^+$	229.077
$C_{10}H_{16}Cl^+$	171.090	$C_{16}H_{11}Cl^+$	238.075
$C_{10}H_{17}Cl^+$	172.099	$C_{18}H_{14}Cl^+$	265.070
$C_{11}H_8Cl^+$	175.026		

References

Alonso, M. J. G., Alvarez, D., Borrego, A. G., Menéndez, R. and Marán, G. 2001. 'Systematic Effects of Coal Rank and Type on the Kinetics of Coal Pyrolysis', *Energy Fuels*, 15, 413-428.

Aronniemi, M., Sainio, J. and Lahtinem, J. 2005. 'Chemical state quantification of iron and chromium oxides using XPS: the effect of the background subtraction method', *Surface Science*, 578, 108-123.

Auriet, F., Poleunis, C., Bertrand, P. 2001. 'Capabilities of static TOF-SIMS in the differentiation of first-row transition metal oxides', *J. Mass Spectrom.*, 36, 641-665.

ASTM, *ASTM Coal Maceral Classification*. Available at: https://energy.usgs.gov/Coal/OrganicPetrology/PhotomicrographAtlas/ASTMCoalMaceralClassification.aspx.

Baxter, L. L., Richards, G. H., Ottesen, D. K. and Harb. J. N. 1993. 'In Situ, Real-Time Characterisation of Coal Ash Deposits Using Fourier Transform Infrared Emissions Spectroscopy', *Energy Fuels*, 7, 755-760.

Beamish, B. B. 1994. 'Proximate Analysis of New Zealand and Australian Coals by Thermogravimetry', *New Zealand J. Geol. Geophys.*, 37, 387-392.

Briggs, D., Fletcher, I. W. and Gonçalves, N. M. 2000. 'Positive secondary ion mass spectrum of poly(methyl methacrylate): a high mass resolution ToF-SIMS study', *Surf. Interface Anal.*, 29, 303-309.

Buckley, A. N. and Lam, R. N. 1996. 'Surface chemical analysis in coal preparation research: complementary information from XPS and ToF-SIMS', *Int. J. Coal Geology,* 32, 87-106.

Campisi, A. and Domazetis, G. 1990. 'Minimising ash fouling from High Sodium Brown Coals, Vol 2A: Experimental and Modelling Investigations of Sodium and Other Ash Forming Inorganics in Flames', End of Grant Report, NERDDP Proj No., 1167, State Electricity Commission of Victoria, ND/90/055 (and references therein).

Carlson, G. A. and Granoff, B. 1991. 'Modeling of Coal Structure by Using Computer-Aided Molecular Design', in Harold H. Schubert, Keith D. Bartle and Leo J. Lynch (eds.), *Coal Science II (American Chemical Society Symposium Series 461)* (Washington, DC: American Chemical Society), 159-170.

Chen, M., Yuana, T., Houa, Z., Wang, Z. and Wang, Y. 2015. 'Effects of moisture content on coal analysis using laser-induced breakdown spectroscopy', *Spectrochimica Acta B*, 112, 23-33.

Choi, C-V., Muntean, J. V., Thompson, A. R. and Botto, R. E. 1989. 'Characterization of Coal Macerals Using Combined Chemical and NMR Spectroscopic Methods', *Energy Fuels*, 3, 528-533.

Ctvrtnickova, T., Mateo, M. P., Yañez, A. and Nicolas, G. 2010. 'Laser induced breakdown spectroscopy application for ash characterisation for a coal fired power plant', *Spectrochimica Acta B*, 65, 734-737.

Domazetis, G. and Buckman, N. 1987. 'The Chemistry of the Formation of Ash for the Aluminium /Iron /Magnesium/ Calcium System', End of Grant Report, Volume 3, NERDDP project 933, Research and Development Department, State Electricity Commission of Victoria, Report ND/87/042.

Domazetis, G., Buckman, N. and Campisi, A. 1987. 'The Chemistry of the Formation of Ash for the Iron/Magnesium/ Calcium System', End of Grant Report, Volume 3A, NERDDP project 933, Research and Development Department, State Electricity Commission of Victoria, Report ND/87/041.

Domazetis, G., James, B. D. and Liesegang, J. 2009. 'Pyrolysis of low rank coal and metal-mediated chemistry preceding catalytic steam gasification', in Walker S. Donahue and Jack C. Brandt (eds.), *Pyrolysis: Types, Processes, and Industrial Sources and Products* (New York: Nova Science Publishers), 165-236.

Domazetis, G., Raoarun, M. and James, B. D. 2006. 'Low-Temperature Pyrolysis of Brown Coal and Brown Coal Containing Iron Hydroxyl Complexes', *Energy Fuels,* 20, 1997-2007.

Domazetis, G., Raoarun, M., James, B. D., Liesegang, J., Pigram, P. J., Brack, N. and Glaisher, R. 2006. 'Analytical and Characterization Studies of Organic and Inorganic Species in brown Coal', *Energy Fuels*, 20, 1556-1564.

Doughten, M. W. and Gillison, J. R. 1990. 'Determination of Selected Elements in Whole Coal and in Coal Ash from the Eight Argonne Premium Coal Samples by Atomic Absorption Spectrometry, Atomic Emission Spectrometry, and Ion-Selective Electrode', *Energy Fuels*, 4, 426-430.

Erdenetsogt, B-O., Lee, I., Lee, S. K., Ko, Y-J. and Bat-Erdene, D. 2010. 'Solid-state C-13 CP/MAS NMR study of Baganuur coal, Mongolia: Oxygen-loss during coalification from lignite to subbituminous rank', *Int. J. Coal Geology,* 82, 37-44.

Galetakis, M. J. and Pavloudakis, F. F. 2009. 'The effect of lignite quality variation on the efficiency of on-line ash analysers', *Int. J. Coal Geology*, 80, 145-156.

Gammidge, L., 'Atlas of coal macerals'. Available at: http://www.newcastle.edu.au/discipline/geology/cfkd/macerals.htm.

Grzyek, T. and Kreiner, K. 1997. 'Surface Changes in Coals after Oxidation. 1. X-ray Photoelectron Spectroscopy Studies', *Langmuir,* 13, 909-912.

Gupta, R. 2007. 'Advanced Coal Characterization: A Review', *Energy Fuels*, 21, 451-460.

Gupta, R. P., Wall, T. F., Kajigaya, I., Miyamae, S. and Tsumita, Y. 1998. 'Computer-controlled scanning electron microscopy of minerals in coal: Implications for ash deposition', *Prog. Energy Combust. Sci.*, 24, 523-543.

Hatcher, P. G. 1988. 'Dipolar-Dephasing ^{13}C NMR of Decomposed Wood and Coalified Xylem Tissue: Evidence for Chemical Structure Changes Associate with Defunctionalisation of Lignin Structural Units during Coalification', *Energy Fuels*, 2, 48-58.

Hurley J. P. and Schobert, H. H. 1992. 'Ash Formation During Pulverized Subbituminous Coal Combustion. 1. Characterization of Coals, and Inorganic Transformations during Early Stages of Burnout', *Energy Fuels*, 6, 47-58.

Ibarra, J. V., Muñoz, E. and Moliner, R. 1996. 'FTIR study of the evolution of coal structure during the coalification process', *Org. Geochem.,* 24, 725-735.

Jurkiewicz, A. 1987. 'Spatial system of the Wiser model of coal structure according to the second moment of the nuclear magnetic resonance line', *J. Appl. Phys.*, 62, 3892.

Kelemen, S. R., Afeworki, M. and Gorbaty, M. L. 2002. 'Characterization of Organically bound Oxygen Forms in Lignites, Peats, and Pyrolyzed Peats by X-ray Photoelectron Spectroscopy (XPS) and Solid-State ^{13}C NMR Methods', *Energy Fuels*, 16, 1450-1462.

Kok, M. V. 2003. 'Coal Pyrolysis: Thermogravimetric Study and Kinetic Analysis', *Energy Sources*, *25,* 1007-1014.

Lachas, H., Richaud, R., Jarvis, K. E., Herod, A. A., Dugwell, D. R. and Kandiyoti, R. 1999. 'Determination of 17 trace elements in coal and ash reference materials by ICP-MS applied to milligram sample sizes', *Analyst*, 124, 177-184.

Liptay, G. 1971-1976. *Atlas of Thermoanalytical Curves*, London: Heyden & Son Ltd.

Liu, S., Weng, L-T., Chan, C-M., Li, L., Ho, N. K. and Jiang, M. 2001. 'Quantitative Surface Characterization of Poly(styrene)/Poly(4-vinyl phenol) Random and Block Copolymers by ToF-SIMS and XPS', *Surf. Interface Anal.,* 31, 745-753.

Ma, S., Hill, J. O. and Heng, S. 1991. 'Kinetic Analysis of the Pyrolysis of Some Australian Coals by Non-isothermal Thermogravimetry', *J. Therm. Anal.*, 37, 1161-1177.

Mathews, J. P., Campbell, Q. P., Xu, H. and Halleck, P. 2017. 'A review of the application of X-ray computed tomography to the study of coal', *Fuel,* 209, 10-24.

Mathews, J. P., van Duin, A. C. T. and Chaffee, A. L. 2011. 'The utility of coal molecular models', *Fuel Processing Technology,* 92, 718-728.

Mayoral, M. C., Izquierdo, M. T., Andres, J. M. and Ruio, B. 2001. 'Different Approaches to Proximate Analysis by Thermogravimetric Analysis', *Thermochim. Acta.*, 370, 91-97.

McKenry, S. A. 2001. 'The release of soluble organic and inorganics species from brown coals into water and the systematic examination of their removal using coagulant, flocculation and precipitation chemistry', Honours Thesis, Department of Chemistry, La Trobe University.

Metz, J. G. H. and Domazetis, G. 1999. 'Analysis of ultra-clean low rank coals using lithium borate fusion – XRF and ICP-AES spectroscopy', *Australian Int. Symposium on Analytical Science*, AISAS-99.

Microbeam Technologies, *Computer-Controlled Scanning Electron Microscopy*. Available at: https://microbeam.com/testing-analysis-methods/computer-controlled-scanning-electron-microscopy/.

Murata, S., Hosokawa, M., Kidena, K. and Nomura, M. 2000. 'Analysis of oxygen-functional groups in brown coals', *Fuel Process. Technol.,* 67, 231-243.

Peters, J., Bartscher, K., Döscher, C., Taute, W., Höft, M., Knöchel, R. and Breitkreutz, J. 2017. 'In-line moisture monitoring in fluidized bed granulation using a novel multi-resonance microwave sensor', *Talanta,* 170, 369–376.

Pyle, S. M., Nocerino, J. M., Deming, S. N., Palasota, J. A., Palasota, J. M., Miller, E. L., Hillman, D. C., Kuharic, C. A., Cole, W. H., Fitzpatrick, P. M., Watson, M. A. and Nichols, K. D. 1995. 'Comparison of AAS, ICP-AES, PSA, and XRF in Determining Lead and Cadmium in Soil', *Environ. Sci. Technol.,* 30, 204–213.

Redoglio, D., Golinelli, E., Musazzi, S., Perini, U. and Barberis, F. 2016. 'A large depth of field LIBS measuring system for elemental analysis of moving samples of raw coal', *Spectrochimica Acta B,* 116, 46-50.

Romero, C. E., De Saro, R., Craparo, J., Weisberg, A., Moreno, R. and Yao, Z. 2010. 'Laser-Induced Breakdown Spectroscopy for Coal Characterization and Assessing Slagging Propensity', *Energy Fuels,* 24, 510-517.

Schulze, D., Ernst, H., Fenzke, D., Meiler, W. and Pfeifer, H. 1990. 'Applicability of the NMR Cross-Polarization Technique to Separate Rigid and Mobile Components in Coal Structure', *J. Phys. Chem.,* 94, 3499-3502.

Shevhenko, S. M. and Bailey, G. W. 1996. 'Life After Death: Lignin-Humic Relationships Re-examined', *Crit. Rev. Environ. Sc. Tech.,* 26, 95-153.

Solomon, P. R., Serio, M. A., Carangelo, R. M., Bassilakis, R., Gravel, D., Baillargeon, M., Baudais, F. and Vail, G. 1990. 'Analysis of the Argonne premium coal samples by thermogravimetric Fourier transform infrared spectroscopy', *Energy Fuels,* 4, 319-333.

Song, H., Liu, G., Zhang, J. and Wu, J. 2017. 'Pyrolysis characterisations and kinetics of low rank coals by TG-FTIR method', *Fuel Processing Technology,* 156, 454-460.

Speight, J. G. 2005. *Handbook of Chemical Analysis,* Hoboken, NJ: John Wiley & Sons.

Stout, S. A., Boon, J. J. and Spackman, W. 1988. 'Molecular aspects of peatification and early coalification of angiosperm and gymnosperm woods', *Geochim. Cosmochim. Acta,* 52, 405-414.

Sun, X. 2001. 'A study of chemical structure in "barkinite" using time-of-flight secondary ion mass spectrometry', *Int. J. Coal Geology,* 47, 1-8.

Vassilev, S. V. and Tascón, J. M. D. 2003. 'Methods for Characterization of Inorganic and Mineral Matter in Coal: A Critical Overview', *Energy Fuels*, 17, 271-281.

Vassileva, C. G. and Vassilev, S. V. 2005. 'Behaviour of inorganic matter during heating of Bulgarian coals 1. Lignites', *Fuel Processing Technology*, 86, 1297-1333.

Wang, J., Sakanishi, K., Saito, I., Takarada, T. and Morishita K. 2005. 'High-yield hydrogen production by steam gasification of hypercoal (ash-free coal extract) with potassium carbonate: comparison with raw coal', *Energy Fuels*, 19, 2114-2120.

Wang, J., Sharma, A. and Tomita, A. 2003. 'Determination of the Modes of Occurrence of Trace Elements in Coal by Leaching Coal and Coal Ashes', *Energy & Fuels*, 17, 29-37.

Xiong, J. and Maciel, G. E. 2002. 'Re-examining the Molecular/ Macromolecular Model of Coal from Comparative in Situ Variable-Temperature 1H NMR Studies of Argonne Premium Coal 601 and Its Pyridine Extraction Residue', *Energy & Fuels*, 16, 791-801.

Zhu, Q. 2014. *Coal sampling and analysis standards*, London: IEA Clean Coal Centre.

Zoller, D. L. and Johnston, M. V. 1999. 'Thermogravimetry–Photoionization Mass Spectrometry of Different Rank Coals', *Energy Fuels,* 13, 1097-1104.

CHAPTER THREE

MOLECULAR MODELS OF LOW RANK COALS

Our chemical understanding of matter revolves around molecules, their composition, structure, and the relationship of these with measured properties. The availability of supercomputing facilities has enabled computational chemistry and quantum mechanics molecular modelling (QM); such molecular modelling usually deals with small, well-characterised molecular structures, and for these, QM modelling is used in wide ranging studies, including chemical synthesis, reaction routes, and catalytic chemistry.

While modern computing facilities and expertise are increasingly used for studies of coal structures, the heterogeneous nature of coal presents particular difficulties in studies using advanced computational molecular modelling; coal cannot be considered as a distinct molecule, and instead the approach has been to develop hypothetical molecular structures that would encapsulate the available experimentally-derived data. This approach often results in the construction of large molecular structures which preclude study with QM techniques due to the unrealistically large computing resources needed for such large molecular structures. The variations in the rank of coal have also resulted in the development of numerous and various molecular representations for particular coals.

Molecular modelling studies of coal have often commenced with simple 2-dimensional molecular (2D) representations, and these were subsequently developed into 3-dimentional (3D) structures (Mathews and Chafee, 2012). These structures have reflected the interests and intuitions of the particular modellers, and despite the many difficulties, molecular models have proven useful in furthering our understanding of coal. With the availability of powerful computers, molecular models of coal have been devised and used in studies of industrially important processes, such as metal mediated pyrolysis, catalytic gasification, and coal transformations (Jones et al., 1999; Mathews et al., 2011).

Most of the molecular structures developed have been for studies of bituminous coal, but structures of low rank coals have also been developed; an early molecular model of brown coal was proposed in 1987 that included cations (calcium, potassium, iron, aluminium, and sodium) in an organic

structural entity, but it did not contain water molecules (Hüttinger and Michenfelder, 1987). Molecular structures were also devised in an endeavour to quantitatively present the distribution of the various bond types (aliphatic and aromatic) in coal, and to incorporate available information concerning the functional groups, particularly on aspects important to coal liquefaction. Interest in representative molecular structures of coal grew when coal liquefaction was considered as a source of oil, in response to the increase in the price of oil. Models were developed depicting structures of coal containing aromatic groups cross-linked by various bridging groups, and various functional groups. These were averaged structures, which were constructed based on information concerning the elemental composition, and on the nature of the various organic moieties identified from the products of coal liquefaction. Coal liquefaction studies, and the utilisation of new analytical techniques, provided substantial amounts of new information on several important aspects of coal at a molecular level. Insights into coal conversion processes, especially when catalysts were used in such processes, were obtained by examining reaction schemes. Molecular models were constructed to enable an understanding of the steps in the conversion process and the nature of the products; these were based on detailed chemical analyses of the coal and the characterising of the products from various liquefaction schemes (Shinn, 1984).

A feature of studies on coal liquefaction is the molecular/macromolecular (or the two phase) structural model proposed for high rank coals, which considers the coal organic matrix to consist of a three-dimensional, cross-linked network, termed the "macromolecular phase", and small organic molecules, termed the "mobile phase"; the latter are soluble in nucleophilic solvents such as pyridine. The macromolecular phase is thought to consist of aromatic clusters that are cross-linked by aliphatic bridging groups, with relatively flexible side chains covalently attached to the aromatic clusters. The mobile molecular phase is considered to be entities trapped in voids of the macromolecular matrix or attached to the macromolecular network *via* non-covalent associative forces, such as hydrogen bonds and other associative forces; these are thought to stabilise the overall structure of coal, which includes the macromolecular portion of the coal. The "two phase" model of high rank coal has been widely discussed and debated in the literature, but the nature of the two phases proposed for high rank coal is not yet fully understood (Derbyshire et al., 1989; Xiong et al., 2002).

The difficulties in devising a general molecular model applicable to all coals are considerable. The chemical composition varies with rank, and the distribution of constituents of the organic matrix varies, as do the amounts of moisture and ash; these variations are observed within the same rank, and

greater variations are observed between the variously ranked coals. Additionally, the computational techniques that can be used in examining structures vary in accuracy. The size of a molecular model increases as more information is added, but the large molecular models that result from such effort can only be studied using low-level techniques such as molecular mechanics. Studies of reaction mechanisms and the catalytic chemistry of coal require quantum mechanics molecular modelling techniques, but the use of large structures for these is restrained by computer capabilities that restrict the size of the molecular models. Consequently, the molecular models discussed in the literature reflect numerous variations stemming from the computer techniques used for molecular modelling, the rank of coal, the size of the molecule, and the nature of the study. As coal is a heterogeneous substance, a discrete coal molecule does not exist, and instead simplified organic molecular structures have been utilised as models to gain insights on specific properties and behaviour of the various coals.

The construction of representative coal molecular models has relied on experimentally measured data, such as elemental analysis, the type of functional groups, and the distributions of aromatic and aliphatic moieties. A recent study indicated 134 molecular models of coal have been proposed, of which 24 were considered representative, and out of these 18 were shown to fall within 10% of experimentally determined values (such as elemental composition, aromatic and aliphatic bonds and C-O bonding) and of these, only 5 were of low rank coal (Zhou et al., 2016).

The particular molecular representations need to reflect the properties and composition of a specific type of coal, and as stated, the differences between low rank and high rank coals are considerable. If proposed molecular models fail to adequately encapsulate the experimental data for the type of coal studied, they cannot be considered sufficient for any related studies that rely on modelling results. Some aspects of the different coals present very large differences; for example, mined brown coal contains ~60wt% of water (compared to <10wt% high rank coal), a relatively low proportion of aromatic groups, and a higher proportion of aliphatic groups. About 26wt% of the dry ash free weight (daf) of brown coal is made up of oxygen, present as functional groups such as carboxylate and phenolic (Hatcher and Lerch, 1991). The ash chemistry of low rank coals also differs significantly from that of high rank coals (Domazetis, 1985; Robins, 1991; Quast and Readett, 1991). In contrast, the molecular representations of high rank coal contain relatively small amounts of moisture, larger amounts of condensed aromatic components relative to aliphatic, less oxygen functional groups, and ash-forming constituents that are mainly present as inclusions in the dense hydrophobic matrix (Larsen, 1992; Carlson and Granoff, 1991).

A particular molecular representation of a coal is constructed to obtain insights on identified aspects of coal utilisation, and the size of the model sets the level of computational optimisation. The studies discussed in this volume deal mainly with coal treatment chemistry to eliminate ash-related problems, and the chemistry of catalytic steam gasification of low rank coals. Studies aimed at providing molecular representations that reflect measured properties may be optimised using the low-level techniques of molecular mechanics and molecular dynamics, and these permit using large structures containing numerous features of interest. Computations that seek to examine, for example, chemical reaction routes and metal mediated chemistry require quantum mechanical computations, so as to obtain changes to the energies of moieties undergoing a specific chemical change, and energy changes resulting from a set of transformations for a given chemical reaction route – these computations can only be carried out using suitably sized molecular representations, and not the large representations often postulated for coal. Simple modelling, such as the distribution of water molecules in as-mined brown coal, however, can be carried out using large molecular representations optimised using molecular mechanics and computations with particular lower level semi-empirical quantum mechanics (SE-QM) packages.

The requirements of a molecular model of brown coal that is suitable for studies on coal treatment methodologies discussed in this volume may be met by modelling an organic matrix as a 3D macromolecule that is based on the averaged measured elemental analysis, distribution of aromatic and aliphatic groups, with oxygen, sulphur and nitrogen functional groups dispersed throughout, and 10-20wt% of the mass made up of water hydrogen bonded within the coal molecular matrix. A brown coal model containing a large amount of water can be constructed by distributing the required amount of water molecules throughout a larger model made up of a number of the 3D molecules with spaces separating them, which mimic micro-capillaries, and the water is distributed through this network of capillaries and at the surface of the coal's molecular structure particles, regarded as "bulk water". The structure would also be capable of modelling inorganic species chemically associated with the oxygen functional groups within the 3D molecule. This molecular model of low rank coal must also be capable of scaling down to a molecular model of a size that is suitable for quantum mechanical molecular modelling computations, and encapsulates averaged measured chemical and physical properties.

Constructing Molecular Models of Coal

Molecular structures are fundamental to the study of materials; elucidating particular molecular structures requires information on the molecular parameters of atoms and bond types, lengths, and angles. Molecular structures can be determined with precision using x-ray or neutron diffraction techniques for solids that can form single crystals. Experimental determination of precise molecular structure is based on spectroscopic as well as diffraction methods, and these have provided structural data for a large number and variety of molecules.

Structural information and molecular properties are provided by computational chemistry, based on molecular orbital theory and density functional theory (DFT). These types of computational methods may be used for studies of coal molecular models to provide bond lengths and angles, the distribution of electrons and calculated partial charges; this information is related to properties such as ionic interactions of inorganics, hydrogen bonds within the coal molecules, and water molecules within the organic macromolecular matrix of low rank coals. The bond distances, angles, and partial charges enable an understanding of the ionic bonding of ash-forming species, and the structures that may be anticipated for inorganic molecules added to the macromolecule for potential catalytic activity. SE-QM computations provide an optimised structure with the minimum energy for proposed individual molecules, and this can be useful in studies of various structures examined for chemical reaction routes related to pyrolysis, char formation and catalytic reactions for brown coal.

The challenge to these studies is in the creation of a suitable structure that is representative of the particular coal.

The various approaches to devising suitable molecular structures for the amorphous substance of coal have been discussed in the literature for decades. An approach adopted in studies of low rank coals commences by using the major organic groups found in coal arranged into 2D configurations, and these are then used to construct a 3D molecular model. All methods endeavour to construct large molecular structures based on the type of groups in coal, and connections between these groups, obtained from experimental data. Computer-assisted approaches have also been used in this arduous effort to construct molecular models, as these may not be as time consuming as the manual construction of such structures; however, the number of conformers and arrangements derived from computer-aided constructions may be large and additional effort is required to select an appropriate molecular model for the particular coal. Faulon (1994) summarises the approaches to coal molecular modelling into three

categories; the conventional, the deterministic, and the stochastic. The software package SIGNATURE is an example of a stochastic approach for computer-generated structures. Additionally, a knowledge-based computer methodology has been reported to generate structures using fragments from the coal organic matrix, and this was demonstrated for a typical Japanese bituminous Akabira coal. This computer-based approach seeks to construct a molecular structure by mimicking the manual method used by coal experts. The computer software speeds up the process for constructing the model, and also enables an evaluation of the tentative structures by optimisation using molecular mechanics. Numerous computer-generated structures may be created, and erroneous structures are removed by the program based on a geometric assessment. This process presumably would develop larger structure(s) to meet predefined parameters, with reduced computational time (Ohkawa et al., 1997).

Proposed structures for coal must conform to experimentally determined parameters and computations must provide an optimised ground state. It is convenient initially to use molecular mechanics (MM) computer optimisation to identify the stable conformer from a group of similar molecular structures, but this is a preliminary examination, as there are cases where MM optimisation of coal molecular models provided significantly different configurations from those obtained using SE-QM computations. MM optimisation, however, is often the only technique that can be used for large molecular structures. The preferred approach, which was adopted in studies of low rank coal discussed here, was to initially optimise suitably sized structures using MM and then carry out further optimisation using SE-QM techniques to arrive at the final structure. This combined approach of MM and SE-QM is restricted to a suitably sized molecular structure, and also increases the time invested in developing a particular molecular structure, but these factors can be offset by the benefits obtained from a structure that has undergone a rigorous assessment during its construction.

A brief description of the construction of two molecular models of coals is presented to illustrate the diverse approaches adopted in these studies; these are of coal models optimised using MM and molecular dynamics (MD) techniques (US bituminous coal, and a Chinese Shenfu sub-bituminous coal). The construction of the molecular model of brown coal is then discussed in detail as this has utilised MM and QM techniques, and it has been applied to the research on the treatment and utilisation of low rank coals.

The first example is of molecular models of high rank coals: A model of a US bituminous coal was constructed based on data for the maceral vitrinite – the modelling results were compared with experimental data obtained

during carbonisation, combustion, solvent swelling, and liquefaction. The study was intended to show that the coal's molecular structure encapsulates the behaviour of the coal it represents. Two samples of vitrinite are considered; one is from the Upper Freeport coal seam, and the other from the Lewiston-Stockton coal seam. The experimental data used for verification purposes were proximate and ultimate analysis, flash-pyrolysis GC/MS at 610°C, ^{13}C NMR techniques, surface area, and density. The SIGNATURE program was used to build a three-dimensional structure from given molecular fragments. Structures that contained a composition and functional groups similar to measured values were then optimised using MM and MD to obtain spatial arrangements in a three-dimensional space. The SIGNATURE program was also used to compute physical properties for this model, which were compared with the experimental data, and the structure was then further refined to achieve a closer comparison (details can be found in Mathews et al., 2001).

A molecular model of Illinois No. 6 Argonne Premium coal was constructed by assembling cross-linked and non-cross-linked molecules, as implemented in the Amorphous Cell module of the Materials Studio package.* In this, molecules were constructed by gradually adding atoms and bonds using a minimum energy criterion. Prior to this, water molecules amounting to 8wt% for the mass of coal were randomly added to the empty simulation cell to account for the moisture content. This 3D structure was built with an initial low bulk density of 0.5 g/cm^3 to avoid the overlapping of aromatic rings during simulation cell construction. The model contained 50,789 atoms within 728 molecules. The aromatic ring size distribution in the molecular modelling space was based on multiple high-resolution transmission electron microscope (HRTEM) lattice fringe micrographs, duplicated with automated construction protocols (Fringe3D). Additional structural data were that of organic oxygen, nitrogen, and sulphur functionalities within the polyaromatic structures, as indicated by XPS and X-ray adsorption near-edge structure spectroscopy. Aliphatic carbons were in the form of bridges and pendant alkyl groups; data were also obtained with laser desorption ionisation mass spectrometry, ruthenium ion catalysed oxidation, elemental analysis, and NMR. During model construction, elemental composition, NMR parameters, molecular weight distribution and simulated helium density were adjusted to agree with the available experimental data. This coal model captured the two-phase model for coal, that is, of a covalently bound cross-linked network (immobile phase) and low molecular weight compounds (mobile phase) physically trapped within macromolecular networks. The elemental composition for the coal model

* Materials Studio Software (2010). Accelrys Inc., San Diego, CA.

compares favourably with the experimental data on a daf basis for Illinois No. 6 coal; the atomic H/C ratio of 0.774 agreed with the literature value of 0.773. The calculated helium density of the dry coal model was 1.32 g/cm^3, compared to the experimental value of 1.30 g/cm^3 (daf), and pore sizes of the model extend up to about 10Å, compared with the average micropore diameter of 6Å for the coal. The automated model construction protocol was validated by the agreement obtained between model and experimental parameters (Castro-Marcano et al., 2012).

The second example is of models of Chinese Shenfu coal and char: These molecular models were constructed with the Dreiding FF using the Materials Studio Forcite module. A number of configurations of functional group were initially created for the models with the ACD/Chemsketch software; a series of polyaromatic hydrocarbon molecules were constructed to represent the char structure. The optimal geometric configuration of functional group fragments was obtained initially, followed by the coal structure constructed with the Amorphous Cell module in the software package. This was performed by constructing the coal molecule and importing the functional group fragments into the unit cell using the construction task in the Amorphous Cell module, and adding the periodic boundary condition to the unit cell. The periodic boundary is the additional condition to keep the system constant. Annealing dynamic simulation was performed on the optimised models to obtain a reasonable coal or char density. The annealing cycle was from 298-700K, compression and decompression at pressures of 0.01 GPa and 0.1 MPa, respectively. The minimising energy configurations were selected from the annealing MD simulation, and the results from this were the optimal geometric configurations of coal or char. The calculated density for the optimised structure was 1.2 gm cm^{-3}, compared to the measured value for the coal of 1.28 gm cm^{-3}, and the elemental analysis of the coal and char models compared well with the measured values (Zhao et al., 2017).

The third example is of models of low rank coals: These have been discussed in detail by Domazetis and co-workers, and a general treatment is presented to illustrate the method used to develop a molecular model, based on elemental composition, carbon distribution as the ratio of one-, two- and three-ring fused aromatics, and oxygen distribution amongst functional groups such as carboxyl, phenolic, methoxyl, hydroxyl, carbonyl and ether (Hüttinger and Michenfelder, 1987; Domazetis et al., 2005; Domazetis and James, 2006). Additional insights are provided from studies of the coalification process, which indicate the distribution of numerous organic moieties within the coalified substance; models have also been proposed based on structural studies of coalified wood found in brown coals deposits

(Dorrestijn et al., 2000; Hatcher, 1990; Hatcher and Clifford, 1997; Faulon et al., 1994; Hatcher and Faulon, 1994; Hatcher et al., 1982; Hatcher et al., 1988).

The molecular model(s) discussed here have been developed specifically for work on the treatment of low rank coals, and of the utilisation of treated coals, with an emphasis on the behaviour of metal complexes within the molecular matrix, and the chemistry that would occur on heating, related to metal mediated pyrolysis and catalysis. Other aspects, however, emerged from the molecular modelling studies, such as the formation of char with the breakdown of functional groups. The size of the molecular model for SE-QM, and for *ab initio* DFT molecular computations, was restricted to the available supercomputer capabilities.

The molecular model(s) of low rank coal were constructed for insights into:

- The distribution of functional groups typifying the hydrophilic properties of low rank coals.
- The distribution of water molecules within the coal matrix.
- The ionic bonding of cations, with hydration spheres, to carboxylate groups.
- The addition of transition metal oxy-, hydroxyl complexes, and with the formation of coordination bonds within the coal molecule.
- The mechanisms of char formation.
- The transformation of transition metals, particularly iron species, in metal mediated pyrolysis.
- The mechanisms for catalytic steam coal gasification.

These studies commenced with the construction of a molecular model of brown coal that encapsulated (the averaged values of) the following:

- Elemental analysis (%C, %H, %O, %S, %N).
- The proportion of H-bonded water molecules within the macromolecular structure.
- The ratio of aromatic carbon to total carbon (C_{ar}/C_{tot}).
- The ratio of aromatic hydrogen to total hydrogen (H_{ar}/H_{tot}).
- The distribution of oxygen amongst the relevant functional groups.
- Data from the modelling of pyrolysis reaction routes for comparison with experimentally observed values.
- Structures of inorganic species and interactions with coal functional groups.

- Modelling transformations of iron species at elevated temperatures, for comparison with experimental data.
- The catalytic activity of steam gasification, and products consistent with experimental values.

A molecular structure for brown coal would be a 3D configuration that conforms to the average values of the relevant experimental data, and would be capable of forming bonds between oxygen functional groups and aqua-metal hydroxyl complexes without undue strain. A pragmatic approach to constructing a model that would meet these requirements is to initially construct smaller 2D structures that encapsulated many of the measured properties of the coal, and then examine ways to link these 2D structures into a 3D structure that would avoid the problems that would arise from steric hindrance when inorganic species are added to the coal model.* By examining various 2D molecules, and adopting the appropriate ones for constructing a 3D model, it is possible to significantly decrease the number of 3D configurations that must be examined; this approach also maintains the measured properties for the coal encapsulated by the 2D fragments since the additions required to form the 3D structure are only appropriate hydrocarbon links. This 'manual' approach is time consuming, but it has the virtue of enabling a chemist to understand in detail how a particular structure would be suitable for the tasks envisaged.

Two examples of 2D structures that proved suitable for the construction of 3D molecular model(s) are shown in Figures 3-1 (a) and (b). The structure in Figure 3-1 (a) contains a three-way link *via* a phenyl group, and Figure 3-1 (b) has an sp^3 carbon for a three-way link – these are significant as Figure 3-1 (a) has a flat link, and Figure 3-1 (b) a three-dimensional link. These 2D structures may then be linked to form particular configurations of 3D molecular models. A judgement is required on the type of links used to construct a 3D molecule; for example, if a number of small links were employed, such as $-CH_2-$, the 3D structure becomes very strained and is judged unsuitable for further study.

The calculated properties of each of these two 2D structures are listed in Table 3-1, and these are within the averaged measured properties of brown coal. A number of 3D structures were examined; a particular 3D configuration was chosen on the basis of the lowest energy obtained from SE-QM computations of various structural configurations of similar elemental compositions. An example of a suitable 3D structure is the molecular model [C_{258} H_{256} N_2 O_{78} S, MWt 4664.8]; this connects three 2D

* Adapted with permission from Domazetis et al., Energy & Fuels, 22, 3994, 2008. Copyright (2008). American Chemical Society.

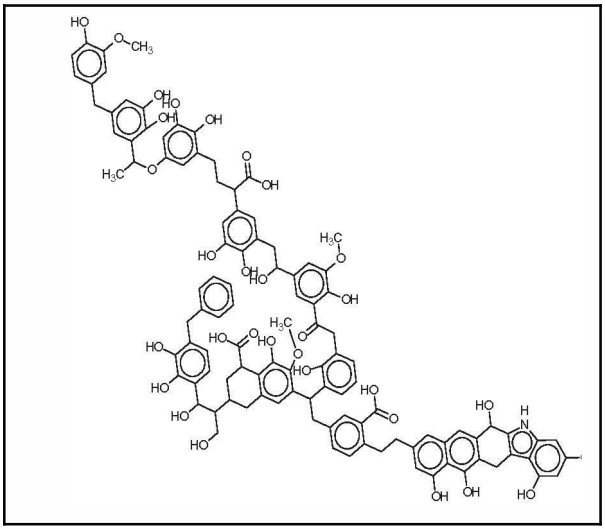

(a)

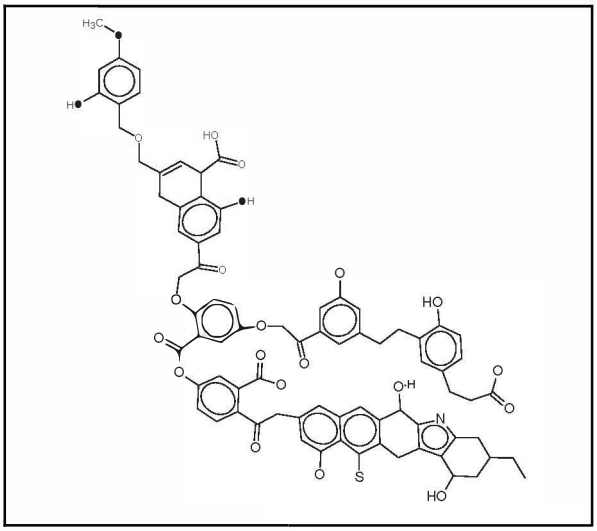

(b)

Figure 3-1. 2D structures connected with (a) phenyl three-way link, and (b) with a sp^3 C three-way link.

structures using hydrocarbon and ether linkages. Table 3-2 lists typical measured properties of brown coal, which are compared to values for the 3D model; the properties of the model are in reasonable agreement with the typical elemental composition and distribution of functional groups of brown coal (Verheyen and Perry, 1991). It has been noted that considerable differences are observed for low rank coals (Murata, 2000), and these variations are illustrated by the values in typical elemental compositions of low ash coals from Australia, Indonesia and the USA (daf), shown in Table 3-3.

Table 3-1. The calculated properties of each of the 2D structures.

2D molecular fragment (a)	
Composition	$C_{79}H_{71}NO_{22}S$
Analysis	C 66.89%; H 5.05%; N 0.99%; O 24.81%; S 2.26%
MWt	1418.5
Density	1.47 ± 0.06 g/cm^3
$C_{(ar)}/C_{(tot)}$	0.61
$H_{(ar)}/H_{(tot)}$	0.28
Oxygen groups as:	$O_{(OH)}$ 33%; $O_{(COOH)}$ 19%
2D Molecular fragment (b)	
Composition	$C_{109}H_{103}NO_{30}$
Analysis	C 68.65%; H 5.44%; N 0.73%; O 25.17%
MWt	1906.9 au
Density	1.50 ± 0.06 g/cm^3.

Table 3-2. Properties for the 3D molecular model [C_{258} H_{256} N_2 O_{78} S MWt 4664.89] (Figure 3-2). Reprinted with permission from Domazetis et al., J Molecular Modelling, 14, 581, 2008, Copyright (2008). Springer.

Elemental	%C	%H	%O	%N	%S
Model	66.4	5.5	26.8	0.6	0.7
Measured	67.8	4.9	26.4	0.6	0.3
Functional	carboxyl $O_{(C●●H)}$	phenolic $O_{(●H)}$	methoxy $O_{(O\text{-}CH3)}$	ether/hydroxyl $O_{(R\text{-}OH)}$	carbonyl $O_{(RC=O)}$
Model	21%	30-35%	7%	7%	11-15%
Measured	17-23%	35-38%	~12%	~4%	~23%
Aromatic/ total	$C_{ar}/C_{t●t}$	$H_{ar}/H_{t●t}$			
Model	0.63	0.2			
Measured	0.57-0.65	~0.3			

Table 3-3 Typical elemental composition of low ash low rank coals.

Coal	%C	%H	%N	%S	%O*
Yallourn (Aust.)	66.9	4.7	0.5	0.2	27.7
South Banko (Indo.)	71.3	5.4	1.2	0.5	21.6
Beulah Zap (US)	72.9	4.8	1.2	0.7	20.4
Adaro (Indo.)	73.1	5.1	1.1	-	20.7

*by difference

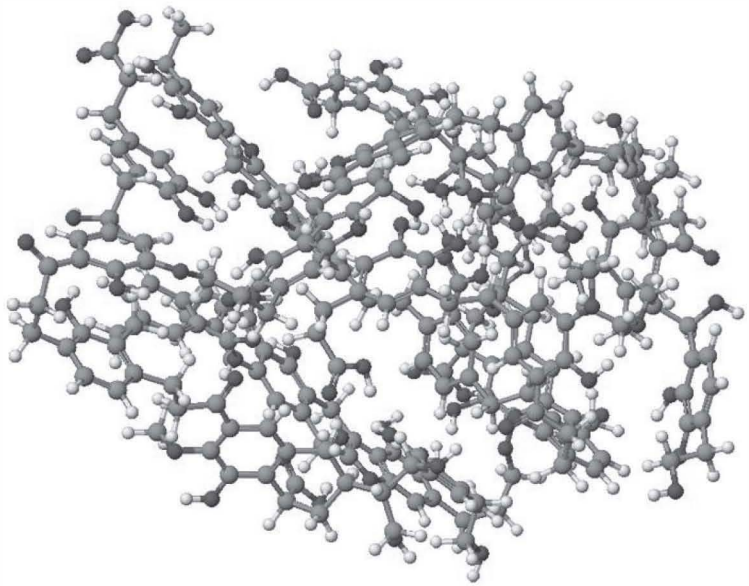

Figure 3-2. Molecular model of brown coal (C = ●black, H = ○white, O = ●red, S = ●yellow, N = ●blue).

The model shown in Figure 3-2 typifies the 3D molecular structure of brown coal used in studies discussed in this volume. 3D molecular models have also been constructed with the various compositions shown in Table 3-3 for lignite and sub-bituminous coal, using the method outlined.

In developing the molecular model of brown coal, a number of configurations were studied using MM and SE-QM computations. These exercises highlighted the importance of hydrogen bonds within the molecular model, and because of the various oxygen functional groups in the molecule, a number of models of similar elemental composition and

functional groups, but with differing configurations, may be optimised to a ground state that maximises the internal hydrogen bonds. Inter H-bonding impacts on the internal configurational stability of the structure. A solid material made up of many of these molecules, however, would experience intra- and inter- hydrogen bonding, which would impact on the overall stability of such a model. In such a solid, portions of a molecule may also encounter interactions from neighbouring groups, and other factors, such as ionic interactions, and those with the hydrogen bonding network throughout the solid matrix, would impact on optimisation results. The molecular models discussed here are of isolated structures, and intra-aspects relevant to solids cannot be included in these computations.

The brown coal optimised structure(s) contained bond lengths and angles typical for organic structures; computations indicating the total energy and enthalpy of the structure are determined by a complicated interplay between the orientations of oxygen functional groups, the arrangement of phenyl groups, and the links between phenyl groups. The arrangement of substituted phenyl groups is especially important, as it may cause crowding, and also adversely impact the hydrogen bonds formed by carboxyl and phenolic groups throughout the structure. Additionally, the SE-QM computations of coal models containing transition metal complexes displayed an acute dependency on steric crowding and strain, related to the orientation of the functional groups. The impact of strain on the energy of optimised structures can be illustrated by two examples (these models were optimised without inorganics added to them): the heat of formation (ΔH_f) for the model [$C_{295}H_{206}N_6O_{32}$] was indicative of lower stability when compared to the less strained, albeit larger model [$C_{327}H_{307}N_3O_{90}$]. Additionally, the ΔH_f value for the smaller model [$C_{259}H_{265}N_3O_{77}$] is of a more stable structure than the larger, crowded model [$C_{279}H_{265}O_{54}S$]. It is noted that structures that could not be optimised to a ground state using SE-QM computations, due to considerable steric hindrance and strain, were (erroneously) computed to a ground state using MM – this shows that results from MM computations should be treated with caution.

The 3D brown coal molecular model shown in Figure 3-2 also encapsulates the hydrophilicity of the low rank coal matrix. The ΔH_f value for the coal model containing H-bonded water within the molecular matrix shows that it is more energetically favoured when compared to the same molecular model optimised with an equal number of water molecules placed at a distance from the molecule (these cannot form hydrogen bonds within the coal structure, but form hydrogen bonds amongst the water molecules). Each of these molecular models, and the same model containing various amounts of water, was optimised to the ground state. The stability due to

water molecules within the coal matrix is -56.9±2.8 kcal per H_2O molecule. A comparison between the 3D model with water molecules situated within the coal structure, and with the same number of water molecules at a distance as water vapour, show a difference of +4.6kcal per H_2O for water outside the coal molecule, illustrating hydrogen bonded water within low rank coal imparts additional stability to the structure. These results are underscored by a linear relationship observed between the computed ΔH_f value and the number of water molecules added to the 3D brown coal model. The ΔH_f values for the low rank coal models also correlate with the number of hydrogen bonds; a plot of ΔH_f and the number of hydrogen bonds for the optimised structures provide a linear fit with a correlation coefficient $R^2 = 0.9$. Larger amounts of water caused an increase in the molecular volume, which corresponds to a lower density; the molecular volume of a coal structure with 53wt% water increased by a factor of 1.8 per coal molecule, consistent with the change in the densities of as-mined brown coal when compared to dried brown coal.

Computational Molecular Modelling

Computational molecular modelling of brown coal is undertaken initially by using MM, followed by SE-QM; the optimised molecular model is then used for studies of reaction routes relevant to coal combustion and catalytic gasification.

Computational quantum chemistry is applied in many fields, and details are found in textbooks, reviews, and other scientific literature (Fernándeza and Cossio, 2014; Cramer and Truhlar, 2009; Stewart, 2004; Murray-Rust et al., 2005). There are a number of open source, academic, and commercial packages available that may be used for computational chemistry dealing with molecular models, molecular dynamics, solid state, and studies of biologically relevant molecules. Our interest is in MM and QM techniques to examine molecular structures that may mimic the properties of low rank coals. This consists of developing models of viable structures suitable for computations using SE-QM and DFT, and these can be performed with packages such as CAChe 5.04 for Windows, MOPAC2002, and Jaguar 6.5 from Schrödinger; details have been discussed elsewhere.*

The molecular models of low rank coal consist of the organic macromolecular matrix with added water molecules, and the model may contain added main group cations (mainly Na, Mg and Ca), or transition

* Adapted with permission from Domazetis et al., Energy Fuels, (2005; 2008) Copyright (2005, 2008). American Chemical Society.

metal complexes. Transition metals are mainly present as octahedral complexes, forming conventional bonds with carboxyl groups, and coordination bonds with ligands, which may consist of water molecules, carboxyl, and phenolic groups from the coal matrix. Models relevant to char formation may also contain transition complexes, such as iron, which may be present as any of the Fe(0), Fe(II) and Fe(III) species, and as multi-nuclear oxy-, hydroxyl, complexes and/or clusters. These aspects of computational molecular modelling increase the complexity of models, and make considerable demands of the software package.

MM is used for the initial examination and optimisation of these models. MM can deal with virtually any sized molecular model, and does not require excessive computer resources (Hinchliffe, 1966). This technique does not use orbitals and electrons in describing chemical bonds; instead, the bonds connecting atoms are imagined as 'sticks' which have optimal lengths and stiffness, and any deviation from this induces strain. A variety of non-bonding interactions, including electrostatic, hydrogen bonding and van der Waal terms, are included in this treatment. Interactions between atoms 1,2 (bond stretching), 1,3 (angle bending) and 1,4 (bond torsions) are considered. The molecular mechanics force field (FF) MM3 has been used in structures discussed here; this has been shown to be an improvement on earlier force fields in calculating the structures and energies, including heats of formation, conformational energies, and rotational barriers. The results using the MM3 force field have been reported to be useful for simple molecules, and also macromolecules. The MM3 force field has also improved the van der Waals' potentials for interactions between carbon and hydrogen in both aliphatic and aromatic systems (Allinger et al., 1989; Lii and Allinger, 1989).

The terms used in the FF are derived from experimental data and, consequently, computed results are dependent on FF parameters that have often been fitted to particular structures (Rappé and Casewit, 1997). The FF derived for transition metal coordination compounds are not based on accurate thermodynamic and vibrational spectroscopic data, as these are not generally available; subsequently, these MM FF parameters are empirically derived and are not related in any strict sense to observables, such as, for example, the stretching force constants derived from infra-red spectroscopy for relevant transition metal complexes. The usual practice is to derive FF by fitting data from crystal structures, and since the parameters are derived by fitting a series of crystal structures, the resulting calculated structure using MM is of a molecule envisaged in an averaged crystal lattice.

The potential energy functions and parameter sets within a FF are interdependent and are not transferable from one force field to another; thus,

to maintain consistency, all work for the low rank coal models discussed here has used the MM3 FF. Electrostatic interactions may pose a particular problem for inorganic compounds, although for relatively small molecules this usually is not a serious problem since Coulomb forces may be included in other potentials (bond stretching, valence angle bending, van der Waal interactions) (Boeyens and Comba, 2001).

MM calculations for inorganic compounds are not abundant as organic and bioorganic structures. This is because important electronic effects arising from, for example, partially occupied d-orbitals in the chemistry of transition metal ions are difficult to model with MM; few FF are able to deal with all metal ions in all their different redox states and coordination geometries. Problems arise from the variety of geometries that can occur at metal centres, and a number of approaches have been devised to deal with them. These approaches essentially use the FF developed for organic compounds and extend this to transition metal complexes. The potential energy equations of organic FF can be adapted to provide suitable potential surfaces for the structure found in metal complexes. The methods used to obtain the parameters for these potential energy equations have been reviewed (Hay, 1993), and while advances are noted, MM cannot address a coal molecular model's electronic structure containing inorganics.

Semi-empirical and *ab initio* quantum mechanics methods are a direct way to study such challenging systems, albeit with increased computational costs. A detailed discussion of the theory of semi-empirical and *ab initio* treatments of molecular structures is outside the scope of this volume; however, the optimisation of the parameters for semi-empirical methods has been discussed by Stewart (2004). Details on the theory and operation of the MOPAC program, used in the present study, are available in the literature, and information on the current version of MOPAC is provided by J. J. P Stewart.* The following is a summary of the software used in studies of molecular models of low rank coals.

As mentioned, the construction of molecular models of brown coal discussed here commenced with molecular fragments used in various 2D structures (to be use in creating 3D structures), examined with ChemSketch Freeware, version 10.00, by Advanced Chemistry Development, Inc. (ACD/Labs); this is a convenient package to draw chemical structures and has been used to calculate elemental distribution, molecular weight, and density for molecular structures.† Suitable molecular structures were then

* Available from http://openmopac.net/manual/index.html.

† ACD/ChemSketch Freeware, version 10.00 (2006). Advanced Chemistry Development, Inc., Toronto, Ontario, Canada. Available from http://www.acdlabs.com.

manually selected to be optimised with the CAChe 5.04 for Windows package* (Domazetis et al., 2008). The CAChe package enables studies using a number of routines (in this case MM3 and MOZYME); the MOZYME algorithm allows rapid semi-empirical calculations of large organic compounds to be performed using a personal computer; it replaces the standard self-consistent field procedure with a localised molecular orbital (LMO) method. Unlike a conventional molecular orbital, which extends over all atoms, a LMO is localised in a small region of the molecule; by using a LMO, the equations can be solved in a relatively short time. MOZYME, however, cannot handle radicals, open-shell systems, or electronic excited states.

After the initial assessment of various molecular models, suitable structures were selected for semi-empirical optimisation using MOPAC2002 (Stewart, 2002); the results and details discussed here were all obtained at the Australian Partnership for Advanced Computing National Facility (currently the National Computational Infrastructure) at the Australian National University, Canberra, Australia (APAC-NF). Computations of structures used in studies of reaction routes were also carried out using Density Function Theory (DFT), with Schrödinger's Jaguar package, at the Victorian Partnership for Advanced Computing facility, Melbourne, Australia (VPAC).†

MOPAC is a general purpose, semi-empirical quantum mechanics package that can calculate numerous chemical and physical properties, such as total energy, heat of formation, Gibbs free energies, activation energies, reaction paths, dipole moments, non-linear optical properties and infrared spectra. MOPAC 2002 includes the semi-empirical Hamiltonians, MNDO, MINDO/3, AM1, PM3, PM5 and MNDO-d (current versions also include RM1, PM6 and PM7). For the studies discussed here, all structures were optimised using MOPAC 2002 with the parametric method 5 Hamiltonian (SE-PM5) and the output includes: total energy, the heat of formation of the compound from its elements in their standard state (ΔH_f), bond lengths, bond angles, bond orders, atomic partial charges, and contributions of σ and π components to bonds with clusters. ΔH_f is defined in MOPAC as $\Delta H_f = E_{elect} + E_{nuc} - E_{isol} + E_{atom}$ (where E_{elect} is the electronic energy, E_{nuc} is the nuclear-nuclear repulsion energy, E_{isol} is the energy required to strip all the valence electrons off all the atoms in the system, and E_{atom} is the total heat of atomisation of all the atoms in the system (this is calculated in eV and converted into kcal mol^{-1} in MOPAC)). Wyberg indices in MOPAC provide bond orders that mirror the simple ideas of single, double, and triple bonds;

* CAChe *ab initio* version 5.04 (2000-2002), Fujitsu Ltd.

† Jaguar, version 6.5 (2005), Schrödinger, LLC, New York, NY.

the bonds matrix is split into σ-π-δ components, and the net charge, or atomic partial charge, on each atom from MOPAC is the Coulson charge; Mülliken populations and atomic partial charges are also computed.

Coal molecular models were optimised to ground states; it is noted that a rigorous treatment of coal molecular models containing transition metal complexes requires multi-electron configuration interactions (MECI) calculations which require extremely large computer wall-times; although a few of these computations were carried out, the majority were restricted to single structure self-consistent field (1scf) MECI calculations. This operation performs energy minimisation to a stationary point on the potential surface, and not necessarily the global minimum. 1scf SE-PM5 computations commence with the structure optimised using MM3, and followed by 1scf SE-PM5 treatment, to provide the heat of formation, partial charges, and, if required, other information such as dipole moment, ionisation potential, and unpaired spin density distribution. Ordinarily calculated parameters of geometries obtained from such computations may be compared with experimental values, but this is not possible for coal as we do not possess a distinct molecule of low rank coal; comparisons were made between measured and computed values of bond lengths, bond angles, and partial charges, all of which are typical for the moieties present in the low rank coal model. The 1scf SE-PM5 methodology is used in studies of reaction routes, using a single coal model structure that undergoes a number of specific single-step changes, which in totality form a reaction sequence.

SE-QM optimisation of some molecular models containing transition metal complexes, for some structures, was complicated by interactions between the transition metal and adjacent hydrogen atoms, which may form short [M…H] and [H..OH_2] distances; in these cases, each optimised structure had to be examined, and an assessment made of the nature of such interactions, by comparing the computed values of bond lengths and partial charges, with those for well-characterised molecules. Distorted structures would be rejected, but in some cases, adjustments were required. In rare cases involving a transition metal complex, SE calculations could be performed by varying the minimum allowed ratio for energy change in MOPAC, and also by optimising the structure to a trust radius of <0.0001.

DFT computations were confined to (the smaller) molecular models of char, and of char containing catalytic species; the bulk of such studies were of char formation with iron active centres and the resulting catalytic reactions between char and steam. DFT calculations of small molecules of transition metal complexes, metal clusters, and organic molecules were carried out with CAChe 5.04 DGauss 4.1/UC-4.1, using Becke '88, Perdew & Wang '91 theory, with a triple-zeta-valence un-contracted, 63321/531/41

Gaussian basis set (DZVP, A1), and Li-Rn pseudopotential, which includes relativistic effects for heavy atoms. DFT computations for chars and related structures were carried with the Jaguar package at 3LYP theory, exact Hartree-Fock, Slater local exchange functional, Becke '88 non-local gradient correction, Vosko-Wilk-Nusair local functional correlation and Lee-Yang-Parr local and non-local functional correlation, and lacvp** or lacvp3** basis sets, which included effective core potentials (ECPs) for iron developed at Los Alamos National Laboratory; the basis set was valence-only, containing the highest s and p shells for the main group atoms and the highest s, p, and d shells for transition metals, including the outermost core orbitals (the 631G basis set was used for atoms not described by ECPs). Polarisation functions were on all atoms except for transition metals, and the effective core potentials included one-electron mass-velocity and relativistic corrections. 1scf-DFT calculations were carried out to assess energy changes for structures undergoing specific chemical steps. Geometries were optimised for selected molecular models using DFT-3LYP and lacvp**; these required a large amount of computer resources and had to be restricted to lower accuracy computations. Jaguar computed a comprehensive array of molecular properties, and those relevant to these studies include partial charges, molecular orbitals, electron density, Fukui functions, and Mülliken population.

DFT geometry optimisation was carried out for all relevant char models, and the data from these computations were consistent with experimental values obtained when char was heated at temperatures of 600°C to 900°C, and also of the char models containing transition metals. 1scf-DFT calculations were also carried out to examine reaction routes for H_2 and CO formation as char underwent heating. DFT computations were also performed to model reaction routes; the modelling data included the energy change for each reaction step, relative to the starting structure, and the data for all of the steps were used to construct an energy profile for the particular reaction sequence.

Modelling Inorganic Species in Brown Coal

The inorganics that are of interest in processing low rank coal are those responsible for the formation of ash during coal combustion, which are: Na, K, Mg, Ca, Fe, SiO_2 and Al_2O_3, with minor amounts of a variety of other species. SiO_2 and Al_2O_3 are mostly present as extraneous mineral and clay particles, mixed with the coal as it is mined. The remainder of the inorganics are chemically associated with the coal molecular matrix. Molecular models of brown coal containing inorganics chemically associated with functional

groups in brown coal will necessarily reflect the 'averaged' molecular structure discussed thus far. The modelling does not include extraneous mineral particles.

Acid treatment of low rank coal removes the inorganics chemically associated with the coal molecular matrix – this is discussed in detail later, and is consistent with the models of inorganics in brown coal.

The main organic coal functional groups are carboxyl, phenolic, and other oxygen groups. A relatively large proportion of water molecules are H-bonded within the coal matrix. The chemistry of inorganics added within brown coal has been studied over a lengthy period, and the views expressed may be summarised as those of ion-exchange, acid extractable and acid-base mechanisms. The inorganic species in brown coal models are: (a) main group solution species, and (b) transition metal solution complexes.

Mined brown coal contains up to 60wt% of water, and it is clear that molecular modelling studies should be of brown coal, water, and the various inorganics; an understanding of the solution chemistry and interactions of the cations with coal functional groups is required for modelling. Generally, main groups' cations are viewed as forming ionic bonds with anion carboxyl groups. The chemistry could be considered similar to reactions of bases, such as NaOH, with carboxyl groups. Additionally, main group solution species, such as Na^{+}, Mg^{2+} and Ca^{2+}, are present as solvated moieties, and these may be added to the coal matrix by adjusting the pH of the coal/solution mixture. The relevant mechanism(s) are thus centred on the chemistry of a macromolecular matrix with carboxyl and phenolic groups, and modelling needs to deal with the nature of dissolved cations chemically interacting with carboxyl groups in coal.

Transition metal aqueous species undergo hydrolysis; an understanding of the chemistry of the uptake of these inorganics by brown coal includes the specific conditions for the chemical interactions of brown coal oxygen functional groups with the various species of the transition metal complex, consistent with their hydrolysis chemistry.

A solution of an inorganic mixed with brown coal would equilibrate as the various coal functional groups interact with the dissolved inorganic compound. Changes in the concentration of any inorganic species may shift this equilibrium, as would changes in the pH of the mixture. The coal-water interactions are significant in this system, and metal species would migrate into the coal matrix as a result of the complex chemical forces that define the coal/water interface and the solvated inorganic species. The modelling would include features of the solution chemistry of the inorganics species that are present in the coal matrix, and from this it is possible to model the various interactions between low rank coals and the inorganics within the

coal molecular matrix; the following discussion outlines the major features of the computational chemistry, with detailed discussions found in Domazetis et al., (2005; 2008) and Domazetis and James (2006).

Low rank coal, water, and solutions of Na^+, Mg^{2+} and Ca^{2+}

The main group species $M(H_2O)_x^{n+}$ (where M = Na^+, Mg^{2+} and Ca^{2+}, x = 2, 4, 6 and n = 1 or 2) exists in solution with hydration shells. The cation species in solution contain relatively shorter [M-O] bond distances, and are subject to electrostatic effects, and to related H-bonds (Mayer et al., 1992); these factors impact on the stability of the inorganic complexes when they are within the coal organic matrix. With the high water content in brown coal, these cations associate with the water molecules and the relevant oxygen functional groups, particularly with negatively charged carboxyl [R-$(COO)^-$] groups in the coal matrix.

Molecular models of brown coal require the optimisation of the coal with water molecules, and then followed with the model containing water molecules and one of the cations.

Computations of a 3D model of brown coal containing the required amount of water are accomplished by placing most of the water molecules in spaces between a large molecule comprising three or four of the structures shown in Figure 3-2. This large structure can be optimised to a ground state using the MOZYME routine; the resulting molecular model conforms to the measured amount of water found in mined coal. Most of the water molecules in this molecular model are present as bulk or liquid water, with only a fraction of these H-bonded to coal functional groups. The molecular volume of the model increases due to the large amount of water molecules, and it decreases when the water molecules are removed. The calculated molecular volume of the coal model was relatively constant when water molecules are hydrogen bonded within the macromolecule (for this, the model molecular weight comprised ≤20wt% water), but when the molecular weight is ≥50wt% of water, the molecular volume increases significantly, consistent with the measured lower density of the mined coal.

The solution behaviour of the main group $[M(H_2O)_x^{n+}]$ systems is dynamic and detailed studies of each cation requires insights related to its hydration spheres. Consequently, rigorous molecular modelling treatments of these systems use various *ab initio* methods; such studies show that an electrostatic attraction to the cation is the major factor in the interaction energy for a molecule in the second hydration sphere, instead of hydrogen bonding with the water molecules in the first hydration sphere (Derepas et al., 2002). We may infer from this that electrostatic interactions within the

organic coal matrix and the cation would contribute to the stability of the coal molecular model, in addition to the hydrogen bonds formed within the coal molecular matrix; the computed partial charges on all atoms of the coal molecular model are indications of these electrostatic properties.

The molecular modelling was carried out by initially comparing the optimised 3D molecular structures with and without a limited number of water molecules, followed by the inclusion of a cation; the results were indicative of the relative stabilities of the coal models with inorganic species. The relevant solution main group metal species used in these models were $[Na(H_2O)_6]^+$, $\{[Na(H_2O)_6]^+[Cl\ (H_2O)_6]^-\}$, $[Mg(H_2O)_6]^{2+}$, and $[Ca(H_2O)_6]^{2+}$.

The chemistry of the various inorganic species added to the coal is illustrated by the following:

1. A solution of NaCl with brown coal (NaCl with the first hydration shell):

$\{[Na(H_2O)_6]^+[Cl(H_2O)_6]^-\} + Coal \rightarrow \{Coal(H_2O)_{10}(Na^+)(Cl^-)\} + 2H_2O$

Modelling shows the structure [brown coal $10H_2O$ (Na^+Cl^-)] is more stable than [brown coal (Na^+Cl^-)] because of H-bonding and electrostatics involving the water molecules, with the cation stabilised by interaction with the oxygen functional groups of the brown coal matrix. Modelling also shows the structure [brown coal $10H_2O$] is more stable than [brown coal $10H_2O$ (Na^+Cl^-)], indicating that the addition of NaCl alone to coal is not energetically favoured. A model containing $[Na^+]$ and $[Na^+Cl^-]$, [brown coal $(COO^-)(2Na^+)(Cl^-)$ $30H_2O$], is stabilised mainly by the interactions of water molecules within the structure, and with the anions and cations interacting with water and oxygen functional groups, resulting in reduced partial charges and the larger $Na^+....Cl^-$ distances of >4.5Å.

2. Acid-base reaction between NaOH and brown coal:
$NaOH + Coal\text{-}COOH \rightarrow [Coal\text{-}(COO^-)(Na^+)] + H_2O$

A model for this chemistry was created by adding $[Na(H_2O)_6]^+$ to the brown coal molecular matrix. The modelling computations provided the stable structure [brown coal $(COO^-)(Na^+)10H_2O$], with a reduction in the partial charge on the cation.

The computes for the structure [brown coal $(COO^-)(Na^+)$] indicated this was not a stable structure, in spite of the reduction in the partial charge on the cation due to the ionic interaction with the carboxyl anion.

Detailed examination of the relative stabilities for a number of such molecular models qualitatively highlights the central role of the hydrophilic nature of brown coal. The relative order of stabilities shows the least energetically favoured models are [brown coal $(COO^-)M^+$], and the energetically favoured models are [brown coal xH_2O] and [brown coal $(COO^-)M^+ xH_2O$]. The total energies calculated using MOZYME-PM5, for the models [brown coal $70H_2O$] and the [brown coal $(COO^-)(2Na^+)(Cl^-)$ $70H_2O$], are within 2%. This is in stark contrast with the results for the brown coal models without water, which compute with significantly higher energies, indicative of lower stabilities.

The interactions of the cations with the first hydration sphere have been assessed in the optimised structures by examining bond lengths and angles, partial charges, and distances between atoms forming hydrogen bonds, and coordination bonds, and these details are discussed by Domazetis and James (2006). The spatial distribution of oxygen functional groups in a 3D molecular structure displays bond lengths and angles typical for aliphatic, aromatic, and oxygen functional groups, with the following atomic partial charges: oxygen groups -0.38 to -0.51, carboxyl hydrogens +0.33 to +0.35, phenolic hydrogens +0.28 to +0.32, and carboxyl carbons +0.48 to +0.44. Extensive hydrogen bonding is evidenced with water molecules and aqua-ionic species in the structure. For example, [O…H] distances between water and carboxyl groups are: 2.01Å for $[(H_2O)..(HOOC-)]$; 2.24Å for the phenolic groups [(OH)…(HOOC-)]; and 2.56Å for the [(OH)…(OH)] groups. The results of these computations are consistent with the experimental observations for brown coal, in which between 10wt% and 20wt% of moisture is hydrogen bonded within the coal matrix, and this contributes significantly to the lower energy conformation of the coal molecular model.

The relative changes in the energy of a molecular model attributed to any particular aqua-ionic species (Na^+, K^+, Mg^{2+}, or Ca^{2+}) in the coal are small, and consistent with the ability of the cation to fit within the coal molecule with minimal disruption to hydrogen bonds. These have been assessed from the computed ΔH_f values, by comparing those for the coal molecular model with a given number of water molecules, and the same model containing each of the cations sodium, or calcium, or sodium and sodium chloride added to the model. The relatively small computed changes in energies of models with and without cations are consistent with the general observations, in that NaCl can be washed out from brown coal with water, and mild acidic conditions would remove cations such as Na^+, Mg^{2+} and Ca^{2+}.

A model of coal containing Na^+ and a (COO^-) group, surrounded by water molecules, formed an energetically favoured structure; the sodium

was situated ~2.5Å to six oxygens, comprising two H_2O, one carboxylate, and three hydroxyls. Partial charges were: sodium +0.4; and of the carboxylate anion -0.5.

Ca^{2+} is a bulky cation which requires greater space within the molecular structure, and the modelling results indicated the cation was associated with suitably situated carboxyl groups, and steric factors were relevant to stabilising the 3D structure. These observations are consistent with the chemistry:

$$Ca(OH)_2 + \{Coal(COO^-)_2\ 2H_3O^+ \rightarrow \{Coal(COO^-)_2\ [Ca^{2+}]\} + 4H_2O$$

The coal's molecular structure contained a partial charge of Ca^{2+} at +0.6, and the cation was surrounded by five H_2O molecules (Ca ←--OH_2 distances 2.27Å, 2.36Å, 2.29Å), a hydroxyl group (Ca←--OH at 2.72Å), a monodentate carboxylate (Ca..O 2.28Å) and a bidentate carboxylate (Ca..O 2.42Å and 2.69Å). The computed partial charges on carboxylate oxygens were -0.7 to -0.5, those for water oxygens were -0.45, and those for the phenolic oxygens were -0.44. A coal model containing 43 water molecules and a calcium cation provided an optimum structure in which the cation was surrounded by water, with coal oxygen functional groups at a considerable distance, and the carboxylate groups forming strong hydrogen bonding with two water molecules and two hydroxyl groups. The stability of this model was enhanced by placing the cation in an unhindered space within the molecule.

The decrease in partial charges observed for the cations Na^+ and Ca^{2+} is indicative of chemical interactions that lead to electron density donated from the coal matrix to the cations. The partial charge on Mg^{2+}, however, was virtually unchanged compared to that on the aqua species, while the distances between the cation and oxygen groups were shorter relative to the other cation models, consistent with an increase in the ionic interactions.

Figure 3-3 displays the ΔH_f values for coal molecular models containing a given number of water molecules and sodium, or calcium, or sodium and sodium chloride. This illustrates that the major impact on the stability of the coal molecular matrix is due to the water molecules, with relatively small variations in the energy of the molecule attributed to the various cations.

Thermodynamic studies of the interactions of ionic metal-humic substances have shown the enthalpy terms are endothermic, and the major contribution to the Gibbs energy change arises from a large increase in the entropy term on the discharge of the humic-associated electrical double layer. Further studies have also indicated that dehydration of the cation, and changes in the electrical double layer, may also increase the entropy of such systems (Bryan et al., 1998; 2000).

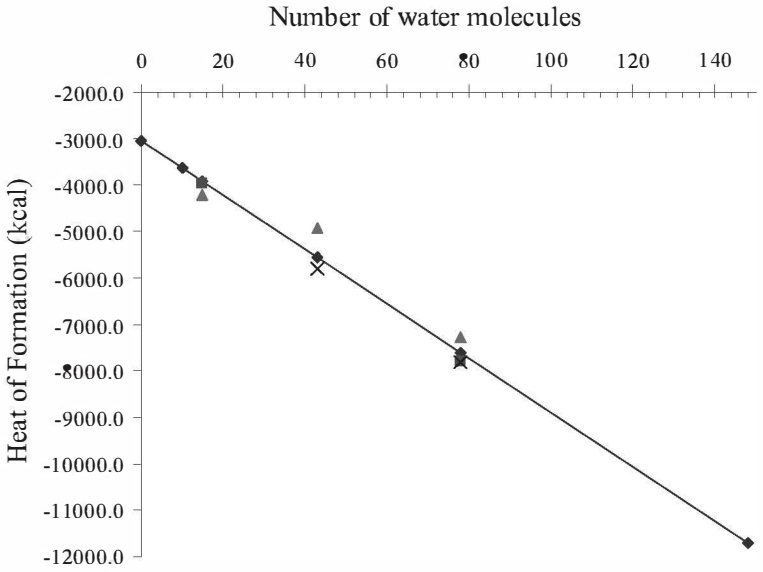

Figure 3-3 Heat of formation (ΔH_f) for coal with water (♦); coal with water and Na^+(■); Ca^{2+} (▲); Na^+, NaCl (x) Reprinted with permission from Domazetis et al., J. Mol. Mod., 14, 581, 2008. Copyright (2008) Springer.

Low rank Coal with Transition Metal Complexes

Computations of low rank coal models containing transition metal complexes are particularly challenging; the aqueous chemistry of transition metals, such as iron, nickel and cobalt, includes hydrolysis and the formation of multi-nuclear hydroxyl complexes, as exemplified by the chemistry of aqueous iron (Cornell and Schwertmann, 1996; Flynn, 1984; Hong-Xiao and Stumm, 1987). Aqueous complexes of transition metals contain six water molecules coordinated to the metal atom, and a second shell of 12 to 16 water molecules. DFT computations for transition metals cations in water have been reported, but for the purpose of examining such complexes in brown coal, these may be modelled with six water molecules (Uudsemaa and Tamm, 2004).

Experimentally, the amounts of transition metal complexes added to brown coal by mixing the coal with a solution of the salt (e.g. $Fe(NO_3)_2$), depend on the pH of the mixture. Only a small amount of the metal complex is added to the coal by simply mixing the solution with the coal, which is at

about pH 2.5, and at this pH, the metal species in the solution are predominately the octahedral aqua complexes $[M(H_2O)_6]^{n+}$ (n = 2 or 3, M = Cr, Fe, Co, Ni). As the pH is increased, increasing amounts of multi-nuclear aqua complexes form in the solution, and concurrently increasing amounts of the particular transition metal complex are added to the coal molecular matrix.

The chemistry of aqua mono-nuclear metal species and brown coal is summarised by (n = 2 or 3):

$$\{Coal(COOH)_n\} + [M(H_2O)_6]^{n+} \leftrightarrows \{Coal(COO)_n[M(H_2O)_{(6-n)}]\} + nH_3O^+$$

The equilibrium is shifted to the right by adding a base to remove $[H_3O]^+$. Iron complexes added to coal are of particular interest; the relevant aqueous chemistry has been discussed by Domazetis et al., (2005). The addition of multi-nuclear iron complexes to brown coal is summarised by the following equation:

$$\{Coal(COOH)_4\} + [Fe_2(OH)_2{\cdot}8H_2O]^{4+} \leftrightarrows Coal\{(COO^-)_4[Fe_2(OH)_2{\cdot}4H_2O]^{4+}\} + 4H_3O^+$$

The amount of iron added to brown coal can be determined by measuring the amount of the base, [OH], needed to adjust the pH of the mixture of coal and iron multi-nuclear complexes, and by accounting for the mass balance of iron distributed in the coal, and the solution. The addition of [OH] impacts on the hydrolysis chemistry of iron complexes. Overall, the aqueous chemistry relevant to a mixture of coal and Fe(III) complexes is:

$$\begin{aligned}
&Coal\ (COOH) + H_2O \leftrightarrows Coal\ (COO^-) + H_3O^+ \\
&Fe^{3+} + 2H_2O \leftrightarrows [Fe(OH)]^{2+} + H_3O^+ \\
&2Fe^{3+} + 4H_2O \leftrightarrows [Fe_2(OH)_2]^{4+} + 2H_3O^+ \\
&3Fe^{3+} + 8H_2O \leftrightarrows [Fe_3(OH)_4]^{5+} + 4H_3O^+ \\
&Fe^{3+} + 4H_2O \leftrightarrows [Fe(OH)_2]^{+} + 2H_3O^+
\end{aligned}$$

The complexes that may be added to the coal are: Fe^{3+}; $[Fe_2(OH)_2]^{4+}$; $[Fe(OH)]^{2+}$; $[Fe_3(OH)_4]^{5+}$; $[Fe(OH)_2]^{+}$; $[Fe_5(OH)_{12}]^{3+}$; $[Fe_4(OH)_{10}]^{2+}$; $[Fe_5(OH)_{13}]^{2+}$; $[Fe_5(OH)_{12}(H_2O)_2]^{3+}$; and $[Fe_7(OH)_{16}(H_2O)_5]^{5+}$.

The distribution of the various iron complexes resulting from the hydrolysis can be calculated as a function of the iron concentration and the pH, using the Phreeqc program; this computer program has extensive capabilities, including calculations of the equilibrium chemistry of aqueous solutions of a wide variety of materials (Parkhurst and Appelo, 1999).

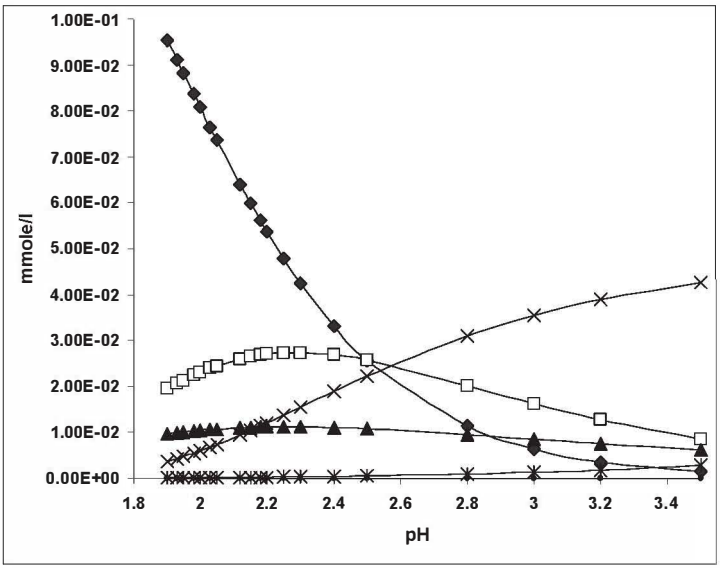

Figure 3-4. Calculated concentrations of species for a given total concentration of Fe(III), with changes in pH
(◆Fe^{3+}; □$[Fe_2(OH)_2]^{4+}$; ▲$(FeOH)^{2+}$; ×$[Fe_3(OH)_4]^{5+}$; ✱$Fe(OH)_2^{+}$; •$Fe(OH)_3$).
Reprinted with permission from Domazetis, et al., J. Mol. Mod., 14, 581, 2008. Copyright (2008). Springer.

Figure 3-4 is the calculated distribution of Fe(III) species in the range of pH 1.8-3.5 at a typical concentration of Fe(III). At lower total concentrations of Fe(III), a pronounced decrease in the concentration of monomeric Fe^{3+} is observed. An increase in pH distributes iron to the poly-nuclear species $[Fe_2(OH)_2]^{4+}$ and $[Fe_3(OH)_4]^{5+}$, and the concentrations of mono-nuclear Fe^{3+} and $[Fe(OH)_2]^{+}$ are reduced. During the latter part of the addition of iron to coal, the predominant complexes in the solution are $[Fe_3(OH)_4]^{5+}$ and $[Fe_2(OH)_2]^{4+}$. These various iron hydroxyl complexes are added to the coal molecular matrix by bonding with carboxyl groups, and by forming coordination bonds with water and with phenolic hydroxide. Figure 3-5 shows the increase in the uptake of iron complexes as the pH of the coal/solution mixture is increased.

The calculated distribution of iron species, after 62% of the iron had been added to the coal, is shown in Figure 3-6. This shows that the predominant iron species added to coal are dimeric and trimeric iron complexes.

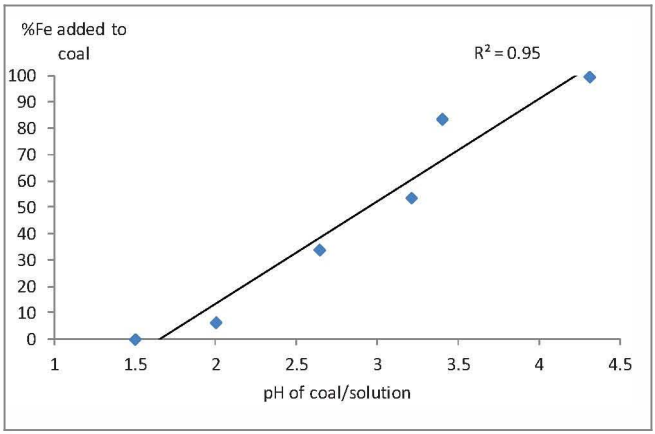

Figure 3-5. Addition of Fe(III) to brown coal with changes in pH of an iron/coal mixture.

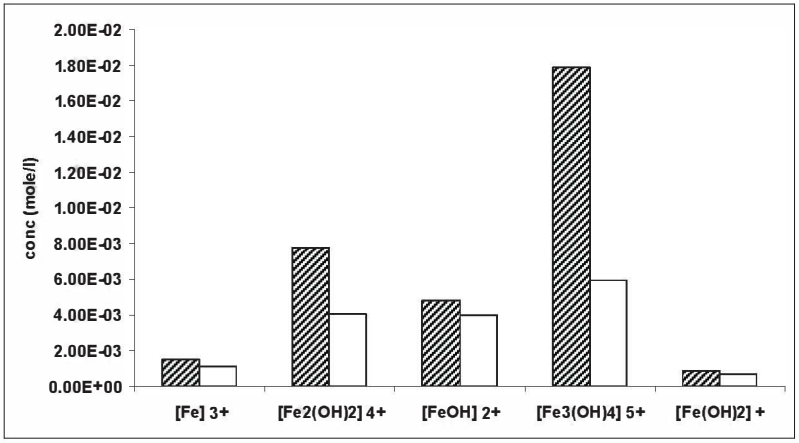

Figure 3-6. Distribution of Fe(III) complexes in solution at pH 3.1 before (shaded) and after (unshaded) 62% Fe(III) was added to coal. Reprinted with permission from Domazetis et al., Energy Fuels, 19, 1047, 2005. Copyright (2005). American Chemical Society.

SE-PM5 molecular modelling provides the relative changes in the energy of a coal structure containing mono-nuclear transition metal complexes, compared to the total energy computed for the same coal model without the metal complexes. Coal models containing Cr, Fe, Co, and Ni

complexes are generally less stable than the coal model without the transition metal complex. Coal models containing water molecules, with and without transition complexes, show water exerts a pronounced influence on the energy of the model. Figure 3-7 displays the heat of formation computed for coal containing 6 and 43 water molecules, and the same model containing transition metal species, obtained with 1sf-PM5 and SE-PM5 techniques. These models contained the μ-hydroxyl poly-nuclear complex with H_2O and OH moieties equivalent to $6H_2O$, and thus the energies in Figure 3-7 are compared to the ΔH_f value of the coal molecular model with $6H_2O$. The ΔH_f values for coal models containing mono-nuclear metal complexes are similar to [Coal $43H_2O$], indicating the water in coal exerted the major influence on the energy of these molecular models. The atomic partial charges on the metal centres for these coal models were lower for Cr and Ni, and higher for Fe and Co, suggesting a differing change of electron density occurred for the latter.

XPS data of coal particles with iron complexes are consistent with the proposed hydroxyl-iron species. Di-iron oxy fragments are also observed with TOF-SIMS, which is also consistent with poly-nuclear iron complexes in a treated coal sample. The coal models containing octahedral metal complexes provided bond lengths and angles typical for transition metals (Domazetis et al., 2008).

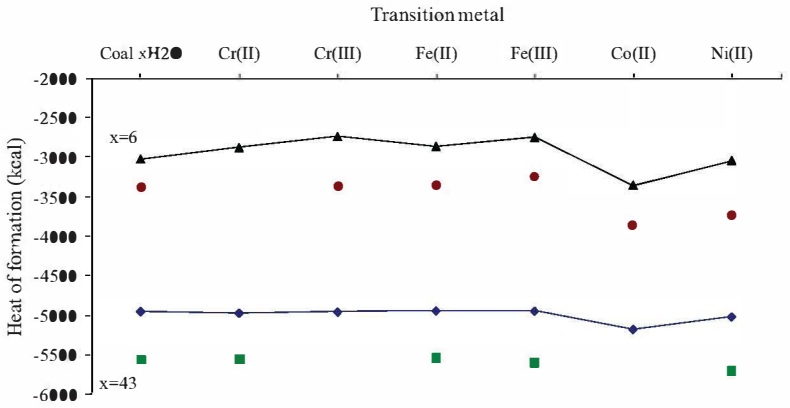

Figure 3-7. Heats of formation (ΔH_f) for coal and transition metal complexes: {coal[M] $43H_2O$} (♦1scf, ■SE) and {coal[$M_2(OH)_2(H_2O)_6$]} (▲1scf, ●SE). Reprinted with permission from Domazetis et al., J. Mol. Mod., 14, 581, 2008. Copyright (2008). Springer.

1scf-MECI computations for mono-nuclear complexes provided singlets for Cr(II), Fe(II), Ni(II), and doublets for Cr(III), Co(II) and Fe(III) calculated at -1.2eV to -2.5eV lower energy. Molecular modelling of coal with nickel octahedral complexes in coal were optimised with nickel bonded to mono-dentate carboxyl groups, which also formed hydrogen bonds between water molecules coordinated to the nickel, and other water molecules and hydroxyl groups in coal. Modelling also indicated that a distorted nickel structure with one carboxyl group acting as a bidentate ligand was less stable when compared with the undistorted octahedral nickel structure. The atomic partial charges on the metal centres within the coal models are relatively lower for Cr and Ni, and higher for Fe and Co. The atomic partial charge on the Cr(II) complex is unusually low, due to shorter coordination bond lengths in the structure (Cr ←-OH_2 and Cr ←-OH, 1.99Å and 2.00Å) and higher bond orders. This result is likely due to an increased donation of electron density by the ligand lone-pair to the metal. The partial charge on the oxygen coordinated to Cr(II) is lower (-0.2 to -0.3), and that on the hydrogen is higher (0.3 to 0.4), compared to the values for these in the original coal molecular model.

1scf-MECI computations for the same coal molecular model containing di-nuclear complexes provided lower energy levels, indicating stable structures. The energy differences, compared to the coal model, were as follows: Co(II) singlet -0.01eV, Cr(III) triplet -1.15eV, and Fe(III) triplet -2.26eV. Generally, the energy of the coal model containing transition metal structures was stabilised by the formation of [M-O] and coordination [M ←-OH] bonds; however, the molecular structure was destabilised if an octahedral complex was placed in a region that caused significant steric strain, particularly if this disrupted the hydrogen bonding between water molecules and the coal oxygen functional groups.

Coal molecular models with an amount of iron similar to that added to brown coal (5.4wt%, 6.5wt% and 13wt% of iron in coal) were created by adding various amounts of the $[Fe_3(OH)_n]^{(9-n)+}$ and $[Fe_4(OH)_n]^{(12-n)+}$ complexes to the coal macromolecule. These molecular models were also employed for computations on the formation of brown coal char, and the concurrent formation of iron clusters with char formation. Examples from this modelling are shown in Figure 3-8 (a) for brown coal containing a mono-iron complex, and Figure 3-8 (b) for coal containing a di-iron complex, Figure 3-9 displays a coal model with various iron species, and Figure 3-10 displays a model of char containing an iron cluster formed by transforming the iron-hydroxyl complexes into iron-oxides, consistent with experimental data.

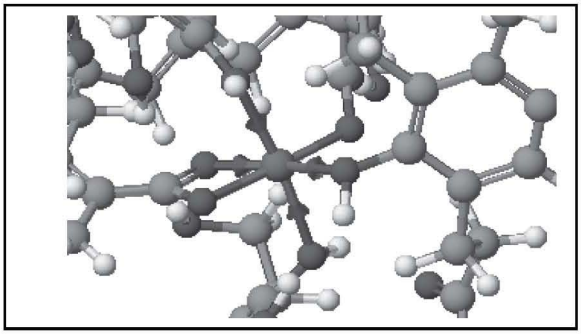

(a)

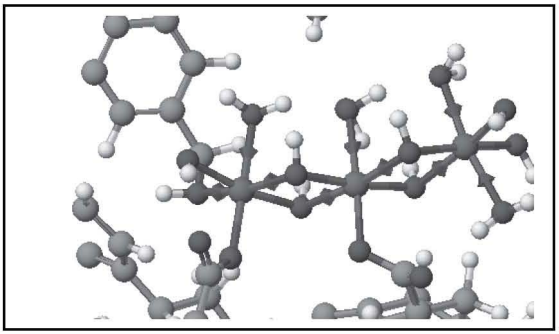

(b)

Figure 3-8. Examples of iron octahedral complexes within the coal molecular model (C = ●black, H = ○white, O = ●red, S = ●yellow, N = ●blue, Fe = ●purple). (a) [Fe(II)] bonded to two carboxyl groups and three (coal-OH) coordination bonds. (b) [Fe_3(III)$(OH)_7(H_2O)_5$] bonded to carboxyl groups, coordinated water, and coal-OH coordination bond.

The results of computations of coal molecular models containing the various iron complexes show these form relatively stable structures, particularly with water molecules incorporated by the iron complexes within the coal model. Stable structures were also obtained by placing the large multi-nuclear complexes in spaces between two or more coal molecules. The data emphasise the importance of hydrogen bonds, and steric factors, on the stability of molecular models of low rank coals containing transition metal complexes, and reinforces the notion that these large poly-nuclear hydroxyl complexes would be situated in regions of the coal macromolecule with space to accommodate them, and with coordinated water molecules. The models are transformed into char containing iron clusters by the loss of CO_2, H_2O and some CO, as observed during pyrolysis.

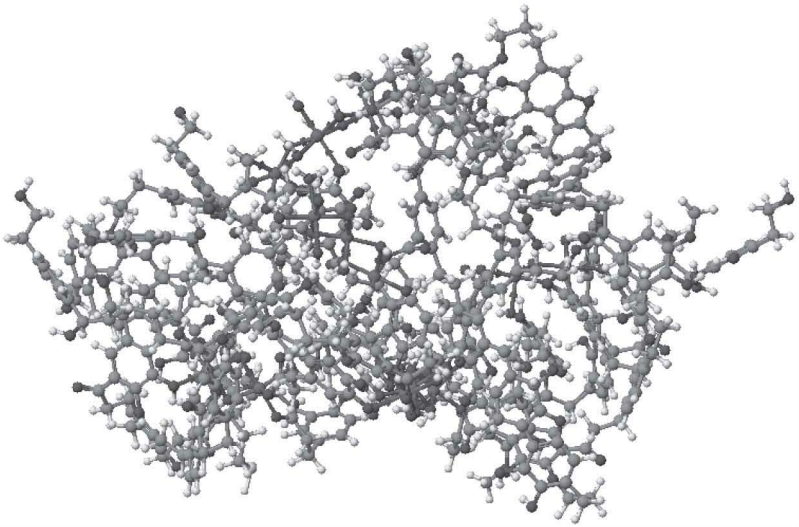

Figure 3-9. Molecular model of coal containing various Fe complexes: $C_{258}H_{(256+32)}O_{(78+32)}N_2S_2Fe_{14}$; MWt 6003.5; Fe=13.2wt% (C = ●black, H = ○white, O = ●red, Fe = ●purple).

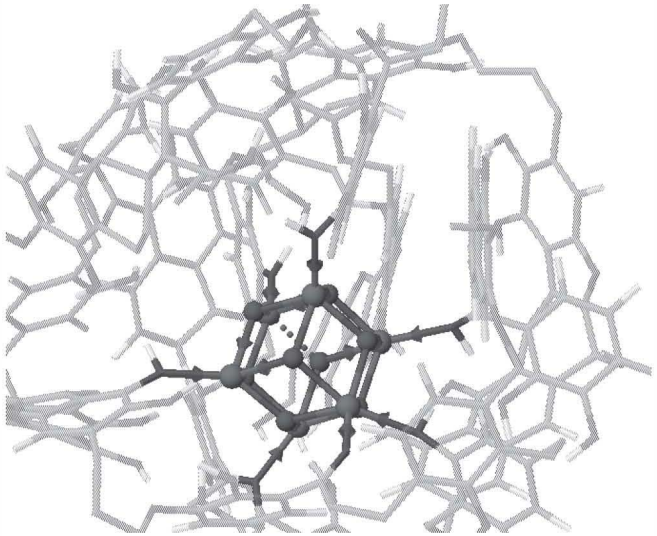

Figure 3-10. Molecular model of char containing the cluster $[Fe_6O_8]$ (C = ●black, H = ○white, O = ●red, Fe = ●purple). Reprinted with permission from Domazetis et al., Energy Fuels, 21, 2531-2542, 2007. Copyright (2007). American Chemical Society.

Coal with added Inorganics and Char Formation

Computational molecular modelling has been utilised to develop a sequence of chemical transformations of brown coal pyrolysis and char formation. This development in molecular modelling also included transformations of inorganics within coal as it undergoes thermal chemistry. The modelling has been performed for pyrolysis and char formation from coal without inorganics, and pyrolysis and char formation of coal containing inorganics. The results from molecular modelling are compared with experimental data, to provide insights on molecular events on the chemistry of coal combustion and gasification, discussed in subsequent chapters.

Insights from the thermal chemistry of well-characterised inorganic complexes that contain suitable organic ligands have also been useful in unravelling the complex chemistry of coal pyrolysis and char formation from low rank coal containing inorganics.

Coal pyrolysis is studied experimentally by measuring the yield of products and weight losses as the coal sample is heated. The initial weight loss is due to the loss of bulk water (100°C), followed by the loss of hydrogen bonded water (and also water within coal micro-capillaries) over the temperature range 100-180°C. Inorganic species present in the coal may contain hydrogen bonded water which would be lost >100°C, and also coordinated water which may be lost over a greater temperature range. Multi-nuclear aqua-metal hydroxyl species would also undergo reactions at higher temperatures and would form metal oxides with the elimination of water molecules. Water lost at higher temperatures (200-300°C) may be derived from transition metal hydroxides, minerals, and organic reactions involving hydroxyl functional groups. The formation of CO_2 also commences at relatively low temperatures and some CO is detected soon after CO_2. The formation of CO_2 and CO has been related to the decomposition of oxygen functional groups in brown coal. A correlation is observed between CO_2 and H_2O evolved on heating that shows a greater amount of CO_2 is obtained from coal containing inorganics.

As coal is heated to increasingly higher temperatures, after the initial loss of bulk water, volatiles are released as the coal is transformed into char. The modelling of brown coal pyrolysis with the 3D molecular model is performing by subjecting it to the following steps, which concurrently result in the formation of a molecular model of char:

1. Loss of carboxyl groups to form CO_2,
2. Loss of carboxyl groups to form CO,
3. Loss of carbonyl groups to form CO,
4. Loss of carboxyl and hydroxyl groups to form CO and H_2O, and

5. Loss of various groups and links to form CO, H_2O, H_2 and hydrocarbons.

The coal model can be subjected to changes reflecting steps (1) to (5); the weight losses of the model that result from these changes can be compared to the experimentally measured weight losses of brown coal as it is heated at increasing temperatures. The measured amounts of evolved CO_2 and CO can also be compared to the amounts obtained during the changes of the coal model as it is transformed into char.

The experimental pyrolysis technique discussed in Chapter Two provides the amounts of CO_2 and CO from the pyrolysis of aw brown coal, and also from the same coal sample containing iron species. The total amounts, and ratios, of CO_2 and CO show a dependence on the temperature-time ramp used in the pyrolysis experiments. All pyrolysis data displayed a change in the ratio of CO relative to CO_2 with an increase in temperature; a greater yield of CO_2 was also observed from coal that contained added inorganic species, relative to aw coal. At a constant temperature in the range 200-300°C, an increase in CO_2 was observed with an increase in the amount of iron in the coal.

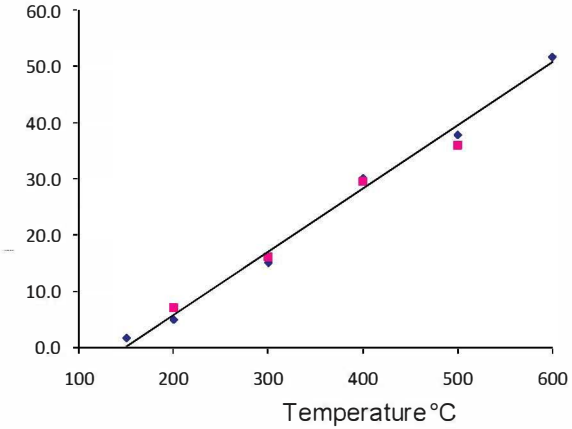

Figure 3-11. Weight loss from brown coal with temperature: model data (♦) experimental data (■).

Figure 3-11 is a comparison of the weight loss obtained by transforming the coal molecular model into a model of char, with the weight loss measured experimentally from heating brown coal. The model was then

subjected to the loss of all carboxyl, carbonyl, ether, and ~40% of phenolic groups, resulting in a total weight loss of ~44%; this result was similar to the experimentally observed weight loss from brown coal heated at 600-700°C. The elemental composition of the char model was also comparable to that obtained for the char, and with similar CO_2:CO ratios (e.g. measured CO_2:CO ratios 2.7-4, from the model CO_2:CO ratio of 2.8).

The transformations of the coal's molecular model into a char model, and of the inorganics within it during pyrolysis, are relevant to studies of catalysed reactions of coal with steam. Detailed molecular modelling of brown coal, and that of brown coal containing iron complexes, has been carried out to map out reaction schemes for the chemistry of coal pyrolysis. For example, metal carbonates have been postulated to explain the changes in the amounts of CO_2 and of H_2O evolved from low rank coal containing inorganics; the models of char with iron complexes, including a carbonate intermediate, are shown in Figure 3-12. XPS data have shown that carbonate intermediates are formed during the pyrolysis of brown coal containing Fe(III) species. XRD data identify the iron phases listed in Table 3-4; at temperatures of 600-700°C, iron oxides in the char are reduced mainly to Fe(0), consistent with molecular models of char containing the iron clusters [Fe_2O], [Fe_3O], [Fe_3], [Fe_4O] and [Fe_4]. An optimised char molecular model similar in composition to char samples obtained at 800°C has been used for *ab initio* DFT computations. DFT treatment of this char model containing the [Fe_3O] cluster, {Char [Fe_3O]}, provided a structure with distances between parallel phenyl groups at 4.4Å for DFT (and 4.3Å for SE-PM5), which conform to distances experimentally observed between sheets in char from low rank coal.

Molecular modelling using DFT provided a series of structures obtained for the loss of H_2 and CO, and these structures form parts of the reaction routes for the formation of these gases.

Table 3-4. Iron phases detected using XRD from a coal sample with 7.8% Fe heated for 15 min.

Temp. (°C)	XRD, iron phases	Species in char models
200-600	γ-Fe_2O_3 / Fe_3O_4 [a]	[$Fe(CO_3)(O)Fe$][b], Fe_2O_3, 2(Fe_3O_4)
700	α-Fe [c]	Fe_3O_2, Fe_3O, Fe_2O, Fe_4O, Fe_4, Fe_3
800	α-Fe [c]	Fe_3, Fe_3O

[a] Broad overlapping peaks; could not resolve γ-Fe_2O_3 from Fe_3O_4
[b] CO_3 detected using XPS
[c] Small amounts of γ-Fe_2O_3

Small organic molecules have been used to obtain details of the breakdown of various carboxyl groups, which cannot be provided for the larger coal molecular models, and these computations have provided: (a) a potential energy map, (b) a saddle point for a reaction, (c) the transition state, and (d) the reaction path to the products. Results from such modelling obtain a trend of the relative rate of decarboxylation for each of the differing carboxyl functional groups in coal. Additional calculations were also performed using the same organic molecules containing sodium, to assess the impact of the inorganics on the reaction routes for the corresponding carboxylate molecules (discussed in Chapter Seven).

The experimental and coal modelling effort has shown that Fe(III) hydroxyl species added to the coal underwent a series of reactions to form a mixture of Fe(III) and Fe(II) oxides, carbonate complexes, and finally various Fe(0) species. The reaction sequences envisaged are: (i) the formation of iron carbonato intermediate complexes that decompose with the loss of CO_2 to form an iron complex containing a μ-oxo iron bond, and (ii) the loss of CO_2 and CO by bond cleavage, the reduction of Fe(III) to Fe(II), and the formation of a radical centre. At lower pyrolysis temperatures, CO_2 is formed by the loss of carboxyl groups bound to iron. This is modelled as a breakage of the [C-COO] bond and transfer of hydrogen from [Fe-OH] to form an [R-CH_3] group; the intermediate [CO_2…O-Fe] forms the carbonato complex with [CO_3] moiety as a bridging ligand.

The reaction sequence for the iron-carbonato complex decomposing into CO_2 and a μ-oxo iron complex is summarised as:

Coal (RCH_3)[(COO)Fe(CO_3)(OH)Fe($COO)_2$R] → Coal (RCH_3)[(COO)(OH)Fe(O)Fe($COO)_2$R] + CO_2

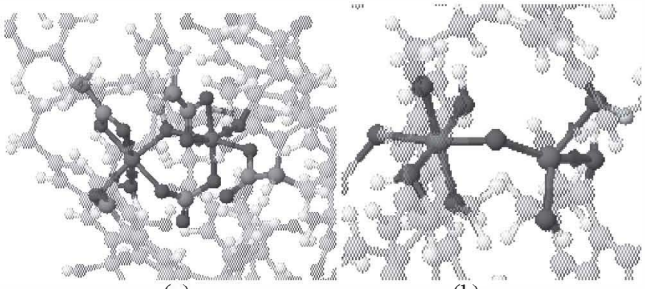

(a) (b)

Figure 3-12. Structures of coal models with: (a) iron carbonato, and (b) μ-oxo-Fe(III)/Fe(II) complexes. Reprinted with permission from Domazetis et al., Energy Fuels, 20, 1997-2007, 2006. Copyright (2006). American Chemical Society.

Figure 3-12 (a) is the model of the carbonato intermediate $[Fe_2(OH)(CO_3)]^{4+}$, prior to the loss of a CO_2 molecule, from a coal model initially containing $[Fe_2(OH)_2]^{4+}$. Figure 3-12 (b) is a model of the μ-oxo bonds connecting the iron centres, derived from a coal model with $[Fe_3(OH)_6]^{3+}$ that had lost two CO_2 molecules *via* the formation of two carbonato complexes; the reduced Fe(II) centre formed a tetrahedral structure. Further reactions may occur with an increase in temperature to form H_2O and the oxidative formation of a [Fe-O-Ph] bond. The loss of CO_2 and CO will occur from these models until the Fe(0) species is formed.

Results from SE-PM5 and 1scf-PM5 computations for these features using the molecular model $[C_{172}H_{170}N_2O_{54}Fe_2]$ are summarised, for illustrative purposes, as:

Coal model: Coal $[(COO)_4Fe_2(OH)_2]$
SE=PM5: Total Energy = -39517.92eV; ΔH_f = -2128.08 kcal; Partial charges Fe = +1.08, +1.05.
1scf=PM5: Total Energy = -39503.90eV; ΔH_f = -1806.11kcal; Partial charges Fe = +1.08, +1.04.

Carbonato complex: Coal $[(COO)_3Fe_2(OH)(CO_3)]$
SE-PM5: Total Energy = -39517.19eV; ΔH_f = -2111.13kcal; Partial charges Fe = +1.31, +0.78.
1scf-PM5: Total Energy = -39504.90eV; ΔH_f =-1827.21kcal; Partial charges Fe = +1.31, +0.78.

μ-oxo-Fe complex (loss of CO_2*): Coal* $[COO)_3Fe(\mu\text{-}O)Fe(OH)]$ $[C_{171}H_{170}N_2O_{52}Fe_2]$
SE-PM5: Total Energy -38837.99 eV; Partial charges Fe = +1.15, +0.83.
1scf-PM5: Total Energy -38822.20eV; Partial charges Fe = +1.01, +0.98.

The ΔH_f for the carbonato complex (compared to the initial coal model) increases by 17kcal to 21kcal, consistent with endothermic chemistry; other models for the formation of a μ-oxo-Fe complex with the loss of CO_2 also show a 1.7% increase in the total energy. 1scf-PM5 calculations for the model undergoing a loss of $4CO_2$ sequentially yielded a linear change in ΔH_f per additional CO_2, indicative of the continuous formation of carbonato intermediates and with the loss of CO_2; this reaction sequence shows that all Fe(III) centres are reduced initially to Fe(II), and ultimately to a mixture of Fe(II) and Fe(0) centres.

Molecular models can also be used to examine radical chemistry during char formation. SE-PM5 and 1scf-PM5 calculations on these coal models,

in which CO_2 was lost and either an alkyl or aryl carbon centred radical was formed, were performed with: (i) the elimination of hydrogen and the formation of a C=C double bond, or (ii) hydrogen abstraction from a suitably situated phenoxyl group, to form a phenoxy-radical. These calculations were carried out with coal models that contain mono-nuclear, di-nuclear and tri-nuclear iron hydroxyl species. The 1scf-PM5 data for the model {coal[$(COO)_2Fe(OH)$]}, and a C or O radical, provided an increase of 1.8% in the total energy compared to the initial model, consistent with an endothermic reaction, and with the subsequent hydrogen elimination to form a carbon double bond slightly energetically favoured. The partial charge for Fe(III) in the initial model of +1.02 was reduced to Fe(II) with a partial charge of +0.71 for the coal model containing the radical, and of +0.74 for the model with the carbon double bond. Similar calculations for the coal model containing a di-nuclear iron complex $[Fe_2(OH)_2]^{4+}$ also provided an increase of 1.8% in the total energy after loss of CO_2; the heat of formation values favoured a carbon centred radical over the formation of a phenoxy radical by hydrogen abstraction; the partial charges on the iron centres changed from +1.09 and +1.04 for the initial model, and after the loss of CO_2 and the reduction of one Fe(III) to Fe(II), the partial charges were +0.82 and +0.57 with a carbon radical; with a phenoxy radical, the partial charges were +1.06 and +0.57.

Pyrolysis chemistry and subsequent catalytic coal gasification are discussed further in Chapters Seven and Eight.

References

Allinger, N. L., Yuh, Y. H. and Lii, J-H. 1989. 'Molecular Mechanics. The MM3 Force Field for Hydrocarbons. 1', *J. Am. Chem. Soc.*, 111, 8551-8566.

Boeyens, J. C. A. and Comba, P. 2001. 'Molecular mechanics: theoretical basis, rules, scope and limits', *Coordination Chemistry Reviews*, 212, 3-10.

Bryan, N. D., Hesketh, N., Livens, F. R., Tipping, E. and Jones, M. N. 1998. 'Metal ion-humic substance interaction-a thermodynamic study', *J. Chem. Soc., Faraday Trans.*, 94, 95-100.

Bryan, N. D., Jones, D. M., Appleton, M., Livens, F. R., Jones, M. N., Warwick, P., King, S. and Hall, A. 2000. 'A physicochemical model of metal-humate interactions', *Phys. Chem. Chem. Phys.*, 2, 1291-1300.

Carlson, G. A. and Granoff, B. 1991. 'Modeling of Coal Structure by Using Computer-Aided Molecular Design', in Harold H. Schubert, Keith D. Bartle and Leo J. Lynch (eds.), *Coal Science II (American Chemical*

Society Symposium Series 461) (Washington, DC: American Chemical Society), 159-170.

Castro-Marcano, F., Lobodin, V. V., Rodgers, R. P., McKenna, A. M., Marshall, A. G. and Mathews, J. P. 2012. 'A molecular model for Illinois No. 6 Argonne Premium coal: Moving toward capturing the continuum structure', *Fuel*, 95, 35--49.

Cornell, R. M. and Schwertmann, U. 1996. *The Iron Oxides*, 2nd ed., Weinheim, Germany: VCH.

Cramer, C. J. and Truhlar, D. G. 2009. 'Density functional theory for transition metals and transition metal chemistry', *Phys. Chem. Chem. Phys.*, 11, 10757-10816.

Derbyshire, F., Marzec, A., Schulten, H-R., Wilson, M. A., Davis, A., Tekely, P., Delpuech, J-J., Jurkiewicz, A., Bronnimann, C. E., Wind, R. A., Maciel, G. E., Narayan, R., Bartle, K. and Snape, C. 1989. 'Molecular structure of coals: A debate', *Fuel*, 68, 1091-1106.

Derepas, A-L., Soudan, J-M., Brenner, V., Dognon, J-P. and Millie, P. H. 2002. 'Can We Understand the Different Coordinations and Structures of Closed-Shell Metal Cation-Water Clusters?', *J. Computational Chemistry*, 23, 1013-1030.

Domazetis, G. 1985. 'Ash Formation from Inorganics in Victorian Brown Coal', *Proc 1985 Int Conf Coal Science* (Sydney: IEA), 389-392.

Domazetis, G. and James, B. D. 2006. 'Molecular models of brown coal containing inorganic species', *Organic Geochemistry*, 37, 244-259.

Domazetis, G., Raoarun, M. and James, B. D. 2006. 'Low-Temperature Pyrolysis of Brown Coal and Brown Coal Containing Iron Hydroxyl Complexes', *Energy Fuels,* 20, 1997-2007.

Domazetis, G., Raoarun, M. and James, B. D. 2007. 'Semiempirical and Density Functional Theory Molecular Modelling of Brown Coal Chars with Iron Species and H_2, CO Formation', *Energy Fuels,* 21, 2531-2542.

Domazetis, G., James, B. D. and Liesegang, J. 2005. 'Studies of inorganics added to low rank coals for catalytic gasification', *Fuel Processing Technol.*, 86, 463-486.

Domazetis, G., James, B. D. and Liesegang, J. 2008. 'Computer molecular models of low rank coal and char containing inorganic complexes', *J. Mol. Model*, 14, 581-597.

Domazetis, G., James, B. D. and Liesegang, J. 2008. 'High-Level Computer Molecular Modelling for Low Rank Coal Containing Metal Complexes and Iron-Catalysed Steam Gasification', *Energy Fuels*, 22, 3994-4005.

Domazetis, G., Raoarun, M., James, B. D. and Liesegang, J. 2005. 'Studies of Mono- and Polynuclear Iron Hydroxy Complexes in Brown Coal', *Energy Fuels*, 19, 1047-1055.

Dorrestijn, E., Laarhoven, L. J. J., Arends, I. W. C. E. and Mulder. P. 2000. 'The occurrence and reactivity of phenoxyl linkages in lignin and low rank coal', *J. Anal. Appl. Pyrolysis*, 54, 153-192.

Faulon, J-L. 1994. 'Stochastic generator of chemical structure. 1. Application to the structure elucidation of large molecules', *J. Chem. Inf. Comput. Sci.*, 36, 1204-1218.

Faulon, J-L., Carlson, G. A. and Hatcher, P. G. 1994. 'A three-dimensional model for lignocellulose from gymnospermous wood, *Org. Geochem.*, 21, 1169-1179.

Fernándeza, I. and Cossio, F. P. 2014. 'Applied computational chemistry', *Chem. Soc. Rev.*, 43, 4906-4908.

Flynn, C. M. 1984. 'Hydrolysis of Inorganic Iron(III) Salts', *Chem. Rev.*, 84, 31-41.

Hatcher, P. G. 1990. 'Chemical structural models for coalified wood (vitrinite) in low rank coal', *Org. Geochem.*, 16, 959-968.

Hatcher, P. G., Breger, I. A., Szeverenyi, N. and Maciel, G. E. 1982. 'Nuclear magnetic resonance studies of ancient buried wood – II. Observations on the origin of coal from lignite to bituminous coal', *Org. Geochem.*, 4, 9-18.

Hatcher, P. G. and Clifford, D. J. 1997. 'The organic geochemistry of coal: from plant materials to coal', *Org. Geochem.*, 27, 251-274.

Hatcher, P. G. and Faulon, J-L. 1994. 'Coalification of lignin to form vitrinite: a new structural template based in a helical structure', *ACS Division Fuel Chem., Reprints*, 39, 7-12.

Hatcher, P. G., Lerch III, H. E., Kotra, R. K. and Verheyen, T. V. 1988. 'Pyrolysis gc-ms of a series of degraded woods and coalified logs that increase in rank from peat to subbituminous coal', *Fuel*, 67, 1069-1075.

Hatcher, P. G. and Lerch III, H. E. 1991. 'Survival of Lignin-Derived Structural Units in Ancient Coalified Wood Samples', in Harold H. Schubert, Keith D. Bartle and Leo J. Lynch (eds.), *Coal Science II (American Chemical Society Symposium Series 461)* (Washington, DC: American Chemical Society), 9-19.

Hay, B. P. 1993. 'Methods for molecular mechanics modelling of coordination Compounds', *Coordination Chemistry Reviews*, 126, 111-236.

Hinchliffe, A. 1996. *Modelling Molecular Structure*, New York: John Wiley & Sons.

Hong-Xiao, T. and Stumm, W. 1987. 'The coagulating behaviours of Fe(III) polymeric species – I. Preformed polymers by base addition', *Water Res.*, 21, 115-121.

Hüttinger, K. J. and Michenfelder, A, W. 1987. 'Molecular structure of a brown coal', *Fuel*, 66, 1164-1165.

Jaguar. 2005. JAGUAR, version 6.5 (2005), Schrödinger, LLC, New York, NY.

Jones, J. M., Pourkashanian, M., Rena, C. D. and Williams, A. 1999. 'Modelling the relationship of coal structure to char porosity', *Fuel*, 78, 1737-1744.

Larsen, J. W. 1992. 'The Physical and Macromolecular Structure of Coals', in Yuda Yürüm (ed.), *Clean Utilisation of Coal, Coal Structure and Reactivity, Cleaning and Environmental Aspects (NATO ASI Series, Vol. 370)* (Dordrecht: Springer), 1-14.

Lii, J-H. and Allinger, N. L. 1989. 'Molecular Mechanics. The MM3 Force Field for Hydrocarbons. 3. The van der Waals' Potentials and Crystal Data for Aliphatic and Aromatic Hydrocarbons. 3', *J. Am. Chem. Soc.*, 111, 8576-8582.

Mathews, J. P. and Chafee, A. L. 2012. 'The molecular representations of coal – A review', *Fuel*, 96, 1-14.

Mathews, J. P., Hatcher, P. G. and Scaroni, A. W. 2001. 'Proposed Model Structures for Upper Freeport and Lewiston – Stockton Vitrinites', *Energy Fuels*, 15, 863-873.

Mathews, J. P., van Duin, A. C. T. and Chafee, A. L. 2011. 'The utility of coal molecular models', *Fuel Processing Technol.*, 92, 718-728.

Mayer, I., Lukovits, I. and Radnai, T. 1992. 'Hydration of cations: H-bond shortening as an electrostatic effect', *Chem. Phys, Letters*, 188, 595-598.

Murata, S., Hosokawa, M., Kidena, K. and Nomura, M. 2000. 'Analysis of oxygen-functional groups in brown coals', *Fuel Processing Technol.*, 67, 231-243.

Murray-Rust, P., Rzepa, H. S., Stewart, J. J. P. and Zhang, Y. 2005. 'A global resource for computational chemistry', *J. Mol. Model.*, 11, 532–541.

Ohkawa, T., Sasai, T., Komoda, N., Murata, S. and Nomura, M. 1997. 'Computer-aided construction of coal molecular structure using construction knowledge and partial structure evaluation', *Energy Fuels*, 11, 937-944.

Parkhurst, D. L. and Appelo, C. A. J. 1999. U.S. Geological Survey Water-Resources Investigations, U.S. Department of the Interior, Denver, Colorado, Report 99-4259, 310.

Quast, K. B. and Readett, D. J. 1991. 'Minerals and Inorganic Components Associated with South Australian Lignites', in Harold H. Schubert, Keith D. Bartle and Leo J. Lynch (eds.), *Coal Science II (American Chemical Society Symposium Series 461)* (Washington, DC: American Chemical Society), 20-30.

Rappé, A. K. and Casewit, C. J. 1997. *Molecular Mechanics across Chemistry*, New York: University Science Books.

Robins, G. A. 1991. 'Coal Structure: The Problem with Minerals', in Harold H. Schubert, Keith D. Bartle and Leo J. Lynch (eds.), *Coal Science II (American Chemical Society Symposium Series 461)* (Washington, DC: American Chemical Society), 44-60.

Shinn, J. H. 1984. 'From coal to single-stage and two-stage products: a reactive model of coal structure', *Fuel,* 63, 1187-1196.

Stewart, J. J. P. 2002. 'MOPAC 2002', Fujitsu Limited, Tokyo, Japan.

Stewart, J. J. P. 2004. 'Comparison of the accuracy of semi-empirical and some DFT methods for predicting heats of formation', *J. Mol. Model.,* 10, 6-12.

Stewart, J. J. P. 2004. 'Optimization of parameters for semi-empirical methods IV: extension of MNDO, AM1, and PM3 to more main group elements', *J. Mol. Model.,* 10, 155-164.

USGS, *PHREEQC (Version 3)-A Computer Program for Speciation, Batch-Reaction, One-Dimensional Transport, and Inverse Geochemical Calculations*. Available at: https://wwwbrr.cr.usgs.gov/projects/GWC_coupled/phreeqc/

Uudsemaa, M. and Tamm, T. 2004. 'Calculation of hydration enthalpies of aqueous transition metal cations using two coordination shells and central ion substitution', *Chemical Physics Letters,* 400, 54-58.

Verheyen, T. V. and Perry, G. J. 1991. 'Chemical structure of Victorian brown coal', in R. A. Durie (ed.), *The Science of Victorian Brown Coal* (London: Butterworth Heimann), 280.

Xiong, J. and Maciel, G. E. 2002. 'Re-examining the Molecular/ Macromolecular Model of Coal from Comparative in Situ Variable-Temperature ^{1}HNMR Studies of Argonne Premium Coal 601 and Its Pyridine Extraction Residue', *Energy Fuel*, 16, 791-801.

Zhao, L., Ding, Y., Yun-he, Z. and Ping, C. 2017. 'Constructions of coal and char molecular models based on the molecular simulation technology', *J. Fuel Chem. Technol.,* 45, 769-779.

Zhou, B., Shi, L., Liu, Q. and Liu, Z. 2016. 'Examination of structural models and bonding characteristics of coals', *Fuel,* 184, 799-807.

CHAPTER FOUR

COAL COMBUSTION, ASH, AND POLLUTANTS

Coal-fuelled power generation utilises the heat released from the combustion of coal to raise steam in a boiler, and this is fed into a steam turbine coupled to an electromagnetic power generator. Demand for power has increased historically, as it has underpinned economic growth and technological advances, and the ever increasing demand for electricity was often met by designing and constructing larger capacity plants to take advantage of the economy of scale. These coal-fuelled plants are capital intensive and have been constructed based on long term projections of demand and supply, which is required for a secure supply of power, and the result has been an effective system of power generation, transmission and distribution, capable of meeting the variable demand for power in a modern community. Generally, the modern grid has been designed to respond to the variable demand for electricity by using baseload coal-fuelled plants (nuclear and hydro power stations may also supply power), with gas-fuelled plants that could be brought online rapidly to respond to the higher demand at peak load. The addition of renewable power has been a recent development and the smart grid is increasingly being implemented to cope with the intermittent nature of renewable power generation.

In this context, plants fuelled by low rank coal suffer unexpected outages of boilers, caused mainly by the formation of ash deposits on heat transfer surfaces. Other problems are also encountered in these boilers, such as erosion and corrosion of heat transfer surfaces. These problems require various maintenance and cleaning measures which increase the costs of low rank-fuelled baseload power generation. It is recognised that improving the quality of low rank coal is an effective remedy for these problems.

A strategy that could address lower emissions intensity, and also meet the increasing demand for power, would include utilising higher efficiency coal-fuelled power plants with low carbon emissions. This approach, however, incurs greater capital expense, and cannot be implemented with low quality fuel that would cause problems of outages and corrosion to a new plant. A process that maintains the low cost of these coals and provides high quality fuel would be an attractive option.

An effective coal treatment process may be regarded as refining crude as-mined low rank coals into fuels specifically designed for modern high efficiency plants, using process conditions that avoided creating environmental problems. To this end, the hydrocarbon components in the coal, which provide the energy, would remain intact, while ash constituents, S-, Cl- and N-derived pollutants, and trace heavy metals are reduced or removed.

An understanding of the chemistry of coal combustion, ash, and pollutants formation is required to provide insights on the degree of coal processing required to produce the high quality products.

Coal combustion is a complex phenomenon; general treatments of coal combustion are found in the literature (Sajwan et al., 2006; Stöllinger et al., 2013) with numerous studies carried out using thermodynamics, chemical kinetics, and computational fluid dynamics for heat and mass flow using global, or simplified, chemical kinetics. The clean coal concept requires particular studies that provide an understanding of the problems stemming from the coal properties and its combustion behaviour relevant to the design of plants, and to determine the treatments required to reduce or eliminate the problems stemming from the poor quality of low rank coals.

This chapter will discuss low rank coal combustion chemistry to obtain insights on the causes of the problems posed by low quality coal. From this, we can elucidate aspects that are important for the production of high quality fuel. In addition to the various techniques used to characterise low rank coals discussed previously, it has proved convenient for these studies to use particular descriptive models and computer simulation programs for the chemistry of ash formation during coal combustion.

Detailed chemical kinetics and thermodynamic calculations for low rank coal necessarily adopt a simple physical model, as this enables a detailed treatment of the chemistry specific to the deleterious impacts of the poor quality fuel, such as: burning of char particles and solid phase reactions of inorganics within it, the release of alkali into the vapour phase, and reactions involving mineral particles, such as clays and silica.

In well-mixed coal flames, up to half of the coal organic matrix of brown coal volatilises as gases, including hydrocarbons, that burn quickly, while the resulting char undergoes solid-gas reactions which take a longer time to burn compared to the gas-phase reactions. At flame temperatures of $\geq$1100°C, low rank coal containing relatively high levels of alkali will release a considerable proportion of alkali as very reactive gas species, which would exacerbate the fouling of ash deposits and form molten phases (slag) on heat transfer surfaces (Domazetis and Campisi, 1986; Domazetis et al., 1988).

Energy from Coal

The overall chemistry of coal combustion is exemplified by the following exothermic reaction:

$$C_nH_mO_x(\text{other}) + \text{xs}[O_2/(N_2)] \rightarrow (n\text{-}x/2)CO_2 + (x/2)CO_2 + (m/2)H_2O + (\text{ash/other}) + \text{heat}$$

where $C_nH_mO_x$ represents the organic components of the low rank coal; excess (xs) oxygen from air is mixed with the pulverised coal to create a flame (other = S and N pollutants, HCl and N_2 fine particles).

A molar distribution of combustion products can be given based on a generalised molecular formula from the elemental composition of the brown coal organic matrix, reacting with excess oxygen from air (moisture is not included in this equation as it evaporates and is part of the mass flow; SO_2 and NO represent sulphur and nitrogen pollutants):

$$C_{258}H_{256}N_2O_{78}S + \text{xs}[O_2(N_2)] \rightarrow 258CO_2 + 128H_2O + SO_2 + 2NO + (N_2)$$

A description of the behaviour of inorganics chemically associated with the burning coal matrix requires detailed solid and gas phase chemistry; this may be illustrated by the generalised reaction that exemplifies sodium in coal-forming gaseous species as the coal particles are heated rapidly to form burning char:

$$[\text{Char(ash)(Na)(NaCl)}] + \text{xs}[O_2\,(N_2)] \rightarrow (\text{char/ash}) + (CO_2) + Na_2O(g) + NaOH(g) + HCl(g) + (N_2)$$

At typical peak coal flame temperatures, the release of some gaseous magnesium and iron occurs, but these are short lived and form aerosols in regions of the coal flame. Reactions of inorganics occur within the burning char, and these form Ca/Mg/Fe/Al solid phases that may eventually mix with deposits from a variety of alumina-silicate mineral particles present as extraneous particles, and depending on the composition of the mined coal, these can form molten and semi-molten particles. Some of the resulting ash would be deposited on heat transfer surfaces, and the remainder is collected as fly ash. In practice, small amounts of unburnt char may be present in the fly ash, and fine particulates may be emitted into the atmosphere.

Typical composition and heat content for a number of low-ash brown coals from a number of mines in Victoria, Australia, are shown in Table 4-1, and the average heat content in these as-mined brown coals is 8.1MJ/kg.

Heat content in coal is stated as higher heating value (HHV) and lower heating value (LHV); other relevant terms are net wet specific energy, and gross dry specific energy. HHV (or gross energy or gross calorific value) is the value obtained by bringing all the products of combustion back to the original pre-combustion temperature, and condensing any vapour produced at a standard temperature of 15°C. LHV (or lower calorific value) is determined by subtracting the heat of vaporisation of the water vapour from the higher heating value. LHV assumes that the water from combustion remains a vapour, while HHV assumes that all of the water in a combustion process is in a liquid state (and releases the heat of vaporisation) after a combustion process. These values are expressed for coal as follows: as received (ar), dry basis (db), and dry ash free (daf).

Table 4-1. Typical data for Victorian brown coals.

Location	Yallourn	Yallourn Nth	Loy Yang	Morwell	Flynn
Moisture (wt%)	66.5	52.3	62.8	61.3	64.1
Ash (wt%db)	1.7	5.0	1.3	3.0	1.3
Fixed carbon (wt%db)	48.0	47.6	48.9	48.7	48.1
Oxygen (wt% daf)	26.9	24.7	25.8	26.2	26.2
GDSE (MJ/kg)	26.1	26.0	26.2	26.3	26.3
NWSE (MJ/kg)	6.9	10.7	7.1	7.5	7.5

GDSE – gross dry specific energy. NWSE – net wet specific energy

A linear relationship is observed between the water content and heating value of these mined low rank coals with relatively low ash, as shown in Figure 4-1. From this correlation, an estimate of the energy of completely dry brown coal would be ~29MJ/kg. In practice the moisture in low rank coals would be reduced to between 12-15wt% of water, because this amount of water is hydrogen bonded to the coal matrix, which requires additional heat to remove completely. The heat content of processed low ash coal with about 15wt% moisture is estimated at 22-26MJ/kg.

Typical compositions for brown coal, lignite, and sub-bituminous coal are shown in Table 4-2, and the lower heating values for these fall in the range 7-10MJ/kg for brown coal, 10-12MJ/kg for lignite, and 15-20MJ/kg for sub-bituminous.

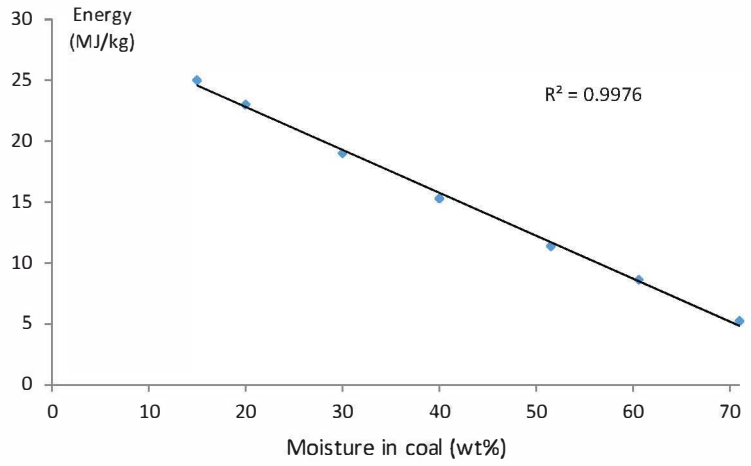

Figure 4-1. Energy (LHV) of low rank coals as a function of moisture content. Reprinted with permission from Domazetis et al., Fuel Processing Technology, 89, 68-78, 2008. Copyright (2008). Elsevier.

Table 4-2. Typical Composition of Brown, Lignite, and Subbituminous Coals

Region / Component	Victoria		W.A.	S.A.	Ger any
	Yallourn*	Loy Yang*	Collie$	Lochiel#	Rhenish*
Moisture (%)	61-66	60-62	21-29	50-61	55
Ash (%)	0.6	1.2	4-9	6-12	3.5
VM (%)	17.5	19.3	24-29	25	-
FC (%)	15.8	16.8	39-45	34	-
S (%)	0.3	0.4	0.3-1.0	3.3	0.8
Cl (%)	0.1	0.2	-	0.5	-
HHVdaf (MJ/kg)	~26	26.4			25.6
LHVar (MJ/kg)	(~7)	(~7)	~19	9.1	10.0

$Sub-bituminous. #Lignite. *Brown coal.

The energy of coal is the heat released when organic matter undergoes combustion; thus, a comparison between the heat content of as-mined low rank coal and the same coal processed into a low ash coal with 15% moisture would provide the difference in the organic matter for a given weight. For example, one kilogram of mined brown coal typically consists of 370-340gms of organic matter, 600gms of moisture, about 30-60gms of ash, and its heat content is 8-10MJ/kg. After treatment to remove moisture and aggressive ash, typically one kilogram of the processed coal would consist of 848-845gms of organic matter, 150gms of water, and 2-5gms of non-fouling ash, and its heat content is estimated at 22-24MJ/kg. Thus, 2.3 tons of as-mined brown coal are required to yield 1 ton of good quality non-fouling coal.

An important aspect of a coal-fuelled plant is the mass flow through a boiler – the high moisture in mined brown coal would give a higher mass flow for a given heat rating of a boiler, and would therefore require a larger plant. The plants fuelled with mined low rank coal must be relatively larger to accommodate the greater mass flow, and consequently would incur higher capital costs; these plants would also suffer from ash fouling and the corrosion of heat transfer surfaces and, because of their low efficiency, would produce higher emissions of CO_2/MWh. If the as-mined low rank coal was simply dried to remove moisture, it would burn at higher peak flame temperatures, which would be unsuitable for boilers designed to operate with high moisture mined coal, and additionally, the higher coal flame temperatures would result in greater ash fouling.

A coal treatment process must be designed to produce the quality of fuel that would maximise the benefits for power generation, and this requires low moisture, non-problematic ash, and very low amounts of pollutants. The processed coal would fuel high efficiency plants with higher power outputs, lower levels of pollutants, and lower emission intensities.

A brown coal processing plant would incur costs; the largest component of these costs is the heat required to remove the moisture in the coal. This cost may be reduced substantially by using low-grade heat from the power station to process the coal. An efficient process would use this low-grade heat to accelerate the action of acid to remove ash and also to lower the moisture in the coal. Capital costs would also be incurred to construct the coal treatment and drying plants, and some of these costs would be offset by the relatively smaller boiler and related plants that could be fuelled with the clean coal. High quality non-fouling processed coal can fuel a supercritical power plant operating at high efficiencies. The reduction of moisture is an obvious way to increase the calorific value of low rank coal, while removing fouling ash increases plant availability and lowers operational

costs, and these would justify the expense incurred in processing these coals. It is axiomatic that the quantifiable costs of processing plants, and benefits from using processed coal for power generation, are dependent on the properties of the mined coal and the performance of the higher efficiency power plants.

The Chemistry of Low Rank Coal Combustion

Coal combustion chemistry can be studied using detailed chemical kinetics schemes, but a rigorous treatment requires a very large number of elementary reactions. This can be illustrated by considering the following: the simplest combustion scheme is a hydrogen-oxygen flame, and a typical chemical kinetics scheme for this consists of 9 species and 21 elementary reaction steps. A hydrocarbon combustion kinetics scheme, such as a methane-oxygen flame, consists of 53 species and 400 reactions; a detailed chemical kinetics mechanism for isooctane consists of 860 species and 3,606 reactions. Additionally, the chemistry of char burning is influenced by the char morphology, which adds to the complexity of a chemical kinetics scheme due to the heterogeneous nature of these coals (Wu et al., 2006).

Computer modelling of the chemical kinetics of low rank coal combustion requires the following routines:

- coal devolatilisation as coal particles are heated,
- combustion of volatiles,
- combustion of char,
- ash formation, and
- pollution formation.

Additional routines would be required to deal with the fluid flow and heat transfer relevant to the coal-fuelled plant. The resulting model would be very large, requiring unrealistically large computer resources (McAllister et al., 2011).

With the rapid progress in super-computational modelling, various approaches have been discussed to model combustion processes, utilising chemical kinetics and computational fluid dynamics (CFD). Computer modelling of these phenomena can now be used to predict flow fields and heat transfer with reasonable accuracy, but it is not sufficient for a rigorous treatment of all facets of coal combustion chemistry; additional constraints stem from an inadequate understanding of all reactions needed to provide a detailed treatment of coal combustion and ash formation chemistry

(Williams et al., 2002). Nonetheless, advanced computer packages that incorporate global chemical kinetics with fluid flow schemes have been developed and are used commercially in designing combustion systems. Detailed reaction kinetics of hydrocarbon combustion is available. Simmie (2003) and Miller et al. (2005) have discussed the development of chemical kinetics of combustion; an example of a commercially available comprehensive code for chemical kinetics of combustion is CHEMKIN.*

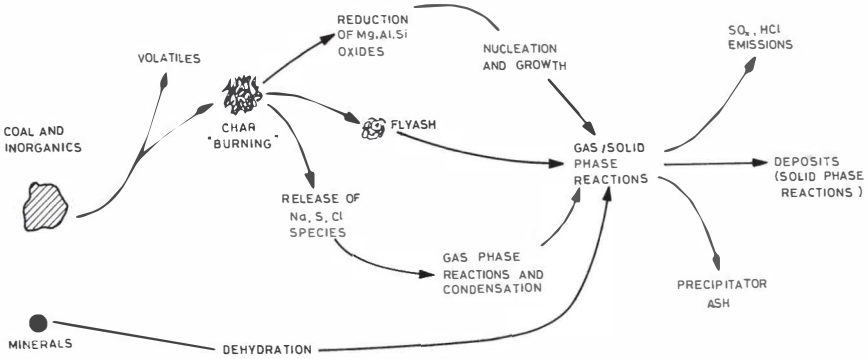

Figure 4-2. Descriptive model of low rank coal combustion and ash formation (Domazetis, 1985).

The present discussion is concerned primarily with a coal combustion chemistry scheme for low rank coal that would incorporate the mechanisms, and subsequent causes, of ash fouling and the emission of pollutants. Such a simulation would simplify the physical parameters, and provide a detailed treatment that relates the coal properties to the chemistry of coal combustion and post-flame events that cause boiler ash fouling, corrosion, and the emission of pollutants. The description would encapsulate the combustion phenomena by considering a cloud of coal particles undergoing rapid heating as they are mixed with air to create a flame. A descriptive model is shown in Figure 4-2, that is, of a perfectly mixed reactor at atmospheric pressure that undergoes an imposed temperature-time, typically found in pilot-plants and full scale coal-fuelled plants. This is a pragmatic approach that avoids a CFD treatment, and instead is focussed on a detailed treatment of the chemistry.

* ANSYS Chemkin-Pro: Comustion Simulation Software. Available from http://www.ansys.com/products/fluids/ansys-chemkin-pro.

The following discussion outlines the essential chemical reactions used in this model – further details of rate constants and modelling assumptions are found in the references cited. The chemistry of the model outlined here has applications for all problems arising from the unwanted properties of ash and pollutants in low rank coals.

Chemical Kinetics

Reactions in combustion chemistry often exhibit high energy barriers and the chemical rates are sensitive to temperature. Reactions need to surmount the energy barrier and provide sufficient heat to sustain combustion; thus, low rank coal flames are stable if the moisture in the fuel is removed, or measures are taken to negate the impact of moisture. A coal flame in a boiler is initiated using an oil or gas burner to heat a boiler to a temperature required to sustain the pulverised low rank coal burner. Moisture in the mined low rank coal is removed by mixing the coal with hot gases extracted from the boiler in the coal pulveriser, so that a stream of pulverised coal particles and evaporated moisture with hot gases is fed to the burner.

As coal particles are heated to higher temperatures, volatiles are released and these and char burn to form a coal flame. The various products formed from coal devolatilisation have been measured experimentally, and from these data rate constants have been derived for these products. The approach adopted for models of devolatilisation is based on the assumption that various functional groups in coal particles break down to yield specific products (Kautman, 1982; Solomon and Hamlen, 1983). This has been illustrated in the discussion on molecular modelling, in which, for example, carboxyl groups undergo thermal chemistry to form CO_2 and CO. In this manner, a correlation is established between the rate of appearance of the various products from devolatilisation and the coal composition. The gaseous products from coal devolatilisation are H_2O, CO_2, CO, H_2, CH_4, tar, and minor amounts of S, Cl and N pollutants – these, char, and the ash constituents make up the total mass of the coal. The total products from combustion are expressed as molecules and, based on the elemental composition of the coal, a mass balance for the reaction scheme is obtained. Tar is thermally cracked into simple hydrocarbons and CO. The inorganic ash-forming constituents are partitioned as (a) volatiles (Na, NaOH, NaCl), and (b) as solid/liquid phases from reactions involving various (Fe/Ca/Al/Mg/Na/Si) species.

Chemical kinetics consists of reactions written to represent individual molecular transformations, and a set of such reactions can form a mechanism to describe a chemical process. Elementary reactions may be written in the form:

$$A + B \underset{k'}{\overset{k}{\leftrightarrow}} C + D$$

The nett rate for this elementary reaction is the difference between the forward and reverse rates.

Forward rate	=	k[A][B]
Reverse rate	=	k′[C][D]
Nett rate	=	{k[A][B]} – {k′[C][D]}

The reaction rate is equal to the product of the concentrations of the reactants multiplied by the rate constant. The equilibrium constant K is given by:

$$K = k/k'$$

The rate constants are usually given by the Arrhenius equation:

$$k = A\, e^{(-Ea/RT)}$$

where T is temperature, R is the gas constant, E_a is the activation energy, and A is the pre-exponential factor, which is related to the collision frequency (a general equation can be written as $k = A_0\, T\, e^{(-Ea/RT)}$).

The gas-phase combustion chemistry can be described as a complex series of coupled elementary reactions. All of the reactions may occur simultaneously, often involving intermediates common to many of the reactions. Gas-phase schemes include an atom or radical (R_1) produced in an initiation step by the thermal dissociation of a starting material (A).

$(A + R_1)$ Initiation step

Radicals ($R_1 \ldots R_n$) are highly reactive and rapidly undergo reactions that yield product molecules and also generate active radical(s); these reactions are termed as propagation steps.

$$R_1 + B \rightarrow R_2 + C \qquad \text{Propagation steps}$$

$$R_n + X \rightarrow R_1 + Y \qquad \text{Branching steps}$$

Branching steps can also take place, where two radicals are produced from one radical. Branching has the effect of increasing the radical pool and thus causes an acceleration of the overall reaction rate. Some radicals, however, will be removed by recombination with other radicals from stable molecules and this terminates the reaction route.

$$R_1 + R_n \rightarrow Z \qquad \text{Termination step}$$

Pollutants are formed from nitrogen, sulphur and chloride species. The formation of nitrogen pollutants is modelled by initially releasing NH_3 and HCN in two regions, one during the early heating of a coal particle and the second as the char burns. Sulphur is released from coal particles as H_2S, but some is retained in char, mainly as $CaSO_4$, which decomposes at higher temperatures into CaO and SO_3. Chloride is considered part of the $Na/O/Cl/SO_2$ scheme, but some organic chloride is modelled for convenience as the hydrocarbon C_2H_5Cl in gas-phase combustion to yield reactive chloro-species.

Following the release of gases during the devolatilisation of coal, gas phase combustion chemistry and char burning ultimately yield the stable products CO_2 and H_2O (and other minor compounds). Volatile inorganics are mainly sodium (and potassium if it is in the coal) and small amounts of other inorganics often present in coal. The volatilisation of sodium is assumed to occur as the coal particle is heated and as the char burns; rate constants of sodium release from heated coal particles are obtained experimentally.

The simulation scheme discussed here has been constructed to use a given temperature-time profile (typically observed in coal-fuelled boilers, pilot plant, or laboratory burners), imposed on the coal combustion chemistry scheme. The model is of a perfectly mixed reactor with the stipulated chemical kinetics scheme, and with additional routines to deal with the devolatilisation, formation and condensation of NaCl and Na_2SO_4, and solid-gas phase reactions. Imposing a measured gaseous temperature-time ramp on a perfectly mixed reaction mechanism avoids the intractable situation presented by the large number of chemical reactions coupled to heat and fluid flow computations. Details of the software architecture, equations and rates data are found in Domazetis et al., (1988). This

simulation treats the chemical reactions scheme as a set of stiff ordinary differential equations solved using Gear's method (Deuflhard et al., 1981; Domazetis and Campisi, 1986).

The gaseous temperature-time profile for the reaction scheme is specified at a number of small intervals; the time is increased by a small amount, and with it a new temperature is obtained from the ramp, and reaction rates recalculated. The temperature and reaction rates are assumed to be constant over the small increments in time. The scheme is at atmospheric pressure. The concentrations of all species are adjusted for each incremental change in temperature by the application of the ideal gas law. This adjustment is performed for every integration step, with an internal check on the "stiffness" of the scheme for the particular step – the computations are not carried out if the step is larger than required; instead a smaller step is computed and the procedure repeated, until a sufficiently small integration step is obtained.

The temperature of the coal particles is taken as the mean of the gas temperature and the centre of the particle temperature, calculated from the general solution of the equation for the heat conduction of a sphere, neglecting radiation; i.e. the mean particle temperature at each given time. The temperature of a burning char particle's surface is assumed to be 200K above the particle temperatures. These computed temperatures of coal and char particles are used in the rates for devolatilisation and char burning.

Low Rank Coal Devolatilisation and Char Burning

A descriptive model for the devolatilisation from coal particles consists of a series of first order chemical equations; the mechanism assumes a first-order scheme with respect to the concentrations of the respective species in coal (Domazetis and Campisi, 1986). The input file stipulates sized coal particles reflecting the coal particle size distribution for given systems, such as, for example, of pulverised coal combustion, and with a distribution of the functional groups (or species) based on the composition of the particular coal. The functional groups undergo chemistry at the calculated rates as the coal particles undergo rapid heating to yield proportions of CO_2, CO, H_2O, tar, and char, with the subsequent breakdown of tar into hydrocarbons, CO_2, and CO:

$d_i/d_t = k(i_0 - i_t)$ $\quad$ di/dt = rate of formation of product i

$\xrightarrow{k}$ $\quad$ i_0 = concentration of species i at t=0

coal species(i) $\rightarrow$ product(i) $\quad$ i_t = concentration of species i at t=t

The rate constant is obtained experimentally from the measured rate of formation of each product during coal devolatilisation. This approach is consistent with devolatilisation models which show products are derived from the thermal breakdown of functional groups in low rank coals. Product concentrations can also be obtained from experiments carried out at specified heating rates to given maximum temperatures (Cliff et al., 1984; Doolan et al., 1985).

A chemical scheme for gas phase combustion includes tar decomposition into gaseous hydrocarbons that undergo combustion – these may be any or all of CH_4, C_2H_4, C_4H_6, C_6H_6, and C_2H_2; a suitable hydrocarbon scheme is chosen based on practical considerations for the total size of the chemical reactions for a simulation, e.g.: Tar composition $\rightarrow C_2H_2 + C_2H_4 + CO$

Choosing a comprehensive hydrocarbon scheme may require so many additional reactions that it results in an impractically large reaction scheme. Sensitivity analysis can identify reactions that would not exert a significant overall impact on the simulation; for example, the above tar breakdown into the selected hydrocarbons feeds into a reaction scheme involving the following:

$C_2H_2 + OH \rightarrow CH_2 + CHO$
$C_2H_2 + O \rightarrow CH_2 + CO$
$C_2H_2 + O \rightarrow C_2HO + H$
$C_2H_4 + OH \rightarrow C_2H_3 + H_2O$
$C_2H_4 + O \rightarrow CH_3 + CHO$
$C_2H_4 + H \rightarrow C_2H_3 + H_2$

Detailed hydrocarbon combustion schemes are available, and generally the size of the scheme used would require a judgement on what is adequate for the chemistry under consideration.

CO is a major intermediate, formed during coal devolatilisation, and accumulates before CO_2 is formed (and is a major product from coal gasification). The formation of CO_2 by the reaction

$CO + OH \leftrightarrow CO_2 + H$

is complex, pressure dependent, and displays a non-Arrhenius temperature dependence. The conversion of CO to CO_2 is pronounced in flames with significant amounts of H/O species and is modelled by reactions involving O, OH, HO_2, O_2 and H. The reaction:

$$CO + O + M \leftrightarrow CO_2 + M$$

is slow; high temperatures and oxidising conditions favour oxidation by OH as mentioned above, and by the chain initiating step:

$$CO + O_2 \leftrightarrow CO_2 + O$$

Char burning occurs over a longer period than gas phase reactions, and provides a good deal of the heat from coal combustion. The study of the char combustion rate is important for a coal burner design and combustion process control, and consequently there exists a very large amount of literature dealing with char burning for various coals (e.g. Smith, 1982; Liu and He, 2015; Naredi and Pisupati, 2008), as well as modelling studies of the reactions of carbon (graphitic) molecules with oxygen, and phenomenological approaches.

The fundamental reactions of carbon and oxygen have been studied using DFT molecular modelling. These use small graphitic molecules to examine oxygen binding at edge carbons, followed by the loss of CO. The reactions of a ketone surface oxide group may occur on two configurations: the zigzag edge and the armchair edge of the molecule. Rearrangement and surface migration reactions are faster than desorption reactions on both the zigzag and armchair edges. Desorption pathways explain the broad activation energy profile for CO desorption observed experimentally. Separate desorption processes obtained on the zigzag surface show activation energies of 275 and 367 kJ mol^{-1}, while the armchair surface provides activation energy of 296 kJ mol^{-1}. A larger size model provided an extra desorption step with activation energy of 160 kJ mol^{-1}, even though activation energies are generally insensitive to the size of the char model (Sendt and Haynes, 2005).

Phenomenological modelling of the solid-gas reactions of burning char particles require calculations of the available surface area for reaction, the diffusion of the reactant (O_2) to the char surface, and of the products (CO, CO_2) moving away from the reacting solid into the bulk gases. Additionally, ash chemistry occurs as char burns; modelling and experimental investigations of char burning with ash inhibition have shown a restricted diffusion through the ash film, and this has a significant impact on the char burnout rate. Char dilution by ash only inhibits combustion significantly when most of the char has been consumed and the combustion shifts from predominantly external diffusion control to that of mixed diffusion control, which exhibits both external and internal diffusion resistance (Hecht and Shaddix, 2015; Niu and Shaddix, 2015).

Numerous approaches to developing models of char combustion have been discussed in the literature (Barranco et al., 2009; Rojas et al., 2012). The modelling discussed in this chapter is descriptive and the approach is primarily concerned with the combustion chemistry resulting from poor quality coal, which includes ash formation and pollutants. Generally, char burning is treated as occurring in three regions:

I. Chemical control, in which oxygen penetrates the particle at low temperatures of ≤800°C, the particle size remains constant, and the density is reduced.
II. Intermediate, pore diffusion limited, when oxygen is consumed before it can penetrate to the centre of the char particle, at temperatures of 800°C-1000°C, and the char particle size decreases with a small decrease in density.
III. Film diffusion limited, where the oxygen is consumed on contact with the surface of the char particle. The reaction rate is equal to the mass transfer rate at temperatures >1000°C, and the char burns with a decreasing particle size.

The amount of carbon in char available for reaction with oxygen is determined by the particle size and the accessible surface area of the char. Low rank coals yield porous char particles which qualitatively track the coal particle size (in contrast with the morphology of high rank coals). Although it is recognised that char combustion is influenced by the inorganics present within the char, the chemistry for relatively low-ash coal is initially simplified to that of the reaction between the accessible carbon in char and O_2 with inorganics, treated as volatile and non-volatile. The volatile inorganics are released into the gas-phase at experimentally determined rates and undergo gas-phase reactions, whereas the non-volatile inorganics undergo solid phase reactions within the burning char.

The changes in the size, apparent density, and specific surface area of a burning char particle depend upon the region in which the particle burns. In region (I), the char-oxygen reaction is at relatively low temperatures, rendering the rate of mass loss as limited to the chemical reaction rate, and a particle burns more or less uniformly throughout its volume. Its size is relatively unchanged and its apparent density varies proportionally with mass loss; in this region the intrinsic chemical reaction rate is used in the model. The char surface area per unit volume initially increases as pores are enlarged, reaching a maximum before decreasing with increasing conversion. The surface area of char is related to pores developed during pyrolysis, and these are classified as micro- and macro-pores. Micro-pores

constitute most of the surface area but do not contribute significantly to char combustion, while macro-pores are important; pore geometry has been examined and related to gas diffusion within pores, and consequently the char burning rate (Chen et al., 2011).

The descriptive model inputs a number of coal particle sizes that approximate the particle size distribution of pulverised coal, and compute the diffusion of reactant(s) to the char surface and of products moving away from the char. It is generally understood that char particles burn mostly in region (II) under conditions typical of industrial, pulverised coal-fired boilers and furnaces; particle burning rates are due to the combined effects of the chemical reaction and pore diffusion of gaseous reactants and products. Due to the oxygen concentration gradients established inside particles, and the associated distribution of the rate of mass loss due to the chemical reaction, particle diameters, apparent densities, and the specific surface areas vary with mass loss when burning in region (II). If the burning of char occurs at higher temperatures, the reaction of oxygen with char would occur in region (III), and the mass losses for the various char particles are limited by the rates of oxygen diffusion to the outer surfaces of the char particles; thus the char particle burns primarily at its periphery. The char particle's apparent density is relatively unchanged in region (III) and its diameter varies to the one-third power with mass loss.

Reaction rates (intrinsic, or chemical rate) have been obtained experimentally for region (I), but there are fewer determinations of rates for region (II) (Tseng and Edgar, 1984; Hamor et al., 1973; Libby and Blake, 1979). Models for char burning in region (II) use rate data expressed in terms of the available external surface area of the char, S, the surface pressure of oxygen, P_s, and the temperature of the burning char particle, T_p:

$$\text{Rate} = S(P_s)^n A e^{[-E/(R\ Tp)]}$$

This is expressed in terms of the available external surface area, and char combustion in region (II) occurs partly inside char pores; an account of the porosity on surface area available for reaction is factored into this approach. The char surface area for lignite particles that has undergone rapid heating found in pulverised coal flames has been measured and shown to increase the porosity under these conditions, and these data are useful in estimating the available surface for reaction (Nsakala et al., 1978). Considerable work has been undertaken to model char combustion and char morphology, and discussions in the literature point out that, in addition to describing the initial char surface area and porosity as it develops during coal combustion, modelling should include parameters that reflect the type of coal and

petrographic structure, and, in cases where appropriate, the fragmentation of char particles needs to be considered, as does the impact of various temperature-time profiles on char reactivity. Research on this area is ongoing.

The reaction of char with a molecule of O_2 produces two molecules of CO, and this leads to an increase in the total molecules of this gas at the char surface, causing a radial bulk flow of gas – individual gases diffuse relative to the bulk gaseous flow, and an assessment of this can be carried out. Equations have been derived for the steady state flow for multi-component gas around a spherical particle, assuming negligible thermal diffusion and pressure gradient with a constant total concentration.

H_2/O_2 and Hydrocarbon Reactions

The hydrogen/oxygen chemical reaction mechanism is central to combustion chemistry due to an almost ubiquitous involvement of the radicals OH and H in reactions in the flame; the major reactions are:

$H + O_2 \leftrightarrow OH + O$	primary chain branching
$O + H_2 \leftrightarrow OH + H$	regeneration of H
$OH + H_2 \leftrightarrow H_2O + H$	continuation of the chain reaction

The main competition for H is the parallel reaction (which is the primary inhibitor in H_2/O_2 flames):

$$H + OH + M \leftrightarrow HO_2 + M$$

and

$$H + OH + M \leftrightarrow H_2O + M \quad \text{primary chain termination step}$$

The formation of water consumes two radicals; the third body combination of H and O to form H_2 and O_2 is also a termination step. This scheme is minimal and does not include other reactions, such as those of H_2O_2, which are relevant at lower temperatures. A detailed discussion is given by Miller et al., (2005). It is noteworthy that comprehensive schemes of fuel oxidation chemistry and kinetics have been developed for studies of internal combustion engines, and the complete mechanism consists of 9,220 reactions and 2,768 species, with 481 reactions and 179 species specific to the iso-octane sub-mechanism. Nonetheless, this scheme is still considered incomplete – further illustrating the extreme complexity of the chemical

kinetics of combustion. The results from such comprehensive modelling have been compared with experimental data and, where the data required, rates have been modified to better model measurements (Atef et al., 2017).

The combustion scheme discussed for the descriptive model of brown coal combustion and ash fouling studies uses 31 reactions dealing with the combustion of CH_4 and C_2H_6; the computed results have been compared to published values of concentration and temperature profiles for the representative species (Quiceno et al., 2002). Additional insights on pollutants, such as NOx, are obtained, for example, from lean premixed methane combustion, discussed in the literature on turbulent methane flames with detailed chemical kinetics (Aspden et al., 2016).

The computed results from the coal combustion and ash chemistry scheme outlined here have been shown to be in reasonable agreement with measured values of the concentrations of selected radicals, sulphur, nitrogen, sodium, and chloride species.

Sulphur and Nitrogen Chemistry

Coals containing relatively high levels of sulphur are problematic as they create sulphur oxides, which contribute to atmospheric pollution and acid rain. A detailed sulphur chemical kinetics scheme requires reactions involving hydrogen sulphide and sulphur oxide species that yield SO_2 and SO_3 during combustion, which then would react with inorganics to form sulphates (gasification chemistry yields sulphides). The descriptive scheme discussed here requires an additional routine to deal with the formation of Na_2SO_4, which may also undergo homogeneous and heterogeneous condensation.

As coal particles are heated, organic sulphur, pyrites and sulphates undergo thermolytic reactions to release gaseous sulphur species. Sulphur is distributed between char and tar, and, as gaseous H_2S and SO_2, the relevant proportions of these depend on the temperature, coal composition, and availability of oxygen. Detailed sulphur reaction schemes for coal flames have been proposed; the scheme discussed here used 38 reactions after the release of sulphur during devolatilisation. A sulphur reaction scheme of 48 reactions has been reported for a coal combustion model (Ströhle et al., 1986; Baruah and Khare, 2007).

The major reactions commence with the release of sulphur from coal as H_2S, which then undergoes hydrogen abstraction, oxidation and branching:

$H_2S + X \leftrightarrow SH + HX$	(where X = H, OH, or O)
$SH + O \leftrightarrow SO + H$	the SH radical undergoes oxidation, producing SO and S
$SH + O \leftrightarrow S + OH$ $SH + H \leftrightarrow S + H_2$	
$S + H_2S \leftrightarrow SH + SH$	concentrations of O are depleted, branching is predominant
$S + OH \leftrightarrow SO + H$ $S + O_2 \leftrightarrow SO + O$	S oxidation to SO
$SO + O_2 \leftrightarrow SO_2 + O$ $SO + OH \leftrightarrow SO_2 + H$	major routes to SO_2 formation
$SO_2 + O + N_2 \leftrightarrow SO_3 + N_2$	oxidation into SO_3

SO_3 formation is slow and does not reach equilibrium in a flame, whereas other reactions involving sulphur species are rapid and reach equilibrium concentrations. The major reactions shown above are of a scheme that has proven sufficient for modelling the chemistry of sulphur during combustion and the formation of Na_2SO_4, $CaSO_4$, and SO_2/SO_3.

The combustion chemistry involving nitrogen is determined to a large extent by fuel rich and fuel lean conditions, and these reflect the availability of oxygen to take part in reactions with nitrogen species. The interplay between fuel rich and fuel lean conditions is the basis for low NOx burners. A combination of low NOx coal burners with other primary measures has been shown to reduce NOx levels by up to 74%, and low NOx coal burners have been developed for full scale plants; these have been reported to be used in over 370 coal-fired units, totalling a generation capacity of more than 125 GWe (DOE, 1996; Chacón et al., 2007).

Nitrogen is present as organic groups in coal, and the formation of NOx has been extensively studied; the chemical kinetics and combustion phenomena relevant to NOx formation and reduction are well-developed. The overall chemistry relevant to the combustion and ash formation scheme discussed here can be summarised as:

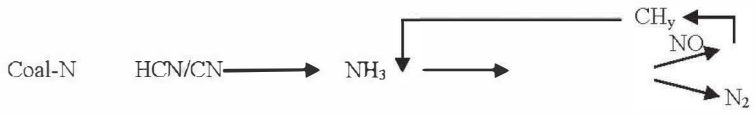

Generally, a nitrogen chemistry scheme requires the species HCN, CN, NCO, NH_3, NH_2, NH, N_2, N_2O, NO, and HNO. Fuel nitrogen forms mainly HCN, CN, and NH_3, which then undergo rapid gas phase reactions. The rate of NO formation from atmospheric N_2 is given by the Zeldovich reactions:

$$O + N_2 \leftrightarrow NO + N$$
$$N + O_2 \leftrightarrow NO + O$$
$$N + OH \leftrightarrow NO + H$$

Prompt NO has been thought to result from reactions of nitrogen with hydrocarbon radicals that form the following species (Fenimore, 1972; Iverach, 1973):

$$CH + N_2 \leftrightarrow HCN + N$$
$$C + N_2 \leftrightarrow CH + N$$

Mechanistic studies also indicate the involvement of CH and C_2O radicals in the formation of prompt NO in hydrocarbon flames (Konnov, 2009). A number of factors impact on the amounts of HCN and NH_3 released from coal particles, including heating rates and residence times in a coal flame (Tsuouchi, 2003).

The Chemistry of Inorganics and Minerals with Coal

The descriptive model of coal combustion and ash formation includes the following pathways:

1. Release of volatile alkali, particularly sodium, and potassium if present in the coal.
2. Reactions of magnesium, iron and calcium as char burns, to form ash.
3. Formation of various solid phases of ash within burning char.
4. Condensation of gaseous inorganics.

The relative proportion of ash in char particles increases as the carbon is consumed, while sodium volatilises and forms mainly NaOH, NaCl, and

Na_2SO_4 (Srinivasachar et al., 1990); the sodium species undergo heterogeneous condensation on particulates as the gaseous temperature is reduced with the gas passing through the boiler. If conditions warrant, homogeneous condensation may also occur. Magnesium, iron, calcium and aluminium species form various phases within burning char, and small amounts of these are released as gas-phase species in a coal flame, which can form aerosols. Some low quality coals contain trace amounts of toxic inorganics, such as mercury, and these are released from burning char and exit the boiler as part of the ash. Some of the ash impacts on heat transfer surfaces to form deposits. If there is sufficient sodium, silicates, and low melting point phases of the Mg/Ca/Fe mixture, the result is liquid and semi-liquid particles that accumulate on surfaces to form molten deposits.

The remainder of the ash exits the boiler and is captured as fly ash. Fine particulates often escape with SOx and NOx (and HCl for high chloride coals) in the flue gas which is released into the atmosphere. Acidic gases may form a corrosive condensate with the moisture in the flue gas, causing dew point corrosion, which can be prevented by maintaining high flue gas temperatures (usually 150-200°C). High flue gas temperatures, however, would further reduce the efficiency of power generation.

The major ash forming inorganics in low rank coals include sodium, potassium, magnesium, calcium, silica, aluminium, iron, sulphur and chloride – but coals can often contain numerous other minor inorganic species.

Sodium is a major factor in ash fouling and numerous studies have been carried out on sodium chemistry during the combustion of coal (Gronhovd et al., 1967; Guo et al., 2017). Sodium may be present as NaCl inclusions (less frequently as Na_2SO_4 inclusions), and as Na bound in the coal structure *via* carboxylic acid groups. These forms of sodium vaporise at the high coal flame temperatures, generating atomic Na, with NaOH and NaCl. Sodium and potassium may also be present as components in extraneous minerals such as feldspar [$(K,Na)_2OAl_2O_36SiO_2$], which form molten particles in a coal flame, and at high temperatures may also release vapour sodium and potassium species. The degree and rate of the volatilisation of sodium has been shown to vary depending on the forms of sodium and the nature of the ash-forming constituents, and this is particularly relevant to advanced fluid-bed coal technology (Naruse et al., 1998). Recent studies of biofuels also show that the behaviour of potassium and sodium compounds present in these substances are important factors in their utilisation as fuels; the morphologies of deposits observed from these fuels indicate that the deposition path for alkali salts includes the thermophoresis of aerosols, which may occur in the thermal boundary layer next to the deposition surface, and in the external gas stream (Capablo, 2016).

Sodium species in coal undergo various chemical changes on heating, and are released into the gas phase where they are rapidly distributed as steady state concentrations. The rate of release of sodium can be determined by measuring the concentrations of atomic Na as a coal particle is rapidly heated, using a graphite tube furnace and atomic absorption spectrometry (AA), discussed in Chapter Two. The concentrations of atomic sodium can be directly related to the concentrations of the other gaseous species using kinetics and thermodynamic computations, and in this way the behaviour of sodium *in toto* is obtained from the experimental data. Measurements of the concentrations of atomic Na can also be made using AA at specific heights of a methane burner fed with a constant stream of narrow-sized coal particles. Gaseous sodium species are also measured using laser techniques, such as excimer laser fragmentation fluorescence (Schürmann et al., 2007), and excimer laser photodissociation of gaseous NaOH and NaCl (Chadwick et al., 1995).

An example of a measurement of the release of sodium from low rank coal particles is shown in Figure 4-3; this is the growth and loss curve for the vaporisation of sodium from rapidly heated brown coal particles, and also from NaCl, measured in a graphite furnace heated at a rate of 1200°C s^{-1} in an inert atmosphere. The data show gaseous Na is observed at temperatures below peak coal-flame temperature typical for pulverised coal-fuelled plants. Additional experimental data show that sodium carboxylate dissociates over the temperature range 400-800°C, forming Na_2CO_3, which then decomposes to yield gaseous sodium moieties, including atomic Na, as the temperature approaches 900°C. As shown in Figure 4-3, a solution of NaCl also yields a similar Na profile on heating, and complete vaporisation occurs at temperatures of 1000-1100°C. The following is a summary of the chemistry of NaCl and sodium in coal as small particles of low rank coal are heated:

$$[\text{coal(NaCl)}] \rightarrow \text{char} + \text{volatiles} + \text{Na(g)} + \text{HCl}$$
$$[\text{coal(COO)(Na)}] \rightarrow Na_2CO_3 \rightarrow \text{Na(g)} + \text{NaOH(g)} + \text{char} + \text{volatiles} + CO_2$$

The experimental data on sodium atomisation are consistent with a mechanism of the form:

$$[\text{Na}] \xrightarrow{k_f} [\text{Na}](g) \underset{k_r}{\overset{k_d}{\leftrightarrow}} [\text{Na}](d)$$

In this scheme, [Na] is the concentration of un-atomised sodium, [Na](g) is the concentration of detected gaseous sodium, and [Na](d) represents atomic sodium outside of the analytical path length; k_f and k_d are first order forward rate constants, and k_r is the reverse rate.

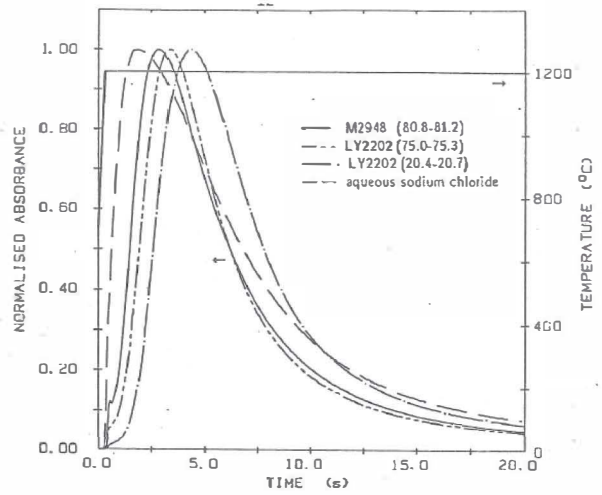

Figure 4-3. Profile of atomic Na released from brown coal particles (diameter in brackets, μm) heated within a graphite tube; brown coal samples from Morwell and Loy Yang mines (Campisis and Domazetis, 1990).

Na atomisation profiles for a number of coal particles of 75 to 106 μm size, heated at a rate of 1667°C sec^{-1} from 700°C to 1200°C, are similar to those from a solution of NaCl and Na_2SO_4, but as shown in Figure 4-3, the NaCl profile appears before that of coal particles, indicative of additional time required to heat the coal particle prior to volatilisation. Results for larger coal particles confirmed that this increase in the time taken to reach the Na peak profile is due to the coal particle size. Additional experiments using slower heating rates indicate sodium present in coal associated with carboxyl groups is volatilised before the NaCl present in the coal particles. The measured release profiles of sodium from Beulah lignite and Loy Yang brown coal are similar, but the Beulah Na peak occurs before that of Loy Yang – the observed difference is due to a higher proportion of Na in Beulah lignite.

Rate constants in the Arrhenius form obtained from the experimental measurement of Na and the temperature profile of the gas provided activation energy of 102 ±8 kJ mol^{-1}; if the graphite furnace wall

temperature profile is used, the activation energy is 146 ±10kJ mol^{-1}. These rate constants k are:

$k=3200 \exp(-102000/RT)\ s^{-1}$ (based on the measured temperature of the gas phase)
$k=4200 \exp(-146000/RT)\ s^{-1}$ (based on the temperature of the wall of the graphite furnace)

Experimental measurements, coupled with chemical kinetics modelling in lean flames, demonstrate that Na profiles roughly track the decay of H atoms. The release of a great deal of sodium from brown coal would occur as char burns. Measurements have also been reported for sodium release from a 6mm coal particle suspended in a methane burner (van Eyk et al., 2008)–these data are based on larger coal particles that differ from the mean diameter of ~40μm for pulverised coal particles fed to boilers, for which the large size cuts off at ~110μm (or 0.1mm). A mechanistic scheme has been proposed for sodium release from such a large coal particle, based on the forms of sodium present, but it is unclear how this scheme may deal with the chemical kinetics of sodium in a coal flame (van Eyk et al., 2011).

The chemical kinetics of sodium in coal may be described by >20 reactions; the dominant ones are (Hynes et al., 1984):

$$Na + H_2O \leftrightarrow NaOH + H$$
$$Na + O_2 + M \leftrightarrow NaO_2 + M$$
$$NaO_2 + H \leftrightarrow NaO + OH$$
$$NaOH + OH \leftrightarrow NaO + H_2O$$

The important H_2/O_2 reactions relevant to the gas-phase sodium chemistry are:

$$H + O_2 + M \leftrightarrow HO_2 + H$$
$$OH + M \leftrightarrow O + H + M$$

Sodium concentrations closely follow H-atom decay. Reactions sensitive to flame conditions are:

$$Na + O_2 + M \leftrightarrow NaO_2 + M$$
$$Na + H_2O \leftrightarrow NaOH + H$$
$$NaO_2 + H \leftrightarrow NaO + OH$$

Sodium hydroxide is the dominant sodium compound in coal flames, but at a high flame temperature of >2000°C, atomic sodium persists for longer periods of time at levels comparable to NaOH. These sodium species would subsequently react with chloride, sulphur, and alumina-silicates; experimental data is consistent with this, as shown by a decrease in atomic sodium concentrations measured in mixtures of sodium, chloride, sulphur, and silica moieties.

The following Na-Cl mechanism has been used to model its behaviour in a flame:

$$\begin{aligned} Na + Cl + M &\leftrightarrow NaCl + M \\ Na + ClO &\leftrightarrow NaCl + O \\ NaO_2 + Cl &\leftrightarrow NaCl + O_2 \\ Na + HCl &\leftrightarrow NaCl + H \\ Na + Cl_2 &\leftrightarrow NaCl + Cl \\ NaOH + HCl &\leftrightarrow NaCl + H_2O \end{aligned}$$

The bulk of chloride in coals is present as NaCl (occasionally, small amounts of organic chloride have been detected). Chloride originates from the NaCl kinetics scheme, and the major chloride species is HCl, with Cl, Cl_2, and ClO forming the relevant species in a Cl kinetics scheme.

$$\begin{aligned} H + Cl_2 &\rightarrow HCl + Cl \\ ClO + CO &\rightarrow CO_2 + Cl \end{aligned}$$

Organic chloride may be modelled as C_2H_5Cl.

$$\begin{aligned} C_2H_5Cl + H &\rightarrow HCl + C_2H_5 \\ C_2H_5Cl + Cl &\rightarrow Cl_2 + C_2H_5 \end{aligned}$$

The final products from coal combustion are HCl and NaCl. Results from the chemical kinetics simulation for the distribution of sodium species have been compared to data obtained using standard thermodynamics calculations (Srinivasachar et al., 1990), and some of these results are shown in Table 4-3.

As noted previously, thermodynamics calculations are equated with those obtained from chemical kinetics when equilibrium has been reached for the particular system. It is reasonable to assume that both thermodynamic and chemical kinetics computations should provide similar results given an appropriate temperature and time, and results are listed in Table 4-3 for a relatively short period of 10 seconds and a higher temperature, which would

be relevant for kinetics, and for 100 seconds and a lower temperature, when equilibrium is anticipated. At 100 seconds, both kinetic schemes and thermodynamic computations provide comparable results for concentrations of NaOH, HCl and NaCl.

Table 4-3. Sodium and chloride species from chemical kinetics and thermodynamics calculations.

Species	Temperature K	Time (secs)	Mole fractions	
			Kinetics	Thermodynamics
Na	1800	10	0.72×10^{-7}	0.13×10^{-6}
	1400	100	0.12×10^{-8}	0.39×10^{-8}
NaOH	1800	10	0.29×10^{-5}	0.19×10^{-5}
	1400	100	0.15×10^{-5}	0.16×10^{-5}
NaCl	1800	10	0.73×10^{-7}	0.37×10^{-7}
	1400	100	0.61×10^{-6}	0.40×10^{-6}
HCl	1800	10	0.20×10^{-5}	0.20×10^{-5}
	1400	100	0.14×10^{-6}	0.16×10^{-6}

Gas phase sodium and sulphur chemistry for the formation of Na_2SO_4 are based on condensation schemes, but the scheme is difficult to model due to the absence of experimental data on vapour phase Na_2SO_4. A simple sodium sulphate formation scheme may be used, based on rapid gas phase chemistry, and on the hypothetical intermediates $NaSO_2$ and $NaSO_3$ (Campisi and Domazetis, 1990):

$$NaOH + SO_2 \leftrightarrow NaSO_2 + OH$$
$$NaSO_2 + OH \leftrightarrow NaSO_3 + H$$
$$NaOH + SO_3 \leftrightarrow NaSO_3 + OH$$
$$NaSO_3 + NaOH \leftrightarrow Na_2SO_4 + H$$

As measured rate constants are not available, this speculative scheme uses estimated forward rates, combined with equilibrium constants, to reproduce concentrations of sodium sulphate measured experimentally (Fryburg et al., 1977). A global approach can also be used which relies on the thermodynamic constant for Na_2SO_4 formation, coupled to computational routines dealing with the condensation of gaseous sodium compounds:

$$2NaOH + SO_3 + O_2 \leftrightarrow Na_2SO_4 + OH + O + H \quad \text{(gas phase)}$$
$$Na_2SO_4 \leftrightarrow Na_2SO_4\,(c) \quad \text{(condensed phase)}$$

Gaseous atomic species have also been observed for Mg, Fe and Ca from coal particles heated in a graphite furnace over the temperature range 900-2500°C, and results for Loy Yang brown coal are shown in Figure 4-4. At post-coal flame, these would rapidly form fine particulates, while the bulk of Mg, Fe and Ca species remains in the char particles and undergoes solid/liquid phase reactions, discussed below. The surface temperature of a burning char particle is greater than the bulk temperature in coal-fuelled boilers, which indicates that small amounts of gas-phase Mg and Fe are present at the high temperatures of burning char particles (Mitchell et al., 2007).

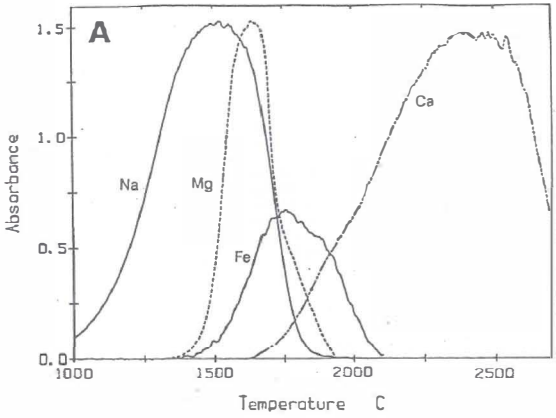

Figure 4-4. Gaseous profiles of atomic species from Loy Yang brown coal.

Pronounced concentrations of vapour magnesium have been observed when coal particles are heated at rates of 1000°C s^{-1} at temperatures between 1162°C and 1262°C. The activation energy correlates well with the Mg-O bond dissociation energy (Sturgeon et al., 1976):

$$MgO(s) \leftrightarrow MgO(g) \rightarrow Mg(g) + O(g)$$

Measurements of the Fe atomisation profile indicate Fe(g) formation from coal particles at about 1300°C. The reduction of FeO by carbon is thermodynamically favoured at >727°C. The onset of Fe(g) formation from aqueous solutions placed in a graphite furnace occurs at 1350°C.

Calcium sulphide is thought to form within coal particles, which subsequently decomposes into CaO in the coal flame. $CaSO_4$ is formed post flame by reactions between CaO and SO_2/SO_3. Simplified reaction schemes

may be constructed for calcium in coal with sulphur species, such as reactions with H_2S and SO_2, and for the formation of CaS during coal devolatilisation (Freund, 1984). The main interest is in the retention of SO_2/SO_3 by CaO; reaction(s) of CaO with sulphur species is mostly centred on sulphur capture, particularly in coal fluid-bed combustion. The reactions of sulphur dioxide with 35–85 μm diameter particles of porous CaO have been studied with TG, which indicate two reactions may occur:

$$CaO + SO_2 \rightarrow CaSO_3$$
$$CaO + SO_2 \rightarrow \tfrac{3}{4}CaSO_4 + \tfrac{1}{4}CaS$$

The small porous CaO particles used in this study prevented the reaction rates from being controlled by the diffusion of SO_2; further reaction with SO_3 is not considered to play a part, as $CaSO_3$ is unstable above 850°C, and the slower reaction that forms $CaSO_4$ occurs above this temperature (Allen and Hayhurst, 1996). Sulphur oxides are removed using calcium oxide/hydroxide.

A quantitative study has been carried out to determine the influence of inlet sulphur dioxide concentration over the range of 600ppm to 3000 ppm, at a relative humidity, with a reactor temperature of 56-86°C, and different amounts of inorganic additives (NaCl, $CaCl_2$ and NaOH) on gas desulphurisation. The results of this study show that the reaction rate does not depend on sulphur dioxide partial pressure and that the temperature and the relative humidity have a positive influence on the reaction rate. A lower apparent activation energy per mol-$Ca(OH)_2$ was estimated for the sulphur retention reaction, and the addition of calcium chloride can result in higher sulphur dioxide removal (Izquierdo et al., 2000).

The reaction between sodium and silica has been shown to occur at temperatures between 1000°C and 1200°C with gaseous NaO(g) and Na(g); the reverse occurs at temperatures above 1200°C. The chemistry is summarised as:

$$[Na(OOC\text{-}coal)]\{(coal)\ NaCl, Na_2SO_4\} \text{ on combustion yields } Na(g), NaO(g)$$
$$NaO(g) + Na(g) + SiO_2 \xrightarrow{<1200^\circ C} Na_2SiO_3$$
$$Na_2SiO_3 + 3C \xrightarrow{>1200^\circ C} 2Na(g) + Si + 3CO$$

Additional chemistry has been proposed for reactions between sodium carbonate and silica during the gasification of brown coal (Kosminski et al., 2006).

$$Na_2CO_3 + 4SiO_2 \rightarrow Na_2SiO_3 + 3SiO_2 + CO_2$$

The chemistry of mineral particles is complex; generally, minerals form semi-molten and molten phases at elevated temperatures (Vargas et al., 2001). Minerals containing sodium and potassium also undergo reactions leading to the formation of gaseous sodium and potassium.

Condensation of Gaseous Inorganic Compounds

Coal combustion chemistry involves numerous gaseous and solid species, and the detailed chemical kinetics model briefly discussed here provides a distribution of all products, including gaseous species in a coal flame; these reach steady-state concentrations, and ultimately an equilibrium distribution at post-coal flame. The gaseous inorganics consist of numerous compounds, and the ultimate distribution of the gaseous and solid compounds at post-flame may be estimated using thermodynamics computations. In this manner, experimental data from a coal flame can be compared with data obtained from chemical kinetics calculations, and data obtained post-flame can be compared with results from thermodynamic computations. An example of the number of inorganic compounds distributed in boilers post-flame, particularly sodium compounds, is given in Table 4-4. Thermodynamic computations can be carried out using as input the coal composition, the amount of air, and the temperature in boilers, and the output is the distribution of compounds that form in a boiler. The inorganic compounds NaCl, Na_2SO_4 and NaOH may undergo reactions with solid phases such as SiO_2 and also condense into liquid or solid phases. As the gases flow over heat transfer surfaces, the gas temperature falls, and the condensation of sodium compounds can occur through two processes:

- Heterogeneous condensation – gas phase molecules make contact with solid and liquid ash particles in the gas flow and condense as a liquid at the surface.
- Homogeneous condensation – gas molecules come together to form a droplet of a size such that surface tension keeps the molecules bound to the droplet.

Small amounts of vaporised MgO and FeO form fine particulates, and these may also provide nucleating centres for the condensation of sodium sulphate and sodium chloride.

Table 4-4. Thermodynamic distribution of major inorganics from Loy Yang brown coal

Gases: N_2, O_2, CO, H_2O, SO_2, SO_3, NO, NO_2, Na, NaCl, NaOH, NaCl, NaO, Na_2SO_4, Na_2Cl_2, HCl
Liquids/Solids: NaCl, NaOH, Na_2CO_3, Na_2SO_4, $CaSO_4$, $MgSO_4$, $FeSO_4$, $Fe(OH)_3$, Al_2O_3, Na_2O, Na_2SiO_3, Na_2SiO_5, $NaAlSiO_4$, $NaAlSi_2O_6$, $MgSiO_3$, $MgSiO_4$, CaO, $CaSiO_3$, $CaMgSi_2O_6$, $MgFe_2O_4$, $MgAl_2O_4$, Fe_2SiO_4, MgO, SiO_2.

A distribution of condensed particulates and of ash has been determined experimentally with a drop-tube furnace, and Table 4-5 lists the results obtained for Loy Yang brown coal. The data show the proportion of ash (ash collected with a cyclone) is greater than condensed ash (collected using a filter). The collected condensed ash consists of sodium compounds with small amounts of other inorganics, which are likely to be fine particulates formed from small amounts of gaseous Mg, Fe and Al that form aerosols. With increasing temperature, the proportion of Cl increases relative to S, indicating NaCl is favoured at higher temperatures. Ash collected at 500-600°C contained condensed salts and some molten ash. At the collection disc temperature of 700°C, the deposit consisted of strongly adhered ash of the following elemental composition: 19% Na, 16% Cl, 10% Mg, 5% S, 5% Si, 5% Al, and 40% Fe (Vuthaluru et al., 1990).

Chemical kinetics simulation for a methane burner fed with aerosol solutions of sodium compounds provided concentration profiles of sodium at various vertical distances of the burner, at fuel rich (reducing) and fuel lean (oxidising) burner operation. Additional data were provided by experiments using laser-induced photo-dissociation and fluorescence, which confirms sodium chloride vapour levels in coal combustion gases at 950-1000°C. Results from high chlorine Loy Yang coal show a linearly increasing fluorescence signal with an increasing coal particle feed rate. The relative measurements from the combustion of five U.S. coals with differing chlorine contents yielded normalised NaCl signal intensities strongly dependent on coal type, and an increase in signal strength with an increasing total chlorine content of the coals. This chlorine level was consistent with equilibrium calculations at the dilute conditions of the experiments, and at realistic post-flame oxygen concentrations. Chemical kinetics calculations for the sodium/chlorine/oxygen/hydrogen system indicated that steady state

concentrations would be achieved rapidly under the conditions of these experiments (Helble et al., 1992).

Table 4-5. Distribution of ash (a), and analyses of condensable particles (b).

(a) Amounts of ash

Gas temp. (°C)	**1000**	**1100**	**1250**
Cyclone ash (gm)	0.0096	0.0129	0.0084
Filter ash (gm)	0.0063	0.0048	0.0150
Coal used (gm)	1.9	2.82	4.05
Ash recovery (%)	28.8	21.7	19.9

(b) Composition of condensed ash

Temperature(°C) / Element(%)	1000	1100	1250
Na	45	45	45
Mg	3	2	1.7
Ca	<0.1	0.4	-
S	30	25	22
Fe	8.5	5.2	3.5
Al	6	3.5	2.8
Si	2	2	1.8
Cl	4	15	23
Na/Cl (ratio)	11	3	2

Drop-tube furnace experiments have also been reported on the formation of particulates and alkali compound interactions for two coals. A bimodal particle size distribution of ash was observed for both coals, due to different inherent minerals in them. Sodium- and potassium-enriched fine particulates were also observed for both coals. The enrichment of alkali compounds' vapour was due to the chemical reactions of the particulates, and the homogeneous condensation of alkali compounds (Takuwa et al., 2006). Adding kaolin to these coals enhanced heterogeneous condensation, causing a decrease in the amounts of fine particles (<1 μm size) produced by the homogeneous condensation of sodium compounds (Takuwa and Naruse, 2007).

Heterogeneous condensation of Na_2SO_4 and NaCl is the dominant mechanism when the gas stream contains particulates that provide a large surface area, and the rate of cooling of the gaseous mixture is not too rapid. Under conditions typical for low rank coal-fuelled plants, the cooling rates

and dust loadings are sufficient to ensure these compounds undergo heterogeneous condensation. If the amount of sodium compounds is relatively high, and/or the cooling rates of the gaseous stream were greater, some homogeneous condensation of sodium compounds would occur; if rapid cooling occurred, this would create super saturation leading to the homogeneous condensation of sodium compounds as fine particulates.

Routines may be added to the chemical kinetics schemes to model the condensation of sodium compounds. The mathematical description of this uses equations on condensation rates in terms of the diffusion parameter and vapour pressures. At each incremental temperature-time step of the simulation, the distribution between a gas and a liquid is assessed from the equilibrium vapour concentration. The equilibrium vapour pressure P_i can be obtained using the expression

$$P_i = r\, e^{(-s/T)}$$

where r and s are constants; P_i can be replaced with an expression relating temperature and density:

$$P_i = [g]\, R\, T$$

From these, a first-order polynomial in [g], the gas phase concentration, is obtained, which can be expressed as a simple polynomial in [g] and a similar expression in [l], the concentration of liquid:

$$d[g]/dt = -A[g] + B \qquad d[l]/dt = A[l] - B$$

These equations form part of the simulated kinetics scheme which generates rates of change of gas and liquid concentrations. Details of the mathematical equations and sources of the values for the parameters are provided in the references cited. Data from simulations and measured experimental values, for typical conditions in brown coal-fuelled plants, indicate that the heterogeneous condensation of sodium compounds would usually occur, and atypical conditions are required for significant homogeneous condensation of sodium compounds.

Chemistry of Inorganics within Char

The main inorganic ash forming constituents in burning char particles (Na, Mg, Ca, Fe, and to varying degrees Al) are chemically associated

within the coal matrix and undergo a chemistry that is distinct from the minerals present as extraneous particles mixed with the mined coal.

Studies have been carried out of the thermal chemistry of various mixtures of Mg, Ca, Fe, and Al compounds, such as acetates or oxalates, mixed in a slurry of water and brown coal, and from these it may be inferred that the coal matrix plays a role in the transformations of these inorganics as the coal mixture is heated (Domazetis and Buckman, 1987). DTA/TG studies of these coal/slurry mixtures identified the formation of carbonate intermediates, which are likely to form during the pyrolysis of carboxylate groups in coal. Without aluminium compounds in the coal slurry, mixed carbonates were observed, which then decomposed on further heating into Fe/Ca and Fe/Mg mixed phases, mainly $CaFe_2O_4$, $CaFe_4O_5$, and $MgFe_2O_4$. At temperatures above 1200°C, further decomposition occurred to yield Fe_2O_3, MgO and CaO. This chemistry is summarised as follows:

$$FeCO_3 + MgCO_3 \xrightarrow{220\text{-}400^\circ C} (Fe,Mg)CO_3$$

$$FeO + CaCO_3 \xrightarrow{450\text{-}600^\circ C} FeO.CaCO_3$$

$$3(Fe,Mg)CO_3 \xrightarrow{700\text{-}750^\circ C} (Fe,Mg)Fe_2O_4 + 2MgO + 3CO$$

$$2(FeO)CaCO_3 \xrightarrow{840^\circ C} CaFe_2O_4 + CO$$

$$2CaFe_2O_4 \xrightarrow{1156^\circ C} CaFe_4O_7 + CaO$$

The formation of the Fe/Ca/Mg complexes indicates that solid solution and eutectic phases may form at the temperatures encountered in the coal flame, and these would further exacerbate the fouling of boiler surfaces.

High rank coals contain appreciable amounts of pyrite, which is the main source of iron in these coals. The variability in the composition of low rank coals is also evident regarding pyrite; a TG/DTA study of two lignites, one without pyrite and another with significant amounts of pyrite, show, in the case of the latter, decomposition beginning at 400°C to form pyrrothite, which is converted into troilite (FeS) at 600°C. FeS slowly decomposes to form elemental iron during lignite pyrolysis. In these studies, the chars produced at 700°C and 800°C had a S/Fe ratio of <1.0 (Yani and Zhang, 2010). The chemistry of pyrite during coal combustion is complicated and various kinetics schemes have been developed; the products include FeO,

FeS, Fe_2O_3, $Fe_2(SO_4)_3$, S, SO_2, and SO_3. A 13-reaction kinetics scheme has been considered for FeS_2 and O_2. Components in the Fe-O-S system may coexist as intermediates in the combustion process producing a low-melting phase. In the simulation scheme discussed here, it is assumed the iron has undergone the solid phase formation chemistry outlined in the above equations.

Aluminium in brown coal generally reduces the fouling propensity because of its refractory properties, and this has prompted experiments with aluminium additives to reduce fouling from low rank coals. Additional phases thought to form with aluminium, at temperatures between 940°C and 1260°C, are $MgAl_2O_4$, $FeAl_2O_4$, $FeAl_2O_4$, $MgAl_2O_4$ and $CaFe_2O_4.3CaOAl_2O_3$. TG/DTA data for Ca/Al and Mg/Al systems indicate that, at 439°C and 462°C, the following occurs:

$$x(CaCO_3)\bullet y(Al_2O_3)\bullet zH_2O \rightarrow x(CaO)\bullet y(Al_2O_3) + xCO_2 + zH_2O$$
$$x(MgCO_3)\bullet y(Al_2O_3)\bullet zH_2O \rightarrow x(MgO)\bullet y(Al_2O_3) + xCO_2 + zH_2O$$

The presence of many of the extraneous mineral particles in low rank coals would add to their fouling propensity, as many of these minerals may form molten and semi-molten ash particles, and those containing sodium and potassium also contribute to the concentration of the gas phase species discussed above.

Validation of Models and Chemical Reaction Schemes

The purpose of the simulation scheme developed for low rank coal combustion and ash formation was to identify the species and reactions that are the cause of ash fouling in boilers and from this devise an approach to mitigate or eliminate ash fouling. The chemical scheme discussed here has included a wide range of chemical reactions, and as mentioned, the size and complexity of the scheme has necessitated a number of simplifications, and consequently the results from these calculations need to be validated by comparing them with experimental measurements, as far as is practical. Data may be obtained from measurements of laboratory flames, drop-tube furnaces, pilot plants, and to a lesser extent from large plants. Measurements using laboratory flames provide data on the kinetics, particularly on the combustion of hydrocarbons, while data from coal-fuelled plants are usually at steady-state or equilibrated conditions. Schemes of hydrocarbon flames that contain the inorganics discussed in this chapter require measurements of the gas phase concentrations of various species of these inorganics. Events at post-flame conditions include ash and pollutants formations, and

these are often validated with data obtained by collecting and analysing ash samples from drop-tube furnaces and pilot plants for analysis, while samples of sulphur oxide and hydrogen chloride can be obtained from flue gases.

Advanced computational models can provide a general treatment of coal combustion applicable to the design and performance of relevant plants, but these often do not provide the required details of the chemistry that encompasses coal combustion with ash formation and pollutants. This is because the complexity of such a scheme increases enormously if it is applied to full scale coal-fuelled boilers. Commercial packages, however, can be configured to deal with specific details. CHEMKIN™ is an example of a comprehensive chemical kinetics scheme that has been developed over a number of decades; this software suite has a wide range of applications, including combustion and chemical processing, and was developed at the Sandia National Laboratories. It has capabilities that incorporate complex chemical kinetics into simulations of reacting flow. This package is a good example of models with the capability to investigate many reaction schemes, and is used for a comprehensive understanding of a particular process involving multiple chemical species, concentration ranges, and gas temperatures. The literature also contains examples of flame simulations and various experiments that can be considered for the validation of a particular model. GateCycle™ is an example of a package that deals with the design of coal-fuelled plants that uses very general treatments of ash formation and fouling.

The validation of reaction schemes for hydrocarbon flames often consider data on the rate of consumption of fuel (e.g. methane) and the concentrations of O/H radicals in the flame. There is a growing body of work in the literature that deals with turbulent premixed methane flames with detailed kinetics. Two examples can briefly illustrate such computations; one is of a two-dimensional rich premixed laminar methane-air flame and the other is a 3D numerical simulation of a premixed methane burner. In these, the emphasis was on the comparative analysis of spatial distributions of CO concentrations with temperature for a range of mixtures using two reaction mechanisms to examine the suitability of such mechanisms. Computed results were compared with experimental data; simulations were conducted using a mechanism involving 16 reactive species with 46 reactions steps. Measured and calculated data were in good agreement in terms of spatial distributions as well as in their peak values of CO concentration and temperature for given cases. A second study used a reduced mechanism (16 reactive species and 25 reactions) for richer flames, yielding a good quantitative agreement for CO concentration and temperature.

A significant difference in the CO concentration was observed near the diffusion flame zone. The estimated CO concentration reached a maximum at a distance of 8.5mm in the lateral direction away from the axis line, while the experimental values fell to zero at 6 mm. Calculations exhibited acceptable trends at all elevated flame heights, showing that, with the increase in the equivalence ratio, the flame height increased and the maximum CO concentration decreased (Reddy Muppala et al., 2007).

The second example consists of the study of turbulence with lean premixed methane flames using direct numerical simulation with detailed chemistry. The conditions were close to those found in atmospheric laboratory experiments. The diffusion of atomic hydrogen was shown to be related to the observed curvature correlations, but this did not have a significant impact on the thickening of the preheat zone (Aspden et al., 2016).

The modelling and measurements of large scale coal-fuelled plants are not as detailed as laboratory flames; an example is a tangentially lignite-fuelled boiler. For this, in the near-field of the burner jets, the coal particles undergo pyrolysis and volatile matter is driven from the particle, but only a limited amount of combustion occurs, therefore turbulent mixing in the near-field of the jets is thought to be less crucial. These coal burners are designed to heat the coal and air by mixing them with entrained hot furnace gases and delivering them to the correct location in the centre of the furnace. Near-field aerodynamics is important for entrainment and to ensure the jets of coal and air reach the centre of the furnace at the correct location and with sufficient momentum to generate the required swirl. The level of combustion in the near-field is low enough that aerodynamics is sufficiently decoupled from the effects of intense chemical reaction and radiative heat transfer, which would otherwise alter the physical properties of the flow. Isothermal modelling is expected to give a reasonably good indication on how the jets from different burner geometries deliver the fuel stream and mix it with the surrounding hot combustion gases within the furnace (Hart et al., 2009).

Validation of the hydrocarbon kinetics scheme outlined here for combustion and ash-forming inorganics has been performed by comparing computed results with data from flat-flame methane burners (Peeters and Mahnen, 1973); the data compared reasonably well with simulated results for the consumption of methane and oxygen, and the concentrations CO_2 and CO, with time (or burner height), but the simulated results occurred at a period of between 3-5ms, whereas the measured profiles were from 0.5-5msec. The concentrations as mole fractions of measured and computed radicals are:

Species (mole fraction)	Measured	Computed
OH	0.03	0.02
H	0.005	0.01
O	0.02	0.04

The differences in time are due to the assumption of an idealised perfectly stirred reactor for the simulation scheme, whereas in reality, fluid flow and heat transfer are important factors that increase the time factor.

Simulation results for sulphur species for an $H_2/O_2/SO_2$ flat-flame burner were also compared with measured values by Zachariah and Smith (1987):

Species (mole fraction)	Measured	Computed	Time (ms)
SO_2	0.015-0.03	0.03	15-30
SO	0.035	0.05	3-10

Measured concentrations of SO_2, SO_3 and HCl from a pilot furnace burning brown coal have been compared to calculated data from the chemical kinetics scheme outlined here, with additional routines added to simulate events relevant to coal and air fed to the pilot plant. The averaged measured data for SO_2 were 260-560 mg m^{-3} at normal temperature and pressure (NTP) on a dry volume basis, and these agreed to within 10% of the simulation data; the measured values from the pilot plant flue gases displayed a maximum variation of 20%. The measured concentrations of SO_3 were between 8mg m^{-3} and 1 mg m^{-3} at NTP on a dry volume basis, which are within the results obtained from the computer simulation scheme.

Four techniques have been evaluated to measure SO_3 by Fleig et al., (2012) in combustion gases, discussed for the oxy-combustion of coal. Average differences of less than 20% of the SO_3 concentrations were observed. Measured HCl values showed similar agreement with the simulated data, but the measured data displayed greater variation.

A sulphur chemistry sub-model has been incorporated within a computational fluid dynamics combustion simulation code to deal with heterogeneous and homogeneous reactions of sulphur species during the combustion of lignite. This dealt with the release of coal sulphur into gaseous products, the homogeneous conversion of sulphur species, and retention by alkaline earth oxides in the coal ash. The simulations included obtaining data for comparison with that from a 500kW furnace. The results for sulphur in the fuel agreed with the general trends observed for the species concentrations, but deviations were observed between the results from the simulation and the experimental data. The deviations may be

attributed to the adoption of a single-step scheme for the release of inorganic sulphur, and to the simplified treatment of SO_2 formation within the global gas phase scheme (Müller et al., 2013).

Comparisons of modelling results and experimental data have been reported for the combustion of pre-dried lignite in an entrained flow reactor. A gas stream sample was extracted and the concentrations of CO, CO_2, CH_4, SO_2 and O_2 were obtained using online gas analysis, and the concentrations of H_2S and COS were measured using gas chromatography with a mass spectrometer. The agreement between the calculated and measured values was good for CO_2, while that of CO was slightly under-predicted by the simulations at low air ratios, because of a lower char conversion rate performed by the model. The overall coal combustion process and sulphur chemistry was captured by the simulations; H_2S was released during devolatilisation and was converted into SO_2 under the oxidising conditions, and transformed into SO and H_2S under reducing conditions. Although the calculated gas concentrations were generally in agreement with experimental measurements, the model provided lower values of SO_2 because part of the sulphur remained in the coal within the devolatilisation routine, and gaseous sulphur species which would react with minerals in the fly ash were not accounted by the model. The generality of the chemical kinetics and fluid dynamics modelling enables its applicability to the combustion of fossil fuels and biomass (Capablo, 2016). The restrictions inherent in the phenomenological approach to modelling have been recognised, and it is understood that the ultimate goal for computational modelling is to perform computations at the molecular level; these matters have been discussed, for example, by Williams et al., (2001).

References

Allen, D. and Hayhurst, A. N. 1996. 'Reaction between gaseous sulphur dioxide and solid calcium oxide mechanism and kinetics', *J. Chem. Soc., Faraday Trans.*, 92, 1227-1238

Aspden, A. J., Day, M. S. and Bell, J. B. 2016. 'Three- dimensional direct numerical simulation of turbulent lean premixed methane combustion with detailed kinetics', *Combustion and Flame*, 166, 266–283.

Atef, N., Kukkadapu, G., Mohamed, S. Y., Al Rashidi, M., Banyon, C., Mehl, M., Heufer, K. A., Nasir, E. F., Alfazazi, A., Das, A. K., Westbrook, C. K., Pitz, W. J., Lu, T., Farooq, A., Sung, C-J., Curran, H. J. and Sarathy, S. M. 2017. 'A comprehensive iso-octane combustion model with improved thermochemistry and chemical kinetics', *Combustion and Flame*, 178, 111-134.

Barranco, R., Rojas, A., Barraza, J. and Lester, E. 2009. 'A new char combustion kinetic model 1. Formulation', *Fuel*, 88, 2335-2339.

Baruah, B. P. and Khare, P. 2007. 'Pyrolysis of High Sulphur Indian Coals', *Energy Fuels*, 21, 3346–3352.

Capablo, J. 2016. 'Formation of alkali salt deposits in biomass combustion', *Fuel Processing Technology*, 153, 58-73.

Chacón, J., Sala, J. M. and Blanco, J. M. 2007. 'Investigation on the Design and Optimization of a Low NOx-CO Emission burner both Experimentally and through Computational Fluid Dynamics (CFD) Simulations', *Energy Fuels*, 21, 42-58.

Chadwick, B., Domazetis, G. and Morrison, R. 1995. 'Multiwavelength Monitoring of Photofragment Fluorescence after 193 nm Photolysis of NaCl and NaOH: Application to Measuring the Sodium Species Released from Coal at High Temperatures', *Anal. Chem.*, 67, 710-716.

Chen, Y., Wang, X. and He, R. 2011. 'Modelling changes of fractal pore structures in coal pyrolysis', *Fuel*, 90, 499-504.

Cliff, D. I., Doolan, K. R., Mackie, J. C. and Tyler, R. J. 1984. 'Products from rapid heating of brown coal in the temperature range 400-2300C', *Fuel,* 63, 394.

Deuflhard, P., Bader, G. and Novak, U. 1981. 'Larkin – a software package for the numerical simulation of LARge systems arising in chemical KINetics', in K. H. Ebert, P. Deuflhard and W. Jager (eds.), *Modelling of chemical reaction systems* (Berlin: Springer-Verlag), 38-55.

DOE, 1996. *Reducing Emissions of Nitrogen Oxides via Low-NO_X burner Technologies (DOE Report Number 5)*. Available at: https://www.netl.doe.gov/File%20Lirary/Research/Coal/major%20demonstrations/cctdp/Round3/topical5.pdf ; http://www.iea-coal.org.uk/site/ieacoal/dataases/ccts/low-nox-urners

Domazetis, G. 1985. 'Ash Formation from Inorganics in Victorian Brown Coal', *Proc 1985 Int. Conference on Coal Science* (Sydney: IEA), 389-392.

Domazetis G. and Campisi, A. 1986. 'Chemical Kinetics of Coal Combustion and Pollution Formation', Research and Development Department, State Electricity Commission of Victoria, Report SO/86/104.

Domazetis, G. and Buckman, N. 1987. 'Fly Ash Formation and Sulphation During the Combustion of brown Coal, Vol 3, The Chemistry of the Formation of Ash for the Aluminium/Iron/Magnesium/Calcium System', NERDDP End of Grant Report, ND/87/049.

Domazetis, G., Campisi, A., Legg, G., Skomra, B. and Song, W. 1987. 'SCCOFF-a code for the Simulation of the Chemistry of Coal Fired Furnaces', End of Grant Report, Volume 2A, NERDDP project 933,

Research and Development Department, State Electricity Commission of Victoria, Report ND/88/046.

Domazetis, G., Campisi, A. and Zeglinski, P. 1988. 'Chemical Kinetics of Coal Combustion and Pollution Formation', End of Grant Report, Volume 2, NERDDP project 933, Research and Development Department, State Electricity Commission of Victoria, Report ND/87/047.

Doolan, K. R., Mackie, J. C. and Tyler, R. J. 1985. 'The secondary decomposition of tar vapours produced by flash pyrolysis of coal', *Int. Conference on Coal Science,* Sydney, 961.

Kautman, F. 1982. 'Chemical kinetics and combustion: intricate paths and simplest steps', *19th Symposium (Int) on Combustion,* 19, 1-10.

Fenimore, C. P. 1972. 'Formation of nitric oxide from fuel nitrogen in ethylene flames', *Combustion Flame*, 19, 289.

Fleig, D., Vainio, E., Andersson, K., Brink, A., Johnsson, J. and Hupa, H. 2012. 'Evaluation of SO_3 Measurement Techniques in Air and Oxy-Fuel Combustion', *Energy Fuels*, 26, 5537-5549.

Freund, H. 1984. 'Intrinsic global rate constant for the high-temperature reaction of CaO and H_2S', *Ind. Eng. Chem. Fundam.*, 23, 338.

Fryburg, C. C., Miller, R. A., Stearns, C. A. and Kohl, F. J. 1997. 'Formation of Na_2SO_4 and K_2SO_4 in flames doped with sulphur and alkali chlorides and carbonates', NASA-TM-73794.

Gronhovd, G. H., Wagner, R. J. and Wittmaier, A. J. 1967. 'A study of the ash fouling tendencies of a North Dakota lignite to its sodium', *Trans. Soc. Of Mining Engrs. Quarterly*, 240, 313-322.

Guo, S., Jiang, Y., Yu, Z., Zhao, J. and Fang, Y. 2017. 'Correlating the sodium release with coal compositions during combustion of sodium-rich coals', *Fuel*, 196, 252-260.

Hamor, R. J., Smith, I. W. and Tyler, R. J. 1973. 'Kinetics of combustion of pulverised brown coal char between 630 and 1200K', *Combustion and Flame*, 21, 153-162.

Hart, J. T., Naser, J. A. and Witt, P. J. 2009. 'Aerodynamics of an isolated slot-burner from a tangentially-fired boiler', *Applied Mathematical Modelling*, 33, 3756–3767.

Hecht E. and Shaddix, C. 2015. 'Coal Combustion and Gasification Science', Combustion Research Facility, Sandia National Laboratories. Available at: https://www.netl.doe.gov/File%20Library/Events/2015/crosscutting/Crosscutting_20150427_1530B_SNL.pdf

Helble, J. J., Srinivasachar, S., Boni, A. A., Charon, O. and Modestino, A. 1992. 'Measurement and Modelling of Vapour-Phase Sodium Chloride

Formed During Pulverized Coal Combustion', *Combust. Sci. Technology*, 81, 193-205.

Hynes, A. J., Steinberg, J. and Schofield, K. 1984. 'The Chemical Kinetics and Thermodynamics of Sodium Species in Oxygen-rich Hydrogen Flames', *J. Chem. Phys.*, 80, 2585-2597.

Iverach, D., Basden, K. S. and Kirov, N. Y. 1973. 'Formation of nitric oxide in fuel-lean and fuel-rich flames', *Symposium (International) on Combustion,* 14, 767-775.

Izquierdo, J. F., Fité, C., Cunill, F., Iborra, M. and Tejero, J. 2000. 'Kinetic study of the reaction between sulphur dioxide and calcium hydroxide at low temperature in a fixed-bed reactor', *J. Hazardous Materials*, 76, 113-123.

Konnov, A. A. 2009. 'Implementation of the NCN pathway of prompt-NO formation in the detailed reaction mechanism', *Combustion Flame*, 156, 2093–2105.

Kosminski, A., Ross, D. P. and Agnew, J. B. 2006. 'Reactions between sodium and silica during gasification of a low rank coal', *Fuel Processing Technology*, 87, 1037-1049.

Libby, P. A. and Blake, T. R. 1970. 'Theoretical study of burning carbon particles', *Combustion and Flame*, 36, 139-169.

Liu, Y. and He, R. 2015. 'Variation of apparent reaction order in char combustion and its effect on a fractal char combustion model', *Combust. Sci. Technol.*, 187, 1638–1660.

McAllister, S., Chen, J-Y. and Fernandez-Pello, A. C. 2011. *Fundamentals of Combustion Processes (Mechanical Engineering Series)*, New York: Springer.

Miller, J. A., Pilling, M. J. and Troe, J. 2005. 'Unravelling combustion mechanisms through a quantitative understanding of elementary reactions', *Proc. Combustion Institute*, 30, 43-88.

Mitchell, R. E., Ma, L. and Kim, B. J. 2007. 'On the burning behaviour of pulverised coal chars', *Combustion and Flame,* 151, 426-436.

Müller, M., Schnell, U. and Scheffknecht, G. 2013. 'Modelling the fate of sulphur during pulverized coal combustion under conventional and oxy-fuel conditions', *Energy Procedia*, 37, 1377-1388.

Naredi, P. and Pisupati, S. V. 2008. 'Interpretation of Char Reactivity Profiles Obtained Using a Thermogravimetric Analyzer', *Energy Fuels,* 22, 317-320.

Naruse, I., Murakami, T., Noda, R. and Ohtake, K. 1998. 'Influence of coal type on evolution characteristics of alkali metal compounds in coal combustion', *Twenty-Seventh Symposium (International) on Combustion* (The Combustion Institute), 1711–1717.

Niu, Y. and Shaddix, C. R. 2015. 'A sophisticated model to predict ash inhibition during combustion of pulverized char particles', *Proceedings of the Combustion Institute*, 35, 561-569.

Nsakala, N. Y., Essenhigh, R. H. and Walker Jr, P. L. 1978. 'Characteristics of chars produced from lignites by pyrolysis at 808°C following rapid heating', *Fuel,* 57, 605-611.

Peeters, J. and Mahnen, G. 1973. 'Reaction mechanisms and rate constants of elementary steps in methane-oxygen flames', *Fourteenth Symposium (International) on Combustion* (The Combustion Institute), 133-141.

Quiceno, R., Chejne, F. and Hill, A. 2002. 'Proposal of a Methodology for Determining the Main Chemical Reactions Involved in Methane Combustion', *Energy & Fuels*, 16, 536-542.

Reddy Muppala, S. P., Sannala, S. K. R., Aluri, N. K., Dinkelacker, F., Beyrau, F. and Leipertz, A. 2007. 'Detailed 2-D numerical simulations of rich premixed lamina methane flames for CO concentrations and temperature', *Combustion Science and Technology,* 179, 1797-1822.

Rojas, A., Barraza, J., Barranco, R. and Lester, E. 2012. 'A new char combustion kinetic model – Part 2: Empirical validation', *Fuel,* 96, 168-175.

Sajwan, K. S., Twardowska, I., Punshon, T. and Alva, A. K. (eds.). 2006. *Coal Combustion products and Environmental Issues*, New York: Springer.

Schürmann, H., Monkhouse, P. B., Unterberger, S. and Hein, K. R. G. 2007. 'In situ parametric study of alkali release in pulverized coal combustion: Effects of operating conditions and gas composition', *Proceedings of the Combustion Institute,* 31, 1913-1920.

Sendt, K. and Haynes, B. S. 2005. 'Density Functional Study of the Reaction of Carbon Surface Oxides: The Behaviour of Ketones', *J. Phys. Chem. A,* 109, 3438-3447.

Simmie, J. M. 2003. 'Detailed chemical kinetic models for the combustion of hydrocarbon fuels', *Prog. Energy Combust. Sci.,* 29, 599-634.

Smith, I. W. 1982. 'The combustion rates of coal chars: a review', *19th Symp. (Int) on Combustion* (The Combustion Institute), 1045-1065.

Solomon, P. R. and Hamlen, D. G. 1983. 'Finding order in coal pyrolysis kinetics', *Prog. Energy Combust. Sci.,* 9, 323.

Srinivasachar, S., Helble, J. J., Ham, D. O. and Domazetis, G. 1990. 'A kinetic description of vapour phase alkali transformations in combustion systems', *Prog. Energy Combust. Sci.*, 16, 303-309.

Stöllinger, M., Naud, B., Roekaerts, D., Beishuizen, N. and Heinz, S. 2013. 'PDF modelling and simulations of pulverized coal combustion – Part 1: Theory and modelling', *Combustion and Flame*, 160, 384-395.

Ströhle, J., Chen, X., Zorbach, I. and Epple, B. 1986. 'Validation of a Detailed Reaction Mechanism for Sulphur Species in Coal Combustion', *Combustion Science and Technology,* 4-5, 540-551.

Sturgeon, R. E., Chakrabarti, C. L. and Langford, C. H. 1976. 'Studies pf the mechanism of atom formation in graphite furnace atomic absorption spectrometry', *Anal. Chem.*, 48, 1792-1807.

Takuwa, T., Mkilaha, I. S. N. and Naruse, I. 2006. 'Mechanisms of fine particulates formation with alkali metal compounds during coal combustion', *Fuel*, 85, 671-678.

Takuwa, T. and Naruse, I. 2007. 'Detailed kinetic and control of alkali metal compounds during coal combustion', *Fuel Processing Technology*, 88, 1029-1034.

Tseng, H. P. and Edgar, T. F. 1984. 'Identification of the combustion behaviour of lignite char between 350 and 900 °C', *Fuel*, 63, 383-393.

Tsuouchi, N., Abe, M., Xu, C. and Ohtsuka, Y. 2003. 'Nitrogen Release from Low Rank Coals during Rapid Pyrolysis with a Drop Tue Reactor', *Energy Fuels*, 17, 940-945.

Van Eyk, P. J., Ashman, P. J., Alwahabi, Z. T. and Nathan, G. J. 2008. 'Quantitative measurement of atomic sodium in the plume of a single burning coal particle', *Combustion and Flame*, 155, 529-537.

Van Eyk, P. J., Ashman, P. J. and Nathan, G. J. 2011. 'Mechanism and kinetics of sodium release from brown coal char particles during combustion', *Combustion and Flame*, 158, 2512-2523.

Vargas, S., Frandsen, F. J. and Dam-Johansen, K. 2001. 'Rheological properties of high-temperature melts of coal ashes and other silicates', *Prog. Energy Combust. Sc.*, 27, 237-429.

Vuthaluru, H. B., Gupta, R. P. and Wall, T. F. 1990. 'Minimising ash fouling from high sodium brown coals. Vol 4. Laboratory experiments to examine the fouling characteristics of Loy Yang coal', NERDDP End of Grant Report, ND/90/058.

Williams, A., Backreedy, R., Habib, R., Jones, J. M. and Pourkashanian, M. 2002. 'Modelling coal combustion: the current position', *Fuel*, 81, 605-618.

Williams, A., Poukashanian, M. and Jones, J. M. 2001. 'Combustion of pulverised coal and biomass', *Prog. Energy Combustion Science*, 27, 587-610.

Wu, T., Lester, E. and Cloke, M. 2006. 'A Burnout Prediction Model Based around Char Morphology', *Energy Fuels*, 20, 1175-1183.

Yani, S. and Zhang, D. 2010. 'An experimental study into pyrite transformation during pyrolysis of Australian lignite samples', *Fuel*, 89, 1700-1708.

Zachariah, M. R. and Smith, O. I. 1987. 'Experimental and numerical studies of sulphur chemistry in $H_2/O_2/SO_2$ flames', *Combustion and Flame*, 69, 125-139.

CHAPTER FIVE

COAL POWER GENERATION AND ASH FOULING

Low rank coals are used as fuel for generating power in numerous countries, including Germany, Bulgaria, Greece, USA, Indonesia, India, China, and Australia. The power stations fuelled by low rank coals have often experienced adverse impacts, and financial penalties, resulting from ash deposits on boilers, fireside fouling and slagging, convective pass fouling, and corrosion; this has been extensively discussed in the literature (e.g. Fernandez-Turiel et al., 2004; Miller and Schobert, 1994; Xu et al., 2002; 2005; Harding and O'Connor, 2007). The cost of ash fouling to the US electric power industry is reported at up to $590 million per year and is the cause for about half of all unscheduled outages. A survey of US power station operators identified ash-related outages lead to poorer performances of boilers, and fuel blending was an option used by some operators to mitigate against poor boiler availability and to lower pollution emissions. Currently, the majority of low rank coal power generation is from aging subcritical power stations which experience ash-related problems and operate at low efficiency, and consequently it is highly unlikely that any future power generation would be from subcritical technology fuelled with as-mined low rank coal.

The difficulties experienced from the ash fouling of heat transfer surfaces by low rank coals have motivated empirical studies on ways to alleviate operational problems. Chemical kinetics and thermodynamics computations are useful to identify important causal factors on the fouling and slagging of plants fuelled by pulverised coal, such as the formation of gaseous alkali species and the formation of molten ash particles. Although the mechanisms of ash deposition and the growth of deposits are not completely understood, the chemistry of ash formation discussed thus far provides an understanding of the major events contributing to the fouling of boiler surfaces by low rank coals, and from this it has been possible to determine the properties required for non-fouling processed coal, and to

develop coal treatment methodologies to produce the required high quality fuel.

Ash Deposition and Fouling of Boilers

The basic features of ash fouling are of hot gases containing variable amounts of particulates, moving past heat transfer surfaces which are at lower temperatures than the hot gases. The events related to the build-up of ash deposits on heat transfer surfaces may be summarised as:

- Condensation of NaCl and Na_2SO_4 (and potassium analogues if present).
- Aerosol deposition consisting of fine particulates produced from burning char.
- Ash particles impacting on heat transfer surfaces.
- Growth of deposits as a consequence of the above events.

The composition of the fuel is responsible for the formation of particles and gases, and these behave differently for the different coals during their combustion, and thus the extent of fouling and corrosion differs for different coals. The degree of fouling and slagging from ash, which is dependent on the coal composition, is also dependent on the impact of the local gas temperatures, tube temperatures and temperature differentials, gas velocities, tube orientation, and the local heat flux. The formation of ash deposits from coal combustion is one of the most important fuel property considerations in the design and operation of commercial coal-fuelled plants, significantly influencing furnace sizing, heat transfer surface placement, and convection pass tube spacing (Bryers, 1996).

The major factors in ash-related problems in coal-fuelled boilers are:

- The formation of ash agglomerates and clinkers.
- The fouling of the convective heat recovery surfaces *via* the condensation of volatiles, the heterogeneous condensation of sulphate submicron species, and ash deposition on the tube surfaces.
- The erosion/corrosion by fly ash, and wear from the impact of soot blowers used to prevent the build-up of ash deposits.
- Tube wastage due to corroding deposits.
- Surface oxidation of tube surfaces due to higher gas temperatures created by lower heat transfer because of an excessive build-up of fouling.

- Design factors causing an imbalance in air distribution, poor burner adjustments, and poor coal particle size distribution of the fuel.

The formation of ash and slag deposits results in:

- Loss in furnace heat absorption due to excessive accumulation of molten or sintered deposits and the resulting changes in the thermal properties as the slag layer grows.
- Damage due to excessive slag falling onto heat exchange surfaces.
- Freezing of slag on hopper slopes, and build-up, leading to boiler shutdown for cleaning.
- Slag accumulations about the periphery of burners.

An approach to dealing with these problems has been to seek good quality coal to blend with poor quality coals, in proportions that would produce a feed with a lower fouling propensity; however, the wide variation in coal quality within mine locations could make blending difficult and this has caused uncertainty in the planning of the plant's performance. Consequently, the design of boilers has included measures to mitigate the impact of ash deposits on plant performance, such as using soot blowers, and operating parameters. The following is a summary of the major design and operational features that must be considered within the context of low rank coal properties:

- Coal crushing, drying, and a coal burner, for high moisture coal.
- Furnace exit temperature.
- Furnace heat absorption.
- Furnace configuration, tube size spacing, orientation, and temperature distribution.
- Specific steam conditions of temperature and pressure.
- Air distribution between burners, burner operation, and excess air/O_2 level.
- Soot blower operation.
- Changes in boiler load with ash deposit formation.

Plants fuelled with low rank coals need larger boilers and associated equipment to cope with the greater mass flow due to the high moisture in the coal, and the coal burner must be designed specifically to achieve a stable coal flame. Overall the coal quality imposes penalties, in that it requires equipment for a greater total mass flow and measures to deal with the aggressive fouling behaviour of ash (Borio and Levasseur, 1986).

Measures used to remove or inhibit ash deposit build-up have relied mainly on physical devises such as soot blowers, in addition to natural gravity-induced deposit shedding during boiler operation. Natural shedding in combustion systems may be caused by any or all of erosion, gravity shedding, and thermal shock. Gravity shedding will occur when the weight of the deposit is sufficient to fall; in the case of molten deposits, build-up causes molten deposits to flow to the hopper region and eventually force a shutdown of the boiler. The chemical composition of coal ash will determine the deposit strength, the melting temperature, and the thermal expansion of the deposit. The gas temperature will influence the deposit surface temperature and the temperature gradient within the deposit; the ash deposits formed in boilers, and the mechanism of deposits shedding, have been reviewed by Zbogar et al., (2009).

Ash fouling and boiler performance have also been examined using modelling techniques. Models have been developed which utilise a description of the flow of coal, the transport, and the sticking of ash on surfaces, and which have approximated the observed ash deposition rates in coal-fuelled boilers. A brief review of work on this area, and a modelling strategy that includes ash deposition within a coal combustion model, is given by Wang and Harb (1997). A predictive scheme based on computer controlled scanning electron microscopy (CCSEM) flyash data, and computational fluid dynamics (CFD), has been applied to model the slagging propensity of three UK coals, and to predict the deposition in a pilot scale single burner ash testing facility. The results of this model are in qualitative agreement with the pilot results, and the predictions of the relative slagging propensity of the three coals are consistent with observations. This effort has shown a preferential deposition of iron during the initial stage of ash deposition for black coal. The average compositions of the deposits became closer to that of the bulk ash when the accumulation of ash deposits was taken into account (Lee and Lockwood, 1999).

CFD modelling has been discussed for brown coal combustion using a mixture of oxygen and recycled CO_2 (oxy-combustion). This model was based on a 375 MW tangentially fired furnace at the Yallourn W power plant in Australia. Although a substantial effort has been expended to validate the model against measured operating data, this modelling did not include ash formation and fouling (Tian et al., 2009). Empirical correlations have been used to relate the ash fusion temperature with the ash chemical composition (Seggiani and Pannocchia, 2003; Browning et al., 2003). All such correlations are based on the chemistry of silicates formation, and endeavour to relate the transformations from solid to liquid phases with the relative proportions of inorganic species, such as CaO, MgO, Na_2O, K_2O,

Fe_2O_3, SiO_2, and Al_2O_3. Modelling has shown molten silicate particles are deposited when they impact on the boiler surface, and small ash particles (<5 micron) follow the flow of gases, while the motion of larger ash particles is dominated by inertia and not by turbulence, and these are likely to impact on boiler surfaces (Tu et al., 1997). Solid particles that may impact on the molten sticky surface will subsequently be incorporated within the molten silicate to form complex silicate mixtures. For such coals, an increase in coal flame temperature would usually cause an increase in ash fouling and slagging (Laursen et al., 1998).

The heterogeneity of these coals means that ash-forming components are often found in more than one chemical environment in the coal, and as a result, they exhibit several types of behaviour; it is difficult, therefore, to arrive at a general mechanism that relates all fouling behaviour with the elemental composition of the various low rank coals. This presents great difficulties to approaches that seek to reduce ash fouling by modifying a particular aspect of ash, such as, for example, adding kaolin or alumina to mined coals (Vuthaluru et al., 1996), or upgrading methodologies that may increase the calorific value of coal by moisture reduction, but which do not significantly modify the ash chemistry. For example, Indonesian low rank coal that is dried to increase its calorific value, when burnt, forms deposits that commence with a thin layer of molten slag on the surface of the heat transfer tube. Equilibrium computations for ash formation identify the molten slag fraction in ash, and experimental results show that such ash deposition behaviour is closely related to the ash melting temperature (Akiyama et al., 2010). Experimental investigations have been carried out on the combustion behaviour of Greek brown coal with varying moisture content, and this has demonstrated the need for a fuel consisting of a mixture of raw and up to 30wt% of dry lignite. This approach resulted in an increased efficiency of only about 1.5% in existing boilers (Agraniotis et al., 2012).

The complex mechanisms of ash formation and fouling include the formation of amorphous silica phases and the crystallisation of ash and slag. These too involve alkali ash constituents; gas phase sodium chloride and sulphate condense on heat transfer surfaces, and inorganics (including sodium, potassium, calcium and iron) participate in the formation of various molten phases, including silicates (Pyykönen et al., 2003; Glarorg and Marshall, 2005). There are many minerals of varying composition present in the as-mined coals and these all exhibit various softening and melting points. A number of the minerals present in low rank coals contain inorganics, such as Na, K, Mg, Ca and Fe; for example: Illite, [$K(MgAl,Si)(Al,Si_3)O_{10}(OH)_8$]; Montomorillonite, [$(MgAl)_8(Si_4O_{10})_3(OH)_{10}$]; Prochlorite,

[2FeO 2MgO Al_2O_3 2SiO_2 2H_2O]; Ankerite, [$CaCO_3$ (Mg,Fe,Mn)CO_3]; and Feldspar, [$(K,Na)_2OAl_2O_36SiO_2$].

Studies by Hurley and Schobert (1993) on the ash behaviour during the combustion of sub-bituminous coal in a pilot plant revealed complex behaviour and problems arising from ash fouling. The causes for ash-related problems include gas-phase attack by sulphur species formed under the fuel-rich conditions of low-NOx firing systems, with ash deposits that included unburnt fuel forming on furnace water walls; these lead to sulphatising and chloride chemistry that attacks materials under local high heat flux and reducing conditions (Valentine et al., 2007).

Soot-blowing of deposits in coal combustion systems causes thermal and mechanical shock, due to the jet impingement used to fracture the deposit. The strength of the deposit depends on the porosity and its crystalline nature. These properties are, in turn, related to the composition of the ash particles in the deposit. Measurements of the thermal and mechanical properties of a number of ash-slag deposits indicated that as the porosity of the deposit decreased, the compressive strength increased. These data show the change in compressive strength is greatest with a ≥25% drop in the porosity; it is noted that measures are needed to avoid this reduction in the ash deposit's porosity, as this is critical for deposit removal by soot-blowing (Senior, 1997).

Numerous studies have shown that the efficient use of low rank coals for power generation is limited by their ash fouling propensity and moisture content. Consequently, low rank coal subcritical PC technologies operate at low overall efficiencies, with lower boiler availability, and the highest emissions of GHG gases per unit of electricity generated. Fouling of boiler surfaces reduces heat transfer, and eventually the build-up of ash deposits necessitates closing the boiler to remove the ash deposits. The results are a loss of revenue for the power station, loss of power supply to consumers, costs incurred in cleaning boiler surfaces, and, where corrosion and erosion has taken place, additional costs of repair and maintenance; overall higher emissions are due to lower efficiencies and more frequent re-starting of power stations.

Power generation using low rank coals benefits from low mining costs, but incurs higher capital and operational costs, and power plant operators have sought to preferentially mine good quality coal. The result has been an accumulation of relatively poor quality low rank coal deposits for future use. This works against the need for lower carbon intensity, which requires good quality fuels for plants that would operate with high efficiencies of power generation.

The design of any new high efficiency coal-fired power-generating plant would require operational methods that may negate ash deposition. Alternatively, new plants must be fuelled with non-fouling high quality coal. These new high performance power systems operate at 40-50% efficiencies, with corresponding lower GHG emissions.

We conclude that the composition of low rank coals causes considerable difficulties when used to fuel current power generation plants. The previous detailed discussion of coal combustion and ash formation chemistry has clarified a cause-effect relationship between the composition of the heterogeneous low rank coal and its poor performance as a fuel. The low heat content of the mined coal is due to its high moisture content, the aggressive chemistry of sodium and potassium in a coal flame is a major factor in boiler fouling, and with sulphur and chloride, fouling and corrosion would occur, along with emissions of sulphur and chloride pollutants. Magnesium, calcium iron, and silicates increase fouling propensity, rendering the fuel problematic, and overall, these are unsuitable properties in a fuel for high efficiency power generation plants.

If all of the ash in coal were removed, then ash fouling would be eliminated, but often this approach must be economically practical to provide fuel for pulverised coal (PC) boilers. A practical approach for any future new plant would be to remove only the ash species that significantly contribute to ash-related problems from low rank coals – this approach may be an economically acceptable way to provide coal of a quality designed for the maximum performance of a PC power plant. A process that would provide such high quality coal with lower moisture, while maintaining the relatively low cost of low rank coals, would be a major advance in coal-fuelled power generation.

Sodium is chemically bound to oxygen functional groups in low rank coal, and NaCl is present as aqua-solvated cations and anions in mined coal. These are not tightly chemically bound to the coal matrix and thus can be removed with mild acid washing. The sodium (and potassium) present in mineral particles, however, is more tightly chemically bound, and removing these requires stronger acid treatment; these stronger acidic conditions should also remove calcium and magnesium, and most forms of iron, from the coal matrix and from most mineral particles. The practical treatment methodology would remove ash species that are responsible for ash fouling and slagging in all sections of a boiler. The remaining ash would consist of acid-washed clay and, in some cases, small amounts of sand and quartz; if only these ash constituents are in treated coal, ash formation and fouling would cease to be problematic for pulverised coal-fuelled plants.

The treatment of low quality coal containing large amounts of ash would require larger amounts of acid and this would increase the costs of treatment for commercial application. Costs of coal processing must therefore be examined against the benefits of removing the ash-forming inorganics from coal, and also of removing inorganic chloride and sulphur; the benefits would be the elimination of ash fouling and of corrosion caused by the build-up of chloride and sulphates in ash deposits on heat transfer surfaces. The overall economics for processing these high ash low rank coals would require detailed assessments of the cost-benefit analysis for each and any coal deposit. These considerations would include the role of sulphur in the build-up of ash deposits if significant amounts of iron sulphides were present in the coal, because such ash deposits are the result of complex chemistry involving sulphur and chloride, with sodium, potassium, and iron. Iron-rich ash deposits have been shown to form on heat transfer surfaces, and these can cause numerous fouling and corrosion problems. The acid treatment process must be able to remove such problematic causes of fouling while maintaining the cost advantage of low rank coals.

When these low rank coals are treated with acid to remove the inorganics that are the primary cause of ash fouling and corrosion, organically bound sulphur remains unaffected. This would not pose a problem for major brown coal deposits, such as are located in Germany and Australia, because these contain low amounts of organic sulphur, and sulphur emissions from these treated coals are expected to fall within environmental regulations. In cases where organic sulphur levels in coal are high, additional measures may be required, such as adding calcium hydroxide to the coal, or using a flue gas sulphur removal plant.

All of the deposits of low rank coals worldwide could be processed into non-fouling fuel, but the conditions and costs of the processes would differ. The treated coal would be non-fouling with low ash, and would meet the requirements for high quality fuel for pulverised coal-fuelled plants. A method that removes virtually all of the ash-forming constituents would provide the highest quality coal.

Low Rank Coal Power Generation and Future Development

Coal is used to fuel a variety of power generation plants, and the majority of these are PC combustion plants. In PC plants, the coal is crushed to a small particle-sized distribution and mixed with excess air to ensure complete combustion in the coal flame. Usually, low rank coal mining and transport is situated in relatively close proximity to the power station, and

the coal is conveyed to the power station where it is fed into a crusher/drier in which hot gases extracted from the boiler are used to vaporise the coal moisture, and the mixture of crushed hot coal, water vapour and air are fed into the coal burner.

Typically, subcritical plants and supercritical plants are configured as PC boilers, and the basic differences between these are related to the coal burner design, the steam temperatures and the pressures generated to drive the steam turbines. During the years when environmental factors were not considered, the design of coal combustion system power generation was motivated by economies of scale. The current concerns include general environmental outcomes, costs and security of power supply, and the need for increasingly lower pollution that meets regulations (Beér, 2000). Future coal-fuelled plants will be designed with non-ash-fouling combustion, high thermodynamic efficiency, and low CO_2 emissions.

The IEA predicts a trend of continuing lower CO_2 emissions for future coal-fuelled plants, decreasing from the current worldwide average emission intensity of 1116kg/MWh to 743 kg/MWh, and down to 669 kg/MWh with advanced systems. It is hoped that the utilisation of CO_2 capture will lead to further reductions (Topper, 2011). Currently the EU's average coal power emission intensity is 881 kg/MWh. The goal of future power generation coal-fired systems is higher efficiency, and this is obtained using SC and USC steam boilers for PC plants. Where applicable, SC and USC conditions may be used with pressurised fluid-bed combustion without, or with, topping combustion, and higher efficiencies would be obtained with integrated gasification with combined cycles. The ultimate goal is zero-emissions coal-fuelled plants, which would capture CO_2 for use as a feedstock. An attractive future concept is a hybrid catalytic coal steam gasification plant with combined-cycle power and the capacity to produce hydrocarbon liquids; captured CO_2 may be used for CO_2/H_2 synthesis. These developments hold out the promise for low- to zero-emissions power generation. The readiness of the technology for advanced coal-based power generation systems is discussed by Sloss (2019).

The current advances in low rank coal-fuelled power generation are in integrated coal drying in a SC plant. RWE Power commissioned a lignite-fired power-plant unit in 2003 at Niederaussem operating at 43.2% LHV efficiency.* The unit is reported to operate at 27.5 MPa/580°C/600°C steam pressure and temperature at the turbine. This is an example of converting an aging lignite-fuelled power unit into a modern one with significantly lower

* On the Niederaussem Coal Innovation Centre, see https://www.group.rwe/en/innovation-and-knowlegde/innovation-and-technology/technology-research-development/coal-innovation-centre.

emissions for a BoA unit with a gross output of 1,000 MW (BoA – German abbreviation for a lignite-fired power station with optimised plant engineering). The higher efficiency of the unit lowered the annual CO_2 emissions by up to three million tons, with dust, sulphur-dioxide and nitrogen-oxide emissions reduced by ~30%.

Problems stemming from high sulphur coal can also be addressed with sulphur retention by calcium oxide/hydroxide additives in circulating fluidised bed combustion (CFBC). CFBC can use a variety of fuels, and operates at lower temperatures to mitigate sulphur emissions; plants of 460-330 MWe SC capacity have been installed in Russia, as has a 600 MWe SC unit in China, and the Lagisza SC 460 MWe CFBC in Poland. The latter is reported to achieve emissions of SOx, NOx and particulates lower than required by the latest EU limits. CFBC use locally supplied low quality coals, biomass and wastes, but an increasing number operate as an alternative to PC boilers. Further incremental efficiency improvements are envisaged, and future developments include 700°C steam temperature, with resulting higher efficiency power generation.

The IEA reports work being undertaken in the EU, Japan, USA, India, and China to develop USC high temperature (700°C plus) systems to increase the efficiency of generation to around 50% (LHV), with reduced CO_2 emissions intensity. For example, the construction of a coal-fuelled Batang power plant has been discussed for Central Java, Indonesia, and India is reported to be considering an 800 MW USC demonstration plant. This effort envisages using advanced alloys to cope with the high temperature, high pressure steam. A USC plant using advanced alloys is expensive and it is unlikely to be fuelled with coal that causes fouling, corrosion and erosion to the alloy surfaces. High quality, high rank coal is also relatively expensive. It follows that high quality, low cost, low rank coals would be the optimum fuel for these advanced power generation plants.

Integrating a low rank coal processing plant with a high efficiency power station needs to be developed for commercial use. The fundamental chemistry and conceptual engineering features have been elucidated by the CCT R&D program. Figure 5-1 is a schematic of a concept based on the CCT R&D program of a futuristic supercritical power station with a fully integrated coal treatment plant. A fully integrated plant would achieve generating efficiencies of 43-45% for SC, and >45% efficiency for an USC plant; the schematic is modelled to operate at a total thermal efficiency of ≥80%. Figure 5-2 illustrates the difference in power and thermal efficiencies

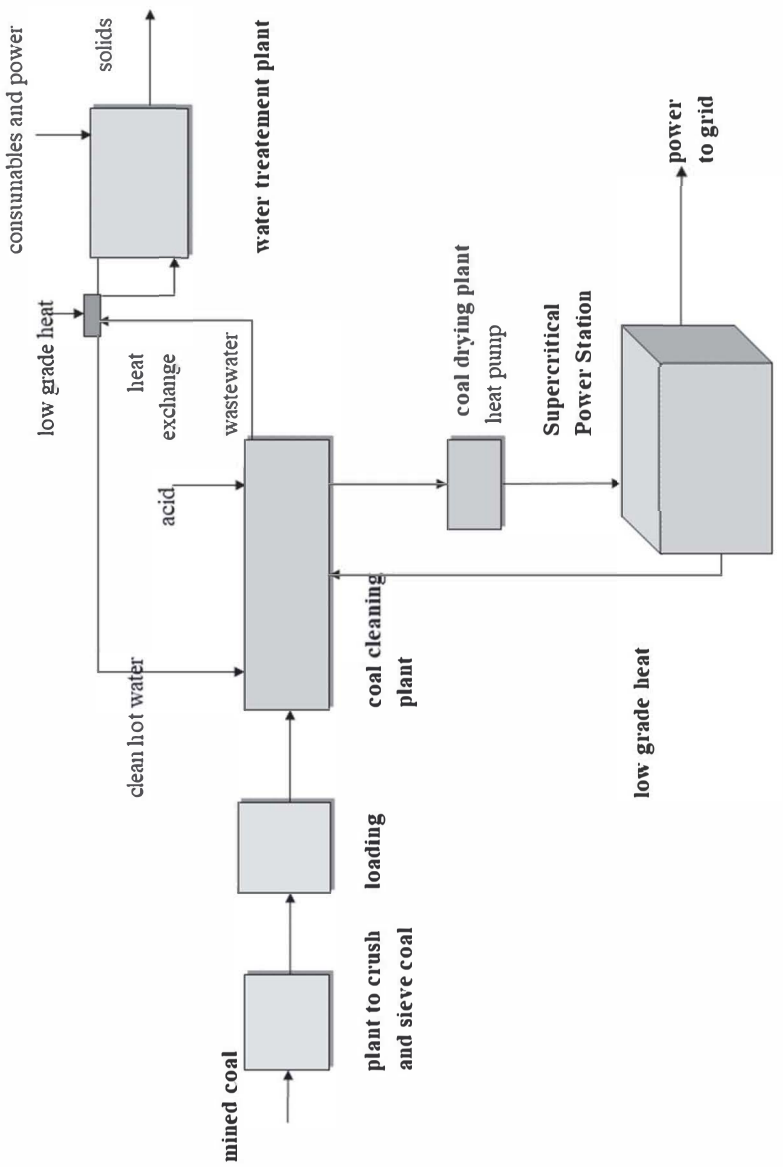

Figure 5-1. Schematic of a futuristic SC power station with integrated coal treatment.

for a subcritical plant fuelled with brown coal, compared to those for an integrated SC plant, as outlined in Figure 5-1. Comparative modelling of a brown coal-fuelled subcritical plant and the integrated SC and USC options, based on 29-30% efficiency for the subcritical, 43% efficiency for the SC, and 46% for the USC plant, provides the following CO_2 emissions ($kgCO_2/MWh$):

- Subcritical PC plant –1290
- SC PC plant – <830
- USC plant – <700
- DCFTCC plant – ≤600

Financial modelling indicates a processed brown coal-fuelled fully integrated supercritical plant would generate power at a lower cost than a current brown coal-fuelled subcritical plant (see further discussions in Chapter Nine).

The concept of coal treatment and drying, integrated to achieve high thermal efficiency, can be developed for zero-ash coal to fuel a combined-cycle plant, as schematically illustrated in Figure 5-3, operating at ≥50% power generation efficiency. This concept, if successfully commercialised, has the potential to operate with an emission intensity of ≤600 kg CO_2/MWh.

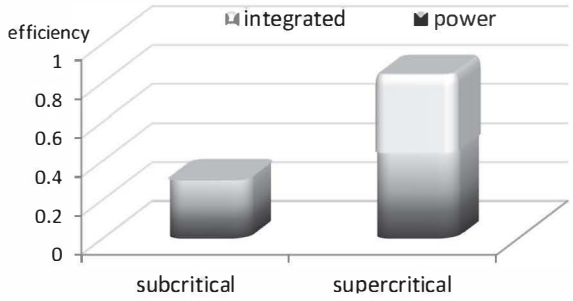

Figure 5-2. Comparing total thermal and power generation efficiencies of subcritical and future integrated supercritical plants.

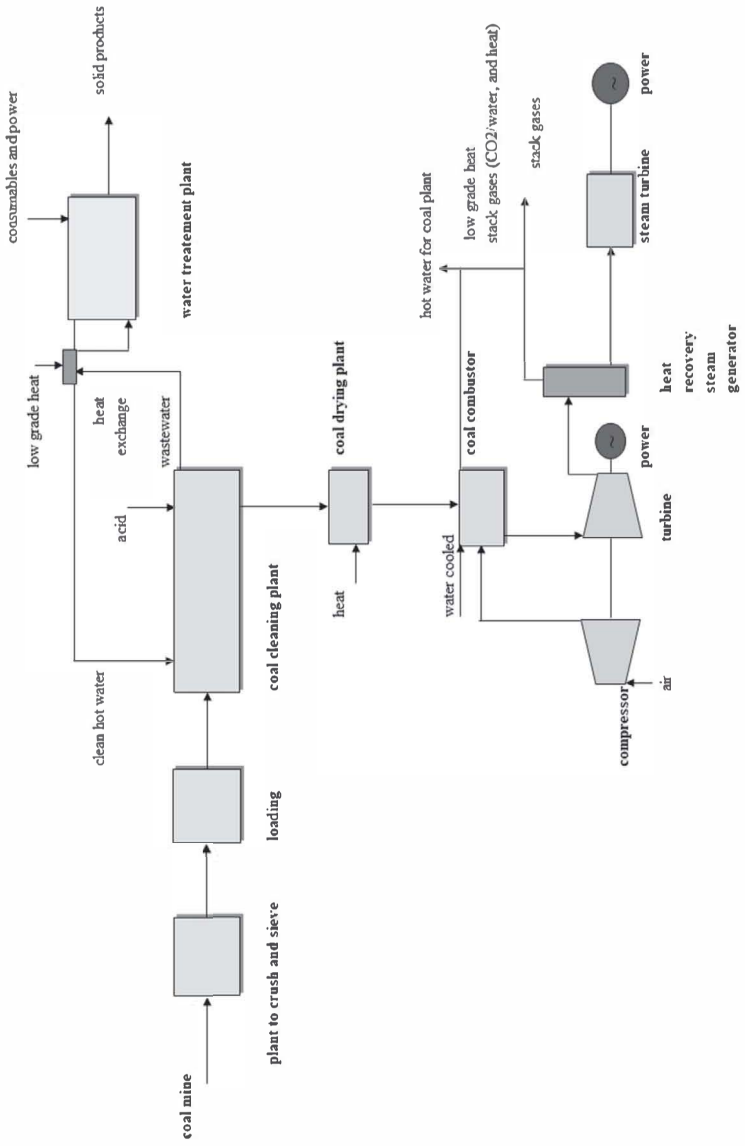

Figure 5-3. Schematic of a combined-cycle plant using zero-ash coal for a direct-fuelled turbine.

The CCT coal process for low rank coal includes a fuel for catalytic steam gasification; this is a new concept which requires considerable development for commercial application. The schematic shown in Figure 5-4 is of a CCT-Hybrid concept that includes a coal processing unit integrated with a fluid-bed coal gasification plant, modified to add steam at high temperatures to gasify the dry processed catalytic coal. The reaction between coal and steam is endothermic and requires heat. A small amount of oxygen may be used to create additional heat in the gasifier, but a futuristic plant can be envisaged that would maximise the reaction with steam by heating it before it enters the gasifier. For example, steam from the gas cooling plant at 400-600°C would be heated to 900-1000°C as it enters the gasifier. Heat supplied with plasma may also be envisaged. Such a CCT-Hybrid catalytic gasifier would be designed with a residence time sufficient to gasify >99% of the coal feed. Fluid-bed gasifiers currently in use, such as the High Temperature Winkler, may be modified for steam gasification. The design of the CCT gasifier is a futuristic concept that would include capturing CO_2 and using it to produce valuable material, such as methanol.

The CCT-Hybrid catalytic gasifier concept would produce synthesis gas with a higher hydrogen content, which would be cleaned from S, N and Cl pollutants and ash particulates, and cooled using a heat exchange plant; the clean and cooled synthesis gas can be fed into a Fischer-Tropsch (F/T) plant to produce hydrocarbons. The tail gases from the F/Tropsch plant would be used as fuel for oxy-combustion in a direct-fuelled turbine, combined-cycle power plant. The gases exiting the power plant would consist of CO_2 and H_2O; CO_2 would be separated and stored for use in reactions with hydrogen in a methanol synthesis plant. Hydrogen and oxygen may be obtained by using the captured water in an electrolysis plant. The major cost associated with conventional water electrolysis is the electricity used in such a plant. A CCT-Hybrid plant would produce relatively inexpensive power with the combined-cycle plant, but this may be insufficient to provide power for sale to the grid, and would also provide H_2 to achieve zero CO_2 emissions. Additional power can be obtained using a solar plant adjacent to the electrolysis plant and/or power provided from the grid during low demand periods. An electrolysis plant would produce H_2 for the reaction of CO_2 into methanol, and also O_2 for the gasifier and the oxy-combustor of the combined-cycle power plant. This scheme would remove the need for an air separation plant, used to provide oxygen for a conventional gasifier, and would also avoid the cost of CO_2 storage.

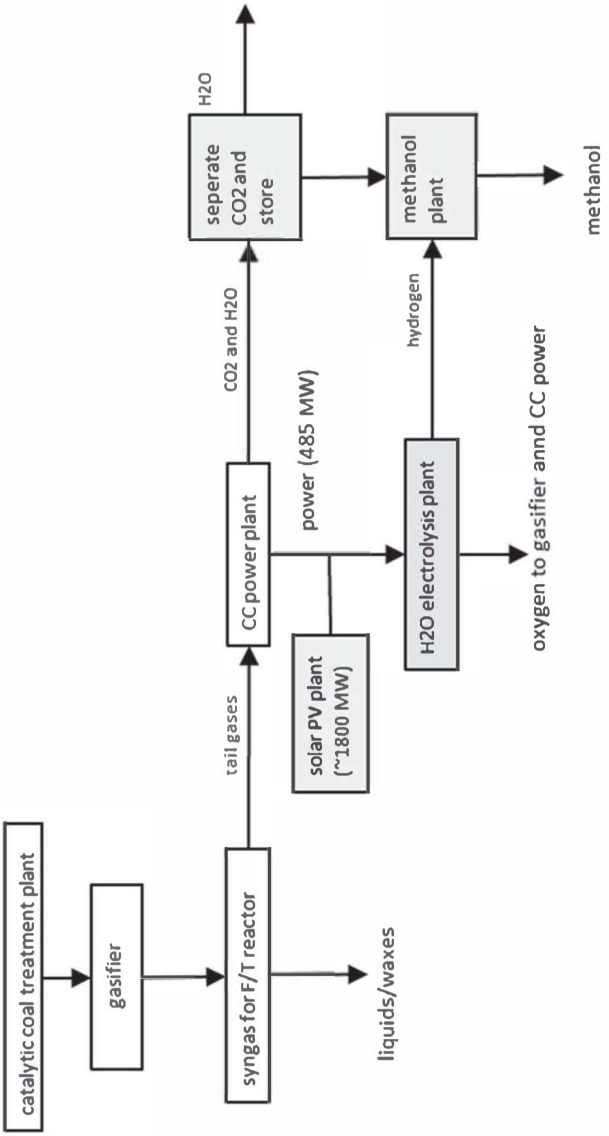

Figure 5-4. Futuristic concept of a CCT-Hybrid zero-emissions plant.

References

Agraniotis, M., Karellas, S., Violidakis, I., Doukelis, A., Grammelis, P. and Kakaras, E. 2012. 'Investigation of pre-drying lignite in an existing Greek power plant', *Thermal Science,* 16, 283-296.

Akiyama, K., Pak, H., Tada, T., Ueki, Y., Yoshiie, R. and Naruse, I. 2010. 'Ash Deposition Behaviour of Upgraded Brown Coal and Bituminous Coal', *Energy Fuels*, 24, 4138-4143.

Beér, J. M. 2000. 'Combustion technology developments in power generation in response to environmental challenges', *Prog. Energy Combust. Sc.*, 26, 301-327.

Borio, R. W. and Levasseur, A. A. 'Overview of coal ash deposition in boilers'. Available at: https://web.anl.gov/PCS/acsfuel/preprint%20archive/Files/29_4_PHILADELPHIA_08-84_0193.pdf.

Browning, G. J., Bryant, G. W., Hurst, H. J., Lucas, J. A. and Wall, T. F. 2003. 'An Empirical Method for the Prediction of Coal Ash Slag Viscosity', *Energy Fuels,* 17, 731-737.

Bryers, R. W. 1996. 'Fireside slagging, fouling, and high-temperature corrosion of heat-transfer surface due to impurities in steam-raising fuels', *Prog. Energy Combust. Sci.,* 22, 29-120.

Fernandez-Turiel, J-L., Georgakopoulos, A., Gimeno, D., Papastergios, G. and Kolovos, N. 2004, 'Ash Deposition in a Pulverized Coal-Fired Power Plant after High-Calcium Lignite Combustion', *Energy Fuels*, 18, 1512-1518.

Glarorg, P. and Marshall, P. 2005. 'Mechanism and modelling of the formation of gaseous alkali sulphates', *Combustion and Flame,* 141, 22-39.

Harding, N. S. and O'Connor, D. C. 2007. 'Ash deposition impacts in the power industry', *Fuel Process. Technology,* 88, 1082-1093.

Hurley, J. P. and Schobert, H. H. 1993. 'Ash Formation during Pulverize Subbituminous Coal Combustion. 2. Inorganic Transformations during Middle and Late Stages of burnout', *Energy Fuels*, 7, 542-553.

Laursen, K., Frandsen, F. and Larsen, O. H. 1998. 'Ash Deposition Trials at Three Power Stations in Denmark', *Energy Fuels*, 12, 429-442.

Lee, F. C. C. and Lockwood, F. C. 1999. 'Modelling ash deposition in pulverized coal-fired applications', *Prog. Energy Combust. Sc.,* 25, 117-132.

Miller, S. F. and Schobert, H. H. 1994. 'Effect of the Occurrence and Modes of Incorporation of Alkalis, Alkaline Earth Elements, and Sulphur on

Ash Formation in Pilot-Scale Combustion of Beulah Pulverized Coal and Coal-Water Slurry Fuel', *Energy Fuels*, 8, 1208-1216.

Pyykönen, J. and Jokiniemi, J. 2003. 'Modelling alkali chloride superheater deposition and its implications', *Fuel Processing Technology*, 80, 225-262.

Seggiani, M. and Pannocchia, G. 2003. 'Prediction of Coal Ash Thermal Properties Using Partial Least-Squares Regression', *Ind. Eng. Chem. Res.*, 42, 4919-4926.

Senior, C. L. 1997. 'Predicting Removal of Coal Ash Deposits in Convective Heat Exchangers', *Energy Fuels*, 11, 416-420.

Sloss, L. 2019. 'Technology readiness of advanced coal-based power generation systems', IEA CCC Report Number CCC/292.

Tian, Z. F., Witt, P. J., Schwarz, M. P. and Yang, W. 2009. 'Numerical Modelling of Brown Coal Combustion in a Tangentially-Fired Furnace', Seventh International Conference on CFD in the Minerals and Process Industries CSIRO, Melbourne, Australia.

Topper, J. 2011. *Status of Coal Fired Power Plants World-Wide*. Available at: https://www.iea.org/media/workshops/2011/cea/Topper.pdf.

Tu, J. Y., Fletcher, A. J. and Behnia, M. 1997. 'Numerical modelling of three-dimensional fly-ash flow in power utility boilers', *Int. J. Numer. Methods Fluids*, 24, 787-807.

Valentine, J. R., Shim, H-Sh., Davis, K. A., Seo, S-I. and Kim, T-H. 2007. 'CFD Evaluation of Water Wall Wastage in Coal-Fired Utility boilers', *Energy Fuels*, 21, 242-249.

Vuthaluru, H. B., Domazetis, G., Wall, T. F. and Vleeskens, J. M. 1996. 'Reducing fly ash deposition by pre-treatment of brown coal: effect of aluminium on ash character', *Fuel Processing Technology*, 46, 117-132.

Wang, H. and Harb, J. N. 1997. 'Modelling of ash deposition in large-scale combustion facilities burning pulverised coal', *Prog. Energy Combust. Sc.*, 23, 267-282.

Xu, Z. M., He, X., Azevedo, J. L. T. and Carvalho, M. G. 2002. 'An advanced model to assess fouling and slagging in coal fired boilers', *Int. J. Energy Res.*, 26, 1221-1236.

Xu, Z. M., Yang, S. R., Guo, S. Q., Zhao, H. and Zhang, Q. Z. 2005. 'Costs Due to Utility Boiler Fouling in China', *Heat Transfer-Asian Research*, 34, 53-63.

Zbogar, A., Frandsen, F., Jensen, P. A. and Glarborg, P. 2009. 'Shedding of ash deposits', *Progress Energy Combust. Sc.*, 35, 31–56.

CHAPTER SIX

PROCESSING LOW RANK COALS INTO HIGH QUALITY FUELS

Low rank coals constitute about 47% of all worldwide coal deposits. The discussion in the previous chapters has shown the properties of low rank coals render them problematic fuels, but their low cost and abundance has resulted in fuelling a considerable portion of power generation worldwide. Power generation plants using low rank coal incur ash fouling problems and higher CO_2 intensity. The concern about GHG emissions has become a powerful force for adopting low intensity emissions technology in coal power generation and coal gasification. If costs are imposed for CO_2 emissions, this, associated with the costs for maintenance and cleaning fouling in boilers, negates the advantages provided by the low cost of the poor quality fuel.

Research has been undertaken to create coal power generation with lower emissions of CO_2, but progress has been slow in developing advanced low rank coal-fuelled plants. Currently the impetus is to adopt other power generation technologies, such as solar and wind. Switching to carbon neutral fuels for power generation has also been examined (e.g. fuels such as straw and wood) but these too pose serious problems.

Traditionally, the economy of scale had favoured the construction of large, expensive, low efficiency coal power stations; nowadays, however, high efficiency, lower emissions coal-fuelled plants are chosen for power generation. A high efficiency plant requires expensive alloys for constructing boilers to generate steam at the high temperature and pressure required for supercritical (SC) and ultra-supercritical (USC) plants, and for these it is imperative that fuel-related problems are minimal or eliminated. The worldwide clean coal effort has also considered additional options, such as the capture and storage of CO_2 from coal-fuelled power stations, and improving the performance of coal gasification plants. The capture and storage of CO_2 from coal-fuelled plants is expensive and renders conventional subcritical power generation uncompetitive.

The practical results from the worldwide clean coal effort have often been modifications that improved a power plant's performance, with a lesser emphasis on developing coal processes to improve the quality of mined coals, and to use these in new high efficiency plants. Yet it is widely recognised that an economical method that would produce low cost, high quality coal would be a major advance in the economic implementation of high efficiency power plants, and ultimately could contribute to the development of low- to zero-emissions coal-fuelled power generation. In this chapter, major coal treatment projects aimed at improving the quality of coals are briefly discussed, as background to a detailed discussion on the chemical processing of low rank coal into high quality fuel.

Coal Treatment Processes

Coal treatment processes are generally categorised as physical or chemical methodologies (biological treatments are not included in this discussion). The literature is replete with an almost bewildering number of attempts to upgrade various coals. Most processes are aimed at increasing the calorific value of low rank coals by reducing their moisture content, and in some cases with sulphur reduction; only a few coal treatment processes aim to reduce both moisture and ash (Willson et al., 1997; DOE, 2003). Physical methods include mild pyrolysis, crushing and sieving, gravity separation, froth flotation, oil agglomeration, magnetic separation, electrostatic separation, and air fluidisation. Chemical treatment methods include the use of alkalis, acids, and solvent extraction. Of the various approaches to upgrade the quality of coals none has yet been commercialised, with the exception of a drying process for brown coal which has been scaled-up for commercial application; the quality of product coals from the various treatment methodologies varies considerably (Katalamula and Gupta, 2009; Rahman et al., 2017). Many of these methods progressed to pilot-plants, but were subsequently abandoned because of multiple problems encountered in the handling and storage of the product, and in many cases, because the quality of the product failed to meet expectations. These methodologies were developed for upgrading a specific coal, and few (if any) methods have been designed for application to all low rank coals.

The following are the major processes for coal treatment, and are briefly discussed to illustrate the methods and plants used for upgrading various coals:

AMAX Coal Company's Coal Drying Project

This commenced during the early 1990s, and was a fluidised-bed coal drying system, operating at 94-120°C. Coal was mined at Amax's Belle Ayr mine with an average of 0.3-0.4wt% sulphur, and with moisture at about 30wt%. A 1.1-Mt/a thermal coal-drying facility was built and operated at the Wyoming mine. The process reduced the moisture of the coal to 10wt%. Formation of coal fines caused problems and the process was modified to reduce fines by binding the dried product into pellets; eventually this project was abandoned (Wen et al., 1991).

Rosebud SynCoal's Advanced Coal Conversion Process

The schematic of the plant is shown in Figure 6-1. Coals were upgraded from a moisture of 25-55wt% and sulphur from 0.5-1.5wt% into a product with 1wt% moisture and 0.3wt% sulphur. The DOE provided 41% of the total funding of $105.7 million. Tests commenced in 1992, and the project was completed in 2001 with the design of a plant with a capacity of 68.3 tons of feed coal per hour.

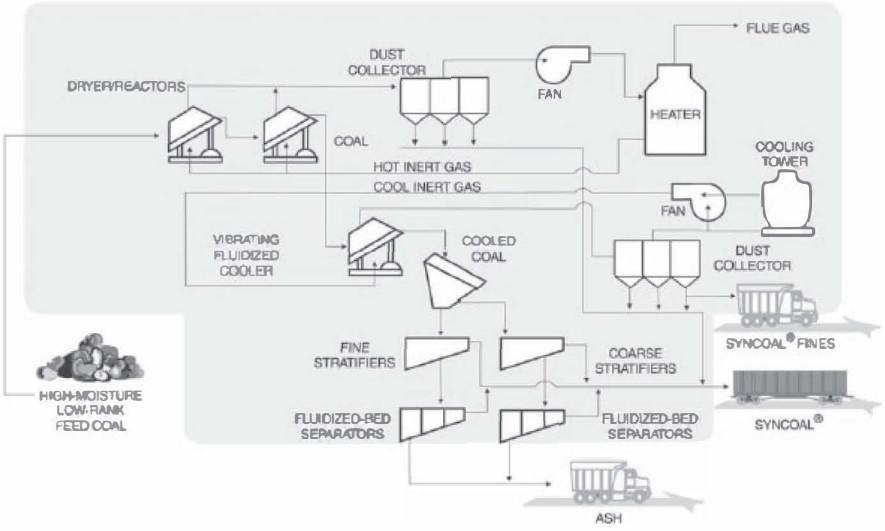

Figure 6-1. Outline of SynCoal Process (Clean Coal Technology Programs: Program Update 2003, DOE/FE-0459-1; available at https://www.osti.gov/search/semantic:syncoal).

The process consists of a first-stage dryer/reactor, a second-stage thermal reactor, and a product cooler. Raw coal, sized at 1-3 cm, is heated in the dryer/reactor to remove surface water by using hot combustion gas (from a natural gas-fired heater) that is mixed with recirculated gas from the dryer. The dried coal is further heated in the second thermal reactor using a recirculating gas stream, to remove water bound in the pores of the coal and to promote some pyrolysis. Particle shrinkage occurs in this stage, which liberates mineral matter and enables the physical separation of some ash from the coal. The coal then contacts cool inert gas in a vibratory cooler. After the coal is cooled to below 40°C, it is screened into four size fractions. The low gravity stream is sent to the product conveyor. The high gravity stream of the smallest size fraction is discarded, and the medium-heavy stream is split into light and heavy streams with fluidised bed separators. The light streams are collected and sent to product handling, and the heavy streams, which contain high concentrations of mineral matter, are discarded. Problems stemming from the spontaneous combustion of the product require storage in an inert gas (DOE, 2005).

ENCOAL's Mild Gasification Process[†]

This was developed from an earlier liquid from coal project. The cost of the initial ENCOAL plant was $90 million, with 50% provided by the DOE. This process dries the coal and then it is pyrolysed at about 540°C. The solids are cooled, quenched, treated with a dust suppressant, and stored. The gas/liquids are cleaned from dust and condensed to produce a coal-derived liquid. The solid fuel (char) contains twice the original ash content in the raw coal. The schematic of the plant is shown in Figure 6-2.

Low rank coal from the US Powder River Basin, mined with moisture of 25-32wt%, was processed to almost zero moisture, and this was followed by mild pyrolysis to remove about 60% of the original volatile matter and a portion of the sulphur. The resulting char was subjected to a multiple-step process to produce the solid fuel. Volatile matter driven off during the pyrolysis process was partially condensed into a hydrocarbon coal liquid. The non-condensed gaseous hydrocarbons were used to provide heat for the drying and pyrolysis. Each ton of raw coal produced about half a ton of solid fuel, half a barrel of liquid, and 70% of the hydrocarbon gas required to provide heat for the process.

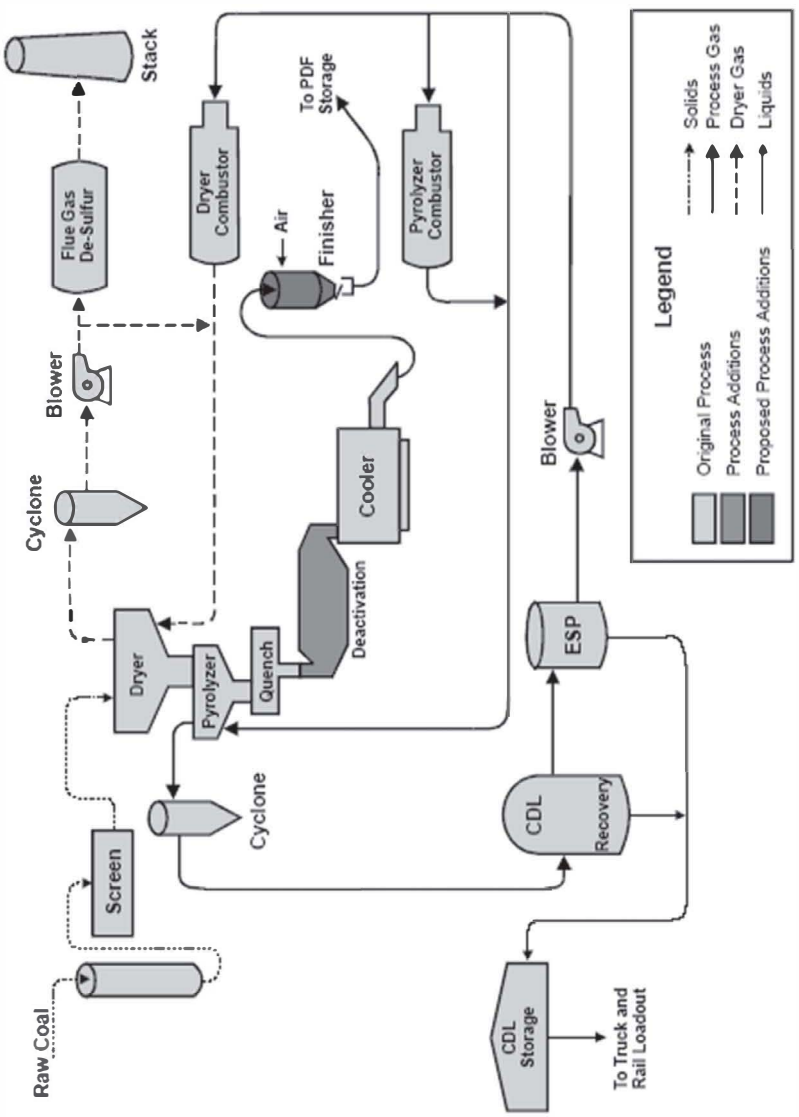

Figure 6-2. Schematic of ENCOAL Process (ENCOAL, 1997).

The liquid product was a low-sulphur, highly aromatic heavy hydrocarbon, similar to low-sulphur fuel oil. The market for the liquid fuel did not materialise, and consequently it was further treated with a centrifuge to reduce solids, and upgraded into: (1) crude cresylic acid, (2) pitch, (3) refinery feedstock (low-oxygen middle distillate), and (4) oxygenated middle distillate (industrial fuel). A commercial plant feasibility study was completed in 1996 for a 15,000-metric-ton/day, three-unit liquid from coal plant, with an independent 80 MWe cogeneration unit, at a capital cost of $475 million. An assessment by the DOE was concluded in 2002 and commercial feasibility activities were planned (DOE, 2002). No further activities have been reported.

Carbontec's SynCoal® Process

This process is designed to upgrade low rank coal from the US Powder River Basin into a high quality fuel. The process was demonstrated at a 45 ton/hr test facility adjacent to Western Energy Company's Rosebud Mine near Colstrip, Montana. The treated product was dusty with a propensity for spontaneous combustion that created shipping and storage problems; spontaneous combustion could occur if the product was piled or shipped in quantities larger than about two tons. These concerns limited large scale commercial applications and options were sought to use the fuel onsite at power generation facilities. More than 2.8 million tons of raw coal was processed to produce almost 1.9 million tons of the treated coal over the life of the project. The product, however, faced difficulties for commercial exploitation because of spontaneous combustion and dustiness (Sheldon, 2006).

Drying Indonesian lignite

This technology has been developed to upgrade Indonesian low rank coal by mixing it with oil, and the mixture was then subjected to a stipulated temperature, followed by separation and recovery of the oil for re-use. The process is illustrated by the block diagram in Figure 6-3, and includes crushing low rank coal, dispersing the crushed coal in light oil (which contains heavy oil such as asphalt), and dewatering the dispersion at a temperature of 130°C to 160°C under a pressure of about 4 to 5 atmospheres.

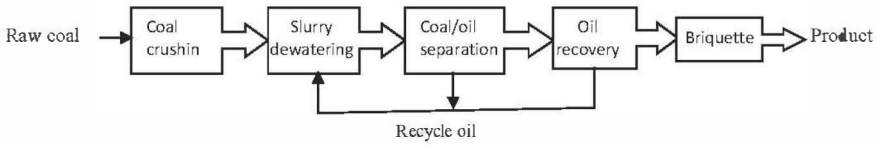

Figure 6-3. Block diagram of the process to upgrade Indonesian low rank coal.

The mild conditions of the dewatering ensure that thermal breakdown of coal does not occur, which avoids serious wastewater treatment problems. The coal moisture is driven off as steam and subsequently removed from the coal as it is mixed with the hot oil. The steam is compressed and reused as a heat source, and this lowers the energy consumption. The coal pores absorb heavy oil (asphalt), which stabilises the coal to prevent spontaneous combustion (Kinoshita et al., 2010). The treated coal was tested for combustion characteristics (Umar et al., 2006).

Hydrothermal treatment

This was conceived in the mid-1970s and has been developed to pilot scale in the USA and Australia (Favas and Jackson, 2003; Racovalis et al., 2002). The concept is that of heating a coal/water mixture to high temperatures to destroy oxygen groups in low rank coals, and thereby render the product as hydrophobic, due to decarboxylation and the release of tar within the pores of coal particles. The resulting product is thought to contain lower moisture, and the loss of some inorganics is anticipated. The product is touted as a coal/water slurry that could be fed as a liquid to fuel plants as a replacement for heavy oil.

The process causes the coal/water slurry to undergo thermolysis at high temperatures, which involves the decomposition of oxygen functional groups, and the release of water soluble organics and tar from the organic matrix of the low rank coal. This is an irreversible process that is accompanied by the release of organic moieties into the water phase, as shown by the very high levels of total organic carbon (TOC) in the wastewater.

Nakajima et al., (2013) carried out studies to determine the ecotoxicity of wastewater from this coal treatment process. The ecotoxicity of wastewater obtained by a hot water extraction at ~80°C of coal was assessed to show virtually zero mutagenicity, but treatment of the coal/water mixture at high temperatures produced highly toxic wastewater; chlorination of the wastewater also resulted in high mutagenicity, implicating chloro-organo species for the high toxicity. Tests were also conducted on the wastewater

produced by subjecting two lignite and two sub-bituminous coals to the high temperatures of the hydrothermal coal treatment. The wastewater from these tests was assessed for mutagenicity by the *Ames Salmonella* assay. The tests included the impact of reaction temperature, and the ratio of liquid to solid (coal) on the mutagenicity of the wastewater. The wastewater was also tested for acute toxicity on the freshwater organisms *D. magna* (water flea) and *Oryzias latipes* (Japanese medaka), which are frequently used in ecotoxicity testing. When the coal/water mixture was subjected to 350°C and the solid to liquid ratios of the coal/water slurry were varied at 3 and 20, the TOC in the wastewater was measured at 4,500 and 18,000 mg-C/L, respectively. The wastewater produced from the treatment of low rank coal at high temperatures gave high toxicities for both *D. magna* and *O. latipes*, which is comparable to the toxicity of phenols. Analysis of wastewater indicated that lower molecular weight compounds were formed due to the decomposition of the treated coal, and these low molecular compounds include highly toxic phenolic compounds. The mutagenicity of the wastewater was almost zero when the coal/water mixtures were heated to between 80°C and 200°C, but was observed to increase when the temperature was raised from 300°C to 350°C, indicating an increase in mutagenicity at elevated temperatures; an appreciable mutagenicity was also observed for wastewater from all mixtures of lignite and sub-bituminous coals heated in the temperature range from 300°C to 350°C.

The hydrothermal coal treatment concept suffers from the serious flaws of toxic wastewater and poor quality fuel; the coal matrix breaks down at the temperatures of the process, producing large volumes of toxic wastewater with very high amounts of soluble organic compounds. The temperatures required to produce the hydrophobic product are between 300°C and 450°C, and at the higher temperatures, numerous decomposition reactions take place, as does the formation of organic radicals; organo-chlorides can be particularly toxic and traces of these have been detected from brown coal using TOF-SIMS (discussed previously). Low rank coals subjected to these conditions greatly increase the formation of oxy-radicals, especially phenoxy-type radicals, and these take part in recombination and addition reactions. Free-radical mechanisms are ubiquitous for pyrolysis and thermolysis of organics' substrates, and complicated reaction schemes include bond-breaking radical formation and radical-interconversion that would lead to a variety of species (Poutsma, 2000). It is highly likely the wastewater contains carcinogenic species; such toxic waste is difficult and expensive to treat, and the production of such toxic waste is prohibited by law.

The quality of the coal slurry as fuel derived from the hydrothermal treatment is relatively poor as the moisture levels are marginally lower and most of the ash remains in the coal.

Treatment with Caustic

There are numerous reports and patents dealing with processes that use sodium hydroxide to treat high rank coal, converting the ash into soluble sodium silicates and clays into sodium aluminosilicates. As has been noted for the hydrothermal process, it is likely that waste from this process would be toxic if the process is carried out for low rank coal at elevated temperatures. A process patented in 1989 (US patent 4859212) commences with heating the coal at between 420°C to 450°C (to remove volatiles) for 10-30 minutes, followed by leaching with molten caustic. This removes 95wt% of ash and 90wt% of sulphur. After leaching, the coal-caustic mixture is washed with water to remove the soluble salts and then with diluted acid to remove ionically bound alkali metals and base-insoluble species such as iron hydroxides. The coal is finally washed with water to remove any residual acid. A counter current washing procedure may be used for the water washing of the coal-caustic mixture and for the acid washing step, or alternatively concurrent washings may be used.

Generally, after the treatment of the coal with caustic, the mixtures are treated with acid which dissolves the silicates, and then separates the coal by filtration. Any remaining minerals are removed at various temperatures by washing the treated coal to obtain a low ash content. Various coal treatment processes have been tested, some using molten NaOH, and $NaOH/Ca(OH)_2$, at temperatures of 325-415°C and 250-300°C. The general features are similar to the process developed by the CSIRO for black coal, which has been reported to produce ultra-clean coal (Brooks et al., 2000).

The chemistry for this process is summarised as the dissolution of minerals, such as $[Al_2SiO_5](OH)_4$ by NaOH, to form sodium aluminosilicates, such as $Na_4Si_3Al_3O_{12}(OH)_2$, which are dissolved with sulphuric acid into the soluble salts Na_2SO_4, $Al_2(SO_4)_3$ and H_2SiO_3.

An international patent (WO/2010/026600) claims to have improved the beneficiation of coal by using caustic leaching, with acid treatment and washing, to reduce high ash Indian coal to an ash content of 4-5wt% with a yield of clean coal of 75-85wt%.

The treatment of high ash low rank coals with caustic and acid have met with limited success. Reports include treating high sulphur coal from Assam, India, with aqueous sodium hydroxide followed by hydrochloric acid, resulting in a significant removal of mineral matters and sulphur from

the coal. The report states 43-50wt% of the ash, 10wt% of the total inorganic sulphur, and about 10wt% of the organic sulphur were removed with a 16wt% sodium hydroxide solution followed by 10wt% hydrochloric acid (Mukherjee and Borthakur, 2001). The resulting product is nonetheless of a relatively poor quality. An attempt to upgrade low grade Indian coal using caustic leaching, followed by sulphuric acid at 100°C, resulted in reductions of ash by 28-48wt% (Behera et al., 2017). A grinding and alkaline leaching process was applied to lignite and black coals, resulting in a reduction of total sulphur and arsenic, and a reduction in ash of 43wt% for the brown coal. The wear of equipment due to grinding the coal was a drawback (Baláž, 2001).

Treatments with Acids

There are numerous patents that discuss the de-ashing of coals using a variety of acids. The important processes use a mixture of acids (HCl, HNO_3) with hydrofluoric acid (HF); these methods are well researched, and can produce ultra-clean black coal with ash of 1wt% to 0.1wt%. The treatment by HF precipitates a number of insoluble inorganic fluorides and subsequent treatment with HNO_3 is required to remove these, and also to dissolve a portion of FeS_2, but this also oxidises some of the organic matrix (Steel and Patrick, 2001). A partial reduction in the ash of high sulphur coal from Assam, India, was reported using various concentrations of acid and temperatures of up to 95°C (Mukherjee and Borthakur, 2004). Other examples of chemical treatments for coals have been discussed (Couch, 1990), and a number of processes have been patented (for example, US patents 4780112, 4743271, 4618346, 4741741, 4695290 and 4569678). Nearly all are acid leaching processes using a combination of acids, including hydrofluoric acid, to remove silicates from hydrophobic black coals. Black coals mostly encapsulate ash-forming entities within the coal matrix, and the hydrophobic properties of high rank coals repel aqueous acid solutions. Consequently, measures are required to expose the ash-forming species to attack by acid and also to enhance the rates of the reaction of acid with ash entities. These processes include significant crushing of the coal to release ash and a usage of elevated temperatures, with a combination of various acids. This requires a complicated plant operating at elevated temperatures, and using strong acids.

These conditions are in contrast to the CCT P/L process, which is carried out at moderate temperatures and relatively lower acidity, discussed below.

Solvent extraction

This approach extracts the organic matter from coals using various solvents at elevated temperatures. For example, ash-free coal is extracted from low rank Canadian coals with a non-polar organic solvent and an organic polar-non-polar solvent mixture; in some cases, the mixture may contain hydro-treated heavy aromatic hydrocarbon solvents from the coal-tar industry. High temperature solvent extraction may be carried out in the range of 200°C to 500°C. Yields vary from about 30% (daf) using 1-methylnaphthalene, a non-polar solvent, to 73% (daf) using hydrotreated aromatic hydrocarbons at 400°C. The heating value of the product is estimated at 36-37 MJ/kg, and with a 12.5-61.1% decrease in sulphur content (Rahman et al., 2013). The treatments of various ranks of coal have been reported using several organic solvents, including tetralin, 1-methylnaphthalene, dimethylnaphthalene and light oil, at temperatures of 200°C to 380°C, followed by solid/solution separation at room temperature. The ash in seven of the nine treated coals was reported at ≤0.1wt% (Yoshida et al., 2002).

Moisture Reduction of Low Rank Coals

Moisture content in low rank coals varies from ≥60wt% for brown coal to 30-40wt% for lignite, and below 30wt% for sub-bituminous coal. Low rank coal moisture consists of surface (free) water, inherent or physically bound water, and water molecules hydrogen bonded within the coal molecular matrix. In order to process low rank coals into high quality fuels, the moisture content is usually reduced down to 10-20wt%; further drying requires additional heat to remove water that is hydrogen bonded to coal functional groups, and further reduction in moisture may be considered impractical. With an increase in the reduction in moisture, low rank coal particles shrink and undergo some fragmentation, producing coal fines. The dry coal can also undergo spontaneous combustion when stored. A number of methods have been developed solely for moisture reduction; the most common is flash (evaporative) drying, in which hot gases from a boiler are recycled through the pulverising mills to crush and dry the coal prior to entry into the coal flame. This method has been widely used for many years as an integral part of subcritical boilers in power stations fuelled with brown coal.

Numerous drying methods have been developed, or are being developed, including steam tube drying, rotary drum drying, batch Fleissner process, and fluidised-bed drying. When water is removed as a liquid, the energy requirement for drying is lower than that required for evaporative drying. A

number of processes have been derived from this concept, all using pressure and temperature to ultimately remove moisture as liquid water. The specific energy requirements for these are 0.6 to 1.7 MJ/kg of liquid water removed (compared with 3.0 to 4.5 MJ/kg for plants that evaporate water). Most low rank coal drying technologies suffer from losses of fines, spontaneous combustion, and the production of polluting wastewater. Other drying techniques under development include using hot oil to drive off moisture, which also coats the dry coal particles with oil; this concept offers the capability for producing a dry coal, suppressing dust, and rendering the coal suitable for transport.

Fluidised bed dryers have been used successfully for drying sub-bituminous, lignite, and brown coal. Fluidised bed drying variations include using hot air, flue gas, or steam to fluidise a bed of lignite/brown coal particles, and have been designed to use single, two, and three stage processes. The advantages of fluidised bed drying include the large contact surface area between solids and gas, the high thermal inertia of solids, and the rapid transfer of heat and moisture between solids and gas, which shortens drying time considerably. There are a number of challenges in using this drying technology for low rank coals at the large scale required for power plants; a major concern is the self-ignition of low rank coals when using hot air as the fluidising medium. The high moisture content and particle agglomerate of low rank coals can also be detrimental to fluidisation. However, the technology offers a fast drying speed, resulting in high production, relatively low energy consumption, and automatic control. Consequently, numerous studies have been performed to clarify the mechanism, and various innovations have been examined, in attempts to improve the technology, such as microwave heating, vibration, and agitation (Si et al., 2015).

Drying methods developed for commercial implementation have included the tubular drier, the WTA* drier and the Coal Creek fluidised bed coal dryer by Great River Energy (Bullinger et al., 2006).

The Coal Creek pilot fluidised bed coal dryer examined drying rates for North Dakota lignite at low temperatures, and results indicated neither coal oxidation nor appreciable devolatilisation occurred, nor were any operational difficulties encountered. The fluidised bed coal dryer separates the denser materials in the coal, such as pyrites, small rocks, and sand, before it is fed to the power station. The process removes substantial fractions of sulphur and mercury from the coal. A prototype coal dryer has been built and integrated to use waste heat with the Coal Creek 1,090 MW

* WTA is the German abbreviation for fluidised-bed drying with internal waste heat utilisation.

subcritical lignite-fired power station (schematic shown in Figure 6-4). Operations began in 2006, at a nominal coal flow rate of 75 tons/hr. The moisture of the lignite was reduced by 8.2% (from 38wt%), providing a coal flow rate reduction of 2.0wt% and a coal pulverising mill power reduction of 4.5%. The boiler efficiency improved by 0.27%, with a net unit heat rate improvement of 0.34%. NOx mass emissions were lower by 8.5%, and SOx mass emissions were lower by 2.0%. Great River Energy has expanded the project into full-scale dryer modules used for the entire Coal Creek station. The technology is commercialised as DryFining™, a fuel enhancement system that uses a plant's waste heat and a proprietary fluidised-bed drying process to remove moisture and impurities from low rank coals (Ridderbusch, 2016).

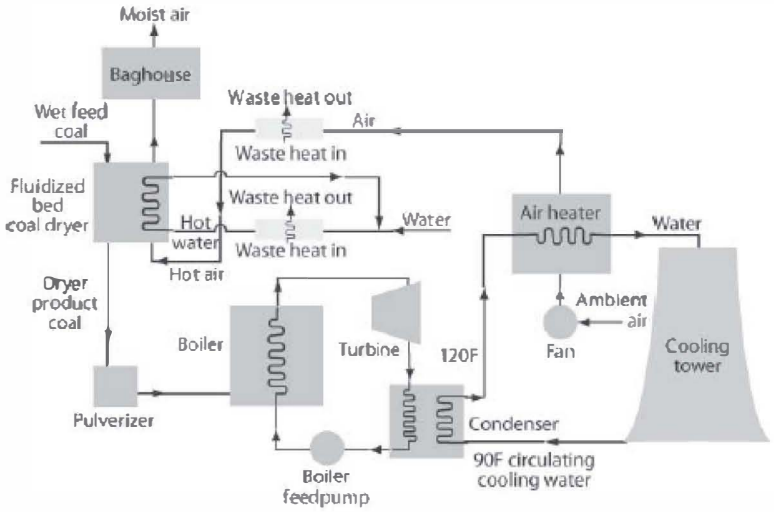

Figure 6-4. Schematic of the Great River Energy Lignite Drier, integrated with a power station, using waste heat from a condenser and flue gas (Sarunac et al., 2014).

Computer simulation studies have been carried out for the integration of an external dryer into a Greek lignite-fired power plant (Kakaras et al., 2001; Bergins, 2003).

The WTA fluid-bed drier has been developed to a commercial scale, and this is illustrated in Figure 6-5. This technology uses a stationary fluidised-bed with steam, and the heat for drying is supplied by using heat exchangers within the fluidised-bed drier. German brown coal is dried to 12wt% moisture

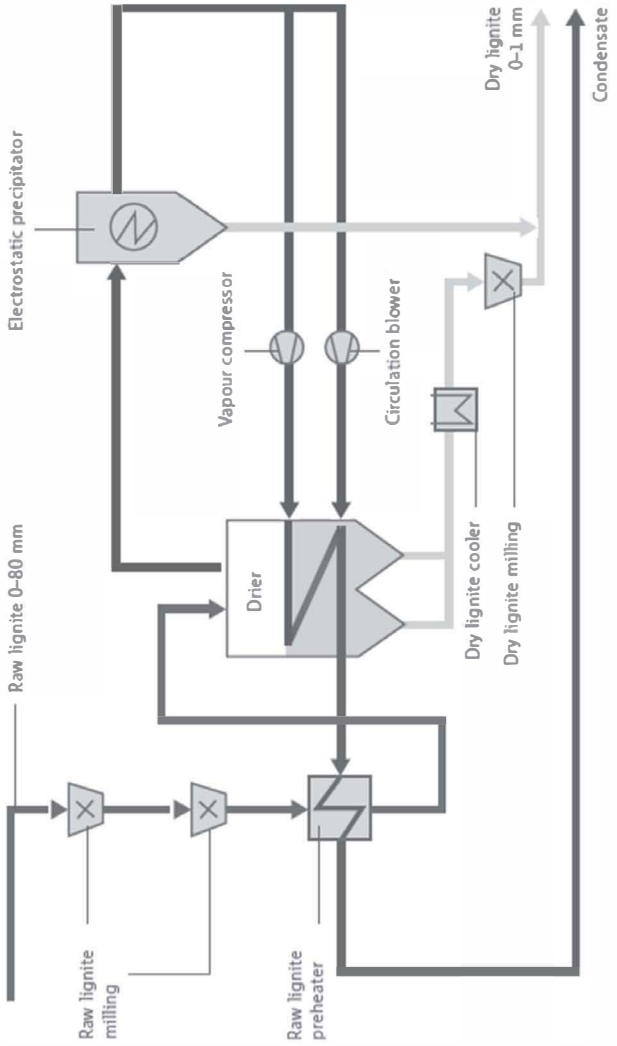

Figure 6-5. Illustration of the WTA brown coal drier with compressor (www.rwe.com).

at 110°C, and Victorian (Australia) brown coal at 107°C. Heat is provided for drying by using a compressor to compress the steam released from the coal into hot water, and the hot water is passed through the heat exchangers

(alternate designs may use low pressure steam to provide the heat for drying). This drier can be integrated with a high efficiency coal-fuelled plant; the technology has successfully operated commercially in a German brown coal-fuelled supercritical power station (Klutz, 2010). This technology is the most advanced brown coal and lignite drying process, which is reported to consume 80% less energy compared to the rotary steam tube drying process, with significantly less dust emissions and relatively lower costs (Zhu et al., 2015). Improved drying may be achieved by using vibration-fluidised bed technology. This option enables the fluidised bed to operate at a lower gas velocity, which would avoid the problem of fine particles' entrainment, and improve the gas-solid contact efficiency, resulting in improved heat and mass transfer.

Future coal-fuelled power generation requires coal processing and drying technologies that would be integrated with a power station to utilise waste heat, to be fed as fuel after being processed into high quality fuel, in plants that would operate at the highest power generation efficiencies. An integrated processing plant would avoid problems posed by a stand-alone coal drying plant, which would require heat supplied by burning coal and thereby create CO_2 emissions, with additional costs being incurred to store and transport the dried coal. Unless suitable measures are implemented, the coal dried in a stand-alone plant will re-absorb moisture, and would be faced with spontaneous combustion, a problem encountered when dried low rank coal is stored for transport.

Treatment of Coal and the CCT P/L Process

The discussion on the properties and behaviour of low rank coals has shown that any process to upgrade these into high quality fuel(s) must be applicable to all low rank coals. The process must meet environmental requirements, ensure high efficiency, and avoid the formation of coal dust and spontaneous combustion. A viable process for the production of high quality fuel must address all of the following:

- Remove ash constituents in the coal responsible for fouling and slagging.
- Increase the heating value of the product.
- Remove sulphur and chloride in coal to eliminate corrosion and emissions that cause acid rain.
- Avoid spontaneous self-combustion.
- Use waste or low-grade heat to process and dry the coal.

- Produce fuel suitable for high efficiency power generation and coal gasification.

Additionally, the coal treatment process must not produce pollutants, or toxins in the wastewater, and the high quality fuel must be economically competitive for power generation plants. The process must be a concept that can be developed to a commercial scale, and used in plants designed for a low carbon footprint.

The coal treatment plant could also be modified to add inorganic species that would act as catalysts for steam gasification of the processed coal.

The discussion on coal combustion and the chemistry of ash formation identified the predominant factors that cause ash fouling and slagging; these are volatile alkalis, various inorganic phases that form within burning char particles, and the formation of molten alumina-silicate particles. While a number of measures have been used in attempts to deal with the fouling and build-up of deposits in boilers, these have been limited in their scope, are not applicable to all low rank coal, and add to the expense of power generation. Coal blending is a practical approach if an abundant supply of good quality low-ash coal is available for blending with high ash coal, but once the supply of low-ash coal has been exhausted, the ash fouling problems for such plants would increase as the remaining fuel is of poor quality.

A coal treatment process should remove all fouling and slagging moieties, and the boilers should be designed to operate using fuel without ash fouling problems.

Moisture reduction can produce a coal with a higher calorific value, but this approach to producing high quality fuel is only viable if an abundant supply of low-ash coal is available. For most low rank coals, moisture reduction would produce a coal that burnt at higher coal flame temperatures and this would worsen ash fouling and slagging problems.

Any process that operates by heating low rank coal, or a coal/water mixture, to temperatures exceeding 250°C will yield unacceptable amounts of pollutants, and would often face spontaneous combustion problems. These difficulties have been experienced by numerous methods; a viable upgrading methodology must avoid these problems, and also maintain the economic advantages of low rank coals.

These difficulties, and the variability of the properties of low rank coal, necessitate a comprehensive coal treatment process that can be applied to all low rank coals, and one that is economical for commercial exploitation; such a comprehensive approach, in addition to eliminating ash-related problems, would also be carried out at temperatures that enhance the rate of

ash removal to ensure good production rates. The heat added to reduce ash should also be used to reduce the moisture in the coal, and, in this way, provide a non-fouling coal with higher heat content at a lower cost. Such a process would also remove inorganic forms of sulphur and chloride, thereby reducing SOx and HCl emissions, and low NOx burners would be used to lower NOx emissions.

A general coal processing methodology that meets these requirements must be grounded in a comprehensive R&D program to define the general conditions applicable for all low rank coals' upgrading into high quality products, and avoid problems such as wastewater pollutants and spontaneous combustion. The CCT P/L Program has provided fundamental data that are the basis of such a general concept for processing low-rank coals.

An economical process would integrate the coal treatment plant with the power plant to use waste heat (or low grade heat) to process the coal into non-fouling fuel for high efficiency power generating, operating at higher thermal efficiency, and thus achieve lower emissions (values typical for combined heat and power plants). The integrated process does not expose the processed coal to atmospheric oxygen, thereby avoiding spontaneous combustion. An ultra-clean coal (virtually zero-ash) should fuel a direct or indirect coal-fired combined-cycle plant operating at very high efficiency.

The CCTP/L Process is fully integrated to remove ash and moisture from low rank coals and produce fuel specifically designed for high efficiency power plants. This general concept may also be modified to add inorganics to the coal that would act as catalysts for coal-steam gasification. The concept is applicable to all hydrophilic coals, and has been devised to produce three categories of high quality fuel: (a) non-fouling coal, (b) virtually zero-ash coal, and (c) coal with catalysts for steam gasification.

Removal of Inorganic Ash Constituents from Low Rank Coals.

The hydrophilic property of low rank coals ensures water and acid can penetrate the coal matrix, and consequently acid treatment would attack all functional groups in the coal matrix and solubilise the chemically associated inorganic ash-forming species. The remaining ash-forming moieties are extraneous mineral, sand, and clay particles that are obtained from interseam layers during the mining of the coal seam, and these may also be by subject to attack with acid. The thermal instability of low rank coal, however, requires a process temperature that would enhance the rate of acid attack, but avoid the thermal breakdown of the organic coal matrix, as this would produce toxic wastewater.

The general features of this process need to:

1. Remove inorganics associated with the coal matrix.
2. Remove inorganics present in mineral particles mixed with the coal.
3. Remove the remaining alumina-silicates present in the coal.
4. Add selected inorganics for catalytic chemistry.

A process that achieves (1) and (2) would produce non-fouling coal, and one that achieves (1), (2) and (3) would produce virtually zero-ash coal; achieving (4) would produce catalytically-loaded coal.

Ash-forming components are often found in more than one chemical environment in coal and thus exhibit several types of behaviour. Treatment with acid can solubilise ash constituents chemically associated with the coal matrix (including sodium, potassium, calcium and iron), while more aggressive methods are needed to remove the inorganics present in the mineral particles mixed with the coal. Finally, virtually zero-ash coal would require dissolving all remaining extraneous mineral particles, and this can be carried out in an additional step with an appropriate fluoro-acid.

The action of acid renders the chemically associated sodium, magnesium, and calcium (and some iron) into soluble cations, and these must be washed out of the hydrophilic coal as dissolved salts using clean water. Washing the coal is of practical significance, since without an adequate washing of the treated coal, the inorganics remain as a solution within the coal. Figure 6-6 illustrates the impact of washing the coal after it is treated with acid. A relationship between pH and the extent of the removal of inorganics is shown in Figure 6-7.

The chemistry is summarised by the following equation:

$$\text{Coal-(n)M} + n\text{H}^+ \rightarrow \text{Coal-(n)H} + \text{M}^{n+}$$

where (n)M are inorganics and M^{n+} represents cations dissolved in the water phase of the coal/water mixture. Simple filtration would leave a considerable proportion of these cations in the water within the coal pores, and for brown coal, this water content would be >60wt% of the coal, which would contain a corresponding proportion of solubilised inorganics. The CCT Process is designed to completely remove the dissolved inorganics from the treated coal by a number of washing cycles.

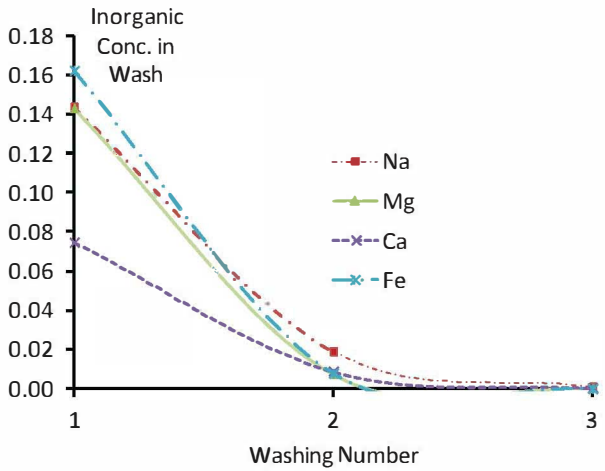

Figure 6-6. Inorganics removed from coal by washing after acid treatment.

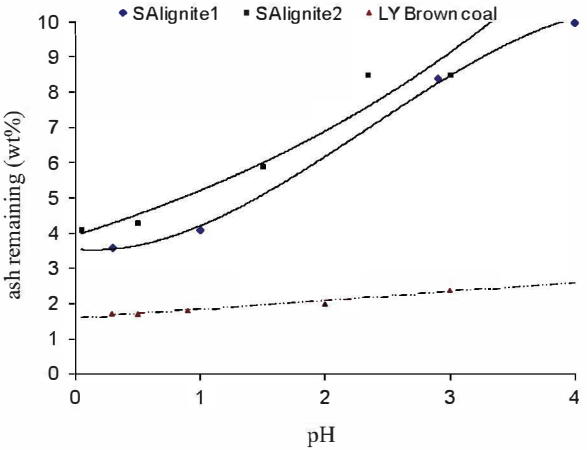

Figure 6-7. Amount of ash remaining after treatment at various pH levels.

XRD and elemental analysis of ashes from treated coals show that water washing after acid treatment can remove most of the dissolved Ca/Mg/Fe/Na/K. The ash remaining in the treated coals consists mainly of quartz and aluminosilicate (clays); data for SAlignite1 below show that ~90wt% of the ash in the treated coal consists of SiO_2 and Al_2O_3, and 80wt% of this is silica. This can be compared to the raw coal, in which 46.3% in

the ash consists of SiO_2 and Al_2O_3. Na/K/Mg/Ca for this coal were reduced by acid treatment from a total of 33% of the ash to ≤2.5%. The total ash was reduced from 11.5wt% to 4.5wt% of the dry coal. The analyses data of the ash from ar Salignite1 and the same aw coal cleaned are:

	$\%SiO_2$	$\%Al_2O_3$	$\%Fe_2O_3$	%MgO	%CaO	$\%Na_2O$	$\%K_2O$	$\%SO_3$	%Cl	TiO_2
ar	38.03	8.26	5.33	11.31	15.65	5.14	0.86	11.94	2.32	1.15
aw	80.41	9.71	2.26	0.46	1.73	0.10	0.21	0.59	0.50	2.60

Similar results were obtained for a high ash coal sample (SAlignite2); after acid treatment and water washing, ~90wt% of the ash in the cleaned coal consisted of SiO_2 and Al_2O_3. The total ash was reduced from 17wt% to about 4wt%, and total Na/K/Mg/Ca levels were reduced to <0.1wt%.

The CCT acid treatment of a sub-bituminous coal caused a reduction of Mg/Ca/Na to low levels, while the proportional sum of SiO_2 and Al_2O_3 changed from 75wt% of the ash in the untreated coal to 92wt% of the treated coal. Although the action of acid on minerals can be complicated due to the large and diverse range of mineral that may be found in coals, and many of these contain inorganic cations, laboratory results have shown the appropriate acid treatment removes the bulk of all inorganics, and often may remove some silica and alumina. For example, acid and water washing treatment of a high ash sub-bituminous coal (28.9wt% ash in the untreated coal, reduced to 20.5wt% after acid treatment, with the remaining ash predominately being formed of silicate minerals) removed most of the Fe/Mg/Ca/Na in the ash, as shown by the analysis data:

	$\%SiO_2$	$\%TiO_2$	$\%Al_2O_3$	$\%Fe_2O_3$	%MgO	%CaO	$\%Na_2O$	$\%K_2O$	$\%SO_3$	%Cl
ar	50.40	2.23	24.69	7.46	2.48	5.73	2.80	1.12	1.42	0.37
aw	61.87	2.89	30.18	1.05	0.35	1.07	0.02	1.13	0.57	0.72

Further data on lignites, in which the ash of the untreated coal consisted of ~75% of SiO_2 and Al_2O_3, show the acid treatment provided ash consisting of 92% SiO_2 and Al_2O_3; acid treatment also reduced the alumina content due to the removal of some aluminium as aqua-compounds from the coal matrix, and also some silica and alumina dissolved from mineral phases, as shown by the following coal ash analysis data:

Coal	SiO_2		Al_2O_3	
SAlignite1	Ar 3.8%	Aw 2.0%	Ar 1.2%	Aw 0.1%
SAlignite2	Ar 4.0%	Aw 3.4%	Ar 0.5%	Aw 0.1%

Results for German and Victorian brown coals (containing 3-5wt% ash) also show acid treatment can effectively remove inorganics. The small amount of ash from these coals consists of clays and silica.

While laboratory experiments show that acid treatment at the appropriate pH, followed by effective washing, can produce non-fouling coal, the rate that de-ashing occurs under laboratory conditions is insufficient for an industrial process. The action of acid at pH~2 at mild temperatures is slow, and higher temperatures are required to enable the rapid removal of ash in a practical process. The CCT P/L process operates at an elevated temperature (above 100°C and below 200°C), and the treatment plant is designed to enable the rapid removal of inorganics, while avoiding creating toxic organics from the decomposition of the coal organics matrix, and to wash out dissolved species from the treated coal. The wastewater is collected and treated to provide clean water, and is then recycled for further coal treatment.

Demineralising Low Rank Coals

Acid treatment at appropriate conditions can remove virtually all aggressive inorganic ash constituents from low rank coal, and also removes some of the inorganics found in extraneous mineral particles mixed with the mined coal. A list of the common minerals that may be found in coals is provided below.

Mineral found in mined coal		Mineral found in mined coal	
Muscovite	$KAl_2(AlSiO_3O_{10})(OH)_2$	Staurolite	$2FeO\ 5Al_2O_3\ 4SiO_2\ H_2O$
Kaolinite	$Al_2Si_2O_5(OH)_4$	Topaz	$(AlF)_2SiO_4$
Siderite	$FeCO_3$	Pyrophyllite	$Al_2Si_4O_{10}(OH)_2$
Hematite	Fe_3O_4	Illite	$K(MgAl,Si)\ (Al,Si_3)O_{10}\ (OH)_8$
Quartz	SiO_2	Montomorillonite	$(MgAl)_8\ (Si_4O_{10})_3\ (OH)_{10}\ 12H_2O$
Zircon	$ZrSiO_4$	Prochlorite	$2FeO\ 2MgO\ Al_2O_3\ 2SiO_2\ 2H_2O$
Diaspore	$Al_2O_3.H_2O$	Chlorite	$(Mg,Fe,Al)_6\ (Si,Al)_4\ O_{10}(OH)_8$
Lepidocrocite	$Fe_2O_3.H_2O$	Gypsum	$CaSO_4\ 2H_2O$
Kyanite	$Al_2O_3SiO_2$	Penninite	$5MgO\ Al_2O_3\ 3SiO_2\ 2H_2O$
Calcite	$CaCO_3$	Ankerite	$CaCO_3(Mg,Fe,Mn)CO_3$
Magnetite	Fe_2O_3	Garnet	$3CaO\ Al_2O_3\ 3SiO_2$
Pyrite	FeS_2	Hornlende	$CaO\ 3FeO\ 4SiO_2$
Marcasite	FeS_2	Apatite	$9CaO\ 3P_2O_5\ CaF_2$
Augite	$CaO\ MgO\ 2SiO_2$	Epidote	$4CaO\ 3Al_2O_3\ 6SiO_2\ H_2O$
Feldspar	$(K,Na)_2OAl_2O_36SiO_2$	Biotite	$K_2O\ MgO\ Al_2O_3\ 3SiO_2\ H_2O$

Conventional methods for dissolving alumino-silicates and silica use hydrofluoric acid, and the rate of silicates dissolution increases when using a mixture of mineral and hydrofluoric acids. Studies have shown that the overall dissolution of silicates comprises parallel catalysed and un-catalysed reactions, and the catalysed reactions are related to the adsorption of H_3O^+ at the dissolving mineral surface (Langmyr and Paus, 1968; Kline and Fogler, 1981). However, if the low rank coal were initially treated with hydrofluoric acid, reactions with K, Na, Ca and Mg within the coal can form fluoride precipitates (e.g. CaF_2, MgF_2 and $NaAlF_4$) and these could remain in the coal. If elevated temperatures are employed, it is possible that reactions of HF with the organics matrix of low rank coals may form organo-fluoro species. Chemistry that forms fluoro by-products is undesirable and the correct conditions must be chosen to dissolve the mineral particles present in low rank coals, and avoid undesirable by-products.

The chemistry involving hydrofluoric acid to produce ultra-clean black coal has been discussed in great detail, and it differs from that used in the CCT Process. This black coal treatment method commences by mixing HF with the coal, followed by a step to remove fluoro products using a mineral acid such as HNO_3 or HCl. This work has shown that HF reacts preferentially with aluminosilicate compounds in mineral matter present within the black coal. Two distinct HF concentration regions were identified in which different chemical mechanisms occur. Treating the mineral matter with sub-stoichiometric concentrations of HF yields mainly AlF_3, SiF_4 and SiF_6^{2-}, with minor amounts of AlF_2 and AlF_4, in equilibrium with the AlF_3. This equilibrium produced H_3O^+ ions that dissolved the inorganics in the mineral matter, producing soluble Na^+, Ca^{2+} and Mg^{2+} species. The available F^- in the equilibrium with the AlF_3, SiF_4 and SiF_6^{2-} is insufficient for the formation of CaF_2 and MgF_2 precipitates, nor is the concentration of AlF_4^- sufficient to create a complex with Na^+ and form the precipitate $NaAlF_4$, or the precipitate $MgAlF_5$. This chemistry provides a foundation for de-ashing high rank coals and addresses costs by devising a strategy for recovering reagents, such as HF, from the spent liquors (Steel et al., 2001).

Numerous patents also disclose various processes that use hydrochloric and hydrofluoric acid solutions on coals (e.g. US patent 4695290). The products from such processes often include gaseous HF and perhaps SiF_4, both of which are extremely toxic and should be avoided in commercial coal treatment processes.

The CCT P/L process avoids forming fluoride precipitates in the coal by initially removing cations prior to demineralisation with fluoro-acid. It has been found that the action of acid in removing inorganics from minerals

renders the remaining clays and amorphous silicates more susceptible to dissolution using dilute fluoro-silicic acid. The effects of strong acids such as HNO_3 and HCl on this chemistry are not related to the consumption of H_3O^+ by any silicate, but instead they are considered a catalytic action at the solid-liquid interface of HF dissolution of silicate complexes.

Overall, the CCT P/L coal treatment process consists of two distinct steps performed separately: (1) acid solubilisation and washing out inorganics in the coal, and (2) fluoro-silicic acid dissolution of remaining alumina-silicates, and washing out the mixture, resulting in virtually zero-ash coal. The washing is critical for the quality of the product, and virtually zero-ash coal needs a final wash with ultra-pure water.

Generally, the CCT P/L process avoids the chemistry of hydrofluoric acid on silica, alumino-silica, and complex minerals, as this could form toxic gaseous SiF_4; the chemistry avoided by the CCT P/L process is illustrated by the reactions of HF with SiO_2 and kaolin to form SiF_4 and AlF_3:

$$SiO_2 + 4HF \rightarrow SiF_4 + 2H_2O$$
$$SiO_2.Al_2O_3 + 10HF \rightarrow SiF_4 + 2AlF_3 + 5H_2O$$

Additionally, the action of HF on a mineral can also form insoluble compounds such as calcium fluoride CaF_2. The chemical reaction for garnet ($3CaO.Al_2O_3.3SiO_2$) with HF illustrates this:

$$[3CaO.Al_2O_3.3SiO_2] + 24HF \rightarrow 3SiF_4 + 2AlF_3 + 3CaF_2 + 12H_2O$$

Sodium aluminium fluoro-complexes of low solubility (e.g. $NaAlF_3$) will also form if Na is present. These unwanted compounds are avoided in the CCT P/L process by adopting the chemistry summarised as follows:

1. Remove inorganic cations from the coal matrix and discreet mineral particles using mineral acid (H_2SO_4 or HCl):

$$Coal\text{-}[M^{n+}] + nH_3O^+ \rightarrow CoalH + [M^{n+}] + nH_2O$$
$$\{SiO_2.Al_2O_3.[(M)OH]\} + H_3O^+ \rightarrow SiO_2.Al_2O_3 + [(M^+)] + 2H_2O$$

$[(M^+)]$ and [(M)OH] are cations found in the coal matrix, and in mineral particles. M = K, Na, Mg, Fe, Ca.

2. Remove silicates and alumino-silicates using dilute fluorosilicic acid.

$$2[\text{-}SiO(OH)] + HF + H_3O^+ \rightarrow [\text{-}Si(OH)_2F] + [\text{-}Si(OH)_2\text{-}] + H_3O^+$$
fluorosilicic acid *silica gel* *acid*

The chemistry illustrated by reaction sequence (1) (termed step 1) solubilises the cations in coal, and the plant is designed to completely wash these out of the coal. Once this has been done, reaction sequence (2) (termed step 2) is carried out with dilute HF which forms a water soluble mixture of fluorosilicic acid and silicic gel; protons from the mineral acid used in "step 1" may participate in dissolving silicates, and are considered to exert a catalytic action. "Step 1" also removes cations from the silicate particles, and these cations are replaced by H_3O^+ added to the alumino-silicate matrix, and this facilitates the formation of water soluble silicic acid species.

Fluoride can be recovered from the wastewater used to wash out dissolved species from reaction sequence (2) for re-use by using a mixture of $Ca(OH)_2$ and $CaCl_2$, e.g.:

$$2Ca(OH)_2 + H_2SiF_6 + CaCl_2 \rightarrow 3CaF_2 + Si(OH)_4 + 2HCl$$
$$Ca(OH)_2 + 2HCl \rightarrow CaCl_2 + 2H_2O$$

Hydrofluoric acid may be regenerated using established techniques, e.g. reacting CaF_2 with H_2SO_4:

$$CaF_2 + H_2SO_4 \rightarrow 2HF\uparrow + CaSO_4$$

The efficacy of the chemistry summarised by "step 1" is illustrated by laboratory results obtained for a suite of low rank coals from Victoria, Western Australia, South Australia and Germany. These coal samples were treated using mineral acid (H_2SO_4 or HCl); the analysis of the remaining ash is shown in Table 6-1.

Table 6-1. Analysis of ash after acid extraction – Reaction 1 (%wt, dry coal; ND=not detected)

Sample	%SiO_2	%Al_2O_3	%Fe	%Mg	%Ca	%Na	%K	%Cl	%Ash
SAlignite1	2.20	0.25	0.03	ND	0.01	0.001	0.003	0.01	2.5
SAlignite2	4.66	0.23	0.15	0.01	0.01	0.002	0.026	-	5.3
Loy Yang	0.07	0.01	0.01	ND	0.00	0.001	-	-	0.1
German I	ND	ND	0.01	ND	0.01	0.004	-	-	0.3
German II	ND	ND	0.04	0.01	0.02	0.005	-	-	0.4
Sub-bituminous – (untreated, %ash = 5.6; treated, %ash = 2.4)									

The results from employing reaction sequence (2) to coal samples, treated after they had undergone reaction sequence (1) followed by being thoroughly washed with distilled water and then with ultra-pure water after

reaction sequence (2), are shown in Table 6-2 (these brown coal samples were subjected to a variety of conditions of HF concentration, temperature and washing, and were analysed for ash constituents using ICP-AA). The variations observed are directly related to the conditions and equipment used in treating the coal, which are background concentrations (e.g. sodium was shown to increase if soda-glass beakers were used in handling ultra-pure water used in washing the coal samples subjected to "step 2", because small amounts of sodium were leached out of the glass container).

Table 6-2. Analysis of virtually zero-ash coal samples from the CCT P/L process (ppm)*

Sample	V	Na	Mg	Al	Si	K	Ca	Fe	Ti	Total
Loy Yang1	<3	10	< 2	20	233	<5	7	22	20	<322
Loy Yang2	<2	20	<2	<20	20	<10	9	8	8	<99
German1	-	7	41	37	46	-	97	149	27	460
German2	-	5	7	19	94	<5	23	42	35	231

The CCT P/L Low Rank Coal Process

The notable differences between the CCT P/L methodology and other coal treatment methods are:

- Producing virtually zero-ash coal (the levels of ash-forming species are at the background amounts set by the process materials)
- Maintaining the relative cost advantage of low rank coals
- Avoiding the creation of pollutants

This concept achieves the often conflicting goals of relatively low cost and non-polluting outcomes. Ordinarily, coal processes incur additional costs when pollution avoidance measures are employed, and if toxic substances are created, there are additional concerns for the safe disposal of toxic waste.

The chemistry discussed here forms the basis for the coal process developed by Domazetis; the research on the fundamental chemistry has been part of the CCT/LTU R&D collaborative program (Raetz, 2009). The

* Amended with permission from Domazetis et al., Fuel Processing Technology, 89, 2008, 68-78. Copyright (2008) Elsevier.

concept has since been developed into the design of a plant; the design considerations include a number of aspects, such as the impact of coal particle size distribution, the compressibility of a coal bed under pressure, the materials of a vessel suitable for performing the acid treatment chemistry at the appropriate temperature and pressure, water washing, and water recovery. The concept includes drying the coal after acid treatment with a fluidised coal drying unit that is loaded with the hot clean coal to reduce its moisture. The dry clean coal is directly used to fuel a high efficiency power plant. Figure 6-8 outlines a schematic of a CCT processing plant with the capability of using low grade heat by integrating the process with a power plant.

The coal treatment process must include the efficient separation of the coal from the wastewater for the large scale production required for commercial application. This is achieved with a vessel used to process the coal, which is designed to filter the wastewater from the bed of coal particles. The coal bed porosity and bed depth will determine the rate at which the water may move through the bed and the filter at the given pressure. The coal bed porosity will be determined by the size distribution of the coal particles, as well as the compression of the coal bed subjected to the pressure used to force the liquid out. The packing of the coal particles, with a selected particle distribution range, may cause any fine particles to form dense regions, particularly at the filter membrane situated at the bottom of the coal bed, as fines are more easily carried by the flow of liquid. This could reduce the flow rate. Coal bed compression is related to the pressure, which results in decreasing particle-particle voidage. The extreme case would be compression of the coal that ultimately causes low particle-particle voidage, so that water cannot flow through the bed at a sufficient rate for a practical process. Compression of the coal bed can be avoided by designing the treatment vessel with the capability to initially adjust the flow rate of liquid through the porous coal bed, and minimise compression. Measures are also taken to reduce the proportion of coal fines during the crushing of the mined coal.

The CCT P/L process uses a proprietary design that includes a self-cleaning filtration membrane and fluid flow control through the bed of a given size distribution of coal particles. The features of the process include crushing and sieving to ensure that a minimum amount of fines is formed. A typical calculation of the impact of compression on the flow rate through a bed of brown coal particles envisaged for a commercial coal treatment process is shown in Figure 6-9.

Calculations have been carried out to obtain an indication of the impact of the size distribution of the coal particles on the flow rate and pressure drop across the coal bed. Various approaches have been used in these empirical

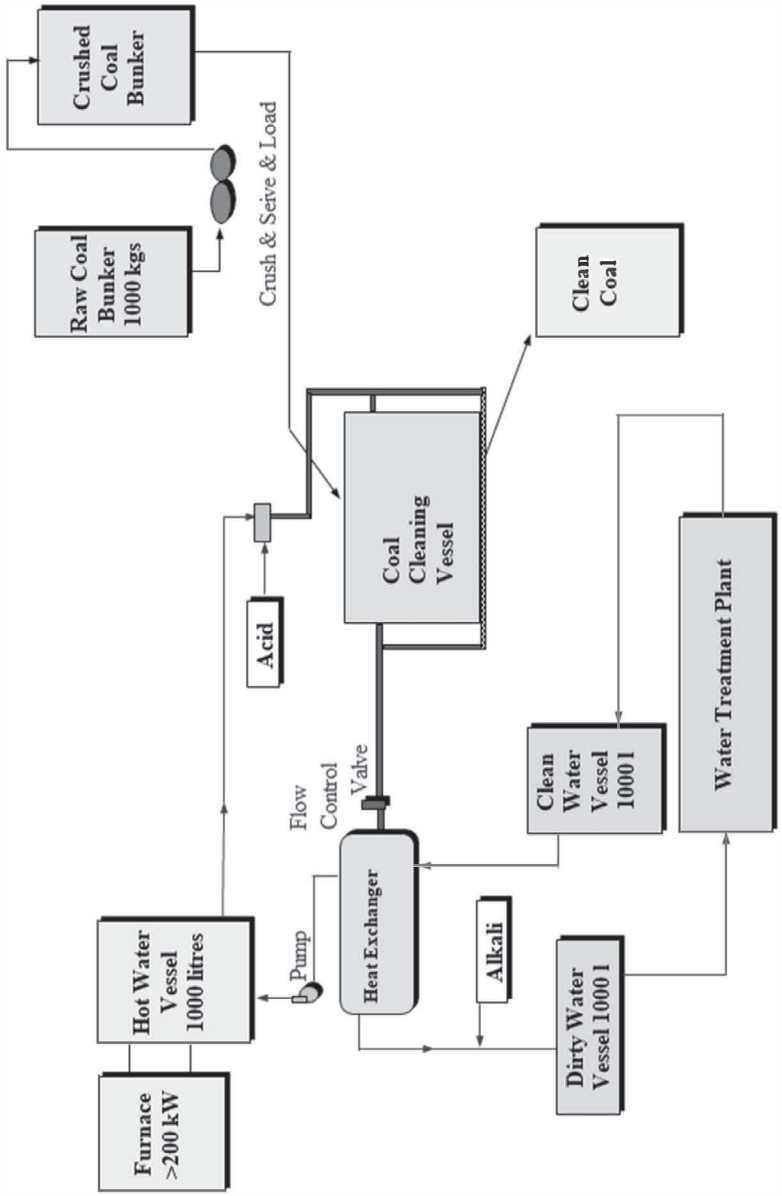

Figure 6-8. Schematic outlining major aspects of the CCT P/L low rank coal processing plant.

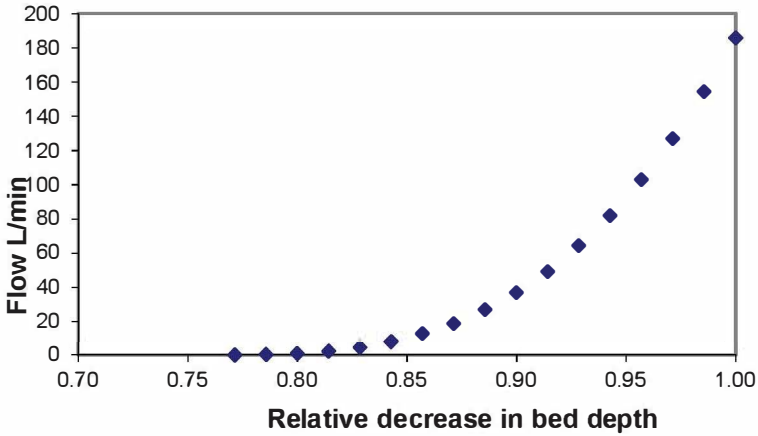

Figure 6-9. Impact of compression of a bed of low rank coal particles on the flow rate of wastewater.

calculations, including partitioning the coal into bins that represent the particle size distribution, and also placing particles into a given volume to obtain an estimate of porosity with particle size distribution. These calculations highlight the impact of very fine coal particles (1 to .01-micron diameter) on the flow rate, even when they are a relatively small portion of the total coal, especially when the coal bed undergoes compression.

The calculated results have compared well with experimental data for coals from Victoria, Germany, South Australia and Western Australia, treated using a laboratory apparatus with the required design features, operating at elevated temperatures and pressures. These experiments provided rates of flow at the upper range of calculated flows, indicating coal cleaning may proceed well within acceptable flow rates. The analysis of the coals treated using acid provided data that are consistent with the predicted values, namely, sodium was reduced to the levels of the distilled water used in the experiment, magnesium was likewise reduced to the background levels, while calcium and other inorganics were reduced by 90-98% of the original levels. The ash in such coals was reduced to the level consistent with non-fouling coal.

The impact of one and two washing cycles on ash removal from brown coal after acid treatment is illustrated by the data in Table 6-3. The ash remaining in the coal after one washing cycle is reduced by 68-90wt%, and, after a second washing cycle, to levels consistent with non-fouling processed coal. The levels of sodium are reduced by almost 100% after two water washing cycles, which are similar to calculated values.

Table 6-3. Ash and sodium in coals with cleaning cycles of the CCT P/L process.

Coal Sample	% Ash in Coal (db)			% Na in Coal (db)		
	Untreated	Cycle 1	Cycle 2	Untreated	Experimental	Calculated
SAlignite1	11.8	3.8	2.8	0.50	0.001	0.002
Loy Yang	2.3	0.17	<0.01	0.15	<0.001	<0.001
German	4.3	0.40	0.02	0.05	<0.001	<0.001

The coal samples obtained after the treatment outlined above as "Step (2)" contained ash ranging from <99ppm to 460ppm, with sodium often at the limits of detection. The CCT P/L ultra-clean coal contains considerably lower levels of ash compared to the CSIRO ultra-clean product, as shown in Table 6-4 (these have been discussed previously); the CSIRO product contains a total ash of about 1350ppm, compared to 99-460ppm ash for the CCT product.

Results reported for the acidic treatment of black coal (Gordonstone Thermal Coal) with aqueous HF and HCl or HNO_3 removed ≥96% of the ash. The ash in the raw black coal for this process is 13-14wt%, and the ash content in the clean black coal is estimated at 0.5wt%; coal with 0.1wt% ash has also been reported (these amounts are 1,000-5,000ppm).

Table 6-4. Analysis of black coal before and after treatment by the CSIRO process.

	Si	Al	Fe	Ca	Mg	Na	K	V	Ti	Total ash
Raw (ppm)	24,800	12,300	3,383	437	431	919	464	29	733	8.3wt%
Clean (ppm)	78	~0	215	36	12	542	29	1	513	0.5wt%

Ultra-clean coal is envisaged as fuel for future high efficiency direct coal-fired turbines, and the critical components are the amounts of the volatile inorganics sodium and potassium, and the total ash. The expected concentrations of volatiles in the hot gases entering the turbine are 100-300ppb. These levels are required because higher levels of volatile sodium and potassium species can condense on turbine blades, causing corrosion, and particulates would impact and cause a build-up of ash on turbine components. GateCycle™ models of direct coal-fuelled combined-cycle plants indicate that the CCT P/L processed virtually zero-ash coal would meet the criteria for volatile species and ash loading stipulated to fuel direct coal-fuelled turbine plants.

Wastewater Treatment

Water recovery and reuse is crucial to the viability of an environmentally benign coal treatment process; this is because relatively large amounts of water are needed to wash the treated coal. It is useful to note that low-rank coals contain significant amounts of moisture, and a good portion of this would also be recovered; for high moisture brown coal, the CCT P/L process would produce a surplus of water.

As mentioned previously, the wastewater produced from a low rank coal/water mixture at an elevated temperature will contain organic and inorganic substances. The amount of soluble organics that may be released into the aqueous phase depends on the type of coal treated and the temperature of the coal/water mixture.

The CCT P/L process avoids conditions that would create pollutants from the thermal decomposition of the coal; systematic studies have shown that the formation of pollutants can be avoided at process temperatures below 200°C.

The wastewater from the CCT P/L process, when the coal is treated with mineral acid (step 1) would contain:

- Soluble organic species
- Soluble salts, mainly Na^{+}, Mg^{2+}, Ca^{2+} and Fe^{3+}
- Colloidal suspensions of clay and coal
- Coal fines

Experimental data have shown that the total dissolved solids (TDS) for the mixture of coal and water heated at temperatures between 100°C and 220°C varied for different coals; brown coal from Australia and Germany typically provided TDS of 400-650 mg/l, and lignites gave TDS levels of between 150-200 mg/l. The organics measured by chemical oxygen demand (COD) were 600 mg/l for brown coal and 250-600 mg/l for lignite over the process temperature range.

The TDS values in the wastewater depended on the amount of material removed from the coal, the temperature of the coal/water mixture, and the pH of the mixture. Brown coal treated with acid produced wastewater containing Fe^{3+}, Al^{3+}, Na^{+}, Mg^{2+}, Ca^{2+}, K^{+}, Cl^{-}, $SO_4^{=}$, silica and alumina complexes, and, if carbonates and sulphides were present, relatively small amounts of CO_2 and H_2S. Figure 6-10 illustrates the increase in TDS with temperature of a lignite/water mixture.

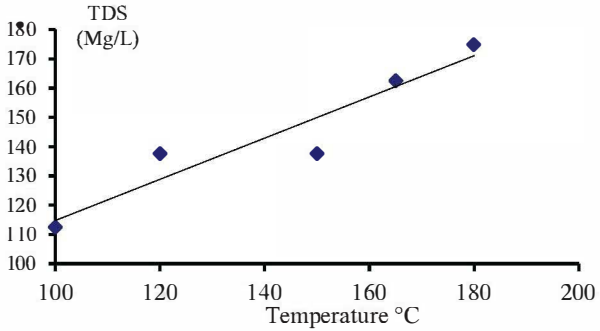

Figure 6-10. TDS in wastewater from a slurry of water and SAlignitel with temperature. Amended with permission from Domazetis et al., Fuel Processing Technology 91, 255-265, 2010. Copyright (2010). Elsevier.

The COD and TDS levels from these coals are well within the range that can be treated using conventional wastewater treatment, commencing with water clarification with coagulants and flocculants. The experimental data show that the wastewater obtained after treating brown coal and lignite contains appreciable amounts of dissolved aluminium and iron; the process takes advantage of this by developing coagulants and flocculants with iron and aluminium salts and with pH adjustment.

The chemistry of iron species in acidic and alkaline solutions is dominated by a number of hydroxyl-species. For example, at low pH, Fe^{3+} exists predominantly as the hexa-aqua ion $[Fe(H_2O)_6]^{3+}$, but at higher pH values, poly-iron hydroxyl species form. The hydrolysis and polymerisation reactions may be summarised as:

$$xFe^{3+} + yH_2O \rightarrow Fe_x(OH)_y^{(3x-y)+} + yH^+$$

Aluminium hydroxide polymeric species are created by a slow addition of a base (e.g. NaOH) and clarification is observed with an OH/Al ratio of 2.7. The relative proportions of the major aluminium species depend on factors such as the ionic strength of the wastewater, aluminium concentration, rate of addition of base, the temperature of the wastewater, and time. The polymeric species are mostly $Al_{13}(OH)_{32}^{7+}$ and some Al^{3+}, $Al(OH)^{2+}$ and $Al(OH)_2^+$.

The CCT P/L process also removes some silica from the coal, and this is present as colloidal silica and silica hydrates in wastewater. Colloidal species are removed by the coagulant; silica removal is primarily determined

by the pH of the coagulant/wastewater mixture. Experiments have identified the optimum pH as 7-7.5 for wastewater from brown coal treatment, but this value will vary for different coals. The wastewater clarification method also reduces dissolved organics present in the wastewater, measured as COD. Experimental data obtained using a proprietary Fe/Al coagulant, at the particular pH adopted, also lowered the proportion of dissolved Fe, Al and Si, leaving a clear product containing mainly dissolved Na, Mg and Ca salts. A reduction in COD of 80% was obtained using the clarification method outlined.

The clarified water would undergo further purification with reverse osmosis (RO) to produce distilled grade water and a concentrate containing the inorganics extracted from the coal. If sufficient amounts are present in the raw coal, it is possible to obtain Na/Mg sulphate from the concentrate by crystallisation; alternatively, a solid mixture of the remaining inorganics can be obtained by flash evaporation.

A summary of the results of two of the CCT P/L proprietary coagulant/flocculent mixtures, and RO data, used in water treatment for two coals is shown in Table 6-5.

The wastewater from the demineralisation (reaction sequence (2)) is also treated to recover all fluoride, and the recovered fluoride can be used to produce hydrofluoric acid, thus re-using this acid. As mentioned previously, the fluoride can be fully recovered as CaF_2 by using a solution of $CaCl_2$ and a suspension of $Ca(OH)_2$ at pH 2-4. The precipitated CaF_2 is separated by filtration. Analysis of the dry CaF_2 powder shows the complete recovery of fluoride. The wastewater treatment and water/CaF_2 recovery is shown schematically in Figure 6-11.

Table 6-5. Analysis results from the CCT P/L process wastewater treatment (mg/L).

Sample	Si	Fe	Mg	Ca	Na	K	COD
Untreated-sample 1	1440	3.98	8.02	9.91	100.0	68.3	201
Treated using CCT Flocculent 1							
Clarified water	137	0.02	7.57	14.5	206.8	2.4	29
ROreject	272	0.04	20.40	53.4	727.8	10.2	34
RO clean water	0	0	0.02	0.04	0.6	0.0	4
Untreated-sample 2	1165	0.56	9.25	4.1	84.1	23.4	310
Treated using CCT Flocculent 2							
Clarified water	61.6	0	8.38	8.7	268.7	11.2	9
RO reject	206	0	0	33.7	970	13.8	60
RO clean water	0	0	0.01	0	0.9	0.08	0

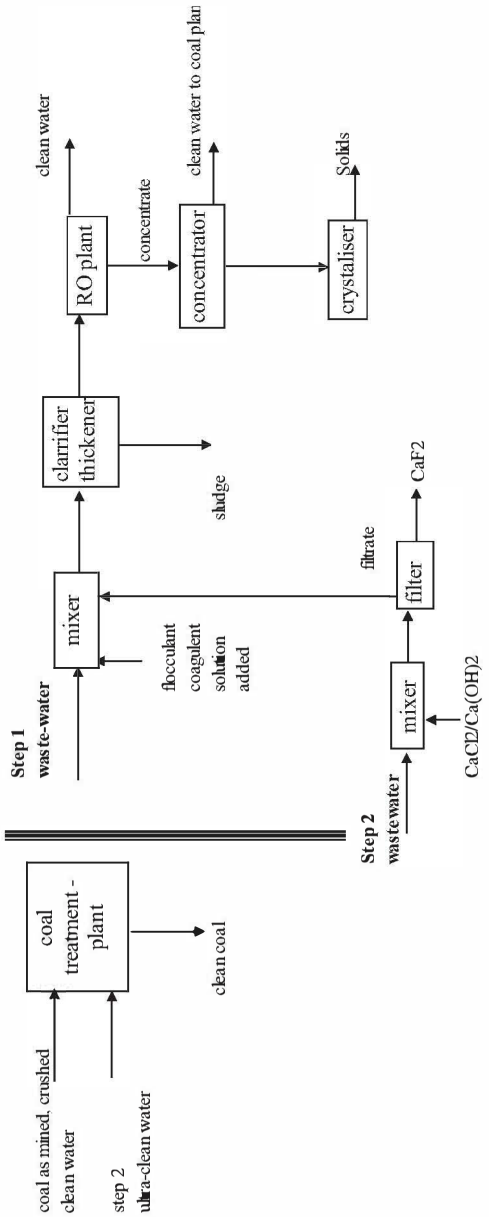

Figure 6-11. Schematic of wastewater treatment for the CCT process.

References

Baláž, P., LaCount, R. B., Kern, D. G. and Turčániová, L. 2001. 'Chemical treatment of coal by grinding and aqueous caustic leaching', *Fuel*, 80, 665-671.

Behera, S. K., Chakraborty, S. and Meikap, B. C. 2017. 'Chemical demineralization of high ash Indian coal by using alkali and acid solutions', *Fuel*, 196, 102-109.

Bergins, C. 2003. 'Kinetics and mechanism during mechanical/thermal dewatering of lignite', *Fuel,* 82, 355-364.

Brooks, P., Clark, K. and Waughet, B. 2000. 'Ultra-Clean Coal as a Gas Turbine Fuel'. Presented at the 10th Japan/Australia Joint Technical Meeting on Coal.

Bullinger, C., Ness, M. and Sarunac, N. 2006. 'Coal Creek Prototype Fluidized Bed Coal Dryer: Performance Improvement, Emissions Reduction, and Operating Experience Coal Creek Prototype Fluidized Bed Coal Dryer', 31st International Technical Conference on Coal Utilization and Fuel Systems, Clearwater FL, May 21-25.

Couch, G. R. 1990. *Lignite upgrading* (IEACR/23), London: IEA Coal Research.

Couch, G. R. 1991. *Advanced coal cleaning technology* (IEACR/44), London: IEA Coal Research.

DOE. 2002. *The ENCOAL® Mild Coal Gasification Project. A DOE Assessment.* DOE/NETL-2002/1171. Morgantown, WV: U.S. Department of Energy.

DOE. 2003. *Clean Coal Technology Programs: Program Update 2003.* Available at: https://www.osti.gov/biblio/827244.

DOE. 2005. *Advanced Coal Conversion Process Demonstration. A DOE Assessment.* DOE/NETL-2005/1217. Morgantown, WV: U.S. Department of Energy.

ENCOAL. 1997. *Encoal Mild Coal Gasification Project: Commercial Plant Feasability Study.* DE-FC21-90MC27339. Morgantown, WV: U.S. Department of Energy.

Favas, G. and Jackson, W. R. 2003. 'Hydrothermal dewatering of lower rank coals.2. Effects of coal characteristics for a range of Australian and international coals', *Fuel,* 82, 59-69.

Kakaras, E., Ahladas, P. and Syrmopoulos, S. 2001. 'Computer simulation studies for the integration of an external dryer into a Greek lignite-fired power plant', *Fuel,* 81, 583-593.

Katalamula, H. and Gupta, R. 2009. 'Low-Grade Coals: A Review of Some Prospective Upgrading Technologies', *Energy Fuels*, 23, 3392-3405.

Kinoshita, S., Yamamoto, S., Deguchi, T. and Shigehisa, T. 2010. 'Demonstration of Upgraded Brown Coal (UBC●) Process by 600 tonnes/day Plant Processes', *Kobelco Technology Review*, 29, 93-98.

Kline, W. E. and Fogler, H. S. 1981. 'Dissolution Kinetics: Catalysis by Strong Acids', *J. Colloid Interface Sci.*, 82, 93-102.

Klutz, H. J., Moser, C. and Block, D. 2010. *Development status of WTA fluidized-bed drying for lignite at RWE Power AG*. Available at: http://www.rwe.com/web/cms/mediablob/en/606202/data/183490/2/rwe/innovations/power-generation/coal-innovation-centre/fluidized-bed-drying/Development-status-of-WTA- fluidized-bed-drying-for-lignite-at-RWE-Power-AG-Article-taken-from-Kraftwerkstechnik-Sichere-und-nachhaltige-Energieversorgung-Volume-2.pdf.

Langmyr, F. J. and Paus, P. E. 1968. 'The Analysis of Inorganic Siliceous Materials by Atomic Absorption Spectrophotometry and the Hydrofluoric Acid Decomposition Technique', *Anal. Chim. Acta.*, 43, 397-408.

Mukherjee, S. and Borthakur, P. C. 2001. 'Chemical demineralization/ desulphurization of high sulphur coal using sodium hydroxide and acid solutions', *Fuel*, 80, 2037-2040.

Mukherjee, S. and Borthakur, P. C. 2004. 'Demineralization of subbituminous high sulphur coal using mineral acids', *Fuel Processing Technology*, 85, 157-164.

Poutsma, M. L. 2000. 'Fundamental reactions of free radicals relevant to pyrolysis reactions', *J. Analytical Applied Pyrolysis*, 54, 5-34.

Racovalis, L., Hoday, M. D. and Hodges, S. 2002. 'Effect of processing conditions on organics in wastewater from hydrothermal dewatering of low rank coal', *Fuel*, 81,1369-1378.

Raetz, E. 2009. 'Clean coal studies in European energy award', *LaTrobe University Bulletin*, Autumn 2009, 7-8.

Rahman, M., Pudasainee, D. and Gupta, R. 2017. 'Review on chemical upgrading of coal: Production processes, potential applications and recent developments', *Fuel Processing Technology*, 158, 35-56.

Rahman, M., Samanta, A. and Gupta, R. 2013. 'Production and characterization of ash-free coal from low rank Canadian coal by solvent extraction', *Fuel Processing Technology*, 115, 88-98.

Ridderbusch, G. L. 2015. 'DryFining™ to Improve Efficiency and Lower Emissions 5+ Years of Commercial Operations', *Great River Energy*. Available at: https://www.usea.org/sites/default/files/event-/Greg%20Ridderbusch.pdf.

Sarunac, N., Ness, M. and Bullinger, C. 2014. 'Improve Plant Efficiency and Reduce CO_2 Emissions When Firing High-Moisture Coals', *Power*.

Available at: http://www.powermag.com/improve-plant-efficiency-and-reduce-co2-emissions-when-firing-high-moisture-coals/.

Sheldon, W. R. 2006. *Advanced coal conversion process demonstration.* DOE/FE-0496. Washington, DC: Western Syncoal LLC.

Si, C., Wu, J., Wang, Y., Zhang, Y. and Shang, X. 2015. 'Drying of Low Rank Coals: A Review of Fluidized Bed Technologies', *Drying Technology*, 33, 277-287.

Steel, K. M., Besida, J., O'Donnell, T. A. and Wood, D. G. 2001. 'Production of Ultra Clean Coal: Part I—Ionic equilibria in solution when mineral matter from black coal is treated with aqueous hydrofluoric acid', *Fuel Processing Technol.,* 70, 171-192.

Steel, K. M., Besida, J., O'Donnell, T. A. and Wood, D. G. 2001. 'Production of Ultra Clean Coal: Part II—Ionic equilibria in solution when mineral matter from black coal is treated with aqueous hydrofluoric acid', *Fuel Processing Technol.,* 70, 193-219.

Steel, K. M. and Patrick, J. W. 2001. 'The production of ultra-clean coal by chemical demineralisation', *Fuel*, 80, 2019-2023.

Umar, D. F., Usui, U. and Daulay, B. 2006. 'Change of combustion characteristics of Indonesian low rank coal due to upgraded brown coal process', *Fuel Processing Technology*, 87, 1007-1011.

Wen, W. W., Nowak, M. A. and Killmeyer, R. P. 1991. 'Drying and reconstitution of subbituminous coal, CRADA 90-004, Final Report', DOE/FETC-97/1049.

Willson, W. G., Walsh, D. and Irwinc, W. 1997. 'Overview of Low Rank Coal (LRC) Drying', *Coal Preparation*, 18, 1-15

Yoshida, T., Takanohashi, T., Sakanishi, K., Saito, I., Fujita, M. and Mashimo, K. 2002. 'The effect of extraction condition on 'HyperCoal' production (1)—under room-temperature filtration', *Fuel*, 81, 1463-1469.

Zhu, J., Wang, Q. and Lu, X. 2015. 'Status and Developments of Drying Low Rank Coal with Superheated Steam in China', *Drying Technology*, 33, 1086–1100.

CHAPTER SEVEN

COAL GASIFICATION

Gasification is a process that can use a variety of solid and gaseous fuels to produce synthesis gas (syngas), and is used around the world to produce chemicals, fertilisers, transportation fuels, substitute natural gas (SNG), and electricity. Eastman Chemical Company, for example, has produced chemicals using coal gasification since the mid-1970s, initially producing acetic anhydride, and then expanding to include other chemicals such as methanol, vinyl acetate, and methacrylic acid (Zoeller, 2009). The gasification and syngas technologies council reports that there are more than 272 operating gasification plants worldwide with 686 gasifiers. Amick (2007) states that about 94% of the fuel used in gasifiers in the US is low rank coal. There are currently 74 plants under construction worldwide that will have a total of 238 gasifiers; China has the largest number of gasification plants.* The output from gasifiers worldwide in 2014 was 60% as syngas used in the production of chemicals (including fertilisers), and 24% for the production of liquid transportation fuels. Power and gaseous fuels accounted for 8% of the total global syngas production.† SASOL has produced transportation fuel for South Africa and currently 106 Sasol-Lurgi fixed bed dry bottom gasifier plants are operational worldwide (Baumann, 2005).

Gasifiers may be grouped into three types or variants:

1. **Entrained-flow gasifiers**, in which pulverised coal particles and gases flow concurrently at high speed. The majority of high throughput coal gasifiers developed in the past 60 years are slagging entrained-flow gasifiers. For this gasifier, the behaviour of inorganic ash-forming components of the coal can be the determining factor in its design and operation, and fouling or plugging of the gasifier by ash is a major concern.

---

* Figures according to the Global Syngas Technology Council's Worldwide Syngas Database, available at http://gasification-syngas.org/resources/.

† For further information, see https://www.netl.doe.gov/research/Coal/energy-systems/gasification/gasifipedia/markets

Refractory wear is largely related to the interaction with ash inorganic matter, and may lead to poor plant availability. The distribution of potentially toxic inorganic matter in fly ash and slag is an environmental concern.

Entrained-flow gasifiers operate at high temperature and pressure, and with an extremely turbulent flow – this causes rapid fuel conversion and high throughput. The gasification reactions occur at a very high rate (typical residence time is on the order of a few seconds), with high carbon conversion efficiencies (98-99.5%). The tar, oil, phenols, and other liquids produced from the devolatisation of coal are decomposed into hydrogen, carbon monoxide and small amounts of light hydrocarbon gases. Entrained-flow gasifiers can handle practically any coal feedstock and produce a clean, tar-free syngas, but most are fuelled with high rank coal. At the high operating temperatures of these gasifiers, the ash in coal melts into slag which flows out of the gasifier, and measures are often taken, such as adding flux, to obtain the required flowing properties of the molten ash (Marc et al., 2014).

The finely crushed coal feed can be fed to the gasifier in either dry or slurry form. The former uses a lock hopper system, while the latter relies on the use of high-pressure slurry pumps. The slurry feed is a simpler operation, but it introduces water into the reactor which needs to be evaporated. The result of this additional water is a product syngas with a higher H_2 to CO ratio, but with a lower thermal efficiency. Thus the feed preparation system is important within the overall process design alternatives for a particular application to ensure optimal performance. The high temperatures in this type of gasification tend to shorten the life of components, including the gasifier vessel's refractory lining.

Commercial gasifiers include: GE Energy (formerly Chevron Texaco) Gasifier; CB&I E-Gas™ Gasifiers; Shell Gasifiers; Siemens Gasifiers; PRENFLO Gasifier; MHI Gasifier; EAGLE Gasifier; ECUST Gasifier; HCERI Gasifier; MCSG Gasifier; and Tsinghua OSEF Gasifier.

2. **Fluidised-bed gasifiers** operate as a bed of coal particles suspended in the gas flow; the feed of coal particles is mixed with the particles undergoing gasification in the coal bed. Small coal particle sizes (<6 mm) are suspended as a bed in the gasifier. Coal is fed into the side of the reactor, while steam and oxidants flow from the bottom at a velocity needed to fully fluidise the reactor bed. The thorough mixing within the gasifier maintains a constant temperature in the reactor bed, which is at a moderately high temperature to achieve a carbon conversion rate of 90-95% and to decompose most of the tar, oils, phenols, and other liquids from the

coal. The operating temperatures need to be lower than the ash fusion temperature so as to avoid clinker formation and the de-fluidisation of the bed. Thus, fluidised-bed gasifiers are suited to relatively reactive low rank coals, and other fuels such as biomass, but not for high sodium ash coal. High moisture coals would normally be dried before being fed to the gasifier, or measures are taken to reduce the high moisture in coal. Some char particles are entrained in the raw syngas as it leaves the top of the gasifier, and are recovered and recycled back to the reactor *via* a cyclone. Ash particles are removed below the bed, and are cooled as they heat the incoming steam and recycled gas.

Commercial fluidised bed gasifiers include: KBR Gasifiers; High Temperature Winkler Gasifier; and U-Gas● Gasifier.

3. **Moving bed (also called fixed-bed) gasifiers** are designed for gases to flow relatively slowly through the bed of coal feed.* The Lurgi Dry-Ash Gasifier and the British Gas/Lurgi Gasifier are the major commercial gasifiers. These gasifiers usually operate at pressures of 25-30 atmospheres, and are fed with large coal lumps loaded at the top of the refractory-lined gasifier vessel. The fuel moves slowly downward through the bed, while reacting with the gas which is high in oxygen; in counter-current design the gas is added at the bottom of the gasifier and flows upwards to the exit.

These gasifiers may operate in dry-ash mode (e.g. Lurgi dry ash gasifier) by maintaining the temperature below the ash-slagging temperature. The temperature in the bed is moderated by the reaction of the char with excess steam. As the ash moves below the combustion zone, it is cooled by the upward flow of steam and oxygen, and at the bottom it is captured as solid ash. As-mined low rank coals are used to fuel these gasifiers (van de Venter, 2005).

The British Gas/Lurgi gasifier can operate in a slagging mode, and it uses less steam in the gas flow to ensure the ash experiences a higher temperature in the combustion zone, so that it melts into a liquid and is captured at the bottom as slag.

The coal particles in these moving bed gasifiers undergo reactions within the gasifier as they move through different 'zones'. Initially the coal is heated and dried at the top of the gasifier (drying zone), and the product gas is cooled as it leaves the reactor. As the coal moves down the gasifier, volatiles are released as the coal encounters a higher temperature (the carbonisation zone). The fuel then enters the gasification zone, where the devolatilised coal initially encounters steam and carbon dioxide, followed

* For further information, see https://www.netl.doe.gov/research/coal/energy-systems/gasification/gasifipedia/fmb.

by the combustion zone, which is at the highest temperature due to the reactions of char with oxygen.

The moisture content of the fuel mainly determines the discharge gas temperature. Lignite, which has a high moisture content, produces raw gas at a lower temperature, while lower moisture bituminous coal produces gas at higher temperatures. The performance and economics of dry bottom and slagging fixed-bed gasifiers have been compared, for example, for Chinese lignite, and the results for this coal indicate that the BGL (slagging) process is superior to the Lurgi (dry ash) process (Yang et al., 2017).

A great deal of R&D on gasification has been conducted on coal-fuelled integrated gasification and combined-cycle power generation (IGCC); from a longer-term strategic perspective, IGCC is seen as the more promising route towards near zero-emissions power generation. This will only be achieved, however, if the technology incurs a lower capital cost. While gasification can be carried out with almost any carbonaceous substance, the quality of the fuel directly impacts on the H_2:CO content of the syngas produced. Good quality syngas has a H_2:O ratio of between 2 and 1, with low amounts of CO_2. Gasifiers fuelled with low rank coal produce lower quality syngas (Minchener, 2005; Zheng and Furinsky, 2005). Gasification plants also utilise gas cleaning to produce syngas free from particulates, sulphur, and nitrogen pollutants.

Catalytic steam gasification is potentially an attractive new technology that would greatly improve the hydrogen content of syngas, and in this way enhance the benefits of coal gasification. The potential for zero-emissions may be realised with hybrid systems that produce valuable products and power, designed into a competitive zero-emissions plant that enjoys a revenue stream from CO_2 utilisation. The chemistry of catalytic steam gasification of low rank coal, however, is very complex and the chemical mechanism(s) for catalytic steam gasification are poorly understood. The catalytic system is further complicated by the chemical transformations of the inorganic compound(s) added to the low rank coal as it is heated, which creates various inorganic species, only some of which may act as catalytic sites for gasification chemistry.

Before addressing the complex chemistry of catalytic gasification, it is important to understand the chemistry of conventional coal gasification. Coal gasification chemistry is described by reaction(s) with oxygen, steam and carbon dioxide to produce a mixture of H_2, CO, CO_2, H_2O, and pollutants from S, N and Cl moieties in the coal. This gaseous mixture requires cleaning before it is used to synthesise various products, or to produce power as fuel in a combined-cycle plant. Gasification can also be

designed to produce SNG. This chapter considers the chemistry of coal gasification.

Chemistry of Coal Gasification

Coal gasification chemistry is summarised by the reactions 1-7 shown in Table 7-1. Reactions with oxygen are exothermic and generate heat in the gasifier to form mainly CO (reaction 6) with small amounts of CO_2 (reaction 5). The breakdown of oxygen functional groups in coal also produces CO_2, H_2O and CO. As the temperature increases, reaction 6 dominates. Gasification of char by H_2O and CO_2 (reaction 1) is an endothermic reaction that yields CO and H_2. The water-gas-shift (reaction 2) reaches quasi-equilibrium in a gasifier. Methane formation and hydrogen are favoured at lower temperatures (reactions 3 and 4). The relative importance of these reactions is understood from their reaction rates, which are of the comparative order:

$$\underset{10^5}{r(O_2)} >> \underset{3}{r(H_2O)} > \underset{1}{r(CO_2)} > \underset{3\times10^{-3}}{r(H_2)}$$

Table 7-1. Heats of formation for coal gasification reactions (degrees Kelvin).

Reaction	ΔH kJ mol^{-1} 800K	1000K	1200K	
Steam				
$C + H_2O \rightarrow H_2 + CO$	+135.6	+136.0	+135.9	(1)
$CO + H_2O \rightarrow H_2 + CO_2$	-36.9	-34.7	-32.8	(2)
$CO + 3H_2 \rightarrow CH_4 + H_2O$		-223.3	-226.3	(3)
Hydrogen				
$C + 2H_2 \rightarrow CH_4$	-87.5	-89.9	-91.5	(4)
Oxygen				
$C + O_2 \rightarrow CO_2$	-394.5	-394.9	-395.3	(5)
$C + ½O_2 \rightarrow CO$	-222.0	-224.2	-226.6	(6)
Carbon dioxide				
$C + CO_2 \rightarrow 2CO$	+172.5	+170.7	+168.7	(7)

The final product from a coal gasification plant is synthesis gas (syngas), which is a mixture of H_2 and CO (with small amounts of CO_2). The gas mixture is used to synthesise hydrocarbons and other products. Syngas from

low rank coals has a low H_2 content, but higher quality syngas may be produced by increasing the reaction of char with steam. Industrial gasifiers use a mixture of oxygen and steam to improve the hydrogen content of the syngas, and this requires a cryogenic plant to supply oxygen, and steam is supplied from a heat exchanger that cools the syngas. The water shift reaction (which is exothermic) is also used to increase the amount of H_2 in syngas, at the cost of reducing the amount of CO, and increasing the amount of CO_2.

While the reaction of char with steam (reaction 1) would improve the H_2:CO ratio in syngas, the rate of the endothermic steam chemistry is slower. Catalysts have the potential to enhance this chemistry, and significantly increase the yield of H_2 from reactions between coal and steam.

Overall, gasification is carried out using an amount of oxygen required by reaction 6 to produce CO, with some steam added to enhance the hydrogen content. Coal gasifier designs are based on coal properties and the conditions that would maximise the H_2:CO ratios in syngas. The syngas composition from coal gasification and the behaviour of ash have been extensively studied; for example, recent studies reported for three Chinese coals postulate that ash adhesion is related to the formation of adhesive glassy materials, with the enrichment of iron as ferro-aluminate and ferro-alumino silicate (Li et al., 2016). Other studies of low rank, high ash Indian coals using a bubbling fluidised bed reactor, with air and steam as the gasification agents under atmospheric pressure, indicate the supply of steam improves the calorific value of the syngas (Kumar et al., 2017).

The operation of a coal gasifier is impacted by moisture in coal, the ash chemistry and the extent of H_2S, COS, NH_3 and HCl pollutants, which must be removed from the syngas (Mondal et al., 2011). Low rank coal gasification may be described as a series of events:

1. Pre-drying the coal, or designing the gasifier to operate with the as-mined coal.
2. Pyrolysis, as the coal undergoes heating, producing char, CO_2, CO, tar, sulphur and nitrogen, and an initial release of volatile inorganic species.
3. Reactions of O_2, H_2O, and CO_2 with char and tar, the release of volatile inorganics, and the formation of various types of ash.
4. Syngas, which may be treated in a water shift reactor, and then in the gas cleaning plant.
5. Removal of ash.

Gasifiers may be designed to operate at high temperatures to form liquid ash (molten slag) which is removed as a liquid, or to operate at temperatures below the softening point of ash, which can be removed as dry ash. The temperature of a gasifier would be modified if coals with significant amounts of chloride and sulphur are gasified, as these may adversely affect the gasifier through high temperature corrosion, and impose additional cleaning requirements for the syngas.

The initial stage of coal gasification is pyrolysis, which is the behaviour of coal as it is heated. The chemistry of low rank coal pyrolysis is of particular interest as up to half of the coal matrix volatilises on heating, and pyrolysis chemistry of coal with inorganics also provides insights on the transformations of inorganics that may lead to the formation of catalytic sites.

Coal Pyrolysis

Pyrolysis is the chemical transformation of organic materials by the application of heat, usually in an inert atmosphere. Pyrolytic processes are used in a wide variety of industrial processes, including waste treatment, the production of activated carbon, and the production of tars and various chemicals from a wide range of materials, including coal, wood, plastics, biomass, rice husks, tire scrap, and more generally the recycling of carboniferous materials (Donahue and Brandt, 2009). Coal pyrolysis has been an important industrial process since the 19th and early 20th century as a source of coke and coal-derived chemicals. With the growth of the petroleum industry, chemicals' production, such as ammonia, creosote, and aromatic chemicals such as toluene, from oil, has overtaken coal as its source. The pyrolysis of coal and biomass has been reviewed particularly with regard to processing routes for making synthetic liquids, including biomass to liquids, coal to liquids, and waste to liquids (Morgan and Kandiyoti, 2014). Pyrolysis is a vast subject and cannot be discussed fully here; this discussion deals with events in the initial stages of coal gasification, albeit prior to the encounter of the coal with a reactive atmosphere, with an emphasis on the chemistry that may be subsequently related from metal mediated pyrolysis to coal catalytic gasification reactions.

The chemistry of the pyrolysis of low rank coals commences with the breakdown of oxygen functional groups at 100-400°C. For example, brown coal loses ~30wt% of its mass at ~350°C, as CO_2, CO and H_2O amount to the loss of ~66% of the oxygen functional groups in the coal. With increasing temperature, the decomposition of the various oxygen functional

groups increases and additional decomposition yields more gases and tar. The oxygen functional groups in low rank coal may be chemically associated with inorganics in coal, and consequently the coal pyrolysis chemistry would include the reactions of the functional groups and accompanying inorganic transformations.

A summary of the major events in the chemistry of ash-free low rank coal pyrolysis is shown in Table 7-2, in which oxygen functional groups in coal break down to yield mainly H_2O, CO_2, CO, and H_2. The compositions of char, and the amounts of gases and tars, are determined by the temperature and the rate of heating used during pyrolysis. Although the equations in Table 7-2 greatly simplify the complex chemistry, they are used to illustrate the relationship between the functional groups in coal with the gaseous products during pyrolysis; these equations do not include the chemistry of the inorganics associated with the functional groups. The solid material formed as coal undergoing thermolytic reactions is char; in coal containing ash constituents, as the char forms, ash constituents remain and form a greater proportion of the particle mass, and these ash components also undergo transformations.

Table 7-2. Summary of the formation of major products from the pyrolysis of ash-free low rank coal

{coal(H_2O)•xH_2O}	--→	{coal(H_2O)} + xH_2O (bulk water)
{coal(H_2O)}	--→	{coal} + H_2O
{2[R-(COOH)]}	--→	{[R-C(O)-R]} + CO_2 + H_2O
{2[R-(COOH)]}	--→	{[R-R]} + CO_2 + H_2O + CO
{coal(COOH)}	--→	{char-H} + CO_2
{coal(COOH)}	--→	{char(OH)} + CO
{coal(R-CH_2-CH_2OH)}	--→	{char(R-CH_3)} + CO + H_2
{coal(Ph-CH_2OH)}	--→	{char(Ph-CH_3)} + CO

The pyrolysis of coal is central to understanding coal combustion and gasification, and there is extensive literature which often deals with experiments that have examined all ranks of coal. The following is a brief discussion of experimental and modelling studies dealing mainly with the pyrolysis of low rank coals. The majority of these studies have dealt with coal as it is received, although there are some studies that included aw coal, and also aw coal to which specific inorganics have been added.

TG/DTA experiments have demonstrated that during the early stages of coal pyrolysis, H_2O, CO_2 and CO are produced, with increasing amounts of CO and H_2 with increasing temperature; these gases are due to the

breakdown mostly of the coal functional groups, with contributions from minerals and inorganics. The pyrolysis of Beulah-Zap (lignite) and Wyodak (sub-bituminous) coals illustrates this behaviour. The evolution of water is observed at 166°C and 241°C from "bulk" H_2O, and at 465°C and 606°C from H_2O due to the breakdown of functional groups in coal. Water from minerals such as illite, kaolinite, and montmorillonite also evolves at 225°C, 395°C, 500°C, 580°C, and 700°C. Beulah-Zap lignite yields CO_2 at 418°C, and at 502°C to 755°C (CO_2 at 694°C due to carbonate from clays). The predominate CO_2 peak for Wyoming coal is at 439°C, and continues at 505°C and 640°C (CO_2 is also observed from siderite at 554°C, and from calcite at 743°C). The major CO peak for Beulah-Zap is at 758°C, but features are also observed at 469°C, 608°C, and 944°C; the CO peak profiles for Wyoming coal are at 455°C, 602°C, 773°C, and 955°C, with the major peak at 773°C. A major H_2O peak (at 460°C) for Beulah-Zap is assigned to the decomposition of a coal-aromatic-OH group, and a peak at 504°C from the decomposition of carboxylic acids or esters (Giroux et al., 2006).

Hill et al., (1989) and Ma et al., (1991) identify two activation energies from an examination of the Arrhenius plot based on TG data for brown coal; this indicates a primary pyrolysis associated with chemical decomposition, and a secondary pyrolysis dominated by heat and mass transfer, but a distinct change in the chemistry at a given temperature cannot be observed. The yield of volatile matter depends on temperature and heating rates; cations added to brown coal may affect the total volatile matter release over a large temperature range, and an increase is observed in the relative amount of CO_2 at lower temperatures. Examination of the pyrolysis kinetics indicates that adding either of Cu^{2+} or Fe^{2+} to aw coal lowers the activation energy compared to that of the aw coal.

It is important to note that the relative yields of gases, tars, and char are also determined by the experimental parameters and sample preparations used during pyrolysis. These parameters include the size of coal particles, rates of heating, temperature gradients and mass transfer within coal particles, and the design or type of reactor used for the experiment. Thus the chemistry is related to the molecular composition and functional groups of the coal that decompose to yield products, and the rates and distribution of products are also determined by the experimental conditions. Generally, with the increase in temperature, radical chemistry is increasingly favoured. Free-radical reactions are ubiquitous for the thermal decomposition of organic compounds and the mechanisms often involve various elementary reactions that make up the overall mechanism. It may be speculated that parallel, and perhaps competing, reactions may occur in different areas of the heterogeneous coal matrix. Reactions may also include the formation of

intermediates, whose relative concentrations may depend on many factors, including heating rates and final temperature.

Radicals have been observed experimentally during the pyrolysis of brown coal, using electron paramagnetic resonance (EPR) in chars obtained by heating the coal at temperatures between 100°C and 800°C. An EPR signal at 550°C-600°C results from the formation of organic radicals, but above 700°C the signal intensity sharply decreases. The formation of carbon centred radicals generally begins at ~400°C, reaching a maximum at ~550°C. At higher temperatures, the increasing formation of condensed polyaromatic hydrocarbons ultimately results in lower radical concentrations, as shown by the lower EPR signal strength at increasingly higher temperatures (Gavalas, 1982; Czechowski, 1997).

The formation of char during pyrolysis involves the condensation of aromatic groups, and perhaps bond forming reactions such as cross-linking. Reactions that require participation by different functional groups for cross-linking in coal could only take place if these groups were suitably situated within a 3D molecular structure. The molecular models of low rank coal discussed previously have provided insights into these complicated phenomena. Modelling has also enabled a comparison between experimental and predicted yields of major volatile species, and kinetics modelling has indicated a mechanism with one to three independent parallel first-order reactions. Pyrolysis has been described as primary and secondary processes, but various stages have also been postulated, subject to a given temperature-time ramp. For example, five principal stages have been proposed, with two stages at 100°C-450°C for the loss of H_2O and CO_2 *via* the breakdown of carboxylate groups, the third stage at 500°C-700°C yields H_2O and some CO, the fourth stage at 700°C-900°C yields tars, CO, hydrocarbons, and hydrogen, and the final stage is the high-temperature loss of CO (Suuberg et al., 1978).

Physico-chemical modelling of the pyrolysis of a single coal particle can be carried out by considering the coal as the source of gases and liquids/tars released on heating, leaving behind a porous char particle. If extremely rapid heating rates were employed in the experiment, the gases and liquids may be released with explosive force; secondary reactions may be avoided if the reactive species were rapidly swept away. If the heating rates are relatively slow, the formation and loss of reactive intermediates would occur within the particle undergoing a slow increase in temperature. Rapid heating rates, however, may lead to an increase in reactive intermediates whose concentrations may grow if their subsequent rate of decomposition is slower than their rate of formation. This general, and necessarily vague, description indicates slow heating rates would yield a different distribution of products

compared to those from very fast heating rates. Further complications would arise from thermal gradients and mass transfer aspects from rapid heating rates, especially for larger coal particles.

These complicated aspects of coal pyrolysis have resulted in numerous kinetic expressions, some of which are single-reaction models, and others are multi-reaction models. The following are summaries of the major pyrolysis models; details are found in the references provided. These are phenomenological models, some of which may provide predictions of the yields of individual components (Saxena, 1990).

The chemical percolation devolatilisation model has been used to predict the gas, tar, and char formation in lignite, sub-bituminous coal, and in high-volatile bituminous coal; this models coal as clusters, ridges, side chains, and loops (Grant et al., 1989; Fletcher et al., 1990; Fletcher et al., 1992). FLASHCHAIN is an example of a pyrolysis kinetic mechanism and an analytical expression for chain statistics and their time evolution. Coal is divided into four pseudo-components based on the ultimate analysis, carbon aromaticity, aromatic cluster size, proton aromaticity, and extract yields in pyridine. The model uses a four-step reaction mechanism; labile bridges comprise all aliphatic and oxygen functionalities in the coal, and are the key reaction centres. The release of oxygen functional groups is modelled by the simultaneous release of CO_2, H_2O, and small amounts of CO when labile bridges are converted into char links, and the release of CO is from the residual oxygen in nascent char links at high temperatures. Predictions for the devolatilisation of 15 coals at temperatures from 227°C to 927°C and reaction times of 10 sec have been reported to be within experimental error (Niksa and Kerstein, 1991; Niksa, 1996).

The distributed activation energy model (DAEM) provides yields of the various products from coal pyrolysis by simulating coal pyrolysis using a number of parallel reactions, each with a rate expression with an activation energy and pre-exponential factor. This may be simplified by assuming that one, two or three parallel reactions are sufficient to describe the formation of the key products (Anthony et al., 1975). The multiple independent parallel reaction model and functional group models are examples that use a Gaussian distribution of activation energies. These do not explicitly include the effects of transport and secondary tar-cracking reactions (Ko et al., 1988). The limitations of using global kinetics for complex systems are noted, and a distribution of activation energies causes the effective activation energy determined by simple kinetic analysis to be lower than the true average value. Calculations can be made to determine simpler effective kinetic parameters that can be applied at particular temperatures or heating rates; the Gaussian distribution model(s) should be applied with caution

(Braun and Burnham, 1987). The DAEM provides a trend for the increase in volatiles with variation in coal rank, and a reasonable agreement between the experimental and calculated data. A simple expression for the devolatilisation rate for a given distribution of reactants may provide a rapid estimate of kinetic parameters and the distribution of activation energies (Yu and Zhang, 2003; Please et al., 2003).

The pyrolysis of Chinese low rank coals has been studied with TG under the non-isothermal temperature program, and the DAEM was utilised to investigate kinetics based on the chemical structures. ^{13}C cross-polarisation magic angle spinning NMR was carried out to characterise carbon functional groups of low rank coal samples. The calculated activation energy and frequency factor were shown to differ at various conversion degrees for the coals, and this was attributed to various functional groups in the macromolecular structures of low rank coals. The differing bond strengths of the various chemical bonds in coal are proposed to need different activation energy as they decompose in the varied pyrolysis temperature range. Average activation energies for the four coal samples were proposed at 331 kJ mol^{-1}kJ, 298 kJ mol^{-1}, 302 kJ mol^{-1}, and 196 kJ mol^{-1}, and the activation energy at low conversion was considered to be a lower value. The NMR data from this study were interpreted as the decomposition of aliphatic methyl in side chains, methylene groups at lower temperature, and oxygen-containing carbon functional groups considered to cleave at higher temperatures; this study did not identify gaseous products required to confirm this speculation (Song et al., 2016).

The major kinetic models deal with small coal particles in isothermal conditions, but large coal particles undergo a different intra-particle mass and heat transfer. These variables are in addition to differences in the structures and compositions of coals, and differences in the pyrolysis reactors. Reported kinetic parameters, together with the activation energy distributions in DAEM, were obtained firstly by non-isothermal TG analysis and then a particle model, based on the obtained kinetic parameters, was proposed to predict the temperature distribution and the evolution of the volatiles during heating. The model was used to predict the mass fraction of the solid residue, the temperature profiles inside the coal particle, and the time for complete pyrolysis. The obtained kinetic parameters E_0, k_0 and σ were 186.5 kJ mol^{-1}, 3.96x10^{10}/sec., and 39.5 kJ mol^{-1}, respectively. The DAEM is reported to depict the main features in coal pyrolysis; these were used to develop a single particle model coupling with heat transfer and pyrolysis reactions to simulate the chemical and physical phenomena occurring within a coal particle in a fluidised bed. The results of this simulation show complicated and strongly coupled heat transfer and

pyrolysis reactions. A long heating-up time, and pyrolysis time, was obtained for a large particle; for example, for a coal particle with a diameter of 3 mm, a temperature difference of 300K was observed within the particle. The reactions, simulated as the shrinking core mechanism, gave a complete pyrolysis time of 6.2 sec, which was compared to the measured pyrolysis time of 0.35 sec, for a coal particle with a diameter of 0.3 mm (Wang et al., 2017).

The theoretical analysis of the isothermal pyrolysis of a coal particle led to the conclusion that under kinetic control, a particle's temperature does not change during thermal decomposition, while under external heat transfer control, an increase to the particle's temperature of up to 100K may occur. This study proposed a mean value of the activation energy for the devolatilisation of many coals of 240 kJ mol^{-1}, which is higher than many measured values that are thought to have been measured under heat transfer controlled conditions. The temperature during the pyrolysis of 'thermally thin particles' is suggested to remain unaltered by fragmentation, swelling, or change of shape (Chern, Hayhurst, 2010).

The difficulties inherent in devising a general chemical kinetics scheme for coal pyrolysis covering all rates of temperature increases is well understood; the following example illustrates that neither the simulation scheme developed for brown coal devolatilisation (rapid heating rates) nor a published scheme (Hinserg et al., 1996) could adequately reproduce experimentally measured CO_2 and CO concentrations from the pyrolysis of brown coal. However, the measured wt% loss for the coal sample could be reproduced by modelling the phenomena using a series of first order reactions (with Arrhenius rate constants), in which the coal functional groups were made available for decomposition into CO_2 and CO. In spite of this result, this model could not reproduce the experimentally derived values of the ratio of CO_2:CO with changes in temperature (and time).

A pragmatic approach can be devised using a scheme that could successfully reproduce the experimentally measured CO_2 and CO concentrations over 200°C to 500°C. This reaction scheme consisted of competing reactions for CO_2 and CO formations at 200°C to 400°C, and an additional competing reaction to provide significant amounts of CO at temperatures >300°C. The proportion of oxygen functional groups stipulated as 'A' decomposes at low temperatures into mostly CO_2, and some CO. The portion 'B' represents the oxygen functional groups in coal that decompose into CO at higher temperatures. This model is not generally applicable to all coals; instead, the observed concentration profiles for brown coal can be qualitatively simulated by performing step calculations, using a hypothetical reaction mechanism involving three reactants '$R_{(n)}$'

undergoing a sequence of one or two reactions, including the formation of an intermediate '$Int_{(n)}$' with a numerically determined rate constant $k_{(n)}$ (n = 1 to 3). Thus, the formation of the products P (CO_2 or CO), with rate constants $k_{(a)}$, or $k_{(b)}$, could be simulated to occur *via* a one-step or a two-step mechanism, where 'R' is the reactant. An explanation of why this treatment has provided the observed concentration profiles is that varying the amounts of the reactants during each sequential step of the reaction scheme leads to changes in the reaction rate as the temperature increases. This approach to a simulation of brown coal pyrolysis does not provide a unique combination of reaction rates, nor a specific chemical reaction scheme. Rather, it demonstrates that the observed concentration profiles of CO_2 and CO are due to a number of reactants undergoing differing reactions; these are the differing oxygen functional groups in brown coal undergoing different reactions during heating, and are likely to include reactions involving intermediates. As decomposition takes place, the relative concentrations of the functional groups changes with time, and, as the temperature increases with time, the type of reaction, and the reaction rates, are also thought to change.

A mechanism involving intermediates is important, as this may be related to metal mediated pyrolysis and catalytic steam gasification chemistry. Inorganic species chemically associated with oxygen functional groups could form intermediates (such as carbonates) that decompose into inorganic oxide complexes that are chemically bound to char, and the formation of CO_2 and CO; ultimately, the metal centres are reduced to lower oxidation states. This is further elaborated with molecular models involving inorganic species.

Molecular Modelling of Coal Pyrolysis

Computational molecular modelling can be used to examine reaction routes for the loss of the various functional groups in the coal, and to relate these with the type and amount of major gases observed experimentally. Molecular modelling is also valuable in developing reaction routes involving inorganic species bound to these functional groups, providing insights on the structures of inorganic species present in the particular coal and the changes to inorganic species as the coal is heated.

As discussed previously, detailed *ab initio* or semi-empirical molecular computations provide energy barriers to specific chemical events. It is instructive to initially use DFT and SE-PM5 for the detailed studies of the breakdown of simple compounds containing carboxyl groups into CO_2 and CO for an examination of likely reaction routes, and to follow this with

modelling of the same simple molecules, but now containing an inorganic ionically bound to the functional group. These computations would be valuable as indications of events that may be modelled using the molecular model of brown coal discussed in Chapter Three.

Detailed discussions of pyrolysis have been provided by Domazetis et al. (2006), and the main features related to carboxyl groups are here presented.* Models of simple molecules provide an initial assessment of factors on the breakdown of typical carboxyl groups found in low rank coals. These simple molecules are well characterised, can be used for extensive computations and, in some cases, the modelling can be directly compared to experimental data. It needs to be emphasised that these simple molecules are not substitutions for coal models, and are intended to provide a relative comparison on the behaviour of differing carboxyl groups.

The three molecules used for these studies are substituted benzoic acid [A], substituted tetrahydronapthoic acid [B], and 4-(phenyl) butanoic acid [C]. The molecular modelling of pyrolysis chemistry of these molecules would commence with the initial step observed at 150°C to 300°C, which is decarboxylation that yields mainly CO_2 and smaller amounts of CO. SE-PM5 Hamiltonian, on the loss of CO_2 from these molecules, provide relative trends for decarboxylation, based on the activation energies of the particular reactions.

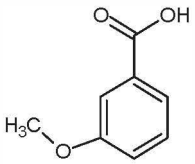

[A]

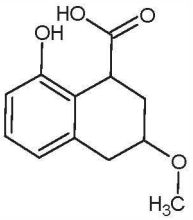

[B]

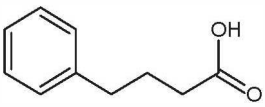

[C]

The reactions for the elimination of CO_2 are: (I) addition of hydrogen to the β-carbon, (II) elimination of CO_2 from a carboxylate anion, and (III) elimination of CO_2 or CO involving radicals. Modelling provides activation energies and these are indicative of which reaction(s) is likely to dominate CO_2 formation from the breakdown of these carboxyl groups.

* Portions of discussions on pyrolysis are adapted here with permission from Domazetis et al., (2006) Energy Fuels, 20, 1997-2007, 2006. Copyright (2006). American Chemical Society.

I. Elimination of CO_2 by the addition of hydrogen to the β-carbon.

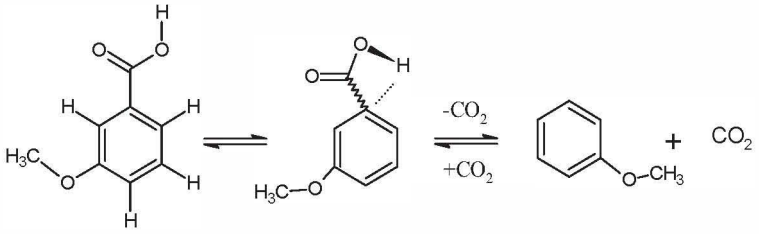

(1)

Modelling of reaction (1) for molecules [A] and [B] provides similar activation energies. Reported decarboxylation rates for various benzoic acids indicate a dependence on the conditions used for decarboxylation (Dabestani et al., 2005; Kelemen et al., 1994; Manion et al., 1996). Measured activation energies for a series of hydroxyl derivatives of benzoic acid are in the range 90-97 kJ mol^{-1}, indicating these reactions occur at a lower temperature, but higher theoretical values for these reactions have also been reported (Li and Brill, 2002; 2003).

Decarboxylation of molecule [B] may be postulated to occur either as in reaction (1), or *via* an intermediate involving the carboxyl hydrogen and the phenoxyl hydrogen, with proton transfer, as in reaction (2).

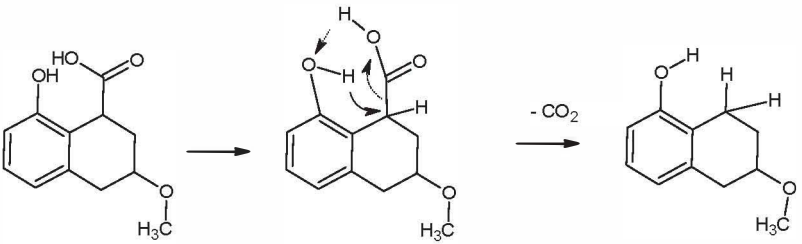

(2)

While the calculated activation energy for molecule [B] and reaction (1) is similar to that for molecule [A], calculations for molecule [B] in reaction (2), involving the intermediate structure, are energetically favoured compared to reaction (1). The activation energy for the decarboxylation of 4-phenyl butanoic acid [C], however, is considerably larger than for molecules [A] and [B] and thus is less likely to occur.

II. Elimination of CO_2 from a carboxylate anion.

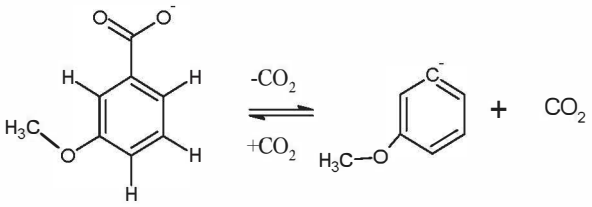

(3)

Calculations for reaction (3) gave relatively large activation energy for a carbanion. Reaction (4), however, in which the carboxylate anion is lost to form a carbanion, followed by the formation of the phenoxide by the transfer of hydrogen, is energetically favoured over reaction (3).

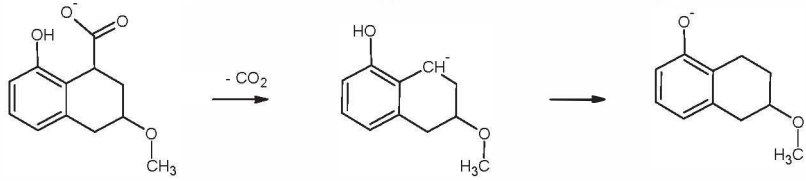

(4)

The activation energy for a similar reaction for compound [C] is considerably larger, indicating decarboxylation *via* this route for this functional group is less likely.

The conclusion from this molecular modelling is that functional groups similar to 3-benzoic acid [A] and substituted tetrahydronapthoic acid [B] are likely to break down and yield CO_2 at lower temperatures, whereas functional groups resembling [C] are unlikely to yield CO_2 at these temperatures.

III. Elimination of CO_2 or CO involving radicals.

Reaction routes involving radicals are likely to form CO_2, H_2, CO, and H_2O [i.e. (R′)-(COOH)n → (R˙) + CO_2 + CO + H_2O + H_2].

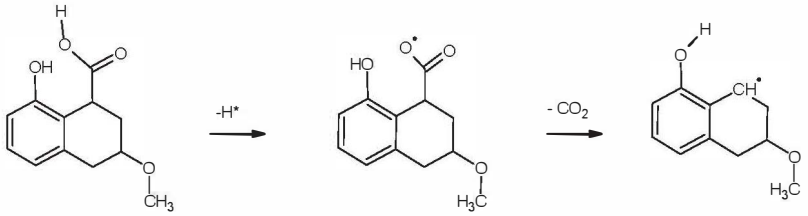

(5)

The formation of H_2 and H_2O may result from a radical combination (e.g. $H^* + H^* \rightarrow H_2$; $OH^* + H^* \rightarrow H_2O$). Although radical formation requires large activation energy, radicals present in coal may initiate such chemistry and provide an energetically favoured reaction route. A larger activation barrier is encountered for the loss of CO_2 in reaction (5) compared to reactions (2) and (3).

The elimination of H_2O and CO_2 *via* anhydride formation may occur if carboxyl groups are suitably situated in the 3D molecular models of brown coal:

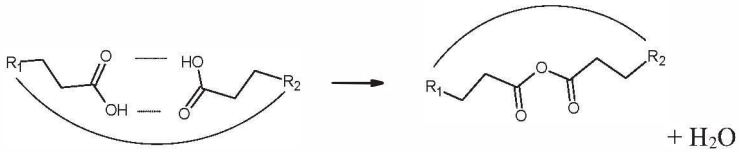

(6)

This type of reaction has been discussed for the pyrolysis of poly(methacrylic acid), in which decarboxylation to form CO_2 was assisted by an adjacent acid group, with anhydride and H_2O formation (Lazzari et al., 1998). Adjacent carboxyl groups forming strong H-bonds have been observed in 3D low rank coal molecular models. It is possible that a reaction scheme resembling reaction (6) may contribute to cross-linking in coal during heating (Solomon et al., 1990).

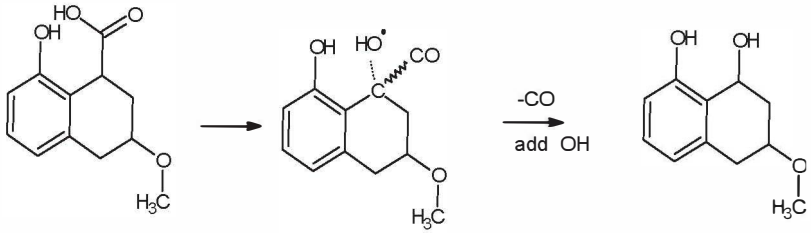

(7)

Pyrolysis at increasingly higher temperatures includes the decomposition of carboxylic, carbonyl, phenolic, and carbonyl groups, which may also yield CO. Modelling the decarboxylation of alkyl carboxylic acids, similar to compound [C], indicates these would occur at higher temperatures. Radical reactions often produce a mixture of CO_2 and CO; the formation of CO is illustrated by reaction (7), which requires the simultaneous loss of CO and addition of OH.

Pyrolysis of phenols involves phenoxyl radicals that undergo dimerisation and also form dibenzofuran (Wiater et al., 2000). A direct molecular elimination to CO and C_5H_6 at high temperatures can also be considered (Brezinsky et al., 1998). Modelling the decomposition of phenol to the cyclopentadiene radical provides larger activation energy than for the decarboxylation reactions discussed above, indicating this route for the decomposition of phenoxyl groups requires high temperatures to overcome the larger energy barrier.

The modelling of the decomposition of carbonyl groups provides large activation energy, indicating this chemistry could occur at elevated temperatures to give CO; however, a number of reaction routes and products need to be considered at these temperatures, including the transfer of hydrogen with the formation of a double bonded alkyl group (CH_2=CH_2-R), the formation of radicals and further bond cleavage, or the formation of a new [C-C] bond.

The modelling chemistry discussed for the three simple molecules can be repeated for these molecules containing sodium to assess the impact of an inorganic on the activation energies for CO_2 and CO formation.

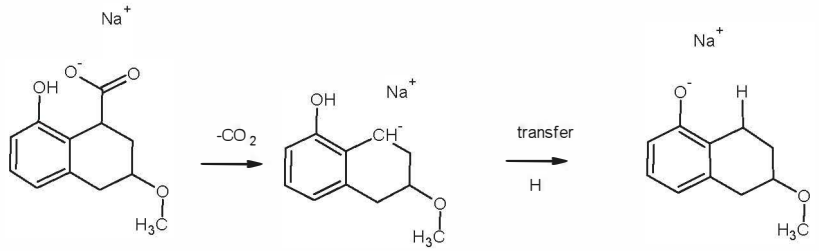

(8)

These models need to be initially assessed by placing sodium in different positions, as various configurations provided significantly different values of the activation energy for the decomposition of the sodium compound of [A]. The lowest activation energy is obtained with sodium situated between the methoxyl and carboxylate groups, and the ionic nature of the compound is shown by the calculated partial charges (Na = +0.56, PhC = -0.44).

Reaction (8) yields CO_2 and the chemistry includes a transfer of the phenolic hydrogen to the carbanion. Calculations show the phenoxide product is energetically favoured over the carbanion, with a moderately low activation barrier for the transfer of the hydrogen from the phenol group. The activation barrier for the loss of CO_2 from the sodium salt of molecule [B] is similar to that of the sodium salt of molecule [A].

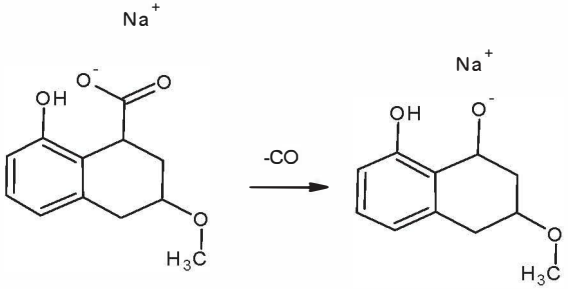

(9)

Reaction (9) is the loss of CO, and the activation energy for this reaction indicates CO formation may compete with CO_2 formation for these types of compounds. The activation energy for the decomposition of the sodium salt of molecule [C] into CO_2 was also dependant on the conformations of the molecule, and although the value was larger than for the sodium salts of

molecules [A] and [B], the calculated activation energy indicates these types of groups may also decompose at moderate temperatures. The reaction of the sodium salt of [C] into CO and the sodium alkoxide is calculated with similar activation energy to the decarboxylation reaction, but the alkoxide product is more energetically favoured compared to the carbanion.
These modelling results of decarboxylation during pyrolysis follow the order:

carboxylic acid ~ carboxylate salt » radical

The results also indicate that decarboxylation during pyrolysis follows the order:

substituted tetrahydronapthoic ≥ substituted benzoic >> straight chain alkyl

The 2D and 3D brown coal models discussed previously contain carboxyl groups similar to those displayed in the molecules designated [A], [B], and [C]. The weight loss obtained from changes simulating these pyrolysis events, carried out with the molecular model, is similar to the experimentally measured value. While is it not possible to quantify the distribution of all the types of carboxyl groups in low rank coal, the above results qualitatively show some carboxyl groups would break down into CO_2 at lower temperatures, while others would break down into CO_2 and CO at higher temperatures, and this conforms to experimental results. At higher temperatures, it is shown that almost all carboxyl groups decompose, as do a significant portion of phenoxyl, carbonyl, and ether groups. Computational modelling using a 2D molecular model, containing carboxyl groups similar to molecules [A] and [B] and with sodium ionically bound to a carboxylate, provides transition states with similar configurations, but lower activation energies than those of the smaller molecules, indicating greater thermal breakdown may occur at lower temperatures for low rank coals containing inorganics.

Computations for char models involving radical formation gave overall higher activation energies; however, radicals are naturally present in the coal and this may facilitate radical chemistry. As indicated previously, radical chemistry could also take place at elevated temperatures, consistent with the EPR data for radicals in coals. Small amounts of CO are detected from the pyrolysis of coal at relatively low temperatures, and this may involve radicals in the coal. Radicals have been reported in low rank coals with fairly constant concentrations up to 300°C, increasing at about 400°C

and reaching maximum values at around 550°C (Czechowski and Jezierski, 1997).

A number of conformations of coal models containing sodium may be examined, and of others containing iron hydroxyl-complexes; these computations indicate conformational factors may complicate the modelling of various mechanisms for the decomposition of particular carboxylic groups.

The validity of the reaction routes examined with the coal molecular models is ascertained from an acceptable comparison between experimental results and those obtained with computational models. Experimental data are obtained as the coal undergoes heating, and these consist of the yields of products, and of the weight loss experienced by the coal with an increase in temperature. During the initial stages of brown coal pyrolysis, the gaseous products observed are H_2O, CO_2, CO, H_2 and CH_4. The products and the corresponding weight loss are measured for acid-washed coal, and similar data are obtained for the same coal containing specific inorganic species. While the weight loss of the coal sample and the amounts of CO_2 and CO can be measured with reasonable accurately and reproducibility, it is difficult to accurately measure water obtained from the decomposition of various groups in coal, and thus estimates need to be made for loss of water during pyrolysis at low temperatures (experiments which involved the distillation of condensed liquids have also given reasonable indications of H_2O evolving as coal is heated). These experimental data, coupled with results from computational molecular modelling of brown coal, enable a molecular description of the transformations of coal into char. The changes that may be made to the molecular model that would mimic the experimental data of brown coal as it is heated to higher temperatures, and the formation of brown coal char, are:

(a) loss of carboxyl groups to form CO_2
(b) loss of carboxyl groups to form CO
(c) loss of carbonyl groups to form CO
(d) loss of carboxyl and hydroxyl groups to form CO and H_2O
(e) loss of ester and aliphatic links to form CO, H_2O, H_2 and hydrocarbons (e.g. CH_4, CH_2=CH_2)

The molecular model of char shown in Figure 7-1 is the result of performing the above steps on the molecular model of brown coal; the relative changes to the molecular weight of the model are also similar to the percentage weight loss observed experimentally for brown coal transformed into char.

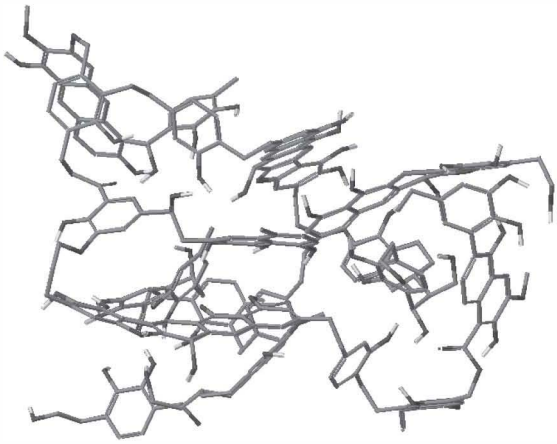

Figure 7-1. Molecule model of a char obtained from transformation of the brown coal molecular model (C = •black; O = •red; H = ○white). Reprinted with permission from Domazetis et al., (2007) Energy Fuels, 21, 2531-2542. Copyright (2007). American Chemical Society.

The resulting char molecular model conforms to data obtained from the pyrolysis chemistry of aw brown coal at 300°C ($C_{249}H_{239}NO_{65}$; FWt = 4285.6). The phenyl groups in this structure mainly form a disordered arrangement, but some two-phenyl groups are arranged in parallel separated by 3.5Å to 4Å, consistent with XRD data of these chars (Wertz, 1999; Sahajwalla et al., 2001; Feng et al., 2003). Overall, the structures of low rank chars are disordered, and the char molecular model reflects this disorder (or non-graphitic arrangement); the char contains an increasing proportion of phenyl groups, and also a greater number of condensed two phenyl ring groups. About 85% of all carbons in the char model are phenyl groups and a number of [C=C] double bonds have also formed as a result of the elimination of functional groups with hydrogen loss (e.g. RCH_2-CH_2-$COOH \rightarrow RCH{=}CH_2 + CO + H_2O$). This chemistry would also include the formation of carbon and oxygen centred radicals through hydrogen abstraction, and probably some recombination of H radicals into molecular H_2.

The resulting char model reflects the available experimental data of char formation at low temperatures, and the model can continue to undergo changes that mimic pyrolysis at higher temperatures; this transformation gives a molecular model of a similar composition to the char obtained from the pyrolysis of aw brown coal heated to 600°C-700°C. The char molecular

model encompassed the loss of all carboxyl groups, over half of the phenolic groups, and most of the carbonyl and ether groups from the brown coal 3D molecular model. Links in this 3D char molecular model may be broken, and this molecular model may form a conformer consisting of three fragments; DFT optimisation of this type of structure provides an optimum configuration. However, a conformer in which all fragments are linked to form a single 3D char molecular model is also optimised to a ground state configuration, indicating links may form within this structure, and these do not significantly impact the configuration of the char molecule.

In the absence of inorganic species in coal, the formation of gaseous products at higher temperatures is thought to involve significant radical chemistry. Chars formed from coal containing inorganic species, however, undergo mainly metal-mediated chemistry. For example, reaction routes for the breakdown of carboxyl groups into CO_2 and CO from coal containing iron complexes may be modelled to include the abstraction of hydrogen by iron centres. Hydrogen abstraction from [Fe←-OH] groups may lead to the oxidative formation of [-C-O-Fe] bonds, iron-hydrides, and ultimately yield H_2; the breakdown of the newly formed [-C-O-Fe] bonds would yield CO. The formation of hydrides in iron clusters, and also hydride formation from reactions between $[Fe_m]^+$ clusters and methane, has been discussed in the literature. Hydrogen abstraction and transfer reactions have been reported for small organic molecules, the dehydrogenation of ethylene by iron, nickel, and cobalt clusters, and for the formation of hydrogen.

Pyrolysis of aw Brown Coal with added Inorganics

Studies of the behaviour of inorganics in low rank coals have often been underpinned by a notion that inorganics are added by an 'ion-exchange' process, or alternatively they form a non-descript slurry of inorganic salts, water, and the coal molecular matrix. The interactions between coal functional groups and various inorganic species, however, are more complex and, as a result, there are scant data on the nature of particular inorganic complexes that are solely chemically associated with functional groups in hydrophilic coal and their impact on the pyrolysis chemistry of the treated coal. The inorganic species that may be added to the coal matrix span almost the entire range of metal complexes, and the chemistry of such species may well be modified by their environment within the coal. Thus, salts such as NaCl and $MgCl_2$ may be added as a solution of dissolved anions and cations to the wet coal matrix, while acid-base chemistry may result in a slurry of water, coal, and for example $Ca(OH)_2$, which dissolves the calcium, which is added to the coal matrix as Ca^{2+} associated with carboxyl anions. As

stated previously, transition metal complexes may be added to brown coal as mononuclear and poly-nuclear species. At high pH levels, however, metal hydroxide precipitates may form in the pores of coal. Thus there are numerous chemical interactions that may involve a variety of chemical species when considering the addition of inorganic species within brown coal. Computer molecular modelling of brown coal and aqua complexes of Na^{+}, Mg^{2+}, Ca^{2+}, Fe^{3+} and Ni^{2+}, discussed previously, provides insights on the nature of these inorganics in low rank coals. These insights enhance our understanding of the chemistry of metal mediated pyrolysis and steam coal gasification catalysis.

Experimental investigations have shown that a wide range of inorganics are added to acid-washed brown coals by adjusting the pH of the mixture of the coal and inorganic solution. Care must be taken during such procedures to ensure inorganic precipitates do not form, and in cases where this cannot be avoided (such as using when an elevated pH to increase the amount of inorganics in coal), the treated coal should be washed with a solution of dilute acetic acid as a precaution to dissolve any precipitated hydroxide, thereby not contaminating the sample.

Table 7-3. Amounts of inorganics added to coal at various pH values, wt%, dry basis.*

Inorganic added to coal	*Ash as oxide in coal*	*pH of coal mixture*
$NiSO_4$	2.3%, NiO	3.8
$NiSO_4$	7.8%, NiO	6.3
$CoCl_2$	0.9%, Co_2O_3	3.4
$CoSO_4$	4.9%, Co_2O_3	6.2
$Al_2(SO_4)_3$	18%, Al_2O_3	4.2
$Zn(CH_3COO)_2/ZnCl_2$	16%, ZnO	5.8
$NiSO_4/Al_2(SO_4)_3$	25.8%, NiO/Al_2O_3	5.9
$Ni(NO_3)_3/Fe(NO_3)_3/CaCl_2$	10.1%, Ni/Fe/Ca/oxides	6.3
$CuCl_2$	6.6%, CuO	4.1
$FeSO_4/CaO$	14.6%, Fe_2O_3/CaO,	5.6

* Reprinted with permission from Domazetis et al., Fuel Processing Technology, 86, 463-486, 2005. Copyright (2005), Elsevier.

Table 7-4. Analysis of ash from brown coal samples with added inorganics (db).*

	As Oxides in Coal									
	$\%SiO_2$	$\%Al_2O_3$	$\%Fe_2O_3$	%MgO	%CaO	$\%Na_2O$	$\%K_2O$	%NiO	% Ash Calc'd	% Ash Measured
Yal Ni	0.07	0.08	0.10	0.03	0.05	0.07	0.00	8.01	8.40	8.5
LY Ni	0.02	0.19	0.44	0.07	0.07	0.48	0.01	10.05	11.32	11.6
GermII Al/Ni	0.11	6.64	0.26	0.10	0.12	0.28	0.03	14.96	22.49	25.8
GermII Ni/Fe/Ca	0.14	0.10	4.03	0.01	3.04	0.01	0.01	1.58	8.93	10.2
GermI Ni/Fe/Ca	1.20	0.25	9.15	0.02	0.63	0.02	0.02	10.60	21.89	19.6
GermIIFe(II)/Ca	0.14	0.16	8.54	0.02	4.46	0.02	0.02	0.00	13.35	14.6
	As Elements in coal (±.01%)									
			%Fe	%Mg	%Ca	%Na	%K	%Ni		
Yallourn Ni	0.07	0.08	0.07	0.02	0.04	0.05	0.00	6.23		
LY Ni	0.02	0.19	0.31	0.04	0.05	0.35	0.01	7.81		
GermII Al/Ni	0.11	6.64	0.18	0.06	0.08	0.21	0.02	11.63		
GermII Ni/Fe/Ca	0.14	0.10	2.82	0.01	2.17	0.01	0.01	1.23		
GermI Ni/Fe/Ca	1.20	0.25	6.40	0.01	0.45	0.01	0.02	8.25		
GermIIFe(II)/Ca	0.14	0.16	5.97	0.01	3.18	0.01	0.01	0.00		

LY – Loy Yang Mine; Yal – Yallourn Mine; Germ I – German; Germ II – German, low clay content.

When the acid-washed coal is added to a solution of a metal salt and the mixture stirred, the pH often drops. The extent of the pH drop in the mixture differs for each of the inorganic salts. For iron and nickel solutions, the pH of a brown coal/water mixture drops to pH <2. This is not observed for zinc and aluminium solutions, however, in which the pH is between 3 and 4. This type of behaviour is due to differing chemistry for the mixture with brown coal and for transition metals, which is due to hydrolysis as the salt interacts with brown coal. Adjusting the pH of these mixtures can control the amounts of inorganics added to the coal; this is illustrated by the data in Table 7-3, which lists a number of coal samples treated with inorganic salts at specific pH values, and the corresponding amount of inorganic(s) added to the coal, expressed as the metal oxide. The analyses of coal with the added inorganics, as components of the ash obtained from the respective coal sample, are shown in Table 7-4.

Pyrolysis experiments have been carried out for these coal samples to measure the amounts of liquids and gases evolved, and the amount of resulting char. This was performed using a glass cold-finger distillation apparatus purged with nitrogen and with a thermometer within the coal bed. The coals were heated at 350°C until gases or tars were no longer released. This apparatus distils all liquids to leave a solid char in the flask. The liquids and tars are condensed with the cold finger and collected in a closed flask. Char remaining in the heated flask was cooled under nitrogen, collected and weighed. The entire apparatus was weighed before and after the pyrolysis experiment to determine the mass of gases by difference. The char remaining in the container was studied with XPS, and underwent elemental analysis. The amount of water was determined by distillation of the tar/liquid mixture at 100°C and weighing the condensed water. The changes in the amounts of solid, liquid and gaseous products from brown coal with inorganics, compared to those obtained from the aw coal, can be attributed to the inorganic added to the aw brown coal. The results show the total volatiles yield at low temperatures, attributed to the added inorganic(s), was between 35wt% and 49wt%, compared to a total volatiles yield of about 15wt% from the same experiment using aw coal, as shown by the data in Table 7-5.

Table 7-5. Distribution of char and volatiles from the pyrolysis of brown coal at 350°C (daf).

Coal Sample	Coal wt	Char wt	%mass	Volatiles wt	% mass	%Ash
Acid washed	2.79 gm	2.33 gm	83.7%	0.41 gm	14.7%	0.1
Coal/Ni/Fe/Ca added	4.06 gm	1.95 gm	48.1%	2.00 gm	49.2%	9.3
Coal/Ni/Fe/Ca added	3.18 gm	2.04 gm	63.9%	1.13 gm	35.5%	9.3
Coal/Al/Zn added	3.02 gm	1.91 gm	56.1%	1.02 gm	40.3%	16.0

An additional observation is the dramatic weight loss from the brown coal samples with added inorganics, when these are heated in air at a relatively low temperature; all of the coal is consumed at ≤300°C due to reaction with oxygen in the air – these data highlight the importance of undertaking studies of pyrolysis of such coal samples in an inert atmosphere, even at relatively low temperatures, and are indicative of catalytic action on the oxidation of coal from the inorganics. The data in Table 7-6 show the loss of mass in air for a sample of aw brown coal, to which 10.4wt% iron was added (*via* the method that adds polynuclear iron hydroxyl chemically bound to oxygen functional groups in the coal macromolecular matrix).

The loss of organic matter from these coal samples heated in air at temperatures ranging from 100°C-350°C is due to the catalytic effects on the reactions of oxygen with coal by the iron added to the coal. These studies were carried out using either an open heating furnace or a tubular furnace, in which weighed samples of either aw coals, or coals with inorganics, were placed in a crucible and heated to temperatures of 110°C, 130-170°C, and 300°C. The samples were then weighed to determine the mass loss.

Table 7-6. Weight loss of dry brown coal containing 10.5wt% Fe, heated in air.

Initial wt: 4.502 gm (ash=10.5wt%)		Weight Loss	Weight loss (daf)
Weight at 110°C	1.780 gm	60.5%	67.6%
Weight at 130-170°C	1.009 gm	77.6%	86.7%
Weight at ~300°C	0.473 gm	89.5%	100%

Numerous experiments have been carried out in an effort to understand the changes in the pyrolysis products arising from inorganics added to aw brown coal. Brown coals containing Fe/Ca and Fe/Ni/Ca catalysts were heated under dry nitrogen, and also under a stream of nitrogen and water vapour, and a nitrogen/oxygen mixture. These experiments were performed at specific temperatures over the range 100°C-350°C. The evolving gas was dried and sampled in a standard gas cell for analysis using a Perkin Elmer 1600-X FTIR instrument, as described previously. The gases obtained under nitrogen were due to pyrolysis, while those produced with a stream of moisture, or air, result from coal gasification. The IR spectrum detected the evolved gases CO, CO_2 and CH_4.

These studies indicate that numerous factors complicate the chemistry of coal pyrolysis, and an elucidation of this requires detailed molecular modelling and systematic experimental studies. An additional motivation

for these studies is the interest in the catalytic gasification of low rank coals with added inorganic species, such as potassium, sodium, or calcium, and transition metal species, such as iron or nickel hydroxyl species (Solomon et al., 1984; Hindmarsh et al., 1995). An understanding of the thermolysis solely attributed to metal species mixed with brown coal, and the chemistry that may be attributed to catalytic species, requires an understanding of the initial molecular structure of the added metal complex, and the molecular transformations of the inorganic complex within the coal substrate on heating. It is necessary, therefore, to relate products' formation (such as H_2O, CO_2 and CO) with the interactions and transformations of particular inorganic species and the coal as this is heated in inert, and in reactive, atmospheres.

Although measured results for pyrolysis can differ due to different coal sample preparations, and also due to the apparatus and experimental conditions used in particular studies, the following general trends can be qualitatively observed. As-received coal initially loses bulk water, followed by a loss of hydrogen bonded water (and also water within coal micro-capillaries) over the temperature range 100°C-180°C. Inorganic species present in the coal may contain hydrogen bonded water, which would be lost at above 100°C, and also coordinated water, which may be lost over a greater temperature range. Multi-nuclear aqua-metal hydroxyl complexes also undergo reactions at higher temperatures that would form metal oxides with the elimination of water molecules. Water lost at higher temperatures (200°C-600°C) may be derived from transition metal hydroxides, minerals, and organic reactions involving hydroxyl functional groups.

The formation of CO_2 commences at relatively low temperatures, and CO is detected soon after CO_2. The formation of CO_2 and CO (and some H_2O) has been experimentally related to the decomposition of oxygen functional groups in brown coal; a greater amount of CO_2 is obtained from coal containing the inorganics Na, K, Mg, Ca and Ba. Product yields commence with mainly CO_2 and, as the temperature increases, the amount of CO increases relative to CO_2. At a constant temperature, there appears to be a correlation of an increase in CO_2 at 200°C-300°C with the amount of inorganics (e.g. iron) in the coal. This is likely to be due to the formation and subsequent decomposition of metal carbonates during pyrolysis, and a carbonate intermediate has been directly identified with XPS for the pyrolysis of brown coal containing iron species.

Otake and Walker (1993) have reported a detailed description of the pyrolysis of demineralised (ash free) Texas lignite, and of this coal with the added cations of Ca, Ba, Mg, Na and K – the data were obtained with a tube furnace which heated the coal sample at 5°C min^{-1} to 1000°C, and gases

were analysed using GC. The gaseous products are attributed to the decomposition of specific coal functional groups: (a) CO_2 from various carboxylates, (b) H_2O qualitatively identified from reactions involving phenolic groups, and (c) CO from thermolysis of ether, methoxy or carbonyl groups. Coal pyrolysis in this study is also postulated to occur in two steps. The first is a primary step during which functional groups are decomposed to liberate gases, cross-links are broken to form aromatic and hydroaromatic moieties, and the loss of hydrogen is accompanied by condensation reactions. The second step consists of secondary reactions by various organic moieties as they diffuse through the micropores of the coal particles. Specifically, the rate of CO_2 evolution reaches a maximum at just below 400°C; in this example, the H_2O evolution profile peaks at 450°C for demineralised coal. For coal with cations, the H_2O yield profile displayed a shoulder near 200°C and a peak at 450°C; the shoulder is attributed to water associated with cations, and this evolved over the temperature range 100-300°C. The coal that contained cations also yielded more CO_2 and H_2 than demineralised coal above 250°C and 500°C respectively. At ~800°C, Ca-loaded lignite yielded more CO than demineralised lignite. XRD analyses of chars prepared at 1000°C from coal containing Ca and Mg identified CaO, $Ca(OH)_2$ and MgO. The weight losses as coal is converted to char are estimated as ~20wt% at 400°C of lignite containing cations; at 1000°C the product distribution for demineralised lignite was measured as 47.3wt% char and 30.5wt% gases (with ~17wt% considered as other unspecified products obtained by difference). The pyrolysis of the lignite containing cations yielded a distribution of 48.0-48.3% char, and 32.2-35.7% gases (a difference of 13.1-16.1% is due to other products).

Additional data for low rank coal pyrolysis are reported from three Chinese coals of increasing rank and a corresponding decreasing oxygen content of 25.5wt%, 16.3wt% and 12.7wt% (daf); the evolved gases were measured using GC/MS. During the pyrolysis of these coals, the oxygen functional groups are shown to be distributed amongst char, tar and gases, and the proportion observed in the gases increased with temperature. The major gases are CO_2 and CO; evolving CO_2 peaked at 300°C-400°C and CO peaked at 500°C-800°C. Less than 10wt% of oxygen is in tar; the amount of phenol in tars is related to the coal type and heating rates, and higher heating rates produce less phenol in tars. The oxygen content in char decreases with the increase in pyrolysis temperature; at 300°C, char from these coals contains between 10wt% and 17wt% oxygen, and this decreases to 6wt%-10wt% at 500°C, and 2wt%-4wt% at 900°C. Pyrolysis of lignite containing ash of between 12-36wt% (db) yielded CO_2, CO and CH_4

profiles that differ significantly from those obtained from the same coal after it was acid treated (Shengyu et al., 2003; Mavridou et al., 2008).

The results from coal pyrolysis are indicative of a general mechanism that applies to the organic matrix of the various types of low rank coals, and a mechanism that differs for those coals containing inorganics within the coal matrix. This has motivated a detailed examination of the reaction route(s) based on molecular modelling and experimental data, particularly for brown coal containing iron complexes.

The chemistry for low temperature pyrolysis of low rank coal containing iron complexes commences with the loss of coordinated carboxyl groups as CO_2 and CO and the reduction of Fe(III) to Fe(II), and ultimately to Fe(0). With increasing temperature, any proposed mechanism must account for the experimental observations with EPR; studies of the effect of iron on the carbonisation of Loy Yang brown coal reveal the increasing intensity of the EPR signal with the rise in temperature to 400°C, but the signal vanished at 450°C and was replaced by a broad absorption. Spectroscopic and gas analysis results indicate these results may be due to iron in the coal forming carboxylate-related species up to 400°C, and with increased heating the iron-carboxylate species breaks down and iron phases form magnetite, initially, and at the highest temperature principally α- and γ-iron. The formation of the magnetically-ordered iron phases coincided with a pronounced broadening of the signal in the EPR spectrum (Ozaki et al., 1999). Additional insights may be obtained from molecular models, and for this, reasonable agreement is required between experimental data and molecular modelling for weight loss and the ratio of CO_2:CO at low temperatures. The experimental CO_2:CO ratio, however, is sensitive to heating rates, and consequently data are needed for low, and also high, heating rates.

Results from experiments and molecular models of brown coal pyrolysis are compared in Table 7-7; the values of the elemental composition of brown coal are typical, and the variation between the experimental data and that of the molecular models is pronounced in the oxygen content of the char that contains iron, because in the molecular modelling it is assumed the hydroxyl groups from iron complexes are instantly lost, whereas experimentally these groups are lost over a temperature range.

The molecular modelling of the pyrolysis of brown coal containing iron complexes commences with CO_2 formation by loss of a carboxylate group *via* an iron-carbonato complex, with hydrogen transfer from [Fe-OH] to an organic group, and the iron-carbonato complex subsequently decomposing to yield CO_2 and the μ-oxo iron complex. The formation of CO and H_2O is also modelled by the breakdown of a carboxylate group into CO, the

formation of a [HO-Fe] hydroxyl group to the iron centre, a carbon double bond (i.e. [coal(H_2C=CH_2)]), and the reaction between a phenoxyl OH and the (HO-Fe) bond to form H_2O. The loss of CO_2 and CO during pyrolysis is accompanied by a reduction of the iron hydroxyl complexes to yield char with Fe(III/II) and Fe(0) species. These have been modelled as [iron-oxy] species in char, and at higher temperatures, the char models contain iron clusters of the forms [Fe_mO] and [Fe_m] (m = 2 to 5). The reduction of iron in char is consistent with XRD data, and Table 7-8 lists the bulk iron phases detected with XRD in char. It is unlikely that the bulk iron phases detected with XRD are identical with the iron clusters used in computational molecular modelling studies, but XPS data for these samples are consistent with the iron clusters used in the molecular models. The oxidation states identified with XRD are applicable to all iron species in the char samples.

Table 7-7. Comparison of experimental data with molecular modelling pyrolysis data.

Sample	Experimental Data				Molecular Model			
	%C	%H	%O	%Fe	%C	%H	%O	%Fe
Coal (aw)	64.3	4.3	31.1	-	65.1	5.0	29.7	-
Char (aw)	70.1	4.1	25.4	-	69.8	5.6	24.3	-
Char and Fe	56.7	3.8	30.2	5.9	62.8	5.4	24.5	7.0
	CO_2:CO		wt loss		CO_2:CO		wt loss	
Coal (aw)	(2.8 – 3.3):1		14%		3.6:1		12%	
Coal and Fe	4:1		16-20%		3.8:1		15%	

Table 7-8. Iron phases detected using XRD for coal samples with 7.8% Fe heated for 15 min.

Temp. (°C)	Crystalline iron phases	Fe clusters in char models
200-600	γ-Fe_2O_3 / Fe_3O_4 [a]	[Fe(CO_3)(O)Fe][b], Fe_2O_3, 2(Fe_3O_4)
700	α-Fe [c]	Fe_3O_2, Fe_3O, Fe_2O, Fe_4O, Fe_4, Fe_3
800	α-Fe [c]	Fe_3, Fe_3O

[a] Broad overlapping peaks; could not resolve γ-Fe_2O_3 from Fe_3O_4
[b] CO_3 detected using XPS
[c] Small amounts of γ-Fe_2O_3

The weight loss for aw coal differs from that observed for this coal with added inorganics. Figure 7-2 shows the total weight loss for aw brown coal and the same brown coal which contained Fe^{3+} or Co^{2+} hydroxyl species; the samples containing the inorganic complexes provide a similar weight loss, which is greater compared to the weight loss observed for aw brown

coal over the same temperature range. The total weight loss of these coal samples, and the yields of CO_2 and CO, is accounted for by attributing virtually all of the weight loss to the total yield of CO_2 and CO to the temperature range 300-400°C. The CO_2:CO ratio changes significantly, however, when the sample is subjected to a different temperature-time ramp. The amounts of CO_2 and CO, and the ratio of CO_2:CO under these conditions, displayed complex behaviour with changes in heating rate; pronounced spikes in the amounts of CO_2 and CO were observed when the temperature was changed with time, but when the temperature became constant, the amounts of CO_2 and CO were similar to the values obtained previously at that constant temperature. These observations are consistent with the complicated chemical kinetics schemes discussed previously for low rank coal pyrolysis.

In summary, as low rank coal undergoes heating, char is formed, and with char formation, inorganics undergo transformations into carbonates, and at higher temperatures transition metals are reduced. Initially the gaseous products are H_2O, and CO_2, and at the latter stages of pyrolysis the gases contain greater proportions of H_2, CO, and small amounts of CH_4. The chemistry of the pyrolysis of coal containing inorganics provides changes to the inorganics that can be detected experimentally with XPS. The overall sequence is the breakdown of carboxyl (and other oxygen-containing groups) in coal, the formation of inorganic carbonates and oxides, and ultimately species such as metal carbides, metal oxide clusters, and metal clusters.

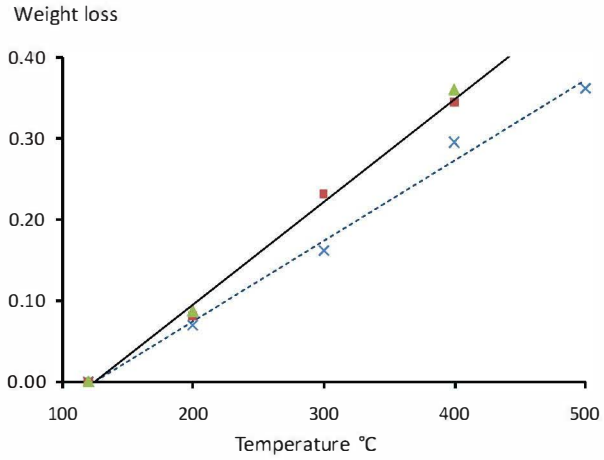

Figure 7-2. Weight losses (db) for brown coal (▲ 5.7% Co(II), ■ 12.4%Fe(III); × aw).

Molecular modelling computations enable an examination of the various chemical transformations during pyrolysis; it is important to consider the differences, and any similarities, between pyrolysis chemistry in an inert atmosphere, and the chemistry in a reactive atmosphere. This point may be illustrated by comparing the phases of iron detected with XRD for coal samples that underwent pyrolysis in an atmosphere of helium, and the same samples that were subjected to the same conditions in an atmosphere of steam.

Table 7-9. Iron phases detected using XRD for a coal sample with 7.8wt% Fe heated for 15 min. Reprinted with permission from Domazetis et al., Applied Catalysis A: General, 340, 105-118, 2008. Copyright (2008). Elsevier.

Temp. (°C)	Pyrolysis	Gasification with steam
200-600	γ-Fe_2O_3 / Fe_3O_4 [a]	γ-Fe_2O_3 / Fe_3O_4 [a]
700	α-Fe	γ-Fe_2O_3 / Fe_3O_4 [a]
800	α-Fe	γ-Fe_2O_3 [b]
900	α-Fe, γ -Fe	γ-Fe_2O_3 [b]
1000	γ -Fe, small amount of α-Fe	-

[a] Broad overlapping peaks, could not resolve γ-Fe_2O_3 from Fe_3O_4; [b] small amount of Fe_3O_4.

Table 7-9 lists the iron phases detected using XRD for a brown coal sample that underwent pyrolysis in an atmosphere of helium and the same sample in identical conditions but in an atmosphere of steam over a 15 min period. The XRD spectra of pyrolysis samples at 200°C to 600°C consisted of broad peaks assigned to a mixture of γ-Fe_2O_3 and Fe_3O_4. Above 600°C, sharper peaks were observed, mainly from α-Fe, with small peaks due to iron oxides; at 900°C, a mixture of α-Fe, γ-Fe was observed, and at 1000°C the predominant phase was of γ-Fe, with some α-Fe. The XRD of samples obtained after steam gasification show only iron oxide phases, and this observation is consistent with XPS data.

It needs to be emphasised, however, that XRD detects major phases and cannot detect active species distributed through the char matrix. Methods that mix iron solutions with coal, with or without adjusting the pH, and then dry the wet sample coal, would form a mixture of crystalline iron salts, ionic aqua-iron species, often iron hydroxyl precipitates within the coal pores, and a fraction as iron complexes bound to ligands within the coal macromolecular matrix. Such a mixture would lead to the formation of various iron species during pyrolysis, and most would form relatively large particles (and crystalline phases) in the char pores and cannot be involved

directly in catalytic chemistry in the char. The data in Table 7-9 are for aw coal samples to which iron species were added using the method of pH adjustment discussed previously, and these coal samples contain only the stipulated aqua-iron species. XPS examination is required for these samples, as XPS data enable the identification of likely iron species in the treated coal, and also those formed in char as the coal is heated.

The discussion has emphasised the importance of creating inorganic species chemically associated with the coal organic matrix that would eventually undergo transformations into catalytically active species. The method discussed here illustrates how active centres involving iron species may be created by exerting control of the distribution of the polynuclear iron complexes added to coal. This can be done by carefully adjusting the pH of a solution of an iron salt mixed with aw coal; the type of polynuclear hydroxyl species formed is ascertained by measuring the amounts of alkali [OH] used to achieve a specific pH value, and relating this to the remaining concentration of the iron in the solution [Fe]. The distribution of the species Fe^{3+}, $[Fe(OH)]^{2+}$, $[Fe_2(OH)_2]^{2+}$, $[Fe_3(OH)_4]^{5+}$, $Fe(OH)_3$, and $[Fe(OH)_4]^-$ in the pH range 1.5-4 is calculated for each step of the addition procedure, at each [Fe(III)] concentration and pH value, using the program Phreeqc. The ratio of hydroxide used to neutralise acid, and the total iron added to the coal during that step, provides a value of the $[OH^-]$:[Fe] ratio, indicative of the type of species added to the coal. It is also necessary to make adjustments for reactions which may involve coal carboxyl groups with the base; this can be ascertained (if NaOH was used) by measuring any sodium added to the coal.

Experimental values of the amounts of NaOH used to neutralise $[H_3O^+]$ released from the coal/iron mixture provide $[OH^-]$:[Fe] ratios of between 3:1 and 2.3:1 for coal samples with differing amounts of iron. The average ratio of ~2.3:1 calculated for coal samples with larger amounts of iron indicates poly-nuclear species. The total amount of [Fe] added to the coal for each experiment is obtained from the elemental analysis of the ash from the treated coal.

Careful stepwise measurements of adding inorganics to aw brown coal, particularly iron, have been carried out by Domazetis et al., (2005), and some of their observations are outlined here. When the pH of the iron solution is adjusted to ~2.5, the amount of hydroxide consumed provided an $[OH^-]$:[Fe] ratio of 1.7:1; the iron species added to the coal were mainly $[Fe_3(OH)_4]^{5+}$ and some $[Fe_2(OH)_2]^{4+}$. Further adjustment, amounting to the cumulative value for the addition of [OH] to provide an $[OH^-]$:[Fe] ratio of ~2:1, results in total iron added of ~6wt% of the weight of the dry coal. A further careful adjustment of the pH can result in >95% of iron in the

solution being added to the coal, giving a total of 10.9wt% iron in the coal (db). The overall value for $[OH^-]$:[Fe] for this is ~2.3:1, indicating a mixture of poly-nuclear iron species were added to the coal. For example, Phreeqc calculations of the iron solution at pH 3.4 indicate that 92wt% of the iron is present as $[Fe_3(OH)_4]^{5+}$ and $[Fe_2(OH)_2]^{4+}$, and these complexes are chemically associated with coal.

XPS examination of coal particles containing iron complexes identified iron and inorganic oxygen, consistent with the proposed hydroxyl-iron species. Di-iron oxy fragments were also observed with TOF-SIMS, also consistent with the poly-nuclear iron complexes in the treated coal samples. The XPS region scans of numerous coal samples containing varying amounts of iron identified the oxygen bound to the iron complex (O1s binding energy 530.5 eV), distinct from oxygen attributed to the coal (O1s binding energy 533.8 and 532.0 eV). The XPS scans of samples with iron provided at% values of Fe and the O 1s that gave [O]:[Fe] ratios consistent with poly-iron-oxy species. These [O]:[Fe] ratios for coal samples with 7-12wt% iron were between 1.9:1 and 1.7:1, slightly lower than the ratios estimated for the bulk samples from the solution data, but indicative of the polymeric iron species. The XPS data also revealed varying concentrations of iron within coal particles; results for a coal sample with a bulk analysis of 12.9wt% iron show a slightly larger amount of iron for the small particles compared to the large coal particles. SEM-EDX examinations of the centre of microtomed large coal particles contained <50% iron compared with the amounts on the outer surface, indicating a lower penetration of soluble iron species to the centre of large coal particles. The ratio of at% of [O]:[Fe] was 1:4 for the surface of both small and large particles, consistent with polymeric iron species being present, but this ratio was ~1 for the centre of cross sections of the largest particles, indicating both lesser penetration of the solution and that the iron species were either $[Fe(OH)]^{2+}$ or the di-nuclear $[Fe_2(OH)_2]^{4+}$.

SE-PM5 computations provided optimised molecular models of brown coal containing polynuclear species of the type $[Fe_x(OH)_y]^{(3x-y)+}$ with a total iron content of ≥10wt% in the coal (this is a similar amount of [Fe] added to coal samples). For example, an energetically favoured structure, $[C_{172}H_{188}N_2O_{69}Fe_6]$, MWt 3722.4, contained six carboxyl groups: two bi-dentate and four mono-dentate ligands bonded to $[Fe_2(OH)_2]^{4+}$ and $[Fe_4(OH)_{10}(H_2O)_2]^{2+}$. For this molecule, the overall atomic ratio [OH:Fe] was 2:1, with partial charges on each of the iron centres of +1.12, +1.1, +0.87, +0.91, +0.84, and +0.97, and all bond lengths and angles for these iron complexes were normal for iron hydroxyl compounds. Similar computations were performed on various molecular models, such as, for

example, a coal molecular model with $[Fe_5(OH)_{12}]^{3+}$ that formed coordination bonds with all carboxyl groups, and with about 13wt% of [Fe].

A large coal molecular model containing a number of the polynuclear iron species was also examined; this consisted of four coal molecules held together by H-bonds and electrostatic interactions and containing a mixture of mono- and poly-nuclear iron complexes that added to a total [Fe] of about 17wt% in the coal. Because of its large size, the model could only be optimised using MM, but it demonstrates that numerous iron-hydroxyl species can be added to brown coal. Some of the polymeric iron complexes occupied spaces between the coal molecules. This molecular structure was stabilised by extensive H-bonding between adjacent coal molecules and water molecules and/or hydroxyl groups of the iron complex. The smaller mono- and di-nuclear iron species in this model were bound to carboxyl ligands in the interior of each coal molecule. All carboxyl groups formed bonds with the iron species and phenol groups formed coordination bonds to iron centres, displacing the coordinated water molecules on iron. The atomic ratio [OH:Fe] averaged over the mono- and multi-iron complexes for this model was 2.1:1.

The thermal decomposition of Fe(III) formate is reported to occur *via* competitive formate anion decomposition, and electron transfer from formate to Fe(III) (to yield Fe(II) formate) with a yield of the gases CO, CO_2, H_2, H_2O, and HCOH (Morando et al., 1987). Thermal decomposition of Fe(III) lactate, Fe(III) tartrate, and Fe(III) citrate, in a static air atmosphere in the temperature range 298K-773K, has been studied with Mössbauer, IR spectroscopies and TG. Under oxidising conditions, decomposition to α-Fe_2O_3 is reported without reduction to Fe(II) intermediates (Randhawa et al., 1997). The thermal decomposition of Fe(III) succinate and Fe(III) adipate pentahydrate, at different temperatures for different time intervals in a static air atmosphere, has been studied using Mössbauer spectroscopy and DTG-DTA-TG. The reduction of Fe(III) to Fe(II) species is reported at 533K and 563K in the case of Fe(III) succinate and Fe(III) adipate, respectively. At higher temperatures, α-Fe_2O_3 is formed as the final thermolysis product (Bassi et al., 1983).

The thermal chemistry for brown coal containing iron-hydroxyl complexes, in an inert atmosphere, includes the elimination of a carboxyl group bound to iron to yield CO_2, the formation of a carbon centred radical, and the reduction of Fe(III) to Fe(II). Additional reaction pathways for coals with less iron may occur to yield a gaseous mixture of CO, CO_2, H_2 and H_2O; further, the elimination of a water molecule from hydroxyl-iron complexes, with the formation of iron oxides, occurred at higher temperatures.

XPS scans of char with iron detected inorganic carbonate associated with the iron in char.

The overall chemistry of CO_2 formation from coal with iron species is summarised by the following (where [•] is a C centred free radical):

$$\text{Coal}\{[(COO)_2(FeIII)(\mu\text{-}OH)_2(FeIII)(COO)_2]\} \rightarrow \text{Coal}[^{\bullet}]\{[(COO)(FeII)(\mu\text{-}OH)_2(FeIII)(COO)_2]\} + CO_2$$

This assumes all of the iron is present as the di-nuclear octahedral complex (to simplify the molecular modelling), with each Fe(III) bonded to two mono-dentate carboxylate groups, and the remaining coordination sites occupied by hydroxyl groups from the coal matrix. The coal model with an iron-hydroxyl complex was calculated to be energetically favoured relative to the coal model without iron (the iron complex contained normal bond lengths and angles, and the Fe(III) partial charges were +1.04 and +1.09). The elimination of a carboxyl group then occurs, with a reduction of one Fe(III) to Fe(II), the formation of a carbon centred radical, and the remaining carboxyl group now acting as a bi-dentate ligand to maintain the octahedral structure about the Fe(II).

Fe_3O_4 has been reported in char produced by the steam gasification of Loy Yang coal with added iron, while Fe_3O_4 and FeOOH are some of the species reported from studies based on Mössbauer, XRD, X-ray Absorption Spectra and Extended X-ray Absorption Fine Structure Spectroscopy of Loy Yang coal heated under nitrogen. The pyrolysis and carbonisation of Loy Yang coal with added iron has been reported to include increased formation of CO_2 and CO (compared with that from acid washed coal), while EPR signals due to radicals have been detected from carbonised samples of coal with iron.

The iron mediated pyrolysis chemistry, including the formation of an intermediate with a carbon centred radical, would lead to further radical chemistry *via* several chemical pathways, dependent on the nature of the radical organic groups formed; for example, if the elimination of the carboxyl group formed a moiety similar to $PhCH_2CH_2^{\bullet}$, the elimination of a hydrogen radical and the formation of a C=C double bond may occur. Molecular models have been constructed to study such reaction sequences. The proposed coal molecule with the Fe(II)Fe(III) hydroxyl (after the elimination of a carboxylate group) and a C=C bond formed by the elimination of an H radical was optimised to an energetically favoured state relative to the original coal model without iron. The octahedral structure of the Fe(II) centre was maintained by changing the mono-dentate into a

bidentate carboxyl; all bond lengths and angles were normal, with partial charges on Fe(II) of +0.73 and on Fe(III) of +0.82.

Further experimental pyrolysis data, and molecular modelling, are consistent with the iron species transformed into iron clusters by the following reaction route: hydrogen abstraction from [Fe←-OH] groups results in oxidative formation of [-C-O-Fe] bonds and iron hydrides that ultimately yield H_2. The breakdown of the [-C-O-Fe] bonds yields CO and a [Fe-C] bond.

Reactions with methane and $[Fe_m]^+$ clusters involve the formation of hydrides (Knickelbein et al., 1998; Liyanage et al., 2001). *Ab initio* calculations on hydrogen abstraction and dissociation reactions have been reported for cyclohexene and for small organic molecules, such as the dehydrogenation of ethylene by iron, nickel and cobalt clusters (Schimmel et al., 1999; Ichihashi et al., 2006; Le Page and James, 2000).

XPS can be employed to detect iron and inorganic oxygen; data for samples of char obtained after the pyrolysis of coal containing iron at 900°C provided an at% ratio [Fe:O] of 1.9:2, indicative of $[Fe_xO_x]$ clusters. The XPS shows the char consisted mainly of carbon (at% = 91.7), with a small but significant amount of organic oxygen (at% = 4.3). It is interesting that the XPS spectra for the same coal with iron heated in an atmosphere of He/H_2O shows higher surface concentrations of iron and inorganic oxygen (consistent with $[Fe_xO_y]$ clusters), and also higher levels of organic oxygen (indicating a reaction of H_2O with char).

The formation of small iron clusters in char is modelled by the transformations of the aqua polynuclear-iron hydroxyl species such as $[Fe(OH)]^{2+}$, $[Fe_2(OH)_2]^{2+}$ and $[Fe_3(OH)_4]^{5+}$ (i.e. polymeric species $[Fe_m(OH)_n]^{(3m-n)+}$) present in coal. On heating, the iron species in coal form carbonate intermediates and then iron oxide clusters; the iron centres would merge to form small iron clusters as hydroxyl groups are lost on heating, and under reducing conditions would form $[Fe_x]$ clusters.

An estimate can be made of the distribution of iron as smaller iron clusters in char for molecular modelling purposes by either (a) assuming the iron in the brown coal is evenly distributed amongst the clusters Fe_3, Fe_5, Fe_{10} and Fe_{20}, or (b) assuming the clusters are formed from the polynuclear-iron hydroxyl complexes added to coal. From these assumptions, most of the iron could be modelled as Fe_3 and Fe_5 clusters. In assumption (a), a coal sample with 8wt% iron would contain either Fe_3 or Fe_5 clusters totalling 3.8wt% Fe in the molecular model, and in assumption (b) a coal sample with 8wt% total iron may contain >4.8wt% of the iron as Fe_3 or Fe_5 in the model, while coal with 12wt% Fe would contain >7 wt% Fe as Fe_3 or Fe_5. The sizes of char molecular models used for computational studies have been

constructed to reflect these concentrations of iron; e.g. a small char model with one Fe_3 cluster contains 8wt% Fe, while a larger model with one Fe_3 cluster would have 4wt% Fe.

An examination of the molecular size of the coal model, and the sizes of various iron clusters, shows large iron clusters cannot be fully involved with functional groups within the molecular matrix of brown coal (and char) in a similar way to small clusters; instead, catalytic sites are formed with the smaller clusters, such as Fe_3 to Fe_5. Larger sized clusters, such as Fe_{10} to Fe_{20}, can be situated in spaces outside of the coal molecule, in micropores, because of their size. Such large iron clusters, if they form when the char has been consumed, are likely to be involved in gas phase reactions post-steam/char gasification chemistry, such as catalysts in reactions between H_2O and CO.

A chemical reaction scheme of char formation and transformation of iron species has been developed using computational molecular modelling that conforms to the available experimental observations. Brown coal molecular models containing chemically bound iron hydroxyl complexes have been transformed into chars with iron clusters, as observed experimentally during low-temperature pyrolysis. This modelling has continued to elucidate reaction routes, with the transformation of iron in char and higher-temperature char formation. The computational modelling shows hydrogen abstraction and the formation of the iron hydride are energetically favoured; SE-PM5 computations show additional H abstraction can be followed by H_2 desorption, with a neutral overall relative change in ΔH_f. This reaction scheme models H_2 formation during pyrolysis, and would also be relevant to H_2 formation from catalytic char gasification chemistry with steam.

Additional DFT calculations (using the char model MF = $C_{144}H_{119}NO_{10}$; FW = 2023.49; elemental composition: C 85.6%, H 5.9%, O 7.9%, N 0.7%), and also assuming for this char model the [Fe_3] cluster ({Char[Fe_3]}; MF = $C_{144}H_{119}NFe_3O_{10}$; elemental composition: C 78.9%, H 5.5%, Fe 7.7%, O 7.3%, N 0.6%) for the formation of H_2 and CO, provide energy profiles for the various reaction steps leading to the yield of these gases. 1scf-DFT computations provide energy changes for the following sequence: (i) a structure with a coordinated [OH-->Fe] bond, {Char[(HO)-->(Fe)$(Fe)_2$]}, (ii) the formation of a hydride by cleavage of the [OH-->Fe] group and the formation of the [C-O-Fe] bond {Char[(C-O-Fe)Fe_2(H)]}, (iii) an additional H abstracted to form the di-hydride, and (iv) the formation and desorption of H_2. This mechanism constitutes hydrogen abstraction, H_2 formation, and the oxidative formation of the [C-O-(Fe_3)] bond, which then leads to the loss

of CO, ultimately forming the catalytic site [Fe-C]. The pyrolysis scheme yielding H_2 and CO may be summarised as:

$$\{Char(OH)C\text{-}OH)(Fe_3)\} \rightarrow \{Char(OH)(C\text{-}O\text{-})(Fe_3)(H)\} \rightarrow$$
$$\{Char(C\text{-}O)_2(Fe_3)(2H)\} \rightarrow \{Char(C\text{-}O\text{-})_2(Fe_3)\} + H_2 \rightarrow$$
$$\{Char(C\text{-}O\text{-})(Fe_3)(CO)\} \rightarrow \{Char(C\text{-}O\text{-})(Fe_3)\} + CO$$

The complicated nature of this chemistry can be illustrated by comparing computations of two schemes that yield H_2 and CO. One scheme is of a mechanism consisting of a number of discrete steps that yield one product, followed by additional steps to yield the next product. The other is a concerted scheme which contains intermediates that would lead to the formation and yield of both H_2 and CO.

A discrete scheme may commence with iron-hydride formation and intermediates leading to CO formation prior to H_2 loss. Modelling concerted reaction schemes, however, is extremely difficult to fully develop due to the increasing possibilities available for these routes. An examination of various possible concerted reaction sequences indicates a loss of CO, and H abstraction from char functional groups by iron clusters is energetically favoured. H_2 and CO may form *via* metal-mediated chemistry by cleavage of [O-H] and [C-H] groups in char; hydride/CO/iron structures and formation of H_2 and CO may continue until either all OH and CH groups were eliminated or the iron moiety became situated at a relatively large distance from such groups.

This has been a necessarily brief discussion of experimental and high level molecular modelling work carried out to elucidate the chemistry of the pyrolysis of low rank coal-containing inorganics. The chemistry of the Fe-mediated coal pyrolysis is illustrated by the reaction scheme displayed in Figure 7-3; this scheme is developed using a molecular model of char with the Fe_3 cluster, and the initial step is the formation of the iron-hydride complex by H abstraction. The loss of CO and H_2 is modelled mainly as discrete reaction steps, although the yield of both H_2 and CO is included to indicate the likelihood of concerted chemistry. Computational molecular modelling of a detailed examination of concerted chemistry involving Fe-hydrides and Fe-carbonyl intermediates has shown that such a scheme is energetically favoured over discrete reaction steps. Importantly, the scheme identifies routes to the formation of active sites relevant to catalytic gasification reactions with H_2O.

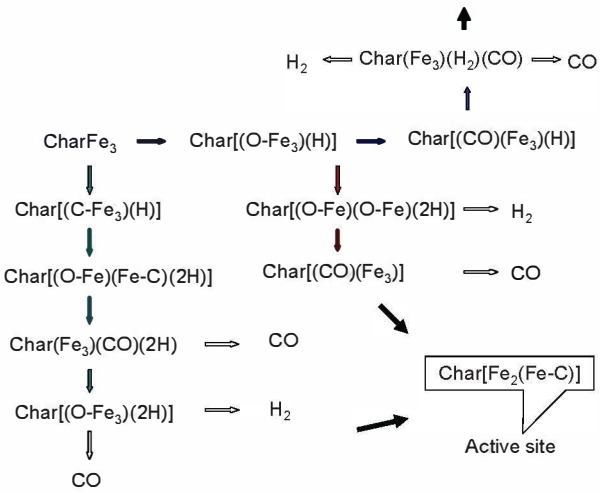

Figure 7-3. Reaction scheme for pyrolysis of coal with iron, yielding H_2, CO and the active site. Reprinted with permission from Domazetis et al., Applied Catalysis A: General, 340, 105-118, 2008. Copyright (2008). Elsevier.

The molecular modelling of the reaction scheme shown in Figure 7-3 commences with the Fe_3 cluster in the char forming [Fe←-OH] coordination bonds with char hydroxyl groups, followed by hydrogen abstraction from one OH group to form [Fe-O] and [Fe-H]. The energy barrier for the initial step in the sequence is about +30kcal, and the overall result is energetically favoured by -30 to -40kcal. A second hydrogen is abstracted to form additional [Fe-O] and [Fe-H] moieties. A lower energy is obtained for a configuration in which the Fe-H groups formed a di-hydrogen group in parallel to the iron cluster. The H_2 is then bonded end-on to one Fe atom in the structure; the H_2 dissociates from the Fe_3 cluster, and is desorbed from the char molecule. Similar modelling can also be carried out using the Fe_3O cluster. 1scf-PM5 calculations for [Char1(Fe_3O)] provided an energy change of +14 kcal; the di-hydride {Char1[$Fe_3O(H)_2$]} was energetically favoured (-110 kcal) while the subsequent formation of hydrogen required almost +60 kcal, yielding an overall result for H_2 formation of -55 kcal. SE-PM5 optimisation of [Char(Fe_3O)], and the sequence for H_2 formation, provided structures containing [Fe..(CO)] interactions typically observed for the concerted sequence of H_2 and CO formation; the initial energy difference from these calculations was +20 kcal, and the iron-hydride species was energetically favoured by -42 kcal, giving a favourable overall energy for the loss of H_2.

Additional computations for a char molecular model containing the [Fe_5] cluster provide an optimised iron hydride structure, [Char(Fe_5H_3)], with three [Fe-H] bonds and three [Fe-C] bonds, all contributing to an energetically favoured structure. The size of the [Fe_5] cluster, however, introduced steric crowding. All of the results show that H_2 formation during pyrolysis may occur *via* the iron clusters [Fe_m] and [Fe_mO] ($m \leq 5$) with a similar energy profile.

Molecular modelling for the formation of CO is *via* the decomposition of [Fe-O-C] groups. Molecular structures with two [Fe-O-C], or one [Fe-O-C] and one [Fe-C], are energetically favoured. 1scf-PM5 data for the loss of CO from {Char[(C-O-$Fe)_2$Fe]}, in which CO was displaced by the Fe forming two [Fe-C] bonds, followed by loss of CO, gave an energy difference of +80 kcal, and the overall endothermic result for the loss of CO (relative to {Char[(C-O-$Fe)_2$Fe]}) was +36 kcal. The energy profile and overall endothermic values for CO formation vary with different configurations of the char molecular models. A reaction scheme that includes an iron-hydride complex during CO formation, with the [Fe_3O] cluster, provides a difference of +30 kcal, with an overall endothermic result of +5 kcal.

These reaction routes are for the pyrolysis of low rank coal that yields char, H_2 and CO *via* iron clusters that ultimately form the [Fe-C] site.

Low Rank Char Formation

The chemistry of char formation from low rank coals without inorganics differs from that of char formation from low rank coal with inorganic species. An understanding of these differences would clarify how catalytic sites may form in the char, and subsequent work would lead to an understanding of the chemistry of catalytic coal steam gasification.

We need to keep in mind, however, that the conditions of laboratory studies of coal gasification may differ from those found in industrial gasification plants. Laboratory studies endeavour to obtain details on pyrolysis and char formation by obtaining samples of char at given times and temperatures. Coal consumption is continuous (akin to steady-state) in a commercial gasifier, and the conditions in industrial coal gasifiers differ considerably for different plants, and events can occur in a relatively short residence time, such as in entrained flow gasifiers, while fixed-bed gasifiers operate within a relatively long residence time.

The transformations that occur as the coal is heated include an increase in the proportion of aromatic groups, with resulting changes to the physical characteristics, ultimately forming char. The coal characteristics relevant to

char formation include particle size, porosity, and the nature of inorganic species within the char. The laboratory data discussed here would be closer to fluid-bed gasification, but additional modelling would be required to assess steady-state chemistry to mimic conditions relevant to fluid-bed gasifiers.

Chars may generally be considered as non-graphitic and graphitic; non-graphitic chars are produced from low rank coals and are mostly disordered structures, and, as the term implies, their structures are not made up of parallel layers of sheets of aromatic rings, as are found in graphite. The char that may be graphitised contains layered planes or groups of layered planes, which can be reoriented by annealing into a graphitic structure containing parallel layers of polyaromatic sheets. The disorder in low rank chars arises from insufficient numbers of large polyaromatic sheets and excessive cross-linking between organic moieties in the molecular structures that cannot be reoriented into parallel arrangements by heat treatment. There are, however, smaller groups of poly-aromatics in low rank char, as indicated by a measure of crystalline grouping (or parallel arrangement of aromatics) by XRD. These groups of polyaromatic layers are 'scattered' throughout the disordered char. The pyrolysis conditions, including heating rates, maximum temperature, and whether reactive or non-reactive atmospheres were chosen, all impact on the molecular structure, porosity, and density of the final char product.

Li et al., (2013) discussed *in situ* studies of pyrolysis and char formation with evolving gases for four demineralised low rank coals. The powdered samples were heated to specific temperatures, at a heating rate of 10°C/min, and kept at constant temperatures for each measurement (25°C, 200°C, 250°C, 300°C, 400°C, 500°C, 600°C, 650°C, 700°C, 750°C, 800°C, 850°C and 900°C) for 10 minutes. The *in situ* XRD profiles were measured for the sample at each temperature, and the gaseous products were analysed using TG coupled with mass spectrometry. A four-stage development of char structure was proposed as the coal underwent heating up to 900°C, based on the XRD parameters d_{002} (interlayer spacing), L_c (stacking height), and L_a (layer diameter). Stage 1 shows an increase of d_{002} and a decrease of L_c and L_a, indicating an increase in imperfections of the aggregate structure, accompanied with the release of small molecules and loss of hydrogen bonds. Stage 2 shows minor structural changes, while stage 3 displays a decrease of d_{002} and increase of L_c and L_a, reflecting the development of an aggregate structure, accompanied by the evolution of H_2. In the final stage, d_{002}, L_c and L_a show minor changes. Analysis of the volatiles (such as CH_4, CO_2, H_2O, C_3H_6 and C_6H_6) shows these are mostly released during stage 2. It is thought aliphatic side chains and oxygen-containing functional groups

undergo decomposition during stage 2; CO_2 and H_2O are derived from the oxygen-containing groups, and CH_4 and C_3H_6 are attributed to the decomposition of aliphatic side chains. The major changes to the char structure are reported to involve aromatic moieties in the development of stacking into layers, indicated by the decrease of d_{002}, increase of L_c, and an increase of layer diameter L_a. The authors proposed that the removal of the functional groups in stage 2 leaves the remaining aromatic nuclei in a reactive state and, during stage 3, the char structure undergoes changes in stacking height and interlayer spacing, providing crystallite carbon structures. The initial decrease of d_{002} and increase of L_c occur at about 500°C, when C_3H_6 and C_6H_6 are detected, both of which are likely to occur from the decomposition of hydrocarbons in the macromolecular structure. The increase in the layer diameter L_a during stage 3 is related to the release of volatile material in stage 2. The increase in the layer diameter L_a during the third stage may also indicate the formation of larger aromatic sheets. A second peak of benzene is observed, which may be released during the condensation of aromatic structures; the increase of L_a is also thought to relate to the evolution of H_2.

Chars are characterised by elemental analysis, porosity, surface area, and by data obtained using XPS, SEM-EDX, ^{13}C NMR, XRD, FTIR, and image analysis. The size distribution of char particles, formed as coal is heated in a reactive atmosphere, is usually related to the size distribution of the coal particles, provided coal particles do not fragment. Char porosity is important for gasification; the overall chemistry is related to the accessibility of gasification molecules to the reactive sites in the char at the operating temperature and pressure of the gasifier. The gasification agents are oxygen, steam and carbon dioxide, and overall, the chemical rate(s) of gasification with oxygen are similar to those of combustion, while lower reaction rates are observed with respect to the gaseous reactants H_2O and CO_2.

The effects of pressure on the evolution of pore structure during pyrolysis, and on the formation of active sites, have been studied for chars subjected to steam gasification. The development of char morphology is complicated and a decrease in the internal surface areas of chars with an increase in pressure is observed for bituminous coals because they go through a softening stage during pyrolysis, but similar changes were not observed for lignite; char that is formed in an atmosphere of steam undergoes the most significant widening of pores (Johnson, 1981; Zeng and Fletcher, 2005). Systematic studies of chars formed from lignite and bituminous coal samples, using a methane flat flame burner and a pressure drop-tube furnace, show the surface areas of the chars are related to the

different conditions used to prepare the chars. Lignite forms chars with an increased mesopore surface area, compared to those from bituminous coal, mainly due to the minerals and inorganics in lignite; dry lignite yielded char with a lower surface area than that containing moisture (Gale et al., 1995).

Experimental and molecular modelling studies of a brown coal structure transformed into a char have shown that the formation of major pyrolysis products (H_2, CO, CO_2) are impacted by metal complexes formed within the coal molecular matrix. The presence of larger sized metal species may increase the char porosity, and the release of gases associated with the inorganic species in the char molecule may further impact on the type of pores developed. As the coal matrix loses weight, its porosity may also be changed as the relative concentrations of inorganics increase in the char particle.

The impact of various inorganic species on the pyrolysis of low rank coals have been discussed previously. These studies usually focus on specific inorganics added to acid-washed coal, and are examined in char formed at various temperatures using techniques such as XRD, XPS, XANES, SEM, and Mössbauer. Char samples prepared at intermediate temperatures from coal samples containing only sodium formed $Na_2CO_3.xH_2O$, Na_2CO_3 and dispersed sodium within char. $Ca(NO_3)_2$, and $CaCl_2$ added to Loy Yang coal by mixing, and also by adjusting the pH, provided char at 650°C-800°C which contained highly dispersed Ca as CaO_6, CaO, and $CaCO_3$, along with $Ca(OH)_2$. Iron salts added to low rank coals provided chars with a number of iron species, including γ-Fe, α-Fe, Fe_3C, Fe_2O_3, Fe_3O_4, and FeOOH. Chars prepared from brown coal containing aqua-multi-nuclear iron hydroxyl species formed Fe_2O_3 at 200°C to 400°C, and Fe_2O_3, $FeFe_2O_4$ (magnetite), γ-Fe, and α-Fe, over the temperature range from 400°C to 600°C; at higher temperatures these were mainly γ-Fe, and α-Fe. XPS surface analysis of these char samples formed at low temperatures identified iron, inorganic oxygen and inorganic carbonate CO_3. Nickel species added to low rank coals form octahedral coordinated complexes with N-O bonds, and char prepared at 400°C contained Ni-O and Ni-Ni complexes, suggesting metal clusters may have formed. Coal with a larger amount of nickel complexes yielded char containing agglomerated nickel at lower temperatures. Sintering (or agglomeration) of oxides and metallic clusters has been proposed by numerous workers as the reason for the deactivation of catalysts in the gasification of low rank coals.

The experimental data generally show that, as the temperature increases, main group metals are transformed into hydroxides, oxides and carbonates. Salts such as NaCl, $CaCl_2$ and $NiCl_2$ would not decompose at low

temperatures, and at high temperatures some salts may melt prior to thermal decomposition. If some of the chloride salts simply exist as particles or crystals mixed with coal, when they are heated they may undergo thermal decompositions to yield HCl and form various hydroxides, oxides and carbonates within the char. The structure of char undergoes significant changes at the molecular level because of the presence of inorganic species, and these changes depend largely on the nature of the coal/inorganic interactions.

Coal contains nitrogen amounts of between 0.5wt% and 2wt%. XPS studies identify organically bound nitrogen present in the tars and chars after pyrolysis. The content of pyrrolic and pyridinic nitrogen increased, while that of quaternary nitrogen decreased with increasing coal rank (Kelemen et al., 1998); 90mol% of the nitrogen in the coals has been reported to remain in the char and tar as a result of the pyrolysis of the raw coals at temperatures of 500°C to 1040°C (Takagi et al., 1999). The effect of the heating rate on the conversion of nitrogen in low rank coals was observed to yield higher levels of HCN from high heating rates, and larger amounts of N_2 from lower heating rates, at maximum temperatures of 1000°C to 1040°C (Kidena et al., 2000). The nitrogen is partitioned into [tar-N], HCN, NH_3 and N_2 from acid-demineralised coals; Fe species catalysed the decomposition of [tar-N], HCN and NH_3 into N_2 at 1000°C to 1350°C. The heating rate can affect the behaviour of coal-nitrogen release at 1000°C, and slower heating rates were observed to produce larger amounts of N_2 from low rank coals (Tsubouchi and Ohtsuka, 2008).

Sulphur in coals is found as organic and inorganic species; sulphur species that evolve during pyrolysis include H_2S and COS, originating from the organic moieties and inorganic sulphides, and sulphates decompose mainly to yield SO_2. Studies have reported 15 European coal samples covering all ranks, with sulphur content ranging from 0.4 to 5.0wt%, in which the ratio of pyritic, sulphate and organic sulphur differed. The pyrolysis products were H_2S, COS, SO_2, CH_3SH, and CS_2, and yields were between 56% and 80% of the total amount of sulphur present in the coal (Selsbo et al., 1996). The evolution of H_2S from high sulphur Indian coals was dependent on temperature up to 850°C, and low concentrations of SO_2 were from the decomposition of inorganic sulphates. Maximum sulphur release was found in the temperature range of 600°C-850°C, and this release decreased as the temperature increased from 850°C to 1000°C (Baruah and Khare, 2007).

References

Amick, P. 2007. 'Experience with Gasification of Low Rank Coals', Workshop on Gasification Technologies, Colorado.

Anthony, D. B., Howard, J. B., Hottel, H. C. and Meissner, H. P. 1975. 'Rapid devolatilisation of pulverized coal', *15th Symposium (International) on Combustion* (Pittsburgh: The Combustion Institute), 1303-1317.

Baruah, B. P. and Khare, P. 2007. 'Pyrolysis of High Sulphur Indian Coals', *Energy Fuels*, 21, 3346-3352.

Bassi, P. S., Randhawa, B. S. and Jamwal, H. S. 1983. 'Mössbauer study of the thermal decomposition of some iron(III) dicarboxylates', *Thermochim. Acta,* 65, 1-8.

Baumann, P. S. 2005. 'Historical Discontinuities within Coal Gasification Technology as Precursors for Future Developments', Gasification Technologies Council, San Francisco, October 2005.

Braun, R. L. and Burnham, A. K. 1987. 'Analysis of chemical reaction kinetics using a distribution of activation energies and simpler models', *Energy Fuels,* 1, 153-161.

Brezinsky, K., Pecullan, M. and Glassman, I. 1998. 'Pyrolysis and Oxidation of Phenol', *J. Phys. Chem. A,* 102, 8614-8619.

Chern, J-S. and Hayhurst, A. N. 2010. 'A simple theoretical analysis of the pyrolysis of an isothermal particle of coal', *Combustion and Flame,* 157, 925–933.

Czechowski, F. and Jezierski, A. 1997. 'EPR Studies on Petrographic Constituents of Bituminous Coals, Chars of Brown Coals Group Components, and Humic Acids 600°C Char upon Oxygen and Solvent Action', *Energy Fuels,* 11, 951-964.

Dabestani, R., Britt, P. F. and Buchanan III, A. C. 2005. 'Pyrolysis of Aromatic Carboxylic Acid Salts: Does Decarboxylation Play a Role in Cross-Linking Reactions?' *Energy Fuels,* 19, 365-373.

Domazetis, G., Liesegang, J. and James, B. D. 2005, 'Studies of inorganics added to low-rank coals for catalytic gasification', *Fuel Processing Technology*, 86, 463-486.

Domazetis, G., Raoarun, M., James, B. D. and Liesegang, J. 2005. 'Studies of Mono- and Polynuclear Iron Hydroxy Complexes in Brown Coal', *Energy Fuels*, 19, 1047-1055.

Domazetis, G., Raoarun, M., James, B. D. and Liesegang, J. 2008. 'Molecular modelling and experimental studies on steam gasification of low-rank coals catalysed by iron species', *Applied Catalysis A: General*, 340, 105-118.

Donahue, W. S. and Brandt, J. C. (eds.) 2009. *Pyrolysis: Types, Processes, and Industrial Sources and Products*, New York: Nova Science Publishers Inc.

Duchesne, M. A., Hall, A. D., Hughes, R. W., McCalden, D. J., Anthony, E. J. and Macchi, A. 2014. 'Fate of inorganic matter in entrained-flow slagging gasifiers: Fuel characterization', *Fuel Processing Technology*, 118, 208–217.

Feng, B., Bhatia, S. K. and Barry, J. C. 2003. 'Variation of the Crystalline Structure of Coal Char during Gasification', *Energy Fuels*, 17, 744-754.

Fletcher, T. H., Kerstein, A. R., Pugmire, R. J. and Grant, D. M. 1990. 'Chemical percolation model for devolatilization. 2. Temperature and heating rate effects on product yields', *Energy Fuels*, 4, 54-60.

Fletcher, T. H., Kerstein, A. R., Pugmire, R. J., Solum, M. S. and Grant, D. M. 1992. 'Chemical percolation model for devolatilization. 3. Direct use of carbon-13 NMR data to predict effects of coal type', *Energy Fuels*, 6, 414-431.

Gale, T. K., Fletcher, T. H. and Bartholomew, C. H. 1995. 'Effects of Pyrolysis Conditions on Internal Surface Areas and Densities of Coal Chars Prepared at High Heating Rates in Reactive and Nonreactive Atmospheres', *Energy Fuels*, 9, 513-524.

Gavalas, G. R. 1982. *Coal Pyrolysis (Coal Science and Technology 4)*, New York: Elsevier.

Giroux, L., Charland, J.-P. and MacPhee, J. A. 2006. 'Application of Thermogravimetric Fourier Transform Infrared Spectroscopy (TG-FTIR) to the Analysis of Oxygen Functional Groups in Coal', *Energy Fuels*, 20, 1988-1996.

Grant, D. M., Pugmire, R. J., Fletcher, T. H. and Kerstein, A. R. 1989. 'Chemical model of coal devolatilization using percolation lattice statistics', *Energy Fuels*, 3, 175-186.

Hill, J. O., Ma. S. and Heng, S. 1989. 'A thermal analysis study of the pyrolysis of Victorian brown coal', *J. Thermal Anal.*, 35, 977-988.

Hill, J. O., Ma. S. and Heng, S. 1989. 'Thermal analysis of Australian coals—A short review', *J. Thermal Anal.*, 35, 2009-2024.

Hindmarsh, C. J., Thomas, K. M., Wang, W. X., Cai, H. Y., Güell, A. J., Dugwell, D. R. and Kandiyoti, R. 1995. 'A comparison of the pyrolysis of coal in wire-mesh and entrained-flow reactors', *Fuel*, 74, 1185-1190.

Hinserg, W., Houle, F., Allen, F. and Yoon, E. 1996. Chemical Kinetics Simulator Program v1.01, IM Almaden Research Center.

Ichihashi, M., Hanmura, T. and Kondow, T. 2006. 'How many metal atoms are needed to dehydrogenate an ethylene molecule on metal clusters?

Correlation between reactivity and electronic structures of Fe^{+}_{n}, Co^{+}_{n}, and Ni^{+}_{n}', *J. Chem. Phys.*, 125, 133404-133409.

Johnson, J. L. 1981. 'Fundamentals of coal gasification', in M. A. Elliott (ed.), *Chemistry of Coal Utilization* (Wiley: New York), 1491-1598.

Kelemen, S. R., Gorbaty, M. I. and Kwiatek, P. J. 1994. *Prepr. Am. Chem. Soc., Div. Fuel Chem.,* 39, 31-35.

Kelemen, S. R., Gorbaty, M. L., Kwiatek, P. J., Fletcher, T. H., Watt, M., Solum, M. S. and Pugmire, R. J. 1998. 'Nitrogen Transformations in Coal during Pyrolysis', *Energy Fuels,* 12, 159-173.

Kidena, K., Hirose, Y., Aibara, T., Murata, S. and Nomura, M. 2000. 'Analysis of Nitrogen-Containing Species during Pyrolysis of Coal at Two Different Heating Rates', *Energy Fuels,* 14, 184-189.

Knickelbein, M. B., Koretsky, G. M., Jackson. K. A., Pederson, M. R. and Hajnal, Z. 1998. 'Hydrogenated and deuterated iron clusters: Infrared spectra and density functional calculations', *J. Chem. Phys.*, 109, 10692-10700.

Ko, G. H., Peters, W. A. and Howard, J. 1988. 'Comparison of tar evolution rate predictions in coal pyrolysis from the multiple independent parallel reaction model and the functional group model over a wide range of heating rates', *Energy Fuels,* 2, 567-573.

Lazzari, M., Kitayama, T. and Hatada, K. 1998. 'Effect of Stereoregularity on the Thermal Behaviour of Poly(methacrylic acids). 2. Decomposition at Low Temperatures', *Macromolecules,* 31, 8075-8082.

Le Page, M. D. and James, B. R. 2000. 'Nickel bromide as a hydrogen transfer catalyst', *Chem. Commun.,* 1647-1648.

Li, F-H., Ma, X-W., Guo, Q-Q., Fan, H-L., Xu, M-L., Liu, Q-H. and Fang, Y-T. 2016. 'Investigation on the ash adhesion and deposition behaviours of low rank coal', *Fuel Processing Technology*, 152, 124-131.

Li, J. and Brill, T. B. 2002. 'Spectroscopy of Hydrothermal Reactions 20: Experimental and DFT Computational Comparison of Decarboxylation of Dicarboxylic Acids Connected by Single, Double, and Triple Bonds', *J. Phys. Chem. A*, 106, 9491-9498.

Li, J. and Brill, T. B. 2003. 'Decarboxylation Mechanism of Amino Acids by Density Functional Theory', *J. Phys. Chem. A*, 107, 2667-2673.

Li, M., Zeng, F., Chang, H., Xu, B. and Wang, W. 2013. 'Aggregate structure evolution of low rank coals during pyrolysis by in-situ X-ray diffraction', *Int. J. Coal Geology,* 116-117, 262-269.

Liyanage, R., Zhang, X-G. and Armentrout, P. B. 2001. 'Activation of methane by size-selected iron cluster cations, Fe^{+}_{n} (n=2–15):Cluster-CHx (x=0–3) bond energies and reaction mechanisms', *J. Chem. Phys.*, 115, 9747-9763.

Ma, S., Hill, J. O. and Heng, S. 1991. 'A kinetic analysis of the pyrolysis of some Australian coals by non-isothermal thermogravimetry', *J. Thermal Anal.*, 37, 1161-1177.

Ma, S., Huang, G. and Hill, J. O. 1991. 'KNIS-a computer program for the systematic kinetic analysis of non-isothermal thermogravimetric data', *Thermochimica Acta.*, 184, 233-241.

Manion, J. A., McMillen, D. F. and Malhotra, R. 1996. 'Decarboxylation and Coupling Reactions of Aromatic Acids under Coal-Liquefaction Conditions', *Energy Fuels*, 10, 776-788.

Mavridou, E., Antoniadis, P., Littke, R., Lücke, A. and Krooss, B. M. 2008. 'Liberation of volatiles from Greek lignites during open system non-isothermal pyrolysis', *Org. Geochem.*, 39, 977-984.

Minchener, A, J. 2005. 'Coal gasification for advanced power generation', *Fuel,* 84, 2222-2235.

Mondal, P., Dang, G. S. and Garg, M. O. 2001. 'Syngas production through gasification and clean-up for downstream applications – Recent developments', *Fuel Processing Technol.,* 92, 1395-1410.

Morando, P. J., Piacquadio, N. H., Blesa, M. A. and Vedova, C. O. D. 1987. 'The thermal decomposition of iron(III) formate', *Thermochim. Acta,* 117, 325-330.

Morgan, T. J. and Kandiyoti, R. 2014. 'Pyrolysis of Coals and Biomass: Analysis of Thermal Breakdown and Its Products', *Chem. Rev.,* 114, 1547−1607.

Niksa, S. 1994. 'FLASHCHAIN Theory for Rapid Coal Devolatilization Kinetics. 5.Interpreting Rates of Devolatilization for Various Coal Types and Operating Conditions', *Energy Fuels*, 8, 671-679.

Niska, S. 1996. 'Flashchain Theory for Rapid Coal Devolatilization Kinetics. 7. Predicting the Release of Oxygen Species from Various Coals', *Energy Fuels,* 10, 173-187.

Niksa, S. and Kerstein, A. R. 1991. 'FLASHCHAIN theory for rapid coal devolatilization kinetics. 1. Formulation', *Energy Fuels*, 5, 647-665.

Otake, Y. and Walker Jr., P. L. 1993. 'Pyrolysis of demineralized and metal cation loaded lignites', *Fuel*, 72, 139-149.

Ozaki, J., Nishiyama, Y., Cashion, J. D. and Brown, L. J. 1999. 'Carbonization of iron-treated Loy Yang coal', *Fuel*, 78, 489-499.

Please, C. P., McGuiness, M. J. and McElwain, D. L. S. 2003. 'Approximations to the distributed activation energy model for the pyrolysis of coal', *Combustion Flame*, 133, 107-117.

Randhawa, B. S., Kaur, R. and Sweety, K. 1997. 'Mössbauer study on thermal decomposition of some hydroxy iron(III) carboxylates', *J. Radioanalytical and Nuclear Chemistry*, 220, 271-273.

Sahajwalla, L. L. V., Kong, C. and Harris, D. 2001. 'Quantitative X-ray diffraction analysis and its application to various coals', *Carbon,* 39, 1821-1833.

Saxena, S. C. 1990. 'Devolatilization and combustion characteristics of coal particles', *Prog. Energy Combust. Sci.,* 16, 55-94.

Schimmel, P. H. A., Ruttink, P. J. A. and de Jong, B. H. W. S. 1999. 'Ab Initio Calculations on Hydroaromatics: Hydrogen Abstraction and Dissociation Reaction Pathways', *J. Phys. Chem. B.,* 103, 10506-10516.

Selsbo, P., Almén, P. and Ericsson, I. 1996. 'Quantitative Analysis of Sulphur in Coal by Pyrolysis-Gas Chromatography and Multivariate Data Analysis', *Energy Fuels,* 10, 751-756.

Shengyu, L., Wenying, L. and Kechang, X. 2003. 'The Fate of Organic Oxygen During Coal Pyrolysis', *Energy Source*, 25, 479-488.

Solomon, P. R., Hamblen, D. G. and Carangelo, R. M. 1984. '5-Analytical Pyrolysis of Coal Using FT-IR', in K. J. Vorhees (ed.), *Analytical Pyrolysis* (Oxford: Butterworth-Heinemann), 121-156.

Solomon, P. R., Serio, M. A., Despande, G. V. and Kroo, E. 1990. 'Cross-linking reactions during coal conversion', *Energy Fuels*, 4, 42-54.

Song, H., Liu, G. and Wu, J. 2016. 'Pyrolysis characteristics and kinetics of low rank coals by distributed activation energy model', *Energy Conversion and Management,* 126, 1037-1046.

Suuberg, E. M., Peters, W. A. and Howard, J. 1978. 'Product Composition and Kinetics of Lignite Pyrolysis', *Ind. Eng. Chem. Process Des. Dev.*, 17, 37-46.

Takagi, H., Isoda, T., Kusakabe, K. and Morooka, S. 1999. 'Effects of Coal Structures on Denitrogenation during Flash Pyrolysis', *Energy Fuels,* 13, 934-940.

Tsubouchi, N. and Ohtsuka, Y. 2008. 'Nitrogen chemistry in coal pyrolysis: Catalytic roles of metal cations in secondary reactions of volatile nitrogen and char nitrogen', *Fuel Process. Technology,* 89, 379-390.

Van de Venter, E. 2005. 'Sasol-Lurgi Coal Gasification Technology and Low Rank Coal', Presentation to the Gasification Technologies Council Conference, 10-12 October.

Vijay Kumar, K., Bharath, M., Raghavan, V., Prasad, B.V.S.S.S., Chakravarthy, S. R. and Sundararajan, T. 2017. 'Gasification of high-ash Indian coal in bubbling fluidized bed using air and steam – An experimental study', *Applied Thermal Engineering*, 116, 372-381.

Wang, J., Lian, W., Li, P., Zhang, Z., Yang, J., Hao, X., Huang, W. and Guan, G. 2017. 'Simulation of pyrolysis in low rank coal particle by using DAEM kinetics model: Reaction behaviour and heat transfer', *Fuel,* 207, 126-135.

Wertz, D. L. 1999. 'Interlayer Structural Models of Beulah Zap Lignite Based on Its Wide Angle X-ray Scattering', *Energy Fuels*, 13, 513-517.

Wiater, I., Born, J. G. P. and Louw, R. 2000. 'Products, Rates, and Mechanism of the Gas-Phase Condensation of Phenoxy Radicals between 500-840 K', *Eur. J. Org. Chem.,* 6, 921-928.

Yang, S., Qian, Y., Liu, Y., Wang, Y. and Yang, S. 2017. 'Modelling, simulation, and techno-economic analysis of Lurgi gasification and BGL gasification for coal-to-SNG', *Chemical Engineering Research and Design*, 117, 355-368.

Yu, J. and Zhang, M. 2003. 'A Simple Method for Predicting the Rate Constant of Pulverized-Coal Pyrolysis at Higher Heating Rate', *Energy Fuels*, 17, 1085-1090.

Zeng D. and Fletcher, T. H. 2005. 'Effects of Pressure on Coal Pyrolysis and Char Morphology', *Energy Fuels.* 19, 1828-1838.

Zheng, L. and Furinsky, E. 2005. 'Comparison of Shell, Texaco, BGL and KRW gasifiers as part of IGCC plant computer simulations', *Energy Conversion and Management,* 46, 1767-1779.

Zoeller, J. R. 2009. 'Eastman Chemical Company's Chemicals from Coal program: The first quarter century', *Catalysis Today*, 140, 118-126.

CHAPTER EIGHT

CATALYSTS FOR LOW RANK COAL GASIFICATION

Catalysts are widely used in numerous processes and are estimated to contribute to about 20% of the US gross domestic product (GDP) (ACS, 2011), and about 25% of the world GDP. Interest in catalytic steam coal gasification has spanned over many decades, as catalysts have the potential to improve the quality of syngas, but in spite of a considerable R&D effort, it has not as yet resulted in the operation of commercial catalytic coal gasifiers (Gallagher and Euker, 1980; Johnson 1976). In the 1970s and 1980s, Exxon (Nahas, 1983) and the US DOE expended effort on catalytic gasification and built a demonstration unit to produce synthetic natural gas (SNG), using bituminous Illinois No. 6 coal.* GreatPoint Energy has undertaken a program for commercialising a catalytic gasification system, which evolved from the development by Exxon, to produce SNG from coal.† Clean Coal Technology Pty Ltd is endeavouring to develop a steam catalytic coal gasification process fuelled by low rank coals containing iron species.

Although the field of catalysis is mature, catalytic coal gasification is novel and an understanding of the mechanisms at a molecular level is challenging. A catalyst modifies the kinetics of a chemical system, accelerating the reactions by providing alternate reaction routes with lower activation barriers. The rate of any reaction is exponentially dependant on its activation energy, so reductions in the energy barrier to a reaction route would exert a significant change on the reaction system. Generally, catalytic coal gasification is classified as heterogeneous catalysis and what constitutes the active sites in coal where the catalysed reaction(s) takes place is an important question (Zaera, 2002; Widegren and Finke, 2003; Nørskov et al., 2008). Related to this is the question of the structural dependence of the reaction rate on the variations of the activity that may be due to particle

* On catalytic gasification, see https://www.netl.doe.gov/research/coal/energy-systems/gasification/gasifipedia/specialapps.

† For details about the GreatPoint program, see http://www.greatpointenergy.com/about.php.

size and the accessible surface area of the char, and also the chemistry of the inorganic compound added for catalytic activity; indeed, some catalysts may exist as discrete particles, while others may be dispersed as part of the char, and these factors further complicate mechanistic studies. General questions on the nature of the active sites and structural dependence of all heterogeneous catalysts have been debated for decades, and particular questions and studies on catalytic (with H_2O and CO_2) coal gasification mechanisms are expected to continue.

Theoretical studies on conventional heterogeneous catalysis based on DFT calculations have provided insights on surface reactivity, and these, coupled with experiments, have shown there could be order of magnitude differences in reaction rates for different surface structures. These modelling techniques have been combined with a number of experimental methodologies to provide insights on heterogeneous catalysis at the molecular level. Application of these techniques to coal catalysis offers greater insight on this complicated chemistry.

Gasification of coal by steam is an important technology for industrial application, with additional interest in gasification using CO_2. An understanding of the catalytic gasification chemistry of low rank coals requires an examination of the structure of these coals with the added inorganic species. The complexity of the process requires considerable effort to clarify the reaction system within the tenets of heterogeneous catalysis. It is necessary to understand the non-catalytic, thermolytic chemistry, which also involves inorganic species within the coal matrix as it undergoes heating (discussed in the previous chapter), and, from these studies, seek to identify catalytic reactions involving the gasification agent and the relevant sites in coal and, ultimately, in the char molecular matrix.

The heterogeneity of low rank coals also poses challenges to experimental methodology. The inorganic species added to these coals must be well characterised, and further, these studies necessitate a systematic treatment of low-temperature pyrolysis chemistry to ascertain reactions that precede catalytic gasification. From these studies, additional data are needed to identify reaction centres and catalytic moieties. Experimental data must be collected that can be used in combination with molecular modelling, to develop reaction schemes that would show the formation of the catalytic species and reactive sites available to the gasification agent.

It is clear that the fundamental aspects of coal catalytic gasification would be understood within the tenets of heterogeneous catalysis; ordinarily, a heterogeneous catalyst is a solid and reactants are mobile phases (liquid or gas) and consequently may react by moving to the solid phase's reactive centre and yield products which are then able to leave the

reactive centre, and in this way the catalytic cycle continues. The chemistry is often carried out under reducing conditions, and thus a change would be expected to occur in the oxidation state of the catalytic substance; often this is an important step in the catalytic cycle.

In coal catalysis, however, the compound added to the coal to act as a catalyst is part of the solid matrix, the reactants are a mobile gas (such as steam) and solid char, and the products are gases. Both the substrate (char) and the inorganic catalytic species form the solid phase in the reaction route – this immobile carbon reactant therefore requires a novel concept for theoretical considerations of catalytic activity in coal.

The overall coal gasification chemistry leading to the formation of syngas would include additional secondary reactions involving ash particles, the breakdown of tar, and reactions with the gases CO and H_2O to form H_2 and CO_2 (the water gas-shift reaction). Data are needed to differentiate between catalytic reactions involving char and the gasification agent from the additional post-gasification solid-gas-phase chemistry. Work that has measured the gasification of coal or char has shown catalytic activity would depend on which inorganics are added to the coal, the chemical nature of these inorganics, and their transformations as the coal is heated; a mixture of inorganics may provide other species that are involved in the additional reactions of post-char gasification. This complicated phenomenon requires extensive experimental research and molecular mechanistic studies to identify the effective catalysis for coal gasification.

Catalysis of Coal Gasification

This section presents a brief review of mechanisms proposed for the catalysis of coal gasification, followed by further detailed discussions on the mechanisms of iron catalysis of processed low rank coals. Generally, while a great number of heterogeneous catalysts have been used in industrial processes, not all of these mechanisms are fully understood; insights available from fundamental research enable applications and improvements to industrial processes, and the classic example of this is the Fischer-Tropsch synthesis in which iron and cobalt catalysts are utilised in the reactions of synthesis gas to form hydrocarbons (Davis, 2001). These remarks are also applicable to catalytic coal gasification.

Early mechanisms' coal gasification, which addressed the catalysts as a solid phase onto char, proposed a scheme in which a distinction is made between 'direct' and 'indirect' catalytic effects. The direct concept involves the transport of the gaseous reagent (in this case steam) to the catalyst to form H_2, and either O is transported by the catalyst or C atoms are dissolved

and transported within the catalyst to form CO. The indirect concept splits H_2O into H_2 and the resulting O reacts (spills over) at an active C site, followed by CO formation; alternatively, the catalyst is involved at a reactive site at which a reaction between C and H_2O occurs to form H_2 and CO. In both cases, CO and H_2 molecules leave the surface (Mims, 1990). The classical picture of a catalyst lowering the activation barrier to a reaction may apply in such a case, but little, if any, molecular mechanistic information, or insights on the chemical nature of an intermediate or catalytic site, is provided by such schemes.

The overall rate of gasification may depend on a number of factors, such as the rate of diffusion of the reactant gas to the active site, the chemical effect(s) arising from localised conditions, such as temperature or gas composition, and the morphology of the catalyst within the char, which could play an important role in the particular mechanism. The morphology of catalysts on char may range from discrete particles to a dispersed phase spread out on a carbon surface, or to active centres chemically formed with the char and the catalyst. The morphology of the char is also related to the inorganic added to the coal, as this may impact on the char's structure and porosity.

The formation of catalytic sites, and subsequent activity, depend on the substance and the method used to add it to the coal matrix, and the subsequent behaviour as the treated coal is heated. The substance added as a catalyst may change during char formation and its dispersion may not be similar to that when it was added to the coal. Thus for higher rank coals, catalysts such as nickel and iron would be expected to exist either as small discrete particles at the carbon surface, whereas potassium and sodium compounds may be dispersed throughout the char. Some substances may undergo melting, particularly if low melting point eutectics were formed at elevated temperatures. The interfacial bonding between carbon/char and the catalyst is strongly influenced by the type of catalytic material. Thus, materials which melt and 'wet' the surface would bond to the carbon by a 'wetting' action, while solid particles may only form weak bonds with carbon. Inorganic complexes which are chemically bonded to coal functional groups may continue as part of the char molecular matrix, and could undergo a series of reactions and transformations which eventually may form catalytically active species.

Low rank coals form disordered char structures which do not display significant graphitic properties, whereas char from high rank coal may be annealed into graphite. The difference(s) in gasification between graphitic and non-graphitic chars is illustrated by studies with scanning tunnelling microscopy, which show that graphite is gasified by the formation of

circular voids that initially have one atomic layer, which may then grow into a depth of many such layers. For example, platinum acts as a catalyst for graphite gasification *via* channel formation within the structure, as it changes the graphite physically during gasification. The relation between interfacial attraction and the mode of catalytic attack of solid dispersions has been clarified by microscopic techniques which may show a metal forming a melting phase, and wetting a carbon surface, and the behaviour of the graphitic carbon layer is to gasify as the catalytic action occurs at the edges. A disordered char structure, however, is expected to behave differently to graphite; for example, it is possible for solids to be lodged into the micro pores of low rank chars and there may act as catalytic sites for gas-phase reactions.

Studies of catalysis for H_2O/CO_2 reactions with low rank and high rank coals have been carried out to examine many inorganic compounds, but the ones of particular interest here are alkali and alkali earth compounds, such as potassium, sodium, calcium, and transition metals, such as iron and nickel, and various mixtures of these (Chu and Schmidt, 1991; Raghunathan and Yang, 1989). Catalysts have also been used in coal gasification to produce methane, or to produce hydrogen by using catalysts for the water shift reaction with syngas. The various compounds examined for catalytic activity are proposed to show a general trend in catalytic activity, such as of the order K>Na and Ca>Fe, but this approach is suspect, as some reports indicate these orders may be reversed. Proposed kinetics and molecular mechanisms have been complicated by differences in the yields of primary products, and in the case of H_2O gasification, because some reports have not made a distinction between the primary reactions of char with steam from those catalysed reactions of steam with CO (e.g. the water shift reaction).

Catalysis using Alkali and Alkali Earth compounds

Catalytic activity has been examined for alkali and alkali earth compounds added to coals, and for mixtures containing one or more of these compounds. Attempts have been made to identify those substances that display higher catalytic activity, and also to assess their potential for applications, determined by matters such as the expense, deactivation, and recovery of the catalyst. For example, potassium compounds have been demonstrated to be active as catalysts, but they are expensive, and can become deactivated by reactions at elevated temperatures with silicates and chlorides; calcium compounds are also shown to be active, but these may be deactivated by reactions with sulphur compounds from coal.

Gasification systems using a potassium catalyst have been of interest for the industrial production of SNG; the deactivation and recovery of the catalyst are major concerns for a commercial operation. The catalyst increases the rate of steam gasification, promotes gas phase methanation, and minimises the agglomeration of caking coals. In the Exxon (and GreatPoint Energy) plant that employs K_2CO_3 as the gasification catalyst with coal, measures are used in a novel processing sequence to maximise the benefits derived from the catalyst. The process combines a relatively low gasifier temperature (700-750°C) and high pressure (500 psig) with the separation of syngas ($CO + H_2$) from the methane product so that the only net products from gasification are CH_4, CO_2, and small quantities of H_2S and NH_3. These impurities are removed to produce SNG. The overall reaction is essentially thermo-neutral and can be represented by the equation:

$$\text{Coal} + H_2O \xrightarrow{\text{Kcat}} CH_4 + CO_2$$

A progression of ideas has been discussed about reaction mechanisms dealing with potassium catalysed coal gasification with CO_2 and H_2O. It has been understood that the interaction of the catalyst with the solid carbon substrate is important for the activity and stability of the resulting system. There has been speculation on whether the reactive catalyst species is the potassium metal, or an intercalate type potassium-carbon compound, or perhaps a surface oxygen-potassium complex. The reactivity at increasing burn off has also been a point of debate; a maximum reactivity at 20-50% burn off, followed by a steady decrease, has been proposed. Speculation has also occurred concerning the potassium catalyses of the methanation reaction, and an equilibrated water-gas shift reaction. A detailed description has been given for the reactivity, selectivity and kinetics in the potassium carbonate catalysed gasification of highly pure activated carbon with low pressures of steam. It has been shown that absolute reactivity increases with an increase in catalyst loading and at increasing burn off, leading to a maximum value of between 40% and 80% burn off, dependent on the initial loading.

In view of the various notions discussed for catalytic action by inorganics on carbon, Espinal et al., (2009) carried out DFT molecular modelling studies on the mechanisms of the steam gasification of carbonaceous materials to assess the thermodynamics of possible reactions that may occur, especially the interactions of water molecules with active sites of clean and oxidised carbonaceous models. These molecular computations consider the pathways for the evolution of molecular

hydrogen and carbon monoxide from the carbon-H_2O reaction. Graphene models have been used in which the boundaries of these finite graphite models were of zigzag and armchair configurations. Dissociative chemisorption of H_2O on the active sites of clean zigzag and armchair models was reported to be exothermic and yielded stable intermediates such as hydroxyl, semiquinone, and cyclic ether functional groups. Semiquinone groups can be produced by further dissociation of the hydroxyl groups, or though the formation of molecular hydrogen. Stable cyclic ether groups can also be produced by H_2 evolution, but only at armchair edges. The reaction of water with the active sites of an oxidised surface can be more exothermic than the reaction with the clean surface due to the stabilisation of the surface hydroxyl groups, which is a key product of the initial dissociation of water, stabilised through strong hydrogen bonds. When water interacts with a hydrogen saturated surface, however, the dissociative chemisorption of the water molecule is endothermic. It was concluded that the presence of hydrogen in the gasification atmosphere should partially retard the gasification reaction by obstruction of the active sites.

Several possible endothermic pathways for the formation of H_2 and CO have been proposed based on DFT computations; the evolution of a hydrogen molecule may occur from an adsorbed hydrogen atom and the hydrogen atom of the hydroxyl group that is formed after the dissociative adsorption of water on the active sites. Another possible route is postulated to occur from two water molecules on contiguous active sites of the model. These involve dissociative chemisorption of the two water molecules to yield two neighbouring hydroxyl groups in zigzag and armchair configurations, respectively, and these are computed to be exothermic; the hydroxyl groups are precursors for subsequent hydrogen evolution, leaving two semiquinone groups on the surface that could desorb as carbon monoxide or carbon dioxide. Reactions have been proposed for carbon monoxide desorption, after the yield of hydrogen, to include the formation of five member rings, after the evolution of carbon monoxide through endothermic reactions for zigzag and armchair configurations. However, for the armchair configuration, the reaction enthalpy for carbon monoxide evolution from a semiquinone group is about half the energy required for carbon monoxide evolution from a cyclic ether, probably due to the high stability of cyclic ether groups and because more bonds need to be broken to release carbon monoxide from cyclic ether groups.

DFT computations and experimental investigations have been carried out by Roberts et al., (2015) on CO_2 gasification of coal chars derived from the vitrinite- and inertinite-rich South African coals at 1000°C. A graphene model was also used in this study and various configurations were

examined; the mean double numerical polarisation basis set nucleophilic Fukui function (DFT-DNP) was employed to compute reaction pathways and transition states, and to obtain the energy of reaction and activation energies for the gasification reactions of CO_2 with active carbon sites. These results were compared with TGA experimental results obtained at 900°C-980°C. The DFT-DNP value of the H-terminated char models and active sites located at similar edge positions decreased with the increasing size of char molecules and followed the sequence: zigzag >armchair tip active sites. The mean DFT-DNP value for the activation energy of 233 kJ mol^{-1} at the reactive carbon edge was in reasonable agreement with the experimental data of 191 ± 25 kJ mol^{-1} and 210 ± 8 kJ mol^{-1} for the respective vitrinite and inertinite chars.

Mechanistic studies of carbon gasification by H_2O and CO_2 using isotopically labelled $K_2{}^{13}CO_3$ show the potassium compound exchanges CO_2 with the carbon surface at <1000K, while at >1000K potassium carbonate decomposes (and potassium may be lost as vapour); carbon surface-oxygen intermediates stabilise the potassium and decrease its rate of volatilisation. A comparison of the catalytic influence of potassium on the reaction of C sites with H_2O, and CO_2 demonstrated that equal amounts of catalysts cause identical increases in the respective reaction rates. It was concluded that potassium catalyses both H_2O and CO_2 reactions with C in the same way. The potassium-salt catalyst is reported to be well dispersed throughout the carbon and 'wets' the carbon surfaces. Surface anionic centres are proposed to form, which provide the strong interfacial energies responsible for the catalyst's self-dispersion. The amount of catalyst needed for maximum activity is thought to correspond roughly to the amount of edge carbon area available for the particular char. Chloride and clays are able to scavenge the potassium (Saber et al., 1986; Schumacher et al., 1986).

The kinetics for potassium catalysis for the CO_2/C reaction is thought to involve reversible oxidation-reduction cycles, with the gasification step taking place in the oxidised state. The reaction with C/CO_2 is usually described by a two-step model, in which the oxidation/reduction cycle represents all steps preceding gasification. A free carbon (C_f), or carbon edge, may be envisaged:

$$CO_2 + C_f \underset{k_{-1}}{\overset{k_1}{\leftrightarrow}} CO + C(O)$$

$$C(O) \xrightarrow{k_2} CO$$

(k_2 is the forward rate constant and the assumed rate determining step)

The nature of potassium catalysis is envisaged to include intermediate oxidised and reduced species. The potassium carbonate forms a carbon supported oxide of unknown structure:

$$K_2CO_3/C \rightarrow 'K_2O/C'$$

Between 900K and 1200K, a reduction of 'K_2O/C' takes place and yields CO:

$$'K_2O/C' + C \rightarrow 'K/C' + CO$$

Catalytic activity has been observed at temperatures where most of the potassium is present as the carbon supported oxide. Phenoxide surface salts have been proposed as the reduced intermediate, and a phenoxide radical analogue may form as a result of oxidation of the catalyst film, which decomposes to release CO. Thus in this proposed mechanism, metallic potassium is not considered the active site, although it may be present during gasification. The proposed mechanism(s) which are consistent with experimental data involve oxidic potassium species with a CO inhibition step:

$$\begin{aligned} CO_2 + K_xO_y &\leftrightarrow CO + K_xO_{y+1} \\ K_xO_{y+1} + C &\rightarrow K_xO_y + C(O) \\ C(O) &\rightarrow CO \end{aligned}$$

The inhibition by CO requires an additional step in the kinetic scheme, e.g.:

$$CO + C(O) \rightarrow CO_2 + C$$

Kinetic studies of alkali metal catalysis of carbon gasification, such as potassium, indicate the catalyst increases the number of active C(O) species; the rate-determining step is the same for both catalysed and un-catalysed gasification, that is, $C(O) \rightarrow CO$, thus the relative effects of a catalyst may be explained by the creation of a greater number of active sites (Mims and Pabst, 1983; Moulijn and Kapteijn, 1986).

The mechanism for the reaction by potassium-char with steam has been observed to produce H_2 and CO_2, which is a novel way to yield the same products as the water-shift reaction (Wang et al., 2005). Catalysis by potassium is also postulated to include a potassium-oxidic-carbon intermediate resembling the above mechanism.

Computer molecular modelling has been carried out using idealised molecular structures of graphite and potassium particles or clusters, defined as non-stoichiometric compounds with an excess of metal. A unified mechanism is proposed for reactions of graphite with CO_2, and H_2O for uncatalysed reactions, and for ones catalysed by alkali and alkaline earth compounds. In this unified mechanism, two oxygen intermediates have been proposed, bonded to the active edge carbon atoms: one is an in-plane semiquinone type, $C_f(O)$, and the other intermediate an off-plane oxygen bonded to two saturated carbon atoms that are adjacent to the semiquinone species, $[C(O)C_f(O)]$. The rate-limiting step is the decomposition of these intermediates by breaking the C-C bonds that are connected to $C_f(O)$. The reaction of a carbon source with 21 Torr H_2O ($26.4x10^{-3}$ atm) at 700°C gave a turn-over frequency (TOF) for the phenoxide [(Ph)C-O-K] of 0.15 s^{-1}, whereas the TOF was 7.8 s^{-1} for KOH particles or clusters, indicating clusters are more effective catalysts. Molecular orbital theory calculations have been carried out on the H_2O-carbon reaction, and also *ab initio* computations for the adsorption of alkali on graphite; these studies have characterised the dispersions of alkali metal atoms on carbon surfaces (Chen and Yang, 1997; Zhu et al., 2002; Zhu and Lu, 2004).

A study of K_2CO_3 catalysis of steam gasification of pure activated carbon shows absolute reactivity increases on increasing initial catalyst loading and increasing burn off, the latter leading to a maximum value of between 40% and 80% burn off, dependent on the initial loading. Activation of the catalyst in the region up to 50% burn off is probably due to the breaking up of [K-O-C] bonds. The lack of activity at low catalyst concentrations is explained by intercalate formation, which makes the catalyst inaccessible to the gaseous reactant. The results suggest that both CO and CO_2 are primary reaction products from different reaction pathways, in which potassium catalysis is basically controlled by the catalyst-carbon interaction. The reaction can be described by a redox mechanism in which the reduction step becomes more important at higher catalyst loadings. The assumption of a water-gas shift equilibrium is doubtful during the potassium catalysed, low pressure, steam gasification of activated carbon. These studies of the potassium catalysed steam gasification of activated carbon indicate potassium acts as an oxygen transferring medium, while water adsorption takes place on a reduced site (Wingmans et al., 1983).

Recent studies of steam gasification of high rank coal with K_2CO_3 indicate potassium causes char to be disordered, and this enhances the reactivity between char sites and steam. A K-char intermediate is postulated and this reacts with H_2O to yield H_2 and a [K-O-char] species which

decomposes into CO, and the reactive intermediate [K-char] is again formed for a cyclic reaction (Zhang et al., 2016). Experimental data show a greater proportion of char is gasified by steam, but no turnover numbers or frequencies are proposed, and a prolonged period is required for char gasification.

A mechanism of K_2CO_3-catalysed steam gasification of ash-free char has been proposed, and in this scheme, [K–O–C*] denotes a reduced intermediate; a portion of active carbon (C*) in this structure reacts with steam to form CO and H_2, with another carbon reacting with oxygen from steam to yield an active carbon site C(O), which reacts with another H_2O molecule to yield CO_2 and H_2 with the oxidation of potassium into a potassium oxide species [K-O]. This potassium oxide species is then reduced to [K-O-C*] thereby completing the catalytic cycle. This mechanism differs from the previous one in that the formation of CO occurs *via* the [K-O-C*] intermediate instead of a [K-O-C(O)] intermediate (Wu et al., 2016).

The activity of alkali metal catalysts such as potassium and sodium during gasification is suggested to be determined by a combination of metal evaporation, metal intercalation (or 'wetting'), metal-oxide surface group formation and the formation of crystalline forms. Catalysis of gasification by sodium carbonate has been demonstrated and mechanisms postulated. Differences in the catalytic activities between potassium and sodium are ascribed to the poorer intercalation properties of sodium. Sodium may possess catalytic activity on an oxygen-rich char surface, but the deactivation of sodium needs to be further studied before its potential for useful catalysis can be realised (Wigmans et al., 1983). Sodium present as NaCl was shown not to possess catalytic activity, but ion-exchanged sodium and sodium carbonate are reported to exhibit good catalytic activity to char gasification with steam. Sodium K-edge X-ray absorption near edge structure (XANES) studies show that the ion-exchanged sodium undergoes chemical changes on heating to form finely dispersed sodium carbonate, although there is no direct evidence that this is the form of the active catalyst. NaCl will only show catalytic activity after conversion to sodium carbonate. Formations of crystals of either NaCl or Na_2CO_3 are reported to deactivate catalysis by sodium (Yamashita et al., 1991).

The gasification of Yallourn brown coal char loaded with about 1% Na_2CO_3 has been studied using a quartz reactor tube coupled to a gas chromatograph, gasified with pulses of steam. After a pulsed gasification run, the sample temperature was decreased to 573K and a temperature programmed desorption run carried out from 573K to 1273K to determine oxygen remaining on the char surface. Results show the formation of

hydrogen at 923K, indicating the oxidation of metal by water molecules to give H_2, and at 1073K corresponding amounts of CO and CO_2 were observed. The reactions postulated involve the formation of H_2 and Na_2O from water, with CO formed by reactions involving the sodium oxide and carbon. The gasification with Na_2CO_3 was compared to that using iron as a catalyst. The iron catalyst did not display a similar temperature dependence. Large amounts of catalyst in the char increased the amounts of H_2 and CO formed, but the increase was not linear with respect to catalyst loading (Suzuki et al., 1989).

Experiments have been reported using a number of chars, including brown coal char, to determine reaction pathways for sodium catalysis. Catalyst oxidation pathways involving two types of sites are postulated, one being a fast reduction of CO_2 on the dispersed sodium metal, and the other a slow oxidation of the sodium cluster through the cluster-CO_2 complex. The reduction step(s) is also believed to involve two paths on the same two sites (such as are observed for oxidation pathways), one being the fast oxidation of carbon with the active oxidant, and the other the slow oxidation of carbon by the sodium oxide cluster. In this work, the mechanism for sodium gasification is thought to be similar to that for potassium (Suzuki et al., 1992).

Ion-exchanged calcium compounds added to North Dakota lignite are reported to increase the reactivity of char by over 30 times, equivalent to about a 100-degree decrease in temperature for a similar reactivity. The char showing greatest reactivity was prepared by pyrolysing demineralised lignite impregnated with calcium compounds, and this was heated at 1275K for about 0.3 seconds. This result is contrasted with that of data obtained from experiments in which residence times were employed for pyrolysis of about 5 minutes, which yielded a reduced char reactivity by a factor of about 25. The greater reactivity of the former sample is attributed to the highly dispersed $CaO/CaCO_3$ in the char particles; in the latter, when the sample is heated to form a char over a prolonged residence time, the calcium compound may agglomerate, and thereby reduce catalytic activity (Radovic et al., 1983).

The reactivity observed with Spherocarb, a high purity synthetic char, was similar to that of char obtained from demineralised Beulah Zap char when both were impregnated with aqueous calcium. Adding $CaCO_3$ increased the reaction rates in 10% oxygen, for both Spherocarb and acid-treated Beulah Zap char, by 100-fold (Bartholomew et al., 1991). Temperature-programmed desorption experiments using labelled $^{13}CO_2$ at 300°C and 500°C distinguished between two types of CO for the Ca carbon system. ^{13}CO was produced by dissociation of $CaCO_3$ at the catalyst-carbon

contact, and ^{12}CO was obtained from carbon gasification *via* decomposition of the oxidised carbon sites. These two CO peaks were of similar concentrations and appear to confirm the steps in the following mechanism of CO_2 gasification catalysed by calcium (Cazorla-Amorós et al., 1991):

$$Ca^{13}CO_3 \leftrightarrow CaO\text{-}C(O) + {}^{13}CO$$
$$CaO\text{-}C(O) \rightarrow CaO\text{-}C + {}^{12}CO$$

Analysis of calcium dispersed in coal by ion-exchange, using X-ray absorption fine structure spectroscopy techniques on samples heated up to 950°C, shows that, at low calcium loading, most of the calcium is present as highly dispersed, amorphous clusters of CaO. As calcium loading increased, the X-ray absorption spectrum was similar to that from bulk calcium oxide, indicating increases in its particle size (Cazorla-Amorós et al., 1991).

Studies of calcium catalysed steam gasification of coal using a micro-reactor produced data consistent with a mechanism in which CaO is the active component, while the reaction between $CaCO_3$ and C is the rate-determining step. Deactivation of the calcium catalyst is attributed to sintering of CaO, which diminishes the contact area between the catalyst and substrate, and the formation of calcium sulphide, which diminishes the amount of catalytically active calcium (Schwar et al., 1991).

Detailed temperature-programmed reaction studies of CO_2 gasification of coal with ion-exchanged calcium, and also calcium acetate mixed into the coal matrix, led to the conclusion that the active phase is $CaCO_3$, owing to the reversibility of the [$CaCO_3$-CaO] transformations which facilitates the reaction between CO_2 and carbon. The role of CaO particles is suggested to be that of transport of CO_2 to the [Ca-C] interface. Thus, larger CaO particles (or sintered particles) would cause a slower diffusion to the [Ca-C] interface, and shift the gasification to higher temperatures. The [Ca-C] contact is thus considered to be responsible for the catalytic activity. The proposed mechanism includes the following steps (Cazorla-Amorós et al., 1992):

$$CaO\text{-}C + CO_2 \leftrightarrow CaCO_3\text{-}C$$
$$CaCO_3\text{-}C \leftrightarrow CaO\text{-}{*}CO_2\text{-}C \leftrightarrow CaO\text{-}C(O) + CO$$
$$CaO\text{-}C(O) \rightarrow CaO\text{-}C + CO$$

The first step in these reactions is the carbonation of the Ca-carbon interface, while the sequence of steps in the second set of equations is the decomposition of the carbonate at the interface through an intermediate that

yields CO. The final step is considered to be the decomposition of an oxidised carbon and constitutes the rate-determining step of the process.

The effects of a 15% K_2CO_3 and 5% CaO_{ES} mixture (CaO_{ES} obtained from eggshells) on the gasification of Indonesian sub-bituminous coal with H_2O and CO_2 have been studied using TG and a fixed-bed reactor operating at atmospheric pressure. Data consisted of syngas compositions and char reactivity. At 800°C, the yield of H_2 is reported to be 123% higher compared to non-catalytic gasification, and 6% higher compared to the results obtained when only K_2CO_3 was used as a catalyst. The CO yield with the mixed catalysts is 19% higher compared to the results from only K_2CO_3 and 100% higher compared to the results without any catalyst. The increase in H_2 yield is equated with the water-shift reaction. The catalytic effect of the mixture (15%K + 5%CaO_{ES}) is estimated to increase the carbon conversion rate by more than three times within the temperature range 700°C-900°C and is reported to be due to a reduction of the activation energy of gasification by about 38% (Fan et al., 2016).

Studies have been reported of mixed inorganic compounds that form low melting point eutectics, with the additional goal of simultaneous sulphur capture. A wide range of combined catalysts have appeared in the scientific literature, such as salts of Ni/Fe, K/Ni, troca, nahcolite (minerals of sodium carbonate/bicarbonate), Na/Fe, Ca/Ni, Na/K as carbonates/chlorides/ sulphates, Mg/K, K/Fe, KCl/$CaSO_4$, K_2SO_4/$FeSO_4$, and many other combinations, including exotic ones such as La/Fe/Pt salts. Studies aimed at improving the activation of potassium catalysts by lowering the melting points of mixtures were carried out using KCl/$MgCl_2$ (MPt 488°C), KCl/NaCl (MPt 625°C) and KCl/NaCl/$MgCl_2$ (MPt 397°C). The results show that the onset of gasification could be lowered from 860°C for pure potassium chloride to about 770°C for the mixtures. The sequence of activity corresponds to the sequence of melting points, but the increase in catalytic activity is not significantly greater than that for pure KCl. Ion-exchange of potassium and magnesium (or calcium) salts in lignite caused a decrease in the temperature of catalytic activation (compared to the initial chlorides/sulphates) and a three-fold increase in catalytic activity compared to pure potassium carbonate, much greater than that shown by KCl. Using a mixture of potassium sulphate and iron sulphate resulted in catalytic activity for the production of CO and CH_4 that was comparable to that of K_2CO_3, but the temperature at which catalytic activity was observed was somewhat higher for the mixed catalyst (700°C-750°C). Gasification rates of coal char and graphite in CO_2 and steam increased on the addition of binary and ternary eutectic alkali salt catalysts. The enhanced catalytic activity is attributed to a reduction in melting points of the eutectic phases,

leading to a better dispersion of the salt phases on the carbonaceous substrates (Kline et al., 1990; Weldon et al., 1986; Hüttinger and Minges, 1986; McKee et al., 1985).

Studies of the gasification of high rank coal using a Li/Na/K salts eutectic mixture evenly distributed in the char resulted in the proposed reaction scheme shown below, which includes the formation of potassium sulphide (K_2S) and carbonates. K_2S may be present as a solid during and after gasification, and most of the Na^+ and Li^+ are carbonates during and after gasification, which may be due to a relatively higher molar fraction of Na_2CO_3 and Li_2CO_3 in the initial eutectic compositions of the mixture. The potassium salt acts as a desulphurising agent to form K_2S. K_2O has a tendency to react with the CO_2 and H_2S, to form K_2CO_3 and K_2S (Godavarty and Agarwal, 2000). The chemistry is summarised as:

$$K_2CO_3 + 2C \rightarrow 2K + 3CO$$
$$2K + CO_2 \rightarrow K_2O + CO$$
$$K_2O + CO_2 \rightarrow K_2CO_3$$
$$K_2O + H_2S \rightarrow K_2S + H_2O$$

The steam gasification of coal has been discussed for advanced steam gasification of a solid fuel (coal, biomass, organic residues, etc.) using a fluidised bed with simultaneous CO_2 capture (Corella et al., 2006). Effects of pressure on coal pyrolysis and char morphology, applied to coal gasification, have been discussed (Zeng and Fletcher, 2005). Catalysis in coal conversion processes at 500°C-750°C is touted as the next generation for a gasification process that would employ alkali metal salts supported on perovskite type oxides as the catalysts (Mochida and Sakanishi, 2000). Ca, K, Na and Fe moieties have also been discussed as catalysts for the gasification of US coals with various approaches to gasification of low- and high rank coals; however, sulphur may poison iron catalysts, while K, Na and Ca compounds are thought to be important catalysts for coal gasification in O_2, CO_2 and H_2O (Walker et al., 1983). A novel coal gasification technology has been suggested which combines catalytic combustion with coal gasification to produce H_2 and CO from coal, and also CO_2 for sequestration (Castaldi and Dooher, 2007).

Experimental results have been reported for coal gasification with and without the addition of calcium oxide and potassium hydroxide to coal, which serve as a catalyst for gasification between 700°C and 900°C. These studies considered the syngas composition, CO_2 and H_2S capture, and the steam-coal gasification kinetic rate. The syngas composition from the gasifier was roughly 20% methane, 70% hydrogen, and 10% other species,

with the CaO/C molar ratio at 0.5. The steam-coal gasification kinetic rates were enhanced when adding small amounts of potassium hydroxide to coal, and the gasification reactor was carried out in a $CaO/CaCO_3$ chemical looping mode. The steam-coal gasification kinetic rate is reported to increase by 250% when mixing dry calcium oxide with a sub-bituminous coal at a Ca/C molar ratio of 0.5; the kinetic rate increased by 1000% when making a slurry by mixing water, calcium oxide and coal at a Ca/C molar ratio of 0.5, and potassium hydroxide at a K/C molar ratio of 0.06. Multi-cycle studies were also carried out in which $CaCO_3$ was calcined by heating to 900°C to regenerate the CaO, which was then reused, thus repeating the $CaO/CaCO_3$ cycle. Increased steam-coal gasification kinetics rates were observed when adding CaO, and CaO+KOH, enabling reuse for six cycles of gasification and calcination; CO_2 capture with recycled CaO decreased by roughly 2-4% per cycle (Siefert et al., 2013).

The catalytic activity of graphite treated with calcium/nickel solutions on gasification was studied using controlled electron microscopy. The results show that calcium catalytic activity was reduced by nickel, possibly as a result of nickel hindering the supply of carbon to the calcium species. Nickel and copper mixtures were studied as catalysts for the steam gasification of graphite. The results indicated that the combined catalyst is more active over a wider temperature range than nickel. The data indicate that copper maintains the catalyst in a well-dispersed state and this prevented deactivation of nickel by sintering. The methane to hydrogen ratio was also significantly affected by the addition of copper, but the activation energy of the reaction remained unchanged compared to that for the nickel system (Baker and Chludzinski, 1985; Baker et al., 1985). Increased catalytic activity has been reported for a Na/Fe catalyst for the steam gasification of Yallourn coal. The catalyst was impregnated into the coal as sodium hydrotetracarbonyl ferrate, which was converted into Fe_3O_4 and Na_2CO_3 during the reaction. Reduction of the iron by chemistry involving sodium is believed to be responsible for the increased activity (Suzuki et al., 1985). Mixtures of potassium sulphate and iron sulphate have been studied as catalysts for water vapour gasification of carbon. A mixture of 1wt%:4wt% Fe:K (total metal 7 wt% of carbon) gave optimum catalytic activity, and an increase in pressure enhanced the total gasification rate with an increased methane yield (Adler and Hüttinger, 1984).

Catalysis with Iron and Nickel Compounds

The catalytic activity of transition metals in coal is of particular interest, especially that of iron salts added to low rank coal due to the relatively low

cost of iron salts. Comparative studies of nickel and iron as catalysts for the gasification of carbon with H_2O, CO_2, and H_2 indicated the activity of nickel was lower than that of iron with H_2O or CO_2. The reaction rate for nickel was greatest at about 550°C while for iron the temperature for high catalytic activity was about 900°C. At 727°C, with H_2O/H_2 ratios $>10^{-5}$, the nickel catalyst involved with the gaseous species would be NiO; reactions with carbon (char) indicate the catalyst would be metallic nickel with an amount of dissolved carbon. The mechanism postulated for nickel catalysed steam gasification is initial carbon dissolution at the Ni/C interface; carbon is postulated to diffuse through to the gas-nickel interface. The carbon reacts with oxygen from the water molecule to form CO and H_2. The kinetic behaviour occurs with a change in the activation energy at about 560°C, and is also thought to show a dependence on the particle size of the catalyst (Tamai et al., 1977).

Steam gasification of Yallourn brown coal treated with a soluble nickel salt, and gasified at 1.9 MPa, 500°C and 600°C, produced a methane concentration of 36% and 31% respectively (dry basis). The steam/coal ratio was 1 for these results. At higher steam/coal ratios, 600°C and 1.1 MPa, methane production fell and hydrogen production increased from 39% to 61%; for ratios of steam/coal at 1.2 and 5.0, methane was reduced from 23% to 5%, with CO_2 at 27% and 28% of the mixture, and CO at 11% and 6% respectively, with about 80% coal conversion at 600°C. The pyrolysis of the coal was strongly influenced by the catalyst, with little tar produced in the presence of the catalyst. High pressures increased the catalytic effect of the nickel; these samples contained 10wt% Ni loading to coal (db) (Takarada et al., 1987).

Steam/air gasification of Indian lignite has been reported to increase the yields of H_2 and methane at atmospheric pressure. A 4wt% Ni loading in coal, and gasification at 400°C, was reported to yield 22.7% methane and 9.3% hydrogen (with 38% N_2) on a dry basis. Increasing the Ni loading to 10wt% of coal caused an increase in hydrogen (from 9% to 26.6%) and a decrease in methane (from 40.6% to 2.1%). Ammonium washing achieved 29-89% Ni recovery from the char/ash residue (Srivastava et al., 1988). A low conversion of coal is anticipated at low temperatures.

Iron catalysis for coal gasification has been studied extensively and various mechanisms have been postulated. Two thermodynamic end-points for the iron catalyst are reported as Fe_2O_3-Fe_3C, but other states of iron, including the metallic state, have also been indicated. This work suggests the active catalyst is Fe iron in the metallic state operating *via* the carbide delivery system. Significant iron catalysed gasification is observed above 700°C, while it is thought the formation of stable iron-oxide surface

complexes occurs below 700°C. A mechanism has been proposed for water vapour iron catalysed gasification (here labelled as the "FeO scheme" for convenience) of polyvinylchloride cokes, based on the temperature-programmed desorption of carbon monoxide (Hermann and Hüttinger, 1986).

The Holstein and Boudart mechanism (here termed as the "FeC scheme" for convenience) has also been proposed for the iron catalysed carbon-steam reaction, summarised by the following equations (McCarthy, 1990):

$(Fe) + (C) \leftrightarrow (FeC) + ( )$

$(FeC) + H_2O \leftrightarrow (FeCO) + H_2$

$(FeCO) \leftrightarrow (Fe) + CO$

(Fe) – a reactive iron site
(FeC) – carbide-like species
(FeCO) – CO chemisorbed on an iron site
( )&(C) – active carbon site

'Poisoning' of the catalyst is postulated to occur by the reaction:

$(Fe) + H_2O \leftrightarrow (FeO) + H_2$ (FeO) – most stable iron-oxygen complex

The above equations provide a mechanism in which carbon reacts directly with iron rather than with an iron-oxygen complex. In this mechanism, the formation of H_2 and CO is proposed to result from reactions with (Fe) as the active site and a (FeC) moiety, while a reduction in catalytic activity may be associated with the formation of stable oxide complexes. The implications of this mechanism for practical gasification systems include poisoning, or the deactivation of the reactive iron centre through oxide formation by introducing oxygen to the system, as this would increase the formation of stable iron oxide complexes.

Experiments have been reported in which iron chloride and sulphate were found to be ineffective as catalysts, indicating that in these compounds the iron may be in a deactivated form. Iron added through ion-exchange with the coal was found to offer good catalytic activity for gasification with steam at 678°C. The bulk form of the catalyst during gasification was proposed to be Fe_3O_4 and its dispersion correlates with catalytic activity (Ohtsuka and Asami, 1991).

Additional mechanistic studies of iron catalysed gasification reactions have been reported, carried out to determine the activation energies and frequency factors of CO formation by desorption in N_2, and gasification in H_2/H_2O. The influence of water vapour partial pressure and metal dispersion in the char were investigated. Iron has been suggested to display an autocatalytic character because the catalyst is stabilised by the H_2 and CO

formed during gasification with water, while the transfer of oxygen from the iron to the carbon has higher activation energy than for water dissociation. Iron was reported to have greater catalytic activity compared to cobalt and nickel. However, the ability to disperse the catalyst, and its agglomeration within char, also influences the overall activity of the particular catalyst. Organically bound sulphur in coal was shown to inhibit the catalytic activity of iron at 0.3wt% sulphur in char. The inhibition of the iron catalyst by sulphur was decreased by lowering the water vapour content and increasing the hydrogen partial pressure (Hüttinger et al., 1986; Hermann and Hüttinger, 1986).

These observations show an eclectic activity on catalysis with inorganics which display varying catalytic effects, and are added to coal in a variety of methods. Clarity is required in developing detailed mechanistic studies that address the entire process, from the addition of well-characterised inorganic species to the coal, to the events occurring during pyrolysis, and ultimately to the chemistry of the formation of active centres for catalytic activity and specifically to steam gasification; these matters are discussed in the following section.

While numerous inorganic species have been tested as catalysts, iron compounds added to low rank coals are especially interesting for commercial applications, and laboratory results show iron species in these coals may display very effective catalysis. The hydrophilic nature of low rank coals enables aqua-chemistry to be used to produce chemically bonded metal complexes to oxygen functional groups in the coal molecular matrix. Processing low rank coals to produce fuel for catalytic steam gasification offers opportunities for the production of high quality syngas. This opportunity can become a practical proposition when all molecular-based events for catalytic coal gasification are understood, and can then be applied on an industrial scale.

The observed catalytic activity of added inorganic(s) is linked with the properties of char as it is formed on heating the coal; the properties of char that impact on catalytic gasification include: particle size, porosity, and the abundance of accessible catalytic sites.

The elucidation of the chemical interaction(s) of inorganic complexes in the coal, and the mechanism(s) of subsequent char transformations leading to the formation of catalytic sites that are accessible to gasifying molecules, is challenging for the following reasons:

- Adding inorganic species to coal that form catalytic sites requires specific details of the chemistry between the aqua-inorganic complex and coal functional groups.

- Non-uniform composition of the char surface results in variations in catalytic sites.
- The surface coverage with adsorbed steam molecules can vary because of the differing morphology of the char, which is related to the type of coal and pyrolysis conditions.
- Methods for identifying reactive sites for catalysis *in situ* at the temperature and pressure found in industrial gasification plants are unavailable.
- Coal particles undergo many reactions and transformations as they are heated to form char, and there is a paucity of experimental data that are directly related to any of the specific mechanisms for char formation with the transformations of the inorganic complexes into catalytic species.
- Relevant molecular modelling is very complicated; it requires reaction routes during coal pyrolysis, thermolytic chemistry of inorganic complexes in coal, and reactions specific to catalytic steam gasification.
- Molecular reaction sequences may be modelled as discrete, but the more complicated concerted mechanisms appear more realistic, involving the breaking of [C-H] and [O-H] bonds, formation of [M-C] and [M-H] bonds, with insertion of O to form [M-O-C] bonds.
- Various events/reactions in an industrial plant may involve further unknown or unexpected structure transformations of the char, which may impact on the accessibility of steam to the catalytic species/sites.

Due to the complexity of the coal chemistry and the difficulties inherent in dealing with such a heterogeneous substance, it is necessary to adopt a fairly rigorous methodology, and to perform experiments on a well-characterised coal sample with well-defined conditions (discussed in Chapters Two and Three) to obtain results that are attributed to the catalyst, and to relate these to results from molecular modelling. Thus, data are sought for the weight loss of each sample of treated coal that is attributed to the catalytic activity. The required methodology would detect this weight loss by making measurements starting from the commencement of pyrolysis, at 200°C, and the temperature is increased by given amounts (such as in 100 degree steps) up to 1000°C, under an inert atmosphere (N_2 or He, for pyrolysis) and also under an atmosphere of the same inert gas containing the gasification agent, steam. The conditions used in the experiments must be the same in terms of the gaseous flow rate and the relatively short time (e.g. ≤15 min) for heating each sample. This approach enables a direct comparison of the weight loss from pyrolysis and that from

steam gasification. As a result, if greater weight loss were observed for any sample when heated under He/steam, this would be directly attributed to reactions with steam. Char samples need to be obtained in an inert gas for analysis, after they are heated to a specific temperature for a given time. At the same time, the gases exiting the reactor are analysed, and the yields of H_2, CO, CH_4 and CO_2 are then compared with the observed coal/char weight losses, to obtain a reasonable mass balance. The experimental data should also be incorporated within molecular modelling to obtain a detailed mechanism of the pyrolysis and steam gasification of low rank coals catalysed by the inorganic (in the present discussion, this is iron complexes). In this way, the proposed mechanism can be postulated based on experimental data, semi-empirical quantum mechanics molecular modelling, and, where practical, *ab initio* DFT computational molecular modelling.

An outline has been presented in previous chapters of experimental data, calculations of solution species, and molecular modelling utilised to clarify the nature of iron complexes added to the coal – further work addressed the transformations of iron species during early pyrolysis chemistry, and identified the active sites that could be involved in catalytic reactions with H_2O molecules as the temperature increases. It is noteworthy that this detailed mechanistic scheme appears to answer the questions posed by the early mechanistic proposals which have been termed here for convenience as the FeO scheme and the FeC scheme. Metal mediated chemistry, discussed previously, identified the iron catalytic site for reaction with steam as [Fe-C], suggestive of the FeC scheme, and experimental and modelling data (to be discussed below) also show [Fe-O] moieties are involved in reactions with H_2O, suggestive of the FeO scheme.

Catalytic Efficacy of Brown Coal with Iron Species

Experimental and molecular modelling results give a measure of the efficacy of the catalysis observed for the treated coal containing poly-nuclear iron hydroxyl compounds chemically bound to oxygen functional groups in the coal matrix.

On heating the low rank coal containing added iron species, transformations occur, with significant changes beginning at 300°C-500°C, and the formation of small iron clusters and the [Fe-C] site beginning at about 600°C, indicating catalytic steam gasification is likely above this temperature. The accessibility of the active site [Fe-C] to H_2O molecules, and the chemi-adsorption of H_2O to a metal centre, would be accentuated by increased char porosity. Experimental data show that pore formation and an increase in char surface area occurs when low rank coal containing

inorganics is pyrolysed in an atmosphere of steam; char porosity is also increased by the presence of any larger sized iron species, even though these may not participate directly themselves in catalytic reactions of steam with char.

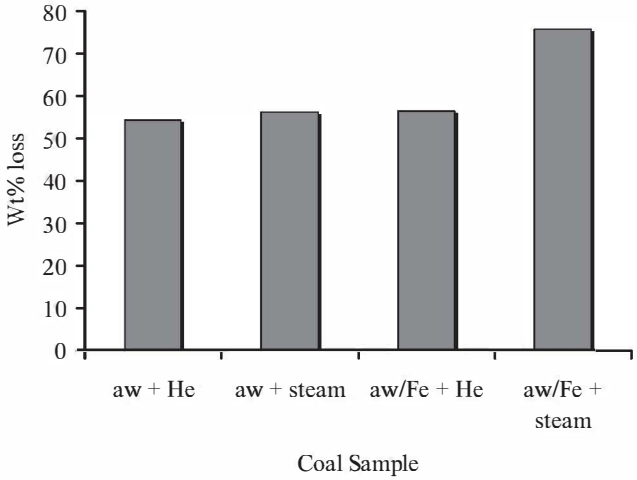

Figure 8-1. Weight loss of coal samples (daf, 900°C, after 15 min). Reprinted with permission from Domazetis et al., Applied Catalysis A: General, 340, 105-118, 2008. Copyright (2008). Elsevier.

Experimental determination of weight losses for aw coal, and the same aw coal containing iron species, is typically illustrated in Figure 8-1; these results were obtained by heating the samples at a temperature of 900°C for 15 minutes, under inert and reactive atmospheres. The weight losses for aw brown coal and brown coal containing iron, under identical conditions, are comparable up to 600°C, but the weight loss with steam for coal with iron then increases with temperature. At 900°C under steam, the weight loss for coal with 7.8wt% Fe is: 76wt% after 15 min, 84wt% after 60 min, and 100wt% after 100 min (daf). Results for the same coal with >10wt% Fe under the same conditions show almost complete char weight loss due to reaction with steam in under 15 minutes.

These results for coal containing aqua-iron species show a significantly greater weight loss over a shorter time when compared to data reported by Yamashita et al., (1991) of the weight losses for gasification of Yallourn brown coal with added Fe catalysts; these reported a weight loss of 40-60wt% of the brown coal in 30 min, and 60-80wt% after 90 min. The coal samples for

these were prepared by soaking them in a solution of iron nitrate and then drying the treated coal. The authors point out that highly dispersed iron species might be the active species. The change(s) of iron species in coal during steam gasification were studied with Mössbauer and extended X-ray absorption fine structure spectroscopy. The chemical forms of highly dispersed iron species that may be responsible for catalytic activity are stated to be FeOOH; the transformation(s) of the iron in coal is illustrated in Figure 8-2.

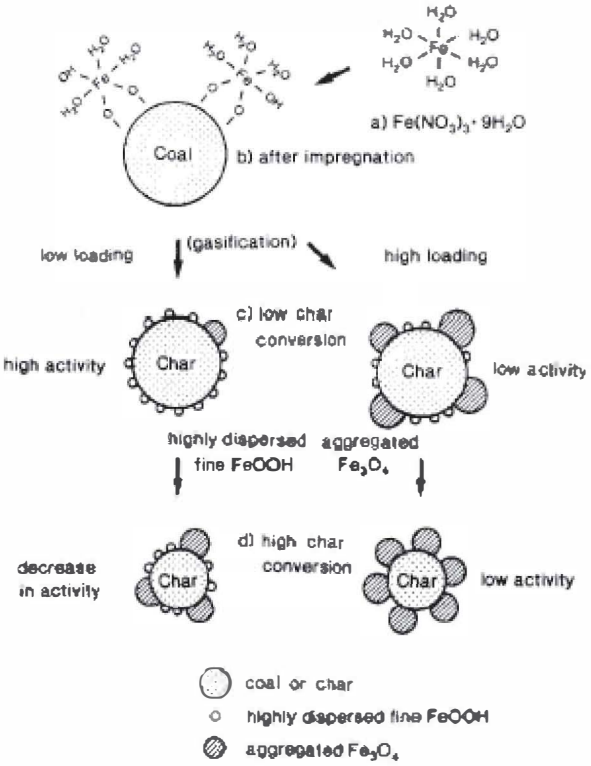

Figure 8-2. Illustration of the proposed transformations of iron species in brown coal during steam gasification. Reprinted with permission from Yamashita et al., Energy Fuel, 5, 52, 1991. Copyright (1991). American Chemical Society.

The higher conversion rate reported by Domazetis et al., (2012) for the samples of brown coal containing aqua-hydroxyl iron complexes is attributed to the method used to add the aqua-iron complexes to the brown coal and the subsequent formation of iron clusters in char. The weight losses

obtained for a number of brown coal samples with increasingly higher Fe, where each sample was subjected to the same conditions, is shown in Figure 8-3. The data clearly show virtually all of the coal with 7wt%-12wt% Fe is consumed at 900°C, over a 15-minute period, by reaction with steam. The weight losses and gaseous composition for aw coal samples, and coal samples with 2-4wt% Fe, indicate undetectable reactions for aw coal, and low to negligible reactions with steam for coal with 2-4wt% Fe over the same period.

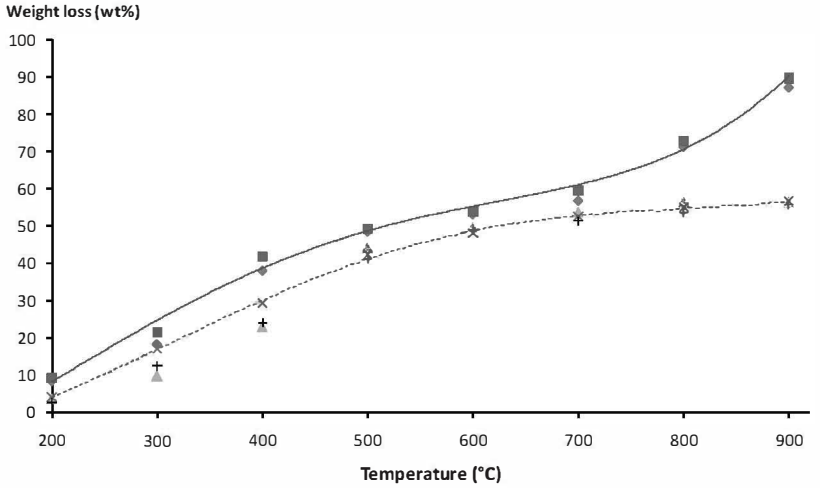

Figure 8-3. Weight losses (daf) from coal samples heated in steam for 15 min. — catalytic (♦7.8wt% Fe, ■12.4wt% Fe); --- non-catalytic (▲aw, x 1.7wt% Fe, + 4.4wt% Fe). Reprinted with permission from Domazetis et al., Fuel 93, 404-414, 2012, Copyright (2012). Elsevier.

The TOF value is the measure of catalytic efficacy; the results discussed for brown coal may be used to obtain an apparent turn-over number for catalytic activity (ATON). The data displayed in Figure 8-3 have been utilised to calculate an ATON by assuming catalytic activity is attributed to the total added iron; i.e., the ATON is the additional amount of char consumed under steam, as moles of carbon, per the total moles of iron in the original coal sample. Although this assumption is necessary, catalytic sites have been shown to be associated with small iron clusters, and these are formed from a portion of the iron species. It is also assumed for these calculations that, at low temperatures, both aw coal and coal containing iron underwent somewhat similar weight losses attributed to pyrolysis. The

additional weight loss observed under steam at higher temperatures is thus due to catalytic steam gasification of the char. Based on these assumptions, the ATON for brown coal containing 7.8wt% Fe is between 12 and 26 moleC/moleFe (i.e., each iron centre catalyses reactions between steam and 12-26 carbon atoms). For these experiments, an apparent turn-over frequency (ATOF), defined as the ATON per min, varies at: 0.8 (15 min), 0.3 (60 min), and 0.2 (100 min) moleC/moleFe per min. While it is difficult to directly compare these ATOF values with data reported for various other catalytic coal-steam systems, it is interesting to note that computational modelling of potassium clusters and the reaction of a carbon source with 21 Torr H_2O (~$27x10^{-3}$ atm) at 700°C have been used to propose a TOF for the phenoxide [(Ph)C-O-K] of 0.15 per sec, whereas the TOF value was 7.8 per sec for KOH particles or clusters – an ATON is not available for these computations.

TG and DTG studies of brown coal samples containing iron hydroxyl species (7.8wt% Fe) heated under helium gave weight losses at 223°C, 322°C and 402°C, and a sharp, distinct weight loss at 696°C. The observed molar weight loss at 696°C was equivalent to the amount of CO_2 lost from an iron carbonate species. The acid-washed coal sample underwent weight losses centred at 320°C and 410°C, and no distinct weight loss was observed at ~700°C. A larger proportion of CO_2 was observed compared to CO for the coal containing iron species, consistent with additional CO_2 from decomposition of an iron carbonate species.

Table 8-1. Gases from iron catalysed brown coal steam gasification at 700°C (as mole% ± 10%).

Aw Coal	H_2	CO_2	CO	CH_4	Total
+ 1.7wt% Fe	ND	2.4	1.2	0.6	4.2
+ 4.4wt% Fe	ND	3.9	1.6	0.7	6.2
+ 7.8wt% Fe	14.7	18.9	3.7	1.4	38.7
+ 12.4wt% Fe	14.6	21.5	2.7	1.1	39.9
Gases from catalytic coal gasification at 900°C					
+ 12.4wt% Fe	54	30	18	~0.8	100

The reactions between the char and steam for the samples that contained 7.8wt% and 12.4wt% Fe yielded H_2, CO, CO_2 and CH_4. The %mole composition of each gas measured at 700°C is shown in Table 8-1, and results obtained at 900°C are also displayed (ND = not detected; the remaining proportion is carrier gas, error at ±10% of the measured value). The gas samples from the coals with 12.4wt% Fe contained between

52mol% and 55mol% (average 54.5mol%) of H_2 at 900°C (Domazetis et al., 2008; 2012).

The amounts of product gases from the coal sample containing 12.4wt% Fe, heated under steam at 900°C over a 15-minute period, were used to obtain a mass balance, and this shows the yields of H_2 were greater than the theoretical values calculated for the mass of char consumed by steam. An account for these experimental data can be made by adding the products from post-gasification chemistry between CO and H_2O to yield additional H_2 and CO_2. This is done by: (1) calculating the moles of H_2, CO and CO_2 attributed to the weight loss from the coal pyrolysis, and the moles of H_2 and CO from the reaction between char with steam at 900°C; i.e. $C + H_2O \rightarrow H_2 + CO$; and (2) adding 50-60mol% of the CO to undergo the post-gasification reaction with steam ($CO + H_2O \rightarrow H_2 + CO_2$). The results from these calculations compare favourably with the experimentally measured values, i.e.:

Experimental ratios for H_2 to CO, and CO_2 to CO = 3.6 H_2:CO; 2.1 CO_2:CO, (<0.1 CH_4:CO).

Calculated ratios for 50-60mol% of CO reacting with steam = 3.1-4.2 H_2:CO; 1.5-2.1 CO_2: CO.

The results from XPS analyses of the coal sample containing 7.8wt% Fe, after heating in steam at 900°C, are shown in Figure 8-4 and Figure 8-5; these show a greater proportion of inorganic and organic oxygen in the char obtained when the coal was heated with steam, compared to the same sample heated under helium. The inorganic at% [O] associated with iron after catalytic steam gasification also increased markedly, as shown in Figure 8-5. The data show that oxygen from H_2O was transferred to the iron cluster, forming the [Fe…O] moiety. There is also an increase in organic oxygen groups [O-C] in the char samples heated in steam; the analyses also show that char provided a decrease in the proportion of [C(C-H)] groups. The observed increases in oxygen were due to oxygen from steam forming [Fe-O] groups with the iron catalytic species, and also to the formation of [C-O] groups in the char molecule, due to the catalysed reaction(s) with H_2O.

The XPS data show that:

- Under steam, the ratios of total organic oxygen to total carbon (O:C) were 0.23:1 at 400°C and 0.16:1 at 900°C for coal containing 7.8wt% Fe, which are three times larger than those obtained after pyrolysis of the same coal sample treated in an inert atmosphere at the same temperature and time.
- The proportion of carbon groups covalently bound to oxygen also increased (i.e. C-O, C=O, O-C=O) compared with the carbon groups

bound to carbon and hydrogen (C/C-H); at 900°C and after 15 min, the at% C ratio [C/C-H:C(O)] was 1:2 after catalytic steam gasification, compared to a ratio of 1:0.6 after pyrolysis in helium.

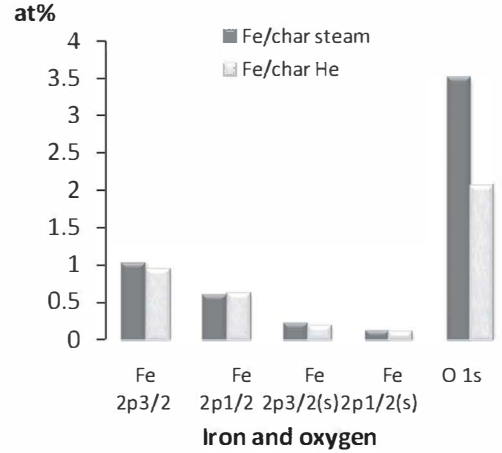

Figure 8-4. XPS data of char samples with Fe after catalytic reaction with steam at 900°C, showing the increase in inorganic oxygen bound to iron obtained from reaction with steam. Reprinted with permission from Domazetis et al., Fuel 93, 404-414, 2012, Copyright (2012). Elsevier.

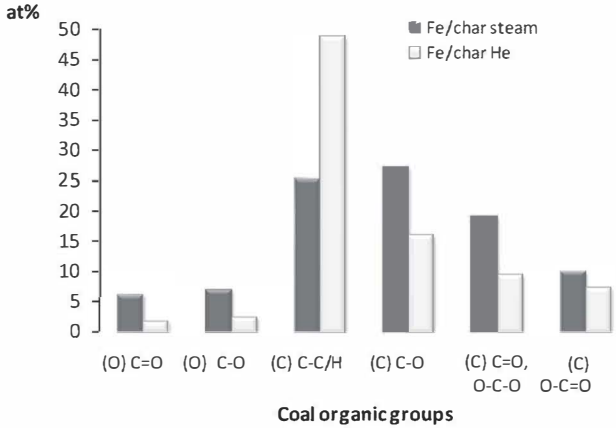

Figure 8-5. XPS data of char samples after catalytic reaction with steam heated at 900°C, showing increased oxygen in char organic groups. Reprinted with permission from Domazetis et al., Fuel 93, 404-414, 2012, Copyright (2012). Elsevier.

The char samples were cooled under helium before being weighed after each experiment; samples from pyrolysis and steam gasification were treated in the same way. The increase in oxygen in char samples, therefore, was derived from steam during gasification, and is consistent with the mechanism for catalytic steam gasification, which includes the insertion of oxygen into the [Fe-C] bonds to form [Fe-O-C] bonds.

The modelling studies of catalytic gasification of iron in char show H_2O would be adsorbed onto the active iron sites *via* the oxygen atom to form the [Fe←--OH_2] coordination bond, followed by H abstraction from H_2O to yield an iron hydride complex, and an additional [H-O-C] functional group, which adds organically bound oxygen to the organic char matrix.

Mechanism of Pyrolysis with the Formation of Active Sites

The experimental results for catalytic steam gasification of brown coal containing aqua-iron species show that catalytic reactions involving steam commence at about 600°C. It is reasonable, therefore, to model mechanisms of pyrolysis of these coals below this temperature, as precursors to the formation of iron active sites for reactions with steam. The previous discussions on molecular modelling, and of the various events during coal pyrolysis, show the complexity of these phenomena, and the numerous reaction routes that need to be considered for detailed studies of the mechanisms. Here, summaries are given of typical molecular modelling of pyrolysis, relevant to the formation of active sites and yielding H_2 and CO, to illustrate the type of computations undertaken in such studies – details of the treatments are found in publications by Domazetis et al.*

Initially, pyrolysis of brown coal containing iron-hydroxyl moieties chemically bonded to carboxyl groups undergoes reactions that ultimately form iron clusters in char. Molecular modelling results provide the various energies for pathways leading to char formation and the [Fe-C] active site, with the yield of H_2 (shown in Figure 8-6). The steps in the formation of H_2 and the [Fe-C] active site will be discussed with an example of SE-PM5 modelling of these reactions for the [Fe_3] cluster; this commences with the [Fe_3] cluster forming the [Fe←--OH] coordination bonds with char hydroxyl groups, as shown in Figure 8-7 (a), followed by hydrogen atom abstraction from one OH group to form [Fe-O] and [Fe-H] (labelled {$CharFe_3$ (1)} in Figure 8-6). A second hydrogen atom is abstracted to form additional [Fe-O] and [Fe-H] groups; this structure is shown in Figure 8-7 (b) (labelled {$CharFe_3$ (2)} in Figure 8-6); the lower energy configuration of this molecular

* Modified with permission from Domazetis et al., Fuel 93, 404-414, (2012), Copyright (2012). Elsevier.

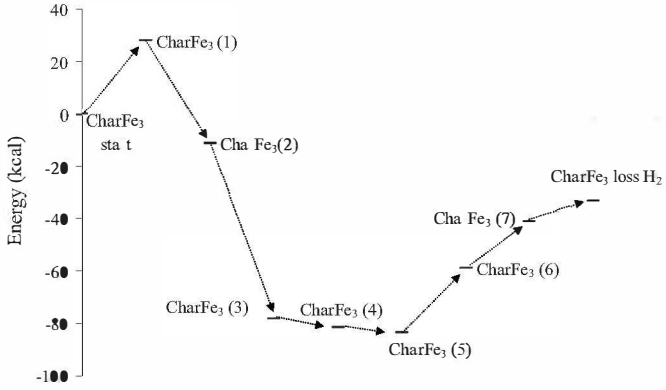

Figure 8-6. Molecular modelling data for H_2 formation during pyrolysis of [Char(Fe_3)]. Reprinted with permission from Domazetis et al., Applied Catalysis A: General, 340, 105-118, 2008.

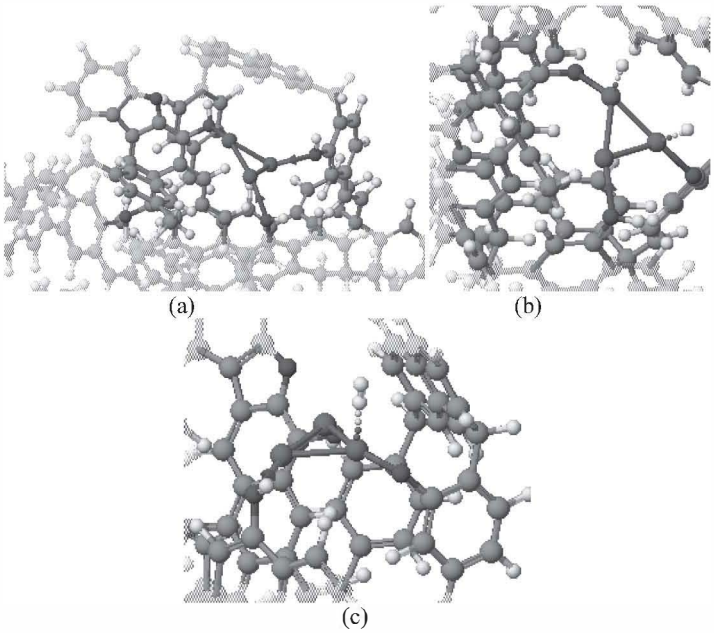

Figure 8-7. Molecular structures for the formation of H_2 during pyrolysis. (a) [Fe←OH] coordination bonds; (b) second hydrogen abstracted to form [Fe-O] and [Fe-H bonds]; (c) H_2 bound end-on to Fe centre. (Fe = ●purple, O = ●red, H = ○white, C = ●grey). Reprinted with permission from Domazetis et al., Applied Catalysis A: General, 340, 105-118, 2008. Copyright (2008). Elsevier.

structure positions the [Fe-H] groups to form a di-hydrogen group in parallel to the iron cluster (labelled {CharFe3. (3)}, {CharFe3. (4)}, and {CharFe3. (5)} in Figure 8-6). The H2. is then bound end-on to one Fe atom in the structure (labelled {CharFe3. (6)} in Figure 8-7 (c)), and the H2. dissociates from the Fe3. cluster (labelled {CharFe3. (7)}) and desorbs from the char molecule.

The formation of H2. during pyrolysis may also include the abstraction of H from [C-H] groups in the proximity of the iron cluster, directly creating the [Fe-C] site.

A rigorous SE-PM5 treatment of this chemistry would require concerted reaction mechanisms, including mapping of the reaction trajectory, and the identification of a specific intermediate for each of the various char molecular models; such a detailed treatment is beyond our present computational capabilities for these large molecules.

SE-PM5 results are also provided for the char model with [Fe_mO] clusters (m = 3 or 5). The computations with the {Char[Fe_3O]} model for the formation of H_2 and CO may typically be carried out as discrete steps for the formation of H_2, and then CO, or they may be carried out to illustrate possible concerted reaction schemes. The computations for the discrete reaction route to yield H_2 provide a near thermo-neutral result, with the largest energy barrier being +20 kcal/mol for the entire reaction sequence. This is followed by the discrete reaction sequence yielding CO, which provided an energy change of +66 kcal/mol. The results for the same reaction sequence modelled as a typical concerted chemistry yielding CO gave a lower energy change of +32 kcal/mol, and a near thermo-neutral overall result. While these SE molecular modellings are not a comprehensive examination of all possible reaction mechanisms, they indicate that the likely chemistry is of the concerted type. A reasonable approximation of the concerted chemical reaction route of pyrolysis yielding H_2 and CO is illustrated in Figure 8-8. The numbers in Figure 8-8 designate the events in the reaction sequence; hydride structures are designated by (..H2), while chemisorbed and molecular hydrogen is designated by (H_2).

This reaction sequence commences with the abstraction of H from the char [OH] groups coordinated to the iron cluster [Fe_3O], i.e. labelled {CharFe3O(..HO)2}, and leads to the iron (hydride)(carbonyl) intermediate labelled {CharFe3O(..H2)(CO)3}; the iron hydride intermediate labelled {CharFe3O(...H2)(CO)3} in Figure 8-8 is shown in Figure 8-9 (a). Figure 8-9 (b) shows the molecule of H_2 adsorbed to the iron (carbonyl) intermediate. Relatively small energy changes are observed for the formation of the iron hydride. The H_2 molecule remains chemisorbed onto the [Char-Fe_3O] structure. Two iron carbonyl species can be examined prior to the loss of

CO, and these are labelled (11) and (11a) in Figure 8-8; species (11) contains CO bonded in parallel to the iron, and species (11a) contains the CO bonded 'end-on' to the iron-CO. These results indicate that, at high temperatures, CO could be formed by the loss of CO from species (11). The results also indicate that the formation of iron-carbonyl compounds is energetically favoured from species (11); an overall endothermic result of about +50 kcal/mol is observed for the approximation of concerted formations of H_2 and CO.

DFT calculations for H_2 and CO formation during coal pyrolysis are consistent with these reaction routes; energy changes are obtained for: (1) the formation of H_2 by H abstraction from [O-H] and [C-H] groups to form {Char[(C-O)-Fe_3(-C)]} species, (2) cleavage of two [OH] groups to form {Char[-O-C)$_2$(Fe_3)]}, and (3) the elimination of CO from an [Fe-O-C-C] group to form the [Fe-C] reaction centre, which is an active site that would participate in catalytic reaction with a water molecule in steam gasification. DFT geometry optimisations of structures involving {Char(Fe_3O)} and hydrogen abstraction, followed by the loss of H_2 and CO, gave similar results to those obtained with the SE-PM5 modelling.

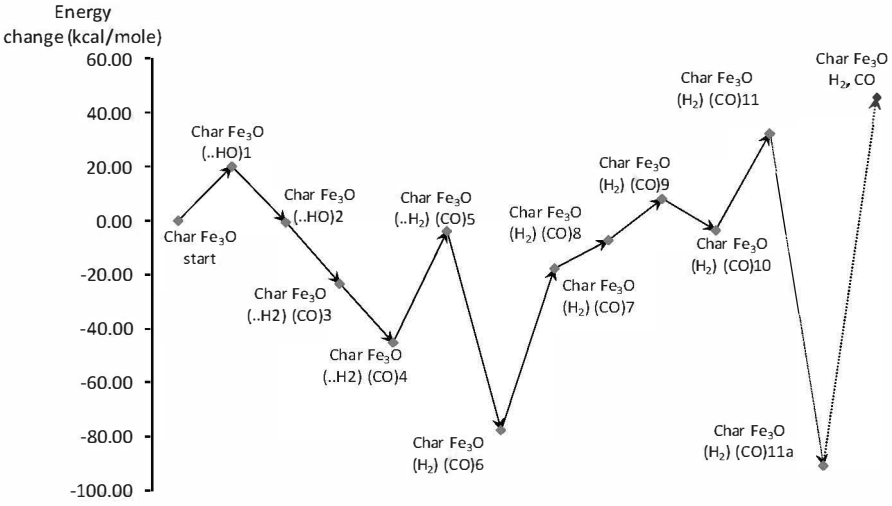

Figure 8-8. Pyrolysis reaction route to model concerted chemistry for Fe_3O and the yield of H_2 and CO. Reprinted with permission from Domazetis et al., Fuel 93, 404-414, 2012. Copyright (2012). Elsevier.

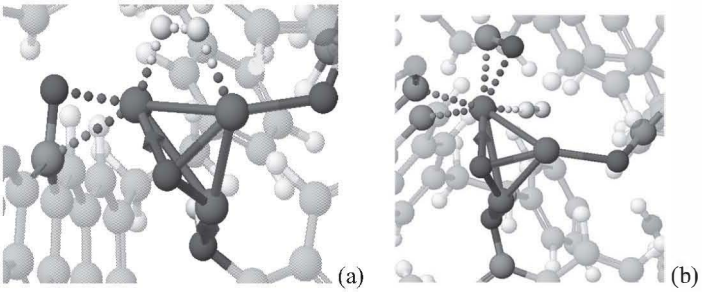

Figure 8-9. (a) Iron (hydride) intermediate, and (b) iron (carbonyl) intermediate prior to loss of H_2 (H = ○white, O = ●red, C = ●grey, Fe = ●purple). Reprinted with permission from Domazetis et al., Fuel 93, 404-414, 2012. Copyright (2012). Elsevier.

Mechanism of Catalytic Steam Gasification

SE-PM5 and DFT molecular modelling of the mechanism for catalytic steam gasification using the model {Char[Fe_3]} may commence with chemisorption of H_2O on either the [Fe-O] or the [Fe-C] site, to form a coordination bond between the oxygen of the water molecule and either of the iron sites [H_2O-->Fe], as illustrated in Figures 8-10 (a) and (b). The subsequent reaction routes include H abstraction from H_2O to form the iron hydride, and this ultimately yields H_2. The reaction routes leading to CO formation included the insertion of oxygen from H_2O into the [Fe-C-C] group to form [Fe-O-C-C]; CO is eliminated and another [Fe-C] site is formed. Additional reaction routes may be contemplated in char containing various iron oxide clusters, such as [Fe_3O], [Fe_3O_2], [Fe_5O_2] and also [Fe_3], [Fe_4] and [Fe_5]. The final step in these reaction routes is the elimination of H_2 and CO as gases; these may be modelled to occur separately, or concurrently.

The experimental data show catalytic activity is observed when brown coal contains a substantial amount of iron species and negligible (or below detection limits) catalytic activity for coal containing small amounts of iron species; this indicates catalytic activity is related to the amounts of iron species added to coal, and the subsequent number of active sites that may form in the char. An estimate of the number of [Fe-C] active sites (and also [Fe-O-C-C] sites) that may form in char would depend on the type of iron clusters, and also on the number of these clusters present in the char. If 7wt%-10wt% of iron complexes were added to the coal, and all of the iron complex in the char were assumed to form only [Fe_3] clusters, the char molecular model would contain two clusters per char molecular model, with

a total of 2-4 active iron sites; based on the experimental data, a TON of 26 is likely, and from this, it may be estimated that these iron sites would undergo reactions with 52-104 carbon atoms and corresponding H_2O molecules per active site. If the iron were present as larger clusters (e.g. [Fe_5]), then a different number of active sites may be available for H_2O chemisorption and reaction to yield H_2 and CO. We have previously seen that iron species added to brown coal using the method of pH adjustment would be distributed as a number of poly-nuclear iron complexes, and more than 60% of the total iron in the coal would form small iron clusters in char. Experimental data discussed previously indicate a similar TON to the estimates made from molecular modelling.

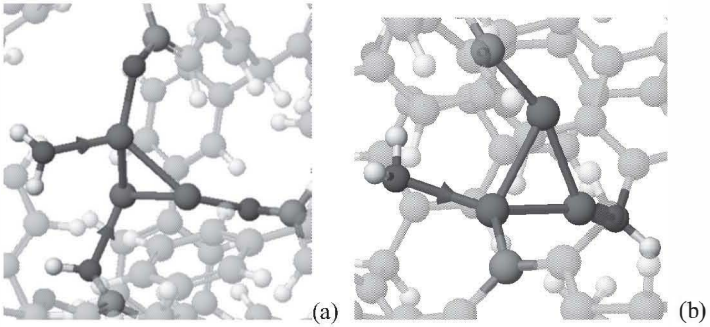

Figure 8-10. (a) Coordination of H_2O to [Fe-O], (b) Coordination of H_2O to [Fe-C] H = ○white, O = ●red, C = ●grey, Fe = ●purple). Reprinted with permission from Domazetis et al., Fuel 93, 404-414, 2012. Copyright (2012) Elsevier.

Computational modelling has indicated that chemisorption of H_2O onto the reactive site of the iron centre in {Char[Fe_3]} is energetically favoured by between -12 kcal/mol and -30 kcal/mol per H_2O molecule. Molecular modelling of chemisorption on sterically hindered iron sites also shows these sites are not as energetically favoured and may not behave as active sites, again indicating accessibility to active sites in char is a significant factor.

The chemisorbed water molecule forms a coordination bond to an iron centre of the [Fe_3] clusters containing either of the groups [Fe-O] or [Fe-C], as shown in Figure 8-10 (a) and (b). The ionic attraction between the [$Fe^{\delta+}$(-C)] group and [$O^{\delta-}$(-H_2)] is shown by modelling to favour the formation of the [(Fe_2)(C-Fe←-OH_2)] coordination bond. An SE-PM5 optimised {Char[Fe_2(Fe←-OH_2)]} molecular structure contains a distorted octahedral Fe centre (with a coordinated H_2O ligand), with one Fe…Fe distance in the

cluster of 0.31 nm (3.1Å), and the other two Fe centres forming distorted tetrahedral structures. From this, reaction routes that would yield H_2 include H abstraction from the coordinated H_2O, leading to the intermediate structure containing an H atom situated between the two Fe centres; the Fe-H bond lengths in this structure are 0.18 nm (1.8Å) and 0.16 nm (1.6Å). The reaction sequence that yields CO would be the insertion of O (from H_2O) into the [Fe-C] group to form [Fe-O-C-], followed by the elimination of CO and formation of another [Fe-C] group, establishing the catalytic cycle.

1scf-DFT calculated energy changes for a discrete reaction scheme, with H_2O forming a coordination bond to the Fe centre of the {Char[Fe_3]} molecular model, provide a maximum energy change of +92 kcal/mol (*cf.* 1scf-SE result of +84 kcal/mol) to yield H_2, indicating a relatively large energy barrier. The subsequent discrete reaction sequence yielding CO from this molecule gave a further overall energy change of about +130 kcal/mol. These energy changes are greater than those obtained for concerted reaction routes. It must be emphasised that rigorous molecular modelling of reaction schemes of concerted chemistry for catalytic steam gasification is extremely difficult, because the size of the char molecule makes it impossible to carry out the highest level *ab initio* computations. Concerted mechanisms have been discussed for numerous reactions; for example, a concerted metalation-deprotonation mechanism is discussed for palladium-catalysed direct arylation for a range of aromatic substrates (Gorelsky et al., 2008). Various molecular-level aspects of classical supported metal catalyst preparations and molecular-level characterisations have been reviewed (Lambert and Che, 2000). The determination of the active site for heterogeneous catalysis is a challenge, and often several possible active sites may compete for reactions on the surface of the particular solid catalyst.

Molecular modelling of the {Char/Fe/H_2O} system has been used to examine a number of reaction routes, including ones which contain major features of concerted chemistry. The SE data obtained for a scheme that mimics concerted chemistry, in that simultaneous loss of H_2 and CO occurred from a reaction with H_2O, show the largest energy change for the particular reaction sequence was +110 kcal/mol. The formation of the hydride [Fe..H] intermediate leading to the formation of H_2 was energetically favoured, as was the insertion of O into [Fe-C] to form [Fe-O-C]; an energy change of +78 kcal/mol was observed for the elimination of CO from [Fe-O-C] to yield CO and a new [Fe-C] group.

A scheme that mimics concerted chemistry in which the loss of CO occurs from an iron hydride intermediate, instead of a simultaneous loss of both CO and H_2, gave a more favourable energetic change, and the results for this reaction scheme are shown in Figure 8-11. This reaction sequence

includes the insertion of [O] from H_2O, into an [Fe-C] to give the [Fe-O-C] group, followed by the formation of the {Char[Fe_3]…(CO)} structure in which CO is chemisorbed onto Fe. Ultimately the loss of CO is accompanied with a new [Fe-C] group to continue the catalytic cycle. The largest energy change for this sequence is +55 kcal/mol, and the overall reaction is almost thermo-neutral, due to the favourable energy change accompanying the formation of the iron hydride intermediate {Char [Fe_3…H]} during the loss of CO.

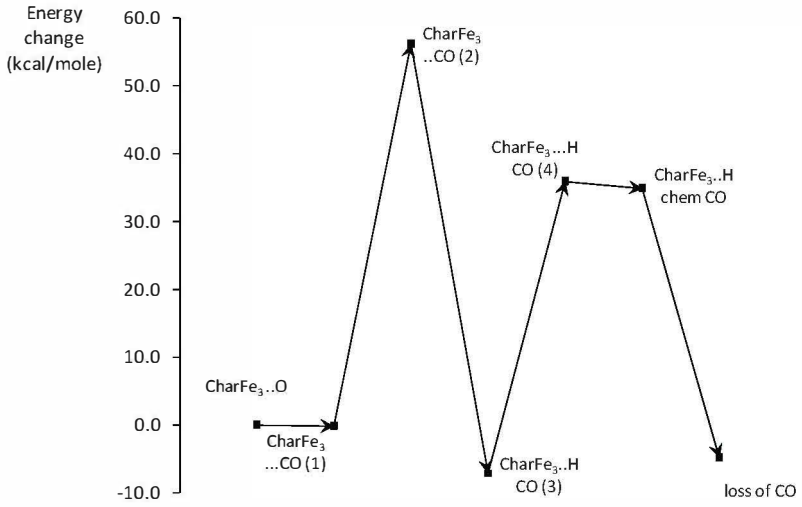

Figure 8-11. Reaction of steam involving iron hydride in CO formation and loss (after H_2 yield). Reprinted with permission from Domazetis et al., Applied Catalysis A: General, 340, 105-118, 2008. Copyright (2008). Elsevier.

A number of additional reaction schemes may be examined that mimic various concerted reaction routes, including the formation of an iron-hydride by the abstraction of [H] from a -CH_3 group in char during steam gasification. This scheme forms H_2 by abstracting [H] from char and [H] from the H_2O molecule, with [O] inserted into the resulting [Fe-C] group to yield CO. This reaction sequence yields H_2 and CO with an overall energy change of +89 kcal/mol.

Additional molecular modelling that examined reaction routes for the formation of CO and H_2, using char molecules that contained iron clusters at different positions (and thus different configurations), gave results

indicating that reaction routes that mimic concerted chemistry, with the formation of iron hydride and carbonyl intermediates, provide pathways with lower energy changes. Generally, this molecular modelling yielding H_2 and CO from catalysed reactions with H_2O provided overall energy changes of between +40 and +90 kcal/mol.

Transition States for Iron Clusters and Water Molecules

Studies of chemical reaction mechanisms include the identification of transition states (TS); for H_2 formation from the reaction of H_2O with iron clusters, the TS may be either (1) the linear [Fe…O-H-H] structure, or (2) the iron hydride [Fe..H-H(O)] structure. A rigorous examination of char models cannot be carried out for either of these intermediates, nor an examination of possible TS for the proposed mechanism to yield H_2 using the molecular model [Char(Fe_m)] and H_2O. Instead, computations of TS can be carried out on the iron clusters with H_2O, to ascertain which of the two possible TS is likely. Conventional calculations can then be performed to obtain the relative energies for reaction sequences using models of [Char(Fe_3)(H_2O] to ascertain if the structure indicated from these TS results would be consistent with energetically favoured reaction routes for these models.

Examinations of the likely TS were carried out using H_2O interacting with the [Fe_5] or the [Fe_3] clusters by comparing the computed results for the following structures: (1) coordination of the water molecule to the iron cluster and the formation of a linear [(Fe_m)-O-(H-H)] intermediate, and (2) coordination of the water molecule to the iron cluster and the abstraction of hydrogen to the adjacent iron through the hydride [Fe..H-H(O)] bonded structure. Examinations of reaction coordinates and the vibrational analyses of the relevant intermediate provided only one imaginary frequency for the TS containing the [Fe….H] bonds, indicating structure (2) is the likely TS for these clusters. The result for the alternate structure (1) does not provide a single imaginary frequency from the vibrational analysis for the [Fe_n..O..H-H] (n=3 and 5) cluster structures containing the linear O..H-H unit, in which the H_2 was end-on to the oxygen; thus, this is not the likely TS.

The [Fe..H] bond lengths for the TS with the [Fe…H-H(O)] structure are 1.92Å and 1.76Å and long [H..O] distances in the water molecule of 2.47Å; SE-PM5 modelling for the breaking of the oxygen-hydrogen bonds, and the formation of H_2, provides a relatively small energy barrier. The formation of the [Fe_5←-OH_2] coordination bond was energetically favoured by -13 kcal, and an exothermic result was obtained for the formation of the iron cluster [Fe_5O]; the subsequent loss of H_2 was endothermic, giving an

overall energy change of +16 kcal for the formation of H_2. Similar results were obtained for computations with the [Fe_3] cluster; the vibrational analysis of the TS for the [Fe_3] and H_2O complex provided only one imaginary frequency; the structure for this transition state contained [Fe..H] distances of 1.89 Å and 1.90 Å. The H atoms were at a distance of 2.5 Å and 3.0 Å from the oxygen atom.

The results from the molecular modelling support the mechanism for H_2 formation from {Char[Fe_n](H_2O)} *via* iron hydride intermediates.

Research and Application of Catalytic Steam Gasification*

The discussion on catalysis and steam gasification has shown that a judicious combination of experimental and molecular modelling efforts has enabled us to identify the major aspects of the catalytic steam gasification of brown coal, namely the formation of active iron sites [Fe-C] and [Fe-O-C], and the reactions routes of these with H_2O to yield H_2 and CO. The insights gleaned from this effort are summarised below for H_2 and CO formation at elevated temperatures from Fe-mediated pyrolysis and the subsequent catalysed reactions of char with H_2O. This summary also illustrates the cyclic nature of the steam coal catalysis chemistry:

$$Char[Fe_3{\leftarrow}(OH)_2] \rightarrow Char[Fe(Fe\text{-}O)_2] + H_2$$
(pyrolysis; yield of H_2)

$$Char[Fe(Fe\text{-}O\text{-}C)_2] \rightarrow Char[Fe_2(Fe\text{-}O\text{-}C)] + CO$$
(pyrolysis; yield of CO)

$$Char[Fe_2(Fe\text{-}O\text{-}C)] \rightarrow Char[(Fe\text{-}C)Fe_2] + CO$$
(pyrolysis, formation of CO and active site)

$$Char[Fe_3] + H_2O \rightarrow Char[Fe_2\,(Fe{\leftarrow}\cdots OH_2)]$$
(chemisorption of H_2O)

$$Char[Fe_3{\leftarrow}\cdots OH_2] \rightarrow Char[Fe_2(Fe\text{-}O\text{-}C)] + H_2$$
(steam gasification; O insertion, H_2 formation)

$$Char[Fe_2(Fe\text{-}O\text{-}C)] \rightarrow Char[Fe_3] + CO$$
(steam gasification; CO formation, new active site)

$$Char[Fe_3O] + H_2O \rightarrow Char[Fe_3O(\leftarrow\cdots H_2O)]$$
(chemisorption of H_2O)

$$Char[Fe_3O{\leftarrow}\cdots H_2O] \rightarrow Char[Fe_3O(\text{-}O\text{-}C)] + H_2$$
(steam gasification; H_2 formation)

$$Char[Fe_3O(\text{-}O\text{-}C)] \rightarrow Char[Fe_3O] + CO$$
(steam gasification; CO formation, new active site)

* Portions modified with permission from Domazetis et al., Fuel 93, 404-414, 2012. Copyright (2012). Elsevier.

$$Char[Fe_3O] \rightarrow Char[Fe_2(Fe\text{-}O\text{-}C)]$$
(O insertion)

$$Char[Fe_2(Fe\text{-}O\text{-}C)] \rightarrow Char[Fe_3] + CO$$
(steam gasification, CO formation, new active site)

$$Char[Fe_3] + H_2O \rightarrow Char[Fe_2\,(Fe{\leftarrow}{-}OH_2)]$$
(chemisorption of H_2O to continue the cycle)

This is a summary of the major steps in the formation of H_2 and CO and shows the integral nature of pyrolysis (in forming active sites and yielding CO and H_2), and the chemisorption of H_2O on the respective active sites. Catalysed reactions of char and H_2O yield further CO through the elimination of CO from an [Fe-O-C] group to yield the active site [Fe-C], while H_2 formation results *via* an iron hydride intermediate. Additionally, experimental data have shown that significant catalytic activity occurs for coal samples containing relatively high loadings of small iron clusters, while XPS data have shown that oxygen is abstracted from steam molecules, and this forms [C-O] and [Fe-O] groups in char; this is consistent with the *in situ* formation of active sites within the char molecule and the Fe-catalysed reactions of H_2O with the char substrate.

The experimental results show the number of active sites is related to the amounts (and number) of poly-nuclear iron hydroxyl species added to the brown coal molecular matrix, as these form iron clusters when the coal is heated; greater amounts of these iron species form a larger number of active sites, leading to enhanced weight loss by reactions with H_2O and subsequent greater yields of the products H_2 and CO. Post-gasification reactions, catalysed by iron oxide particles formed as char undergoes gasification, have not been included in this reaction scheme (these would increase the proportion of H_2 and lower the CO in the gaseous product).

The discussions of the solution chemistry, and of the pyrolysis transformations, strongly indicate the iron species within the char substrate consist mostly of small iron clusters, with some larger ones; small clusters would participate in catalytic reactions with steam, but the larger iron oxide clusters may be involved in the enlargement of pores, and would act as catalysts for post-gasification reactions. An increase in char porosity would also improve the accessibility of steam molecules to catalytic active sites within char.

Iron clusters may be located near the surface and within the char particle. This indicates that the accessibility of active sites to H_2O molecules may vary throughout the char substrate. Further insights into this chemistry may be obtained with molecular dynamics (MD) modelling; visualisation of the output from MD modelling shows that a number of steam molecules impact

at the catalytic active site, as illustrated by a snapshot of such a system shown in Figure 8-12; in this, water molecules may chemi-adsorb on the Fe centre, and additional water molecules not interacting directly with the iron centres surround the char and may adsorb on the surface; additional water molecules (not shown) are situated at larger distances from the char. Thus H_2O molecules act dynamically and impact on the char surface, as well as on accessible catalytic sites. Molecular modelling has also shown that the chemi-adsorption of water on the active Fe site is energetically favoured. This is exemplified by results for the molecular model [$CharFe_3$•$2(H_2O)(4H_2O)$] shown in Figure 8-12, which was optimised with four H_2O molecules physically adsorbed to the char surface, and two molecules chemically adsorbed to the iron active site. The initial structure for this molecular model contained six water molecules randomly distributed at a large distance from the char molecule, and was optimised to the ground state (SE-PM5) with four water molecules physically adsorbed onto the char surface and two water molecules coordinated to the Fe centre. The iron complex is a somewhat distorted octahedral structure, with hydrogen atoms from nearby [C-H] groups situated at distances of between 1.9Å and 2.0Å from the other Fe centres. The difference in ΔH_f for the structure with H_2O at a distance and the optimised one is -94.6 kcal; these computations indicate the structure is stabilised by about -60 kcal from the two coordinated H_2O molecules, with additional contributions of -2 to -8 kcal per H_2O molecule from the four H_2O molecules physically adsorbed on the char surface. The molecular structure is stabilised by the two [Fe←OH_2] coordination bonds to form in an octahedral Fe structure and by [Fe…H] interactions. The [Fe…H] interactions in this structure form an arrangement that would enhance the formation of iron-hydride complexes proposed in concerted catalytic steam gasification chemistry.

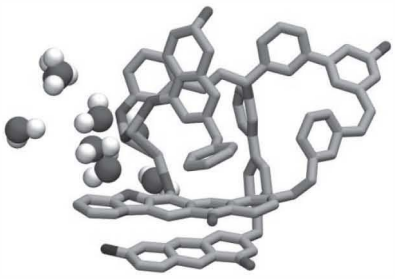

Figure 8-12. Snapshot of [$CharFe_3$•$(H_2O)_2$ $(4H_2O)$] with two steam molecules about the active site and four in the same area (Fe = ●green, O = ●red, H = ○white, C = ●light blue). Reprinted with permission from Domazetis et al., 2012.

Further work is required to assess the accessibility of all of the active sites in char for steam molecules and in this way obtain data on the impact of pressure and temperature relevant to industrial coal gasification. Further SE/DFT molecular modelling, and MD modelling, is required to identify the changes in the energetics of the reaction of char with steam that would result from any changes in temperature and pressure. For example, higher temperatures may cause different configurations of the char molecule containing the small iron clusters, and the energy states for the substrate will need to be re-examined within the context of elevated temperatures; the present SE/DFT modelling has used values for ground states to obtain indications of likely reaction routes. As the temperature of the system increases, the char molecules are expected to undergo conformational changes that may result in different energetics. These considerations may be addressed with MD, but this approach to the modelling of the catalytic steam coal gasification system is in its infancy. The MD results obtained at this early stage show that the [Fe-C] site in the char model would incur a larger number of impacts by H_2O molecules, indicating enhanced reactions at these sites.

Generally, calculations of the dynamics of heterogeneous catalysis are required to obtain the rate that gas molecules impact and stick on the active sites on the char surface, and these computations would correlate with simulations of the chemical kinetics of the system (Oura et al., 2003). Heterogeneous catalysis would correspond to a thermodynamic open system, in which mobile chemicals are efficiently converted at the surface into product(s) that are then transported away. A steady-state rate, measured as a TOF, may be based on the amount of reactants consumed over time, and these would correspond to the product yield. A full treatment of the processes, however, would involve the interplay of all relevant molecular-scale processes, including the spatial distributions of the reactant at the catalyst surface, and any possible post-gasification reactions. This necessitates a dynamic treatment of each individual reaction step for all of the molecular transformations of the char, and this would require extremely large computational resources.

It is clear from the work carried out thus far that the char surface area accessible for catalytic gasification is an important factor, as the distribution of active sites within the char surface is a function of the char/iron molecular composition; the surface area also determines the accessibility of the gasification reacting agent to active sites. The surface coverage of chars by water molecules has been reported to be between 0.2 and 0.7, at pressures of between 1 to 5 H_2O atmospheres; MD modelling would treat reaction rates for these systems as a function of the number of accessible active sites

for a given surface area and the probability of H_2O molecules adsorbing to these active sites (Roberts and Harris, 2006; Gale et al., 1996). While the extent of un-catalysed steam gasification may be negligible compared to the rate of catalytic steam gasification, the extent of coverage of the accessible char surface by H_2O molecules *per se* may impact on events during pyrolysis, and from this, it can be inferred that this would impact on the efficiency of catalytic gasification.

The catalytic chemistry discussed here emphasises the importance of the chemical structure of the char and the transformations of the iron complexes into active sites; the physio-chemical events that are involved in the formation of the char, and the resulting porosity, are important factors that would determine the accessibility of the active sites to H_2O molecules. Additional molecular modelling has examined the energetics of water molecules impacting on char. While the rate of steam molecules hitting the char surface is relatively high, the probability of steam molecules sticking on the active sites is related to the number of available iron sites and the energy change accompanying the sticking of H_2O to form the iron-water complex. Energy changes indicative of the interactions of water molecules were obtained with SE-PM5 molecular modelling as the difference in ΔH_f values calculated for the ground states of the char molecule with water molecules at a large distance, from those for the sticking of the water molecule(s) on the char surface. SE-PM5 values of ΔH_f for water physically adsorbed on char are:

a. [Char (H_2O)] (char model with one water molecule, indicative of char with a lower surface area) -2 kcal and -3 kcal, and
b. [Char# ($2H_2O$)] (char model with two water molecules, indicative of char with a larger surface area), -6 kcal and -10 kcal (or -3 kcal and -5 kcal per H_2O molecule).

Energy changes for water chemi-adsorbed on the active site for molecular models of char with [Fe_3] and also with char containing the [Fe-C] site are:

a. [CharFe_3], in which the [Fe_3] cluster has formed coordination bonds with hydroxyl groups in char, and H_2O has formed the [Fe←-OH_2] coordination bond, and provided an energy change of -12 kcal, and
b. [CharFe_2(Fe-C)], in which H_2O stuck onto the [Fe-C] group, and provided an energy change of -30 kcal.

Model (b) indicates an energetically favoured mechanism. While these data indicate water would readily stick to the [Fe-C] site, the data are

sensitive to steric constraints in char molecules and the resulting position of the active site. The ΔH_f values differed if the H_2O molecule encountered steric hindrance; for example, a molecular configuration in which the [Fe-C] group encountered significant steric hindrance gave a lower ΔH_f value of -18 kcal; an extreme example of steric hindrance gave an unfavourable ΔH_f energy change of +14 kcal.

Typical results from 1scf-DFT calculations are ΔH_f of -8 kcal for the physical adsorption of one water molecule on the char surface and -17 kcal for the formation of $[CharFe_3(H_2O)]$ with the $[Fe\leftarrow OH_2]$ coordination bond; however, differing conformations of the molecular model indicate considerable variation in the respective energy of a particular conformer. Thus DFT geometry optimisation of the char molecule alone gives an energy profile that differs with changes in the configuration by about -20 kcal; optimisation of the char molecule containing the $[Fe_3]$ cluster shows variations in the configuration to give ΔH_f values of between -30 kcal and -60 kcal. The DFT results for char models containing the metal centre are also sensitive to steric hindrance caused by particular changes in the char molecular configuration. 1scf-DFT calculations for char structures in which the metal centre forms a distorted octahedral structure and also distorts the macromolecule are not energetically favoured. The chemi-sorption of H_2O on the $[Fe_3O]$ cluster in the model $[Char(Fe_3O)]$ to form a $[Fe\leftarrow OH_2]$ coordination bond is also sensitive to steric constraints.

The experimental data of steam gasification of catalytic brown coal indicate an enhanced reaction by H_2O with char, resulting in the production of a higher content of hydrogen in syngas.

The potential for the industrial application of catalytic steam gasification of low rank coal can be understood by comparing the composition of syngas from catalytic and non-catalytic chemistry, illustrated by the following equations (S and N pollutants would be cleaned from the syngas):

1. The theoretical yields from catalysed char/steam chemistry are greater compared to the yield from the conventional gasification of uncatalysed chemistry (composition of brown coal expressed as molecular distribution, dry ash free, excluding S and N).

The yield for catalysed chemistry is:

$$C_{5.7}H_{4.9}O_{1.63} + 5.4H_2O \rightarrow 5.4CO + 5.4H_2 + 2.25H_2 + 0.3CO_2 + 0.2H_2O$$

The yield for non-catalysed chemistry is:

$$C_{5.7}H_{4.9}O_{1.63} + 2.3O_2 \rightarrow 5.4CO + 2.25H_2 + 0.3CO_2 + 0.2H_2O$$

These equations show catalysed gasification would potentially increase the yield of H_2 by about three-fold, without a reduction in the yield of CO. In practice, conventional gasification would also involve some reaction with steam, which would also increase the H_2 content. Nonetheless, catalytic steam gasification can produce a considerable increase in the H_2 content in syngas.

2. The subsequent production of H_2 can be obtained from the syngas by employing water-shift chemistry:

$$5.4CO + 5.4H_2 + 2.25H_2 + 0.3CO_2 + 0.2H_2O + 5.2H_2O \rightarrow 13.25H_2 + 5.7CO_2 \text{ (catalysed)}$$

$$5.4CO + 2.25H_2 + 0.3CO_2 + 0.2H_2O + 5.2H_2O \rightarrow 7.65H_2 + 5.7CO_2 \text{ (non-catalysed)}$$

This chemistry would almost double the yield of hydrogen when compared to the uncatalysed reaction, and highlights the potential for hydrogen production using catalytic steam gasification of low rank coals – the water shift reaction also increases the amount of CO_2, however. In practice, the water-shift chemistry may be used to provide the desired combination of CO and H_2 in the syngas; for example, shifting CO in the catalysed reaction to yield syngas containing 4.4CO and $8.65H_2$ would optimise the yield of liquids from a Fischer-Tropsch plant.

These equations illustrate the potential for improvements in industrial processes offered by catalytic gasification of low rank coal, and this is explored further in the next chapter.

References

ACS. 2011. *Catalysis - A key technology for sustainable development.* Available at: https://catl.sites.acs.org/.

Adler, J. and Hüttinger, K. J. 1984. 'Mixtures of potassium sulphate and iron sulphate as catalysts for water vapour gasification of carbon, 1. Kinetic studies', *Fuel,* 63, 1393.

Baker, R. T. K. and Chludzinski, Jr., J. J. 1985. 'Catalytic gasification of graphite by calcium and nickel-calcium', *Carbon,* 23, 635.

Baker, R. T. K., Dudash, N. S., Lund, C. R. F. and Chludzinski, Jr., J. J. 1985. 'Comparison of the catalytic influence of nickel and Cu-Ni alloys on the graphite steam reaction', *Fuel,* 64, 1151.

Bartholomew, C. H., Gopalakrishanan, R. and Fullwood, M. 1991. 'Catalysis of char gasification in O_2 by CaO and $CaCO_3$', *JACS Proceedings Div. Fuel. Chem.*, 36, 982.

Castaldi, M. J. and Dooher, J. P. 2007. 'Investigation into a catalytically controlled reaction gasifier (CCRG) for coal to hydrogen', *Int. J. Hydrogen Energy*, 32, 4170-4179.

Cazorla-Amorós, D., Linares-Solano, A., Salinas-Martínez de Lecea, C., Meijer, R. and Kapteijn, F. 1991. 'Further evidence on the mechanism of the CO_2 carbon gasification catalyzed by calcium: TPD after $^{13}CO_2$ chemisorption', *JACS Proceedings Div. Fuel. Chem.*, 36, 975.

Cazorla-Amorós, D., Linares-Solano, A., Salinas-Martínez de Lecea, C., Yamashita, H., Takashi K. and Tomita, A. 1991. 'Nature and structure of calcium species dispersed on carbon, XANES and EXAFS study', *JACS Proceedings Div. Fuel. Chem.*, 36, 998.

Cazorla-Amorós, D., Linares-Solano, A., Salinas-Martínez de Lecea, C. and Joly, J. P. 1992. 'A temperature-programmed reaction study of calcium-catalyzed carbon gasification', *Energy Fuel,* 6, 287.

Chen, S. G. and Yang, R. T. 1997. 'Unified Mechanism of Alkali and Alkaline Earth Catalysed Gasification Reactions of Carbon by CO_2 and H_2O', *Energy Fuels*, 11, 421-427.

Chu, X. and Schmidt, L. D. 1991. 'Gasification of Graphite Studied by Scanning Tunnelling Microscopy', *Carbon,* 29, 1251.

Corella, J., Toledo, J. M. and Molina, G. 2006. 'Steam Gasification of Coal at Low-Medium (600-800°C) Temperature with Simultaneous CO_2 Capture in Fluidized Bed at Atmospheric Pressure: The Effect of Inorganic Species. 1. Literature Review and Comments', *Ind. Eng. Chem. Res.*, 45, 6137-6146.

Davis, B. H. 2001. 'Fischer-Tropsch synthesis: current mechanism and futuristic needs', *Fuel Processing Technology*, 71, 157-166.

Domazetis, G., James, B. D. and Liesegang, J. 2008. 'Computer molecular models of low rank coal and char containing inorganic complexes', *J. Mol. Model*, 14, 581-597.

Domazetis, G., James, B. D. and Liesegang, J. 2008. 'High-Level Computer Molecular Modelling for Low Rank Coal Containing Metal Complexes and Iron-Catalysed Steam Gasification', *Energy Fuels*, 22, 3994-4005.

Domazetis, G., James, B. D., Liesegang, J., Raoarun, M., Kuiper, M., Potter, I. D. and Oehme, D. 2012. 'Experimental studies and molecular modelling of catalytic steam gasification of brown coal containing iron species', *Fuel,* 93, 404-414.

Domazetis, G., Raoarun, M., James, B. D. and Liesegang, J. 2008. 'Molecular modelling and experimental studies on steam gasification of

low rank coals catalysed by iron species', *App. Catalysis A: General*, 340, 105-118.

Espinal, J. F., Mondragón, F. and Truong, T. N. 2009. 'Thermodynamic evaluation of steam gasification mechanisms of carbonaceous materials', *Carbon*, 47, 3010-3018.

Fan, S. M., Yuan, X. Z., Zhao, L., Xu, L-H., Kang, T-J. and Kim, H-T. 2016. 'Experimental and kinetic study of catalytic steam gasification of low rank coal with an environmentally friendly, inexpensive composite K_2CO_3-eggshell derived CaO catalyst', *Fuel*, 165, 397-404.

Gale, T. K., Bartholomew, C. H. and Fletcher, T. H. 1996. 'Effects of Pyrolysis Heating Rate on Intrinsic Reactivities of Coal Chars', *Energy Fuels,* 10, 766-775.

Gallagher, Jr., J. E. and Euker, Jr., C. A. 1980. 'Catalytic Coal Gasification for SNG Manufacture', *Energy Research*, 14, 137-147.

Godavarty, A. and Agarwal, A. 2000. 'Distribution and Catalytic Activity of Eutectic Salts in Steam Gasification of Coal', *Energy Fuels,* 14, 558-565.

Gorelsky S. I., Lapointe, D. and Fagnou, K. 2008. 'Analysis of the Concerted Metalation-Deprotonation Mechanism in Palladium-Catalyzed Direct Arylation Across a Broad Range of Aromatic Substrates', *J. Am. Chem. Soc.,* 130, 10848-10849.

Hermann, G. and Hüttinger, K. J. 1986. 'Mechanism of iron-catalysed water vapour gasification of carbon', *Carbon*, 24, 429-435.

Hermann, G. and Hüttinger, K. J. 1986. 'Mechanisms of non-catalysed and iron-catalysed water vapour gasification of carbon', *Fuel*, 65, 1410-1418.

Hüttinger, K. J., Adler, J. and Hermann, G. 1986. 'Iron-catalysed water vapour gasification of carbon', in J. L. Figueiredo and J. A. Moulijn (eds.), *Carbon and Coal Gasification (NATO ASI Series E, No. 105)* (Dordrecht: Martinus Nijhoff), 213-229.

Hüttinger, K. J. and Minges, R. 1986. 'Alkali metal catalysed water vapour gasification of carbon using mineral catalyst raw materials', in J. L. Figueiredo and J. A. Moulijn (eds.), *Carbon and Coal Gasification (NATO ASI Series E, No. 105)* (Dordrecht: Martinus Nijhoff), 197-212.

Johnson, J. L. 1976. 'The Use of Catalysts in Coal Gasification', *Catalysis Reviews, Science and Engineering,* 14, 131-152.

Kline, S. D., Mason, D. M., Carty, R. H. and Babu, S. P. 1990. 'The effects of limestone on ash behaviour in fluidized-bed gasification of coal', in R. Markuszewski and T. D. Wheelock (eds.), *Processing and Utilization of High-Sulphur Coals III* (Amsterdam: Elsevier), 687-695.

Lambert, J-F. and Che, M. 2000. 'The molecular approach to supported catalysts synthesis: state of the art and future challenges', *J. Mol. Cat. A.,* 162, 5-18.

McCarthy, D. J. 1990. 'Discussion of the kinetics of the carbon-steam reaction catalysed by iron and a new mechanistic proposal', *Carbon,* 28, 661.

McKee, D. W., Spiro, C. L., Kosky, P. G. and Lamby, E. J. 1985. 'Eutectic salt catalysts for graphite and coal char gasification', *Fuel,* 64, 805.

Mims, C. A. 1990. 'Catalytic Gasification of Carbon: Fundamentals and Mechanisms', in J. Lahaye and P. Ehrburger (eds.), *Fundamental Issues in Control of Carbon Reactivity (NATO ASI Series E, Vol 192)* (Dordrecht: Springer), 383-407.

Mims, C. A. and Pabst, J. K. 1983. 'Role of surface salt complexes in alkali-catalysed carbon gasification', *Fuel*, 62, 176-179.

Mochida, I. and Sakanishi, K. 2000. 'Catalysts for coal conversions of the next generation', *Fuel*, *79,* 221-228.

Moulijn, J. A. and Kapteijn, F. 1986. 'Catalytic Gasification', in J. L. Figueiredo and J. A. Moulijn (eds.), *Carbon and Coal Gasification (NATO ASI Series E, No. 105)* (Dordrecht: Martinus Nijhoff), 181-196.

Nahas, N. C. 1983. 'Exxon catalytic coal gasification process: Fundamentals to flowsheets', *Fuel,* 62, 239-241.

Nørskov, J. K., Bligaard, T., Hvolbæk, B., Abild-Pedersen, F., Chorkendorff, I. and Christensen, C. H. 2008. 'The nature of the active site in heterogeneous metal catalysis', *Chem. Soc. Rev.*, 37, 2163-2171.

Ohtsuka, Y. and Asami, K. 1991. 'Steam gasification of low rank coals with a chloride-free iron catalyst from ferric chloride', *Ind. Eng. Chem. Res.,* 30, 1921-1926.

Oura, K., Lifshits, V. G., Saranin, A. A., Zotor, M. and Katayama, A. V. 2003. *Surface Science – An Introduction (Advanced Texts in Physics)*, Berlin: Spinger-Verlag.

Radović, L. R., Walker, Jr., P. L. and Jenkins, R. G. 1983. 'Effect of lignite pyrolysis on calcium oxide dispersion and subsequent char reactivity', *Fuel,* 62, 209-212.

Raghunathan, K. and Yang, R. Y. K. 1989. 'Unification of coal gasification data and its applications', *Ind. Eng. Chem. Res.*, 28, 518-523.

Roberts, D. G. and Harris, D. J. 2006. 'A Kinetic Analysis of Coal Char Gasification Reactions at High Pressures', *Energy Fuels*, 20, 2314-2320.

Roberts, M. J., Everson, R. C., Domazetis, G., Neomagus, J.M., Jones, H. W. J. P., Van Sittert, C. G. C. E., Okolo, G. N., Van Niekerk, D. and Mathews, J. P. 2015. 'Density functional theory molecular modelling

and experimental particle kinetics for CO_2 – char gasification', *Carbon,* 93, 295-314.

Saber, J. M., Falconer, J. L. and Brown, L. F. 1986. 'Interaction of potassium carbonate with surface oxide carbon', *Fuel*, 65, 1356-1359.

Schumacher, W., Muhlen, H-J., van Heek, K. H. and Juntgen, H. 1986. 'Kinetics of K-catalysed steam and CO_2 gasification in the presence of product gases', *Fuel*, 65, 1360-1363.

Schwar, J., Jahn, P. W., Wiedmann, L. and Benninghoven, A. 1991. 'Combined chemical and surface analytical investigation of the calcium catalyzed coal gasification process', *J. Vac. Sci. Technol*., A9, 39.

Siefert, N. S., Shekhawat, D., Litster, S. and Berry, D. A. 2013. 'Steam-Coal Gasification Using CaO and KOH for in Situ Carbon and Sulfur Capture', *Energy Fuels,* 27, 4278-4289.

Srivastava, R. C., Srivastava, S. K. and Rao, S. K. 1988. 'Low temperature nickel-catalysed gasification of Indian coals', *Fuel*, 67, 1205-1207.

Suzuki, T., Inoue, K. and Watanabe, Y. 1989. 'Steam pulsed gasification of Na_2CO_3 or $Fe(NO_3)_3$ loaded Yallourn coal char', *Fuel*, 68, 626-630.

Suzuki, T., Mishima, M., Takahashi, T. and Watanabe, Y. 1985. 'Catalytic steam gasification of Yallourn coal using sodium hydridotetracarbonyl ferrate', *Fuel,* 64, 661-665.

Suzuki, T., Ohme H. and Watanabe, Y. 1992. 'A mechanism of sodium-catalysed CO_2 gasification of carbon investigation by pulse and TPD techniques', *Energy Fuels,* 6, 336-351.

Takarada, T., Sasaki, J., Ohtsuka, Y., Tamai, Y. and Tomita, A. 1987. 'Direct Production of Methane-Rich Gas from the Low-Temperature Steam Gasification of Brown Coal', *Ind. Eng. Chem. Res.,* 26, 627-629.

Tamai, Y., Watanabe, H. and Tomita, A. 1977. 'Catalytic gasification of carbon with steam, carbon dioxide and hydrogen', *Carbon,* 15, 103-106.

Walker, Jr., P. L., Matsumoto, S., Hanzawa, T., Muira, T. and Ismail, I. M. K. 1983. 'Catalysis of gasification of coal-derived cokes and chars' *Fuel*, 62, 140-149.

Wang, J., Sakanishi, K., Saito, I., Takarada, T. and Morishita, K. 2005. 'High-yield hydrogen production by steam gasification of hypercoal (ash-free coal extract) with potassium carbonate: comparison with raw coal', *Energy Fuels,* 19, 2114-2120.

Weldon, J., Haldipur, G. B., Lewandowski, D. A. and Smith, K. J. 1986. 'Advanced coal gasification and desulphurization with calcium based sorbents', *JACS Proceedings Div. Fuel Chem.,* 31, 244-252.

Widegren, J. A. and Finke, R. G. 2003. 'A review of the problem of distinguishing true homogeneous catalysis from soluble or other metal-

particle heterogeneous catalysis under reducing conditions', *J. Mol. Catalysis A: Chemical,* 198, 317-341.

Wigmans, T., Elfring, R. and Moulijn, J. A. 1983. 'On the mechanism of the potassium carbonate catalysed gasification of activated carbon: the influence of the catalyst concentration on the reactivity and selectivity at low steam pressures', *Carbon,* 21, 1-12.

Wigmans, T., Haringa, H. and Moulijn, J. A. 1983. 'Nature, activity and stability of active sites during alkali metal carbonate-catalysed gasification reactions of coal char', *Fuel,* 62, 185-189.

Wigmans, T., van Doorn, J. and Moulijn, J. A. 1983. 'Temperature-programmed desorption study of Na_2CO_3-containing activated carbon', *Fuel,* 62, 190-195.

Wu, X., Tang, J. and Wang, J. 2016. 'A new active site/intermediate kinetic model for K_2CO_3-catalyzed steam gasification of ash-free coal char', *Fuel*, 165, 59-67.

Yamashita, H., Yoshida, S. and Tomita, A. 1991. 'Local Structures of Metals Dispersed on Coal. 3. Na K-edge XANES studies on the structure of sodium gasification catalyst', *Ind. Eng. Chem. Res.,* 30, 1651-1655.

Yamashita, H., Yoshida, S. and Tomita, A. 1991. 'Local Structures of Metals Dispersed on Coal. 2. Ultrafine FeOOH as Active Iron Species for Steam Gasification of Brown Coal', *Energy Fuels,* 5, 52-57.

Zaera, F. 2001. 'Outstanding Mechanistic Questions in Heterogeneous Catalysis', *J. Phys. Chem. B*, 106, 4043-4052.

Zeng, D. and Fletcher, T. H. 2005. 'Effects of Pressure on Coal Pyrolysis and Char Morphology', *Energy Fuels*, 19, 1828-1838.

Zhang, J., Zhang, R. and Bi, J. 2016. 'Effect of catalyst on coal char structure and its role in catalytic coal gasification', *Catalysis Communications*, 79, 1-5.

Zhu, Z. H., Finnerty, J., Lu, G. Q., Wilson, M. A. and Yang, R. T. 2002. 'Molecular Orbital Theory Calculations of the H_2O−Carbon Reaction', *Energy Fuels*, 16, 847-854.

Zhu, Z. H. and Lu, G. Q. 2004. 'Comparative Study of Li, Na, and K Adsorptions on Graphite by Using ab Initio Method', *Langmuir,* 20, 10751-10755.

CHAPTER NINE

FUTURE PROCESSED COAL POWER GENERATION

A worldwide effort is underway to develop new coal-fuelled power generation technologies with low- to zero-emissions. Impetus for this has stemmed from environmental concerns, particularly global warming and climate change. The report by the UN Intergovernmental Panel on Climate Change (IPCC, 2001) states:

> Relative to the reference case, the coal industry, producing the most carbon-intensive of products, faces almost inevitable decline in the long term…

Broadly, the power generation sector supplies power using a variety of plants, including fossil fuel (coal, gas, and oil), hydro, nuclear, solar, wind, and, to a lesser extent, biomass. Power is supplied to the end users *via* the grid, which is designed to respond to continuous and changing demand; the grid transmits and distributes power to communities, and, increasingly, the smart grid is developed to enable a better response to the intermittent supply from renewable power sources. In some regions that endeavour to favour solar and wind, coal-fuelled power stations are designed to operate with variable power output to compensate for the intermittent nature of solar and wind power (which incurs additional costs). The supply and demand of power, however, is increasingly designed to encompass higher efficiency measures and devices when practical, and also to deal with the intermittent behaviour of solar and wind power supply.

Processed Coal within the Context of the Mitigation of Emissions

It is noted that addressing global warming requires reductions in emissions of GHGs from all sectors. An appropriate mix of energy resources is required to achieve the goal of secure, affordable power with the required reductions in emissions. Activities in various sectors are discussed, for

example, in the 'Climate Action Now – Summary for Policy Makers 2017' by the UN Climate Change Secretariat (2017). One senses a consensus for reductions in all sources of GHG emissions; this consensus began from the scientific community, and is increasingly being adopted by the wider population – however, predictions for the demand for power in the coming decades are believed to exceed the power generated in the entire 20th century, and this adds to the urgency to develop clean carbon-free power generation. The IEA has assessed 26 technologies to determine their green credentials, and concluded only three of these met the requirements for emission reductions: renewables, electric vehicles, and energy storage. Some progress was noted for the nuclear, industrial, and transport sectors. Coal continues to dominate power generation, and in spite of the need for higher efficiency, 30% of new coal power plants in 2015 were subcritical plants (OECD/IEA, 2017).

The IEA has discussed the importance of higher efficiencies in detail in its 'Energy Efficiency 2018: Analysis and Outlooks to 2040' report (IEA, 2018a):

> The right efficiency policies could enable the world to achieve more than 40% of the emissions cuts needed to reach its climate goals without new technology.

Within the wider background, the R&D effort to process low rank coals into high quality fuel(s) is simply one of the many activities to lower emissions, and its overall goal is to provide high quality, low cost fuel for high efficiency plants that offer secure and economically competitive power generation that meets low emission targets – the ultimate goal is economically competitive zero-emissions coal-fuelled power generation. Processing low rank coal offers a paradigm shift in the way low rank coals can be used for future power generation.

The proportion of electricity worldwide today accounts for 19% of total energy consumed and is predicted by the IEA to increase to 24% by 2040, and consequently the demand for coal-fuelled electricity is growing. About 95% of all CO_2 emissions are from power plants, refineries, cars and trucks, industrial boilers, and home heaters; such diverse sources of emissions require a comprehensive approach to achieve the desired reductions (IEA, 2018b). The IEA also reports that the potential benefits from energy efficiency are as yet not fully realised; additionally, as improvements in energy efficiency are implemented, their global impact on emissions is countered by increasing economic activity. In 2017, energy demand increased across all sectors, resulting in increased GHG emissions.

Lior (2008) reviewed the sources of energy available worldwide and the future prospects of fossil, nuclear, renewable, hydrogen, fuel cell, and micro power systems. Lior also discussed ways to address the problem of the availability, cost, and sustainability of energy resources alongside the rapidly rising demand, and suggested governments should invest in efforts to develop commercial ways for: (1) energy conservation, (2) efficient energy conversion and transmission that encompasses the entire system's life cycle, and (3) global warming mitigation by decarbonising when using fossil fuels, by a judicious use of renewable energy, and by a safe use of nuclear power.

The impact of GHG on global temperatures has been modelled to assess the types of measures needed to limit global warming, and a comparison has been made by Dessens et al. (2016) of major input assumptions and outputs of recent mitigating studies to the 2°C level of global average temperature increase by 2100. This comparison indicated that mitigation to 2°C is feasible, but may be delayed if the deployment of key technologies is limited and progress is not made on energy efficiency. The scenario of avoiding action now, and rapid mitigation efforts being made at a later date, can potentially lead to thousands of fossil fuel plants being retired globally, which would result in political and economic turmoil. Tokimatsu et al. (2015) modelled a number of scenarios on mitigation measures and identified forestry (carbon sinks) and CO_2 capture as the major measures for emissions reduction required to limit global warming to the 2°C level.

China and India are anticipated to increase fossil-fuelled power generation. India requires additional power for further development, and consequently more coal-fired power plants are being built. The ash content of Indian coals is generally high, and because of this larger boilers and associated plants are required; the high ash coals pose additional challenges as India seeks to utilise UC and USC plants. India is also aiming at 40% of non-fossil fuel capacity by 2030. This may result in a lower proportion of coal in the country's energy, and importantly, coal plants will need to operate with increased flexibility to back up intermittent energy sources. It is thought that increasing the flexibility of coal plants will be more important than efficiency gains to meet the requirements of India's current energy policy (Wiatros-Motyka, 2018).

China is the world's largest consumer of both total primary energy and energy from coal, and is also the world's largest emitter of carbon dioxide. Coal is expected to account for 50% of China's total primary energy consumption by 2030 and will continue to be a major source of energy until at least 2050; an increasing reliance on coal upgrading and more efficient coal power generation technologies is anticipated, and the economic

implications from these need to be carefully examined (Zhang et al., 2017). China has progressed its clean coal project, and this includes the installation of ultra-supercritical coal-fired plants exceeding 100 GW, and the operation of a 250 MW integrated gasification combined-cycle demonstration power plant, which includes water slurry gasification; dry feed pressurised gasification technology with a >2000 ton/day capacity is also reported. Additional activity includes a direct coal liquefaction plant with an annual capacity of >1 Mt (oil) and the demonstration of CO_2 capture and storage, including enhanced oil recovery. Research on high temperature heat resistant alloy material has led to the demonstration of a 600 MW USC unit that exceeds 700°C to enable a system efficiency level of 50-52%. A considerable proportion of China's coal reserves are low-rank coals, and research is also ongoing into more efficient ways to utilise these coals (Chang et al., 2016). Feng (2018) discusses the design and optimisation of USC plants in China that combine innovative technologies to achieve an annual average net efficiency of 48.8% (LHV). This operational efficiency provides lower CO_2 emissions, and is expected to halve NOx emissions compared to other similar coal-fuelled power generation units.

China has also undertaken activities towards carbon capture and CO_2 utilisation, particularly enhanced oil recovery. The IEA report on carbon utilisation in China includes plans to retrofit 420 GW of coal power into ultra-low emissions by 2020 by providing an incentive of higher wholesale electricity tariffs to ultra-low emissions units (Lochwood, 2018).

The US DOE examined the factors applicable to an increase in the efficiency and security of coal-fuelled electricity generation. The performance of aging coal generation plants inevitably decreases, and market pressures on the coal sector present opportunities to promote early-stage technologies to retrofit, or replace, components that will result in improvements in the plant's performance. Research and development in materials, fluid dynamics, fuel preparation, and the use of new plant controls can lead to new components that would help improve the efficiency and reliability of coal-fired power plants' baseload power. Falling prices for non-dispatchable renewable energy and environmental concerns have encouraged efforts to improve the efficiency of coal-fired power generation. The uptake of natural gas has also spurred efforts to increase the reliability of coal power (Taylor, 2018).

Nsanzineza et al. (2017) have undertaken a unique study to assess the emissions from US power generation, focusing on the Rocky Mountain region, which has abundant wind and solar resources as well as coal and natural gas. They examined key factors that could shape future electricity generation for a range of natural gas prices and GHG mitigation policies,

and included dispatch results for future electricity generation, reflecting plans for retiring or repowering coal plants. Gas prices, GHG fees, and the availability of renewable power affected the generation mix; a cheap price for natural gas was modelled to account for 22% of generation, but this was 12% if a cost was imposed for GHG emissions. Coal provided about 25% of generation, declining to 17% if a cost for emissions was included. They noted that if transmission lines were at their flow limits, or in regions where the power needed to be exported encountered congested transmission, then renewable generation would be curtailed. Additional variations would result from seasonal factors that would impact on solar and wind power generation.

The US has increasingly used gas as an energy source (see Figure 1-1). The policy of the US government is also undergoing changes, and it is difficult to assess how this may impact on emissions in the USA; the EPA inventory reports the following US GHG emissions (the figures are all stated as million metric tons (MMT) CO_2 equivalent):

> Overall, from 1990 to 2016, total emissions of CO_2 increased by 189.6 MMT (3.7 percent), while total emissions of CH_4 decreased by 122.5 MMT (15.7 percent), and N_2O emissions increased by 14.8 MMT (4.2 percent). During the same period, aggregate weighted emissions of HFCs, PFCs, SF_6 and NF_3 rose by 73.8 MMT (74.0 percent). From 1990 to 2016, HFCs increased by 115.8 MMT (248.5 percent), PFCs decreased by 19.9 MMT (82.1 percent), SF_6 decreased by 22.6 MMT (78.5 percent), and NF_3 increased by 0.5 MMT (1,110.2 percent). Despite being emitted in smaller quantities relative to the other principal greenhouse gases, emissions of HFCs, PFCs … are significant because many of these gases have extremely high global warming potentials and, in the cases of PFCs and SF_6, have long atmospheric lifetimes. Conversely, U.S. greenhouse gas emissions were partly offset by carbon sequestration in forests, trees in urban areas, agricultural soils, landfilled yard trimmings … and coastal wetlands, which, in aggregate, offset 11.5 percent of total emissions in 2016 (EPA, 2018).

The IEA has examined the impact of high efficiency, low emissions coal-fired power plants in reducing emissions of CO_2 in Bangladesh, Indonesia, Malaysia, the Philippines, Thailand and Vietnam. The implementation of high efficiency coal power stations of greater than 800 MW capacity would reduce emissions by about 40% compared to old plants, and by 13-19% compared to new subcritical plants. There are factors, such as geographical ones in Indonesia and Thailand, that may require smaller units and a fragmented grid, and these would inhibit the use of large power stations. Currently the majority of coal-fuelled electricity generation in these countries is from subcritical plants (Barnes, 2018).

Changes to the mix of power sources are also evident in Europe; Germany is an example of a country increasing its uptake of renewables, as nuclear power generation is being phased out, and the amount of coal power generation is decreasing. The ongoing transformation of German energy policy now poses major challenges to uninterrupted electricity supply in the near future. Consequently, the German Federal Government has introduced a provision, and with costs, to ensure power plants considered to be indispensable for the security of supply are kept as reserves; measures are also in place to deal with interruptible loads. A new design for the German electricity market has been suggested to ensure security of energy supply, and the ongoing expansion of renewable energy would also pose special challenges resulting from the intermittent nature of renewables (Coester et al., 2018).

This brief discussion provides a context of the global clean coal activity, and within this context, low rank coal processing for low- to zero-emissions power is one of many concepts that require implementation to achieve an overall mitigation of global warming. The IEA has examined current and future coal-fuelled plants to assess the reduction in emissions that would result from greater efficiencies, and pointed out that advanced R&D efforts could reduce emissions down to 669 kg CO_2/MWh, but beyond this, carbon capture is required for lower emissions (Topper, 2011).

In this chapter, the potential benefits that may be derived from processed high quality, low rank coals into high quality fuel for advanced power generation are illustrated by modelling plants' performance and emission intensities, and there is a general discussion on the corresponding economics; these models can be used to indicate the trajectory required for the desired outcomes for coal-fuelled low- and zero-emissions technology. These are models of the major power plants used to illustrate the potential benefits obtained with CCT processes, and comprise supercritical power plants, direct coal-fuelled turbines, and catalytic steam coal gasification – the latter may be configured to produce hydrogen-rich syngas for a hybrid power and liquids plant.

The CCT P/L processed coal concept proposes low- to zero-emissions technology by capturing CO_2 as a raw material for the synthesis of valuable products. A promising approach to CO_2 capture and utilisation is oxy-combustion, followed by CO_2 capture, and synthetic routes to valuable products using CO_2 and H_2. Work on oxy-combustion is being conducted by a number of organisations, such as, for example, the University of Utah's Clean and Secure Energy from Coal Program (which includes work on gasification and chemical looping).*

* For more information, see http://www.cleancoal.utah.edu/.

The development of higher efficiency and the flexible operation of coal-fuelled power plants is being undertaken by multinational firms involved in the construction and supply of power generation equipment. The supply of high quality, low-cost coal to fuel these new plants would contribute to commercially competitive power generation with lower emissions. The CCT P/L process provides three high quality coals:

1. Non-fouling coal.
2. Ultra-clean coal (or virtually zero-ash coal).
3. Catalytic coal for gasification.

An assessment of the efficiencies and emissions from plants fuelled with these coals has been carried out with models available in the GateCycle™ software package. Modelling studies show that an SC plant fuelled with non-fouling coal and a direct coal-fuelled turbine in a combined-cycle plant fuelled with ultra-clean coal (DCFTCC) achieve high thermal and power efficiencies (USC power plants would be fuelled with non-fouling coal to operate at higher efficiency levels and with lower emissions than SC plants).

Supercritical Plants Fuelled with Non-Fouling Coal

The benefits from processed low rank coals as fuel for high efficiency power plants have been discussed by Domazetis et al. (2008; 2010), and illustrated with models of SC plants from GateCycle™ (a typical model is shown in Figure 9-1), which show efficiencies of 41-45%. These models use CCT P/L non-fouling coal with various amounts of moisture and ash. The benefits from this fuel are based on an assessment of capital costs, efficiency, maintenance and operating costs, and additional costs estimated for the coal processing plant. The output of the model in Figure 9-1 is about 400 MW power at 41% efficiency (LHV). The non-fouling coal composition included an ash content that varied from 1wt% to 5wt%. The CO_2/MWh emissions for the SC models were 700-800 kg/MWh, and SOx emissions were 0.94 kg/MWh, with the stack gas temperature at 126°C, which is above the dew-point temperature for these particular coals. The CO_2/MWh emissions for the SC plant are considerably lower than (old) subcritical brown coal power stations, which operate with emissions of 1200-1400kg CO_2/MWh.

Numerous GateCycle™ modelling studies have been conducted using the composition of various non-fouling coals, discussed in Chapter Two, obtained by acid treatments of brown coal, lignite and sub-bituminous coal.

The efficiencies for these models were in the range of 41-45% and with corresponding lower emissions.

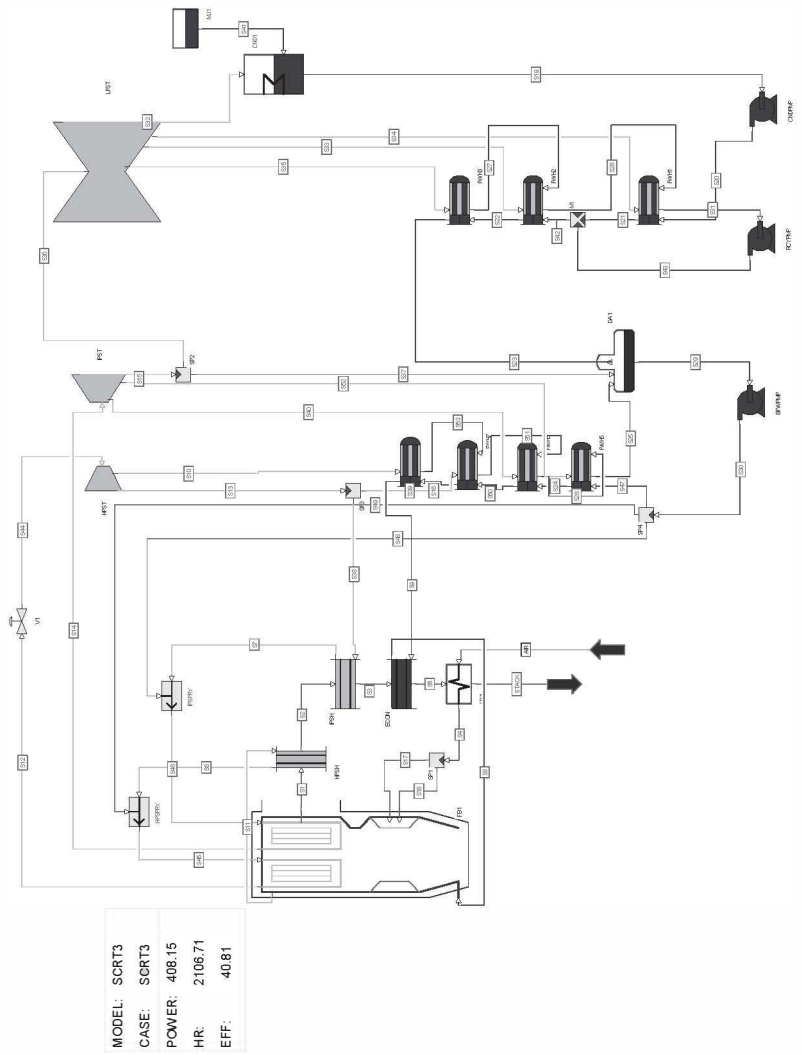

Figure 9-1. Typical GateCycle™ model of a supercritical power station fuelled with non-fouling coal.

The SC (or USC) models of power plants would integrate a coal cleaning and drying module (shown in the schematic in Figure 5-1) to use low grade heat for coal treatment and drying; this concept is similar to a plant that generates power and utilises low-grade heat to provide hot water (CHP). A large number of modelling exercises have shown that extracting heat for coal processing in such a manner may reduce the power sent to the grid, and would result in an overall reduction in the power generating efficiency of 1-2%, and operate at a total thermal efficiency of about 80%. Power is required for the coal drying plant for high moisture coal (60% moisture), and this has been calculated to be equivalent to reducing the efficiency by up to 1.5%; thus a 400-500 MW SC plant that would normally operate at 44% (LHV) power efficiency (and ≥80% thermal efficiency) would be expected to utilise 3.5% of the power output for coal processing and the drying of brown coal mined with 50-60wt% moisture, and the output to the grid would correspond to ~40.5% power efficiency. Mined coal with lower moisture would require less power, and such a plant would send out more power to the grid. Additional modelling has shown a USC plant would operate at ≥45% generation efficiency using processed non-fouling brown coal dried to 10-20wt% moisture.

An SC power station integrated with a CCT processing plant would consist of:

- Open-cut mining operations in close proximity to the power station, providing low-cost coal
- Crushing and conveying of the coal to the CCT processing plant
- Ash reduction using acid washing, utilising low-grade heat
- Water recovery and recycling
- Drying the hot clean coal
- Feeding pulverised processed coal to fuel a supercritical boiler

The amounts of moisture and ash in the raw coal would impact on the heat and power required for the coal cleaning process, and on the acidity of the coal treatment. These factors, in turn, determine the size and operation of the coal treatment vessels, and the size of the water treatment plant. The CCT R&D Program has examined a suite of coals that are typical of low-rank coals worldwide; the heterogeneity of low rank coals makes it necessary to separately assess each coal deposit for commercial exploitation.

Direct Coal-Fuelled Turbines in Combined-Cycle Plants Fuelled with Ultra-Clean Coal

The development of a cleaner and more efficient use of coal for power generation has favoured combined-cycle power generation systems as these operate at the highest efficiencies, resulting in the lowest emissions per MWh. A number of coal-based combined-cycle plants may be developed, including:

- Direct coal-fuelled turbine combined cycles (DCFTCC)
- Integrated gasification combined cycles (IGCC)
- Combined cycles with pressurised fluidised bed combustion (PFBC)
- Externally-fired combined cycles (EFCC)

The essential feature of all of these technologies is the cleanliness of the hot gases that enter the turbine, comprising the concentrations of sodium and potassium, and the particulate ash loading. Turbines are expected to tolerate 100-300 ppb concentration of volatile alkalis (Na+K) and low inlet particulate loading. Generally, the specifications required for cleaning intervals of 2,500 hrs and re-blading intervals of 20,000 hrs stipulate solids at 2-3 ppm for 2μm sized particles (some stipulate 5-6 ppm for 1-20 μm sized particles); further developments may enable turbines to exceed these limits (LeCren, 1992; Wenglarz et al., 1995). Various approaches may be adopted to clean the hot gases before they enter the turbine, or alternatively a plant would use ultra-clean coal that provides gases on combustion that meet the required limits for entering the turbine. The exception to these options is the externally-fired combined-cycle process; in this process, a high-temperature heat exchanger is used to avoid the problems of hot gas cleaning. The energy yielded by combustion is transferred to a clean working medium in a heat exchanger. This working medium is suitable to drive the gas turbine.

The DCFTCC plant incurs lower capital costs relative to the SC and USC plants, operates at higher efficiency and with lower emissions. Consequently, considerable effort has gone into developing this concept. For example, a pilot plant was constructed by Westinghouse, utilising black coal, with hot gases cleaned using slagging combustion equipped with slag/ash removal capabilities (Newby and Bannister, 1998). The coal quality and associated combustion equipment, however, proved inadequate because the concentrations of volatile sodium and potassium compounds in the hot gases were too high, and the levels of particulate ash were higher than required for turbine operation.

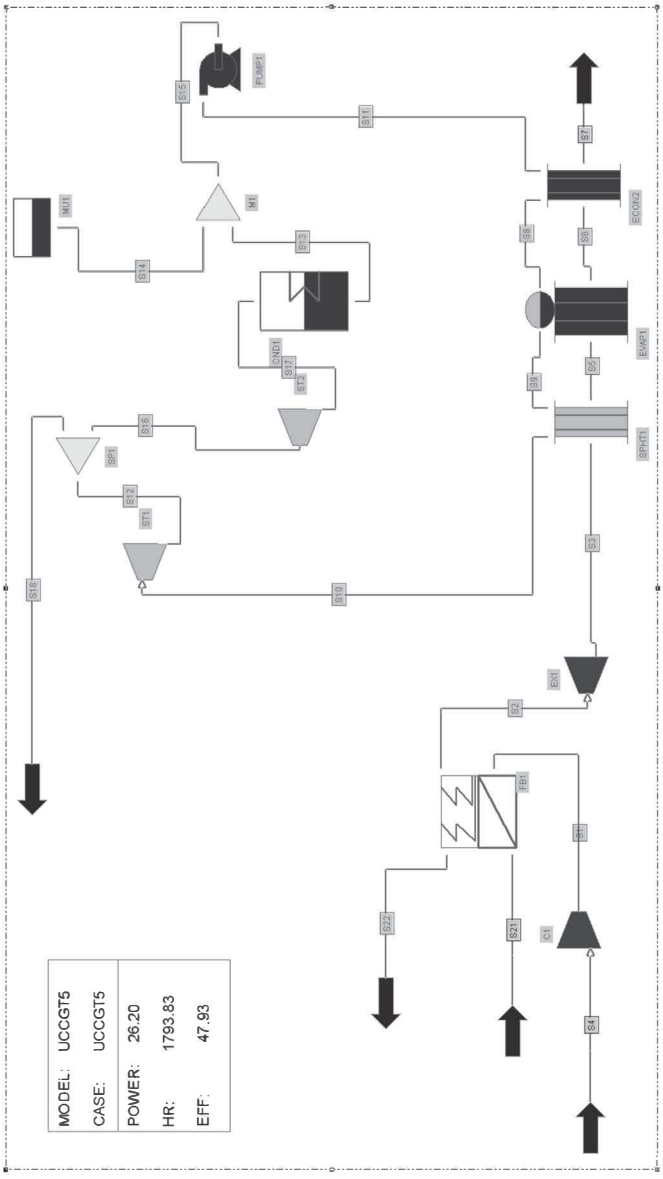

Figure 9-2. GateCycle™ Model of a 26 MW DCFTCC power plant operating at 47.9% efficiency.

The GateCycle™ package contains models of commercially available gas-fuelled turbine combined-cycle plants. A number of these models were modified by replacing the gas combustor module with a pulverised coal combustor module, and also extracting hot water from the power plant for use in the coal treatment plant. The CCT R&D Program has provided laboratory samples of ultra-clean coal, and these compositions were used as input for the fuel for these DCFTCC models. The results indicate the processed ultra-clean coal would meet the specifications required for turbines, assuming complete combustion of the ultra-clean coal (to avoid burning char particles from entering the turbine).

The CCT P/L process of low-rank coals removes Na, K, Fe, Mg and Ca present in the coal matrix, salts such as NaCl, inorganic sulphur, and also mineral particles mined with the coal to produce virtually zero-ash coal. An economical treatment of low rank coals into ultra-clean coal would bring significant benefits to the power generation industry, and would result in the reduction of emissions of CO_2, SOx and HCl. The DCFTCC modelling studies show a sensitivity to the temperature of the gases exiting the coal combustor and entering the turbine; coal with very low moisture would result in excessively high coal flame temperatures, and these gases would need to be cooled to suitable temperatures before they enter the turbine. Temperatures of between 1200°C and 1300°C could be obtained using ultra-low ash coal with moisture of 30-40wt%.

An example of a GateCycle™ model of DCFTCC is shown in Figure 9-2; this uses a wall-cooled coal combustor, and gases enter a three stage expander; the compressor feeds air into the coal combustor. This model produces a hot water flow rate of 3,680 kg/hr at 152°C for use in coal cleaning. The inlet temperature to the gas turbine is 1230°C, the stack flue gas temperature is 127°C, and the coal composition is 30wt% moisture, virtually zero ash, with a heating value of 18.2MJ/kg. The coal flow is 10,903 kg/h and the total mass flow is 174×10^3 kg/h, with a total ash loading of 0.4ppm, which is within the gas turbine's tolerance limits. The CO_2 emissions for this model are 648 kg of CO_2/MWh, and 0.79kg of SOx/MWh.

Figure 9-3 shows a GateCycle™ model that operates at about 52% efficiency; in this model, the coal combustor is not water-cooled, and the gases are expanded with an inlet temperature of 1315°C through the turbine. The coal flow is 26,723 kg/hr (the excess air in the coal combustor is 0.28 of the required amount for combustion), and the model generates 36.4 MW. The flue gas temperature is 130°C. Hot water (at 217°C) is extracted at 15,000 kg/h for cleaning and drying the required amount of coal, integrated for maximum efficiency. The coal moisture is 39wt%, and the ash loading

at the burner is 0.1121 kg/h for a total mass flow rate of 189,705.3 kg/h (particulates at 0.5-0.6 ppm), providing a gaseous stream with <300ppb volatile sodium.

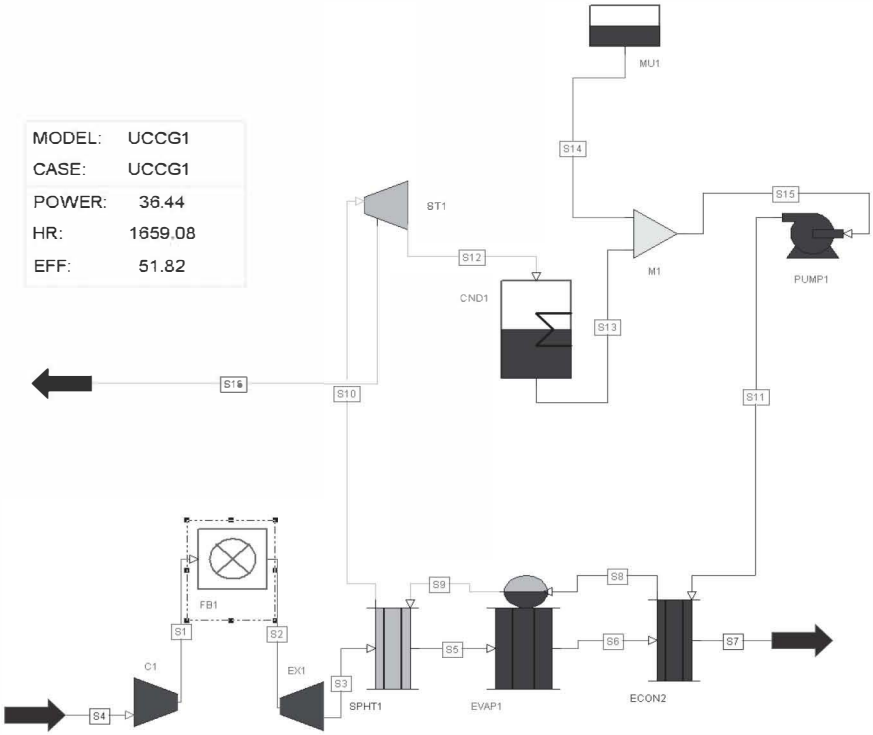

Figure 9-3. Model of a 36 MW DCFTCC power plant operating at 52% efficiency.

Figure 9-4 shows a GateCycle™ model of a larger power station; this design provides power generation efficiency of between 48% and 53% – we may speculate that a heat recovering system providing supercritical steam would increase the steam turbine output, and the plant would operate at a higher efficiency. Coal is fed at 160,020 kg/hr, and the coal contains 40.7wt% moisture with very low ash. If 50,000 kg/hr of hot water is taken at 469.9°C, the efficiency of power generation is 52%. If the amount of the hot water was increased to 150,000kg/hr, the efficiency would be 48.5%; the total thermal efficiencies of these configurations are 70-80%.

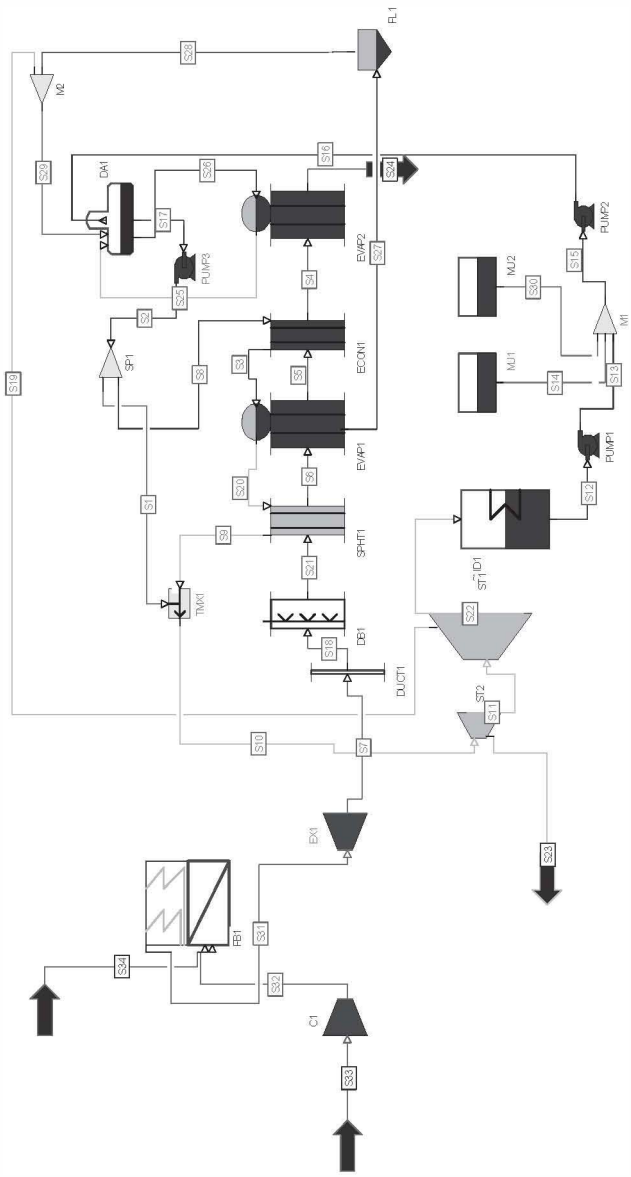

Figure 9-4. Model of a DCFTCC power plant that operates at 48-53% power generation efficiencies.

These three GateCycle™ DCFTCC models:

- Use coal burners interfaced to a turbine; this is a new component that needs to be developed for a commercial plant.
- Show that the quality of the CCT processed coal meets the specifications for turbine operation.
- Illustrate how low-grade heat can be used from the power block to provide hot water for the coal de-ashing and drying.

These computations show that a coal processing plant integrated to a DCFTCC power generation plant would operate at high overall thermal efficiency levels of about 80% and with power generation efficiency levels in the range of 48-52%.

Catalytic Coal Gasification

Integrated coal gasification in combined cycles (IGCC) has been extensively studied because it currently offers the cleanest coal-fuelled option. Stiegel and Maxwell (2001) made the prediction that

> ...gasification will be the heart of a new generation of energy plants, possessing both feedstock and product flexibility, near-zero emission of pollutants, high thermal efficiency and capture of carbon dioxide, with low feedstock and operating/maintenance costs.

Government and industry have sought to develop IGCC power plants, but in spite of significant advances and numerous developmental programs, the capital cost of such advanced new plants, and the risks involved with first-of-a-kind technologies, has prevented the widespread application of IGCC for power generation. The CCT programs discussed in Chapter One all included a zero-emissions goal for coal-fuelled power generation, and IGCC is considered an attractive option for this goal. Coal-based IGCC power generation is predicted by the DOE to achieve a large share of the electricity market due to the abundance and stable price of coal. * Majoumerd et al., (2014) examined the impact of coal rank (and quality) on commercially mature gasification plants (Shell, GE, Siemens, and ConocoPhillips gasifiers) within the context of the European H2-IGCC Project and CCS. They noted gasification performance is significantly affected by coal quality, which varies widely with rank; this is particularly

* Retrieved from https://www.netl.doe.gov/research/coal/energy-systems/gasification/gasifipedia/clean-power.

relevant to low quality coal, which contains high levels of ash, sulphur, chlorine, alkali metals, low heat value and low melting ash. These studies examined the performance of bituminous, sub-bituminous and lignite, and showed that the lowest overall efficiency penalty with coal quality was 5% (LHV basis) for the Shell gasifier when the fuel was changed from bituminous to lignite; GE's gasification technology had the highest CO_2 emissions for lignite coal. Conventional coal gasification incurs significant capital costs, and an additional drawback is the energy lost through the production of the high purity O_2 required in the gasifier. For example, a Shell entrained-flow gasifier with a 300 MW-IGCC power plant is reported to require 39.4-40.2 MW for the gasification system, air separating unit, coal treatment, and steam consumption (Ju and Lee, 2017).

Coal gasification, discussed in Chapters Seven and Eight, would produce varying quality syngas which is dependent on coal quality and the type of plant. The syngas is cleaned by removing ash particulates and pollutants such as are derived from chloride, sulphur and nitrogen in coal. The syngas may be used to fuel a combined-cycle power plant, or as feed for a Fischer–Tropsch plant (F/T) (van Dyk et al., 2006). In a typical commercial plant, the unconverted syngas is recycled, or reformed, to increase the amount of liquids produced in the plant. An alternate, hybrid plant would use these tail gases to fuel a combined-cycle power plant. The hybrid coal gasification plant may be designed to produce power and other products, such as methanol, F/T liquids, or various chemicals. This hybrid concept has attracted a great deal of research interest as it may offer ways to reduce CO_2 emissions with improved economics.

Coal gasification can also be designed to produce hydrogen by converting the coal-derived syngas into a mixture of H_2 and CO_2 using the water gas shift reaction, followed by removing about 90% of the CO_2 (usually with a solvent-based process); the hydrogen can be used with fuel cells to produce power.

Catalytic steam coal gasification is particularly interesting as it provides higher quality syngas with increased hydrogen. The higher quality clean syngas can be used to synthesise hydrocarbons of different chain-lengths in the F/T plant, as indicated by the following equation:

$$CO + 2H_2 \rightarrow 1/nC_nH_{2n} + H_2O$$

This chemistry ideally requires a H_2/CO ratio of two. The proportion of hydrogen in syngas from low rank coal gasification is low, and it may be increased *via* the water-gas shift reaction:

$$CO + H_2O \rightarrow H_2 + CO_2$$

The minimum H_2:CO ratio required for the syngas input stream to a F/T plant is reported at 0.67; however, syngas from brown coal has an upper theoretical ratio of 0.43 and would require a significant shift reaction to obtain the required ratio in the syngas, and this means a lower production of hydrocarbons, because CO is consumed to increase the H_2:CO ratio, and as the above equation shows, CO provides the C in the hydrocarbon molecule. These matters are important as the economics of an industrial plant are determined by capital costs and the production yields of liquids, and, for hybrid plants, the amounts of liquids and power (Mantripragada and Rubin, 2013).

Plants designed for liquids and power, or power only, are assessed on the basis of their capital costs and production rates, and the hydrogen content of the syngas directly affects production. Thus, methods that can increase the hydrogen content of syngas would be commercially attractive. Currently, steam is added to the oxygen to gasify the coal to provide additional hydrogen from the reaction:

$$C + H_2O \rightarrow H_2 + CO$$

The reaction between carbon and steam is slow and endothermic, and as discussed previously, the yield of H_2 can be increased if effective catalysts are used for this chemistry. Catalytic steam gasification offers a route to a higher yield of hydrogen in syngas. The theoretical increase in hydrogen from catalytic steam gasification is quantified by the following equation (the composition of brown coal is expressed as %molar, dry ash free; small amounts of sulphur and nitrogen pollutants are not shown and would be removed from the syngas):

$$C_{5.7}H_{4.9}O_{1.63} + 5.4H_2O \rightarrow 5.4CO + (5.4 + 2.25H_2) + 0.3(CO_2) + 0.2H_2O$$

The reaction of brown coal with steam yields an upper H_2:CO ratio of 1.4; this upper limit, however, would be difficult to achieve in conventional fluid-bed gasifiers. The endothermic chemistry needs heat, and this is provided by the exothermic reaction of char with oxygen ($C + \frac{1}{2}O_2 \rightarrow CO$ + heat).

Futuristic catalytic coal steam gasifiers may employ steam with perhaps a small quantity of oxygen, for thermoneutral operation, to facilitate catalytic chemistry between coal and steam. Laboratory results indicate that

the required chemistry between coal and steam would occur with iron catalysts in low rank coal at temperatures between 800°C and 900°C.

Catalytic steam gasification at lower temperatures has been used to produce a hydrogen/methane rich gas stream, with alkali and alkaline earth catalysts (Mondal et al., 2011).

Solar coal gasification concepts, consisting of hybrid solar/fossil gasification, have received some attention; such autothermal gasification of fossil fuel uses concentrated solar power as the source of process heat. With solar energy, the endothermic catalytic steam-gasification of processed coal would produce high quality syngas. The major drawback to such concepts is the intermittent nature of solar radiation, with additional challenges regarding an efficient heat transfer to the coal/gas mixture undergoing gasification. Kaniyal et al. (2013) present a conceptual design that uses concentrated solar radiation for a coal-to-liquids plant in an atmospheric pressure vortex reactor. This would accommodate the variability in the solar resource by utilising pressurised storage of syngas and oxygen to continue the plant's operation in the absence of solar heat. Zedtwitz and Steinfeld (2005) discuss the steam-gasification of coal in a fluidised-bed or a packed-bed chemical reactor, using an external source of concentrated thermal radiation for high-temperature process heat. They modelled temperature profiles, product gas composition, and the extent of the reaction, and compared these with measured values, obtained with a laboratory tubular quartz reactor directly exposed to high-flux irradiation. For the packed bed, the temperature increases monotonically because the internal radiative exchange approaches a conduction-like heat transfer within the bed. For the fluidised bed, the temperature increases rapidly in the first quarter of the bed and then reaches a constant value because of the strong fluidisation in the upper bed region derived from the 5-fold volumetric growth due to gas formation and thermal expansion. Above 1450K, the product composition was of an equimolar mixture of H_2 and CO. The syngas composition was significantly better than that obtained in autothermal gasification reactors which use the internal combustion of coal for process heat.

Catalytic plasma reformation of hydrocarbons for hydrogen production is of particular interest (Chen et al., 2008), and this technology has been applied to catalytic coal gasification using steam heated with plasma technology to enable the endothermic reaction between catalytic coal and steam, but this has not yet been commercialised. Messerle et al. (2016) discuss experimental investigations on the arc-plasma gasification of bituminous coal in steam and air, with thermodynamic calculations of various species over a wide temperature range. Their calculations indicate that specific power consumptions at lower temperatures for steam

gasification are 1.5-2 times higher than specific power consumption for air gasification. The power consumption, however, decreases for reactions with steam at elevated temperatures. Experimental results indicate the syngas yield for the coal steam gasification was 1.7-1.9 times higher than that obtained for air gasification of the coal. A high carbon gasification rate required temperatures 1.2-1.5 greater for steam gasification, compared to air gasification. An estimation of the economics for the production of syngas with plasma-steam gasification of low grade coal, based on laboratory experiments, is reported to be 40% less than that using conventional methods of syngas production. It is likely that plasma-assisted catalytic coal steam gasification would provide an improved syngas composition.

Plasma technology has undergone development mainly for hydrocarbon reforming with steam and with a mixture of steam and oxygen. Non-thermal plasma processes have been developed with lower power consumption, and these have been reviewed by Petitpas et al., (2007), who discuss the major characteristics of plasma reforming and compare the performances of a number of systems.

Further developmental work on a thermoneutral approach is required for application to catalytic coal gasification with steam. This concept has the potential to be developed into a zero-emissions coal-fuelled plant. The available experimental data show that processed low rank coal containing iron-hydroxyl complexes undergoes rapid catalytic chemistry with steam, with a higher yield of hydrogen in syngas. These data have been used to model configurations for zero-emissions catalytic steam coal gasification that utilises CO_2 as a feedstock for methanol production.

Power Generation with CO_2 Utilisation

The ultimate goal of all CCT R&D programs worldwide is viable zero-emissions coal-fuelled power generation plants. A zero-emissions concept that uses processed low rank coals discussed in this volume, with CO_2 utilisation, is the basis for general modelling to indicate the factors that would impact on commercialisation. Schematics of the integrated CCT processed coal plant with higher efficiency power generation were presented in Chapter Five.

Interest in CO_2 utilisation is considerable, and a number of marketable products from synthesis with CO_2, may provide the impetus for commercialisation. Converting CO_2 into fuels and materials, particularly methanol, offers a strategy to tackle the immediate issue of global climate change and the long term issue of fossil fuel depletion. Currently, global estimates of low-cost high-concentrated CO_2 are estimated at around 500

million tons (<US$20/ton) annually, mostly from natural gas processing and fertiliser plants. CO_2 produced from power, steel, and cement is estimated at 18,000 million tons annually, captured at higher costs (US$50-100/ton). This is contrasted with utilisation of CO_2 globally of about 80 million tons per year, and the bulk of this is for enhanced oil recovery in North America (Zhu 2018; Styring et al., 2014). The cumulative amount of anthropogenic CO_2 that needs to be stored and captured to meet the 2°C target by 2050 is estimated at 90 gigatons (CCS, 2011). These data emphasise the need for lower emissions of anthropogenic CO_2, and also illustrate the scale of the problem; the major barriers to the implementation of zero-emissions power with the utilisation of large amounts of anthropogenic CO_2 are costs of capture and subsequent synthesis. A combination of low fuel cost, high efficiency, use of surplus (low cost) power, and a revenue stream from valuable products synthesised with CO_2 may go some way to addressing costs. A regulatory framework that mitigates risks in the development and commercialisation of CO_2 utilisation may encourage investment in such technology.

A systematic approach to CO_2 reduction from plants fuelled by low cost processed coal would be to commence with SC and USC power plants designed initially for high efficiency air combustion, with the ability to upgrade to an oxy-combustion coal boiler and to a zero-emissions plant by adding a CO_2/H_2 synthesis plant. Oxy-combustion has been discussed in the report 'Oxy-Combustion Technology Development for Industrial-Scale Boiler Applications' (Levasseur, 2014). Such work has shown that there are no technical barriers to the continued development and commercialisation of oxy-combustion, and these developments show performance, emissions, and thermal behaviour similar or better than air-fired boilers. General Electric (GE) has developed oxy-fuel combustion boilers for fossil fuels with a mixture of pure oxygen and re-circulated flue gas, resulting in CO_2-rich flue gas. Pure oxygen is supplied in this example by a cryogenic air separation unit. This is adaptable to most boiler and fuel types, and can be scaled up to the 1,000 MWe range of power plants.*

Conceptually, a zero-emissions plant may include a water electrolysis plant to supply O_2 for coal combustion, and H_2 for reaction with CO_2.

Cau et al., (2018) have modelled conventional air-blown coal-fired steam power plants, and compared these with full and partial oxy-combustion units to provide a detailed techno-economic analysis of a USC steam power plant equipped with CCS. They varied the oxygen concentration from about 21% (conventional air-blown combustion) to 95%

* For more information, see https://www.ge.com/power/steam/co2-capture/oxy-combustion.

(full oxy-fuel), and evaluated the performance using simulation models with Aspen-Plus 7.3 and Gate-Cycle™ 5.40. Their results indicate oxy-combustion can be used for CO_2 remediation.

Future plants may also utilise power cycles running on carbon dioxide at supercritical pressure and temperature (Crespi et al., 2017). This cycle converts thermal energy into electrical energy using supercritical CO_2 as the working fluid medium, with efficiencies that may exceed 50%, with a smaller size and a simpler layout, which, coupled with other technological innovations, may result in reductions in capital and fuel cost. While some technical challenges need to be addressed, supercritical CO_2 cycles for power generation may use energy sources such as processed coal, gas, nuclear, solar thermal, and waste heat (Zhu, 2017).

It is understood that these concepts require considerable development for commercial application, and CO_2 capture and utilisation technology needs to balance incurred costs with the revenue stream. A future is envisaged that would mimic nature, in that CO_2 would be used as a raw material for the production of valuable material. The impediments to CO_2 usage, however, are considerable, due to the scale and cost of capture, and also the cost of additional precursors required for a synthesis; for example, converting CO_2 to methanol requires hydrogen. Cormo et al., (2018) carried out simulations of carbon capture from a number of plants to assess the performance of chemical gas-liquid methyl-di-ethanol-amine absorption and gas-solid CO_2 calcium looping technologies. They showed poly-generation improved a plant's flexibility with the co-production of various totally and partially decarbonised energy carriers (e.g. hydrogen, SNG, methanol, and synthetic F/T fuel).

High efficiency power generation (SC, USC, CFTCC, and catalytic gasification), with oxy-combustion (and catalytic steam gasification), ultimately yield flue gas consisting of CO_2 and H_2O. The CO_2 is separated from H_2O and stored for reaction with H_2. Water is a by-product that would be used in a water electrolysis plant to provide the required H_2 and O_2; costs are curtailed if the electrolysis plant uses low-cost surplus power from the grid, made available during periods of low demand. The additional costs incurred for such a zero-emissions plant would be offset by revenue from the sale of methanol (or other valuable products).

Ultimately, the concept is to develop methanol-fuelled power generation with oxy-combustion, fuelling a DFTCC, in which the resulting CO_2 is converted into methanol, recycling CO_2, and thereby achieving zero-emissions power generation utilising H_2 and O_2 produced from the electrolysis of recycled water. Methanol can be used as fuel for power generation, and for producing valuable materials. Olah et al., (2009) and

Goeppert et al., (2014) discuss the chemical recycling of carbon dioxide into methanol and/or dimethyl ether, and the synthesis of other valuable products. The concept is of an inexhaustible source of recyclable CO_2, while mitigating human-caused climate change. Hydrogen needed for the chemical recycling of carbon dioxide can be obtained in the long term from water electrolysis, and in the short term from existing significant hydrocarbon sources.

Methanol can also be utilised for producing ethylene and propylene, with acidic zeolitic solid catalysts commonly used for the chemistry:

$$2CH_3OH \underset{+H_2O}{\overset{-H_2O}{\leftrightarrow}} CH_3OCH_3 \overset{-H_2O}{\rightarrow} \underset{\text{ethylene}}{H_2C{=}CH_2} \text{ and } \underset{\text{propylene}}{H_2C{=}CH{-}CH_3}$$

Ethylene and propylene are used to make polyethylene and polypropylene, or a variety of other products. Methanol is also the starting material in the methanol to gasoline process for the direct production of gasoline, diesel fuel, and aromatics. Olah et al., (2009) conclude:

> Carbon dioxide thus can be chemically transformed from a detrimental greenhouse gas causing global warming into a valuable, renewable and inexhaustible carbon source of the future allowing environmentally neutral use of carbon fuels and derived hydrocarbon products.

Currently a commercial plant operates in Iceland that captures CO_2 and converts it into methanol, using geothermal power with a water electrolysis plant to provide the required H_2 (Kauw et al., 2015). This demonstrates the commercial viability of CO_2 remediation through methanol synthesis, which can play an important role in an anthropogenic carbon cycle, and may ultimately move towards a methanol economy.* It is emphasised that methanol has many uses – as a fuel for internal combustion engines, fuel cells, fuel for turbine power plants, etc. (GE, 2001) – and can be transformed into numerous valuable products, including the petrochemical products that are currently obtained from fossil fuels.

Achieving the ultimate goal of zero-emissions requires considerable development and testing. Consequently, the CCT P/L modelling effort discussed here has used a general approach that considers a spread of results, which may meet various expectations. The CCT P/L models should be considered within the context of an orderly route to commercialisation. Practical considerations would require that future power generation plants use processed low rank coals initially as low-cost fuel for high efficiency,

* For more information, see http://www.methanex.com.

with resulting lower CO_2 emissions, but with the capability to upgrade to capture CO_2 for use in the production of high value products.

The availability of hydrogen is a critical component for coal-fuelled electricity generation with zero-emissions. The current technologies available for industrial hydrogen production are the gasification of fossil fuels (which provide H_2 and CO_2), and water electrolysis, which provides H_2 and O_2. Renewable energy-based processes of hydrogen production are solar photochemical and photobiological water decomposition, and the electrolysis of water coupled with photovoltaic cells or wind turbines. Water electrolysis currently accounts for less than 1% of total hydrogen production, but this is an active area of research, particularly with renewable power (Buriak et al., 2018). For example, work has shown that nano-TiO_2 is more effective as a photocatalyst for water decomposition, and semiconducting nanoparticles of less than 10 nm exhibit significant improvement in the photocatalytic performance due to the quantum size effect (Singh and Dutta, 2018). It is generally understood, however, that these types of renewable sources would not reduce the costs of hydrogen production in the foreseeable future.

Hydrogen as an energy source has been widely discussed, and Veras et al., (2017) have reviewed hydrogen production technologies. Industrial production of hydrogen during 2007 is reported to have been about 48 million metric tons, mainly from fossil fuels, with about half of this coming from methane reforming (global consumption of hydrogen is reported for 2018 at 290 billion cubic meters). Most of the hydrogen is used to produce ammonia, and refineries use the second largest amount of hydrogen for chemical processes such as removing sulphur from gasoline and converting heavy hydrocarbons into gasoline or diesel fuel. Food producers use a small percentage of hydrogen to add to some edible oils through a catalytic hydrogenation process (Navarro et al., 2007; Baykara, 2018).

The costs of hydrogen production have been critically examined (NREL, 2009) and research is ongoing; for example, a solid oxide electrolysis cell (SOE) has been developed that can operate at higher conversion efficiency levels than current commercial electrolysers, achieving more than a three-fold increase in hydrogen production rates (Wood et al., 2016). Work on various approaches for water electrolysis is discussed by Zhu (2018).

General Considerations of Economics and Efficiency

Financial (or economic) models of power generation plants are used to assess the commercial viability of the various plants for generating electricity. The outcome from these models is a levellised cost of electricity (COE) which is a measure for all commercially available power generation

options, based on data from operational plants found in various regions in the world. This enables a comparison of the performance and cost for each of the commercially operational plants. A detailed economic analysis, required for the construction of a new plant, provides the constant real wholesale price of electricity that meets the financing costs, debt repayments, income tax and cash flow constraints associated with the construction, operation and maintenance of a power generating plant (Gross et al., 2009; Shuster, 2009).

It is difficult to apply this approach to futuristic coal processing technologies discussed in this volume, focussed as they are on integrating a plant to provide high quality processed coals to fuel proposed future plants, because data are not available from such operational plants. Investment in the proposed new technology is usually assessed with the internal rate of return (IRR), which establishes theoretical long-term profitability and potential risks, while net present value analysis (NPV) is used to provide confirmatory results.

The appropriate model for investment discussions has, as its primary goal, the factors that yield an IRR (and NPV) that would meet investors' requirements, which relate risk to reward. The World Energy Council's report 'Cost of Energy Technologies' (2013) states:

> The likelihood of a significant amount of new coal generation coming online in Western Europe, the US and Australia is low. For the purposes of this report we have assumed a 10% cost of equity for our base hurdle rate, but indications are that the actual hurdle rates demanded by investors in order to induce them to supply capital to a new build coal plant may be on the order of 18% or higher, pushing the levelised COEs up even further.... In the case of both Europe and Australia any new plant would be subject to an uncertain future carbon price, which is the main reason why investors consider these plants so risky. Despite this – in continental Europe, new coal plants continue to come online in Germany where the nuclear ban and other market-specific factors will likely drive new additions for the next few years.

Currently, policy needs to be developed to encourage the closure of aging plants and the introduction of new, higher efficiency plants; policymakers should consider how fixed and sunk costs are treated by policy changes. While it is not the role of policymakers to deliver profits to power companies, investors will consider risks, and need to feel confident that a new plant would be profitable over the business cycle, or, for a power plant, would operate profitably over its lifespan. Models may be used to assist policy development, such as the multi-regional, multi-sector, general equilibrium model, discussed by Zhang et al., (2017), which is designed to simulate existing and proposed energy and climate polices in China, and

assess their impact on the deployment of new energy technologies; such models include factoring fuel competition, environmental outcomes, and the impact of energy policy on the economy within a global context. Zhao et al., (2017) demonstrate the uncertainty in predicting the demand and supply for power generation in China. They employ a levelised COE as criteria in models of a nationwide survey on the economics of coal power. This economic analysis highlighted the unusual recent boom of coal power investment in China, considered to be due to incomplete market reform in the power sector. The changes in the demand and supply of electricity in China have occurred at an unprecedented speed, and this modelling indicates gloomy future prospects for coal power. They predict that, by 2020, the IRR for coal power in most provinces in China will fall to below the average, or in some cases will fall to a negative value.

Phillips and Newell (2013) examined the importance of politics and the nature of India's economy in understanding the development of clean energy sources and technologies. A broad range of institutions exert political influence regarding benefits and costs. The authors go beyond an analysis of technocratic aspects of governance to provide an appreciation of the political nature of the trade-offs and debates about India's energy future. They note that even if India increases its renewables 40-fold by 2032, this will only amount to 5.6% of India's total energy requirement. Kumar et al., (2015) examine factors related to the NPV method of estimating coal-fired power plant economics in northern India, using data and the performance of a 210 MW subcritical electricity generation unit. This parametric study indicated how sensitivity to plant life, interest rates, and the escalation rate impacted on plant economics. The payback period was estimated at ~10 years, and beyond that the plant begins to make a profit. The fuel cost was noted to be sensitive to these calculations, while operating and maintenance costs increased with the plant life. India has an aspirational goal that 40% of its electricity will come from non-fossil fuel capacity by 2030. This would lower the proportion of coal in the country's energy supply, and coal plants will need to operate with a flexibility that would enable backing up intermittent energy sources to meet the requirements of India's energy policy.

The potential for commercial applications of future coal-fuelled power generation may be assessed *via* comparative techno-economic modelling to obtain an indicator of the costs of CO_2-free power generation using the appropriate configuration of available technologies. These models compare the technical and economic aspects of plants' configurations. Pettinau et al., (2017) discuss such a comparative assessment of USC and IGCC plants to estimate potential applications of CCS technologies. In this case, the

comparison was between plants without CCS and plants with CCS, using conventional technology for a reference thermal input of 1000 MW, with simulation models by Aspen Plus 7.3 and Gate-Cycle™ 5.40. Aspen-Plus can simulate gasification with conditioning and purification processes of syngas and flue gas, and Gate-Cycle™ models power generation. This type of economic assessment highlights the uncertainties arising from the variability of the cost of fuel and of CCS. The assessment indicated USC could be preferable for power generation without CCS, with a levelised COE of 38.6 €/MWhr, compared to the IGCC with 43.7 €/MWh. With CCS, however, the COE was 59.6 €/MWh for the IGCC, compared to 63.4 €/MWh for the USC. The COE for USC oxy-coal combustion with CCS was 62.8 €/MWh.

As data from a commercially operational power plant using new CCT coal processing technology are not available, a conventional economic assessment of the levelised COE modelling study cannot be carried out. Clearly, the potential for improved coal-fuelled power generation is indicated by the R&D data, and an alternate approach is needed to model economic factors that would illustrate the potential of integrated CCT coal processing for high efficiency power generation. This alternate approach uses models that emphasise the potential economic outcomes that may be derived from adding a new coal processing unit onto a commercially operational coal-fuelled power plant. All available data derived from commercially operational plants are applied to the model, and these are supplemented with assumptions on the likely costs for additional modules required for the future coal processing plant. For example, data are available for a SC power plant with facilities to dry low rank coal. Data from developmental work on coal processing may then be added to the model, to illustrate the potential benefits that may be derived from this addition to the power generation plant. Additional information may be derived from ongoing developments, such as oxy-combustion, as well as data on water electrolysis to produce oxygen and hydrogen.

The results from this modelling approach are encouraging, and indicate a new coal treatment plant may be integrated with a commercially mature power generation plant to provide data that support the potential for relatively lower COE and lower emissions. Additional modelling may be carried out on the ways a high efficiency power plant could be upgraded to zero-emissions performance. Positive outcomes from these models would encourage and support the development of policies that would support low- to zero-emissions outcomes. These models would give an indication of the potential returns on investment (and identify risks from fuel treatment

innovations), and of the anticipated reductions in emissions from such future power generation.

This comparative economic modelling that has been carried out considered current brown coal-fuelled subcritical plants and a future model that would encapsulate the CCT P/L coal treatment. This commenced by specifically using data from an operational low-rank coal-fuelled plant as a reference case for a comparison of the COE with that for a future CCT P/L SC power plant. Data have been used from current brown coal-fuelled subcritical power stations operating in the Latrobe Valley, Australia. It is understood that we are comparing future CCT plants with current operational plants to indicate the potential benefits of a future SC power plant with an integrated CCT P/L coal processing plant. The input data for this modelling consisted of the plant's availability, efficiency, the amount of mined brown coal fed to the 1000 MW subcritical plant, the cost of mined coal per year, the plant's utilisation per year, capital and finance costs, and operating and maintenance costs. The output consisted of cost per MWh of electricity, and CO_2 emissions as kg/MWh for a specified plant life of 30 years.

The comparative modelling discussed here cannot provide a conventional levelised COE for the CCT P/L SC plant, but instead provides a comparative calculated cost/MWh of electricity, and emissions intensity, to illustrate the differences with conventional subcritical plants. Positive results for the CCT P/L SC model result from the low cost of the mined brown coal, the higher efficiency, and the higher plant utilisation, accompanied with lower CO_2 emissions. This exercise illustrates the benefits that may be derived from using the CCT P/L process to convert low quality, low rank coal into high quality coal to fuel high efficiency plants. The CCT P/L SC model output has also been compared to results for a model of a SC plant fuelled with Australian black thermal coal.

The modelling provides a comparison between:

- A reference brown coal-fuelled subcritical power station using operational data averaged over a given period.
- A CCT P/L processing unit integrated with a SC plant, which is fed with the same brown coal used for the reference case.
- A SC plant fuelled with Australian black thermal coal.

The data are sourced from 'Electricity and Gas Australia 2009' by the Electricity Supply Association of Australia and 'Energy in Australia' 2008 and 2009 by the Australian Bureau of Agriculture and Resource Economics. The models were constructed using the tonnage and heat content data averaged for all brown coal-fuelled power plants in Australia. The reference

model provides data on CO_2 emissions and overall COE values for a brown coal-fuelled plant, and these are shown to be similar (to within variations observed in the operational plant) to the reported data, averaged for four operational brown coal power stations.

The schematic in Figure 9-5 is an outline of the CCT SC plant operating at 43-45% efficiency. Capital costs are typical for a SC plant (see below), with an addition to these costs of 15-20% for the coal treatment plant. The assumptions in the comparative modelling were:

- Same quality of mined coal and the same cost, fed to each plant.
- Efficiencies of 30% for the subcritical plant, and 43-45% for the SC plant.
- The CCT P/L SC plant was fuelled with non-fouling coal fed from the integrated coal processing unit.
- Plant availability was 85% for the subcritical plant, and 95% for the SC plant.
- Similar operating and maintenance (O&M) costs – the higher efficiency for the SC plant resulted in lower O&M costs per MWh for the SC plant.

The favourable comparison of the CCT P/L SC model with the SC model fuelled with black coal highlights the impact of the low cost of the fuel, compared to the higher cost of black thermal coal, resulting in a lower COE for the CCT P/L SC plant.

The calculations were repeated to examine the impact on COE from changes in any of the following:

- Increase and decrease in capital costs.
- Variations in O&M costs.
- Variations in plant availability.
- Variations in the price of black coal.
- An emissions trading scheme imposing a cost on CO_2.

The calculated COE for the reference case was similar to published values for brown coal subcritical power plants in Australia; the value of COE for the CCT P/L SC plant was lower by 25-30% and CO_2/MWh emissions were lower by 38-40% relative to the reference brown coal subcritical plant.

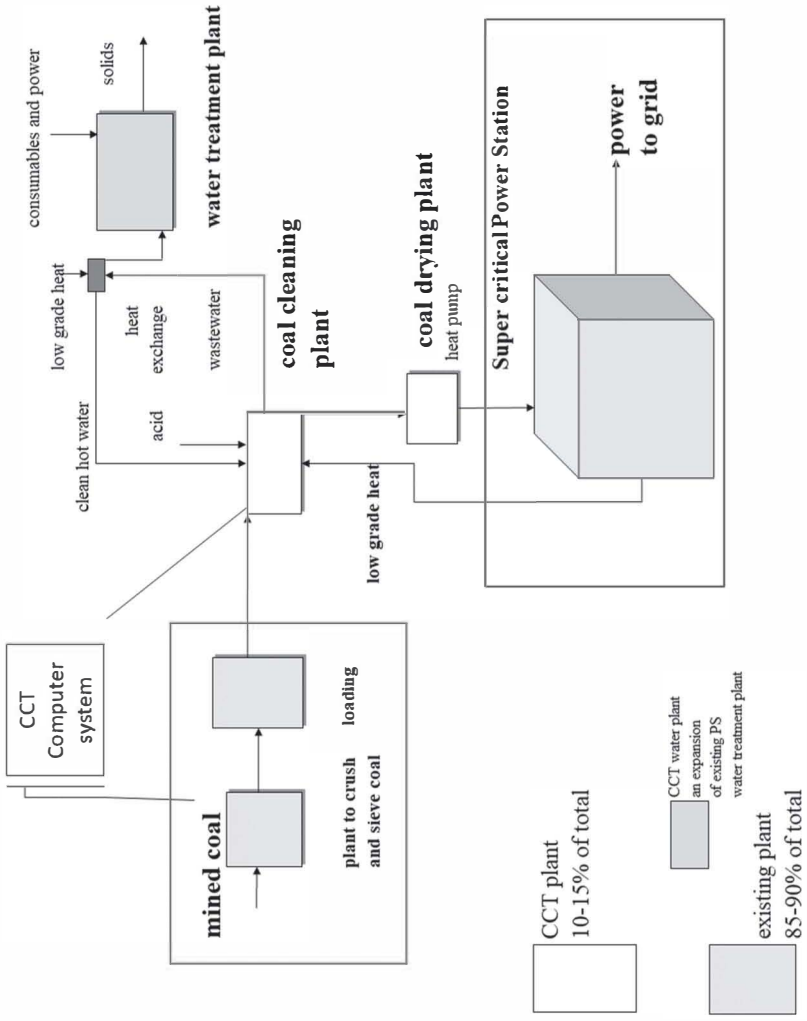

Figure 9-5. Components of a future CCT P/L-SC power plant used in modelling.

Comparative modelling was also carried out for DCFTCC using CCT P/L processed coals. The results for models using ultra clean coal were compared to those for a gas-fuelled combined-cycle plant. The high cost of gas resulted in a higher COE for a gas-fuelled combined-cycle plant relative to the CCT-DCFTCC option, but the overall risk in commercialising is high

for the CCT P/L option as it requires a constant feed of virtually zero-ash coal.

Models were also constructed of a hybrid catalytic coal gasification plant in which various compositions of syngas were computed that reflected the proportion of hydrogen obtained in laboratory measurements from the catalytic coal gasification with steam. Based on the composition of the syngas, an estimate was made of the yield of liquids from the Fischer-Tropsch (F/T) hydrocarbons synthesis. The remaining gas was used to fuel a combined-cycle power plant (Figure 5-4 shows an outline of this concept). It is not possible to use a reference case for this model of the gasification of Victorian brown coal; instead this modelling was used to test a number of syngas compositions that may be obtained from catalytic steam gasification of processed catalytic coal, with the F/T output reflecting these various syngas compositions.

The hybrid model was also extended to examine methanol production from CO_2 and H_2, to speculate on the benefits that may occur from processing the low cost brown coal and lignite into the stipulated high quality catalytic coals. The various models examined for catalytic steam gasification cannot provide a valid assessment of the risks that would be relevant to investment decisions on commercialising the new technologies. Financial models, however, may be employed to examine the information that may be relevant to future decisions, based on given values for discount rates, IRR and NPV.* This financial modelling may also be used to show the value(s) for the selling price of electricity that would encourage the replacement of old plants with new plants for power generation.

It is impossible to create a model that would fully capture all difficulties, benefits, or improvements in environmental outcomes for innovations in all generating options. Variations in regions, and the increasing emphasis on environmental impact(s), make standardised modelling extremely difficult; environmental factors also require a clear regulatory framework to assess their impact on IRR. Currently, such regulations differ in global regions. Other variations include matters such as labour and material costs.

Variables and Estimates – **CCT P/L SC**: The initial model provides a calculated value of the COE based on costs for coal, capital, finance, and O&M – unknown factors may indicate greater risk for future coal-fuelled plants; consequently, we may use the initial calculated COE as a starting point, and from this we may speculate on how assuming higher values for the selling price of electricity would impact on estimates of calculated IRR and NPV. The capital costs for the CCT model were varied over a range that

*An example of financial analysis is the paper by Simshauser and Ariyaratnam (2014).

would reasonably cover the likely cost of coal treatment. The data were varied to reflect variations due to regional and plant configuration factors, and the model thus necessarily provides a range of values for IRR and NPV. Eventually, the impact of better environmental outcomes would also need to be quantified, and in this way the CCT modelling would be further refined. Variables that cannot be captured by the current financial modelling include uncertainty in particularities of any specific plant configurations that may impact on costs, and electricity supply and demand situations in regions that may result in differing prices at which power is sold to the grid.

Capital costs for a supercritical coal-fuelled plant are available from a number of organisations.* Costs are often based on a plant configured with carbon capture and storage, and in these capex is considerably higher than for a conventional SC plant. Additional capex estimates are needed for a plant required to meet Hg, SOx and NOx emission regulations in various regions. Thus capital costs could span a very wide range for differing plants, as values have been published from a low of US$1,000/kWh to an upper value of US$3,500/kW.

The CCT SC model, operating with non-fouling brown coal, has low sulphur and extremely low mercury levels, and a flue gas cleaning plant is not required; the assumed efficiency is 45% (overall thermal efficiency at 80% with an integrated CCT coal treatment plant), the utilisation factor is >95%, and the power station is situated adjacent to an open-cut brown coal mine that provides coal at AU$5 per ton.† It is reasonable to use capex for this in the range $1,800-$2,200/kW. Additionally, the CCT treatment plant is able to remove inorganic/mineral pollutants from the brown coal, resulting in lower emissions of pollutants. The modelling considered a range of capex estimates to assess the impact of higher capital costs on IRR. Interest charges are additional variables, and the models varied these between 4% and 12%. Assessing financial instruments for assets such as power stations requires specialised input which is outside the scope of this general treatment. The modelling results of IRR and NPV, with the selling electricity price varying between $50-$80/MWh and a capex of $2,000/kWh, at a 5% interest rate, are listed below.‡

* World Energy Council report (2013) and data from the IEA.

† Henceforth, all prices are given in AU$ unless otherwise specified.

‡ These results are purely illustrative.

Selling Power Price	IRR (pre-tax)	NPV (post-tax)	NPV (pre-tax)
$50	6.1% (8.6%)	-1,715,142,431	- 1,067,316,374
$70	11.2% (15.1%)	-256,567,028	+1,010,764,074
$80	13.5% (18.2%)	+472,720,673	+2,049,804,297

- *DCFTCC Power Plant*: The results for models of CCT P/L ultra-clean coal, integrated to fuel a DCFTCC plant, are lower calculated COE and low emissions; this is because of the lower capex relative to SC plants and the low cost of mined low rank coal. The critical assumption for this model is the ability to produce coal that would continually meet the stringent properties at the scale required for baseload power generation. Thus, while this option presents the greatest potential for lower COE with low emissions (and higher IRR), it is also an option that needs considerable development.

Hybrid catalytic steam gasification: This modelling is exploratory, and is discussed here to illustrate why this concept presents great potential for zero-emissions technology. A futuristic hybrid plant was modelled as a complex consisting of three production streams: power, hydrocarbons suitable for premium quality diesel production, and methanol. The model uses 10 million tons of mined brown coal annually, and from this, a syngas composition is based on ≥50% of carbon in coal reacting with steam, and the remainder with oxygen. This model's annual production is 2.1 million tons of liquids, 490 MW of power, and 1.8 million tons of methanol. The production rate, or yield of hydrocarbons, is based on established data that directly relate the yield of hydrocarbons with the amount and H_2:CO ratio of the syngas. The yield of methanol is also based on published data for a plant using CO_2 and H_2 to produce 99% pure methanol. The model assumes surplus power is available for a water electrolysis plant at off-peak prices (assumed at $20/MW). The capital costs, for simplicity, are divided between these three streams (total capex $7 billion): (1) the combined-cycle power plant at ~$0.5 billion, (2) the gasification and F/T hydrocarbon synthesis plant at $2.5-$3 billion, and (3) the methanol and electrolysis plant at $3-$4 billion. The higher capex for methanol is appropriate as this includes CO_2 storage and the production of oxygen and hydrogen from water electrolysis.

For illustrative purposes, a range of selling prices were used for this model: power sold to the grid of up to $100/MWh, hydrocarbons at $70-$75/barrel ($560-$600/ton), and methanol with a very wide price range of $400-$1500/ton. Interest rates were 8%, dividends 12%, and tax 30%. The results from this model indicate large returns on investment may be realised at high selling prices for power, hydrocarbons, and methanol. For example, a selling price for power of up to $100/MWh results in an IRR of up to 27%, while the stipulated range of the price for methanol results in an IRR of 8%-

17%, and for hydrocarbons an IRR of 12% (a positive NPV was obtained for all products).

A fully integrated complex presents the best option for a viable zero-emissions concept, but assessing the long term profitability requires greater sophistication in modelling that would include historic data on price movements, and forecasts of future demand and supply for power, hydrocarbons, and methanol. The potential for zero-emissions power, however, should attract significant support from industry and governments for this concept.

We can illustrate the variations in the modelling outcome for the CCT catalytic-hybrid by considering the price movement for industrial grade methanol. Historically, industrial (bulk) methanol has been reported at ~€430/ton (about $683), but prices as low as ~€200/ton (about $320) have also occurred, and at this price the IRR and NPV for methanol would be considerably lower. Additional variation occurs in the price of oil, and this would impact on the price for hydrocarbons or diesel from the F/T plant; however, a good price may be anticipated for sulphur-free premium quality diesel. Investment in a coal-hybrid zero-emissions plant would be more likely if surplus power were to be made available at low prices from the grid for the water electrolysis production of H_2 and O_2.

There are also difficulties with distributing capital costs for a CCT integrated complex into three distinct plants; this is especially difficult if a solar power plant is included in the complex. Finally, methanol is one of a number of valuable products that can be produced from CO_2 and H_2. If the model of the CCT-hybrid uses the lower selling prices for hydrocarbons and methanol, as well as the high estimates of capex, the IRR and NPV would be significantly lower than those discussed above. The return from power is again estimated to yield a high IRR, and a combined liquids and methanol plant is likely to provide an IRR in the range 8-18%. This model does not include royalty payments.

Kler et al., (2018) discuss modelling for the production of methanol and electricity from the gasification of brown coal, and they show the economics are sensitive to the price of methanol. Their modelling considers the specific cost of methanol from US$310/ton to US$420/ton; the lower value corresponds to the natural gas cost and the upper value to the cost of methanol used in the chemical industry. This study points out the potential for an acceptable IRR (in the range 13-22%) and NPV for the production of power and methanol.

A life cycle assessment (LCA) is discussed by von der Assen and Bardow (2014) for the production of CO_2-based polyethercarbonate polyols from a lignite power station with a pilot plant extracting CO_2. The LCA

methodology may be used to evaluate the environmental impacts of products and processes along their entire life cycles, but it has not been standardised; these authors use an industrial setting to show that the production of polyols with 20wt% CO_2 in the polymer chains would result in a reduction of GHG emissions of 2.65-2.86 kg CO_2-eq per kg utilised. When they compared the production of conventional polyether polyols, GHG reductions would be 11-19%, which can be shown to result in up to 3 kg CO_2-eq emissions avoided per kg CO_2 utilised, and the use of fossil resources can be reduced by 13-16%. These reductions may increase by increasing the CO_2 content in the polyols. They indicate that with an average CO_2 content of 20wt%, a theoretical production of polyethercarbonate polyols could utilise up to 1.6 Mt/yr CO_2 as feedstock.

Sakamoto and Zhou (2000) modelled a plant with CO_2 capture, which includes solar power for a CO_2/H_2 synthesis of methanol. They discuss a CO_2 recycling system utilising photovoltaic power generation for water electrolysis. They quantify the costs of materials and also provide an energy analysis for the life cycle of this system. The amounts of concrete and steel that would be used to construct the plant represent the major costs, and the largest fraction of energy consumption is for the construction of the photovoltaic power generation facilities.

The synthesis of methanol from hydrogen and carbon dioxide has additional value due to the social and environmental returns from zero-emissions of GHG. It is preferable to manage a grid so as to use inexpensive power (and renewable power if available) during low demand periods, to provide the electricity needed for the green methanol production. This would require management of the grid for a long term supply of low-cost power to the facility.

Methanol is currently produced using syngas obtained from natural gas, but coal gasification is the alternative for large scale production in regions without gas, or if the price of gas is high. Riaz et al., (2013) reviewed the use of methanol worldwide, discussed the major processes for its production, and highlighted areas for further development to enable good economies. They outlined the multiple uses of methanol, and pointed out that methanol is preferable to hydrogen as a source of energy, as it is easier to store and distribute. In addition to its current uses, methanol can be blended with gasoline for use in transportation, used to fuel turbines, and used in fuel cells.

The chemistry for methanol production is summarised by the following reactions:

$CO + 2H_2 \rightarrow CH_3OH$ ΔH -128 kJ mol^{-1} at 298K
$CO_2 + 3H_2 \rightarrow CH_3OH + H_2O$ ΔH -87kJ mol^{-1} at 298K

The reverse WGS reaction occurs in parallel:

$CO_2 + H_2 \rightarrow CO + H_2O$ ΔH +41kJ mol^{-1} at 298K

The production of methanol from CO_2 hydrogenation has been the subject of many studies. More active catalysts may permit operations at a lower temperature and/or improve the economics through higher conversion rates leading to higher production. Yang et al., (2013) have provided insights into the reaction mechanism of methanol synthesis from $CO/CO_2/H_2/H_2O$ mixtures using copper-based catalysts, to determine whether the carbon in the methanol product comes from CO or CO_2. They show that as the temperature is lowered, the dominant source of carbon in the methanol product gradually shifts from CO_2 to CO, but the TOF is lower. Their results also show that water or water-derived surface species play a critical role in the conversion of both CO_2 and CO into methanol.

Van-Dal and Bouallou (2013) discuss the design and simulation of CO_2 capture from the flue gas of a coal-fuelled power station, using the captured CO_2 for methanol production. The hydrogen is produced by water electrolysis using carbon-free electricity. They conclude from this study, based on the CO_2 balance of the process, that it is possible to abate 1.6 tons of CO_2 per ton of methanol produced, if a selling price of oxygen (from water electrolysis) is included in the model; if it is not included, this figure is 1.2 tons.

The investment for CO_2 remediation *via* methanol synthesis is related to the costs of CO_2 capture, of the production of H_2 (and O_2) from water electrolysis, and of the methanol production plant. These costs are offset by revenue from the sale of methanol. CO_2 capture is assumed to be carried out with oxy-combustion, using O_2 from the electrolysis of water.

Two technologies available for the electrolytic production of O_2 and H_2 are alkaline and proton exchange membrane (PEM) electrolysers. Alkaline electrolysers are cheaper in terms of investment (they generally use nickel catalysts), but are less efficient; PEM electrolysers, conversely, are more expensive (they generally use expensive platinum-group metal catalysts) but are more efficient and can operate at higher current densities, and can therefore be cheaper for large scale hydrogen production. Rivera-Tinoco et al., (2016) conducted a techno-economic assessment using ASPEN of a power-to-methanol technology; this model is coupled either to a polymer electrolyte or a solid oxide water electrolyser with a catalytic CO_2/H_2

reactor. The capital costs were predominantly for the solid oxide/methanol process. Cost reductions would be found in the lifespan improvement of solid oxide electrolyser technologies, and from the speed at which the facility is constructed. The cost breakdown for the polymer electrolyte/methanol process shows operating costs (which are mainly the cost of power used for electrolysis) are predominant, and a higher energy efficiency of the electrolyser offers the greatest potential for the reduction of methanol production costs. Their estimate of the cost of methanol production using current plants was at between 2.5 and 15 times the current market price for methanol; these costs are predicted to be lower if low cost power were available and if water electrolysis technologies were to be improved.

Kauw et al., (2015) discuss methanol production in Iceland, which uses renewable power for water electrolysis to produce H_2 and O_2, and geothermal CO_2, to yield about 340 million litres of methanol per year, and they note the potential of using available geothermal energy and hydropower for the production of about 2,150 million litres of methanol per year. They extend their discussion to a hypothetical situation, using Germany as a case study, to illustrate that the electricity oversupply in Germany is predicted to be 24 TWhe/year by 2050, and if this were used to produce H_2 and O_2, it could translate into a methanol production of about 2,360 million litres/year using CO_2 from fossil fuel power plants.

Currently, it is estimated that <2% of anthropogenic CO_2 is utilised commercially. The impetus for carbon capture and utilisation would stem from the need to reduce emissions as part of climate change mitigation measures within a reasonably commercial setting. The approach would be transformative to the economy, in that it would provide a commercially viable way to ensure manufacturing industries and the energy sector achieve a sustainable low-carbon performance by offsetting the carbon capture costs with the production of valuable materials. This would be part of an overall strategy, along with improved efficiencies and renewable power, to mitigate climate change. Zhu (2018) provides a detailed discussion of the various technologies that utilise CO_2, and new concepts that may be commercialised. While we are cognisant of the larger effort needed to curtail and reduce emissions, the discussion here is confined to the potential offered by relatively low cost, high quality processed coal, particularly the increased hydrogen production from catalytic coal steam gasification. This option would be augmented with additional hydrogen and oxygen from water electrolysis to develop a commercially viable zero-emissions concept.

It needs to be restated that the amounts of CO_2 that need to be removed are considerable for an overall zero-emissions outcome, and as mentioned previously, this requires a worldwide effort from numerous sectors.

A Zero-emissions Trajectory for Future Power Generation

The worldwide CCT programs offer significant technical advances for higher efficiency and cleaner power generation plants. This is consistent with the recommendations in the Executive Summary of the Stern Review:

> The technical potential for efficiency improvements to reduce emissions and costs is substantial. Over the past century, efficiency in energy supply improved ten-fold or more in developed countries, and the possibilities for further gains are far from being exhausted. Studies by the International Energy Agency show that, by 2050, energy efficiency has the potential to be the biggest single source of emissions savings in the energy sector. This would have both environmental and economic benefits: energy-efficiency measures cut waste and often save money. [...] Climate-change policy can help to root out existing inefficiencies. At the company level, implementing climate policies may draw attention to money-saving opportunities. At the economy-wide level, climate-change policy may be a lever for reforming inefficient energy systems and removing distorting energy subsidies, on which governments around the world currently spend around $250bn a year.

The outlook for the future for coal-fuelled plants, as they are currently utilised, is considered by some as grim. For example, Bloomberg (2018) reports:

> By 2050, wind and solar technology provide almost 50% of total electricity globally – "50 by 50" – with hydro, nuclear and other renewables taking total zero-carbon electricity up to 71%. By 2050, we expect only 29% of the electricity production worldwide to result from burning fossil fuels, down from 63% today. This dramatic shift to "50 by 50" is being driven by cheap solar PV, cheap wind, and falling battery costs. The cost of an average PV plant falls by 71% by 2050. Wind energy is getting cheaper too, and we expect it to drop 58% by 2050. PV and wind are already cheaper than building new large-scale coal and gas plants. Batteries are also dropping dramatically in cost.

The predictions from Bloomberg may be contrasted with those of Zhang et al., (2017), who state:

> Coal accounted for 66% of China's total primary energy consumption in 2014 (National Bureau of Statistics of China, 2015), is expected to account for 50% of the total primary energy consumption by 2030, and will continue to be a major source of energy until at least 2050 ... and (for) the urgent need to cut emissions, 'clean coal' technologies are regarded as a promising

solution for China to meet its carbon reduction targets while still obtaining a considerable share of energy from coal. Using an economy-wide model, (their paper) evaluates the impact of two existing advanced coal technologies – coal upgrading and ultra-supercritical (USC) coal power generation – on economic, energy and emissions outcomes when a carbon price is used to meet China's CO_2 intensity target out to 2035. Additional deployment of USC coal power generation lowers the carbon price required to meet the CO_2 intensity target by more than 40% in the near term and by 25% in the longer term. It also increases total coal power generation and coal use. Increasing the share of coal that is upgraded leads to only a small decrease in the carbon price.

Progress worldwide on utilising new low-emissions coal-fuelled power generation has been sporadic, and this is in some measure due to the uncertainty of future policy, and also due to a reluctance to retire old inefficient coal-fuelled plants. Increases in solar power must include measures to reduce and eliminate emissions of extremely potent GHG created during the production of components for solar plants.

The relationship between the poor efficiency of a low-rank coal subcritical power station and higher CO_2 emissions has been modelled, and subsequent comparative models have shown that high quality processed coal improves the performance of SC-PS. China, the largest emitter, is at the forefront of utilising higher efficiency power generation and of examining coal upgrading options. New pulverised coal power generation plants above 600 MW in China will be SC, and half of them are reported to be USC by 2020; these units may account for over 30% of the country's total power capacity, exerting a significant impact on the economic and environmental performances of China's power industry (Zhang et al., 2017).

The direct coal-fuelled turbine combined-cycle concept requires coal with virtually zero-ash, and this model predicts the lowest COE because of the very high efficiency and relatively lower capex of combined-cycle plants. Computer simulations using a standard design of combined-cycle plants fuelled with virtually zero-ash processed low rank coal show high generating (≥50%) and thermal (80-90%) efficiencies, as well as the lowest emissions of CO_2/MWh for coal-fuelled plants.

The ultimate zero-emissions concept is of a coal-fuelled hybrid catalytic steam gasification plant that offers high quality syngas, coupled with a water electrolysis plant for O_2 and H_2; CO_2 would be captured for synthesis with H_2 to produce valuable materials (e.g. methanol).

The models discussed here indicate the zero-emissions concept could be commercially viable, if it uses relatively low-cost fuel and obtains revenue from liquids and power. Zero-emissions plants would also need off-peak power from a judicious mix of new coal-fuelled power generation and

renewable sources of power. This concept, if developed commercially, would secure the power supply needed for the prosperity of communities worldwide.

A trajectory for achieving low and eventually zero-emissions low rank coal power generation may be implemented by methodically replacing low rank coal-fuelled subcritical power plants with:

1. A CCT-SC unit, resulting in a calculated reduction of CO_2 by about 30%.
2. A CCT-DCFTCC unit, resulting in a calculated reduction of CO_2 by about 50%.
3. A planned conversion of each high efficiency unit into a zero-emissions complex by modifying these into an oxy-combustion plant. To do this, a water electrolysis plant is constructed adjacent to each of the units, and this is supplied with excess power from the grid to produce O_2 and H_2. A methanol plant is constructed and CO_2 is collected and used as feedstock with H_2 to produce methanol.
4. A CCT P/L USC plant, which would result in a >40% reduction in emissions, and can be converted into a zero-emissions oxy-combustion plant with methanol production.
5. Methanol may be recycled as fuel for new DFTCC power generating plants to operate at >50% efficiency.

The reductions in emissions stated above are calculated against the reference case of brown coal-fuelled subcritical power generation in Australia. Estimates of reductions for low emissions from high efficiency coal-fuelled plants are also provided by Barnes (2019).

The amount of anthropic CO_2 emitted to the atmosphere is very large, and many measures are required to limit global warming to 2°C by 2050. This volume has discussed some of the measures that are needed to mitigate global warming. High quality processed coal offers a secure and affordable supply of power to the community, with a means to achieve low- and ultimately zero-emissions.

Hopefully, this trajectory may be part of a greater worldwide effort that will result in the reduction in the atmospheric concentrations of GHG, and in this way avoid the extreme scenarios of climate change and rising sea levels.

References

Barnes, I. 2018. 'HELE perspectives for selected Asian countries', IEA report number CCC/287. Available at: https://www.iea-coal.org/hele-perspectives-selected-asian-countries/.

Barnes, I. 2019. 'Hele Technologies and Outreach in Japan and South Korea,' IEA report number CCC/293. Available at: https://www.iea-coal.org/hele-technologies-in-japan-and-south-korea-2/.

Baykara, S. Z. 2018. 'Hydrogen: A brief overview on its sources, production and environmental impact', *Int. J. Hydrogen Energy,* 43, 10605-10614.

Bloomberg. 2018. *New Energy Outlook 2018*. Available at: https://bnef.turtl.co/story/neo2018.

Buriak, J. M., Toro, C. and Choi, K-S. 2018. 'Chemistry of Materials for Water Splitting Reactions', *Chem. Mater.*, 30, 7325-7327.

Cau, G., Tola, V., Ferrara, F., Porcu, A. and Pettinau, A. 2018. 'CO_2-free coal-fired power generation by partial oxy-fuel and post-combustion CO_2 capture: Techno-economic analysis', *Fuel,* 214, 423-435.

CCS. 2011. *Accelarating the Uptake of CCS: Industrial Use of Captured Carbon Dioxide*. Available at: https://hub.globalccsinstitute.com/sites/default/files/publications/14026/accelerating-uptake-ccs-industrial-use-captured-carbon-dioxide.pdf.

Chang, S., Zhuo, J., Meng, S., Shiyue Qin, S. and Yao, Q. 2016. 'Clean Coal Technologies in China: Current Status and Future Perspectives', *Engineering,* 2, 447-459.

Chen, H. L., Lee, H. M., Chen, S. H., Chao, Y. and Chang, M. B. 2008. 'Review of plasma catalysis on hydrocarbon reforming for hydrogen production – Interaction, integration, and prospects', *Applied Catalysis B: Environmental,* 85, 1-9.

Coester, A., Hofkes, M. W. and Papyrakis, E. 2018. 'An optimal mix of conventional power systems in the presence of renewable energy: A new design for the German electricity market', *Energy Policy,* 116, 312-322.

Cormos, A-M., Dinca, C., Petrescu, L., Chisalita, D. A., Szabolcs Szima, S. and Cormos, C-C. 2018. 'Carbon capture and utilisation technologies applied to energy conversion systems and other energy-intensive industrial applications', *Fuel,* 211, 883-890.

Crespi, F., Gavagnin, G., Sánchez, D. and Martínez, G. S. 2017. 'Supercritical carbon dioxide cycles for power generation: A review', *Applied Energy,* 195, 152-183.

Dessens, O., Anandarajah, G. and Gambhir, A. 2016. 'Limiting global warming to 2 deg C: What do the latest mitigation studies tell us about

costs, technologies and other impacts?' *Energy Strategy Reviews,* 13-14, 67-76.

Domazetis, G., Barilla, P., James, B. D. and Glaisher, R. 2008. 'Treatments of low rank coals for improved power generation and reduction in Greenhouse gas emissions', *Fuel Processing Technology,* 89, 68-76.

Domazetis, G., Barilla, P. and James, B. D. 2010. 'Lower emission plant using processed low-rank coals', *Fuel Processing Technology,* 91, 255-265.

EPA. 2018. *Inventory of U.S. Greenhouse Gas Emissions and Sinks: 1990-2016*. Available at: https://www.epa.gov/ghgemissions/inventory-us-greenhouse-gas-emissions-and-sinks-1990-2016.

Feng, W. 2018. 'China's national demonstration project achieves around 50% net efficiency with 600°C class materials', *Fuel,* 223, 344-353.

GE. 2001. *GE Position Paper: Feasibility of Methanol as Gas Turbine Fuel.* Available at: https://www.cmsgx.com/wp-content/uploads/2015/12/GE-White-Paper-Feasibility-of-Methanol-as-a-gas-turnbine-fuel.pdf.

Goeppert, A., Czaun, M., Jones, J-P., Surya Prakash, G. K. and Olah, G. A. 2014. 'Recycling of carbon dioxide to methanol and derived products – closing the loop', *Chem. Soc. Rev.,* 43, 7995-8048.

Gross, R., Blyth, W. and Heptonstall, P. 2010. 'Risks, revenues and investment in electricity generation: Why policy needs to look beyond costs', *Energy Economics,* 32, 796-804.

IEA. 2018a. *Energy Efficiency 2018: Analysis and outlooks to 2040.* Available at: https://www.iea.org/efficiency2018/.

IEA. 2018b. *World Energy Outlook 2018: The gold standard of energy analysis.* Available at: https://www.iea.org/weo2018/electricity/.

IPCC. 2001. *Climate Change 2001: Synthesis Report: Third Assessment Report of the Intergovernmental Panel on Climate Change*, Cambridge: Cambridge University Press.

Ju, Y. and Lee, C-H. 2017. 'Evaluation of the energy efficiency of the shell coal gasification process by coal type', *Energy Conversion and Management,* 143, 123-136.

Kaniyal, A. A., van Eyk, P. J., Nathan, G. J., Peter, J., Ashman, P. J. and Pincus, J. J. 2013. 'Polygeneration of Liquid Fuels and Electricity by the Atmospheric Pressure Hybrid Solar Gasification of Coal', *Energy Fuels,* 27, 3538-3555.

Kauw, M. Benders, R. M. J. Visser, C. 2015. 'Green methanol from hydrogen and carbon dioxide using geothermal energy and/or hydropower in Iceland or excess renewable electricity in Germany', *Energy,* 90, 208-217.

Kler, A. M., Elina A. T. and Mednikov, A. S. 2018. 'A plant for methanol and electricity production: Technical-economic analysis, *Energy*, 165, 890-899.

Kumar, R., Sharma, A. and Tewari, P. C. 2015. 'Cost analysis of a coal-fired power plant using the NPV method', *J. Ind. Eng. Int.*, 11, 495-504.

Levasseur, A. 2014. 'Oxy-Combustion Technology Development for Industrial-Scale Boiler Applications', Topical Report DE NT-0005290. Alstom Power, Windsor, CT. Available at: https://www.netl.doe.gov/Library/events/2013/co2capture/A-Levassuer-Alstom-Oxy-combustion.pdf.

LeCren, R. T. 1992. 'Advanced Combustion Systems for low-Grade Fuels', Turbomachinery Technology Seminar, Caterpillar Solar Turbines.

Lior, N. 2008. 'A review of Energy resources and use: The present situation and possible paths to the future', *Energy,* 33, 842-857.

Lockwood, T. 2018. 'Reducing China's coal power emissions with CCUS retrofits', *IEA Coal Centre.* Available at: https://www.iea-coal.org/reducing-chinas-coal-power-emissions-with-ccus-retrofits/.

Majoumerd, M. M., Raas, H., Sudipta De, S. and Assadi, M. 2014. 'Estimation of performance variation of future generation IGCC with coal quality and gasification process – Simulation results of EU H2-IGCC project', *Applied Energy,* 113, 452-462.

Mantripragada, H. C. and Rubin, E. S. 2013. 'Performance, cost and emissions of coal-to-liquids (CTLs) plants using low-quality coals under carbon constraints', *Fuel,* 103, 805-813.

Messerle, V. E., Ustimenko, A. B. and Lavrichshev, O. A. 2016. 'Comparative study of coal plasma gasification: Simulation and experiment', *Fuel,* 164, 172-179.

Mondal, P., Dang, G. S. and Garg, M. O. 2011. 'Syngas production through gasification and clean-up for downstream applications – Recent developments', *Fuel Processing Technology,* 92, 1395-1410.

Navarro, R. M., Penã, M. A. and Fierro, J. L. G. 2007. 'Hydrogen Production Reactions from Carbon Feedstocks: Fossil Fuels and Biomass', *Chem. Rev.,* 107, 3952-3991.

Newby, R. A. and Bannister, R. I. 1998. 'A Direct Coal-Fired Combustion Turbine Power System Based on Slagging Gasification with in-situ Gas Cleaning', *J. Eng. Gas Turbines Power,* 120, 450-454.

NREL. 2009. *Current (2009) State-of-the-Art Hydrogen Production Cost Estimate Using Water Electrolysis.* NREL/BK-6A1-46676. Available at: https://www.hydrogen.energy.gov/pdfs/46676.pdf.

Nsanzineza, R., O'Connell, M., Brinkman, G. and Milford, J. B. 2017. 'Emissions implications of downscaled electricity generation scenarios for the western United States', *Energy Policy,* 109, 601-608.

OECD/IEA. 2017. *Tracking Clean Energy Progress 2017.* Available at: https://www.iea.org/publications/freepublications/publication/TrackingCleanEnergyProgress2017.pdf.

Olah, G. A., Goeppert, A. and Prakash, G. K. S. 2009. 'Chemical Recycling of Carbon Dioxide to Methanol and Dimethyl Ether: From Greenhouse Gas to Renewable, Environmentally Carbon Neutral Fuels and Synthetic Hydrocarbons', *J. Org. Chem.,* 74, 487-498.

Petitpasa, G., Rolliera, J-D., Darmonb, A., Gonzalez-Aguilara, J., Metkemeijera, R. and Fulcheria, L. 2007. 'A comparative study of non-thermal plasma assisted reforming technologies', *Int. J. Hydrogen Energy,* 32, 2848-2867.

Pettinau, A., Ferrara, F., Tola, V. and Cau, G. 2017, 'Techno-economic comparison between different technologies for CO_2-free power generation from coal', *Applied Energy,* 193, 426–439.

Phillips, J. and Newell, P. 2013 'The governance of clean energy in India: The clean development mechanism (CDM) and domestic energy politics', *Energy Policy,* 59, 654–662.

Riaz, A., Zahedi, G. and Klemeš, J. J. 2013. 'A review of cleaner production methods for the manufacture of methanol', *J. Cleaner Production,* 57, 19-37.

Rivera-Tinoco, R., Farran, M., Bouallou, C., Auprêtre, F., Valentin, S., Millet, P. and Ngameni, J. R. 2016. 'Investigation of power-to-methanol processes coupling electrolytic hydrogen production and catalytic CO_2 reduction', *Int. J. Hydrogen Energy,* 41, 4546-4559.

Sakamoto, Y. and Zhou, W. 2000. 'Energy analysis of a CO_2 recycling system', *Int. J. Energy Res.,* 24, 549-559.

Shuster, E. 2009. *Tracking New Coal-Fired Power Plants.* Available at: https://insideclimatenews.org/sites/default/files/Tracking%20New%20Coal.%20NREL%20Report.pdf.

Simshauser, P. and Ariyaratnam, J. 2014. 'What is normal profit for power generation?', *Journal of Financial Economic Policy*, 6 (2), 152-178.

Singh, R. and Dutta, S. 2018. 'A review on H_2 production through photocatalytic reactions using TiO_2/TiO_2-assisted catalysts', *Fuel,* 220, 607-620.

Stiegel, G. J. and Maxwell, R. C. 2001. 'Gasification technologies: the path to clean, affordable energy in the 21st century', *Fuel Processing Technology,* 71, 79-97.

Styring, P., Quadrelli, E. A. and Armstron, K. (eds.). 2014. *Carbon Dioxide Utilisation. Closing the Carbon Cycle*, Oxford: Elsevier B.V.

Taylor, E. 2018. *Coal-Powered Electric Generating Unit Efficiency and Reliability Dialogue*. Available at: https://www.osti.gov/servlets/purl/1422993.

Topper, J. 2011. *Status of Coal Fired Power Plants World-Wide*. Available at: https://www.iea.org/media/workshops/2011/cea/Topper.pdf.

United Nations Climate Change Secretariat. 2017. *Climate Action Now: Summary for Policymakers 2017*. Bonn: United Nations Climate Change Secretariat. Available at: https://unfccc.int/resource/climateaction2020/media/1307/unfccc_spm_2017.pdf.

Van Dyk J. C., Keyser, M. J. and Coertzen, M. 2006. 'Syngas production from South African coal sources using Sasol–Lurgi gasifiers', *Int. J. Coal Geology,* 65, 243-253.

Van-Dal, E. S. and Bouallou, C. 2013. 'Design and simulation of a methanol production plant from CO_2 hydrogenation', *J. Cleaner Production,* 57, 38-45.

Veras, T. da S., Mozer, T. S., dos Santos, D da C. R. M. and Cësar, A. da S. 2017. 'Hydrogen: Trends, production and characterization of the main process worldwide', *Int. J. Hydrogen Energy,* 42, 2018-2033.

Von der Assen, N. and Bardow, A. 2014. 'Life cycle assessment of polyols for polyurethane production using CO_2 as feedstock: insights from an industrial case study', *Green Chem.,* 16, 3272-3280.

Wenglarz, R. A., Nirmalan, N. V. and Daehler, T. G. 1995. 'Rugged ATS Turbines for Alternate Fuels', *ASME 95-GT-73*, New York: American Society of Mechanical Engineers.

Wiatros-Motyka, M. 2018. 'Improving Power Plant Flexibility – Paving the Way for Greening the Grid', *IEA Clean Coal Centre*. Available at: https://www.iea-coal.org/improving-power-plant-flexibility-paving-the-way-for-greening-the-grid/.

Wood, A., He, H., Joia, T., Krivy, M. and Steedman, D. 2016. 'Communication-Electrolysis at High Efficiency with Remarkable Hydrogen Production Rates', *J. Electrochemical Society,* 163, F327-F329.

World Energy Council. 2013. *World Energy Perspective: Cost of Energy Technologies*, London: World Energy Council.

Yang, Y., Mims, C. A., Mei, D. H., Peden, C. H. F. and Campbell, C. T. 2013. 'Mechanistic studies of methanol synthesis over Cu from $CO/CO_2/H_2/H_2O$ mixtures: The source of C in methanol and the role of water', *J. Catalysis,* 298, 10-17.

Zedtwitz, P. and Steinfeld, A. 2005. 'Steam-Gasification of Coal in a Fluidized-Bed/Packed-Bed Reactor Exposed to Concentrated Thermal Radiation Modelling and Experimental Validation', *Ind. Eng. Chem. Res.,* 44, 3852-3861.

Zhang, X., Winchester, N. and Zhang, X. 2017. 'The future of coal in China', *Energy Policy,* 110, 644-652.

Zhao, C., Zhang, W., Wang, Y., Liu, Q., Guo, J., Xiong, M. and Yuan, J. 2017. 'The economics of coal power generation in China', *Energy Policy,* 105, 1-9.

Zhu, Q. 2017. *Power generation from coal using supercritical CO_2 cycle (CCC/280)*, London: IEA.

Zhu, Q. 2018. *Developments in CO_2 utilisation technologies (CCC/290)*, London: IEA.